The potential therapeutic role of selenium in diffuse large B-cell lymphoma

Kassam, Shireen

The Potential Therapeutic Role of Selenium in Diffuse Large B-cell Lymphoma

Dr Shireen Kassam

A dissertation submitted to the University of London for the degree of Doctor of Philosophy

Centre for Medical Oncology
Barts Cancer Centre
Queen Mary University of London

ABSTRACT

The clinical background to this work confirms the very poor outcome of patients with recurrent diffuse large B-cell lymphoma (DLBCL) and highlights the need for better therapies. One such potential option would be to add selenium (Se) to conventional chemotherapy. Previous work has demonstrated the ability of non-toxic concentrations of Se to sensitise DLBCL cell lines to chemotherapy and to protect normal cells from chemotherapy-induced toxicity. The aims of this study were therefore to identify mechanisms of Se action and potential biomarkers of Se activity. The form of Se used was methylseleninic acid (MSA), a precursor of methylselenol, which is the metabolite thought to be responsible for the anti-tumour effects of organic Se compounds.

DLBCL cell lines differed in their sensitivity to MSA, which may relate to differences in intracellular glutathione depletion by MSA. MSA sensitivity, however, was not related to the induction of DNA damage or to the *p53* status of lymphoma cell lines. Although cytotoxic concentrations of MSA induced apoptosis, chemo-sensitising concentrations did not enhance apoptosis or alter pro-apoptotic pathways. MSA induced endoplasmic reticulum (ER) stress in a concentration-dependent manner, however, in an MSA-resistant cell line, this led to autophagy and cell survival. Thus, ER stress induction is not a mechanism of chemo-sensitisation. MSA inhibited HDAC activity in DLBCL cell lines but only in a cell-based assay, suggesting that a metabolite of MSA is responsible for this effect. In addition, MSA inhibited the hypoxia-induced induction of HIF-1α in DLBCL cell lines.

Peripheral blood mononuclear cells (PBMCs) were relatively resistant to MSA and this was associated with increased expression of two pro-survival proteins, GRP78 and NF-κB. In addition, the metabolism of MSA differed between PBMCs and DLBCL cell lines, suggesting that methylselenol is formed more efficiently in the latter. In contrast, keratinocytes and fibroblasts were relatively sensitive to MSA, but MSA was unable to protect keratinocytes from the toxicity of chemotherapeutic agents. These results differ

from those obtained in DLBCL cell lines in which MSA enhances the activity of chemotherapeutic agents.

Combining MSA and bortezomib in mantle cell lymphoma cell lines unexpectedly resulted in an antagonistic interaction. This was associated with the induction of ER stress and autophagy and increased expression of two pro-survival proteins, Bcl-2 and Mcl-1.

A proteomics approach identified novel protein changes induced by chemo-sensitising concentrations of MSA in two DLBCL cell lines.

Several potential biomarkers of Se activity were identified; GRP78, NF-κB, vascular endothelial growth factor and acetylated histone H3.

In conclusion, Se in the form of MSA affects many intracellular pathways in DLBCL cell lines, such that it has not been possible to identify a single unifying mechanism of Se action. However, differences have been observed between PBMCs and DLBCL cell lines and this work has identified novel protein changes and mechanisms of Se action.

TABLE OF CONTENTS

ABSTRACT **2**
TABLE OF CONTENTS **4**
LIST OF FIGURES **10**
LIST OF TABLES **21**
ACKNOWLEDGEMENTS **23**
ABBREVIATIONS **24**

CHAPTER 1: Introduction **31**
1.1 Background **31**
1.2 Diffuse Large B-cell lymphoma **32**
1.2.1 Classification 32
1.2.2 Clinical features and staging 33
1.2.3 Prognostic factors 34
1.2.4 Treatment 38
1.2.5 Response assessment 45
1.2.6 Recurrence 46
1.2.7 Treatment of recurrent DLBCL at St Bartholomew's Hospital 48
1.3 Selenium **49**
1.3.1 Background 49
1.3.2 Selenocysteine Synthesis and Selenoproteins 51
1.3.3 Dietary sources of selenium, intake and requirements 55
1.3.4 Chemical forms of selenium, bioavailability and metabolism 56
1.3.5 Selenium transport and uptake into cells 60
1.3.6 Selenium toxicity 62
1.3.7 Selenium and cancer prevention 63
1.3.8 Selenium in established cancer 68
1.3.9 Anti-cancer mechanisms of selenium in cancer prevention and established cancer 72
1.3.9.1 Selenoproteins 73
1.3.9.2 Selenoprotein polymorphisms 73
1.3.9.3 Redox modification of proteins 76
1.3.9.4 Cell cycle arrest and induction of apoptosis 77
1.3.9.5 Induction of phase II enzymes 81
1.3.9.6 Activation of p53 protein 81
1.3.9.7 Nrf2-Prx1 pathway 83
1.3.9.8 PI3-kinase/Akt and MAP kinase pathways 85
1.3.9.9 Inhibition of the NF-κB pathway 87
1.3.9.10 Suppression of survivin expression 89
1.3.9.11 Endoplamic reticulum stress and the unfolded protein response 90
1.3.9.12 Autophagy 95
1.3.9.13 Inhibition of angiogenesis 99
1.3.9.14 Tumour specific effects of selenium 102
1.3.10 Selenium and its effect on normal tissue 102

1.3.11 Functional markers of selenium status 103
1.3.12 Studies of selenium in lymphoma 105
1.4 HYPOTHESIS AND AIMS 112

CHAPTER 2: Materials and Methods 113
2.1 Cell Culture 113
2.1.1 Cell line characteristics 113
2.1.2 Culture of cell lines under hypoxic conditions 114
2.1.3 Harvesting peripheral blood mononuclear cells 114
2.2 Drug preparation 114
2.2.1 Methylseleninic acid 114
2.2.2 Methylselenocysteine 115
2.2.3 Doxorubicin 115
2.2.4 4-hydroperoxycyclophosphamide 115
2.2.5 Bortezomib 115
2.2.6 Suberoylanilide hydroxamic acid 115
2.2.7 Staurosporine 116
2.2.8 Bafilomycin A1 116
2.3 Cell proliferation and cytotoxicity assays 116
2.3.1 Trypan blue exclusion 116
2.3.2 ViaLight® HS assay (ATP assay) 116
2.3.3 Gauva® Viacount® Assay 117
2.4 Sample preparation for western blot analysis 119
2.4.1 Treatment of cell lines 119
2.4.2 Methylseleninic acid treatment of peripheral blood mononuclear cells 119
2.4.3 Whole cell protein extraction 119
2.4.4 Nuclear and cytoplasmic protein separation 119
2.4.5 Whole cell, nuclear and cytoplasmic protein quantification 120
2.5 Western blot analysis 121
2.5.1 Electrophoresis of proteins 121
2.5.2 Transfer of proteins from the gel to the polyvinylidene fluoride membrane 121
2.5.3 Antibody staining of western blots 122
2.5.4 Antibodies used for protein detection 122
2.5.5 Visualisation of protein bands 124
2.5.6 Validation of loading control 125
2.6 Intracellular glutathione measurement 126
2.7 Analysis of cell cycle distribution using flow cytometry 128
2.7.1 Sample preparation 128
2.7.2 Staining with propidium iodide and cell cycle analysis 128
2.8 Intracellular doxorubicin measurement by flow cytometry 128
2.9 Measurement of mitochondrial membrane potential 129
2.10 Real-time polymerase chain reaction 129
2.10.1 Sample preparation 129
2.10.2 RNA extraction and quantification 130
2.10.3 Synthesis of complementary DNA from RNA 130

2.10.4 Real-time quantitative polymerase chain reaction for GADD153 131
2.11 LC3 immunofluorescence 132
2.12 Acridine orange staining using flow cytometry 133
2.13 Quantification of the phosphinositide 3-kinase/Akt signal transduction pathway - 'Aktide assay' 133
2.13.1 Principle of the assay 133
2.13.2 Sample preparation 134
2.13.3 Aktide assay 135
2.13.4 Product extraction by strong cation exchange 135
2.13.5 Quantification of the enzymatic reaction by ultra-high performance liquid chromatography and mass spectrometry 136

CHAPTER 3: Patterns of survival in patients with diffuse large B-cell lymphoma. Long follow-up from St Bartholomew's Hospital. 140
3.1 INTRODUCTION 140
3.2 PATIENTS AND METHODS 141
3.2.1 Patients 141
3.2.2 Treatment at diagnosis and recurrence 141
3.3 RESULTS 145
3.3.1 Clinical characteristics at diagnosis 145
3.3.2 Response to initial treatment and remission duration 146
3.3.4 Recurrence 154
3.3.5 Survival 160
3.4 DISCUSSION 170

CHAPTER 4: The activity of selenium in B-NHL cell lines 177
4.1 INTRODUCTION 177
4.2 AIMS 178
4.3 MATERIALS AND METHODS 178
4.4 RESULTS 179
4.4.1 The activity of MSA in DLBCL cell lines 179
4.4.2 Combining MSA with standard chemotherapeutic agents 180
4.4.3 The effect of MSA on the generation of DNA damage 181
4.4.4 The effect of MSA on intracellular glutathione concentration 182
4.4.5 Mitochondrial membrane potential 184
4.4.6 Pro-apoptotic signalling 191
4.4.7 Effect of MSA on the p53 wild-type cell line JVM2 195
4.4.8 The effect of MSA on doxorubicin uptake 201
4.4.9 The activity of methylselenocysteine in B-NHL cell lines 204
4.5 DISCUSSION 206

CHAPTER 5: Cellular stress induction by methylseleninic acid 215
5.1 INTRODUCTION 215
5.2 AIMS 216
5.3 MATERIALS AND METHODS 216

5.4 RESULTS 217
5.4.1 Induction of endoplasmic reticulum stress in RL and DHL4 cell lines exposed to MSA 217
5.4.2 Endoplasmic reticulum stress-induced apoptosis 221
5.4.3 Protein degradation 225
5.4.4 The effect of MSA on other stress-induced proteins 231
5.5 DISCUSSION 234

CHAPTER 6: Inhibition of histone deacetylase activity by selenium 241
6.1 INTRODUCTION 241
6.2 AIMS 246
6.3 METHODS 246
6.3.1 Measurement of histone deacetylase activity 247
6.3.2 Preparation of DHL4 cell lysates as a source of histone deacetylase activity 248
6.3.3 Measurement of vascular endothelial growth factor 249
6.4 RESULTS 250
6.4.1 The effect of MSA on protein acetylation 250
6.4.2 The effect of MSA on histone deacetylase activity 253
6.4.3 The effect of MSC on protein acetylation 256
6.4.4 Effect of MSA on HIF-1α expression and vascular endothelial growth factor production 257
6.4.5 Acetylation of Histone H3 in peripheral blood mononuclear cells 259
6.5 DISCUSSION 259

CHAPTER 7: The activity of methylseleninic acid in non-malignant cells 266
7.1 INTRODUCTION 266
7.2 AIMS 268
7.3 MATERIALS AND METHODS 268
7.3.1 Cell lines 268
7.3.2 Chemicals 269
7.3.3 NF-κB activity in peripheral blood mononuclear cells treated with MSA 269
7.4 RESULTS 270
7.4.1 The activity of MSA in three in vitro models of normal cells 270
7.4.2 The activity of chemotherapeutic agents in keratinocytes and HFFF2 cells 272
7.4.3 Cell cycle analysis in keratinocytes exposed to MSA 273
7.4.4 Combining MSA and chemotherapeutic agents in keratinocytes 274
7.4.5 Induction of endoplasmic reticulum stress in peripheral blood mononuclear cells exposed to MSA 277
7.4.6 Effect of MSA on NF-κB activity in peripheral blood mononuclear cells 279
7.4.7 The effect of MSA on other stress-induced proteins in peripheral blood mononuclear cells 285
7.5 DISCUSSION 286

CHAPTER 8: Combining methylseleninic acid and bortezomib in mantle cell lymphoma cell lines **293**
8.1 INTRODUCTION **293**
8.2 AIMS **296**
8.3 METHODS **296**
8.3.1 Cell lines, cell culture and treatment of cell lines 296
8.3.2 Proteasome activity assay 297
8.4 RESULTS **298**
8.4.1 The effect of MSA and bortezomib on cell viability and number 298
8.4.2 Simultaneous combination of MSA and bortezomib 300
8.4.3 Pre-treatment with MSA followed by the addition of bortezomib 302
8.4.4 Protein changes associated with the antagonistic combination of MSA and bortezomib 304
8.4.5 Proteasome inhibition 307
8.5 DISCUSSION **309**

CHAPTER 9: The investigation of methylseleninic acid uptake and metabolism by diffuse large B-cell lymphoma cell lines and peripheral blood mononuclear cells. **315**
9.1 INTRODUCTION **315**
9.2 AIMS **318**
9.3 METHODS **318**
9.3.1 Sample preparation for total selenium determination and intracellular selenium species 318
9.3.2 Determination of total intracellular selenium concentration 318
9.3.3 Measurement of intracellular selenium species 320
9.3.4 Measurement of volatile selenium compounds 322
9.3.5 Tumour selenium measurements 323
9.3.6 β-lyase activity in lymphoma cell lines 324
9.4 RESULTS **326**
9.4.1 Total intracellular selenium concentration in DLBCL cell lines and peripheral blood mononuclear cells exposed to MSA 326
9.4.2 Intracellular selenium species in DLBCL cell lines and peripheral blood mononuclear cells 328
9.4.3 Cell lysates spiked with MSA 334
9.4.4 Volatile species generated by DHL4 cells and peripheral blood mononuclear cells exposed to 20µmol/L MSA 335
9.4.5 β-lyase activity in lymphoma cell lines 343
9.4.6 Tumour selenium concentration at diagnosis in patients with DLBCL 345
9.5 DISCUSSION **346**

CHAPTER 10: A proteomics approach to investigating the chemo-sensitising action of methylseleninic acid **356**
10.1 INTRODUCTION **356**
10.2 AIM **359**
10.3 METHODS **359**

10.3.1 Sample preparation 360
10.3.2 Cell lysis..... 361
10.3.3 Protein digestion 361
10.3.4 Peptide desalting 361
10.3.5 Phospho-peptide enrichment by immobilised metal ion affinity chromatography 361
10.3.6 Nanoflow-UPLC® coupled to tandem mass spectrometry (LC-MS/MS)..... 362
10.3.7 Data analysis 362
10.4 RESULTS 363
10.4.1 DHL4 cell line..... 363
10.4.2 RL cell line..... 371
10.4.3 Classification of the differentially expressed proteins by function 377
10.5 DISCUSSION 384

CHAPTER 11: Conclusions and future studies 393

REFERENCES..... 406
APPENDIX..... 462
Appendices to Chapter 4..... 462
Appendices to Chapter 5..... 471
Appendices to Chapter 6..... 473
Appendices to Chapter 7..... 476
Appendices to Chapter 8..... 484
Appendices to Chapter 9..... 489
Appendices to Chapter 10..... 491

PUBLICATIONS AND PRESENTATIONS ARISING FROM THIS WORK..... 500

LIST OF FIGURES

Chapter 1

Figure 1.1 Selenocysteine biosynthesis pathway. 52
Figure 1.2 Reaction catalysed by glutathione peroxidase. 53
Figure 1.3 Reaction catalysed by thioredoxin reducatase. 54
Figure 1.4 Chemical forms of selenium. 57
Figure 1.5 Metabolic pathway of dietary selenium in humans. 60
Figure 1.6 Toxicity of six chemotherapeutic agents with and without methylselenocysteine (MSC) pre-treatment in nude mice. All chemotherapy drugs were given at doses above the normal maximum tolerated dose. 69
Figure 1.7 Methylselenocysteine (MSC) increased the cure rate of human tumour xenografts treated with irinotecan. 70
Figure 1.8 Cell cycle regulation. 78
Figure 1.9 Cellular apoptosis pathway. 80
Figure 1.10 Proposed effect of selenium on the Nrf2-Prx1 pathway. 84
Figure 1.11 The NF-κB pathway. 88
Figure 1.12 The unfolded protein response resulting from endoplasmic reticulum stress. 91
Figure 1.13 Mediators of endoplasmic reticulum stress-induced apoptosis. 92
Figure 1.14 The autophagy pathway. 97
Figure 1.15 Overall survival of patients with 'aggressive' B-cell NHL split into serum selenium quartiles.. 106
Figure 1.16 Inhibition of NF-κB activity by MSA and BAY 11-7082 in a DLBCL cell line (DHL4) 109

Chapter 2

Figure 2.1 Gauva® Viacount® Assay. Live cells shown in red and dead cells shown in black (a) An example of control cells (b) An example of cells treated with bortezomib. 118
Figure 2.2 An example of a standard curve of bovine serum albumin quantified using the BCA™ assay kit. 121
Figure 2.3 Western blotting of different protein loading. Protein concentration is shown above and densitometry values below each blot. 125
Figure 2.4 An example of the standard curve of glutathione quantified using the glutathione assay kit with a concentration range of 250-4000nmol/L. 127
Figure 2.5 An example of the standard curve obtained for p-Aktide generated by plotting the ratio of the p-Aktide:IS signal on the y-axis and p-Aktide concentration on the x-axis. Concentration range 50-5000nmol/L. 137
Figure 2.6 An example of the chromatograms obtained from the 'Aktide assay'. (a) p-Aktide, by monitoring parent-daughter ion transition of *m/z* 449.7→400.6 (b) Internal standard, by monitoring the parent-daughter ion transition of *m/z* 452.7→403.6. 138
Figure 2.7 The equation used to obtain an EC_{50} value for drug activity. 139

Chapter 3

Figure 3.1 Outcome of newly diagnosed patients with DLBCL. Numbers in brackets are percentages. 148
Figure 3.2 (a) Remission duration in patients achieving CR/CRu (b) Remission duration comparing patients achieving CR and CRu. 150
Figure 3.3 Remission duration according to (a) Age at diagnosis (b) Stage at diagnosis (c) IPI score at diagnosis (d) Remission duration in patients initially achieving PR but subsequently achieving CR/CRu with additional treatment. 151
Figure 3.4 Remission duration in patients with (a) 'composite' and (b) 'discordant' lymphoma at diagnosis. 153
Figure 3.5 Outcome of patients with recurrent DLBCL. Numbers in brackets are percentages. 155
Figure 3.6 Second remission duration in (a) All patients in whom a second CR/CRu was achieved (b) Those patients in second CR/CRu that did and did not receive HDT. 158
Figure 3.7 (a) Overall and cause-specific survival for all 384 patients treated with curative intent (b) Cause-specific survival according to age at diagnosis (c) Cause-specific survival according to the stage at diagnosis (d) Cause-specific survival according to the IPI score at diagnosis. 161
Figure 3.8 (a) Overall survival according to outcome to initial therapy (b) Overall survival in patients achieving CR and CRu after initial therapy (c) Overall survival and cause-specific survival in patients achieving PR after initial therapy (d) OS in patients not responding to initial therapy. 162
Figure 3.9 Overall survival of patients with (a) 'composite' and (b) 'discordant' lymphoma at diagnosis (c) Comparison of the overall survival of patients with 'composite', 'discordant' and 'pure' DLBCL. 166
Figure 3.10 (a) Overall survival from recurrence (b) Overall survival from recurrence according to outcome to first 'salvage' chemotherapy (c) Overall survival from recurrence according to the IPI score at recurrence. 167
Figure 3.11 Overall survival from recurrence based on length of first RD (a) RD ≤ or > 1 year (b) RD ≤ or > 2 years (c) RD ≤ or > 5 years. 168
Figure 3.12 Overall survival from second remission in (a) patients that did and did not receive HDT (b) all patients achieving a second CR/CRu. 169
Figure 3.13 (a) Remission duration and (b) Overall survival in patients referred to St Bartholomew's Hospital from peripheral hospitals for high-dose therapy. 176

Chapter 4

Figure 4.1 EC_{50} concentration-effect curves following 72-hour exposure to increasing concentrations of MSA in 4 DLBCL cell lines using the ATP assay. Data points are the mean +/- SD of three separate experiments. 179
Figure 4.2 Cell viability of (a) RL cells exposed to a simultaneous combination of 1μmol/L MSA and increasing concentrations of doxorubicin (Dox) for 48 hours (b) DHL4 cells exposed to a simultaneous combination of 10μmol/L MSA and

increasing concentrations of 4-HC for 48 hours. Data points are the mean +/- SD of three separate experiments. *p<0.05..... 181
Figure 4.3 Phosphorylated histone H2AX in (a) RL cells and (b) DHL4 cells exposed to MSA for 4 hours. Exposure to UV light was used as a positive control. 182
Figure 4.4 The effect of MSA on intracellular glutathione concentration in DLBCL cell lines after (a) 2-hour and (b) 24-hour exposure. Data points are the mean+/-SD of three separate experiments. *p<0.05 is a comparison with control using one-way ANOVA followed by Tukey's test. 183
Figure 4.5 JC-1 staining in RL cells treated for 24 hours. (a) Control (b) Doxorubicin 250nmol/L (c) MSA 1µmol/L (d) MSA 5µmol/L (e) MSA 20µmol/L. Numbers represent % viable cells determined by the Guava® viacount assay. Green fluorescence is detected in the FL1 channel and red fluorescence in the FL2 channel. Cells with red fluorescence are shown in the right upper quadrant. When red fluorescence is lost, cells appear in the right lower quadrant. 185
Figure 4.6 JC-1 staining in DHL4 cells treated for 24 hours. (a) Control (b) Doxorubicin 500nmol/L (c) MSA 1µmol/L (d) MSA 10µmol/L (e) MSA 100µmol/L. Numbers represent % viable cells determined by the Guava® viacount assay. Green fluorescence is detected in the FL1 channel and red fluorescence in the FL2 channel. Cells with red fluorescence are shown in the right upper quadrant. When red fluorescence is lost, cells appear in the right lower quadrant. 186
Figure 4.7 Decrease in red fluorescence in cell lines treated for 24 hours (a) RL cells (b) DHL4 cells. Data points are the mean+/-SD of at least 3 separate experiments (except DHL4+doxorucibin n=2). The p values are a comparison with control. ... 187
Figure 4.8 JC-1 staining in RL cells treated for 48 hours. (a) Control (b) Doxorubicin 100nmol/L (c) MSA 1µmol/L (d) MSA 5µmol/L (e) MSA 10µmol/L. Numbers represent % viable cells determined by the Guava® viacount assay. Green fluorescence is detected in the FL1 channel and red fluorescence in the FL2 channel. Cells with red fluorescence are shown in the right upper quadrant. When red fluorescence is lost, cells appear in the right lower quadrant. 188
Figure 4.9 JC-1 staining in DHL4 cells treated for 48 hours. (a) Control (b) Doxorubicin 500nmol/L (c) MSA 1µmol/L (d) MSA10µmol/L (e) MSA 50µmol/L. Numbers represent % viable cells determined by the Guava® viacount assay. Green fluorescence is detected in the FL1 channel and red fluorescence in the FL2 channel. Cells with red fluorescence are shown in the right upper quadrant. When red fluorescence is lost, cells appear in the right lower quadrant. 189
Figure 4.10 Decrease in red fluorescence in cell lines treated for 48 hours (a) RL cells, data points are the mean+/-SD of 2 separate experiments (b) DHL4 cells, **data** points are the mean+/-SD of 3 separate experiments. The p value is a comparison with control. 190
Figure 4.11 PARP cleavage in (a) RL and (b) DHL4 cell lines treated with non-toxic and cytotoxic concentrations of MSA. Cells exposed to staurosporine (ST) for 6 hours were used as a positive control. 191
Figure 4.12 PARP cleavage in (a) RL and DHL4 cell lines exposed to MSA, doxorubicin or both for 48 hours. Densitometry values are shown. (b) DHL4 cells exposed to

MSA, 4-HC or both for 48 hours. DHL4 cells exposed to staurosporine (ST) 1µmol/L for 6 hours were used as a positive control. 192
Figure 4.13 (a) p-Akt in DHL4 and RL cell lines exposed to MSA 60µmol/L and 5µmol/L respectively (b) p-Erk and p-Akt in RL and DHL4 cells exposed to MSA, doxorubicin or both for 48 hours. 193
Figure 4.14 The effect of MSA on the expression of Bcl-2 family proteins. (a) RL and (b) DHL4 cell lines. Densitometry values are shown. 194
Figure 4.15 Survivin expression in (a) RL and (b) DHL4 cell lines exposed to MSA.. 195
Figure 4.16 EC_{50} concentration-response curve following 72-hour exposure to increasing concentrations of MSA in the JVM2 cell line. Data points are the mean +/- SD of 8 separate experiments. 196
Figure 4.17 Cell cycle analysis of JVM2 cells exposed to 3.4µmol/L MSA for 72 hours. (a) Representative DNA histograms (b) Cell cycle distribution. Data points are the mean +/- SD of 3 separate experiments. 197
Figure 4.18 (a) PARP cleavage and (b) p53 and p21 expression in JVM2 cells exposed to MSA (c) p53 expression in RL and DHL4 cell lines exposed to MSA. Staurosporine (ST) 0.5µmol/L for 6 hours. 198
Figure 4.19 Expression of Bcl-2 family proteins in JVM2 cells exposed to MSA. 199
Figure 4.20 Aktide assay performed in JVM2 cells exposed to pervanadate (P) for 30 minutes followed by (a) MSA for 30 minutes, data points are the mean+/-SD of 3 separate experiments and (b) MSA for 2 hours, data points are the mean+/-SD of 2 separate experiments. *p=0.003 is a comparison with control using one way ANOVA followed by Tukey's test. 200
Figure 4.21 p-Akt in JVM2 cells exposed to pervanadate (P) for 30 minutes followed by (a) MSA for 30 minutes and (b) MSA for 2 hours. 201
Figure 4.22 Representation histograms of RL cells exposed to doxorubicin (Dox) for 24 hours with and without simultaneous exposure to 1µmol/L MSA. (a) Increasing concentrations of doxorubicin alone, (b) Doxorubicin 10nmol/L, (c) Doxorubicin 50nmol/L, (d) Doxorubicin 100nmol/L, (e) Doxorubicin 250nmol/L, (f) Doxorubicin 500nmol/L. 202
Figure 4.23 Representation histograms of DHL4 cells exposed to doxorubicin (Dox) for 24 hours with and without simultaneous exposure to 1µmol/L and 10µM MSA. (a) Increasing concentrations of doxorubicin alone, (b) Doxorubicin 10nmol/L, (c) Doxorubicin 50nmol/L, (d) Doxorubicin 100nmol/L, (e) Doxorubicin 250nmol/L, (f) Doxorubicin 500nmol/L. 203
Figure 4.24 MFI in RL and DHL4 cell lines exposed to doxorubicin for 24 hours with and without simultaneous exposure to MSA (a) RL cells MSA 1µmol/L (b) DHL4 cells MSA 10µmol/L. *p<0.05. 204
Figure 4.25 EC_{50} concentration-effect curves following 72-hour exposure to increasing concentrations of methylselenocysteine in 3 lymphoma cell lines using the ATP assay. Data points are the mean +/- SD of at least 4 separate experiments. 205

Chapter 5

Figure 5.1 PDI expression in (a) RL and (b) DHL4 cell lines exposed to MSA. 217

Figure 5.2 GRP78 expression in RL cells exposed to MSA. 218
Figure 5.3 GRP78 expression in DHL4 cells exposed to MSA. 219
Figure 5.4 p-eIF2α in RL cells exposed to MSA. (a) Western blot with fold-change corrected to total eIF2α expression (b) Densitometry analysis corrected to total eIF2α expression. Data points are the mean+/- SD of two separate experiments. . 220
Figure 5.5 p-eIF2α in DHL4 cells exposed to MSA. (a) Western blot with fold-change corrected to total eIF2α expression (b) Densitometry analysis corrected to total eIF2α expression. Data points are the mean+/- SD of two separate experiments. . 221
Figure 5.6 Real-time PCR for GADD153 mRNA in the RL cell line. *p=0.02, **p=0.006. Data points are the mean +/- SDs of three separate experiments. p values are a comparison with control. 222
Figure 5.7 Real-time PCR for GADD153 mRNA in the DHL4 cell line (a) MSA 5µmol/L and 10µmol/L (b) MSA 30µmol/L and 60µmol/L. *p<0.05. Data points are the mean +/- SDs of three separate experiments except for 10µmol/L 48 hours, which is the mean+/-SD of 2 data points. p values are a comparison with control. 223
Figure 5.8 Pro-apoptotic signalling in the RL cell line exposed to MSA. (a) Bcl-2 expression (b) p-Jnk (c) and (d) PARP cleavage (as shown in Chapter 4, Figure 4.11, and repeated here). Cells exposed to staurosporine (ST) were used as a positive control. 224
Figure 5.9 Pro-apoptotic signalling in the DHL4 cell line exposed to MSA. (a) Bcl-2 expression (b) p-Jnk (c) PARP cleavage (as shown in Chapter 4, Figure 4.11, and repeated here). Cells exposed to staurosporine (ST) were used as a positive control. 225
Figure 5.10 Level of ubiquitinated proteins in the (a) RL and (b) DHL4 cell lines exposed to MSA and bortezomib. 226
Figure 5.11 LC3B-I and -II in the (a) RL and (b) DHL4 cell lines exposed to MSA. ... 227
Figure 5.12 Immunofluorescence for LC3B in the DHL4 cell line exposed to MSA ... 228
Figure 5.13 Acridine orange staining in the DHL4 cell line exposed to MSA for 24 hours. (a) Control (b) Thapsigarin 3µM, (c) MSA 10µM (d) MSA 20µM. FL1 indicates green fluorescence and FL3, red fluorescence. Cells above the horizontal line have increased red fluorescence. 229
Figure 5.14 Increase in % of red fluorescent cells in DHL4 cell line stained with acridine orange after exposure to MSA or thapsigargin (TG; positive control). Data points are the mean+/-SD of 3 separate experiments. p values are a comparison with control. 229
Figure 5.15 (a) Accumulation of LC3B-II in the DHL4 cell line exposed to 10nmol/L bafilomycin A1 (b) Cell viability assessed by the Guava® viacount assay in the DHL4 cell line exposed to MSA and bafilomycin A1. 231
Figure 5.16 Expression of HSP70 and HSP90 in (a) RL cells exposed to 5µM MSA and (b) DHL4 cells exposed to 60µM MSA. 232
Figure 5.17 (a) Nrf2 expression in RL cells exposed to 5µM MSA; nuclear and cytoplasmic protein separation (b) Prx1 expression in RL cells exposed to 3µM and 5µM MSA (c) Nrf2 expression in DHL4 cells exposed to 60µM MSA; nuclear and cytoplasmic protein separation (d) Prx1 expression in DHL4 cells exposed to 30µM and 60µM MSA. 233

Figure 5.18 Prx1 expression in DHL4 cells exposed to MSA under hypoxic conditions (1% O_2, 5% CO_2, 94% N_2). 233

Chapter 6

Figure 6.1 Simplified diagram representing the action of HDAC inhibitors. 243
Figure 6.2 An example of the standard curve obtained for vascular endothelial growth factor using the MSD cytokine assay. 250
Figure 6.3 Protein acetylation and p21 expression in DHL4 cells exposed to MSA and SAHA 251
Figure 6.4 Representative western blots of protein acetylation in (a) RL, (b) SUD4 (c) DHL4 cell lines exposed to MSA for 2 and 24 hours. These experiments were performed twice. 252
Figure 6.5 p21 expression (a) SUD4 and (b) RL cells exposed to MSA and SAHA 252
Figure 6.6 TSA inhibition of *Fluor de Lys*™ substrate deacetylation by HeLa nuclear extract. Data points are the mean+/-SD of 5 separate experiments. 253
Figure 6.7 Effect of MSA on *Fluor de Lys*™ substrate deacetylation by HeLa nuclear extract. Data points are the mean+/-SD of 3 separate experiments. 253
Figure 6.8 Deacetylation of *Fluor de Lys*™ substrate in (a) DHL4, (b) SUD4 and (c) RL cell lines incubated with MSA or TSA for 2 hours. Data points are the mean+/-SD of at least 3 separate experiments except in the SUD4 cells where experiments were only performed in duplicate. *p<0.05. p values are comparisons with control. 254
Figure 6.9 Fluorescence signal produced after incubation of *Fluor de Lys*™ substrate with different concentrations of DHL4 cell lysate compared with **HeLa nuclear** extract. AFU=arbitrary fluorescence units. 255
Figure 6.10 Deacetylation of *Fluor de Lys*™ substrate by HeLa nuclear extract and DHL4 cell lysate after incubation with MSA or TSA. Data points are the mean+/-SD of 2 separate experiments. 255
Figure 6.11 Deacetylation of *Fluor de Lys*™ substrate by HeLa nuclear extract after incubation with cell medium from DHL4 cells exposed to MSA. Data points are the mean+/-SD of 3 separate experiments. *p=0.02 is a comparison with control. 256
Figure 6.12 Protein acetylation and p21 expression in RL and DHL4 cell lines exposed to MSC for 24 hours. RL cells were also exposed to SAHA 3µmol/L for 24 hours 257
Figure 6.13 HIF-1α expression in (a, b) DHL4 cells and (c, d) RL cell lines exposed to hypoxia and MSA. Western blot and densitometry combining 2 separate experiments; data points are mean+/-SD. 258
Figure 6.14 Vascular endothelial growth factor levels in the supernatant of (a) DHL4 and (b) RL cell lines exposed to hypoxia and MSA. Data points are the mean+/-SD of 2 separate experiments. Values are expressed relative to control and are corrected for cell number ($1x10^6$ cells). 258
Figure 6.15 Histone H3 acetylation in peripheral blood mononuclear cells exposed to MSA for 24 hours. 259

Chapter 7

Figure 7.1 Perpipheral blood mononuclear cell viability determined by trypan blue exclusion after exposure to MSA. Data points are mean+/-SD of at least 3 separate experiments. *p<0.05. p values are a comparison with control. 271
Figure 7.2 EC_{50} concentration-effect curves following 48-hour exposure to increasing concentrations of MSA in (a) Keratinocytes and (b) HFFF2 cells. Data points are the mean +/- SD of three separate experiments. 271
Figure 7.3 EC_{50} concentration-effect curves following 48-hour exposure to increasing concentrations of 4-HC and doxorubicin in (a, b) Keratinocytes and (c, d) HFFF2 cells. Data points are the mean +/- SD of three separate experiments. 272
Figure 7.4 EC_{50} concentration-effect curves following 48-hour exposure to increasing concentrations of (a) 4-HC and (b) Doxorubicin in the RL cell line. Data points are the mean +/- SD of three separate experiments. 273
Figure 7.5 Cell cycle analysis of keratinocytes exposed to MSA (a) 24-hour exposure (b) Representative histogram of 24-hour exposure (c) 48-hour exposure (d) Representative histogram of 48-hour exposure. Data points are the mean+/-SD of at least 3 separate experiments. 274
Figure 7.6 Keratinocytes exposed simultaneously to MSA 0.5μM and (a) 4-HC or (b) Doxorubicin for 48 hours. Data points are the mean+/-SD of 3 separate experiments. 275
Figure 7.7 Keratinocytes pre-treated with MSA 0.5μM for 7 days followed by 48-hour exposure to (a) 4-HC or (b) Doxorubicin. Data points are the mean+/-SD of 3 separate experiments. 276
Figure 7.8 GRP78 expression in peripheral blood mononuclear cells from 3 different individuals exposed to MSA (a) 1μM and 3μM MSA for 24 and 48 hours (b) 5μM, 10μM and 20μM MSA for 24 hours. 277
Figure 7.9 GRP78 expression in peripheral blood mononuclear cells from 6 different individuals exposed to MSA for 4 hours. 278
Figure 7.10 Real-time PCR for GADD153 expression in peripheral blood mononuclear cells exposed to 20μM MSA. Data points are the mean+/-SD of at least 8 separate experiments using peripheral blood mononuclear cells harvested from 10 different individuals. The p values are a comparison with control. 279
Figure 7.11 NF-κB binding activity using the TransAM™ assay kit (a) Positive and negative controls (b) Increasing protein concentration of PBMC whole cell extracts (c) Whole cell extracts of PBMCs exposed to MSA for 24 hours. Data points are the mean+/-SD of at least 2 separate experiments. 280
Figure 7.12 NF-κB binding activity in nuclear extracts of peripheral blood mononuclear cells exposed to TNFα 10ng/ml for 1 hour followed by MSA for a further 4 hours. Experiments on peripheral blood mononuclear cells from 3 separate individuals are shown. Data points are the mean+/-SD of one experiment performed in duplicate. Below each graph is the corresponding western blot. 283
Figure 7.13 (a) NF-κB expression in nuclear extracts of peripheral blood mononuclear cells from 4 healthy subjects after exposure to MSA 20μmol/L or TNFα 10ng/ml for

4 hours (b) Densitometric analysis of western blots of 8 separate PBMC samples exposed to 20µmol/L MSA. *p=0.02. 284
Figure 7.14 p-eIF2α and IκB in peripheral blood mononuclear cells exposed to 20µM MSA. 285
Figure 7.15 (a) HSP70 and HSP90 expression in peripheral blood mononuclear cells exposed to MSA for 24 hours (b) Peroxiredoxin-1 expression in peripheral blood mononuclear cells exposed to a range of MSA concentrations for 24 and 48 hours. 286

Chapter 8

Figure 8.1 An example of a standard curve for AMC. AFU=arbitrary fluorescence units. 298
Figure 8.2 EC_{50} concentration-effect curves following 48-hour exposure to increasing concentrations of MSA and bortezomib using the Guava® viacount assay. (a) MSA cell viability (b) Bortezomib cell viability (c) MSA cell number (d) Bortezomib cell number. Data points are the mean +/- SD of three separate experiments. 299
Figure 8.3 JeKo-1 cells exposed to a simultaneous combination of MSA 10µmol/L and increasing concentrations of bortezomib. (a) Cell viability with bortezomib alone and in combination with MSA (b) The expected and observed cell viability from the combination of MSA and bortezomib. Guava® viacount assay used. Data points are the mean +/- SD of three separate experiments. *p=0.006. 301
Figure 8.4 Granta-519 cells exposed to a simultaneous combination of MSA 10µmol/L and increasing concentrations of bortezomib. (a) Cell viability with bortezomib alone and in combination with MSA (b) The expected and observed cell viability from the combination of MSA and bortezomib. Guava® viacount assay used. Data points are the mean+/-SD of three separate experiments *p=0.01. 302
Figure 8.5 JeKo-1 cells pre-treated with MSA 10µmol/L for 48 hours, followed by increasing concentrations of bortezomib for a further 48 hours. (a) Cell viability with bortezomib alone and pre-treatment with MSA (b) The expected and observed cell viability from the combination of MSA and bortezomib. Guava® viacount assay used. Data points are the mean +/- SD of three separate experiments. *p=0.01 **p=0.04 303
Figure 8.6 Granta-519 cells pre-treated with MSA 10µmol/L for 48 hours, followed by increasing concentrations of bortezomib for a further 48 hours. (a) Cell viability with bortezomib alone and pre-treatment with MSA. (b) The expected and observed cell viability from the combination of MSA and bortezomib. Guava® viacount assay used. Data points are the mean +/- SD of three separate experiments. *p=0.007 **p=0.002. 304
Figure 8.7 Induction of apoptosis, endoplasmic reticulum stress and autophagy in JeKo-1 cells exposed to MSA 10µmol/L and bortezomib 50nmol/L alone and in combination. Densitometry values are shown where relevant..... 306
Figure 8.8 Induction of apoptosis, endoplasmic reticulum stress and autophagy in Granta-519 cells exposed to MSA 10µmol/L and bortezomib 50nmol/L alone and in combination. Densitometry values are shown where relevant..... 306

Figure 8.9 Bcl-2 and Mcl-1 expression in JeKo-1 and Granta-519 cells exposed to MSA 10µmol/L alone for 72 hours, bortezomib alone 50nmol/L for 24 hours and combined pre-treatment with MSA for 48 hours followed by bortezomib for 24 hours. Densitometry values are shown. 307
Figure 8.10 Total ubiquitinated proteins in JeKo-1 and Granta-519 cells treated with 10µmol/L MSA alone, bortezomib 50nmol/L alone and combined pre-treatment with MSA for 48 hours followed by bortezomib. 308
Figure 8.11 Proteasome activity assay in cells treated with MSA 10µmol/L and bortezomib alone and in combination. Bortezomib 20nmol/L, data points are the mean +/- SD of three separate experiments, Bortezomib 50nmol/L, data points are the mean +/- SD of two separate experiments. 309

Chapter 9

Figure 9.1 Standard curve of the Se isotope ^{78}Se, obtained by the standard addition technique (cps; counts per second). 319
Figure 9.2 Chromatographic peak of reagent blank (black line) and 2 replicates of a peripheral blood mononuclear cell control sample (green and yellow lines). 320
Figure 9.3 Standard curve for sodium pyruvate used to quantify β-lyase activity in cell lines. 326
Figure 9.4 Total intracellular selenium concentration in RL and DHL4 cell lines exposed to 20µmol/L MSA. Data points are the means+/-SD of 2 separate experiments.... 327
Figure 9.5 Total intracellular selenium concentration in PBMCs exposed to 20µmol/L MSA. Data points are the mean+/-SD of 5 separate experiments. *p=0.03 comparing 2- and 6-hour exposure. 328
Figure 9.6 Representative chromatograms demonstrating intracellular selenium species generated in the DHL4 cell line exposed to 20µmol/L MSA (a) Control (b) 1-hour exposure (c) 2-hour exposure. Peak A is MSC, peak B is SLM, peak C is dimethylselenide and peak D is unknown. Experiments have been performed in duplicate. 329
Figure 9.7 Representative chromatograms demonstrating intracellular selenium species generated in the RL cell line exposed to 20µmol/L MSA (a) Control (b) 1-hour exposure (c) 2-hour exposure. Peak B is SLM, peak C is dimethylselenide and peak D is unknown. 330
Figure 9.8 Representative chromatograms demonstrating intracellular selenium species generated in peripheral blood mononuclear cells exposed to 20µmol/L MSA (a) Control (b) 1-hour exposure (c) 2-hour exposure. Peak B is SLM, peak C is dimethylselenide and peak D is unknown. Experiments have been performed in duplicate. 331
Figure 9.9 Fragmentation pattern of the unknown parent ion, *m/z* 402, consistent with S-methylselenoglutathione. 332
Figure 9.10 Representative chromatograms demonstrating intracellular selenium species generated in DLBCL cell lines exposed to 20µmol/L MSA for 24 hours (a) DHL4 control (b) DHL4 24 hours (c) RL control (d) RL 24 hours. Peak A is MSC, peak B

is SLM, peak C is γ-glutamyl-MSC, peak D is dimethylselenide, peak E is S-methylselenoglutathione. 334
Figure 9.11 Representative chromatograms demonstrating Se species generated when cell lysates were spiked with MSA (a) DHL4 cell line (b) Peripheral blood mononuclear cells. Peak A is MSA, peak B is SLM, peak C is dimethylselenide, peak D is S-methylselenoglutathione. Experiments were performed in duplicate. 335
Figure 9.12 Representative chromatograms (a) Standards, dimethylselenide and dimethyldiselenide (b) Control/untreated DHL4 cells. SPME fibre held above the headspace of untreated cells and then subjected to COC-GC-TOFMS. 337
Figure 9.13 Representative chromatograms demonstrating the generation of volatile Se species in DHL4 cells exposed to 20µmol/L MSA for 10 minutes. Two replicates shown (a, b) to demonstrate the variability in the peak intensity of dimet**h**yldiselenide. 338
Figure 9.14 Representative chromatogram demonstrating the generation of volatile Se species in peripheral blood mononuclear cells exposed to 20µmol/L MSA for 10 minutes. 339
Figure 9.15 Representative chromatograms demonstrating the generation of volatile species in (a) DHL4 cells and (b) PBMCs exposed to 20µmol/L MSA for 30 minutes. 340
Figure 9.16 Representative chromatograms demonstrating the generation of volatile species in (a) DHL4 cell line and (b) PBMCs exposed to 20µmol/L MSA for 1 hour. 342
Figure 9.17 β-lyase activity in three lymphoma cell lines and the renal adenocarcinoma cell line, ACHN. Data points are the mean+/-SD of at least 3 separate experiments. *p=0.005 **p=0.03. p values are a comparison with the relevant controls. 343
Figure 9.18 EC_{50} concentration-response curve following 72-hour exposure to increasing concentrations of MSC in the ACHN cell line. Data points are the mean+/-SD of three separate experiments. 344
Figure 9.19 Correlation between serum and tumour selenium at diagnosis in 16 patients with DLBCL. 346
Figure 9.20 The proposed cellular metabolism of MSA. 354

Chapter 10

Figure 10.1 Summary of the steps involved in the phospho-proteomics experiments (UPLC; ultra high-performance liquid chromatography) 360
Figure 10.2 Volcano plot showing fold change and p values of peptides identified in DHL4 cells exposed to 10µmol/L MSA. 364
Figure 10.3 Principal component analysis plot for DHL4 cells exposed to 10µmol/L MSA. 365
Figure 10.4 Unsupervised hierarchical clustering, shown as a heat map, of DHL4 cells exposed to 10µmol/L MSA 366
Figure 10.5 'DNA replication, recombination and repair, cell cycle and cell death' network identified by the IPA software in DHL4 cells exposed to 10µmol/L MSA. Shades of red represent proteins that were up-regulated and shades of green

represent proteins that were down-regulated. The intensity of the red and green colour relates to the degree of change..... 369
Figure 10.6 'Cell-mediated immune response, cellular development, function and maintenance' network identified by the IPA software in DHL4 cells exposed to 10µmol/L MSA. Shades of red represent proteins that were up-regulated and shades of green represent proteins that were down-regulated. The intensity of the red and green colour relates to the degree of change..... 370
Figure 10.7 'Cellular growth and proliferation, cellular development and cancer' network identified by the IPA software in DHL4 cells exposed to 10µmol/L MSA. Shades of red represent proteins that were up-regulated and shades of green represent proteins that were down-regulated. The intensity of the red and green colour relates to the degree of change. 371
Figure 10.8 Volcano plot showing fold change and p values of peptides identified in RL cells exposed to 1µmol/L MSA. 372
Figure 10.9 Principal component analysis plot for RL cells exposed to 1µmol/L MSA. 373
Figure 10.10 Unsupervised hierarchical clustering shown as a heat map of RL cells exposed to 1µmol/L MSA..... 374
Figure 10.11 'Cell death, cell cycle, connective tissue development and function' network identified by the IPA software in RL cells exposed to 1µmol/L MSA. Shades of red represent proteins that were up-regulated and shades of green represent proteins that were down-regulated. The intensity of the red and green colour relates to the degree of change..... 377

LIST OF TABLES

Chapter 1

Table 1.1 The 2008 WHO classification of DLBCL. 33
Table 1.2 Outcome of patients with DLBCL according to the IPI score, prior to the use of rituximab. 35
Table 1.3 Outcome of DLBCL according to the IPI score in patients treated with rituximab. 35
Table 1.4 Response assessment in patients with DLBCL 46

Chapter 2

Table 2.1 Primary antibodies used in western blotting experiments 123
Table 2.2 Ultra high-performance liquid chromatography and mass spectrometry conditions for the 'Aktide assay'. 137

Chapter 3

Table 3.1 Clinical Characteristics at diagnosis and recurrence of DLBCL 142
Table 3.2 Histological subtype at diagnosis and recurrence of DLBCL 144
Table 3.3 Treatment at diagnosis and recurrence of DLBCL 145
Table 3.4 Response to treatment at diagnosis and recurrence of DLBCL 148
Table 3.5 Outcome to initial therapy according to age at diagnosis 149
Table 3.6 Outcome to initial therapy according to stage at diagnosis 149
Table 3.7 Outcome to initial therapy according to IPI score at diagnosis 150
Table 3.8 Clinical characteristics of patients with 'composite' lymphoma at diagnosis 152
Table 3.9 Clinical characteristics of patients with 'discordant' lymphoma at diagnosis 153
Table 3.10 Comparison of Stage at diagnosis and at recurrence of DLBCL 157
Table 3.11 Clinical characteristics at diagnosis and recurrence of patients who developed recurrent DLBCL greater than 5 years after initial CR/CRu 159
Table 3.12 Causes of death in patients treated with curative intent 163
Table 3.13 Second malignancies in patients diagnosed with DLBCL 164
Table 3.14 Causes of death in patients with recurrent DLBCL 169
Table 3.15 Causes of death in patients receiving high-dose therapy following recurrence of DLBCL 170

Chapter 4

Table 4.1 EC_{50} values in 4 DLBCL cells lines exposed to MSA for 72 hours 180
Table 4.2 EC_{50} values in 3 lymphoma cells lines exposed to methylselenocysteine for 72 hours 205

Chapter 8

Table 8.1 MSA and bortezomib EC_{50} values for cell viability and number in JeKo-1 and Granta-518 cell lines after 48-hour exposure. EC_{50} values are the mean of 3 separate experiments. 300

Chapter 9

Table 9.1 HPLC-ICP-MS and the HPLC-ESI-MS/MS operating conditions 321
Table 9.2 GC-TOFMS operating conditions 323
Table 9.3 The ratio of dimethylselenide to S-methylselenoglutathione in DLBCL cell lines and peripheral blood mononuclear cells 333
Table 9.4 Summary of MSC EC_{50} and β-lyase activity in three lymphoma cell lines and the ACHN cell line 344
Table 9.5 Tumour selenium concentration in presentation tumour biopsy samples in patients with DLBCL 345

Chapter 10

Table 10.1 The top most up-regulated proteins in DHL4 cells exposed to 10µmol/L MSA 367
Table 10.2 The top most down-regulated proteins in DHL4 cells exposed to 10µmol/L MSA 367
Table 10.3 Up-regulated proteins in RL cells exposed to 1µmol/L MSA 375
Table 10.4 Down-regulated proteins in RL cells exposed to 1µmol/L MSA 376
Table 10.5 Differentially expressed proteins in DHL4 and RL cell lines after exposure to MSA, based on protein function. 378

ACKNOWLEDGEMENTS

There are many people I would like to thank for their help during this project. First and foremost my supervisors, Simon Joel and Ama Rohatiner, for their support, guidance and encouragement and for sharing their immense wealth of knowledge with me. I am very grateful to Andrew Lister for giving me the opportunity to work within his department and for allowing me access to the patient database. I would like to thank the members of the Barry Reed Oncology Laboratory, especially Simone Juliger, for their time and patience in helping me to acquire the necessary laboratory skills. Chapter 3 was only possible due to the hard work and dedication of Andy Wilson. The work on selenium speciation would not have been possible without the expertise of Heidi Goenaga-Infante and her team at LGC. I am also grateful to the Analytical Signalling Group (Barts Cancer Centre), particularly Pedro Cutillas, Alex Montoya and Vinni Sivarajah, without whom the proteomics experiments would not have been undertaken. Thank you also to Essam Ghazaly for helping me to analyse the proteomics data and teaching me about mass spectrometry.

I would also like to thank my funders. For the first year of this work, I was fortunate enough to be supported by a trust fund set up by Katherine Priestly in memory of her husband, David Pitblado, who sadly died of follicular lymphoma. This allowed me the time to generate sufficient data to secure funding from the Medical Research Council for the remainder of this project.

Finally, I would like to thank my family, especially my parents, Amir and Parin, and my husband, Rob, for their unfaltering love, support and patience.

ABBREVIATIONS

aaIPI	age-adjusted international prognostic index
ABC	activated B-cell
ACS	American Chemical Society
ACN	acetonitrile
AMC	7-amino-4-methylcoumarin
AML	acute myelogenous leukaemia
ANOVA	analysis of variance
AO	acridine orange
ASCT	autologous stem cell transplant
ATF	activating transcription factor
Bak	Bcl2-associated killer protein
Bax	Bcl2-associated X protein
Bcl-2	B-cell lymphoma-2
BCA	bicinchoninic acid
CDK	cyclin-dependent kinase
cDNA	complementary DNA
CHOP	cyclophosphamide, doxorubicin, vincristine, prednisolone
CHOEP	cyclophosphamide, doxorubicin, vincristine, etoposide, prednisolone
CI	confidence interval
CNS	central nervous system
COC	cryogenic oven cooling
cps	counts per second
CR	complete remission
CRu	complete remission unconfirmed
CRP	C-reactive protein
CT	computed tomography
CTCL	cutaneous T-cell lymphoma

CVA	cerebrovascular accident
DAPI	4’,-diamidino-2-phenylindole
DEPC	Diethylpyrocarbonate
DDB	DNA damage-binding protein
DLBCL	diffuse large B-cell lymphoma
DMBA	dimethylbenz(a)anthracene
DMSO	dimethyl sulfoxide
DNA	deoxyribonucleic acid
dNTPs	deoxynucleoside triphosphate
DSHNHL	German High-Grade Non-Hodgkin Lymphoma Study Group
DTNB	5,5’-dithiobis(2-nitrobenzoic acid)
DTT	dithiothreitol
ECL	enhanced chemiluminescence
ECOG	Eastern Cooperative Oncology Group
EDTA	ethylene diamine tetraacetic acid
ELISA	enzyme-linked immunosorbent assay
eIF2α	eukaryotic initiating factor 2α
ER	endoplasmic reticulum
Erk	extracellular signal-regulated kinase
ESI	electron spray ionisation
FA	formic acid
FC	fold change
FDA	Federal Drug Administration
FDG-PET	[^{18}F]fluorodeoxyglucose-positron emission tomography
FL	follicular lymphoma
GADD	growth arrest and DNA damage inducible gene
GAPDH	glyceraldehyde-3-phosphate dehydrogenase
GC	gas chromatography

GCB	germinal centre B-cell
GELA	Groupe d'Etude des Lymphoma de l'Adulte
GIT	gastrointestinal tract
GPx	glutathione peroxidase
GR	glutathione reductase
GRP	glucose regulated protein
GSH	glutathione
GSK	glutamine transaminase K
GSSH	glutathione disulphide
HAT	histone acetyltransferase
HBSS	Hanks' Buffered Salt solution
4-HC	4-hydroperoxycyclophosphamide
HDAC	histone deacetylase
HDACi	histone deacetylase inhibitor
HDT	high dose therapy
HEPES	4-(2-hydroxyethyl)-1-piperazineethanesulfonic acid
HIF	hypoxia inducible factor
H_2O_2	hydrogen peroxide
HPLC	high performance liquid chromatography
HRP	horseradish peroxidase
HSP	heat shock protein
HUVEC	human umbilical vein endothelial cell
ICE	ifosphamide, carboplatin, etoposide
ICP	inductively coupled plasma
IGEPAL®	Octylphenyl-polyethylene glycol
IHC	Immunohistochemical
IKK	IκB kinase
IMAC	immobilised metal ion affinity chromatography
IPA	Ingenuity Pathway Analysis

IPI	international prognostic index
IRE1	inositol requiring protein 1
IS	internal standard
JC-1	5,5',6,6'-tetrachloro-1,1',3,3 - tetraethylbenzimidazolylcarbocyanine iodide
Jnk	Jun N-terminal kinase
Keap	Kelch-like ECH-associated protein
KMSB	α-keto-γ-methylselenobutyrate
LDH	lactate dehydrogenase
LPL	lymphoplasmacytic lymphoma
MAPK	mitogen activated protein kinase
MCL	mantle cell lymphoma
Mcl-1	myeloid cell leukaemia-1
MCM	mini-chromosome maintenance
MDC	mediator of DNA damage checkpoint protein
MFI	mean fluorescence intensity
MInT	Mabthera international Trial
M-MLV	moloney-mouse leukaemia virus
MMP	mitochondrial membrane potential
mmu	millimass units
MS	mass spectrometry
MSA	methylseleninic acid
MSC	methylselenocysteine
MSP	methylselenopruvate
MTD	maximum tolerated dose
mTOR	mammalian target of rapamycin
m/z	mass to charge ratio
NADPH	nicotinomide adenine dinucleotide phosphate (reduced form)
NaF	sodium fluoride

Na_3VO_4	sodium orthovanadate
NF-κB	nuclear factor-kappa B
NHL	non-Hodgkin lymphoma
NPC	National Prevention of Cancer
NR	no response
Nrf2	nuclear factor (erythroid-derived 2) related factor 2
OS	overall survival
PARP	poly(ADP-ribose)polymerase
PBMCs	peripheral blood mononuclear cells
PBS	phosphate buffered saline
PBS-T	phosphate buffered saline with Tween-20®
PC	principal component
PCA	principal component analysis
PCR	polymerase chain reaction
PD	progressive disease
PDI	protein disulfide isomerase
PERK	protein kinase RNA(PKR)-like ER kinase
PHD	prolyhydroxylases
PI	propidium iodide
PI3K	phosphoinositide 3-kinase
PKC	protein kinase C
PLP	pyridoxal 5'-phosphate
PMSF	phenylmethanesulfonyl fluoride
PR	partial remission
Prx	peroxiredoxin
PVDF	polyvinylidene fluoride
R	rituximab
RD	remission duration
R-IPI	revised international prognostic index
RNA	ribonucleic acid

ROS	reactive oxygen species
RLU	relative light units
RR	response rate
SAHA	suberoylanilide hydroxamic acid
SBH	St Bartholomew's Hospital
SCX	strong cation exchange
SD	standard deviation
Se	selenium
Sec	selenocysteine
SECIS	selenocysteine insertion sequence
SELECT	selenium and vitamin E cancer prevention trial
shRNA	short hairpin ribonucleic acid
SLM	selenomethionine
SNP	single nucleotide polymorphism
SOD	superoxide dismutase
SPME	solid phase microextraction
ST	staurosporine
TBI	total body irradiation
TBS	Tris buffered saline
TCP	T-complex protein
TFA	trifluoroacetic acid
TG	thapsigargin
TLCK	tosyl-L-lysine chloromethyl ketone
TNB	5′-thio-2-nitrobenzoic acid
TNFα	tumour necrosis factor alpha
TOFMS	time of flight mass spectrometry
TRAIL	tumour necrosis-related apoptosis-inducing ligand
tRNA	transfer ribonucleic acid
TRB3	Tribbles-related protein 3
Tris	tris(hydroxymethyl)aminomethane

Trx	thioredoxin
TrxR	thioredoxin reductase
TSA	trichostatin
UK	United Kingdom
UPLC	ultra high-performance liquid chromatography
UPP	ubiquitin-proteasome pathway
UPR	unfolded protein response
USA	United States of America
UV	ultraviolet
VEGF	vascular endothelial growth factor
VHL	von Hipple-Lindau
WHO	World Health Organisation
XBP1	X-box binding protein 1

CHAPTER 1: Introduction

1.1 Background

The first description of lymphoma came from Thomas Hodgkin in 1832 (Hodgkin, 1832). He described the post-mortem, gross anatomical appearance of seven patients who had presented with lymphadenopathy and splenomegaly. Later, it became apparent that some of these patients had the disease that now bears his name, Hodgkin lymphoma (Wilks, 1865). Rudolf Virchow, in 1863, was the first to use the term lymphosarcoma to encompass the diseases we now know as Hodgkin and non-Hodgkin lymphomas (Jaffe *et al*, 2008). Since that time the classification of lymphoma has developed and changed extensively as different clinical, histological and immunophenotypic subtypes have been recognised and advances in the understanding of the underlying molecular pathogenesis have been made. The most widely used classification is that of the World Health Organisation (WHO) (Swerdlow SH, 2008) which aims at defining specific entities according to their clinical, morphological, immunophenotypic and genetic characteristics.

Non-Hodgkin lymphomas (NHL) account for around 4% of all new cancer diagnoses in the United Kingdom (UK) (http://info.cancerresearchuk.org/cancerstats) and the United States of America (USA) (Jemal *et al*, 2009). However, the incidence varies worldwide with the highest found in North America, Australia and New Zealand and the lowest in Eastern and South Central Asia (IARC). Variations also exist in the types of lymphoma seen in different parts of the world, such that T-cell and NK-cell lymphomas are more common in Asian countries (Swerdlow SH, 2008). The incidence of NHL in Western countries has been increasing over the last 20 years, the reason for which is unclear. In 2007, 10,917 people in the UK were diagnosed with NHL and in 2008 4,438 people died from NHL in the UK (http://info.cancerresearchuk.org). The incidence in men and women is roughly the same but because there are more women than men in the population, the male age-standardised incidence rate of 16.8/100,000 population is higher than the female rate of 11.9/100,000 population. The incidence of NHL increases with age and 70% of all cases are diagnosed in people over the age of 60 (http://info.cancerresearchuk.org).

1.2 Diffuse Large B-cell lymphoma

1.2.1 Classification

Diffuse large B-cell lymphoma (DLBCL) is the commonest subtype of NHL accounting for around 30% of all lymphomas worldwide (Anon, 1997). The disease we now call DLBCL has had many different names in the past. When the cell of origin of NHLs was not known, the classification of lymphoma was based on morphological appearance and growth pattern and terms included reticulum cell sarcoma (Gall & Mallory, 1942) and diffuse histiocytic lymphoma (Hicks *et al*, 1956). In the 1970s it was recognised that NHLs were tumours of the immune system derived from B- or T-cells and this led to an immunologically based classification. During the 1980s and 1990s, the Kiel classification dominated in Europe and what we know as DLBCL was sub-classified into immunoblastic, centroblastic and large cell anaplastic (B-cell) lymphomas (Gerard-Marchant *et al*, 1974). In North America, however, the Working Formulation became the main classification and diffuse mixed, diffuse large cell and immunoblastic lymphomas were the terms used (Anon, 1982). In the late 1990s a new classification by the International Lymphoma Study Group, the 'REAL' classification, incorporated aspects of both the Kiel classification and Working Formulation and the term DLBCL came into use (Harris *et al*, 1994) .

Since 2001, the WHO classification has been most widely used. In the 2001 3rd edition, the term DLBCL was used to encompass all clinical and histological subtypes of the disease. However, in the most recent 2008 4th edition, variants, sub-groups and subtypes of DLBCL are defined on the basis of site of disease, clinical factors and pathological features (Table 1.1) (Swerdlow SH, 2008). After separating these less common, new subtypes of DLBCL, there remains the group that represents the most common type of DLBCL that cannot be further sub-classified based on clinical or pathological features and this is classified as DLBCL, not otherwise specified (NOS). In the rest of this thesis, the term DLBCL refers to DLBCL-NOS as defined in the 2008 WHO classification.

Table 1.1 The 2008 WHO classification of DLBCL.

DLBCL, not otherwise specified Common morphological variants Centroblastic Immunoblastic Anaplastic Rare morphological variants Molecular Subgroups Germinal centre B-cell-like Activated B-cell-like Immunohistochemical subgroups CD5-positive DLBCL
T-cell/histiocyte-rich large B-cell lymphoma
Primary DLBCL of the central nervous system
Primary cutaneous DLBCL, leg type
EBV* positive DLBCL of the elderly
DLBCL associated with chronic inflammation
Other lymphomas of large B-cells
Borderline cases Features intermediate between DLBCL and Burkitt or classical Hodgkin lymphoma

*EBV, Ebstein-Barr virus

1.2.2 Clinical features and staging

DLBCL is an aggressive malignancy of large, mature B-cells which if left untreated has a median overall survival of less than a year. It usually arises *de novo*, but can also arise as a consequence of histological transformation of a less aggressive lymphoma, most commonly follicular lymphoma (FL). DLBCL is slightly more common in males than females and the median age at diagnosis is in the 7th decade (Anon, 1997). The aetiology of the disease remains unknown although underlying immunodeficiency is a significant risk factor. Patients usually present with a rapidly enlarging, symptomatic mass which

may be nodal or extranodal and in up to 40% of patients the disease is initially confined to extranodal sites (Harris *et al*, 1994). The commonest extranodal site is the gastrointestinal tract with the stomach and ileocaecal region most frequently involved (Koch *et al*, 2001). B symptoms consisting of fever, drenching night sweats and significant weight loss are present in around 30-40% of patients at diagnosis (Coiffier *et al*, 2002; Pfreundschuh *et al*, 2008b).

The extent of disease at diagnosis is determined by clinical examination, computed tomography (CT) scanning of the chest, abdomen and pelvis and a bone marrow biopsy. Increasingly, [^{18}F]fluorodeoxyglucose (FDG)-positron emission tomography (PET) is being used to better delineate the extent of disease (Cheson *et al*, 2007). Around half of patients have disseminated disease at diagnosis (stage III/IV) (Anon, 1997).

1.2.3 Prognostic factors

Clinical prognostic factors

At diagnosis, patients can be stratified into prognostic groups based on the International Prognostic Index (IPI) (Anon, 1993) which considers five unfavourable clinical parameters; age >60 years, Eastern Cooperative Oncology Group (ECOG) performance status ≥2, advanced stage (III/IV), ≥2 extranodal sites involved and elevated serum lactate dehydrogenase (LDH). Patients can thus be grouped into four risk groups which predict treatment response, progression-free survival and overall survival (OS; Table 1.2). For patients ≤60 years, the age-adjusted IPI (aaIPI) score can be used which considers three unfavourable variables; poor performance status, elevated LDH and advanced stage, and divides patients into four risk groups (Table 1.2). Since the IPI score was validated in patients who had not received rituximab (R) as part of their treatment (see below in Treatment; section 1.2.4), its prognostic value in the rituximab era needed to be re-assessed. A retrospective analysis of patients treated with combination chemotherapy and rituximab addressed this issue and found that the IPI score remained predictive but was only able to identify two risk groups. However, when the same factors were redistributed

into a revised IPI score (R-IPI), it was possible to identify three distinct prognostic groups (Table 1.3) (Sehn *et al*, 2007).

Table 1.2 Outcome of patients with DLBCL according to the IPI score, prior to the use of rituximab.

IPI score	Risk category	No. of risk factors	% Patients	% Complete remission	% 5-year OS
Full score	Low	0,1	35	87	73
	Low-intermediate	2	27	67	51
	High-intermediate	3	22	55	43
	High	4,5	16	44	26
Age-adjusted ≤60 years	Low	0	22	92	83
	Low-intermediate	1	32	78	69
	High-intermediate	2	32	57	46
	High	3	14	46	32

Adapted from Anon, N Engl J Med, 1993.

Table 1.3 Outcome of DLBCL according to the IPI score in patients treated with rituximab.

IPI score	Risk category	No. of risk factors	% Patients	% 4-year OS
Full score	Low	0,1	28	82
	Low-intermediate	2	27	81
	High-intermediate	3	21	49
	High	4,5	24	59
Revised	Very good	0	10	94
	Good	1,2	45	79
	Poor	3,4,5	45	55

Adapted from Sehn, LH, *et al*., Blood, 2007.

In addition to the IPI score, bulky disease was found to be an independent adverse prognostic marker in the Mabthera international Trial (MInT) (Pfreundschuh *et al*, 2008a).

This was a study evaluating the use of 'CHOP' (cyclophosphamide, doxorubicin, vincristine, prednisolone) or 'CHOP-like' chemotherapy, with or without rituximab, in patients aged between 18 and 60 years with good-prognosis disease; defined as an aaIPI score of 0 or 1, stages II-IV and stage 1 with bulky disease (i.e. a tumour mass >5cm in diameter). A linear prognostic effect on outcome was found in patients with a maximum tumour diameter between 5 and 10cms. In contrast, the Groupe d'Etude des Lymphoma de l'Adulte (GELA) study comparing 'CHOP' with and without rituximab in patients aged >60 years did not find that tumour bulk was a prognostic factor (Coiffier *et al*, 2002). Therefore, whether tumour bulk in the rituximab era is prognostic in all patient groups still needs to be clarified.

Molecular prognostic factors

In addition to the clinical prognostic factors discussed above, molecular characteristics of the disease have also been found to influence patient outcome. Studies using deoxyribonucleic acid (DNA) microarrays to investigate gene expression in tumour samples from patients with DLBCL have identified two distinct molecular subgroups with gene expression patterns reflecting different stages of B-cell development. One subgroup has the gene expression profile of germinal centre B-cells and is termed GCB-like. The other expresses genes normally induced during *in vitro* activation of peripheral blood B-cells and is termed activated B-cell-like (ABC-like). A third subgroup, termed type 3 has also been described but this group is heterogenous and not well defined (Alizadeh *et al*, 2000; Rosenwald *et al*, 2002). The outcome in patients with GCB-like gene expression signature is far superior with a 5-year survival of 60% compared with 35% in the ABC-like and 38% in the type 3 subgroup (Rosenwald *et al*, 2002). Although prognosis has improved in both the GCB-like and ABC-like subgroups with the use of rituximab, there remains a significant difference in outcome between the two groups (Lenz *et al*, 2008a).

The GCB- and ABC-like subgroups have characteristic chromosomal aberrations and alterations in different oncogenic pathways (Lenz *et al*, 2008b). For example, the t(14;18)

translocation, amplification of the *REL* locus on chromosome 2 and deletion of the tumour suppressor *PTEN* on chromosome 10 occurs exclusively in the GCB-like subgroup. In the ABC-like subgroup there is over-expression of Bcl-2 protein in the absence of the t(14;18) translocation and the transcription factor interferon regulatory factor 4 (IRF4). Other frequent aberrations include trisomy 3, deletion of chromosome arm 6q, and deletion of the *INK4a/ARF* (inhibitor of kinase 4A-alternative reading frame) tumour suppressor locus on chromosome 9. In addition, the ABC-like subgroup is characterised by constitutive activation of the nuclear factor-kappa B (NF-κB) pathway which promotes cell survival through activation of a large number of target genes. Activation of the NF-κB pathway is thought to be a mechanism of chemo-resistance in different tumour types and therefore may partly explain the poor prognosis of the ABC-like subgroup (Guo *et al*, 2004).

Since gene expression profiling is not routinely available in clinical practice, immunohistochemical (IHC) staining of tumours has been used as a surrogate to classify patients into GBC and non-GCB subgroups. The most widely used algorithm is that developed by Hans *et al.* (2004), which makes used of three IHC markers; CD10, Bcl-6 and IRF4. This was able to divide patients into two prognostic groups with a 76% and 34% 5-year OS for the GCB and non-GCB groups respectively (Hans *et al*, 2004). However, these results have not been confirmed by all studies and correlation with the gene-expression defined molecular subgroups remains imperfect (De Paepe *et al*, 2005). In addition, the value of IHC-based classification in patients treated with rituximab has not been confirmed (Nyman *et al*, 2007) and the reproducibility and interpretation of some IHC stains remains a problem (de Jong *et al*, 2007).

The GCB and ABC subgroups of DLBCL have not been formally incorporated into the WHO classification for three main reasons. Firstly, gene expression profiling is currently not available in routine clinical practice. Secondly, as mentioned above, the reproducibility and value of IHC-defined subgroups is not clear. Thirdly, the molecular subgroup does not currently influence patient management. With regards to the latter

point, clinical trials have begun to incorporate the molecular subgroup into their treatment protocols. An example of this is the current National Cancer Institute (USA) trial in which patients with non-GCB DLBCL are randomised to receive rituximab plus 'CHOP' chemotherapy with or without bortezomib, a drug that inhibits the NF-κB pathway (www.cancer.gov). A similar study is due to start shortly in the UK.

The gene-expression signature of the non-malignant cells present in the tumour microenvironment has also been shown to influence survival (Lenz *et al*, 2008a). Two gene-signatures termed stromal-1 and stromal-2 have been identified. The stromal-1 signature, associated with a favourable outcome, reflected extracellular matrix deposition and macrophage infiltration of the tumour. In contrast, the stromal-2 signature, associated with an inferior outcome, identified tumours expressing genes related to angiogenesis and this was also associated with increased tumour blood-vessel density.

1.2.4 Treatment

Vincent DeVita and his colleagues from the National Cancer Institute (USA) were the first to report, in 1975, that combination chemotherapy was potentially curative for 'diffuse histiocytic lymphoma', the majority of cases of which were probably DLBCL (DeVita *et al*, 1975). Since that time, DLBCL has been treated with a combination of non-cross resistant chemotherapy agents, the most widely used regimen has being 'CHOP'. This regimen combines cyclophosphamide, doxorubicin, vincristine and prednisolone given every 21 days (McKelvey *et al*, 1976). Subsequently, more intensive regimens were tested and were initially thought to be more effective but when a randomised comparison was made with 'CHOP', no difference was demonstrated in the response rate (RR) or OS and long-term OS was around 40% (Fisher *et al*, 1993). Additional strategies to improve the efficacy of 'CHOP' have consisted of intensifying the regimen by adding drugs such as etoposide ('CHOEP') and by giving 'CHOP' every 14 days instead of every 21 days (Pfreundschuh *et al*, 2004a; Pfreundschuh *et al*, 2004b; Tilly *et al*, 2003). Both these strategies have improved RRs, however, most centres have

continued using ‘CHOP’ every 21 days because of the increased toxicity of the newer regimens.

Localised disease

Localised DLBCL usually refers to patients with stage I disease. However, some patients with stage II disease, where the disease can be incorporated into a single radiotherapy field, are also sometimes referred to as having localised disease. Until recently, an abbreviated course of chemotherapy followed by involved field radiotherapy has been standard treatment in patients with localised DLBCL. This approach was based on a randomised trial by the Southwest Oncology Group in the USA that showed superiority of 3 cycles of ‘CHOP’ chemotherapy plus radiotherapy over 8 cycles of ‘CHOP’ chemotherapy alone, in patients with localised ‘aggressive’ lymphoma (Miller *et al*, 1998). However, updated results from this trial no longer show a survival difference between the two treatment groups, mainly due to late relapses and deaths from lymphoma in patients who received abbreviated ‘CHOP’ plus radiotherapy (Miller *et al*, 2001). Furthermore, a randomised trial conducted by the GELA group in patients older than 60 years with localised, ‘aggressive’ lymphoma, compared 4 cycles of ‘CHOP’ alone or the latter followed by radiotherapy. At a median follow-up of 7 years, there was no significant difference between the two arms in 5-year event-free or OS. Whilst the addition of radiotherapy did reduce recurrence at the initial site of disease it failed to prevent distant recurrence (Bonnet *et al*, 2007). In addition to this study, the GELA trial in younger patients (<60 years) comparing a dose-intensified ‘CHOP’ regimen with 3 cycles of ‘CHOP’ plus involved field radiotherapy in patients with localised ‘aggressive’ lymphoma found that the chemotherapy alone arm had a superior outcome (Reyes *et al*, 2005). In contrast, a study conducted by the ECOG, in which patients were randomised to receive or not to receive radiotherapy following 8 cycles of ‘CHOP’ chemotherapy, did report a significant disease-free survival benefit in the radiotherapy group (Horning *et al*, 2004). It should be noted, however, that this study included patients with less favourable characteristics such as bulky or extranodal disease.

Although the studies discussed above differ in design, patient characteristics, the type of chemotherapy and the number of cycles administered, overall it can be concluded that a 'full course' of combination chemotherapy alone is the optimal treatment for patients with localised DLBCL. Radiotherapy may result in better local disease control but to prevent recurrence at distant sites, adequate systemic chemotherapy is required. It has been extrapolated that the addition of rituximab (see below) to chemotherapy is likely to benefit patients with localised disease and thus 'CHOP' plus rituximab is the standard treatment in most centres.

Disseminated disease

The most significant advance in the treatment of DLBCL in recent years has been the addition of rituximab to 'CHOP' chemotherapy. Rituximab is a chimeric antibody, which targets the CD20 antigen on B-cells. The study that changed practice was conducted by the GELA study group and it was demonstrated that the addition of rituximab to 'CHOP' ('CHOP-R') chemotherapy in 399 previously untreated patients, aged between 60 and 80 years, significantly improved RR and OS. The complete remission (CR)/CR unconfirmed (CRu) rate and 2-year OS in the 'CHOP-R' group was 75% and 70% respectively compared with 63% and 57% in the 'CHOP' group (Coiffier *et al*, 2002). The long-term results of this study have been published and confirm the superiority of the 'CHOP-R' regimen. The 5-year OS survival in the 'CHOP-R' group was 58% compared with 45% in the 'CHOP' group. (Feugier *et al*, 2005). The MInT study subsequently confirmed the superiority of 6 cycles of 'CHOP' (or 'CHOP'-like) plus rituximab given every 21 days over 'CHOP' (or 'CHOP'-like) in 824 patients aged between 18-60 years with good prognosis DLBCL. The addition of rituximab increased the 3-year OS from 84% to 93%. However, significantly different results were obtained according to the aaIPI score. Patients with an aaIPI score of 0 and no bulk had a 3-year event-free survival of 97% compared with 78% in patients with an aaIPI score of 1 +/- bulky disease (Pfreundschuh *et al*, 2006).

Hence, in both young and elderly patients with good or poor prognosis disease, the addition of rituximab to 'CHOP' given every 21 days has become the standard of care in the 'western world'. However, unanswered questions remain regarding the scheduling of the CHOP-R regimen and whether intensification of the regimen yields better results in poor prognostic groups. In addition, patients with a very good prognosis may require less treatment, which could reduce toxicity.

These questions are being addressed in current clinical trials. For younger patients (<60 years) with an aaIPI score of 0 and no bulk the prognosis is very favourable and therefore the FLYER trial being conducted by the German High-Grade Non-Hodgkin Lymphoma Study Group (DSHNHL) is comparing 6 cycles of 'CHOP-R' given every 21 days with 4 cycles. In younger patients with an intermediate prognosis (aaIPI score 1 or 0 with bulky disease), the DSHNHL UNFOLDER trial is addressing whether 'CHOP-R' given every 14 days yields better results than 'CHOP-R' given every 21 days.

In younger patients with an unfavourable prognosis (aaIPI score 2, 3) there is no established standard of care. Randomised trials addressing the role of rituximab in this group of patients are lacking but the benefit of rituximab has been assumed from retrospective analyses and extrapolation from rituximab trials in other patient cohorts. Phase II trials of 'CHOP-R' have yielded disappointing results with one study reporting a CR rate of 74% and a 2-year OS of 68% (Brusamolino *et al*, 2006). Novel high-dose chemotherapy regimens are currently being investigated using cytotoxic agents to their maximum tolerated doses. One such is the DSHNHL 'Mega-CHOEP' trial which compared 8 cycles of conventional dose 'CHOEP-R', given every 14 days, with dose-escalated 'CHOEP-R' ('Mega-CHOEP') requiring haematopoietic stem cell support. Results published in abstract form reported that the 'CHOEP-R' group had a 3-year event-free survival of 71% and an estimated 3-year OS of 84%. These are the best results reported in young, high-risk patients with DLBCL. The 'Mega-CHOEP' arm was discontinued prematurely due to its higher toxicity and inferior survival (Schmitz *et al*, 2009).

The prognosis for elderly patients (>60 years) is worse than in younger patients and thus attempts are being made to improve upon the results of the landmark study by the GELA group which compared 8 cycles of 'CHOP' with 'CHOP-R' every 21 days (Feugier *et al*, 2005). The DSHNHL study group have previously demonstrated that 'CHOP' given every 14 days results in better RR and OS than 'CHOP' given every 21 days (Pfreundschuh *et al*, 2004a). Hence, the same study group conducted the RICOVER-60 trial comparing 6 and 8 cycles of 'CHOP' given every 14 days with and without rituximab. This demonstrated that 6 cycles of 'CHOP' given every 14 days plus 8 doses of rituximab was the best regimen, with significantly improved event-free, progression-free and OS (Pfreundschuh *et al*, 2008b). However, the results of trials formally comparing 'CHOP-R' every 14 days with every 21 days in all age groups are still awaited (Cunningham *et al*, 2009).

Other unanswered questions include the role of radiotherapy in patients with disseminated disease and high-dose therapy (HDT) followed by autologous haematopoietic stem support in the first-line treatment of high-risk patients. Regarding radiotherapy, there have been no randomised trials showing its benefit, in addition to chemotherapy, to areas of bulky or extranodal disease. This question is being addressed in the above mentioned UNFOLDER study. The superiority of HDT followed by autologous haematopoietic stem cell support over conventional chemotherapy in the first-line treatment of high-risk patients has not been established due to conflicting results obtained in clinical trials attempting to address this question (Haioun *et al*, 2000; Linch *et al*, 2010). A meta-analysis of all randomised trials of HDT as first-line treatment of 'aggressive' lymphoma was not able to show an overall survival benefit of HDT (Strehl *et al*, 2003). However, this meta-analysis was performed prior to the routine use of rituximab and thus the role of HDT as first-line treatment with the incorporation of rituximab is currently being investigated. Of note, the 'Mega-CHOEP' trial discussed above concluded that HDT with autologous haematopoietic stem cell support has no role to play in first-line treatment if rituximab is combined with conventional chemotherapy (Schmitz *et al*, 2009).

Central nervous system prophylaxis

The issue of central nervous system (CNS) prophylaxis in the treatment of DLBCL remains unresolved. It is routine practice in most treatment centres to administer CNS prophylaxis to those patients considered at high risk of CNS relapse as this carries an extremely poor prognosis. However, there is considerable variation in practice regarding indications for and methods of prophylaxis. Factors most commonly used to identify patients at high risk include site of disease involvement such as paranasal sinus, testis, epidural, bone marrow. In addition, factors such as stage IV disease, raised LDH, high-risk IPI score and >1 extranodal site involved have been identified as important in predicting CNS relapse (Cheung *et al*, 2005).

The most widely used method of prophylaxis is the administration of intra-thecal methotrexate. However, the results of the RICOVER-60 trial have added more confusion to this area as it reported that the addition of rituximab to 'CHOP' reduced the risk of CNS recurrence but that the addition of intra-thecal methotrexate did not further reduce this risk in patients treated with 'CHOP-R' (Boehme *et al*, 2009). The problem with these results is that this was a post-hoc analysis and the study was not powered to determine reduction in risk of CNS recurrence. It may be that the risk of CNS recurrence is reduced by rituximab purely because it reduces the overall risk of recurrence. Therefore, this issue requires further investigation and clarification.

It can be concluded that the addition of rituximab to 'CHOP' chemotherapy has resulted in significant improvement in the first-line treatment of all patients with DLBCL. However, it is clear that there are sub-groups of patients for which this regimen is not optimal. Therefore, future clinical trials need to concentrate on a more personalised approach to treatment, taking into account clinical and molecular prognostic factors and tailoring treatment accordingly.

Treatment of DLBCL at St Bartholomew's Hospital

At St Bartholomew's Hospital (SBH), NHL of 'unfavourable histology', (which would have included what we now call DLBCL), has been treated with an anthracycline-containing combination since the early 1970's. Initially, the regimen known as 'OPAL' (originally developed as treatment for adults with acute leukaemia) was used (Lister *et al*, 1978b). Consisting of what would now be considered relatively low doses of myelosuppressive drugs given every two weeks, the regimen comprised doxorubicin and vincristine given every 14 days for up to 6 doses, L-asparaginase given daily for 14 days and prednisolone given daily for the duration of treatment (Lister *et al*, 1978a). Subsequently, asparaginase was removed from the regimen to give a three drug combination known as 'VAP'. With the latter, the CR rate was 61% and the 3-year OS, 48% (Blackledge *et al*, 1980).

In the mid-1980's, the results of a regimen known as 'MACOP-B', used to treat patients with DLBCL, were published from Vancouver (Klimo & Connors, 1985). The regimen was derived from the Goldie-Colman hypothesis and was based on the precept that pairs of non-cross-resistant drugs given on alternate weeks would be more effective than conventional dosing schedules (Goldie & Coldman, 1986). Treatment was short, only 12 weeks. The results were indeed impressive, with a CR rate of 84% and, with a median follow-up of 4 years, the OS was 65%. Thus, the regimen was adopted at SBH and at the Christie Hospital, Manchester but with a modification: etoposide was substituted for methotrexate and the regimen was known as 'VAPEC-B' (Radford *et al*, 1994). This was an 11-week schedule of intravenous doxorubicin, cyclophosphamide, vincristine and bleomycin combined with oral etoposide and prednisolone. The CR rate was 62%, with a 4-year OS of 45%.

Between 1980 and 1986, an open-label study was conducted at SBH in which patients with newly diagnosed 'intermediate' and 'high-grade' NHL were treated with 'MACOP' (also known as 'CHOP-M') (Dhaliwal *et al*, 1993). Similar to the 'CHOP' regimen as currently used, it included, in addition, mid-cycle, intermediate dose, intravenous

methotrexate with leucovorin rescue and intra-thecal methotrexate. The regimen was essentially a hybrid between 'M-BACOD' (as originally used at the Dana-Farber Cancer Institute) that included bleomycin and high-dose methotrexate, and conventional-dose 'CHOP'. (Skarin *et al*, 1983) The aim was to try and give the non-myelosuppressive methotrexate mid-cycle, to prevent progression between cycles. In the SBH regimen however, the dose of methotrexate was lower and bleomycin was omitted. The results achieved were similar to those expected had 'CHOP' been used but not as good as those for 'M-BACOD'. However, the patient populations at SBH and the Dana-Farber Cancer Institute are different and this was not a planned, randomised comparison, thus such a comparison is not valid.

In most recent times, the standard 'CHOP' regimen has been used to treat newly diagnosed patients with DLBCL and since 2003, rituximab has been added. Prior to 2001, the policy at SBH was to give all patients prophylactic intra-thecal methotrexate with each cycle of chemotherapy. Subsequently, only those deemed at high risk for CNS relapse received this. These included patients with high LDH, a high-risk IPI score and involvement by DLBCL at specific anatomical sites; bone marrow, testes, the post-nasal space and Waldeyer's ring. Those with a paraspinal mass were also given CNS prophylaxis.

1.2.5 Response assessment

Prior to 1999, assessment of response to therapy varied widely. Therefore, the International Working Group published guidelines on the subject, which were readily adopted. This recommended the following categories based on clinical examination, CT scanning and bone marrow biopsy (if the bone marrow was involved at diagnosis); complete remission (CR), complete remission unconfirmed (CRu), partial remission (PR), stable disease (SD) and relapsed or progressive disease (PD) (Cheson *et al*, 1999). In 2007, these guidelines were revised to incorporate the results of FDG-PET scanning and thus the category of CRu was eliminated (Table 1.4) (Cheson *et al*, 2007).

Table 1.4 Response assessment in patients with DLBCL

	1999	2007
Response	**Definition**	**Definition**
CR	Complete clinical and radiological disappearance of disease.	Complete clinical and radiological disappearance of disease. PET negative.
CRu	A residual lymph node mass greater than 1.5 cm in greatest transverse diameter that has regressed by more than 75% in diameter. Indeterminate bone marrow biopsy.	N/A
PR	≥50% decrease in diameter of up to 6 of the largest dominant masses.	≥50% decrease in diameter of up to 6 of the largest dominant masses. PET positivity in a previously involved site.
SD	Failure to attain CR/PR or PD	Failure to attain CR/PR or PD
Relapsed or PD	Any new lesion or increase by ≥50% of a previously involved site.	Any new lesion or increase by ≥50% of a previously involved site.

Adapted from Cheson, BD *et al*., J Clin Oncol, 1999 and 2007.

1.2.6 Recurrence

Despite improvements in the treatment of newly diagnosed patients with DLBCL, the outcome of recurrent disease remains very poor. A significant proportion of patients, due to advanced age and co-morbidities, are deemed unsuitable for further intensive chemotherapy. For those considered suitable, HDT followed by autologous haematopoietic stem cell support remains the standard treatment for patients with recurrent disease (Philip *et al*, 1995) but it is only of value to patients who remain sensitive to second-line 'conventional dose' chemotherapy (Prince *et al*, 1996). A standard second-line chemotherapy regimen does not exist but such regimens usually contain a platinum agent or cytosine arabinoside. Overall RR to commonly used second-line regimens are around 60% with CR rates of only 25-35% (Moskowitz *et al*, 1999; Velasquez *et al*, 1988; Velasquez *et al*, 1994). Although the IPI score is predictive for overall and progression-free survival in patients with recurrent disease (Guglielmi *et al*, 2001; Hamlin *et al*, 2003), patients (i.e. those being treated with curative intent) are

treated without attention being paid to the IPI score. The importance of re-biopsy at recurrence should also be emphasised as a small proportion of patients have a different histology at recurrence, most commonly FL, and therefore would be treated differently (Larouche *et al*, 2010).

Cure is only possible in around 30-40% of patients with recurrent DLBCL who get to the point of HDT (Vose *et al*, 2004). Several reasons prevent a significant proportion of patients from receiving HDT such as chemoresistance, advanced age and co-morbidities and therapeutic options for those patients are limited. The addition of rituximab to second-line therapy has improved response rates. CR rates in a study evaluating the efficacy of 'R-ICE' (rituximab, ifosphamide, carboplatin, etoposide) as second-line therapy were 53% compared with 27% in historical controls not treated with rituximab (Kewalramani *et al*, 2004). However studies to date have been conducted in rituximab-naive patients and the efficacy of rituximab in patients failing first-line immunochemotherapy is currently being investigated. Interestingly, rituximab monotherapy in patients with recurrent/refractory DLBCL, not previously exposed to rituximab, was shown to result in a RR of 37% (Coiffier *et al*, 1998).

Evidence is now emerging to suggest that the outcome of patients with recurrent DLBCL, who have already been exposed to rituximab, may be even worse. A retrospective study evaluating the influence of prior exposure to rituximab on RR and survival in patients with relapsed/refractory DLBCL found prior exposure to be an independent adverse prognostic factor. Patients previously treated with rituximab had a 3-year progression-free survival of 17% compared with 57% in those not previously receiving rituximab and a 3-year OS of 38% compared with 67% (Martin *et al*, 2008). An interim analysis of the prospective, phase III CORAL study comparing 'R-ICE' with 'R-DHAP' (dexamethasome, cytarabine, cisplatin) has also reported an inferior event-free survival in patients previously exposed to rituximab (Giesselbrecht C, 2007). Thus, rituximab resistance appears to be a significant problem and better second-line therapies are needed.

In contrast to the situation at diagnosis, the molecular subgroup at recurrence does not appear to correlate with outcome in the small number of studies that have been performed, both the GCB and ABC-like subgroups having an equally poor prognosis (Costa *et al*, 2008; Moskowitz *et al*, 2005). There also appears to be concordance between the molecular subgroup at diagnosis and recurrence although this has by no means been widely studied (Moskowitz *et al*, 2005). A recently reported clinical trial studied the role of bortezomib in patients with relapsed/refractory DLBCL. Although bortezomib had no clinical activity as a single agent, when combined with conventional chemotherapy it resulted in a significantly higher RR and OS in patients with the ABC subgroup compared with the GCB subgroup. The overall RR and CR rate were 83% and 42% respectively in the ABC subgroup, compared to only 13% and 6.5% respectively in the GCB subgroup. The median OS was 10.8 months in the ABC subgroup compared to only 3.4 months on the GCB subgroup (Dunleavy *et al*, 2009). This is a potentially important finding, suggesting that the role of bortezomib in both first- and second-line treatment of DLBCL needs to be investigated further. In addition, the study highlights the importance of the molecular subgroup when considering different therapeutic options, thus enabling better tailoring of targeted agents. As mentioned above, a clinical trial is currently open in the USA and another will be opening in the UK to investigate the role of bortezomib in the first-line treatment of patients with non-GCB DLBCL.

1.2.7 Treatment of recurrent DLBCL at St Bartholomew's Hospital

Over a long period of time, the 'second-line' regimen at SBH for patients with recurrent/refractory DLBCL was intermediate dose cytosine arabinoside and etoposide (Whelan *et al*, 1992). Although other centres had reported good results with the platinum-containing 'ESHAP' regimen, at SBH, this was found to have very limited efficacy and was therefore abandoned (Johnson *et al*, 1993). With the advent of HDT, since 1985, patients less than 65 years of age achieving either a CR/CRu or a PR to 'second-line' therapy have been considered for HDT with autologous haematopoietic stem cell support. Prior to 1997, the myeloablative regimen used was cyclophosphamide and total body irradiation. However, this regimen was found to be associated with a significant risk of

secondary myelodysplasia and acute myelogenous leukaemia (AML) (Rohatiner *et al*, 2007). Therefore, in 1997 the 'drug-only' myeloablative regimen 'BEAM' (carmustine, etoposide, cytarabine and melphalan) was introduced.

Clearly there is a need for better therapies for relapsed/refractory DLBCL and a number of new promising targeted agents are currently being investigated. These include the radio-immunoconjugate ^{90}Y-ibritumomab-tiuxetan, the anti-angiogenic agents bevacizumab and lenalidomide and the humanised anti-CD20 monoclonal antibody, ofatumumab. This thesis has investigated the potential therapeutic role of selenium (Se) in DLBCL. The basis for this comes mainly from work performed in solid tumours, in which the addition of Se has been shown to enhance the efficacy of standard chemotherapeutic agents whilst protecting normal tissue from chemotherapy-induced toxicity (Cao *et al*, 2004). The background to the use of Se in cancer therapy will now be discussed in more detail.

1.3 Selenium

1.3.1 Background

Se is a trace element occurring in inorganic and organic forms that is fundamental to human health. It is unique amongst trace elements in that the main form of Se, selenocysteine (Sec) is encoded in DNA by the TGA codon. Sec is the 21st amino acid that is incorporated into selenoproteins, of which there are 25 in man (Kryukov *et al*, 2003). Se was first discovered in 1817 by the Swedish chemist Jon Jakob Berzelius who named it after the Greek goddess of the moon, Selene (Papp *et al*, 2007). The discovery initially came about because of its toxic effects when Berzelius was investigating the cause of illness amongst workers at a sulphuric acid manufacturing plant (Franke, 1934). In fact, it is likely that even before Se was discovered, reports of conditions occurring in animals were in fact due to excessive Se. The explorer, Marco Polo, described the splitting and falling off of hooves in horses and other animals grazing in a particular mountainous region of China (Marco, 1967). On the basis of current knowledge, it is

likely that these animals were grazing in areas where soil Se was at toxic levels. Therefore, research initially focussed on avoiding or ameliorating the toxic effects of Se. In fact, in 1943 Se was reported to be a carcinogen (Nelson *et al*, 1943). However, it soon became apparent that Se was an essential element and that diseases in animals and man could be caused by Se deficiency (Anon, 1979; Muth *et al*, 1958). This changed the emphasis of research and since, much has been learnt about the biological role of Se and the beneficial effects on human health.

Two diseases in man are associated with overt Se deficiency. These were first recognised in an area of China where soil Se is extremely low. Keshan disease is a cardiomyopathy affecting mainly children and women of child-bearing age and is frequently fatal. It is named after the north-east region of China where it was endemic (Cheng & Qian, 1990). Large scale Se supplementation has now reduced the disease incidence. Subsequently, it was discovered that the aetiology of Keshan disease is in part due to infection with an endemic Coxsackie virus which is more virulent in the presence of Se deficiency (Beck *et al*, 1994). Keshin-Beck disease is an osteoarthropathy that occurs in rural areas of China, Tibet and Siberia that is associated with severe Se deficiency but other factors are also important such as iodine status (Moreno-Reyes *et al*, 1998). In addition, it has been demonstrated that a low serum/plasma Se is associated with increased all cause mortality in the elderly (Akbaraly *et al*, 2005), a decline in cognitive function (Akbaraly *et al*, 2007), reduced fertility in men (Scott *et al*, 1998), pregnancy complications such as preeclampsia and miscarriage in women (Barrington *et al*, 1997; Rayman *et al*, 2003) and possibly an increased risk of cardiovascular disease (Flores-Mateo *et al*, 2006). Supplementation with Se above the recommended daily intake has beneficial effects on the immune system, mainly by enhancing cell-mediated immunity (Kiremidjian-Schumacher *et al*, 1994). It may have a role in delaying the progression of HIV infection (Hurwitz *et al*, 2007) and protects against disorders of the thyroid gland (Turker *et al*, 2006).

Se deficiency, therefore, results in a number of disparate effects, which are ameliorated by Se supplementation. However, the mechanism of these effects is not entirely clear. The anti-oxidant function of many selenoproteins is likely to be important although this does not provide a full explanation as some beneficial effects of Se supplementation are observed at levels above that required for full selenoprotein activity.

In addition to the effects of Se mentioned above, there has been much interest and research into the role of Se supplementation in cancer prevention and more recently as an adjuvant treatment in established cancer, mainly in solid malignancies. Pre-clinical work at the Institute of Cancer (Barts Cancer Centre, London, UK) has focused on the potential therapeutic role of Se supplementation in haematological malignancies. The role of Se in cancer will be the focus of the remainder of this chapter.

1.3.2 Selenocysteine Synthesis and Selenoproteins

Sec is unique amongst amino acids in that it is synthesised on its own transfer ribonucleic acid (tRNA) (Figure 1.1). The tRNA is initially aminoacylated with serine, which serves as the backbone for Sec synthesis. The tRNA is therefore known as $tRNA^{[Ser]Sec}$ (Lee *et al*, 1989). Biosynthesis of Sec requires the enzyme selenophosphate synthetase 2, itself a selenoprotein, that is involved in generating the active Se donor, monoselenophosphate (Glass *et al*, 1993). Sec is coded for by the UGA codon in mRNA, which is also a stop codon. In order to distinguish between these two functions, a Sec insertion sequence (SECIS) element, which is a secondary RNA stem-loop structure, is required for the incorporation of Sec into proteins. The SECIS element is located in the 3′-untranslated region of selenoprotein mRNA and recruits additional factors such as the SECIS-specific elongation factor and the SECIS-binding protein that are required for the correct insertion of Sec into polypeptide chains (Berry *et al*, 1993).

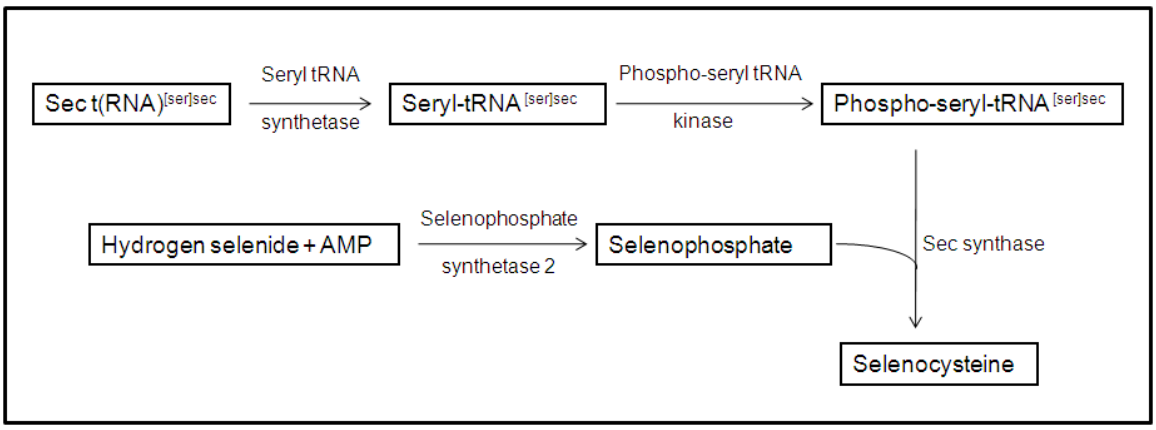

Figure 1.1 Selenocysteine biosynthesis pathway.
Adapted from Papp, LV *et al*., Antioxidants & Redox Signaling, 2007. Sec biosynthesis begins with the attachment of serine to the Sec tRNA$^{[Ser]Sec}$ by seryl tRNA synthetase to produce Seryl-tRNA$^{[Ser]Sec}$. The phosphoseryl tRNA kinase phosphorylates the complex. The phosphate is then replaced by the Se donor selenide, which is activated by selenophosphate synthetase. The resulting molecule, selenocysteyl-tRNA$^{[Ser]Sec}$, delivers the Sec into the growing polypeptide chain.

The function of many of the 25 human selenoproteins is still unknown. The best characterised are the glutathione peroxidases (GPx), thioredoxin reductases (TrxR) and iodothyronine deiodinases. The latter are involved in thyroid hormone metabolism and will not be discussed further. Most selenoproteins have been shown to have a redox regulatory function through the action of Sec within the catalytic sites. Selenoproteins relevant to cancer will be discussed below.

Glutathione Peroxidases

GPx was the first mammalian selenoprotein to be discovered (Rotruck *et al*, 1973). They are a family of antioxidant enzymes which catalyse the reduction of hydrogen peroxide (H_2O_2) and organic hydroperoxides and therefore protect cells from oxidative damage. Glutathione (GSH) is an essential cofactor for the GPx enzymes and reactions involve the oxidation of GSH to glutathione disulphide (GSSG). The GSSG is then reduced back to GSH by glutathione reductase (GR) and nicotinamide adenine dinucleotide phosphate (NAPDH). Sec, located in the N-terminal region of GPx is oxidised to selenenic acid

during the catalytic reaction and GSH is required for reduction back to Sec. In humans there are seven known GPxs but two contain cysteine instead of Sec. The Se containing proteins are GPx1, an enzyme found in the cytosol of all cells; GPx2, mainly a gastrointestinal epithelium enzyme; GPx3, an extracellular enzyme found in plasma; GPx4, a phospholipid hydroperoxide enzyme including a sperm nuclei-specific enzyme; GPx6, located in olfactory epithelium and embryonic tissue (Papp *et al*, 2007). The reaction catalysed by GPx is shown in Figure 1.2.

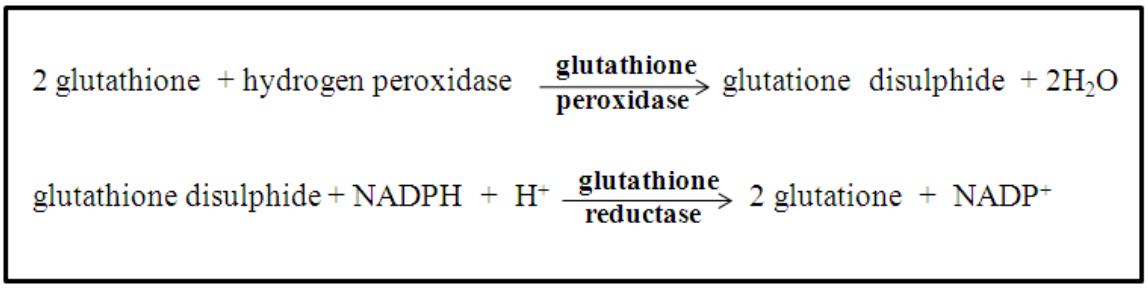

Figure 1.2 Reaction catalysed by glutathione peroxidase.
Glutathione is oxidised to glutathione disulphide. Glutathione disulphide is then reduced back to glutathione by glutathione reductase and nicotinamide adenine dinucleotide phosphate (NAPDH).

Thioredoxin reductases

The thioredoxin system within cells consists of TrxR, thioredoxin (Trx) and NADPH and plays an essential redox regulatory role. Three mammalian TrxR enzymes, containing Sec at the active site, have been identified; TrxR1 which is cytosolic, TrxR2 which is mitochondrial and TrxR3 which is testes-specific. Trx is the major cellular protein disulfide reductase and TrxR is the only enzyme known to catalyse the NADPH-dependent reduction of oxidised Trx (Figure 1.3). Trx has a number of important target proteins that require disulfide reduction for their function. These include ribonucleotide reductase, essential for DNA synthesis, and peroxiredoxins and methionine sulfoxide reductases, important antioxidant proteins. The thioredoxin system is also involved in the control of redox sensitive transcription factors such as NF-κB, p53, Ref1, and apoptosis-regulating kinase. In addition, TrxR has a number of other substrates including protein

disulfide isomerase (PDI) required for protein folding within the endoplasmic reticulum (ER) and glutaredoxin-2 which promotes cell survival. Interestingly, several Se compounds are also substrates of TrxR including selenite, selenodiglutathione and selenocysteine thus the thioredoxin system participates in selenoprotein synthesis and Se metabolism (Arner, 2009; Papp *et al*, 2007).

Given that the Trx system has a wide range of cellular functions, its role in cancer is complex. The effect of the Trx system is dependent on the cell type and various external stimuli such as growth factors. A number of studies describe over-expression of Trx and TrxR in tumours resulting in tumour growth, progression and chemo-resistance, suggesting that Trx would be a good target for cancer therapy (Grogan *et al*, 2000; Wakasugi *et al*, 1990; Yoo *et al*, 2006). In fact, many widely used chemotherapy agents have been shown to inhibit TrxR including, cisplatin, melphalan and arsenic trioxide (Arner, 2009). On the other hand, it has been demonstrated that over-expression of Trx and TrxR may induce apoptosis and reduce tumour proliferation through a p53-dependent mechanism, thus preventing cancer progression (Ueno *et al*, 1999).

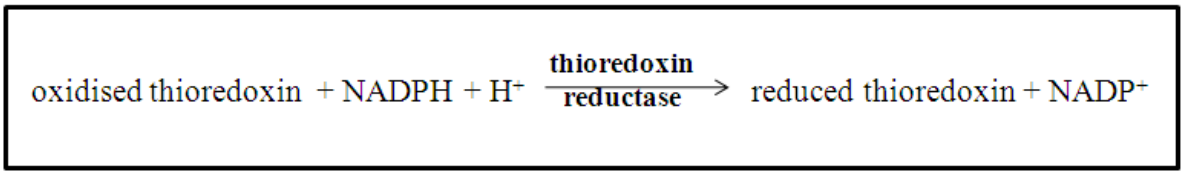

Figure 1.3 Reaction catalysed by thioredoxin reducatase.
Oxidised thioredoxin is reduced by the action of thioredoxin reductase and nicotinamide adenine dinucleotide phosphate (NAPDH).

Selenoprotein P

Selenoprotein P is the most abundant selenoprotein in plasma containing approximately 50% of the plasma Se. It is synthesised in the liver and secreted into the plasma but its expression is detected in all tissues (Hill *et al*, 2003). Selenoprotein P is the only selenoprotein with multiple Sec residues (Kryukov *et al*, 2003). Its main function is the transport and delivery of Se to tissues (discussed further below) (Hill *et al*, 2003).

Selenoprotein P may also have an antioxidant role as it has been shown *in vitro* to reduce phospholipid hydroperoxides (Saito *et al*, 1999). In addition, it may serve as a heavy metal chelator protecting against toxicity (Sasakura & Suzuki, 1998).

Sep15

Sep15 is a selenoprotein so named because of its 15kDa molecular mass. The protein is widely expressed with highest levels in the liver, kidney, testes, brain and prostate (Kumaraswamy *et al*, 2000). Although its precise function is unknown, its localisation to the ER and its interaction with the UDP-glucose:glycoprotein glycosyltransferase suggests it may play a role in protein folding within the ER (Korotkov *et al*, 2001). Studies have reported that Sep15 is required for apoptosis and loss of Sep15 is associated with a malignant phenotype (Papp *et al*, 2007).

1.3.3 Dietary sources of selenium, intake and requirements

Se enters the food chain through the consumption of plants and the amount in food is mainly dependent on the Se content of soil, which varies markedly with geographical location. In addition, plants vary in their ability to accumulate Se and factors relating to the quality of the soil can affect uptake. Thus, the Se content of food is highly variable and the same food produced in different countries may have different Se content (Keck & Finley, 2006). The result is that the Se status of individuals varies from country to country and therefore there is no accepted 'normal' reference range for plasma/serum Se. Brazil nuts are the richest source of Se. Other foods with a high Se content include offal, eggs, fish and cereals and grains (Rayman *et al*, 2008).

In the UK, Se intake and status has fallen over the past two decades. This parallels the change in the sourcing of wheat from Canada, where soil Se is high, to that grown in the UK where soil Se is low (Rayman, 2008). The current recommended daily intake of Se in the UK is 75µg in men and 60µg for women (COMA, 1991). This has been determined based on the intake required for optimal activity of plasma GPx which correlates with a plasma Se concentration of around 1.2µmol/l (Thomson *et al*, 1993). The minimum

intake of Se required to prevent deficiency diseases such as Keshan disease is 17µg/day (Anon, 1979). A higher than currently recommended intake is required for full expression of selenoprotein P (Xia *et al*, 2005) and a supra-nutritional intake is likely to be required for its anti-cancer effects (Rayman & Rayman, 2002). It is therefore probable that the current recommended intake is inadequate to exploit all the benefits of Se.

1.3.4 Chemical forms of selenium, bioavailability and metabolism

Chemical forms of selenium (Figure 1.4)

The biological effects of Se are dependent on the chemical form and dose. The main inorganic species in plants is selenate which is taken up directly from the soil. From this plants can synthesise organic species including selenomethionine (SLM), Sec, Se-methylselenocysteine (MSC) and γ-glutamyl-Se-methylselenocysteine (Rayman *et al*, 2008). Therefore, the majority of dietary Se is available in organic forms. Only a small amount of the inorganic species, selenite, is found in food. However, selenite has been extensively used as a supplement both *in vitro* and *in vivo*. The disadvantage of using selenite and other inorganic forms of Se as a supplement is that they have been shown to be genotoxic, resulting in single strand DNA breaks (Kaeck *et al*, 1997).

To exploit the health benefits of Se, various compounds are available as tablet formulations to buy 'over the counter'. The most commonly available forms are sodium selenite, SLM and MSC. Clinical trials that have investigated the role of Se supplementation in various diseases have mainly used sodium selenite and SLM. SLM is the form that has been most widely used in cancer prevention and cancer therapy trials as it is not genotoxic. In addition, Se-enriched yeast, containing SLM as the main form of Se, has also been used in cancer prevention trials.

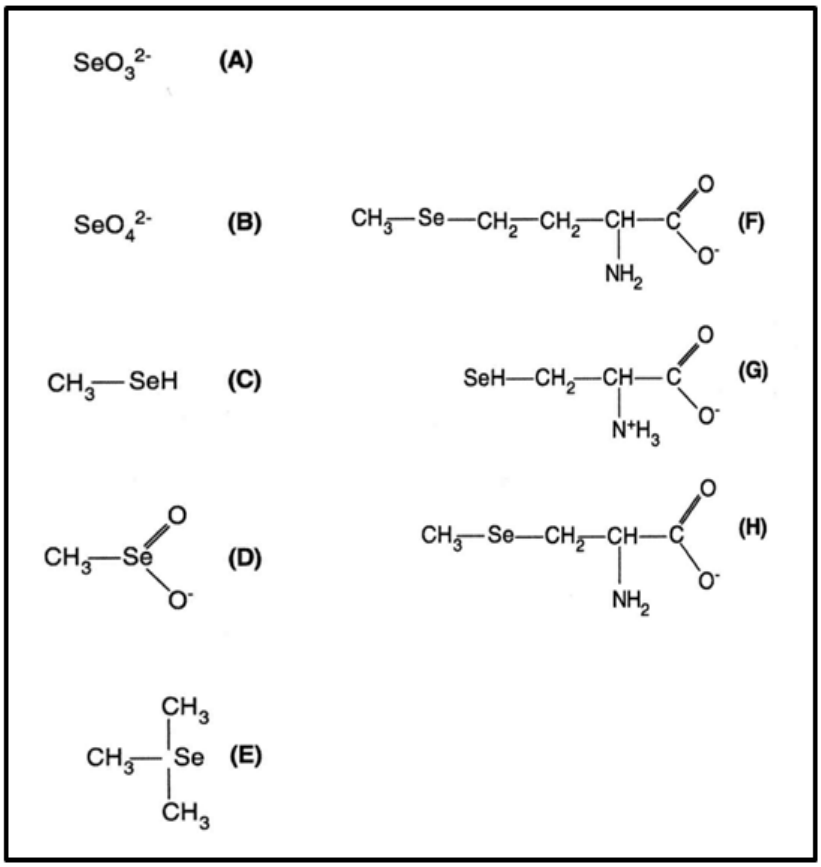

Figure 1.4 Chemical forms of selenium.
Adapted from Abdulah, R *et al*., J Trace Elem Med Biol, 2005. Selenite (A), selenate (B), methylselenol (C), methylseleninic acid (D), trimethylselenonium ion (E), selenomethionine (F), selenocysteine (G), methylselenocysteine (H).

Bioavailability

In humans, SLM has greater bioavailability than selenite. A study in Se-deficient individuals found that almost double the dose of selenite was required compared with SLM to optimise GPx3 activity (Xia *et al*, 2005). In a study in Se-replete individuals, a greater proportion of administered Se was excreted in urine in those given SLM compared with selenite, suggesting absorption of selenite is two-thirds that of SLM (Burk *et al*, 2006). MSC has not been used in clinical trials in humans although it is available as an 'over the counter' supplement. Animal data suggest that it is well absorbed when given orally (Dong *et al*, 2001; Ip *et al*, 1999).

Metabolism (Figure 1.5)

It has become clear that the metabolism of Se compounds is necessary for its anti-cancer activity and that monomethylated metabolites, especially methylselenol are crucial (Ip *et al*, 2000). Once absorbed, both inorganic and organic selenium species can be used with similar efficacy to form selenoproteins. However, Se species differ in their ability to form methylselenol. Conversion to hydrogen selenide is the central reaction in the formation of selenoproteins. Hydrogen selenide is then converted to selenophosphate and incorporated as Sec into selenoproteins. If surplus Se is available, then hydrogen selenide undergoes methylation reactions, firstly to methylselenol which is then converted to dimethylselenide, exhaled in breath, and trimethylselenonium, excreted in urine. Hydrogen selenide can also be directly converted to selenosugars which are excreted in urine. Hydrogen selenide can produce superoxide anion and H_2O_2 through oxidative metabolism and this is responsible for the induction of DNA single strand breaks, particularly a problem with inorganic compounds such as selenite (Rayman *et al*, 2008).

As mentioned above, if excess Se is present, such that selenoprotein synthesis is saturated, hydrogen selenide undergoes methylation to form methylselenol. However, SLM can be non-specifically incorporated into body proteins in place of methionine especially if methionine is in reduced supply. This results in tissue accumulation of Se and SLM is less available for conversion to monomethylated metabolites. Conversion of SLM to methylselenol can occur directly through the action of the enzyme γ-lyase, but the extent of this in humans is not clear (Okuno *et al*, 2006). In contrast, MSC can be directly converted to methylselenol by the enzyme β-lyase and does not have the problem of excessive tissue accumulation as non-specific incorporation into proteins does not occur. Therefore, MSC is a superior source of monomethylated Se species (Ohta *et al*, 2009; Suzuki *et al*, 2006a; Suzuki *et al*, 2007) and it has been demonstrated to have better anti-carcinogenic properties than SLM and selenite (Ip & Hayes, 1989; Ip *et al*, 1991). Studies in rats using enriched stable isotopes of Se suggest that orally administered MSC and SLM can both be delivered in their intact forms to organs and tissues but MSC is a more

efficient source of methylselenol as SLM is preferentially converted to hydrogen selenide (Suzuki *et al*, 2006a; Suzuki *et al*, 2008).

Methylselenol is highly reactive and volatile and therefore cannot be used directly for *in vitro* studies. Therefore, the compound methylseleninic acid (MSA) has been developed. It is a water soluble, stable metabolite that is easily taken up into cells and upon reaction with cellular thiols, such as GSH, is reduced to methylselenol (Ip *et al*, 2000).

A recent *in vivo* study compared the efficacy of MSA, SLM, MSC and selenite in xenograft models of prostate cancer. MSA and MSC were found to be equally effective and more potent than SLM and selenite at inhibiting tumour growth in the DU145 xenograft model but MSA was superior to the other three compounds in the PC-3 xenograft model. The study also examined DNA strand breaks in peripheral lymphocytes and found that MSA, MSC and SLM did not increase DNA strand breaks as assessed by the COMET assay whereas selenite did (Li *et al*, 2008a). This study adds further evidence to the superiority of Se compounds that are directly converted to monomethylated species.

For the reasons discussed above, studies at the Institute of Cancer (Barts Cancer Centre) have focussed on MSA for *in vitro* studies with a view to using MSC in a clinical trial. The remainder of this chapter will focus mainly on organic Se compounds that are precursors of methylselenol.

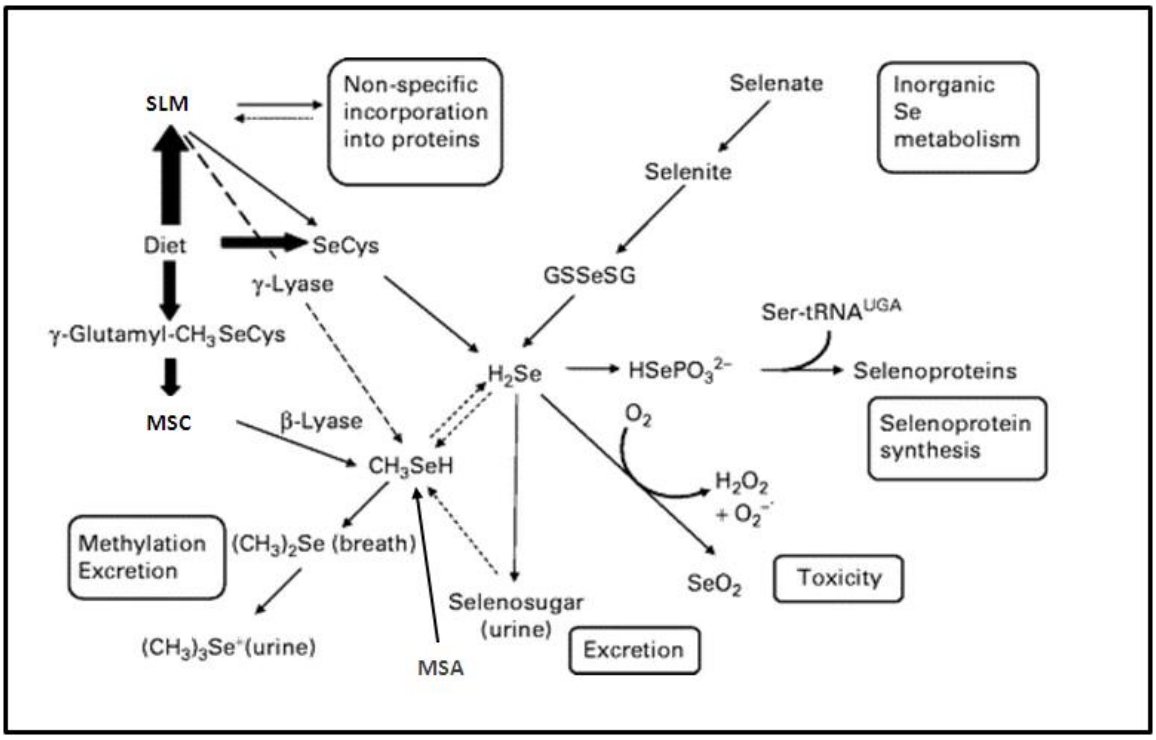

Figure 1.5 Metabolic pathway of dietary selenium in humans.
Adapted from Rayman, MP *et al*., Br J Nutr, 2008. SLM, selenomethionine; SeCys, selenocysteine; GSSeSG, selenodiglutathione; γ-glutamyl-CH_3SeCys, γ-glutamyl-methylselenocysteine; H_2Se, hydrogen selenide; $HSePO_3^{2-}$ selenophosphate; MSC, methylselenocysteine; CH_3SeH, methylselenol; $(CH_3)_2Se$, dimethylselenide; SeO_2, selenium dioxide; $(CH_3)_3Se^+$, trimethylselenonium ion.

1.3.5 Selenium transport and uptake into cells

The uptake of Se into individual cells is poorly understood. From studies in mice with deletion of the selenoprotein P gene (*Sepp*$^{-/-}$) it is apparent that selenoprotein P is important in transporting Se from the liver to other tissues. Deletion of the gene in mice results in a marked decrease in the Se concentration of brain and testes tissue, a modest decrease in kidney tissue, no change in heart tissue and no change or an increase in liver tissue (Hill *et al*, 2003; Schomburg *et al*, 2003). *Sepp*$^{-/-}$ mice develop neurological dysfunction but when fed a high-Se diet, these changes can be prevented. This suggests that Selenoprotein P is required for delivery of Se to the brain but that other mechanisms are involved when selenoprotein P is not present (Hill *et al*, 2004). Male *Sepp*$^{-/-}$ mice are infertile and feeding a high-Se diet does not reverse this (Olson *et al*, 2005). Further

research has identified that the apolipoprotein E receptor-2 is essential for uptake of Se from selenoprotein P into the brain and testes tissue (Burk *et al*, 2007; Olson *et al*, 2007). However, uptake in the brain is likely to be more complex as there is no evidence that apolipoprotein E receptor-2 is present at the blood-brain barrier and hence the full mechanism is not yet elucidated. Selenoprotein P is also required for delivery of Se to the kidney which is the main site of production of GPx3 but the apolipoprotein E receptor-2 is not involved in Se uptake into kidney tissue (Burk *et al*, 2007). It has recently been demonstrated that the lipoprotein receptor, megalin, mediates selenoprotein P uptake in the proximal tubule of the kidney (Olson *et al*, 2008).

The uptake of Se into other cell types, including neoplastic cells, is less clear. Since selenoprotein P deficient mice are capable of distributing Se to most tissues when it is supplemented in the diet, this suggests a small molecule form can be taken up by cells (Hill *et al*, 2003). *In vitro,* it has been demonstrated that selenoamino acids, such as SLM and MSC, are transported into epithelial cells by various amino acid transporters (Nickel *et al*, 2009). Selenite uptake into red blood cells is via an anion transporter (Suzuki *et al*, 1998). A study which investigated the uptake of selenite after reduction to selenide, found that selenide was actively transported into HaCat cells (keratinocyte cell line) through an anion transporter and that this was ATP-dependent (Ganyc & Self, 2008). Another *in vitro* study found that uptake of selenite required it to be reduced and that reduction was dependent on the secretion of cysteine by cells through the multidrug resistance protein efflux pumps. This cysteine secretion was in turn dependent on cystine uptake through the x_c^-cystine/glutamate antiporter in exchange for glutamate, and intracellular NAPDH-dependent reduction to cysteine. The x_c^-cystine/glutamate antiporter is over-expressed in a number of tumours and is associated with resistance to chemotherapy whereas high expression of the transporter is associated with increased sensitivity to selenite (Olm *et al*, 2009). Selenocysteine uptake into red blood cells has been shown to be ATP-dependent and incubation with cysteine inhibited this, suggesting uptake through the cysteine transporter (Imai *et al*, 2009).

Further work is required to identify mechanisms by which clinically relevant Se species are taken up into cells and to compare uptake in normal and tumour cells.

1.3.6 Selenium toxicity

There is both acute and chronic toxicity associated with Se ingestion. There have been reports in the literature of acute Se poisoning (Kise *et al*, 2004; See *et al*, 2006). The ingested dose in these cases was extremely high (2g and 10g). Symptoms included vomiting, garlic-odour breath, mucosal irritation (gastritis, gastric ulcer), abdominal pain, hypersalivation, liver necrosis, cerebral and pulmonary oedema, seizures, cardiovascular collapse and death. Chronic toxicity, known as selenosis, has been more widely documented based on studies in subjects living in seleniferous areas of the USA and China. These studies indicate that selenosis is associated with intakes of greater than 910μg/day over a period of months to years (Yang *et al*, 1983). Most common symptoms are brittle nails and hair (progressing to nail and hair loss), and garlic-odour breath and urine. Other side effects reported include gastrointestinal symptoms (diarrhoea, nausea), skin rashes, fatigue, mottled teeth and a decrease in haemoglobin concentration. Dental caries, irritability, muscle tenderness, tremor, hyperflexia and metallic taste have been reported but a direct causal relationship has not been confirmed (Barceloux, 1999).

Recently, a case series has been reported of 201 individuals who unknowingly ingested toxic concentrations of Se in the form of a liquid dietary supplement, due to a manufacturing error (MacFarquhar *et al*, 2010). The dose of Se, in the form of sodium selenite, was stated as 200μg/fluid ounce but when tested the actual concentration was 40,800μg/fluid ounce. The individuals identified had taken the supplement for a median of 29 days (range 1-109 days) and ingested a median of 41,585μg/day (range 3400-244,800μg/day). Serum Se concentrations were obtained for 8 individuals at a median of 1 day after stopping the supplement and the mean serum concentration was 9.6μmol/l (range 4-19μmol/l) The most frequently reported side-effects were diarrhoea, fatigue, hair loss, joint pain, nail discolouration or brittleness, nausea, headache, foul breath and skin complaints.

Most cancer prevention studies have supplemented Se at a dose of 200μg/day which does not appear to result in overt toxicity when taken over several years (Clark *et al*, 1996). Studies from Roswell Park Cancer Institute (Buffalo, NY, USA) have used high doses of SLM in patients with cancer and doses up to 7,200μg twice daily for a week followed by daily maintenance appear to be safe with the only definite Se-related side effect being garlic-odour breath and urine. Patients received supplementation with SLM for up to 49 weeks (Fakih *et al*, 2008). However, concern has been raised recently that prolonged elevation of serum Se levels, in individuals who, prior to supplementation, had Se concentrations at the high end of the population range, may result in more subtle adverse health effects (discussed below). These finding require further research and remain to be confirmed.

1.3.7 Selenium and cancer prevention

The main body of evidence with regards to cancer is in cancer prevention. This link was first made in the 1960's when it was reported that overall cancer mortality, in both males and females, was lower in states in the USA with high Se containing soils, and therefore a high dietary Se intake (Shamberger & Frost, 1969). This finding is supported by the results of subsequent observational, animal and human interventional studies relating to a wide range of cancers. The strongest evidence for the role of Se in cancer prevention relates to prostate cancer, but there is also good evidence to support its role in the prevention of lung, oesophageal and gastric cancers. Some of these studies are discussed below.

Epidemiological and pre-clinical studies

An epidemiological study investigated the relationship between the Se content of food crops and cancer mortality over a 19-year period in counties of the USA. A significant inverse association was found for the incidence of lung, rectal, bladder, oesophageal, and cervical cancers in rural counties and lung, breast, bladder, rectal, oesophageal, and uterine cancers in all counties (Clark *et al*, 1991). A prospective study of 39,268 Finnish residents found that in men with the lowest serum Se level there was an increased risk of

cancer, with the strongest association for gastric and lung cancers (Knekt *et al*, 1990). Toenail Se levels and the incidence of advanced prostate cancer was investigated in an epidemiological case-control study of 33,737 men in the USA who were followed for 6 years. Those with higher Se levels had a reduced risk of advanced prostate cancer (Yoshizawa *et al*, 1998). A meta-analysis of sixteen epidemiological studies has shown a significantly increased risk of lung cancer associated with low Se exposure, the effect being most marked in populations where daily intake of Se is <55µg/day (Zhuo *et al*, 2004). It would be wrong to suggest, however, that all observational studies had found an inverse correlation between serum/plasma Se and cancer risk. Nonetheless, the data are compelling.

The mammary gland is the most widely studied organ in animals with regards to the inhibitory effects of Se on tumour development. Se has been shown to inhibit tumour development in many rodent models of mammary cancer including virus-induced, chemical carcinogen-induced and spontaneous mammary tumours (El-Bayoumy & Sinha, 2004). An example is a study in which rats injected with the carcinogen methylurea were fed a normal diet or one that contained Se-enriched broccoli. This latter group developed fewer mammary tumours (Finley *et al*, 2001). The predominant species in Se-enriched broccoli has previously been shown to be MSC (Cai *et al*, 1995), which is more effective than SLM in suppressing mammary tumours in rodents (Ip *et al*, 1991).

Interventional studies

On the strength of the observational and animal chemoprevention studies, many interventional studies have been conducted with Se supplementation but the results are far from clear-cut. The Linxian province in China is a region where the mean serum Se concentration in the population is low and which has some of the highest incidences of oesophageal squamous cell cancer and gastric-cardia adenocarcinoma in the world. A significant inverse relationship has been demonstrated between baseline Se and the risk of developing and also dying from these two cancers (Mark *et al*, 2000; Wei *et al*, 2004). The General Population Intervention Trial was a randomised, placebo-controlled, primary

oesophageal and gastric cancer prevention trial conducted in the Linxian province from 1985 to 1991. 29,584 adults participated and were given different combinations of vitamin and mineral supplements to take daily. Results published in 1993 reported that the combination of Se (50μg as Se-enriched yeast), vitamin E and beta-carotene significantly reduced total mortality, total cancer mortality and mortality from gastric cancer (Blot *et al*, 1993). Recently reported, updated results of this trial found that even 10 years after completing active intervention, the group receiving the above supplementation still showed a 5% reduction in total mortality and an 11% reduction in gastric cancer mortality. This protective effect was, however, only apparent in individuals younger than 55 years (Qiao *et al*, 2009).

The strongest evidence for Se in cancer prevention comes from the Nutritional Prevention of Cancer (NPC) trial (Clark *et al*, 1996), the aim of which was to investigate the role of Se supplementation in preventing the recurrence of non-melanomatous skin cancer. This double-blind, placebo-controlled trial of Se-enriched yeast (200μg/day) randomised 1312 patients with a diagnosis of non-melanomatous skin cancer, with the primary end point being recurrence of skin cancer. An interim analysis, however, demonstrated a reduction in the incidence and mortality of other cancers, thus the trial was modified to include various secondary endpoints; incidence and mortality of lung, prostate, colon and total cancer. Results for the first 10 years of the trial were not able to show a reduction in the primary endpoint, but did show a significant reduction in all the secondary endpoints. After longer follow-up, a reduction in total cancer and prostate cancer incidence and mortality was still apparent, but there was no longer an effect on lung or colon cancer incidence and mortality (Duffield-Lillico *et al*, 2003; Duffield-Lillico *et al*, 2002).

For several reasons, the results of the NPC trial required clarification. Firstly, the primary endpoint of incidence of recurrent skin cancer was higher in the Se-supplemented group. However, when cases occurring in the first two years after randomisation were excluded, the risk of developing recurrent skin cancer was non-significant. Secondly, the benefits of Se supplementation were only seen in men, although three quarters of the study

population were male. Thirdly, the benefits of Se supplementation were only seen in those with a low plasma/serum Se level at the start of the trial (Duffield-Lillico *et al*, 2002).

In order to address some of these unanswered questions, the Se and vitamin E cancer prevention trial (SELECT), sponsored by the National Cancer Institute (USA) was initiated. This was a Phase III, randomised, double-blind, placebo-controlled trial designed to test the efficacy of Se (200μg SLM) and vitamin E both alone and in combination, in the prevention of prostate cancer (Lippman *et al*, 2009). Vitamin E, in addition to Se, was investigated because a previous randomised trial studying the effects of vitamin E and beta carotene on the incidence of lung cancer reported, as a secondary end-point, a protective effect of vitamin E against prostate cancer (Anon, 1994). The SELECT trial, the largest cancer prevention trial to date, recruited 35,533 between 2001 and 2004 and planned for a minimum follow-up of 7 years and a maximum of 12 years. However, the study was discontinued in 2008 after a median follow-up of 5.5 years after a planned interim analysis showed no significant difference in the incidence of prostate cancer between the study groups or in the secondary cancer end-points and that the pre-specified 25% risk reduction was unlikely to be achieved with additional study time. In fact there was a statistically non-significant increase in the risk of prostate cancer in the vitamin E alone group and of type 2 diabetes in the Se alone group.

There are a few reasons that may potentially explain the negative results of the SELECT trial and the apparent discrepancy with the results of the NPC trial. Prospective studies suggest that a mean plasma Se concentration between 1 and 1.8μmol/l are required for a reduction in cancer risk (Nomura *et al*, 2000; Wei *et al*, 2004). These plasma concentrations can be achieved with a dietary intake of around 140μg/day (Rayman *et al*, 2006). Recently, however, there has been concern that maintaining too high a plasma Se concentration may have a detrimental effect. In the NPC trial the benefit of Se treatment was restricted to those with a baseline plasma Se ≤1.35μmol/L. In addition, data collected by the NPC trial revealed an increased risk of self-reported type II diabetes in those

supplemented with Se, the effect being greatest in those with a baseline plasma Se concentration >1.54µmol/L (Stranges *et al*, 2007). However, results from studies investigating the relationship between plasma Se and diabetes are conflicting with some reporting a protective effect of high plasma Se (Akbaraly *et al*, 2010). A sub-study of the NPC trial randomised 424 patients to receive 400µg/day of Se or placebo. This dose of Se appeared to have no effect on total cancer incidence, which is clearly in contrast to the finding of the main NPC trial that supplemented 200µg/day. However, due to the small sample size, this study is likely to have lacked sufficient power to detect differences in the primary end-points (Reid *et al*, 2008). Another study which evaluated the association between serum Se levels and all-cause, cancer and cardiovascular mortality found that Se concentrations >1.9µmol/L were associated with a small increase in all-cause and cancer mortality (Bleys *et al*, 2008).

The SELECT trial was conducted in a group of men who were Se-replete at baseline with a mean plasma Se concentration of 1.7µmol/L and after SLM supplementation of 3.2µmol/L. Subgroup analysis of the SELECT trial is still awaited. It appears, therefore, that a balance needs to be struck between exploiting the benefits of Se supplementation and reducing the potential risks associated with prolonged maintenance of high plasma Se concentrations. This is going to be dependent on an individual's baseline Se level which will vary on the basis of country and region of residence. Of note, soil Se, and thus intake, is considerably lower in the UK and other European countries than in the USA (Rayman & Rayman, 2002). Therefore, had the SELECT study been conducted in Europe, the results may have been different.

As alluded to above, it is the monomethylated metabolites, particularly methylselenol, that are thought to be crucial for the anti-cancer effects of Se (Ip *et al*, 2000). These methylation reactions mainly occur when selenoprotein synthesis has been saturated and Se is present in excess. The SELECT trial used SLM whereas the NCP trial used Se-enriched yeast. Although SLM is the major component of Se-yeast, others forms, such as MSC are also present. As discussed above, MSC is thought to be a more effective

chemopreventive agent as it is more efficiently converted to methylselenol and therefore it may be that the best form of Se was not used in the SELECT trial.

An individual's response to Se is also influenced by genetic factors, for example the genotype of antioxidant enzymes. A recent study reported a relationship between plasma Se at diagnosis, the prognosis of prostate cancer and the genotype of the manganese superoxide dismutase (*SOD2*) gene (Chan *et al*, 2009). A *SOD2* variant has a substitution of alanine for valine at amino acid 6. In men with the AA genotype, higher Se levels were associated with a reduced risk of presenting with aggressive disease whereas in men with a V allele, higher Se levels were associated with an increased risk of aggressive disease. The genotype of a number of selenoproteins also appears to be important in determining cancer risk (discussed further below; section 1.3.9.2). This gives further support to the fact that Se requirements vary between individuals and are modified by a number of factors.

Unfortunately, the negative results of the SELECT trial mean that funding for future cancer prevention trials of Se will be difficult to secure. However, should further trials take place they need to be better designed and conducted in subsets of the population taking into account an individual's baseline Se level and antioxidant enzyme/selenoprotein genotype. In addition, trials using MSC need to be performed.

1.3.8 Selenium in established cancer

In addition to its role in cancer prevention, there is evidence to support the role of Se in cancer therapy. Supra-nutritional concentrations have been shown to enhance the efficacy of standard chemotherapeutic agents whilst protecting normal tissue from chemotherapy-induced toxicity. The best evidence for this comes from mice bearing human squamous cell carcinoma of the head and neck and colon carcinoma xenografts (Cao *et al*, 2004). When SLM or MSC was administered orally with standard cytotoxic agents, the result was an increase in the maximum tolerated dose (MTD) of the cytotoxic agents, for some by more than two-fold (Figure 1.6). This effect was apparent across different classes of

drugs. The anti-tumour activity of irinotecan was further investigated and it was found that when combined with MSC, cure rates increased from 0% to 20%, 20% to 100%, 30% to 100% and 10% to 60% in four different tumour models (Figure 1.7). The cure rates in irinotecan-resistant tumours were improved further when irinotecan was given at the increased MTD which was made possible by the co-administration of MSC. The optimal schedule was administration of SLM or MSC for 7 days before and concurrently with chemotherapy. Se was thus shown to be an effective modulator of the therapeutic efficacy of irinotecan and to provide protection against chemotherapy-induced toxicity. It was determined from these studies that plasma concentrations of Se >14µmol/L were needed to achieve maximum protection against chemotherapy-induced toxicity and concentrations >23µmol/L to achieve potentiation of anti-tumour activity. These levels were determined following administration of SLM (Azrak, 2004).

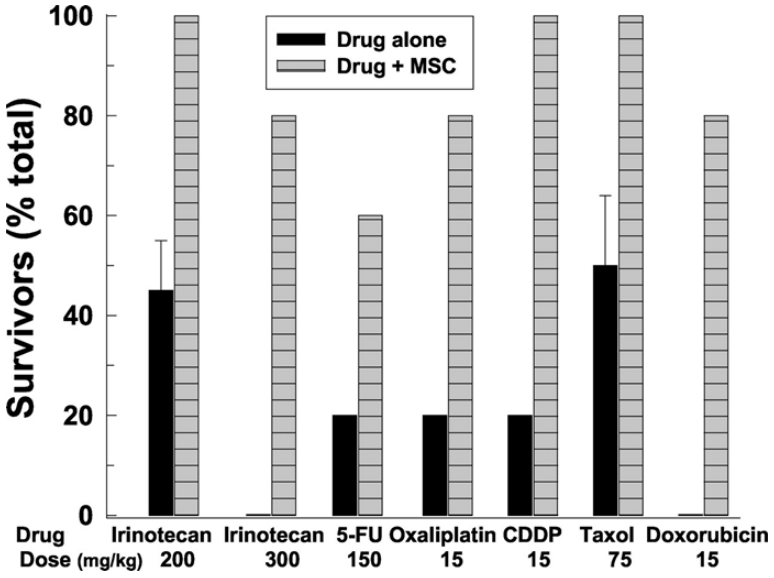

Figure 1.6 Toxicity of six chemotherapeutic agents with and without methylselenocysteine (MSC) pre-treatment in nude mice. All chemotherapy drugs were given at doses above the normal maximum tolerated dose. Methylselenocysteine was able to protect the mice from the toxicity of all the drugs. FU is 5-fluorouracil, CDDP is cisplatin. (Cao S *et al*., Clin Cancer Res, 2004)

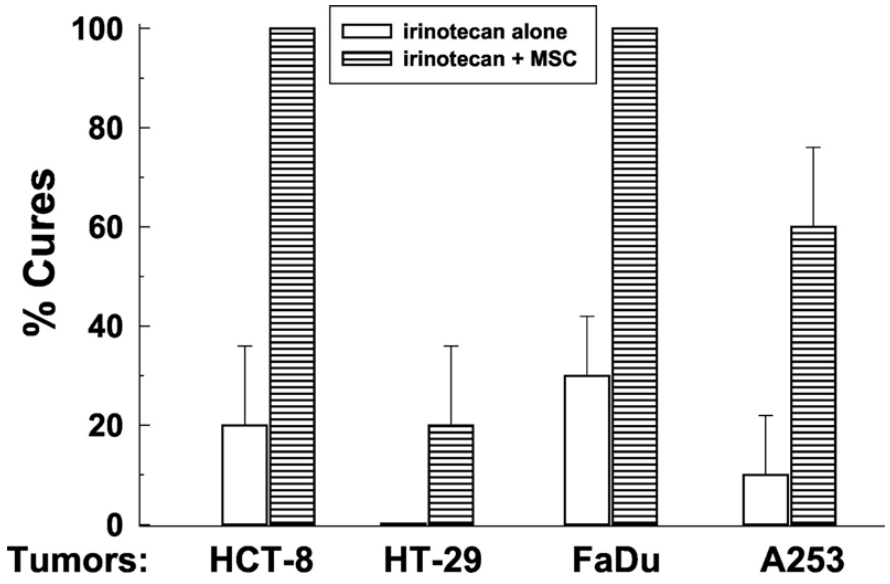

Figure 1.7 Methylselenocysteine (MSC) increased the cure rate of human tumour xenografts treated with irinotecan. HCT-8 and HT-29 are colorectal carcinoma xenografts, FaDu and A253 are head and neck squamous cell carcinoma xenografts. (Cao S *et al*., Clin Cancer Res 2004).

Based on these xenograft studies, investigators from Roswell Park Cancer Institute conducted a phase I trial to determine the MTD of irinotecan with a fixed dose of SLM in patients with advanced solid tumours. SLM at 2,200µg/day was started one week before the first dose of irinotecan and continued throughout the chemotherapy period. However, SLM did not allow escalation of the irinotecan dose beyond the previously documented MTD but SLM at this high dose was well tolerated and the only reported side-effects were garlic-odour breath and urine. Pharmacokinetic studies revealed a slow accumulation of Se, which did not reach a steady state concentration for at least 4-6 weeks. Therefore, the desired plasma concentration of >14µmol/L before the start of irinotecan was not achieved (Fakih *et al*, 2006). The same group, therefore, conducted a phase I dose-escalation study of SLM in combination with fixed dose irinotecan in patients with advanced solid tumours to determine the dose of SLM that achieves a plasma Se concentration >15µmol/L (Fakih *et al*, 2008). Thirty-one patients with advanced solid-tumours were treated at 7 dose levels, with SLM given twice daily for one week prior to commencing irinotecan, followed by once daily maintenance for the

duration of chemotherapy. Dose levels ≥4,800µg resulted in a day 8 plasma Se concentration of >15µmol/L whilst the highest dose level reached of 7,200µg resulted in a day 8 plasma Se concentration of >20µmol/L. SLM was well tolerated and the only toxicity attributable to SLM was mild garlic-odour breath and urine which improved with prolonged treatment. Two patients had dose-limiting toxicities as defined by the study protocol but in the context of advanced cancer these may not have been attributable to the SLM. The study was not designed to evaluate the protective effects of SLM on irinotecan-induced toxicity, however, a major protective effect was not observed. A few patients achieved a better response to treatment than might have been expected considering the advanced nature of their disease. Although conclusions cannot be drawn from these anecdotal cases it perhaps suggests that the clinical use of SLM is worth pursuing. A phase II study has now been initiated by the same group (personal communication from Professor Y.M. Rustum).

The role of Se in reducing chemotherapy- and radiotherapy-induced toxicity has been investigated in human trials but evidence to support its use is not conclusive and is not recommended outside the context of a clinical trial despite some provocative results (Dennert & Horneber, 2006). In a cross-over design study in patients with solid tumours receiving cisplatin chemotherapy, 4000µg of Se (seleno-kappacarrageenan) was administered from 4 days before to 4 days after chemotherapy. Compared with the control group, the supplemented group had higher white cell counts after chemotherapy, a lower requirement for granulocyte-colony stimulating factor and blood transfusions and less nephrotoxicity as determined by the excretion of urinary enzymes. There were no side-effects associated with Se supplementation (Hu *et al*, 1997).

In another study, patients with ovarian cancer receiving various combinations of cytotoxic agents, including cisplatin, were supplemented with 200µg of Se over a 3-month period. Se supplementation resulted in significantly higher neutrophil counts and less nausea, vomiting, stomatitis, and abdominal pain compared with the control group. However, patients in this study received Se in a capsule that also contained vitamin C,

vitamin E, riboflavin, niacin and β-carotene and therefore it is difficult to exclude the possibility that the benefits were derived from the combination rather than Se alone (Sieja & Talerczyk, 2004).

The results of a multi-centre, phase III trial comparing Se supplementation with observation in 81 patients receiving radiotherapy following surgery for cervical and uterine cancer have recently been reported (Muecke *et al*, 2010). The aim of the study was to assess whether Se, in the form of selenite, could improve the post-operative Se status and reduce radiotherapy side-effects. Selenite, 500μg, was given orally on the days of radiotherapy and 300μg on the days without treatment. Most patients had a low plasma Se concentration prior to entry into the study and supplementation increased plasma Se into the lower end of the recommended normal range. In addition, Se reduced the number of episodes and severity of radiotherapy-induced diarrhoea and improved quality of life.

1.3.9 Anti-cancer mechanisms of selenium in cancer prevention and established cancer

The exact mechanism by which Se compounds exert their anti-cancer effects is still not fully understood. However, it is apparent that the effects are dependent on the chemical form and concentration or dose. Thus, high concentrations are cytotoxic (Last *et al*, 2006), intermediate concentrations can modulate the therapeutic efficacy of chemotherapeutic agents (Juliger *et al*, 2007) and low but supra-nutritional concentrations are chemopreventive (Finley *et al*, 2001). Mechanisms differ between these different actions of Se and also between different cancer cell types. Most of the *in vitro* work has been performed in prostate cancer and breast cancer cell lines. As discussed above, the metabolism of Se compounds to monomethylated forms is crucial for the anti-cancer properties and MSC, which can be directly converted to methylselenol, is the most efficacious naturally occurring Se compound available (Abdulah *et al*, 2005).

1.3.9.1 Selenoproteins

Although it is generally accepted that at the supra-nutritional doses of Se, selenoprotein activity will be saturated, there is evidence to suggest that selenoproteins do have a mechanistic role predominantly through the reduction of oxidative stress and hence DNA damage which is important in carcinogenesis (Federico *et al*, 2007). A study conducted in New Zealand men who had a raised prostate specific antigen level and therefore an increased risk of prostate cancer found an inverse relationship between serum Se and DNA stability/damage in blood lymphocytes. This was most apparent in the group of subjects that had a baseline serum Se level <1.2μmol/l and therefore below the level required to saturate GPx activity (Karunasinghe *et al*, 2004). The protective role of GPx is also apparent from genetically modified animals. GPx2 knockout mice were more susceptible to the development of squamous cell cancer of the skin after γ-irradiation (Walshe *et al*, 2007). GPx1/GPx2 double knockout mice had an increased rate of inflammation-induced intestinal cancer (Chu *et al*, 2004).

Baseline Se concentration has been shown to be important in determining the effect of Se supplementation in cancer prevention trials, such that those individuals with low Se concentrations benefit the most (Duffield-Lillico *et al*, 2003). It would therefore appear that, at least in the context of cancer prevention, the activity of selenoproteins is mechanistically important in the action of Se.

1.3.9.2 Selenoprotein polymorphisms

Further evidence for the anti-cancer role of selenoproteins comes from genotype data. It has become clear that individuals differ in their ability to increase the activity of selenoproteins in response to dietary Se and that this may be due to polymorphisms in selenoprotein genes. A recent study described two single nucleotide polymorphisms (SNPs) in the selenoprotein P gene that have functional effects and are associated with differences in plasma Se, GPx and TrxR activity at baseline and in response to Se supplementation. The effects of these two SNPs were influenced by gender and body mass index (Meplan *et al*, 2007). A large study of 2,915 cases of prostate cancer in

Sweden (a low Se area) examined the effect of SNPs in the selenoprotein P and mitochondrial *SOD2* genes on prostate cancer risk. SOD2 is the major detoxifying enzyme in the mitochondria and converts superoxide to H_2O_2 which is then detoxified to water by GPx. Se status has previously been shown to modify the risk associated with a *SOD2* SNPs and prostate cancer (Li *et al*, 2005). In the Swedish study, there was no effect of selenoprotein P genotype alone but an interaction was found between Se status, a combination of a *SOD2* and selenoprotein P SNP and prostate cancer risk/aggressiveness. The SNP in the *SOD2* gene results in an overactive enzyme and a higher generation of H_2O_2. Therefore higher Se and GPx levels are required to remove H_2O_2. It is thought that in the absence of adequate Se and GPx levels, H_2O_2 would promote tumourigenesis. This further supports the notion that Se supplementation may benefit certain individuals more that than others (Cooper *et al*, 2008).

A link between the risk of cancer and polymorphisms in the *GPx1* gene at codon 198 has been reported. In a case-control study, the presence of an allele encoding leucine rather than proline at this position was associated with an increased risk of developing lung cancer in Caucasians (Ratnasinghe *et al*, 2000). Another study which examined tumour tissue from patients with breast cancer found that the leucine-containing allele was more frequently found than the proline-containing allele when compared with a control group that were free of cancer. In addition, it was shown in a human breast cancer cell line that, in the presence of the leucine allele, GPx1 enzyme activity was less responsive to supplementation by Se (Hu & Diamond, 2003). This finding is supported by a study in humans which found that this polymorphism influences GPx1 activity in response to Se, such that in individuals with the leucine allele, GPx1 activity increases to a lesser degree with increasing plasma Se concentration than in individuals with the proline allele (Jablonska *et al*, 2009). However, one study contradicts these results and reported that individuals with the GPx1 leucine allele had a significantly lower risk of developing prostate cancer although no significant difference was found in erythrocyte GPx activity by genotype (Arsova-Sarafinovska *et al*, 2009). Clearly other, yet undefined factors must

be important in influencing the risk of cancer in individuals with polymorphisms of selenoprotein genes.

A SNP in the *GPX4* gene has been reported to have functional consequences influencing GPx4 activity and concentration in lymphocytes and also the activity and concentration of GPx1, GPx3 and TrxR1 (Meplan *et al*, 2008). Another study examined the influence of genetic variations in selenoprotein genes in 832 cases of colorectal cancer and 705 controls and reported an association between SNPs in selenoprotein P, *SelS* and *GPx4* and the risk of developing the cancer (Meplan *et al*, 2010).

Sep15 has been implicated in the effect of Se in cancer prevention. Two SNPs have been identified located at positions 811 (C/T) and 1125 (G/A). The C811 allele only associates with G1125 allele and the T811 allele with A1125. Therefore, there are only 2 possible haplotypes within the human *Sep15* gene (Hu *et al*, 2001). *In vitro*, gene expression of the T811/A1125 variant was found to increase to a lesser degree in response to the addition of Se when compared with the C811/G1125 variant and therefore these SNPs may influence expression of Sep15 and response to Se supplementation *in vivo* (Hu *et al*, 2001; Kumaraswamy *et al*, 2000). Of relevance is that normal prostate tissue has high expression of Sep15 but tissue from prostate cancer expresses a reduced level (Kumaraswamy *et al*, 2000). Amongst African-Americans, allele frequencies were found to be different in DNA obtained from head and neck and breast tumours compared with DNA obtained from lymphocytes of cancer-free individuals suggesting a loss in heterozygosity at the *Sep15* locus in these tumours (Hu *et al*, 2001).

A recent case-control study investigated whether the 1125 G/A polymorphism in the *Sep15* gene combined with Se status was associated with the risk of lung cancer in smokers of Polish origin (Jablonska *et al*, 2008). 325 cases of lung cancer and 287 age-matched controls were analysed. Plasma Se concentration was significantly lower in individuals with lung cancer. At a Se concentration near the population average (0.6μmol/l) the risk of lung cancer was similar for all genotypes. However, at Se levels

below this, individuals with the AA genotype had a much greater increase in lung cancer risk compared with those with the GA and GG genotypes, suggesting that individuals with the AA genotype may benefit most from increasing dietary Se. Of concern, in individuals carrying the GG and GA genotypes, plasma Se concentrations above 1μmol/l were associated with an increasing risk of lung cancer whereas individuals with the AA genotype continued to have a decreasing risk. This supports the suggestion that the potential benefits of Se supplementation will differ between individuals, with some not benefiting at all. The finding of an increased risk of lung cancer with high Se levels needs further research.

In addition to its role in cancer prevention, Sep15 has also been implicated in cancer progression. Knockdown of *Sep15* was able to inhibit colon cancer growth and metastasis in an animal model (Irons *et al*, 2010). A large, prospective, case-controlled study of Sep15 genetic variation in prostate cancer did not find an association between *Sep15* polymorphisms and prostate cancer risk but did find a significant association with prostate cancer mortality (Penney *et al*, 2010).

Thus, the role of selenoproteins in cancer is complex. It is perhaps becoming apparent that selenoproteins do play a role in cancer prevention but once the malignancy is initiated they may also play a role in tumour promotion.

1.3.9.3 Redox modification of proteins

Methylselenol and other Se metabolites have the ability to affect a large number of cellular proteins and pathways due to redox modification of protein thiol groups; sulphur-hydrogen bonds (S-H). Se can modify proteins by the formation of selenotrisulfide bonds (S-Se-S), selenenylsulfide bonds (S-Se), diselenide bonds (Se-Se) and the formation or disruption of disulfide bonds (S-S) (Ganther, 1999). The amino acid cysteine, often found in the catalytic region of proteins, has a thiol as the function group and is therefore susceptible to modification by Se metabolites. Thus, the function of redox-regulated proteins, including transcription factors, can be altered by Se. An example of this is the

inactivation of protein kinase C (PKC) by Se. PKC is a family of intracellular serine/threonine kinases that are involved in signal transduction following the activation of receptor tyrosine kinases. The different family members have distinct but opposing roles in cell proliferation, differentiation, apoptosis and angiogenesis (Griner & Kazanietz, 2007). The effect of Se on PKC activity has mainly been investigated in prostate and breast cancer cells (Gundimeda *et al*, 2008; Sinha *et al*, 1999). MSA and MSC have both been found to inhibit the activity of PKC but the PKC isoenzymes have differing sensitivities. This inhibition of enzyme activity by Se is due to redox modification of cysteine residues in the catalytic domain and in prostate cancer cells, MSA-induced inactivation of PKCε appears to be particularly important in its growth-inhibitory and apoptotic effects (Gundimeda *et al*, 2009).

A more global approach has been taken to characterise protein redox modification by MSA in the prostate cancer cell line, PC-3 (Park *et al*, 2005). This study (discussed further in section 1.3.9.11) labelled proteins containing reactive thiols with a thiol-specific reagent, N-(biotinyl)-N'-(iodoacetyl) ethylenediamine (BIAM), and identified proteins in which the BIAM labelling increased or decreased in response to MSA by 2D-gel electrophoresis and mass spectrometry. 94 proteins were found to be sensitive to redox modification by MSA of which 85 were identified. This study high-lights the potential for Se to affect the function of a large number of cellular proteins. The proteins affected are likely to differ depending on the cell type and the form of Se used and thus may explain, in part, how Se supplementation can result in such differing effects in normal and tumour cells.

1.3.9.4 Cell cycle arrest and induction of apoptosis

Se can induce cell cycle arrest in some cancer cell lines but the effect is dependent on the chemical form and the cell type (Figure 1.8). In prostate and breast cancer cell lines, MSA arrests cells in the G1 phase of the cell cycle, this being associated with a decrease in expression of cell-cycle regulated genes and an increase in cyclin-dependent kinase inhibitors (Dong *et al*, 2002; Zhao *et al*, 2004). In contrast, studies in DLBCL cell lines

performed in our laboratory showed that apoptosis was associated with an increase in the sub-G1 (apoptotic) fraction but was not preceded by cell cycle arrest (Last *et al*, 2006). MSC was found to induce S phase arrest in a mouse mammary cancer cell line and this was associated with inhibition of cyclin-dependent kinase (CDK)-2 activity (Sinha & Medina, 1997). SLM was reported to induce p53-mediated G2/M cell cycle arrest in colon cancer cell lines (Goel *et al*, 2006), however, in lung cancer cell lines SLM did not induce cell cycle arrest (Seo *et al*, 2002a).

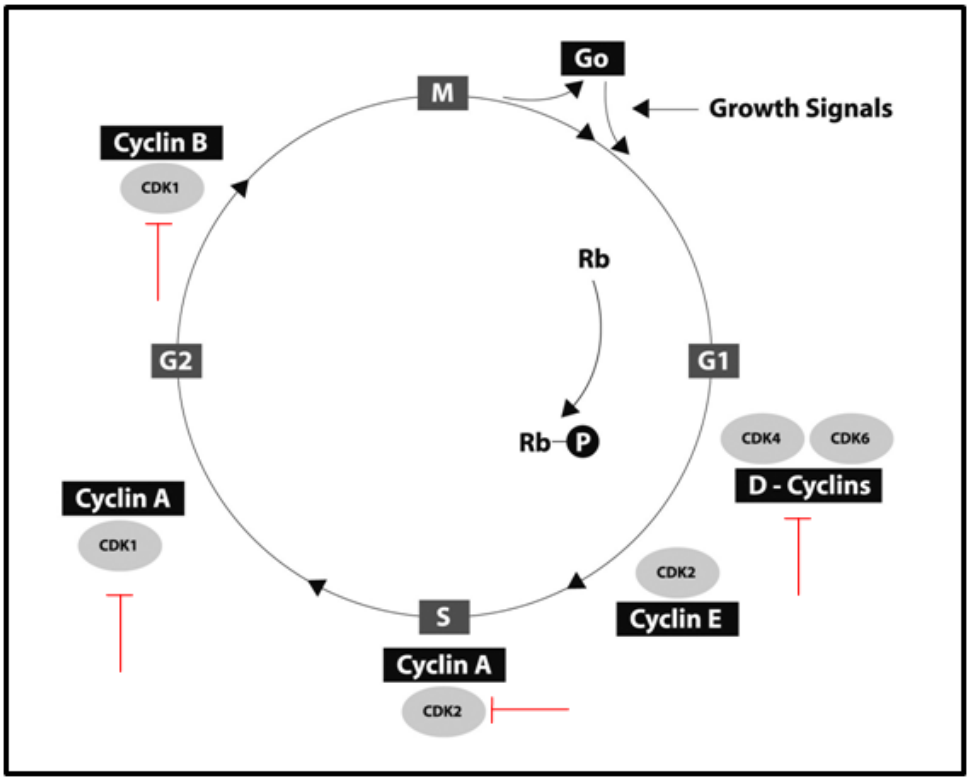

Figure 1.8 Cell cycle regulation.
Red symbols indicate proteins that can be inhibited by the action of Se. Cell cycle progression is a highly regulated process that controls cell growth and proliferation. There are 4 phases; G1 (gap 1) when the cell is preparing for DNA synthesis, S (synthesis) when DNA synthesis occurs, G2 (gap 2) when the cell is preparing for cell division and M (mitosis) when cell division occurs. Cyclins and cyclin-dependent kinases (CDKs) are the main proteins that control transition from one phase to another, CDKs being activated by forming complexes with cyclins. The Rb (retinoblastoma) family of proteins also plays a critical role, as proliferation occurs when Rb is phosphorylated (P) by CDKs and thus inactivated. Most cells remain quiescent in Go until mitogenic signals are received.

Both MSA and MSC have been shown to induce caspase-mediated apoptosis, mainly through activation of the intrinsic, mitochondrial apoptotic pathway, in various cancer cell lines (Figure 1.9) (Jiang *et al*, 2001; Jung *et al*, 2001). In some solid tumour cell lines and *in vivo* tumour models, non-toxic concentrations of MSA and MSC have been shown to interact synergistically with both conventional cytotoxic agents and targeted agents. This interaction was found to involve enhanced apoptosis (Azrak *et al*, 2006; Lee *et al*, 2009b; Li *et al*, 2009). In contrast, in a human head and neck cancer xenograft model, MSC was found to potentiate the activity of irinotecan and hence dramatically increase cure rates but this was not associ**at**ed with increased markers of apoptosis. The results, instead, suggested that the observed synergy correlated with inhibition of angiogenesis. This is discussed further below (section 1.3.9.13) (Yin *et al*, 2006).

The intrinsic apoptotic pathway is regulated by members of the Bcl-2 family of proteins and organic Se compounds have been shown to alter the expression of various family members. A study combining MSC with the pro-apoptotic cytokine TRAIL found that sensitisation of renal cancer cell lines to TRAIL-mediated apoptosis by MSC was due to the down-regulation of the anti-apoptotic protein, Bcl-2 (Lee *et al*, 2009b). In prostate cancer cell lines, MSA was shown to sensitise cells to the apoptotic effects of taxanes through the down-regulation of the anti-apoptotic protein Bcl-xL and also survivin (Hu *et al*, 2008). MSA-mediated apoptosis in the PCa prostate cancer cell line was found to be associated with down-regulation of Bcl-2 and up-regulation of the pro-apoptotic proteins, Bax, Bak and Bid (Reagan-Shaw *et al*, 2008)

Se may also activate the extrinsic, death receptor-mediated, apoptosis pathway but studies reporting this are few. In the MCF-7 breast cancer cell line, MSA enhanced doxorubicin-induced apoptosis by up-regulating FADD protein (Fas-associated death domain) which is involved in transmitting the apoptotic signal after activation of the death receptor signalling (Li *et al*, 2007a).

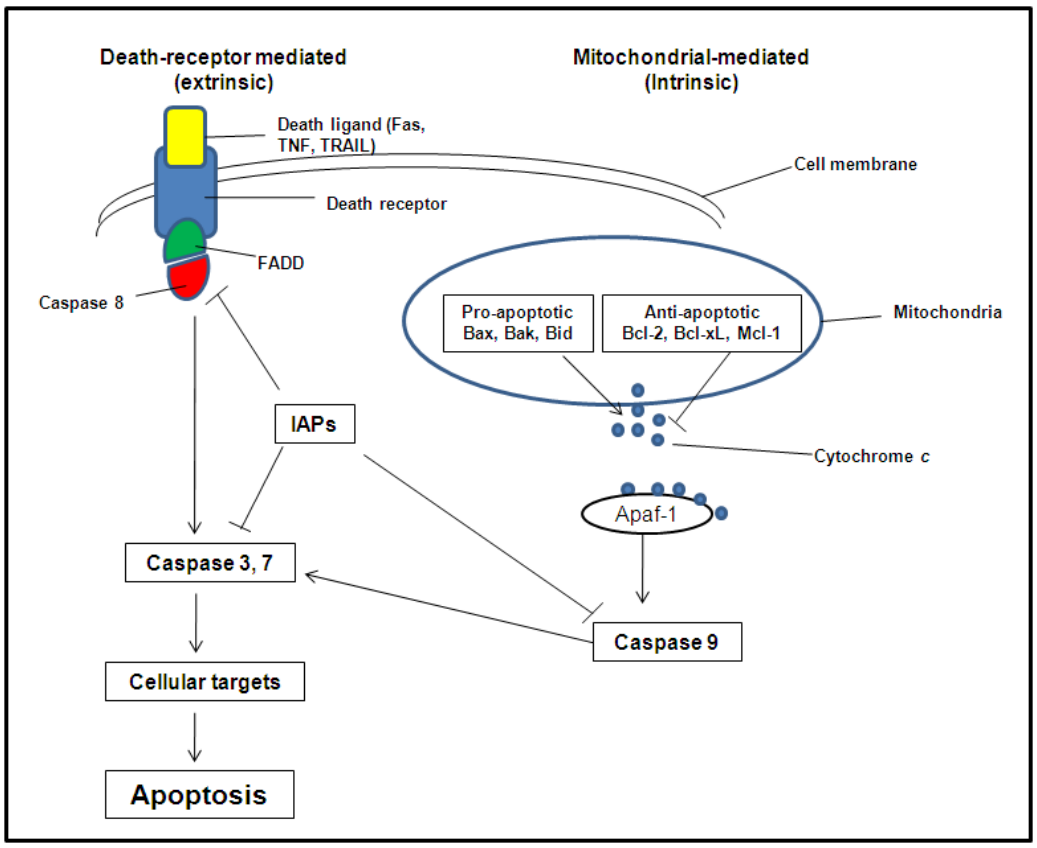

Figure 1.9 Cellular apoptosis pathway.
Adapted from Hotchkiss, RS *et al*., N Engl J Med, 2009. The death-receptor pathway is activated by the binding of death receptor ligands to their corresponding receptor. The adaptor protein Fas-associated death domain (FADD) is recruited to the death receptor which then activates caspase 8. This leads to activation of caspases 3 and 7, the main effectors of apoptosis. The mitochondrial apoptosis pathway requires release of cytochrome *c* from the mitochondria and, in association with Apaf-1 (apoptotic protease-activating factor 1), activates caspase 9 which then activates caspases 3 and 7. Members of the Bcl-2 family of proteins act to either inhibit or promote the release of cytochrome *c*. Activation of caspases 3 and 7 result in cell death by cleaving proteins such as PARP, and activating DNases, which results in DNA fragmentation. (IAPs – inhibitors of apoptosis protein).

There are conflicting *in vitro* data regarding whether apoptosis by methylselenol and its precursors is due to the generation of reactive oxygen species (ROS) such as superoxide (Jiang *et al*, 2002; Zhao *et al*, 2006). This is in contrast to inorganic Se compounds where studies are consistent in demonstrating the production of ROS through redox cycling leading to genotoxicity and apoptosis (Jiang *et al*, 2002; Shen *et al*, 1999). In DLBCL

cells line, studies from our laboratory showed an increase in ROS with the inorganic Se compound, selenodiglutathione, but not with MSA (Last *et al*, 2006).

These studies again emphasise how the effect of Se is very much dependent on the chemical form used and the cell type.

1.3.9.5 Induction of phase II enzymes

Phase II enzymes, such as glutathione-S-transferase and uridine diphosphate glucuronyltransferase, function in metabolising and inactivating xenobiotics and toxins through conjugation with GSH or glucuronic acid, and therefore protect cells against carcinogens. Studies have shown that different forms of Se including MSC and MSA are able to up-regulate phase II enzymes and hence this may be a mechanism of tumour suppression. An example is a study in a dimethylbenz(a)anthracene (DMBA)-induced mammary cancer model in rats. Supplementation with Se-enriched garlic, the main Se component of which is MSC, led to the inhibition of mammary carcinogenesis and a reduction in DMBA-induced DNA adducts. This was accompanied by a 40% increase in urinary excretion of DMBA metabolites and a 2-2.5 fold increase in glutathione-S-transferase and uridine diphosphate glucuronyltransferase activity in liver and kidney. Phase I enzymes, including members of the cytochrome P450 family, were not affected (Ip & Lisk, 1997). Thus, one way in which Se may prevent the development of cancer is by enhancing cellular detoxification mechanisms.

1.3.9.6 Activation of p53 protein

p53 is a transcription factor that activates a number of genes in response to DNA damage. This results in the arrest of cells in the G1 phase of the cell cycle to allow DNA repair and the promotion of apoptosis hence preventing the proliferation of genetically-altered cells. *p53* is thus a tumour suppressor and is mutated or non-functional in a high proportion of human cancers (Riley *et al*, 2008). The effect of Se on p53 is dependent on the chemical form of Se. The organic compound SLM has been shown to differentially affect cells that are *p53* wild-type or mutated. Cancer cells lines that are wild-type appear

to be more sensitive to the apoptotic effects of SLM than *p53*-mutated or -null cells and this is associated with activation of p53 (Goel *et al*, 2006; Zhao *et al*, 2006). SLM has been shown to activate p53 in a human lung cancer cell line, in the absence of DNA damage, through reduction of its cysteine residues which requires the redox factor, Ref1 (Seo *et al*, 2002a). Another study, using a prostate cancer cell line, reported that SLM increased intracellular superoxide resulting in p53 activation, again in the absence of DNA damage. This p53 activation resulted in apoptosis via the mitochondrial pathway (Zhao *et al*, 2006). MSA has also been shown to activate p53 through phosphorylation of threonine residues (Smith *et al*, 2004).

Using mouse embryonic fibroblasts as a model for non-cancer cells, pre-treatment with SLM was able to protect *p53* wild-type cells from DNA damage when exposed to ultraviolet (UV) radiation and DNA damaging cytotoxic agents whereas *p53*-null cells were not protected. In *p53* wild-type cells, SLM led to induction of the nucleotide excision repair pathway which is responsible for DNA repair and regulated by p53. In this study however, MSA did not induce a protective response in mouse embryonic fibroblasts and *p53* wild-type cells were more sensitive to its apoptotic effects compared to *p53* null cells (Fischer *et al*, 2007).

These studies again demonstrate that the effect of Se is dependent on the chemical form and the cell type, but in addition that genetic alterations within the cell influence the action of Se. The ability of Se to activate p53 suggests that this may be a mechanism by which Se prevents cancer development as cells that are in the early phase of neoplastic transformation are likely to still have wild-type *p53*. However, given that mutation or deletion of *p53* occurs commonly in solid tumours, p53-dependent effects of Se are unlikely to be important in established cancer. Activation of p53 in normal cells may be one mechanism by which Se protects these cells from the toxic effects of chemotherapeutic agents and radiotherapy.

1.3.9.7 Nrf2-Prx1 pathway

Peroxiredoxins (Prx) are a family of thiol-specific antioxidant proteins. There are 6 isoforms expressed in mammalian cells that are classified according to the number and position of conserved cysteine residues that participate in the catalytic reactions (Rhee *et al*, 2005). Prx1 is the major cytoplasmic Prx, it has two conserved cysteine residues, is expressed in most cell types and it detoxifies peroxides. The full function of the protein still remains unclear because Prx1 is susceptible to inactivation by oxidative stress. It has been suggested that over-oxidation of the active site promotes a change in function from a peroxidase enzyme to a molecular chaperone under conditions of stress (Moon *et al*, 2005). In addition, Prx1 appears to play a role in the growth and survival of cells and has been found to be elevated in a variety of cancer types including lung (Chang *et al*, 2001), thyroid (Yanagawa *et al*, 1999) and breast (Noh *et al*, 2001). Studies suggest that over-expression of Prx1 plays a part in radio- and chemo-resistance of malignant cells (Chen *et al*, 2006).

In the setting of cancer, Prx1 has been shown to be regulated by the transcription factor nuclear factor (erythroid-derived 2)-related factor 2 (Nrf2) which is activated by various stimuli, including hypoxic and unstable oxygen conditions commonly found within solid tumours (Kim *et al*, 2007d). Nrf2 is kept inactive in the cytoplasm through its association with Kelch-like ECH-associated protein 1 (Keap1), but the mechanism by which Nrf2 dissociates from Keap1 allowing it to translocate to the nucleus remains unclear. Keap1 may act as a redox sensor leading to the modification of cysteine residues and release of Nrf2 under conditions of chemical or oxidative stress (Dinkova-Kostova *et al*, 2002). Phosphorylation of Nrf2 by kinases has also been described as a mechanism for its activation (Huang *et al*, 2002). Once in the nucleus Nrf2 binds to the antioxidant response element in the promoter of target genes thus activating their transcription. Nrf2 regulates a number of genes in addition to Prx1, many of which are involved in the protection of cells against oxidative stress and xenobiotic insult and include the selenoproteins TrxR and GPx2 (Copple *et al*, 2008).

In the study discussed previously by Cao *et al* (Cao *et al*, 2004) where tumour-bearing mice were treated with Se, it was found that Se modulated Nrf2-Prx1 pathways differently in tumour and non-tumour tissue. Se suppressed Nrf2 activation and reduced expression of Prx1 in tumour tissue but increased the expression of Prx1 and other Nrf2 target genes in normal tissue. The authors postulate that this differential response may be related to the different oxygen conditions found in tumour and non-tumour tissue (Kim *et al*, 2007e) (Figure 1.10).

Therefore, the action of Se on the Nrf2-Prx1 pathway may be a mechanism by which it is able to inhibit tumour growth whilst protecting normal tissue from chemotherapy-induced toxicity.

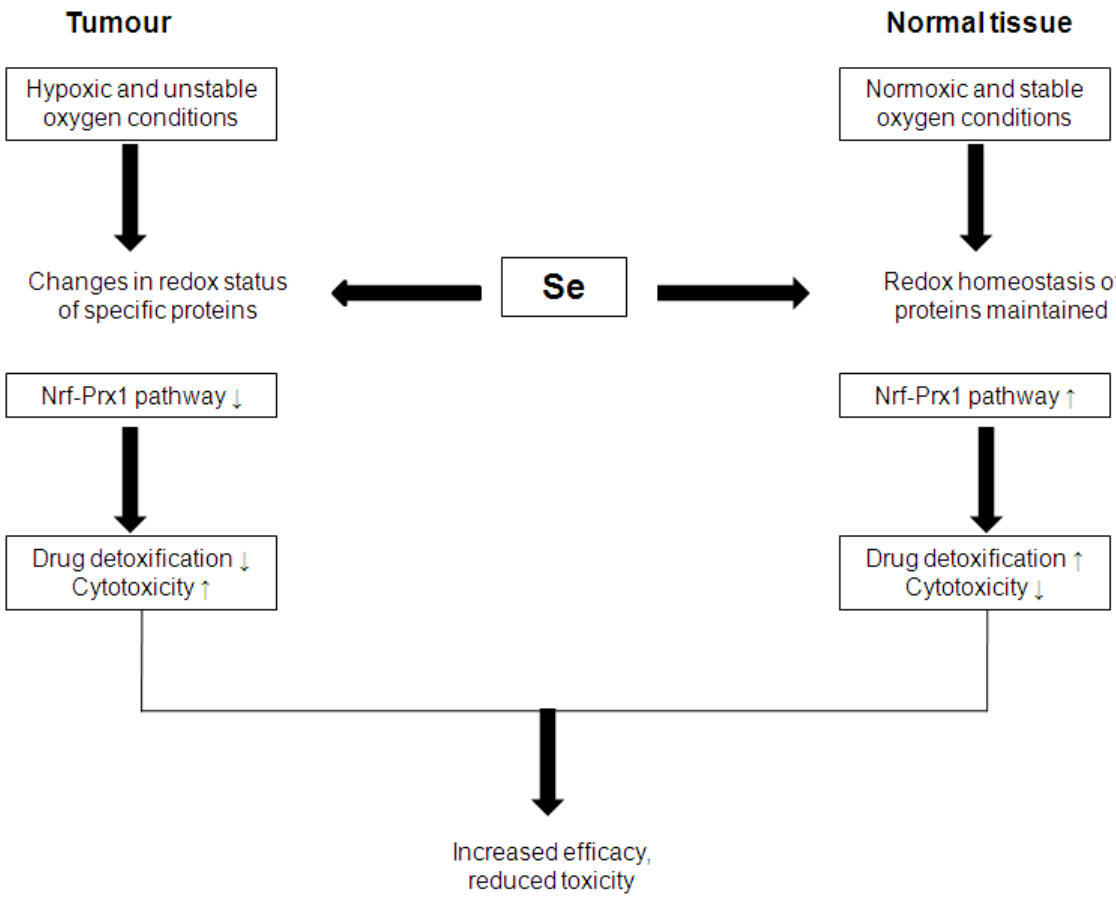

Figure 1.10 Proposed effect of selenium on the Nrf2-Prx1 pathway.
Adapted From Kim, YJ *et al*., Journal of Cancer Molecules, 2007.

1.3.9.8 PI3-kinase/Akt and MAP kinase pathways

The phosphoinositide 3-kinase (PI3K)/Akt pathway is a key pro-survival pathway within cells which is frequently up-regulated in human cancers (Cantley, 2002). Activation of down-stream effector molecules results in increased proliferation, reduced apoptosis and chemo-resistance (West *et al*, 2002). Akt is a serine/threonine kinase that requires PI3K for its phosphorylation and activation in response to growth factor and cytokine stimulation of surface receptors. Akt has a vast number of downstream targets which, in general, promote cell survival (Alessi *et al*, 1997; Sarbassov *et al*, 2005). In a study examining tumour samples from 100 patients with DLBCL, phosphorylated Akt (p-Akt) was detected in 52% of cases and high p-Akt expression was associated with a shorter survival (Uddin *et al*, 2006). A number of inhibitors of the PI3K pathway are currently being investigated for the treatment of several different tumour types.

There have been a number of studies that have reported dephosphorylation of Akt by MSA and this may be a mechanism by which Se sensitises cancer cells to chemotherapy (Gonzalez-Moreno *et al*, 2007; Hu *et al*, 2005b). In a study using the breast cancer cell line MCF-7 it was found that combining doxorubicin with MSA led to enhanced apoptosis compared with doxorubicin alone. Doxorubicin alone led to increased phosphorylation of Akt which was reversed by the addition of MSA. However, MSA was unable to sensitise cells to doxorubicin when Akt was over-expressed (Li *et al*, 2007b). In a prostate cancer cell line, it was shown that MSA dephosphorylated Akt by inhibiting PI3K activity which is required for Akt activation. In addition, Se-mediated calcium release from the ER may also be important since inhibiting calcium release prevented dephosphorylation of Akt by Se (Wu *et al*, 2006). In a mouse mammary cancer cell line, MSC has also been shown to dephosphorylate Akt by inhibiting PI3K activity (Unni *et al*, 2005)

The mitogen-activated protein kinase (MAPK) pathway is another key intracellular signalling pathway involved in the regulation of cell proliferation, survival and differentiation. Six distinct groups of MAPKs have been characterised in mammalian

cells; extracellular signal-regulated kinase (Erk)1/2, Erk3/4, Erk5, Erk7/8, Jun N-terminal kinase (Jnk)1/2/3 and the p38 kinases (p38α/β/γ/δ). Activation of these kinases requires phosphorylation by mitogen-activated protein kinase kinases and in general the Erk1/2 pathway is activated by growth factor-stimulated cell surface receptors, whereas Jnk, p38 and Erk5 are activated by stress and growth factors. Activation of Erk1/2 results in cell proliferation whereas activation of Jnk1/2 and p38MAPK has tumour suppressive effects. These pathways are commonly mutated and disrupted in cancer and attention is being focussed on modulating MAPKs for cancer treatment (Dhillon *et al*, 2007).

In vitro experiments in prostate cancer cell lines have demonstrated that Se has an effect on the MAPK pathway but that different forms of Se have a differential effect. In the DU145 cell line, MSA at apoptotic concentrations led to dephosphorylation of Erk1/2, an effect that preceded the occurrence of caspase-mediated apoptosis suggesting its importance in MSA-induced apoptosis. MSA had no effect on Jnk1/2 or p38MAPK. In contrast, exposure to selenite resulted in increased phosphorylation of Jnk1/2 and p38MAPK but had no effect on Erk1/2 (Jiang *et al*, 2002).

A study examining the effect of MSA on tumour stage-specific prostate cells used three mouse cell lines: Pr111, a slow-growing and non-tumourigenic cell line; Pr14, a tumourigenic cell line derived from a primary tumour; Pr14C1, a subclone of Pr14 explanted from a lung metastasis. MSA decreased phosphorylation of Akt and Erk1/2 in the tumour cells which correlated with its cytotoxic and apoptotic effects. However, in Pr111 cells MSA increased phosphorylation of Akt and Erk1/2 suggesting a differential effect of MSA in tumour and non-tumour cells (Gonzalez-Moreno *et al*, 2007)

These studies support the use of Se in established cancer and suggest that Se may affect pro-survival pathways differently in normal and tumour cells.

1.3.9.9 Inhibition of the NF-κB pathway

NF-κB is a family of inducible transcription factors that consists of five proteins; RelA (p65), RelB, c-Rel, NF-κB1 (p105/p50) and NF-κB2 (p100/52). These proteins form various homodimers and heterodimers that are kept inactive in the cytoplasm by the IκB family of inhibitory proteins (Baldwin, 1996). In response to various stimuli, such as oxidative stress, lipopolysaccaride, viruses and cytokines such as TNFα, NF-κB translocates to the nucleus where it binds to specific DNA sequences in the promoter of target genes and stimulates their transcription (Figure 1.11). These various stimuli first activate the multi-protein IκB-kinase (IKK) that phosphorylates the inhibitory IκB proteins resulting in their polyubiquitinylation and proteolytic degradation by the proteasome. NF-κB dimers are thus released and are able to move to the nucleus (Karin, 1999). The target genes are involved in cell survival and can be grouped into several functional classes such as positive cell-cycle regulators, anti-apoptotic factors (including inhibitor of apoptosis proteins), inflammatory and immunoregulatory genes (Jost & Ruland, 2007). NF-κB activity has been found to be elevated in many tumour types, including lymphoma, and is associated with drug-resistance (Bentires-Alj *et al*, 2003). *In vitro* data suggest that inhibition of the NF-κB pathway can sensitise cancer cells to chemotherapy and favourable clinical results have also been obtained with proteosome inhibitors, such as bortezomib, that indirectly inhibit NF-κB activation (Nakanishi & Toi, 2005).

There have been several studies demonstrating the ability of Se to inhibit NF-κB activity. Work from our own group in DLBCL cell lines found that low, non-cytotoxic concentrations of MSA inhibited NF-κB activity by 50-70% after a short exposure time of 4 hours and that this was a potential mechanism by which MSA enhanced the activity of cytotoxic agents (Juliger *et al*, 2007). In prostate cancer cell lines MSA, at apoptotic concentrations, inhibited NF-κB activation and this was through the inhibition of IKK activity, thus inhibiting IκBα phosphorylation and NF-κB nuclear translocation. In addition, inhibition of NF-κB activity by transfection of cells with an IκBα mutant resulted in increased sensitivity of the cell lines to MSA (Gasparian *et al*, 2002). In

contrast, a study using a different prostate cancer cell line was not able to demonstrate an effect of MSA on IκBα phosphorylation and NF-κB nuclear translocation but did show that MSA inhibited NF-κB binding to DNA (Christensen *et al*, 2007).

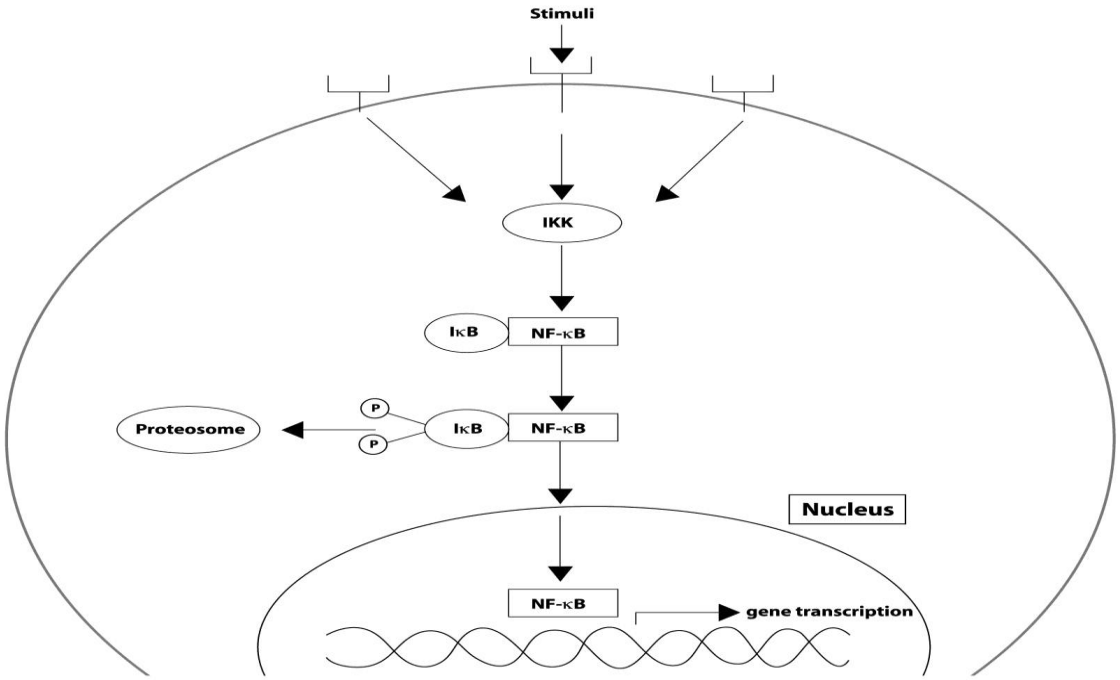

Figure 1.11 The NF-κB pathway.
In response to various stimuli, the multi-protein IκB-kinase (IKK) is activated. This phosphorylates the inhibitory IκB proteins resulting in their polyubiquitinylation and proteolytic degradation by the proteasome. NF-κB dimers are thus released and move to the nucleus where they bind to specific DNA sequences in the promoter of target genes and stimulate their transcription.

In inflammatory conditions, an inverse relationship between serum Se and C-reactive protein (CRP) has been demonstrated. NF-κB is known to up-regulate CRP synthesis by the liver and hence the effect of Se on NF-κB was further investigated in the human hepatoma cell line, HuH-7 (Maehira *et al*, 2003). In this study cells were either deprived of Se in the culture medium or cultured with medium containing Se at physiological levels in the form of sodium selenite. It was found that NF-κB activity and CRP synthesis, induced by TNFα, was inhibited by Se, but when Se was present at a concentration that

was equivalent to the low levels found in subjects with inflammatory conditions, CRP synthesis was maximal.

NF-κB activation has been linked with the development of vascular complications in patients with type II diabetes (Hofmann *et al*, 1999). Therefore the effect of Se supplementation, at a dose of 960μg/day for 3 months, on NF-κB activation, was studied in a group of patients with type II diabetes. When compared to the placebo group, the supplemented group had a significant reduction in NF-κB activation measured in peripheral blood mononuclear cells (PBMCs) reaching the same level as non-diabetic controls (Faure *et al*, 2004).

Given the important role of the NF-κB pathway in tumour promotion and chemo-resistance, these studies provide a sound rationale for the use of Se in established cancer. Of relevance to DLBCL is that this pathway is activated in the ABC-subgroup which has a poor outcome (Alizadeh *et al*, 2000).

1.3.9.10 Suppression of survivin expression

Survivin, which is a member of the inhibitor of apoptosis family of proteins, has been found to be a target of Se. In addition to inhibiting apoptosis, survivin plays an essential role in the control of cell division. It is often over-expressed in malignant tumours and this is associated with aggressive, drug-resistant disease. Survivin is not expressed in most terminally differentiated normal tissues and hence is being investigated as a therapeutic drug target (Altieri, 2003). The Sp1 family of transcription factors have been found to be important in controlling survivin gene expression (Li & Altieri, 1999). In addition, survivin is a downstream target of NF-κB (Tracey *et al*, 2005).

MSA has been shown to down-regulate the expression of survivin both *in vitro* and *in vivo* (Chun *et al*, 2007; Hu *et al*, 2008). In a xenograft model of prostate cancer, orally administered MSA inhibited the expression of survivin in tumour samples. In addition, MSA enhanced the *in vivo* activity of paclitaxel in the xenografts and this was associated

with inhibition of paclitaxel-induced survivin expression (Hu *et al*, 2008). The mechanism by which MSA inhibited survivin in prostate cancer cell lines was reported to be its ability to prevent the binding of Sp1 or Sp1-like proteins to the promoter of the survivin gene (Chun *et al*, 2007). In the ovarian cell line SKOV3, silencing survivin with shRNA resulted in synergy between MSA and paclitaxel which was not apparent in wild-type SKOV3 cells (Azrak *et al*, 2008). Synergy between MSC and docetaxel in prostate cancer cell lines was associated with decreased expression of survivin (Azrak *et al*, 2006).

Inhibition of survivin is currently being investigated for cancer therapy. This action of Se may be important for its use in established cancer especially given that most normal tissue does not express survivin.

1.3.9.11 Endoplamic reticulum stress and the unfolded protein response

The ER is the site where secreted and membrane proteins undergo assembly and folding. This involves the formation of disulfide bonds and the addition of oligosaccharides allowing the tertiary structure of the protein to be formed. A number of insults, including disturbance of calcium homeostasis, changes in redox state and inhibition of protein glycosylation, can lead to protein misfolding in the ER. The accumulation of misfolded or unfolded proteins is known as ER stress and this triggers what is called the unfolded protein response (UPR). The UPR is a survival response which functions to reduce the accumulation of unfolded proteins and restore normal ER functioning. However, if the cellular stress cannot be resolved, the cell will undergo apoptosis (Szegezdi *et al*, 2006).

The UPR is an intracellular signalling pathway mediated by the protein chaperone glucose regulated protein (GRP)-78, a member of the heat shock protein (HSP)-70 family, and three transmembrane ER stress transducers (Figure 1.12). The three transducers are protein kinase RNA (PKR)-like ER kinase (PERK), inositol requiring protein-1 (IRE1) and activating transcription factor-6 (ATF6). In the resting, unstressed state, GRP78 binds to the ER luminal domains of the three transducers keeping them inactive. In response to disturbance of ER homeostasis and the accumulation of unfolded proteins,

GRP78 dissociates from the transducers and moves into the ER lumen where it binds to the misfolded proteins. Once released from GRP78, the three transducers are activated through different mechanisms and the result is the up-regulation of a number of transcription factors (Ron & Walter, 2007). ER chaperones, including GRP78, are also up-regulated by activation of the transducers and hence an increase in GRP78 expression is a good marker of ER stress (Kozutsumi *et al*, 1988; Lee *et al*, 2003).

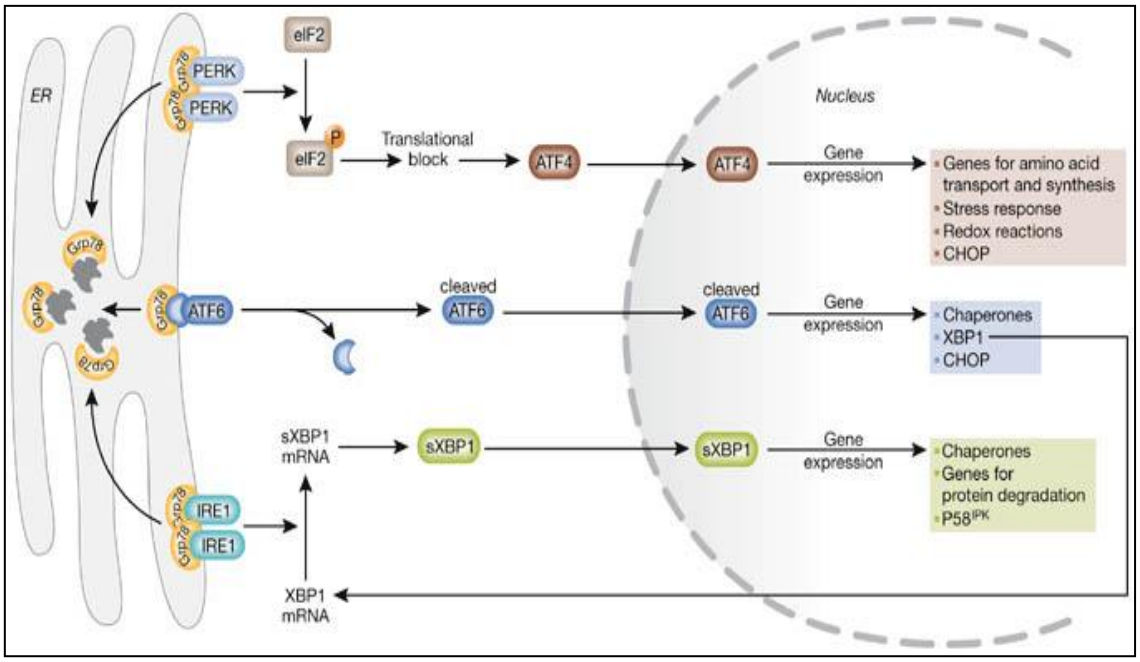

Figure 1.12 The unfolded protein response resulting from endoplasmic reticulum stress. From Szegezdi, E. *et al*., EMBO Rep, 2006. CHOP is also known as GADD153.

When PERK is released from GRP78 it is activated through dimerisation and autophosphorylation. This leads to the phosphorylation of eukaryotic initiation factor 2α (eIF2α) which acts to reduce the rate of general protein translation (Harding *et al*, 2000). However, p-eIF2α also increases the translation of some genes, the best studied being the transcription factor ATF4 involved in promoting cell survival (Scheuner *et al*, 2001). After dissociation from GRP78, ATF6 moves to the Golgi, where it is activated through cleavage by proteases. It then moves to the nucleus where it binds to the ER stress response element of target genes resulting in their induction (Haze *et al*, 1999). IRE1 is

also activated through dimerisation and autophosphorylation when released from GRP78 and it then splices a 26-nucleotide intron from X-box-binding protein-1 (XBP1) mRNA (Calfon *et al*, 2002) . The activated transcription factors, ATF4, XBP1 and ATF6, all function to increase the expression of genes encoding proteins that enhance the protein folding capacity of the ER. This includes GRP78 and proteins that catalyse folding such as PDI. In addition, there is induction of genes required for protein degradation and if the survival response is unsuccessful, there is induction of pro-apoptotic genes. Proteins for degradation are transported to the cytoplasm and degraded mainly by the proteasome (Ron & Walter, 2007; Scheuner *et al*, 2001).

The precise mechanism by which the cell switches to apoptosis in response to ER stress has not been fully elucidated (Figure 1.13). There is evidence to support the role of growth-arrest and DNA damage inducible gene 153 (GADD153; also known as CHOP), Jnk and the Bcl-2 family of proteins in committing the cell to apoptosis, eventually leading to caspase activation and cell death (Szegezdi *et al*, 2006).

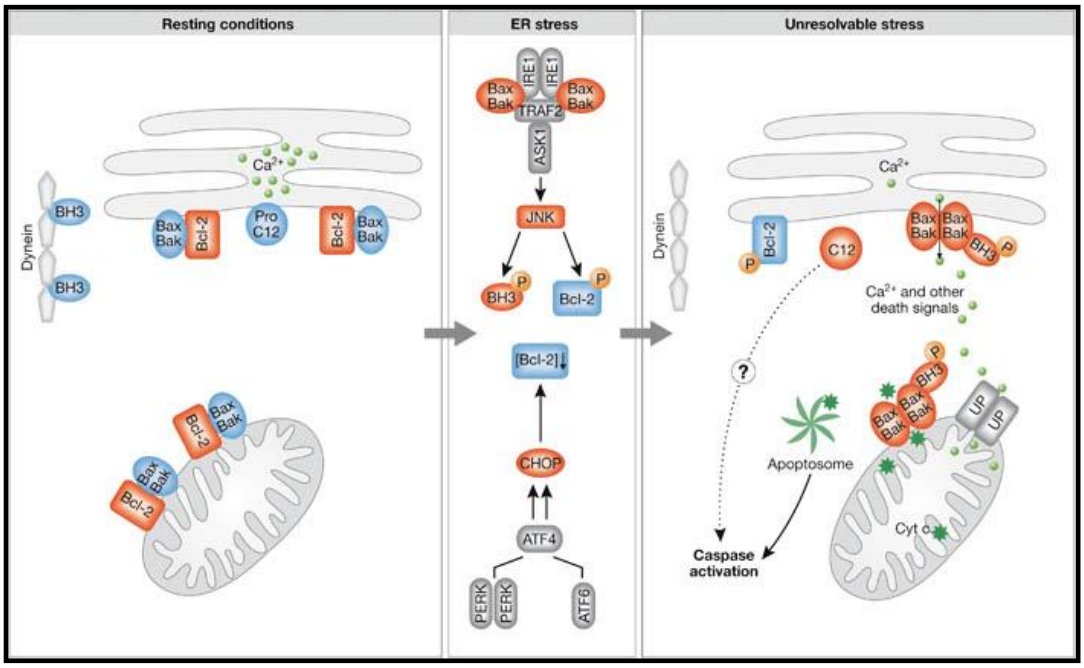

Figure 1.13 Mediators of endoplasmic reticulum stress-induced apoptosis.
From Szegezdi, E. *et al*., EMBO Rep, 2006. CHOP is also known as GADD153.
UP=Uniporter. Blue molecules are inactive, red are active. Rounded shapes are pro-apoptotic and rectangles are anti-apoptotic molecules.

The transcription factor GADD153 appears to be essential for ER stress-induced apoptosis and all three ER transducers can lead to increased transcription of GADD153 (Zinszner *et al*, 1998). Target genes that are up-regulated by GADD153 include, GADD34 (Marciniak *et al*, 2004), which promotes apoptosis through a yet unknown mechanism and Tribbles-related protein (TRB)-3, which can inhibit Akt and hence promote apoptosis (Du *et al*, 2003; Ohoka *et al*, 2005). Bcl-2, an anti-apoptotic protein, is down-regulated by GADD153 (McCullough *et al*, 2001). Of note, GADD34 provides a negative feed-back mechanism whereby it promotes dephosphorylation of eIF2α thus releasing the block on protein translation (Brush *et al*, 2003)

Jnk activation has been reported in response to ER stress and this can promote apoptosis through regulation of Bcl-2 family members. Jnk can phosphorylate Bcl-2, which inhibits its anti-apoptotic effects. It can also phosphorylate Bcl-2 homology domain-3-only members, such as Bim, and enhance their pro-apoptotic effect (Davis, 2000). These changes allow activation of the pro-apoptotic proteins Bax and Bak which promote the release of cytochrome *c*, resulting in the activation of caspases (Lei & Davis, 2003). The exact complement of caspases linked to ER stress-induced apoptosis has not been fully elucidated but may involve caspases 4, 7, 8 and 9 (Jimbo *et al*, 2003; Rao *et al*, 2001).

In general, cancer cells are exposed to conditions within the tumour environment, such as hypoxia and glucose deprivation, that induce a basal level of ER stress. Therefore, as a cyto-protective response, levels of ER chaperones such as GRP78 are over-expressed compared with normal, non-malignant cells. Studies have shown that over-expression of GRP78 promotes tumour growth and chemoresistance and targeting GRP78 can restore chemo-sensitivity (Lee, 2007; Pyrko *et al*, 2007). In addition, therapeutic agents that further induce ER stress, thus over-loading the cell's capacity to deal with misfolded proteins, can promote apoptosis (Davenport *et al*, 2008). For example, in multiple myeloma, the malignant plasma cells produce large quantities of immunoglobulin which increases the cellular protein load resulting in ER stress. Bortezomib, which has shown impressive activity in myeloma, inhibits the proteasome and thus the cells' capacity to

degrade proteins. This leads to increased ER-stress, now shown to be one mechanism by which bortezomib induces cell death (Obeng *et al*, 2006).

Selenium and endoplasmic reticulum stress

Se has been shown to induce ER stress. A proteomics study examined the effect of MSA on reactive protein thiols in the PC-3 human prostate cancer cell line. MSA was found to cause global thiol redox modification of proteins and disruption of disulfide bonds which is a form of cellular stress that can lead to protein misfolding (Park *et al*, 2005). The effect of MSA on markers of ER stress was therefore further investigated. All three UPR transducer arms were found to be up-regulated within a few hours, in PC-3 cells treated with MSA. This was accompanied by increased expression of GRP78 and GADD153 and cleavage of caspase 7, 12 and PARP. A higher concentration of MSA was required to induce the apoptotic proteins compared to the pro-survival proteins. When GRP78 was over-expressed in PC-3 cells, the ability of MSA to up-regulate GADD153 and cleave caspases was reduced. Conversely, when GRP78 was knocked down in PC-3 cells, MSA exposure resulted in a more marked increase in GADD153 expression (Wu *et al*, 2005; Zu *et al*, 2006).

ER stress induction has been reported to be the mechanism by which Se sensitises prostate cancer cell lines to taxanes (Wu *et al*, 2009). In this study a non-cytotoxic concentration of MSA was shown to induce GRP78, p-EIF2α and GADD153. Knock-down of GRP78 enhanced cell death induced by the combination of MSA and paclitaxel, with the reverse being true when GRP78 was over-expressed. Knock-down of GADD153 also inhibited cell death in the combination. Sensitisation was greatest when cells were pre-treated with MSA for 6 hours, suggesting that cells require priming and time to respond to ER stress induction by MSA.

The effect of Se on the ER is not cell-type specific. GADD153 was induced when a mouse mammary cancer cell line was treated with sodium selenite or MSC (Sinha *et al*, 1999). In addition, proteins within normal, non-malignant cells are also likely to undergo

redox modification when exposed to Se and this may also lead to ER stress. It has been demonstrated that Se has a differential effect on tumour and normal tissue and is able to protect normal cells from chemotherapy-induced toxicity (Cao *et al*, 2004). This suggests that different cells handle cellular stress in different ways and it may be that Se triggers a pro-survival response in normal cells. In fact, the induction of ER stress has been reported to protect normal cells from oxidative stress and toxicity from cytotoxic agents (Bedard *et al*, 2004; Hung *et al*, 2003)

In addition to Se compounds that are precursors of monomethylated Se species, two selenoproteins have been implicated in the ER stress response. Both selenoprotein S and Sep15 are induced in response to ER stress and act as molecular chaperones, facilitating protein folding and helping to alleviate ER stress (Kelly *et al*, 2009; Labunskyy *et al*, 2009)

Despite the strong *in vitro* evidence for the mechanistic role of ER stress induction in the action of Se, there has been doubt cast by a recent *in vivo* study (Jiang *et al*, 2009). The action of MSA, MSC and selenite was investigated in a chemically-induced rat mammary carcinoma model and a human DU145 prostate cancer xenograft model. All three compounds were able to inhibit tumour growth, with evidence of increased apoptosis within the Se-treated tumours. However, the levels of GADD153 and GADD34 within the Se-treated tumours, measured by real-time polymerase chain reaction (PCR) and western blotting, were not higher than in untreated tumours. Se treatment did, however, result in decreased expression of the cell cycle protein cyclin D1, increased expression of the cyclin-dependent kinase inhibitor, p27, and activation of Jnk, which may explain the Se-induced tumour growth inhibition and apoptosis. Clearly further work is required to define the role of Se-induced ER stress induction *in vivo.*

1.3.9.12 Autophagy

Autophagy, used here to refer to macroautophagy, is a cellular degradation pathway involved in the clearance of long-lived proteins and organelles (Figure 1.14). It occurs at

low levels in all cells as a normal homeostatic process whereby defective proteins, damaged organelles and abnormal protein aggregates are removed. However, autophagy is activated in response to cellular stress such as starvation and hypoxia, resulting in protein degradation to provide cellular energy and amino acids, fatty acids and nucleotides for the synthesis of essential proteins. Therefore, autophagy is generally considered a cellular survival mechanism (He & Klionsky, 2009). In addition to macroautophagy, there are two other forms of autophagy – chaperone-mediated and microautophagy- but these will not be discussed further as their role in cell death and cancer is less well understood.

The process of autophagy involves the formation of a double-membrane vesicle called an autophagosome, which contains the proteins/organelles to be degraded. The autophagosome fuses with a lysosome to form an autolysosome, which is followed by lysis of the autophagosome inner membrane and degradation of its contents by acid hydrolases. Autophagy is controlled mainly by mTOR kinase, which interacts with a number of signalling pathways such as the PI3K/Akt and MAPK pathways. Downstream of mTOR kinase, a large number of genes, known as *Atg* genes, encode proteins essential for the execution of autophagy (Levine & Kroemer, 2008).

When cells are exposed to excessive stress, autophagy can result in cell death. Morphologically this is distinct from apoptotic cell death and is characterised by massive vacuolisation of the cytoplasm in the absence of chromatin condensation, little or no interaction with phagocytes, and does not involve caspase activation. However, there are difficulties distinguishing between cells that are dying *by* autophagy and those that are dying *with* autophagy. In the latter, autophagy may be activated in an attempt to rescue the cell from death but is not the mechanism of cell death (Kroemer *et al*, 2009).

The induction of ER stress by various stimuli, including the accumulation of misfolded proteins, has recently been shown to activate autophagy. This is mainly thought to be a cyto-protective response preventing the accumulation of abnormal protein aggregates.

However, if the level of ER stress and hence autophagy is excessive, cell death may occur (Hoyer-Hansen & Jaattela, 2007). Both the PERK-eIF2α and the IRE1-Jnk pathways of the UPR have been shown to be important in the activation of autophagy (Kouroku *et al*, 2007; Ogata *et al*, 2006).

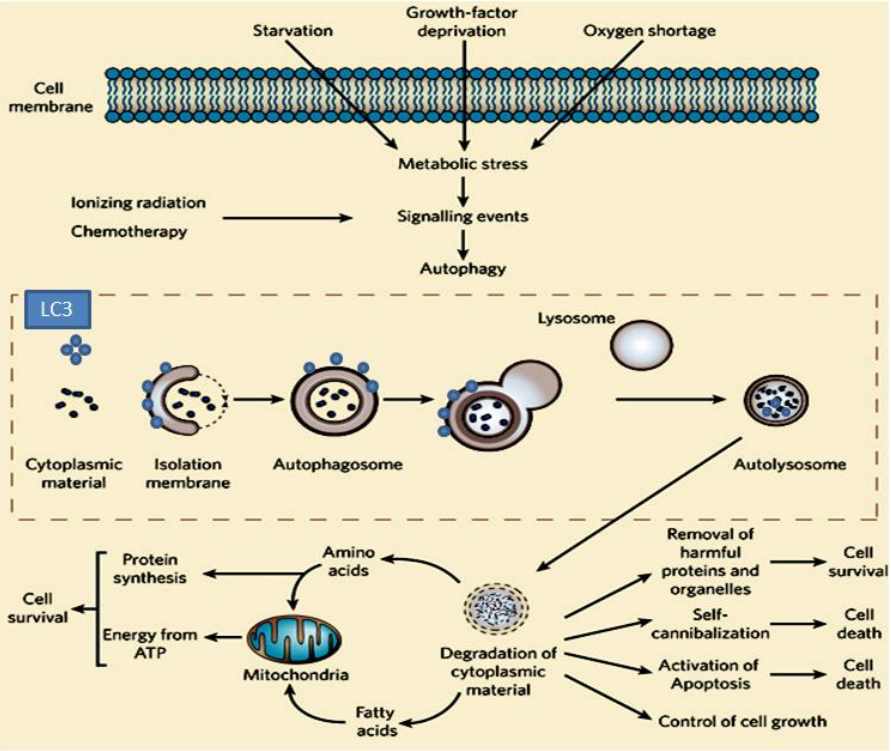

Figure 1.14 The autophagy pathway.
Adapted from Levine, B. Nature, 2007. In response to various signals, cytoplasmic material is sequestered by a membrane-bound vesicle, the autophagosome. This then fuses with a lysosome forming an autolysosome which degrades the cytoplasmic material. LC3 is microtubule-associated protein 1 light chain 3 and after post-translational modification is called LC3-I, which resides in the cytosol. When autophagy is induced, LC3-I is converted to LC3-II by conjugation to phosphatidylethanolamine and relocates specifically to associate with autophagosome membranes. LC3-II is degraded by the autolysosome. Autophagy can lead to cell survival or cell death.

Autophagy and cancer

The role of autophagy in cancer has been the subject of intensive investigation but the data are complicated and somewhat contradictory as evidence supports the role of

autophagy both in cancer development and suppression (Mathew *et al*, 2007). Many oncogenes and tumour suppressor genes have been implicated in the regulation of autophagy (Maiuri *et al*, 2009). Regarding cancer development, there is evidence to suggest that *Atg* genes are tumour suppressors, as many cancers have been shown to have deletions of these genes, for example, inactivation of the *Atg* gene *beclin 1* has been shown to promote tumour growth in mice (Liang *et al*, 1999). However, in established cancer, autophagy can promote cancer cell survival, especially in cells with defective apoptosis (Degenhardt *et al*, 2006) and inhibition of autophagy can sensitise tumour cells to the effects of chemotherapy (Zhu *et al*, 2010). To further complicate the data, it has been reported that certain chemotherapeutic agents induce cancer cell death by autophagy in the absence of apoptosis (Kanzawa *et al*, 2004; Kanzawa *et al*, 2003) and induction of autophagy may explain the synergistic interaction between some cytotoxic agents (Lambert *et al*, 2008). Combining agents that induce ER stress with inhibitors of autophagy is also being explored for cancer therapy (Schonthal, 2009). Clearly targeting autophagy for therapeutic benefit may yield promising results but it is still not apparent in which tumour models autophagy should be inhibited and in which it should be promoted.

Autophagy and selenium

There are little published data describing the effect of Se on autophagy, but given that Se induces ER stress it would be expected to also induce autophagy. Two studies have investigated the effect of selenite on autophagy. In malignant glioma cells lines, selenite was shown to induce autophagic cell death in the absence of apoptosis. This was demonstrated to be a consequence of selenite-induced superoxide generation resulting in mitochondrial damage and mitochondrial autophagy. Pre-treatment of the cells with an inhibitor of autophagy reduced selenite-induced cell death (Kim *et al*, 2007b). In contrast to these results, a recent study using the acute promyelocytic leukaemia cell line, NB4, showed that selenite-induced apoptosis was associated with inhibition of autophagy, through the down-regulation of the PI3K/Akt pathway. Further inhibition of autophagy by specific inhibitors resulted in enhanced selenite-induced apoptosis (Ren *et al*, 2009).

Therefore, from the limited available data it appears that the role of autophagy in the action of Se differs between cell types. In addition, the effect of organic Se compounds on autophagy has not been investigated.

1.3.9.13 Inhibition of angiogenesis

New vessel formation is a crucial component of solid tumour growth, progression and metastasis. There is evidence to suggest that Se has anti-angiogenic properties. When rats with chemically-induced mammary cancers were supplemented with sodium selenite, MSC or Se-enriched garlic, there was a significant reduction in intra-tumoural microvessel density and vascular endothelial growth factor (VEGF) expression compared with the untreated controls. However, the microvessel density of the uninvolved mammary glands was not affected by Se treatment, suggesting a tumour specific effect (Jiang *et al*, 1999). *In vitro*, effects of MSA on HUVEC (human umbilical vein endothelial cell) cells have been studied and MSA induces G1 cell cycle arrest at low concentrations and caspase-mediated apoptosis at higher concentrations. Sub-apoptotic concentrations of MSA led to a dose-dependent reduction in phosphorylation of Akt, Erk1/2 and Jnk1/2 but no change in p38MAPK, while apoptotic concentrations of MSA increased phosphorylation of p38MAPK (Wang *et al*, 2001). MSA-induced G1 cell cycle arrest in telomerase-immortalised microvascular endothelial cells was associated with increased expression of the cyclin-dependent kinase inhibitors p21, p27 and p16 which resulted in the inhibition of the kinase activity of CDK2, CDK4, and CDK6 (Wang *et al*, 2008).

Treatment of HUVEC cells with relatively low concentrations of MSA (2µmol/L) inhibited the gelatinolytic activity of metalloproteinase-2, a protein that is secreted by vascular endothelial cells when stimulated and is required to break down the adjacent tissue matrix. However, this inhibitory effect was dependent on the cellular metabolism of MSA as medium conditioned with MSA did not affect the gelatinase activity of metalloproteinase-2 in a test tube. In addition, selenite was not able to inhibit metalloproteinase-2 activity suggesting that an immediate precursor of methylselenol is

necessary for this effect (Jiang *et al*, 1999). The inhibitory effect of MSA on metalloproteinase-2 activity in HUVEC cells and VEGF expression in epithelial cancer cell lines occurs rapidly, within 30 minutes and 1-2 hours respectively and was apparent at non-apoptotic concentrations of MSA. However, inhibition of metalloproteinase-2 activity appears to be sustained even after removal of MSA from the cell medium whereas inhibition of VEGF secretion required continuous exposure. In addition, inhibition of VEGF expression in the DU145 prostate cancer cell line required only low non-apoptotic concentration of MSA whereas selenite in the same concentration range was not able to decrease VEGF expression once again suggesting that the generation of methylselenol is required (Jiang *et al*, 2000). In a DU145 prostate cancer xenograft model, daily treatment of mice with MSA, 3mg/kg, resulted in significant inhibition of tumour growth, accompanied by a significant decrease in intra-tumoural microvessel density when assessed by IHC staining for CD34 expression (Wang *et al*, 2008).

Inhibition of angiogenesis has been shown to be an important mechanism by which MSC sensitises tumours to the effects of chemotherapy in xenograft models, specifically through the down-regulation of hypoxia inducible factor (HIF)-1α. In a xenograft model of squamous cell head and neck carcinoma, MSC administered 7 days before and during chemotherapy, was able to significantly enhance the anti-tumour activity of irinotecan and increased the cure rate from 30% to 100%. This was not associated with increased levels of apoptosis in tumour samples but was associated with decreased expression of cyclo-oxygenase 2 enzymes and HIF-1α. Both these proteins are important in stimulating angiogenesis by up-regulating VEGF expression and secretion. The combination of MSC and irinotecan was found to decrease microvessel density in the xenografts but this reduction in microvessel density was not seen in normal mouse liver tissue, suggesting a tumour specific effect of MSC (Bhattacharya *et al*, 2008; Yin *et al*, 2006).

In addition to increased vessel density, tumours have morphologically and functionally abnormal vasculature. MSC alone was found to reverse these abnormalities *in vivo* by inducing tumour vessel maturation, reducing tumour vessel leakiness and improving

tumour vascular function. This led to improved delivery of chemotherapy to the tumours in xenograft models of head and neck and colon cancer (Bhattacharya *et al*, 2008; Bhattacharya *et al*, 2009). However, it was found that histological features of the tumour influenced the response to MSC, such that well differentiated, morphologically heterogenous tumours with multiple avascular hypoxic regions responded less well to MSC than well-vascularised, poorly differentiated, homogenous tumours (Bhattacharya *et al*, 2009; Rustum *et al*, 2010).

The effect of Se on HIF-1α specifically has been studied *in vitro* and *in vivo*. In the FaDu xenograft model of head and neck squamous cell carcinoma, HIF-1α knockdown by shRNA had a similar inhibitory effect on tumour growth and microvessel density as treatment with MSC alone, which was also shown to inhibit HIF-1α and VEGF expression in the tumours. In addition, when the FaDu xenografts were treated with irinotecan, the knock-down of HIF-1α had a similar synergistic effect to the administration of MSC resulting in almost 100% cure (Chintala *et al*, 2010). The mechanism by which Se inhibited HIF-1α was further investigated. Prolyhydroxylases (PHDs) are involved in the regulation of HIF-1α such that under normoxic condition they hydroxylate proline molecules of HIF-1α. This facilitates interaction with von Hipple-Lindau (VHL) protein and subsequent ubiquitinylation and degradation of HIF-1α by the proteasome. Under hypoxic conditions, these PHDs are inhibited thus preventing the degradation of HIF-1α (Jaakkola *et al*, 2001). *In vitro*, FaDu cells grown under hypoxic conditions had very low levels of PHDs, however, when these cells were treated with MSA there was up-regulation of PHDs and inhibition of HIF-1α expression. mRNA levels of HIF-1α were unchanged in the MSA-treated cells, suggesting no effect on HIF-1α synthesis In addition, under hypoxic conditions, MSA was found to inhibit the generation of ROS, which are known to be important in inhibiting PHDs and thus activating HIF-1α (Chandel *et al*, 2000). FaDu cells grown under hypoxic conditions were resistant to irinotecan but when treatment was combined with low non-cytotoxic concentrations of MSA there was enhanced cytotoxicity. This sensitisation did not occur under normoxic conditions (Chintala *et al*, 2010).

Inhibition of angiogenesis is a promising target for cancer therapy. These studies suggest that precursors of methylselenol not only inhibit new vessel formation but improve tumour vascular function and reverse chemo-resistance induced by hypoxia. This provides strong evidence for the potential therapeutic use of Se in established cancer.

1.3.9.14 Tumour specific effects of selenium

In addition to the general, common effects of Se compounds that occur in a number of tumour types, there are some effects of Se that are specific to the tumour-type. This is particularly true of prostate and breast cancer. In prostate cancer, both *in vitro* and *in vivo* studies have demonstrated that MSA and MSC can decrease the expression of the androgen-receptor, disrupt androgen receptor signalling and suppress the expression and secretion of prostate-specific antigen. Prostate-specific antigen in known to be controlled through androgen-receptor signalling and is a prognostic marker in prostate cancer (Dong *et al*, 2004; Lee *et al*, 2006). Similarly, breast cancer studies have shown that Se can decrease the expression of the oestrogen receptor and disrupts oestrogen receptor signalling (Lee *et al*, 2005). A synergistic interaction between Se and tamoxifen has been demonstrated and Se appears to be able to reverse tamoxifen resistance (Li *et al*, 2008b). In a breast cancer xenograft model the synergy between MSC and tamoxifen involved enhanced inhibition of oestrogen receptor expression and signalling (Li *et al*, 2009).

1.3.10 Selenium and its effect on normal tissue

Evidence from xenograft models and clinical trials suggest that Se is able to protect normal tissue from chemotherapy-induced toxicity (Cao *et al*, 2004; Hu *et al*, 1997). Additional studies supporting these data include an *in vitro* study that investigated whether the addition of SLM could protect human peripheral lymphocytes from the genetic damage induced by doxorubicin (Santos & Takahashi, 2008). SLM was able to reduce the cytotoxicity, genotoxicity and clastogenicity of doxorubicin. It has been demonstrated, *in vitro,* that pre-treatment of primary human keratinocytes with Se, in the form of selenite or SLM, protects these cells from oxidative damage and apoptosis resulting from exposure to UV radiation (Rafferty *et al*, 2003a; Rafferty *et al*, 2003b).

Work from our group has shown that PBMCs harvested from healthy individuals are relatively resistant to the cytotoxic effects of MSA with a 72-hour EC_{50} of 84.2μM (Juliger *et al*, 2007).

The mechanism by which Se compounds are able to protect normal tissue is not fully understood. As discussed above there are several proposed mechanisms. These include a possible pro-survival response in normal cells to the induction of ER stress (Bedard *et al*, 2004; Hung *et al*, 2003), protection from DNA damage through induction of p53 (Fischer *et al*, 2007) and activation of pro-survival cell signalling pathways such as Akt and Erk1/2 (Gonzalez-Moreno *et al*, 2007).

1.3.11 Functional markers of selenium status

If Se supplementation, at supra-nutritional doses, is going to be used as a therapeutic agent in cancer therapy it would be useful to have a functional marker of its biological effect, a biomarker. Current markers are inadequate. Plasma or serum Se is widely used but this reflects short-term status and is affected by non-nutritional factors. For example, there is an inverse relationship between CRP, a marker of the acute phase response, and serum Se in a number of pathological conditions (Maehira *et al*, 2002). Toenail and hair Se better reflect long-term Se status.

The measurement of selenoproteins may be a more accurate reflection of Se status. However, there are differences between selenoproteins in the response to Se deficiency with preferential incorporation of Se into some. In addition, polymorphisms in the genes coding for selenoproteins have been shown to account for inter-individual variation in the ability to increase the activity of these proteins (this has been discussed earlier in section 1.3.9.2) (Hu & Diamond, 2003; Meplan *et al*, 2007). Within the GPx family, Se deficiency leads to a rapid decrease in activity of GPx-1 and 3 whereas GPx-2 and 4 are depleted more slowly (Weitzel *et al*, 1990; Wingler *et al*, 1999). In addition, plasma selenoproteins such as GPx3 and selenoprotein P plateau at certain Se concentrations. The recommended dietary intake of Se has been determined based on optimising GPx3

activity and hence in individuals who are Se replete, GPx3 does not respond to Se supplementation (Burk *et al*, 2006). This maximal activity is reached at a plasma Se concentration of around 1.2µmol/L (Duffield *et al*, 1999; Thomson *et al*, 1993). Platelet GPx activity however is saturated at higher plasma Se concentrations, 1.2-1.5µmol/L for inorganic forms and 1.4-1.7µmol/L for organic forms (Neve, 1995; Thomson *et al*, 1993). The reason for the difference between inorganic and organic forms of Se is not clear. Selenoprotein P also plateaus but at a higher plasma Se concentration than GPx3, in the range of 1.2-1.7µmol/L (Persson-Moschos *et al*, 1998; Xia *et al*, 2005). However, in a high dose Se supplementation study where individuals were Se replete with an average serum Se concentration of 1.58µmol/L, there was no further increase in selenoprotein P levels (Burk *et al*, 2006). This has been confirmed by a more recent Se supplementation study in which selenoprotein P levels reached a plateau at a plasma Se concentration of 1.57µmol/L (Hurst *et al*, 2010)

Haemolysate TrxR activity was correlated with serum Se levels in a supplementation study (Karunasinghe *et al*, 2006). Activity increased with increasing Se concentration and had not plateaued at concentrations of 1.62µmol/L. However, work in animals suggests that supra-nutritional doses of MSC and MSA are unable to further increase TrxR activity in tissues (Ganther & Ip, 2001).

As discussed above, Se metabolites are excreted in the urine. Until recently it was thought that selenosugars were the major metabolites when Se was ingested at normal dietary doses and that trimethylselenonium became the dominant metabolite when Se was ingested at supra-nutritional doses (Kobayashi *et al*, 2002). However, a recent study in patients with cancer who were supplemented with very high doses of SLM (up to 8000µg/day) found that trimethylselenonium was only a minor metabolite in urine and selenosugars made up the greatest proportion (Kuehnelt *et al*, 2007). These results support those of an earlier study (Kuehnelt *et al*, 2005). Therefore, trimethylselenonium in urine is unlikely to be useful as a biomarker of high Se intake.

Se status will probably best be assessed by a combination of plasma protein markers and others need to be sought to assess the efficacy of supra-nutritional doses.

1.3.12 Studies of selenium in lymphoma

Work at SBH has focussed on the role of Se in lymphoma, particularly DLBCL. Serum Se concentration at diagnosis was found to be independently predictive of treatment response and long-term survival in patients with 'aggressive' B-cell NHL, the majority having DLBCL (Last *et al*, 2003). This retrospective analysis of stored sera in a group of 100 patients found that 73% had a serum Se level below the UK reference range. When the patient group was split into quartiles based on their serum Se level, response to first treatment was 54% in the lowest quartile and 88% in the highest ($p=0.011$) with a lower OS in patients with lower Se ($p=0.03$). Presentation Se was also predictive of delivered dose intensity, reflecting whether cytotoxic chemotherapy could be administered on time and at full dose. Serum Se concentration correlated closely with performance status but with no other clinical variables, including albumin. Figure 1.15 shows the OS, from diagnosis, of the 100 patients split into serum Se quartiles.

Other studies have reported a lower serum Se concentration in patients with NHL. A study in patients with cutaneous T-cell lymphoma found that serum Se was associated with advanced stage and a poorer response to treatment (Deffuant *et al*, 1994). Another study in patients with lymphoid malignancy reported similar findings. Compared with a control group, patients with advanced stage, but not localised disease, had a significantly lower Se level (Avanzini *et al*, 1995). However, serum Se positively correlated with albumin to which a proportion of Se is bound. A smaller study in paediatric patients investigated the hair Se status of newly diagnosed patients with lymphoid malignancies (Ozgen *et al*, 2007). Hair Se, which is a reflection of more long-term status, was lower than that of a control group but this was only statistically significant in malnourished patients.

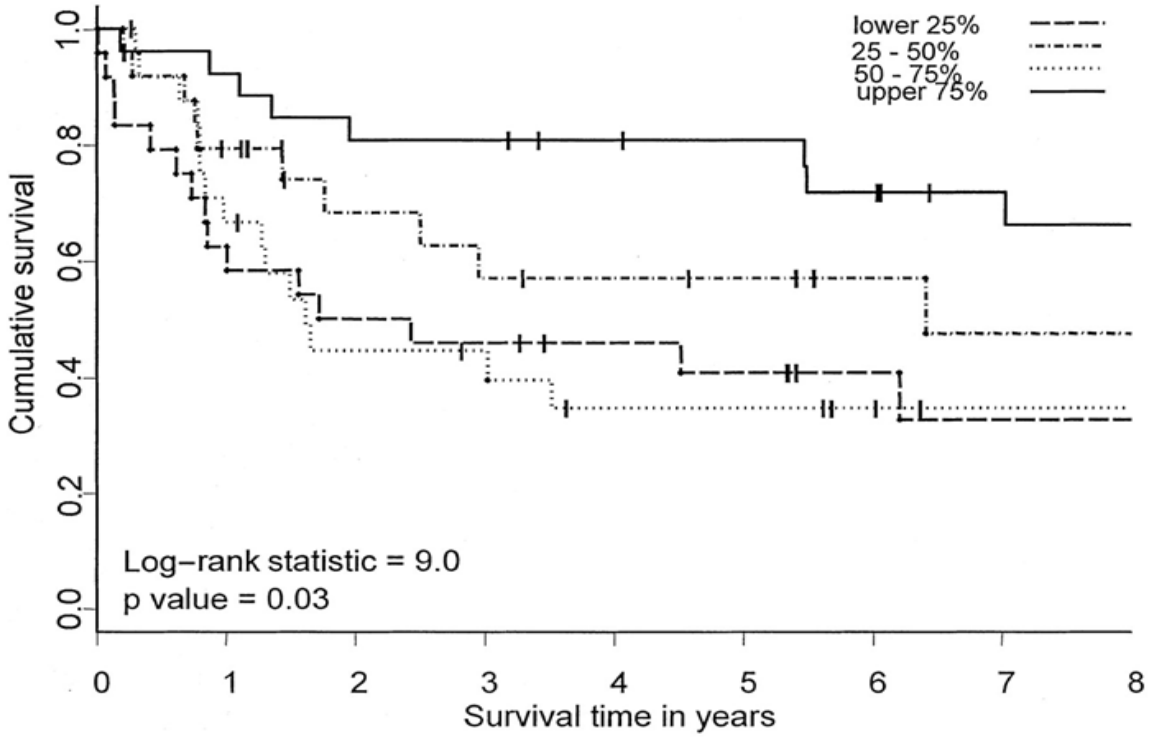

Figure 1.15 Overall survival of patients with 'aggressive' B-cell NHL split into serum selenium quartiles. From Last, KW *et al*., J Clin Oncol, 2003.

There is some debate in the literature about the interpretation of low Se levels in patients with malignancy. It may merely be a reflection of tumour burden, disease progression, an acute phase response and a marker of general nutritional deficiency. With regards to this point it is interesting to note that patients in the intensive care unit with systemic inflammatory response syndrome and multi-organ failure have been found to have low serum Se concentration and GPx activity, and this is associated with increased mortality (Sakr *et al*, 2007). This has led to several clinical trials of Se supplementation, mainly in the form of sodium selenite, in critically ill patients; the rationale being that Se will increase the activity of anti-oxidant selenoproteins. However, the results of these studies have largely been inconclusive (Manzanares *et al*, 2010).

Alternatively, the presence of low serum Se at diagnosis may predict for chemo-resistance and hence a poorer outcome, thus Se supplementation may represent a potential therapeutic intervention. This hypothesis forms part of the rationale for the

proposed clinical trial of Se supplementation in patients with recurrent/refractory DLBCL (discussed further below). Interestingly, studies in solid malignancy have found that a low serum Se level is associated with a significantly increased tumour Se concentration when compared to adjacent non-neoplastic tissue (Charalabopoulos *et al*, 2006a; Charalabopoulos *et al*, 2006b). Whether the increased Se concentration in the neoplastic tissue is responsible for the low serum Se is not clear. Another explanation may be that Se forms part of the defence mechanism in tumour tissue in line with the anti-oxidant properties of some selenoproteins. These findings, however, require further study.

In addition to Se levels, the activity and gene expression of GPx and other antioxidants have been studied in patients with lymphoma. One study measured red cell GPx activity in 50 patients with untreated lymphoma and 47 controls and found that patients with lymphoma had significantly lower levels. Patients also had significantly lower levels of superoxide dismutase, suggesting a general deficiency in the cellular anti-oxidant system. Plasma Se levels were not measured in this study (Bewick *et al*, 1987).

Contradictory results regarding alterations in gene expression of antioxidant enzymes have been reported. One study analysed the expression of a number of antioxidant genes in tumour samples from patients with *de novo* DLBCL and found that decreased expression of GPx (GPx1, 3 and 4) and other antioxidant enzymes was associated with a poor prognosis (Tome *et al*, 2005). However, a similar study found that high expression of GPx1 was significantly associated with early treatment failure and a poor outcome and this remained significant after adjusting for the IPI score and molecular subgroup (Andreadis *et al*, 2007). The Pro197Leu polymorphism in the GPx1 gene has been analysed in patients with lymphoma and a moderate association was found between having the leucine allele and the risk of different NHLs (OR 1.24-1.34) (Lightfoot *et al*, 2006).

It is difficult to pull all these results together as there is evidence in the literature to suggest that oxidative stress may play a role in tumour initiation and progression but also

may be involved in inducing tumour cell death. Suffice to say that the intracellular redox environment is crucial to cellular function and that the selenoprotein GPx plays an important part.

Our laboratory has conducted a number of pre-clinical studies investigating the activity of Se alone and in combination with cytotoxic agents in DLBCL cell lines and primary patient samples. MSA induced apoptosis in DLBCL cell lines, but these cell lines differed markedly in their sensitivity to MSA. Cell death was not associated with cell cycle arrest or with the generation of ROS. In addition, primary lymphoma cultures from 4 patients with B-cell NHL (2 mantle cell lymphoma, 1 FL and 1 chronic lymphocytic lymphoma) showed a concentration-dependent decrease in cell viability in response to MSA (Last *et al*, 2006).

A synergistic interaction was demonstrated between low, non-cytotoxic concentrations of MSA and three cytotoxic agents, etoposide, doxorubicin and 4-hydroperoxycyclophosphamide (4-HC), in DLBCL cell lines. Best results were obtained when MSA was administered simultaneously with the cytotoxic drugs. A potential mechanism for this synergistic interaction with cytotoxic drugs was found to be a Se-induced decrease in NF-κB activity in DLBCL cell lines. To confirm that inhibiting NF-κB activity increased sensitivity to chemotherapeutic agents, the same experiments were conducted with the known NF-κB inhibitor, BAY 11-7082. BAY 11-7082 significantly increased the cytotoxic activity of etoposide and doxorubicin in the DLBCL cell lines. Figure 1.16 shows inhibition of NF-κB activity by MSA and BAY 11-7082. In addition, it was demonstrated that the synergistic interaction between MSA and chemotherapeutic agents was not due to enhanced DNA damage (Juliger *et al*, 2007).

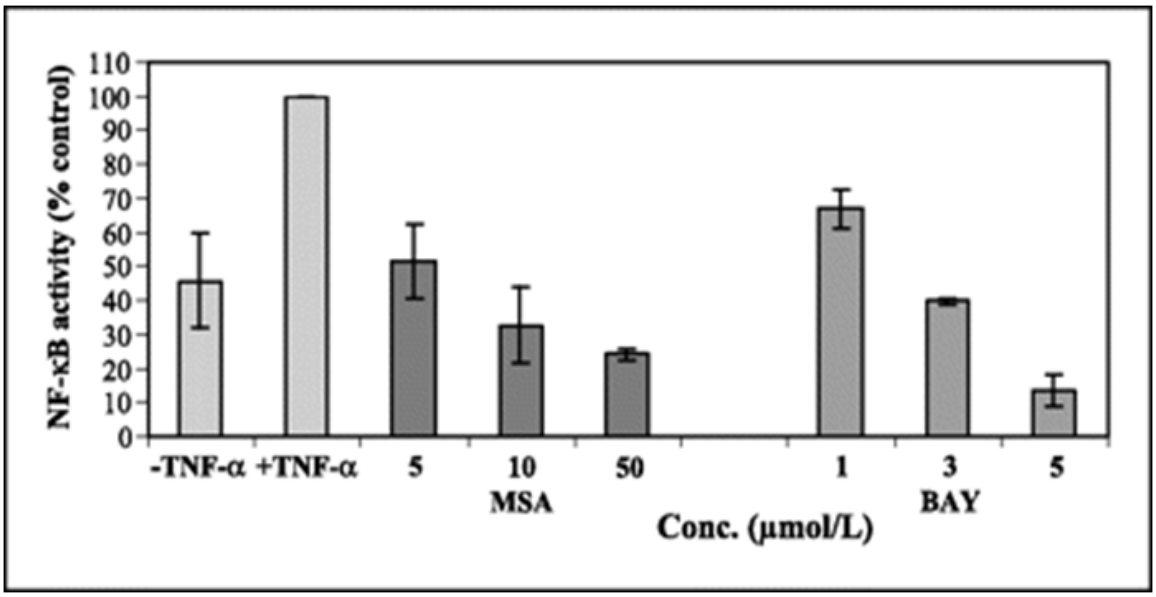

Figure 1.16 Inhibition of NF-κB activity by MSA and BAY 11-7082 in a DLBCL cell line (DHL4). From Juliger, S. *et al*., Cancer Res, 2007.

In a collaboration between our laboratory and LGC (Teddington, London, UK), novel mass-spectrometry methods were developed for quantification of total intracellular Se and the identification of intracellular and volatile Se species. These experiments are important for determining the Se species responsible for the observed effects (Goenaga-Infante *et al*, 2007b). DLBCL cell lines differed in their basal Se concentration. The MSA-sensitive cell line, RL, had a much higher concentration than two resistant cell lines, DHL4 and DoHH2. After 4-hour exposure to MSA, the DHL4 cell line had a much larger increase in Se concentration than the RL cell line.

Intracellular Se metabolites generated after exposure to MSA in DHL4 cells (a resistant DLBCL cell line) were investigated. MSC was detected as the main metabolite with a maximal concentration after 30-minute exposure. SLM and γ-glutamyl-MSC were also detected, but at a much lower level, and were formed at a slower rate than MSC. MSA itself was not detected. Investigation of the volatile Se species generated after exposure to MSA revealed that dimethyldiselenide was formed after 10-minute exposure. There was a

massive increase in dimethyldiselenide generation after 20-minute exposure and the appearance of a second metabolite, dimethylselenide (Juliger *et al*, 2007).

Based on these clinical and *in vitro* studies in lymphoma, a phase I/II multi-centre study of MSC in combination with 'R-ICE' chemotherapy in patients with relapsed/refractory DLBCL will commence shortly. This trial will supplement patients with supra-nutritional doses of MSC aiming to achieve a plasma Se concentration of 20µmol/L prior to commencing chemotherapy. This trial is funded by Leukaemia and Lymphoma Research and will be run from SBH.

There has been a randomised study of high-dose sodium selenite in patients with NHL treated with CHOP chemotherapy (Asfour *et al*, 2009). This was in a group of patients with 'intermediate' and 'high-grade' lymphomas, all of whom had bone marrow involvement. Selenite was given on days 3-7 for the first cycle of chemotherapy only. The main endpoint was the number of apoptotic bone marrow lymphoma cells on day 8 compared with day 0, as assessed by flow cytometric analysis of propidium iodide stained cells. The study reported a significant increase in the percentage of apoptotic lymphoma cells in the selenite-treated group. In addition, a significantly greater reduction in cervical and axillary lymphadenopathy, spleen size and percent bone marrow infiltration was reported in the selenite-treated group. In the control group there was a significant decrease in cardiac ejection fraction after chemotherapy. This was not observed in the selenite group, suggesting a possible cardio-protective effect of selenite.

This study, however, has a number of limitations. Although it is reported that selenite increased the percentage of apoptotic lymphoma cells in the bone marrow, the lymphoma cells were not selected for in the separation process so all mononuclear cells were analysed. It is known that marrow infiltration by lymphoma is patchy and therefore it is unclear what proportion of cells analysed were indeed lymphoma cells and what were normal bone marrow cells. It is not obvious how the reduction in lymphadenopathy was assessed. Given that spleen size was reported 'in fingers' it suggests that the

lymphadenopathy may also have been assessed clinically, rather than by CT scanning. This is clearly a subjective method of assessment and is a source of bias given that the study was not blinded. This study was performed in a heterogenous group of patients and unusually they all had splenomegaly, with over three-quarters of patients also having hepatomegaly. This is unusual given that DLBCL should be the most common subtype.

In summary, there is robust evidence for the therapeutic use of organic Se compounds in solid tumours and evidence is emerging to suggest it may also be of value in treating patients with lymphoma. Clearly, Se has a number of potential mechanisms of action which differ based on the chemical form, concentration and tumour type. Thus, further investigation is required into mechanisms which are important in its action in lymphoma, particularly DLBCL. In addition, the effects of Se differ between normal and tumour cells and the mechanism for this differential activity have not been well defined. For the purposes of the planned phase I/II clinical trial in patients with relapsed/refractory DLBCL, better biomarkers of Se activity are required. Therefore, these areas of investigation form the basis of this thesis.

1.4 HYPOTHESIS AND AIMS

Better therapies are needed for the treatment of DLBCL, particularly at recurrence. One such treatment could be the addition of Se to standard chemotherapy regimens. The hypothesis being tested here is that chemo-sensitisation of DLBCL cell lines by MSA is due to enhanced apoptosis through the induction of cellular stress, and that the response to cellular stress differs between normal, non-malignant cells and lymphoma cells. This was investigated through the following aims:

1. To analyse the patterns of survival in newly diagnosed patients with DLBCL presenting to St Bartholomew's Hospital between 1985 and 2003.
2. To investigate mechanisms by which Se, in the form of MSA, sensitises DLBCL cell lines to chemotherapy.
3. To investigate the effects of MSA in normal cells and identify mechanisms by which Se protects these cells from chemotherapy-induced toxicity.
4. To investigate the uptake of MSA by PBMCs and DLBCL cell lines.
5. To investigate the Se metabolites generated after exposure of PBMCs and DLBCL cell lines to MSA.
6. To identify potential biomarkers for the clinical evaluation of Se.
7. To investigate the combination of Se and bortezomib in mantle cell lymphoma cell lines.

CHAPTER 2: Materials and Methods

This chapter contains methods used throughout the thesis. Methods that are specific to a particular chapter are described in those chapters.

2.1 Cell Culture

A panel of B-NHL cell lines were used in experiments. The DHL4 cell line was obtained from the Dana-Farber Cancer Institute (kind gift from Dr Margaret Shipp). The DoHH2, SUD4, RL and JVM2 cell lines were all obtained from Cancer Research UK cell services. These suspension cell lines were all maintained in RPMI-1640 culture medium (Sigma-Aldrich, Poole, UK) supplemented with 10% foetal calf serum (Sigma Aldrich) and 1% penicillin (100units/ml) and streptomycin (100µg/ml) (both from Invitrogen™, California, USA) at 37°C in a humidified atmosphere with 5% CO_2. Cells were passaged twice weekly and reset at $2x10^5$/ml. For experiments, cells were used in their exponential growth phase. Therefore, cells were reset in fresh culture medium the day before exposure to the various drugs of interest.

2.1.1 Cell line characteristics

The RL cell line is established from the ascites of a patient with DLBCL (Beckwith *et al*, 1991). The SUD4 cell line, also known in the literature as SU-DHL4, is derived from the pleural effusion of a patient with DLBCL (Epstein *et al*, 1978). The DoHH2 cell line is established from the pleural effusion of a patient with FL, which had transformed to DLBCL (Kluin-Nelemans *et al*, 1991). The DHL4 cell line is a drug-resistant variant of the SUD4 cell line, established in the laboratory of Dr Margaret Shipp (Dana Farber Cancer Institute). JVM2 is now accepted as a mantle cell lymphoma (MCL) cell line (Tucker *et al*, 2006), however, it was first reported as being derived from a patient with pro-lymphocytic lymphoma, before the diagnosis of MCL was widely recognised (Melo *et al*, 1988). The RL, SUD4 and DoHH2 cell lines all have the t(14;18) translocation and the JVM2 cell line has a t(11;14) translocation. All the cell lines, except JVM2, have mutated *p53*. The RL, DHL4 and SUD4 cell lines have homozygous mutations whilst the

DoHH2 cell line has a heterozygous mutation (Strauss *et al*, 2007). In this thesis the RL, SUD4, DoHH2 and DHL4 cell lines are collectively termed DLBCL cell lines.

2.1.2 Culture of cell lines under hypoxic conditions

To investigate the effect of MSA on HIF-1α and Prx1 expression and VEGF production, RL and DHL4 cell lines were cultured in a hypoxic incubator (1% O_2, 5% CO_2, 94% N_2) at 37°C in a humidified atmosphere. $5x10^6$ cells, resuspended in 10mls culture medium, were placed in the hypoxic incubator overnight prior to exposure to different concentrations of MSA for a further 24 hours. As a control, cells were also cultured under normoxic conditions. After 24 hours, cells were pelleted by centrifugation at 210*g* for 6 minutes at room temperature and the supernatant collected and stored at -80°C for subsequent determination of VEGF levels. The cells were used for whole cell, nuclear and cytoplasmic protein separation and western blotting was performed.

2.1.3 Harvesting peripheral blood mononuclear cells

Collection of PBMCs from healthy volunteers received a favourable ethical opinion from the East London and City HA Local Research Ethics Committee. PBMCs were obtained through venesection and 20-40mls of blood was collected into blood tubes containing ethylene diamine tetraacetic acid (EDTA; BD Vacutainer®, Plymouth, UK). The blood was then layered over an equal volume of Histopaque® (Sigma-Aldrich), and density-gradient centrifugation (600*g* for 20 minutes at room temperature) was used to isolate the mononuclear cell fraction. The isolated PBMCs were washed once in RPMI-1640 culture medium and then resuspended in RPMI-1640 culture medium supplemented with 10% foetal calf serum, and 1% penicillin (100units/ml) and streptomycin (100µg/ml).

2.2 Drug preparation

2.2.1 Methylseleninic acid

MSA (PharmaSe® Inc., Texas, USA) was dissolved in deionised water as stock solutions of 10mmol/L and 20mmol/L and stored at -80°C. These stocks were further diluted prior to use in cell culture medium to obtain a range of experimental working concentrations.

2.2.2 Methylselenocysteine

MSC (PharmaSe® Inc., Texas, USA) was dissolved in deionised water as a stock solution of 10mmol/L and stored at -80°C. These stocks were further diluted prior to use in cell culture medium to obtain a range of experimental working concentrations.

2.2.3 Doxorubicin

Doxorubicin hydrochloride solution (Sigma-Aldrich), 3.45mmol/L, was made up to the desired concentration in cell culture medium prior to use.

2.2.4 4-hydroperoxycyclophosphamide

4-HC is the active metabolite of cyclophosphamide. It is formed *in vivo* in the liver by the action of p450 oxidases. Thus, for *in vitro* experiments 4-HC (Squarix Biotechnology, Marl, Germany) was used. It forms aldophosphamide, which is in turn converted to phosphoramide mustard, the cytotoxic molecule. A 5mmol/L stock solution of 4-HC was prepared in deionised water and stored at -80°C. These stocks were further diluted prior to use in cell culture medium to obtain a range of experimental working concentrations.

2.2.5 Bortezomib

A 5mmol/L stock solution of bortezomib (LC laboratories, MA, USA) was prepared in dimethyl sulfoxide **(**DMSO, Sigma Aldrich) and stored at -80°C. These stocks were further diluted prior to use in cell culture medium to obtain a range of experimental working concentrations.

2.2.6 Suberoylanilide hydroxamic acid

A 10mmol/L stock solution of suberoylanilide hydroxamic acid (SAHA; synthesised in the Chemistry department, University College London) was prepared in DMSO and stored at -80°C. These stocks were further diluted prior to use in cell culture medium to obtain a range of experimental working concentrations.

2.2.7 Staurosporine

1mmol/L staurosporine solution in DMSO (Sigma-Aldrich) was made up to the desired concentration in cell culture medium prior to use.

2.2.8 Bafilomycin A1

Bafilomycin A1 (Sigma-Aldrich) was dissolved in DMSO to a concentration of 0.1mg/ml and stored -80°C. This stock solution was further diluted prior to use in cell culture medium to obtain a final working concentration of 10nmol/L.

2.2.9 Thapsigargin

Thapsigargin (Sigma-Aldrich) was dissolved in DMSO as a stock solution of 15mmol/L and stored at -80°C. This stock solution was further diluted prior to use in cell culture medium to obtain a final working concentration of 3μmol/L.

2.3 Cell proliferation and cytotoxicity assays

2.3.1 Trypan blue exclusion

Cell count and viability of PBMCs was established by trypan blue exclusion. After mixing, 10μl of cells was mixed with 10μl 0.4% trypan blue (Sigma-Aldrich) and placed onto a haemocytometer for counting under a light microscope. Live cells are colourless and dead cells stain blue since they are unable to exclude the dye due to impaired membrane integrity.

2.3.2 ViaLight® HS assay (ATP assay)

The activity of various drugs in a number of different cell lines was determined using the ViaLight HS bioluminescence kit (Lonza, Basel, Switzerland). Cells were plated in 96-well microtitre plates at a concentration of $2x10^5$/ml for suspension cells and $5x10^4$/ml for adherent cells. After 24 hours, the drug of interest was added to the experimental wells and cells were incubated for a further 48 or 72 hours. The Vialight HS assay is

based on the measurement of ATP and uses the enzyme luciferase to catalyse the reaction between ATP and luciferin, resulting in the generation of light. The reaction is as follows:

$$\text{ATP + luciferin + } O_2 \xrightarrow[Mg^{2+}]{\text{Luciferase}} \text{Oxyluciferin + AMP + } PP_i + CO_2 \text{ + Light}$$

There is a linear relationship between the light emitted and the ATP concentration, this being measured by a luminometer. This assay is based on the observation that as cells lose viability they lose the ability to regenerate ATP, such that intracellular ATP concentration provides a measure of the viability of a population of cells.

After incubating the cells with the drug(s) of interest, 100µl of the nucleotide releasing agent was added to each well and the 96-well plate was incubated at room temperature for 5 minutes. Following this, 180µl from each well was transferred to a white 96-well microtitre plate. The plate was then placed in the POLARstar OPTIMA plate reader (BMG Labtech, Offenburg, Germany), 20µl of ATP monitoring reagent was automatically dispensed into each well and luminescence measured immediately. The results were expressed relative to the control value and data analysis is described in section 2.14.

2.3.3 Gauva® Viacount® Assay

The ViaCount® assay (Millipore, MA, USA) uses a reagent which is a mixture of two DNA binding dyes to obtain absolute cell counts and assess cell viability. One dye is membrane permeable and stains all nucleated cells, the other is membrane impermeable and only enters cells when the membrane has been breached thus identifying apoptotic/dead cells. Cells stained with this reagent were analysed on the Guava® PCA-96 system (Millipore) which has a green laser for excitation, two fluorescence detectors, and a detector of forward scatter that assesses relative size. Data were analysed using the Guava® ViaCount® software (Millipore) and cell viability and cell number data obtained.

Cells were added to 96-well microtitre plates at a concentration of $1x10^5$/ml. After 24 hours, different drugs were added to the experimental wells and plates were incubated for a further 48 hours. Following this, 100µl of the Guava® ViaCount® reagent, diluted 1:400 in cell culture medium, was added to each well. Plates were analysed immediately on the Guava® PCA-96 system. Examples of the results obtained are shown below (Figure 2.1). The results were expressed relative to the control value and data analysis is described in section 2.14.

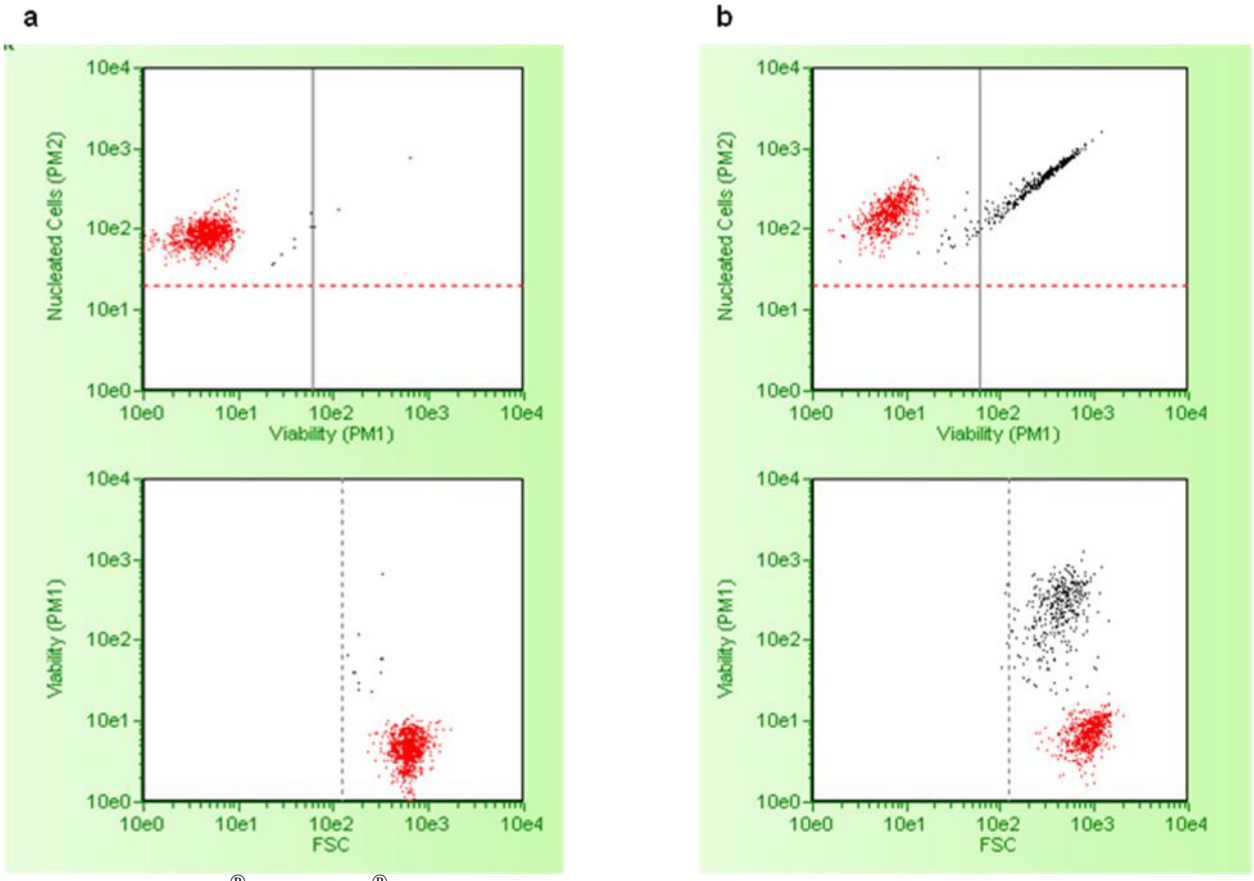

Figure 2.1 Gauva® Viacount® Assay. Live cells shown in red and dead cells shown in black (a) An example of control cells (b) An example of cells treated with bortezomib.

2.4 Sample preparation for western blot analysis

2.4.1 Treatment of cell lines

Cells lines were reset in fresh medium at $5x10^5$/ml in volumes of 6mls. After 24 hours, the drug(s) of interest was added and cells were incubated for various lengths of time.

2.4.2 Methylseleninic acid treatment of peripheral blood mononuclear cells

PBMCs were set in fresh medium at $2x10^6$/ml in volumes of 4mls. MSA was added at a concentration range of 1-20µmol/L and cells incubated for various time-points.

2.4.3 Whole cell protein extraction

Cells were pelleted by centrifugation at 210*g* for 6 minutes at room temperature. The medium was discarded and the cells washed twice in Hanks' Buffered Salt solution (HBSS; Sigma-Aldrich) by centrifugation at 210*g* for 6 minutes at 4°C. The cells were resuspended in lysis buffer [1x phosphate buffered saline (PBS), 1% Triton X-100, 0.5% sodium deoxycholate, 0.1% sodium dodecylsulphate, 1mM EDTA, made up to 500ml with deionised water, pH set to 7.4, stored at 4°C; all chemical were obtained from Sigma-Aldrich]. Protease inhibitor cocktail (Roche, Basel, Switzerland) was added to the lysis buffer at a 1:25 dilution just prior to use. Samples were left on ice for 20 minutes and then centrifuged at 20,800*g* for 10 minutes to remove insoluble cellular debris. The supernatant was removed, placed into fresh eppendorf tubes (Eppendorf UK Limited, Cambridge, UK) and stored at -80°C prior to western blot analysis

2.4.4 Nuclear and cytoplasmic protein separation

All chemicals were obtained from Sigma-Aldrich. Cells were pelleted by centrifugation at 210*g* for 6 minutes at room temperature. The medium was discarded and the cells were washed twice in HBSS by centrifugation at 210*g* for 6 minutes at 4°C. Each cellular sample was then resuspended in 200µl of buffer A [10mM 4-(2-hydroxyethyl)-1-piperazineethanesulfonic acid (HEPES) pH 7.9, 1.5mM $MgCl_2$, 10mM KCl, 0.5mM phenylmethanesulfonyl fluoride (PMSF), 1mM dithiothreitol (DTT), protease inhibitor cocktail, made up to 10mls with deionised water] and incubated for 20 minutes on ice.

0.4% Octylphenyl-polyethylene glycol (IGEPAL® CA-630) was then added and the samples centrifuged at 750*g* for 5 minutes at 4°C. The supernatant containing the cytoplasmic protein fraction was removed and placed into fresh eppendorf tubes. The remaining pellet was washed once in buffer A and then resuspended in 50µl of buffer B [20mM HEPES pH 7.9, 420mM NaCl, 1.5mM $MgCl_2$, 0.2mM EDTA, 0.5mM PMSF, 1mM DTT, protease inhibitor cocktail, made up to 2mls with deionised water]. The samples were incubated on ice for 45 minutes and vortexed every 5 minutes. The samples were then centrifuged at 20,800*g* for 12 minutes and the supernatant containing the nuclear protein fraction removed and placed into fresh eppendorf tubes. Both cytoplasmic and nuclear fractions were stored at -80°C prior to use.

2.4.5 Whole cell, nuclear and cytoplasmic protein quantification

The protein content of each lysate was determined using the BCA™ (bicinchoninic acid) protein assay kit (Pierce, Illinois, USA). This assay makes use of the fact that protein can reduce Cu^{+2} to Cu^{+1} in an alkaline medium. The reagent containing BCA is used for colorimetric detection of Cu^{+1} (purple coloured reaction product is formed when two molecules of BCA are chelated with one Cu^{+1} ion). The absorbance, read at 562nm, has a linear relationship to the protein concentration. 10µl of lysate was pipetted into a 96-well plate with 10µl of lysis buffer. BCA™ reagent A (sodium carbonate, sodium bicarbonate, BCA and sodium tartrate in 0.1M sodium hydroxide) was mixed with BCA™ reagent B (4% cupric sulphate) in a 50:1 ratio and 160 µl added to each well. The plate was incubated at 37°C for 20 minutes and absorbance read at 562nm. The protein content was determined by comparison with a standard concentration curve created by dilutions of bovine serum albumin (2mg/ml) from 0 to 20µg in lysis buffer. The protein concentrations of the samples were calculated by linear regression analysis. An example of the standard curve generated is given below (Figure 2.2; r=0.998).

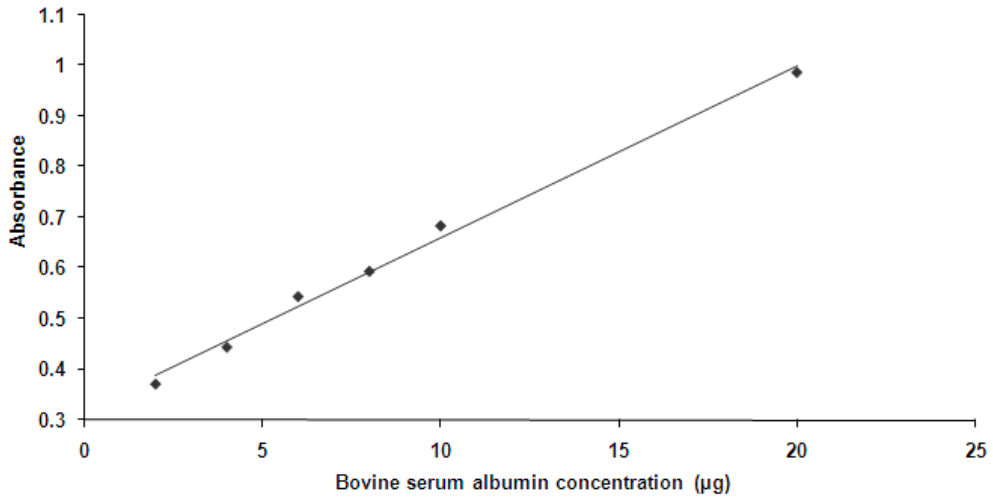

Figure 2.2 An example of a standard curve of bovine serum albumin quantified using the BCA™ assay kit.

2.5 Western blot analysis

2.5.1 Electrophoresis of proteins

20µg to 40µg of cellular protein was added to 1x NuPAGE® LDS sample buffer (Invitrogen™). The samples were heated at 95°C for 5 minutes. Pre-cast gels (NuPAGE® Novex® Bis-Tris midi or mini gel system; Invitrogen™), were placed in a gel tank and running buffer (1x NuPAGE® running buffer, Invitrogen™) added to the tank to a level that covered the gels. The samples were then loaded into the wells of the gels. In the first well of each gel the Novex® sharp standard (Invitrogen™) was loaded. This is a pre-stained standard protein molecular weight marker of between 3.5kDa and 260kDa. For blots that were to be developed using the Fujifilm image analyser (see below in section 2.5.5), a luminescent marker was loaded; MagicMark™ XP Western Protein Standard (Invitrogen™) with bands between 20-220kDa. Electrophoresis of the gel was performed at a constant voltage of 200V.

2.5.2 Transfer of proteins from the gel to the polyvinylidene fluoride membrane

Protein transfer was performed using the iBlot™ gel transfer device (Invitrogen™) for dry blotting of proteins according to the manufacturers' instructions. It is a self-contained

blotting unit with an integrated power supply. The device requires iBlot™ gel transfer stacks which are disposable stacks with an integrated polyvinylidene fluoride **(**PVDF) transfer membrane. Each transfer stack contains a copper electrode and appropriate cathode and anode buffers in a gel matrix. After completion of protein electrophoresis the gels were removed from the gel tank and placed on the anode stack that had the PVDF membrane as its upper most layer. Filter paper, pre-soaked in distilled water, was placed on the pre-run gel and air bubbles removed using a roller device. The cathode stack was then placed on top of the filter paper and the transfer device closed and programmed to perform the protein transfer.

2.5.3 Antibody staining of western blots

Protein expression was determined by antibody staining. After removing the PVDF membrane from the protein transfer device, it was blocked in 1x tris(hydroxymethyl)aminomethane (Tris) buffered saline (TBS) [1L of 10x TBS; 24.2g Trizma® base (Sigma-Aldrich) and 80g NaCl made up with distilled water, pH adjusted to 7.6] with 0.1% (v/v) Tween-20® (Sigma-Aldrich) and 5% (w/v) non-fat dry milk for 1 hour. For phospho-proteins, the membrane was blocked in 5% (w/v) albumin from bovine serum (Sigma-Aldrich). Following 3 washing steps with TBS-tween-20® solution, the primary antibody was added either overnight at 4°C or for 1 hour at room temperature depending on the antibody used. The membrane was again washed three times with TBS-tween-20® solution and then incubated with a horseradish peroxidase (HRP)-conjugated secondary antibody. An HRP-conjugated anti-mouse IgG_1 (1:2000 dilution) was used as secondary antibody for mouse primary antibodies, and an anti-rabbit IgG was used (1:2000 dilution) for rabbit primary antibodies, both from Dako Ltd, (Cambridge, UK).

2.5.4 Antibodies used for protein detection

The following primary antibodies were used in western blot analysis (Table 2.1). All antibodies were diluted in TBS-tween-20®.

Table 2.1 Primary antibodies used in western blotting experiments

Protein	MW*	Company	Dilution
Acetylated histone H3	17	Millipore[1]	1:3000
Acetylated α-tubulin	52	Sigma-Aldrich	1:3000
β-actin	40	Dako[4]	1:3000
Akt	60	Cell Signaling[2]	1:1000
Bak	23	Santa Cruz[3]	1:1000
Bax	30	Santa Cruz	1:1000
Bcl-2	26	Dako	1:1000
Bcl-xL	30	Santa Cruz	1:1000
Cleaved PARP	89	Abcam[5]	1:1000
eIF2α	38	Cell Signaling	1:1000
Erk1/2	42, 44	Cell Signaling	1:1000
GAPDH	36	Abcam	1:1000
GRP78	78	Santa Cruz	1:1000
HIF-1α	120	Abcam	1:500
Histone H3	17	Cell Signaling	1:1000
HSP70	70	Cell Signaling	1:3000
HSP90	90	Santa Cruz	1:3000
IκB-α	35-41	Santa Cruz	1:1000
Jnk	46, 54	Cell Signaling	1:1000
LC3B	14, 16	Cell Signaling	1:1000
Mcl-1	40	Santa Cruz	1:1000
NF-κB p65	65	Santa Cruz	1:1000
Nrf2	57	Santa Cruz	1:1000
p53	53	Dako	1:1000
p21	21	Santa Cruz	1:200
PARP	116, 89	Cell Signaling	1:1000
Peroxiredoxin-1	24	Abcam	1:3000

Phospho-Akt (Ser473)	60	Cell Signaling	1:1000
Phospho-eIF2α (Ser51)	38	Cell Signaling	1:1000
Phospho-p44/42 MAPK (Erk1/2) (Thr202/Tyr204)	42, 44	Cell Signaling	1:200
Phospho-SAPK/Jnk (Thr183/Tyr185)	46, 54	Cell Signaling	1:1000
Phospho-Histone H2AX (Ser139)	15	Cell Signaling	1:1000
Protein disulfide isomerise (PDI)	55	Santa Cruz	1:1000
Survivin	16.5	Santa Cruz	1:500
α-tubulin	52	Cell Signaling	1:1000
Ubiquitin	-	Santa Cruz	1:500

*MW, molecular weight; [1]Millipore™, Billerica, MA, USA; [2]Cell Signaling Technology®, Inc., Danvers, MA, USA; [3]Santa Cruz Biotechnology®, Inc., Santa Cruz, CA, USA; [4] Dako Ltd, Cambridge, UK; [5]Abcam®, Cambridge, UK.

2.5.5 Visualisation of protein bands

The protein bands were visualised using an enhanced chemiluminescence method (ECL reagent, GE Healthcare UK Limited, Little Chalfont, UK). In this method, hydrogen peroxide catalyses the oxidation of luminol in alkaline conditions. This results in excitation of luminol, which subsequently decays whilst emitting light. PVDF membranes were incubated with ECL reagent for 30 seconds then blotted to remove excess reagent. Following this the membrane was placed between two transparent acetate films and exposed to high performance chemiluminescence film (GE healthcare) for up to 20 minutes depending on the strength of the bands. The films were then developed manually using Kodak developer and fixer obtained from Sigma-Aldrich. For the last 7 months of this work, a Fujifilm luminescent image analyser (Fujifilm LAS-4000, Tokyo, Japan) was used for visualisation of protein bands. Densitometric analysis was performed using Gelscan version 5.1 software (BioSciTech, Frankfurt, Germany). Values were normalised to the loading control.

2.5.6 Validation of loading control

For all western blots, equal protein loading was assessed by determining the expression of a 'housekeeping' protein. Commonly used proteins are β-actin, α/β tubulin and glyceraldehyde-3-phosphate dehydrogenase (GAPDH). Proteins of interest were normalised to the 'housekeeping' protein in densitometric analysis of western blots. Therefore, housekeeping proteins were validated by loading increasing concentrations of protein from whole cell lysates of the DHL4 cell line. Figure 2.3 shows western blots obtained for β-actin, α/β tubulin and GAPDH (Figure 2.3). For β-actin, the antibody is saturated at protein concentrations of ≥10µg and beyond this there is no longer a linear increase in band density. For α/β tubulin and GAPDH, the antibody is saturated at concentrations of ≥25µg. GAPDH shows a larger increase in band density between different protein concentrations than α/β tubulin and thus was selected as the loading control for the majority of experiments. For most western blot experiments a maximum of 20µg protein was loaded with the exception of western blots required to assess the expression of phospho-proteins, when 40µg protein was loaded. However, phospho-protein expression was compared to the relevant total protein expression rather than the loading control.

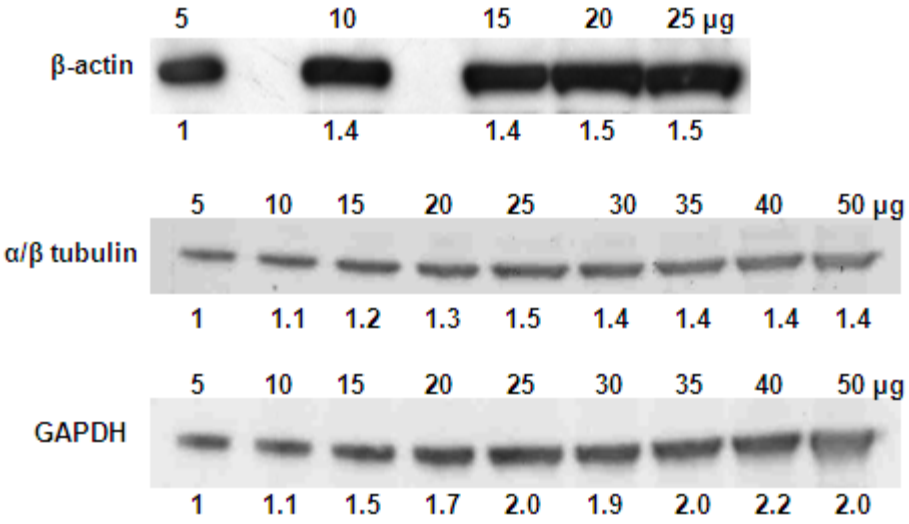

Figure 2.3 Western blotting of different protein loading. Protein concentration is shown above and densitometry values below each blot.

2.6 Intracellular glutathione measurement

The effect of MSA on total intracellular GSH was determined using a 96-well plate-based GSH assay kit (Sigma-Aldrich). Both reduced glutathione (GSH) and the oxidized form, glutathione disulfide (GSSG), are measured by the kit. In the assay, GSH results in the reduction of 5,5'-dithiobis(2-nitrobenzoic acid) (DTNB) to 5′-thio-2-nitrobenzoic acid (TNB). During this reaction, GSH is oxidised to GSSG, which is then converted back to GSH by the action of glutathione reductase and NAPDH. The reaction is as follows:

$$2\ GSH + DNTB \rightarrow GSSG + 2\ TNB$$

$$GSSG + NAPDH + H^{+} \xrightarrow{\text{glutathione reductase}} 2\ GSH + NADP^{+}$$

The reaction rate is proportional to the concentration of GSH. The yellow product, TNB, can be measured spectrophotometrically at 412nm

DHL4, RL and SUD4 cell lines were exposed to a range of MSA concentrations (1-20µmol/L) for 2 and 24 hours. 10 million cells were used for each experimental condition. After exposure to MSA, cells were pelleted by centrifugation at 210*g* for 6 minutes at room temperature. The medium was discarded and cells were washed twice by centrifugation at 210*g* for 6 minutes with 20mls of PBS. The cells were then resuspended in 1ml PBS and transferred to 1.5ml eppendorf tubes. The cells were centrifuged again at 600*g* to obtain a packed cell pellet and the supernatant removed. 200µl of 5% 5-sulfosalicylic acid was added to each sample to deproteinise the cells. The samples were vortexed well and then exposed to 3 freeze/thaw cycles (dry-ice to freeze and a 37°C heated block to thaw). The cell suspension was left on ice for 5 minutes and then centrifuged at 10,000*g* for 10 minutes at 4°C. The supernatant was recovered into fresh eppendorf tubes and used in the assay.

The assay was performed using a 96-well plate. GSH standards (supplied in the kit) were prepared using a concentration range of 250-4000nmol/L and 10µl of each concentration

was added to a 96-well plate in duplicate. 10µl of the cell extracts were also transferred to the 96-well plate, in duplicate. Two wells contained 10µl of 5% 5-sulfosalicylic acid as a reagent blank. 150µl of the freshly prepared working mixture (containing glutathione reductase enzyme 6units/ml and DNTB, 1.5mg/ml) was added to each well and the plate was incubated for 5 minutes at room temperature. 50µl of NADPH solution (0.16mg/ml) was then added to each well and the plate immediately analysed using the POLARstar OPTIMA plate reader (BMG Labtech) to measure absorbance at 412nm. Using the GSH standards, a standard curve was generated and used to determine the GSH concentration in the unknown samples. An example of a GSH standard curve is shown below (Figure 2.4; r=0.986)

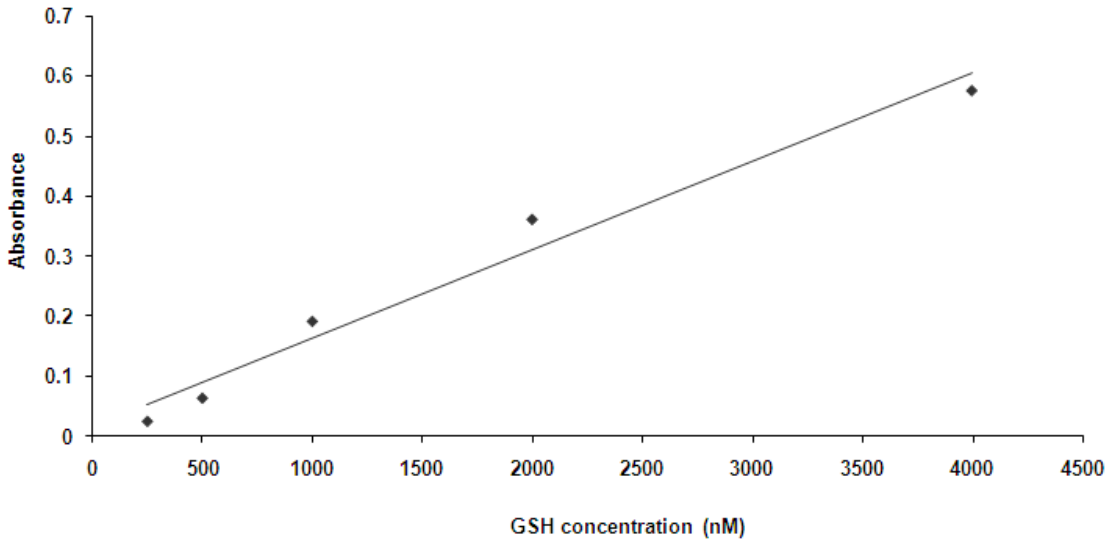

Figure 2.4 An example of the standard curve of glutathione quantified using the glutathione assay kit with a concentration range of 250-4000nmol/L.

2.7 Analysis of cell cycle distribution using flow cytometry

2.7.1 Sample preparation

Cells ($1x10^6$) for analysis were pelleted by centrifugation at 210*g* for 6 minutes at room temperature. The medium was discarded and the cells washed twice in ice-cold HBSS. Cells were fixed in 5mls of 70% ice-cold ethanol (Fisher Scientific, Leicestershire, UK) and incubated at 4°C for 30 minutes or stored at -20°C until further use (maximum 2 weeks).

2.7.2 Staining with propidium iodide and cell cycle analysis

Cells, previously fixed in 70% ethanol, were pelleted by centrifugation at 210*g* for 6 minutes at room temperature. The supernatant was discarded and cells washed once in ice-cold HBSS. 500µl of propidium iodide (PI; Sigma-Aldrich; 50µg/ml PI and 50µg/ml RNAse A in HBSS) was added to each sample and mixed thoroughly. Ten thousand cells per sample were then analysed immediately using a FACSCaliber™ flow cytometer (Becton Dickenson, NJ, USA) with CellQuest ™ software (Becton Dickenson). The percentage of cells in the sub-G1 (apoptotic fraction), G1, S and G2/M phases were determined using the cell cycle analysis program WinMDI (version 2.8).

2.8 Intracellular doxorubicin measurement by flow cytometry

Doxorubicin is fluorescent and therefore the cellular fluorescence intensity measured by flow cytometry can be used to indicate intracellular drug accumulation (Luk & Tannock, 1989). DLBCL cell lines were treated with different concentrations of doxorubicin with and without MSA for 24 hours. Cells ($1x10^6$) were pelleted by centrifugation at 210*g* for 6 minutes at room temperature and then washed twice in PBS. The cell pellet was then resuspended in 500µl of PBS and samples analysed immediately using a FACSCaliber™ flow cytometer (Becton Dickenson) with CellQuest ™ software (Becton Dickenson). Red (560-590nm) fluorescence emission when excited by the 488nm laser was measured for ten thousand cells.

2.9 Measurement of mitochondrial membrane potential

Mitochondrial membrane potential (MMP) was measured using JC-1 (5,5',6,6'-tetrachloro-1,1',3,3-tetraethylbenzimidazolylcarbocyanine iodide), a fluorescent cationic dye. In healthy, non-apoptotic cells the mitochondrial membrane has a negative charge, allowing the JC-1 dye to accumulate in the mitochondria and form aggregates, which fluoresce red. During apoptosis (intrinsic pathway) the mitochondrial potential collapses, therefore the dye is unable to accumulate in the mitochondria and remains in a monomeric form in the cytoplasm, which fluoresces green.

The MMP detection kit (Stratagene, Agilent Technologies, Texas, USA) was used according to the manufacturers' instructions. After exposure to MSA, $5x10^5$ cells were pelleted by centrifugation at 400*g* for 5 minutes at room temperature and the supernatant discarded. The cells were re-suspended in 250µl of 1x JC-1 reagent solution and incubated for 15 minutes in the dark at 37°C. The cells were then pelleted by centrifugation at 400*g* for 5 minutes at room temperature and the supernatant discarded. Cells were washed in 1ml of 1x assay buffer, re-suspended in 500µl of 1x assay buffer and analysed immediately using a FACSCaliber™ flow cytometer (Becton Dickenson) with CellQuest ™ software (Becton Dickenson). Red (590nm) and green (530nm) fluorescence emission when excited by the 488nm laser was measured for fifteen thousand cells.

2.10 Real-time polymerase chain reaction

2.10.1 Sample preparation

RL and DHL4 cells were set in fresh cell culture medium at a concentration of $5x10^5$/ml in 6mls. Harvested PBMCs were set in medium at a concentration of $1x10^6$/ml in 10mls. After 24 hours, RL cells were exposed to 1, 3, and 5µmol/L MSA and DHL4 cells to 5, 10, 30 and 60µmol/L MSA for 4, 6, 24 and 48 hours. PBMCs were exposed to 20µmol/L MSA for 4, 6, and 24 hours. Cells were then pelleted by centrifugation at 210*g* for 6

minutes at room temperature and resuspended in 1ml of TRIzol® reagent (Invitrogen™), incubated at room temperature for 5 minutes and then stored at -80°C till required.

2.10.2 RNA extraction and quantification

Samples were thawed on ice and then 0.2ml chloroform (American Chemical Society, ACS, grade; Thermo Fisher Scientific, Delaware, USA) added per 1ml of TRIzol®. Samples were shaken vigorously for 15 seconds then incubated at room temperature for 2-3 minutes. This was followed by centrifugation at 12,000*g* for 15 minutes at 4°C. Following centrifugation, the colourless, upper aqueous phase containing the RNA was recovered and precipitated with 0.5ml isopropanol (ACS grade, Thermo Fisher Scientific) per 1ml TRIzol®. Samples were incubated at room temperature for 10 minutes followed by centrifugation at 12,000*g* for 10 minutes at 4°C. The supernatant was carefully removed and the precipitated RNA washed once by adding 1ml of 75% ethanol (ACS grade, Thermo Fisher Scientific) per 1ml TRIzol® followed by centrifugation at 7500*g* for 5 minutes. The supernatant was removed and samples allowed to air dry. The RNA was then dissolved in 12µl diethylpyrocarbonate (DEPC)-treated water (Sigma-Aldrich) and samples were vortexed thoroughly. The RNA in each sample was quantified using the NanoDrop™ 1000 spectrophotometer (Thermo Fisher Scientific) using a 260/280nm ratio according to the manufacturers' instructions.

2.10.3 Synthesis of complementary DNA from RNA

1µg of RNA was used to synthesise complementary DNA (cDNA) in 0.5ml micro-centrifuge tubes. All materials were kept on ice following removal from storage. DEPC-treated water was added to the RNA to make up to a volume of 11.5µl. 1.5µl of 50µmol/L random hexamer (Cancer Research UK, Oligonucleotide Synthesis Service, London, UK) was then added to each sample. The samples were incubated at 70°C for 5 minutes, to melt the secondary structure within the template, followed by incubation on ice for 5 minutes to prevent reformation. The following components were then added to each sample to make a final volume of 30µl: Moloney-Murine Leukaemia Virus (M-MLV) reverse transcriptase, RNase H Minus, Point Mutant (Promega Corporation,

Madison, USA), 1µl; M-MLV 5x buffer (Promega Corporation), 6µl; deoxynucleoside triphosphate (dNTPs) (Amersham Biosciences, Amersham UK), 10µl (comprising equal volumes of 2.5mM dATP, dCTP, dGTP, dTTP). The samples were incubated at 42°C for 1 hour followed by 95°C for 5 minutes (to inactivate the remaining enzyme). cDNA was stored at -20°C until use.

2.10.4 Real-time quantitative polymerase chain reaction for GADD153

TaqMan® gene expression assays (Applied Biosystems, Warrington, UK) were used for the detection and quantitation of GADD153 relative to GAPDH, a housekeeping gene. Normalisation to an endogenous reference provides a method for correcting for differing amounts of starting cDNA. The pre-developed TaqMan® gene expression assays contain the primers and probe in a ready to use mix which has already been optimised. The probe for GADD153 is labelled with a FAM™ reporter dye at the 5′ end and a non-fluorescent quencher at the 3′ end. The probe for GAPDH is labelled with VIC® reporter dye and a non-fluorescent quencher at the 3′ end.

For each sample, a 20µl reaction was set up in duplicate in an optical 96-well fast reaction plate (Applied Biosystems), consisting of the following components: TaqMan® universal PCR master mix 2x (Applied Biosystems), 10µl; TaqMan® gene expression assay mix 20x, 1µl; undiluted cDNA, 2µl; water (Sigma-Aldrich), 7µl. Negative controls for both GADD153 and GAPDH were included where water (Sigma-Aldrich) was added rather than cDNA. Real-time PCR amplification was performed using the 7900HT fast real-time PCR sequence detection system (Applied Biosystems). The PCR conditions were 2 minutes at 50°C, 10 minutes at 95°C followed by 40 cycles of 95°C for 15 seconds and 60°C for 1 minute.

The comparative $\Delta\Delta C_T$ method was used to determine relative quantification using the SDS software v2.3 (Applied Biosystems). The C_T or cycle threshold is the number of cycles at which the fluorescent signal of the reporter becomes detectable above background. The ΔC_T is calculated using the mean target gene C_T minus the mean C_T for

the endogenous control. The $\Delta\Delta C_T$ is then calculated by subtracting the ΔC_T of the untreated control sample from the ΔC_T of the treated sample and this is then expressed as a fold difference.

$$\Delta\Delta C_T = (C_T \text{ GADD153} - C_T \text{ GAPDH})_{treated} - (C_T \text{GADD153} - C_T \text{GAPDH})_{untreated}$$

2.11 LC3 immunofluorescence

The DHL4 cell line was exposed to 10μM and 30μM MSA for 24 hours. $1x10^6$ cells were then pelleted by centrifugation at 210*g* for 6 minutes at room temperature and the supernatant discarded. The cells were washed once in PBS and then resuspended in cell culture medium containing 10% fetal calf serum. 10μl of the cell suspension was drawn up in a pipette tip and spread onto a microscope slide. Once the slides had been air-dried, cells were fixed in 4% formaldehyde (diluted in PBS; Sigma-Aldrich) for 20 minutes at room temperature. Slides were then washed in PBS containing 0.1% Tween-20® (PBS-T). Blocking buffer [3% goat serum (Sigma-Aldrich) and 0.1% saponin (Sigma-Aldrich) diluted in PBS] was added to the cells for 30 minutes at room temperature. Without washing the slides, LC3B antibody (rabbit; Cell Signaling) diluted 1:100 in blocking buffer was added to the cells for 1 hour at room temperature. Slides were washed twice in PBS-T followed by the addition of a fluorescent goat anti-rabbit secondary antibody (Alexa Fluor® 488 $F(ab')_2$ fragment, Invitrogen™), diluted 1:100 in blocking buffer, for 1 hour at room temperature in the dark. Slides were washed three times in PBS-T after which DAPI (4',-diamidino-2-phenylindole; Invitrogen™) at a final concentration of 100nmol/L was added as a counter-stain. Once the slides were dry they were mounted with ProLong® Gold antifade reagent (Invitrogen™). Slides were viewed using a Zeiss Axioskop fluorescence microscope (Zeiss, Germany) attached to a CCD camera (Photometric LtD, Tuscon, AZ) which uses IPLLabs Spectrum and SmartCapture (Cambridge, UK) software. The filter wheel was set at green (excitation 450 to 490nm/emission 515 to 565nm) and DAPI (excitation 310 to 380nm/emission 435 to 485 nm).

2.12 Acridine orange staining using flow cytometry

Acridine orange (AO), an acidotropic dye, was used to quantify the formation of acidic vesicular organelles in the cytoplasm of cells. When cells are stained with AO, the cytoplasm and nucleolus fluoresce bright green and dimly red respectively, and acidic vesicles fluoresce bright red (Paglin *et al*, 2001). After exposure of the DHL4 cell line to 10µmol/L and 20µmol/L MSA or 3µmol/L TG for 24 hours, cells ($1x10^6$) for analysis were pelleted by centrifugation at 210*g* for 6 minutes at room temperature. The medium was discarded and the cells washed twice in PBS. AO (Sigma-Aldrich) at a final concentration of 1µg/ml (diluted in PBS) was added and cells incubated for 15 minutes in the dark at 37°C. Cells were then pelleted by centrifugation and the supernatant discarded. Cells were washed once in PBS and then resuspended in 500µl of PBS and analysed immediately using a FACSCaliber™ flow cytometer (Becton Dickenson) with CellQuest™ software (Becton Dickenson). Green (510–530nm) and red (650nm) fluorescence emission when excited by the 488nm laser was measured for ten thousand cells.

2.13 Quantification of the phosphinositide 3-kinase/Akt signal transduction pathway - 'Aktide assay'

2.13.1 Principle of the assay

This assay uses a synthetic Akt substrate peptide, RPRAAFT ('Aktide'), to quantify PI3K/Akt activity in whole cell extracts. The reaction is as follows:

$$\text{RPRAATF} + \text{ATP} \xrightarrow[Mg^{2+}]{\text{Akt kinase}} \text{RPRAApTF (phospho-Aktide)} + \text{ADP}$$

The cell lysate was incubated with Aktide, ATP and Mg^{2+}. When the reaction was stopped, a known amount of phospho-Aktide (p-Aktide) labelled with a stable isotope was added and used as an internal standard (IS) to quantify the amounts of p-Aktide produced. The IS used was RP*PAApTF (Cambridge BioScience, Cambridge, UK), where P*P is L-proline-$^{13}C_5$,^{15}N, a 6-Da heavier version of L-proline. p-Aktide

(Cambridge BioScience) was used to construct a standard curve. In the assay, an excess of Aktide peptide was used but this causes overloading of the HPLC column when the reaction is directly analysed by LC-MS. To avoid this problem, p-Aktide is separated from Aktide in the sample based on their different basicity. The different isoelectric points of p-Aktide (approximately 6.8) and Aktide (approximately 12) makes it possible to separate them by strong cation exchange (SCX). Quantification of p-Aktide produced in the reaction was by mass spectrometry.

2.13.2 Sample preparation

The JVM2 cell line was used for this assay. $1x10^6$ cells were used per reaction and all samples were prepared in duplicate. Cells were stimulated with 100µmol/L pervanadate for 30 minutes at 37°C. 30mM pervanadate solution was prepared in PBS by combining 30mM sodium orthovanadate (Na_3VO_4; Sigma-Aldrich) with 0.18% H_2O_2 (Sigma-Aldrich). This mixture was incubated in the dark at room temperature for 15 minutes prior to adding to the cells. Following stimulation with pervanadate, cells were treated with a range of MSA concentrations for 30 minutes and 2 hours at 37°C. Wortmannin (Calbiochem, San Diego, CA), a known inhibitor of PI3K, was used as a positive control. A stock solution of wortmannin 10mM was prepared in DMSO and aliquots were stored at -20°C. Prior to use, wortmannin was diluted further in cell culture medium to a final concentration of 1µM.

Following treatment with pervanadate and MSA, cells were pelleted by centrifugation at 210*g* for 6 minutes at room temperature. From this stage onwards samples were kept in protein LoBind® eppendorf tubes (Eppendorf UK Limited). Cells were then lysed using 50µl of cold lysis buffer and incubated on ice for 30 minutes. Stocks of lysis buffer consisting of 50mM Tris-hydrochloric acid (Tris-HCl) ph7.4, 150mM NaCl, 1mM EDTA, 1% (v/v) Triton X-100 were prepared and stored at -20°C. Prior to use, 1ml of stock lysis buffer was supplemented with 1µl 0.5N sodium fluoride (NaF; Sigma-Aldrich), 10µl 100mM Na_3VO_4, 20µl of 50x protease inhibitor cocktail (Roche), 1µl 1M DTT, 10ul 100mM PMSF, 2µl 0.5mM okadaic acid (Sigma-Aldrich), 1µl 10mg/ml tosyl-

L-lysine chloromethyl ketone (TLCK; Sigma-Aldrich) and 25µl of 40x phosphatase inhibitor cocktail (Roche). Following incubation in lysis buffer, samples were centrifuged at 20,800*g* for 10 minutes at 5°C and the supernatant transferred to fresh tubes and kept on ice.

2.13.3 Aktide assay

The reaction mix was prepared. This consisted of 20% reaction buffer (20mM Tris-HCl ph-7.4, 1mM Na_3VO_4, 25mM β-glycerol-phosphate, 75mM $MgCl_2$, 0.75mM ATP), 15% Aktide (1mM stock, Millipore) and 65% deionised H_2O. In new tubes, 10µl of the reaction mix and 5µL of cell lysate were mixed and samples were incubated for 30 minutes at 37°C, shaking gently. The reaction was stopped by adding 100µl of stop solution [20% acetonitrile (ACN), 0.1% trifluoroacetic acid (TFA); LGC standards, Teddington, UK] containing 0.05µmol/L IS peptide.

2.13.4 Product extraction by strong cation exchange

2.5µl of Dynabeads® SCX (Invitrogen™) were used per reaction. The total volume of beads required was transferred to an eppendorf tube. The magnetic beads were separated from the solvent using a magnetic rack (MagnaRack™, Invitrogen™). 800µl of conditioning solution (1M NaCl, 50mM ammonium bicarbonate) was added to the beads. The beads were resuspended by vortexing and incubated for 10 minutes at room temperature. The beads were then washed 3 times in 800µl loading solution (25% ACN, 0.1% TFA, 0.01% Tween-20) using the magnetic rack. The beads were resuspended in loading solution (10µl/reaction) ready for use.

10µl of the conditioned Dynabeads® SCX were added to each sample. Samples were vortexed well and then incubated for 45 minutes at room temperature shaking gently. Following this, the samples were placed in the magnetic rack and the solvent discarded. The beads were then washed twice with 200µl of loading solution and once with 200µl washing solution (25% ACN, 0.1% TFA). To elute the reaction products and IS from the beads, 20µl of eluting solution (150mM ammonium bicarbonate, 5% ACN, 0.1% TFA)

was added, samples vortexed and then incubated for 10 minutes at room temperature shaking at 1000rpm. Using the magnetic rack, the eluents were transferred to fresh tubes and samples dried in a speed vac. Dried samples were reconstituted in 25µl of 0.1% TFA in ultrapure H_2O prior to analysis

2.13.5 Quantification of the enzymatic reaction by ultra-high performance liquid chromatography and mass spectrometry

5µl of each sample was injected into a Thermo Scientific Accela™ ultra high-performance liquid chromatography (UPLC) system (Thermo Fisher Scientific) for separation of p-Aktide and the IS. The chromatogram was run over 12 minutes. This was combined with detection of p-Aktide and the IS using a TSQ Vantage triple stage quadrupole mass spectrometer (MS; Thermo Fisher Scientific) by monitoring the parent-daughter ion transition of *m/z* 449.7→400.6 for p-Aktide and *m/z* 452.7→403.6 for the IS (of note, the IS has a double charge, therefore, although it is 6Da heavier than p-Aktide, the *m/z* only differs by 3). The UPLC and MS conditions are shown in Table 2.2. A series of standards were run in parallel with the unknown samples in order to construct a standard curve for absolute quantification of the product. Standards were prepared by serial dilutions of p-Aktide in 0.1% formic acid (FA, Thermo Fisher Scientific)/ultrapure H_2O (concentration range 50-5000nmol/L) containing 0.1µmol/L IS peptide. p-Aktide in the standards and the unknown samples was quantified by measuring the area under the curve of the extracted ion chromatogram for the fragment ion at *m/z* 400.6 and the obtained areas were normalised by the area of the p-Aktide IS fragment at *m/z* 403.6. A standard curve was generated by plotting the ratio of the p-Aktide:IS signal on the y axis and p-Aktide concentration on the x axis and p-Aktide in the unknown samples was calculated by fitting the area values to the linear regression equation. An example of a standard curve for p-Aktide is shown in Figure 2.5 (r=1) and an example of the chromatograms obtained for p-Aktide and the IS are shown in Figure 2.6.

Table 2.2 Ultra high-performance liquid chromatography and mass spectrometry conditions for the 'Aktide assay'.

UPLC conditions	
Column	Vydoc C_{18} (150mm x 800µm id x 5µm)*
Injection loop	5µl
Flow rate	200µl/min
Mobile phase	Solution A 0.1% FA in ultrapure H_2O Solution B 0.1% FA in ACN
Gradient	1) 98% A to 20% A over 4 minutes 2) 20% A for 2 minutes 3) 98% A to 20% A over 6 minutes
MS conditions	
Ionisation	Positive mode
Spray voltage	4501 v
Sheath gas pressure	35 psi
Auxiliary gas pressure	10 arbitrary units
Capillary temperature	270°C
Collision gas	Argon
Collision gas pressure	1.5mTorr

* LC Packings, Dionex Ltd, Surrey, UK

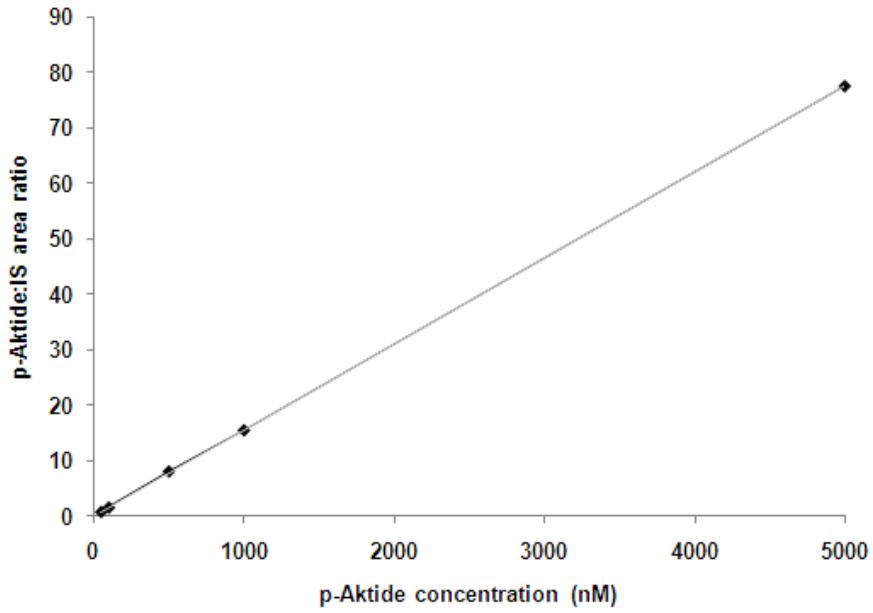

Figure 2.5 An example of the standard curve obtained for p-Aktide generated by plotting the ratio of the p-Aktide:IS signal on the y-axis and p-Aktide concentration on the x-axis. Concentration range 50-5000nmol/L.

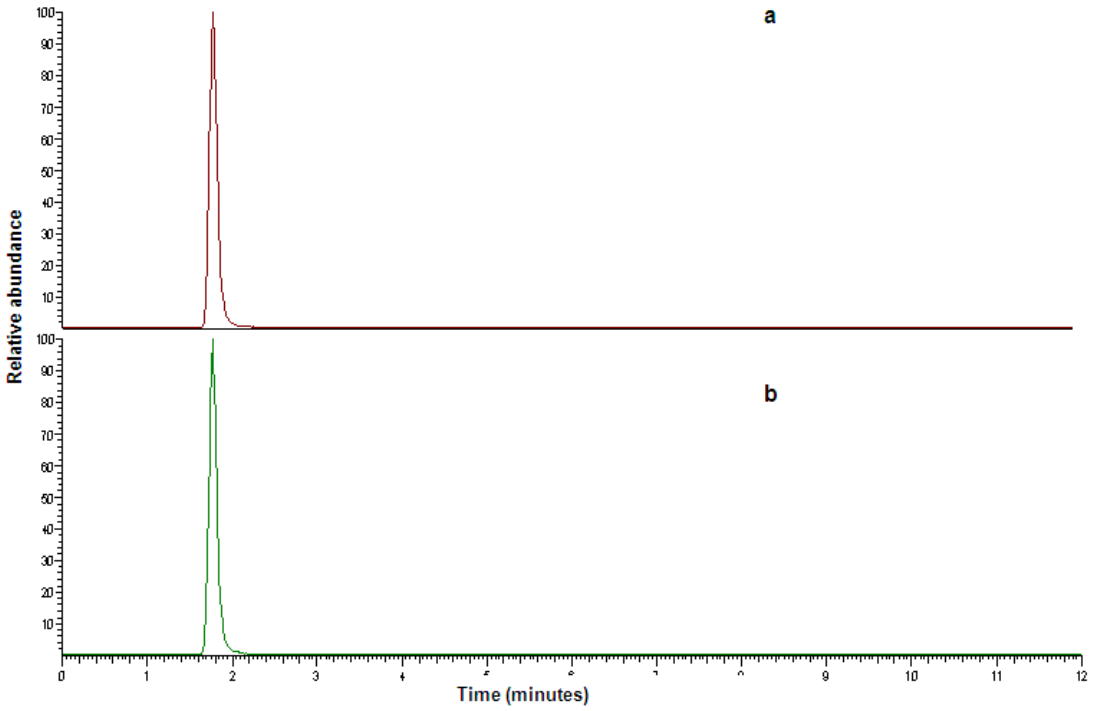

Figure 2.6 An example of the chromatograms obtained from the 'Aktide assay'. (a) p-Aktide, by monitoring parent-daughter ion transition of *m/z* 449.7→400.6 (b) Internal standard, by monitoring the parent-daughter ion transition of *m/z* 452.7→403.6.

2.14 Statistical analysis

Standard statistical methods such as mean and standard deviation (SD) have been used to summarise data. Data have been represented in graphical and tabular form. For most experiments, 3 independent sets of data were obtained. The data were assumed to be normally distributed and parametric statistical tests were used. The paired t-test was used to compare the means of two groups and one-way analysis of variance (ANOVA) followed by Tukey's post hoc test was used to compare the means of more than 2 samples. A p value <0.05 was considered statistically significant.

The activity of various drugs, obtained using the ATP and Gauva® viacount® assays, was summarised to an EC_{50} value (the concentration required to cause 50% of the maximum effect) using the GraphPad PRISM® software (version 5.03). This software fits the data to

a sigmoidal concentration-effect model with variable slope using a modification of the equation shown in Figure 2.7 (Holford & Sheiner, 1982).

$$E_{pred}=E_{cont}-[E_{max} \times C^n/(EC_{50}^n + C^n)]$$

Figure 2.7 The equation used to obtain an EC_{50} value for drug activity.
E_{pred} is the predicted effect, E_{cont} is the effect without the drug, E_{max} is the maximum effect that can be obtained, C is the drug concentration and n is the sigmoid factor.

CHAPTER 3: Patterns of survival in patients with diffuse large B-cell lymphoma. Long follow-up from St Bartholomew's Hospital.

3.1 INTRODUCTION

The outcome of patients with newly diagnosed DLBCL has improved significantly with the addition of rituximab to first-line chemotherapy regimens (Coiffier *et al*, 2002; Feugier *et al*, 2005; Pfreundschuh *et al*, 2006). However, recurrent disease remains difficult to treat. HDT with autologous hematopoietic stem cell support is generally considered to be the 'standard of care' for younger patients with recurrent disease (Philip *et al*, 1995) but is only of value to those who remain 'sensitive' to second-line, 'conventional-dose' chemotherapy (Prince *et al*, 1996).

Overall response rates to commonly used, second-line regimens are around 60%, with CR rates of only 25-35% (Moskowitz *et al*, 1999; Velasquez *et al*, 1988; Velasquez *et al*, 1994). Although the IPI score is predictive for overall and progression-free survival in patients with recurrent disease (Guglielmi *et al*, 2001; Hamlin *et al*, 2003), in general, all patients are treated in a similar way. Therefore, cure is theoretically only possible for the 30-40% of patients who reach the point of HDT (Vose *et al*, 2004). Several reasons prevent a significant proportion of patients with recurrent disease from receiving HDT and therapeutic options for the latter group are limited. Evidence is also now emerging that recurrent disease in those who have already been exposed to rituximab may be even more difficult to treat (Giesselbrecht C, 2007; Martin *et al*, 2008).

This retrospective analysis reports the outcome of a large series of patients with DLBCL with a median follow-up of 12 years. The focus is on patterns of outcome and survival in an unselected group, diagnosed at a single centre.

3.2 PATIENTS AND METHODS

3.2.1 Patients

Between January 1985 and May 2003, 461 patients were diagnosed with DLBCL at SBH. Three hundred and eighty-four (83%) were treated with curative intent and form the basis of this analysis. Clinical characteristics are shown in Table 3.1. Patients with primary CNS lymphoma, primary mediastinal B-cell lymphoma and HIV infection were excluded. Staging investigations comprised clinical examination, bone marrow biopsy and CT scanning (Lister *et al*, 1989). Histological subtype at diagnosis is shown in Table 3.2. Prior to 2001, the Kiel classification (Gerard-Marchant *et al*, 1974) was used and after 2001, the WHO classification (Jaffe *et al*, 2001). The IPI score (Anon, 1993) was assigned retrospectively for patients diagnosed before 2001. Prior to 1989, hydroxybutyrate dehydrogenase was measured instead of lactate dehydrogenase (LDH) and they are assumed to be equivalent (Foo *et al*, 1981; Leung & Henderson, 1981).

3.2.2 Treatment at diagnosis and recurrence

Three hundred and fifty-four of those treated with curative intent (92%) received an anthracycline-containing regimen according to protocols in use at the time (Table 3.3) (Dhaliwal *et al*, 1993; Radford *et al*, 1994). Thirty patients (8%) with localised disease (Stage I, 27 patients; Stage II, 3 patients) received radiotherapy alone. Prior to 2001, the local policy was to give all patients with DLBCL prophylactic intra-thecal methotrexate with each cycle of chemotherapy; 78% of patients actually received this. Subsequently, only those deemed at high risk for CNS relapse did so; 51% received this. Patients considered to be at high risk for CNS relapse were those with a high LDH, a high-risk IPI score and involvement by DLBCL at specific anatomical sites; namely bone marrow, testes, the post-nasal space and Waldeyer's ring. Those with a paraspinal mass were also given CNS prophylaxis.

Table 3.1 Clinical Characteristics at diagnosis and recurrence of DLBCL

	Diagnosis	**Recurrence**
Characteristic	**Number (%)**	**Number (%)**
Number of patients	384	80
Age, years		
Median	60	59
Range	17-95	17-93
Male gender	208 (54)	39 (49)
B symptoms	146 (38)	23 (29)
Bulky disease[1]	161 (42)	20 (25)
Stage		
I/IE[2]	99 (26)	22 (28)
II/IIE	88 (23)	11 (14)
III	55 (14)	18 (23)
IV	142 (37)	26 (33)
Not known		3 (4)
IPI score		
Low-risk	189 (49)	42 (53)
Low-intermediate	110 (29)	24 (30)
High-intermediate	64 (17)	7 (9)
High-risk	21 (5)	4 (5)
Not known		3 (4)

[1]defined as a mediastinal mass >1/3 of the intra-thoracic diameter at the level of T5 vertebra or a mass >10cm in its maximum dimension.
[2] Suffix added if a single extranodal site involved, or if contiguous or proximal to known nodal sites of disease.

At recurrence, patients for whom this was deemed appropriate received further intensive chemotherapy (Table 3.3). In patients less than 65 years of age, the intention was to induce a second remission (CR/CRu or PR) and consolidate this with HDT and autologous hematopoietic stem cell support. Prior to 1997, the myeloablative regimen

used was cyclophosphamide and total body irradiation (TBI). However, this was found to be associated with a significant risk of secondary myelodysplasia and AML, albeit particularly in patients with FL (Rohatiner *et al*, 2007). Therefore, the myeloablative regimen was changed to the 'drug-only' regimen, 'BEAM' (carmustine, etoposide, cytarabine and melphalan) (Mills *et al*, 1995)

3.2.3 Definitions and statistical analysis

Response to treatment was determined at least 4 weeks after completing chemotherapy and was defined according to local criteria used at the time (Dhaliwal *et al*, 1993; Johnson *et al*, 1995). CR is equivalent to CR as defined in the consensus statement by the International Working Group (Cheson *et al*, 1999). 'Good partial remission (GPR)' was defined as the presence of minimal, residual, but equivocal abnormalities on CT scanning or bone marrow examination and is considered to be equivalent to CRu according to the consensus statement. 'Poor PR' is comparable to PR in the consensus statement. For the purposes of this analysis, CR and GPR have been grouped together and are henceforth referred to as CR/CRu. Patients with stable or progressive disease after treatment have been defined as having had 'no response' (NR).

The terms 'composite' and 'discordant' are used to describe the simultaneous occurrence of two different histological subtypes of lymphoma in the same biopsy specimen, or in biopsies from different anatomical sites respectively.

OS was measured from the date of diagnosis to the date of last follow-up or death. Cause-specific survival was measured from the date of diagnosis to the date of death from DLBCL or from complications resulting from its treatment. Survival from recurrence was measured from the date of recurrence to the date of last follow-up or death. Remission duration (RD) was measured from the date of CR/CRu being achieved to the date of recurrence.

Death from treatment-related infection was recorded as the cause of death if death from infection occurred during or within 3 months of completing a cycle of treatment.

The Kaplan-Meier method was used to construct survival and RD curves. Univariate analysis, to test for the prognostic significance of variables, was performed using the log-rank test. Categorical data were compared using the chi-squared test. The Stata® data analysis and statistical software was used. A p value less than 0.05 was considered statistically significant.

Table 3.2 Histological subtype at diagnosis and recurrence of DLBCL

Histology	**Diagnosis**	**Recurrence**
	Number	Number
DLBCL	343	67[3]
Composite i.e. DLBCL with, in addition:	24	1
Follicular lymphoma	22	0
LPL[1]	1	1
Gastric 'MALT'	1	0
Discordant	17[2]	2[4]
Follicular Lymphoma	-	11
Gastric 'MALT'	-	1

[1]lymphoplasmacytic lymphoma
[2]all with follicular lymphoma in the bone marrow
[3]10 patients did not have a biopsy but were treated as DLBCL
[4]1 patient with lymphoplasmacytic lymphoma, 1 patient with marginal zone lymphoma

Table 3.3 Treatment at diagnosis and recurrence of DLBCL

Treatment	Diagnosis	Recurrence
	Number (%) N=384	**Number (%) N=68**
Radiotherapy alone	30 (8)	5 (7)
CHOP[1]	117 (30)	4 (6)
MACOP[2]	69 (18)	10 (15)
VAPEC-B[3]	154 (40)	12 (18)
PMitCEBO[4]	7 (2)	-
Etoposide/cytarabine	-	29 (43)
CHOP+rituximab	-	3 (4)
ICE[5]+rituximab	-	1 (1)
Other	7 (2)	4 (6)

[1]Cyclophosphamide, doxorubicin, vincristine and prednisolone
[2]Methotrexate with leucovorin rescue, cyclophosphamide, doxorubicin, vincristine and prednisolone
[3]Doxorubicin, cyclophosphamide, etoposide, vincristine, bleomycin, prednisolone
[4]Prednisolone, mitoxantrone, cyclophosphamide, etoposide, bleomycin, vincristine
[5]Ifosphamide, carboplatin and etoposide

3.3 RESULTS

3.3.1 Clinical characteristics at diagnosis

Patient characteristics at diagnosis are shown in Table 3.1. Eight-five patients (22%) had primary extra-nodal disease, either Stage IE or IIE. The commonest sites of primary extranodal disease were the gastrointestinal tract (GIT) in 24 patients (6%) and the tonsillar/nasopharyngeal region in 34 patients (9%). In patients with stage IV disease (n=142), the commonest extra-nodal sites were the bone marrow (61%), liver (40%), lung (32%) and GIT (24%). At diagnosis, the CNS was involved in 14 patients (4%).

3.3.2 Response to initial treatment and remission duration

(Figure 3.1, Table 3.4)

3.3.2.1 Patients in whom CR/CRu was achieved following initial therapy

CR/CRu was achieved in 241/384 patients (63%). On univariate analysis, response to initial therapy was significantly associated with age (≤45 years vs > 45 years; p=0.001; Table 3.5), stage (p<0.001; Table 3.6), and the IPI score (p<0.001; Table 3.7) at diagnosis. With a median follow-up for living patients of 12 years (range 2-24 years), the median RD has not been reached (Figure 3.2a) and was not significantly different between patients in whom CR or CRu was achieved (*p*=0.7; Figure 3.2b) On univariate analysis, the following prognostic factors were significantly associated with RD: age (≤45 years vs >45 years p=0.02; Figure 3.3a), stage (I/II vs III/IV p=0.007; Figure 3.3b) and the IPI score (0-II vs III-V p=0.007; Figure 3.3c) at diagnosis.

3.3.2.2 Patients in whom PR was achieved following initial therapy

PR was achieved in 66/384 patients (17%) after initial therapy. Forty-seven of the latter (71%) went on to receive further treatment, in an attempt to improve upon the initial response. CR/CRu was subsequently achieved in 21/47 patients (45%) and a further PR in 9/47. Fifteen had no further response and two died of treatment-related infection. In patients who achieved CR/CRu, the majority (16/21) did so after only one additional regimen, Subsequently 6 patients (5 in CR and 1 in PR) received HDT to consolidate second remission. The patient receiving HDT in PR had no further response and ultimately died of progressive disease. For the 21/66 patients in whom a first CR/CRu was eventually achieved, the median RD was 3.6 years (Figure 3.3d). However, almost half of the 21 patients (48%) developed recurrent disease with a median time to recurrence of 8 months.

Nineteen patients did not receive further treatment with curative intent after initial PR was achieved. Disease progression occurred in 10, with a median time to progression of only 2 months. Six patients died in PR without evidence of disease progression (4 of

infection, 1 of liver disease, 1 of a cerebrovascular accident (CVA) and 3 patients are still alive after a median follow-up of 9 years.

3.3.2.3 Patients in whom initial treatment failed

Twenty-four patients (6%) died of treatment-related infection. Fifty-three of 384 patients (14%) did not respond to initial therapy. Twenty-one received further treatment but in only two was CRu achieved with a second-line regimen (etoposide and intermediate-dose cytarabine (Whelan *et al*, 1992). One who presented with stage IE disease in the tonsil, with a 'low- risk' IPI score, is alive and free of disease at 9 years. The other had stage IV disease with a 'high-intermediate' IPI score and died of heart failure 3 months after CRu had been documented. PR was observed in four patients, two of whom subsequently received HDT; 1 had a further PR and the other progressed. Fifteen patients had no response to further treatment.

Thirty-two patients did not receive further intensive treatment because it was deemed inappropriate to do so; all died of progressive disease, with a median time to death of 3 weeks (range 0 days-3 months). Therefore, of the original 53 patients considered to be refractory to initial therapy, only one is currently alive and free of disease (3 patients having been lost to follow-up).

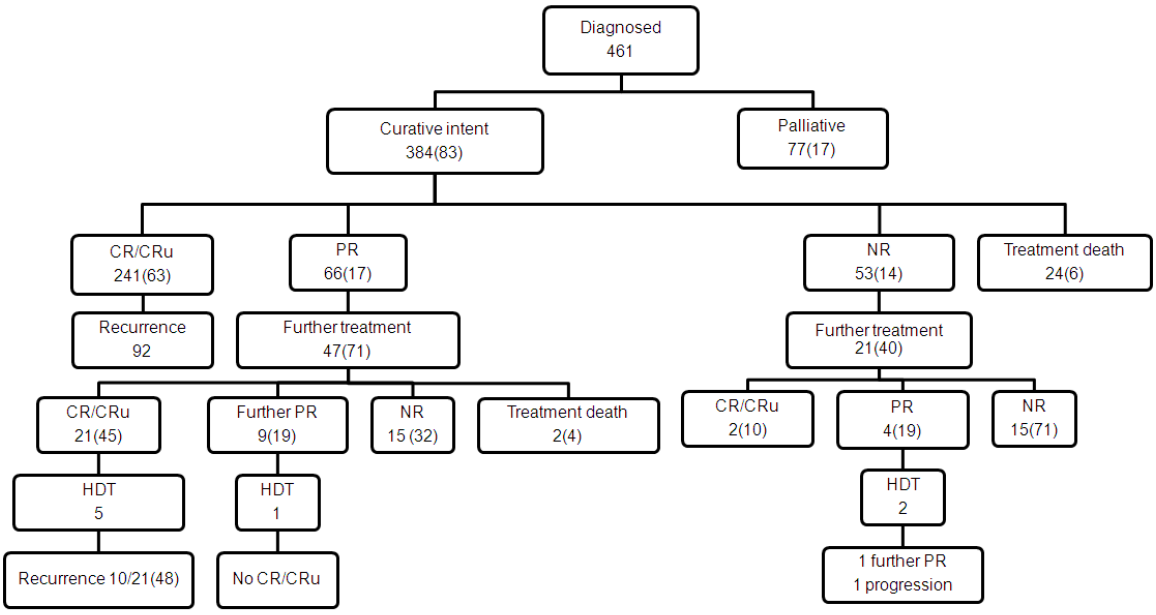

Figure 3.1 Outcome of newly diagnosed patients with DLBCL. Numbers in brackets are percentages.

Table 3.4 Response to treatment at diagnosis and recurrence of DLBCL

	Diagnosis	**Recurrence**
Response to treatment	**Number (%) N=384**	**Number (%) N=68**
CR/CRu	241 (63)	37 (54)
PR	66 (17)	14 (21)
No response	53 (14)	15 (22)
Treatment-related death	24 (6)	2 (3)

Table 3.5 Outcome to initial therapy according to age at diagnosis

Age (years)	Outcome	Number (%)
≤30 (n=22)	CR/CRu	19 (86)
	PR	0 (0)
	NR	3 (14)
	Treatment-related death	0 (0)
31-45 (n=73)	CR/CRu	54 (74)
	PR	7 (10)
	NR	11 (15)
	Treatment-related death	1 (1)
46-60 (n=106)	CR/CRu	63 (59)
	PR	25 (24)
	NR	13 (12)
	Treatment-related death	5 (5)
61-70 (n=92)	CR/CRu	55 (60)
	PR	17 (18)
	NR	15 (16)
	Treatment-related death	5 (5)
>70 (n=91)	CR/CRu	50 (55)
	PR	17 (19)
	NR	11 (12)
	Treatment-related death	13 (14)

Table 3.6 Outcome to initial therapy according to stage at diagnosis

Stage	Outcome	Number (%)
I (n=99)	CR/CRu	76 (77)
	PR	11 (11)
	NR	9 (9)
	Treatment-related death	3 (3)
II (n=88)	CR/CRu	62 (70)
	PR	12 (14)
	NR	11 (13)
	Treatment-related death	3 (3)
III (n=55)	CR/CRu	34 (62)
	PR	15 (27)
	NR	6 (11)
	Treatment-related death	0 (0)
IV (142)	CR/CRu	69 (49)
	PR	28 (20)
	NR	27 (19)
	Treatment-related death	18 (13)

Table 3.7 Outcome to initial therapy according to IPI score at diagnosis

IPI score	Outcome	Number (%)
0, 1 (n=189)	CR/CRu	141 (75)
	PR	26 (14)
	NR	16 (8)
	Treatment-related death	6 (3)
2 (n=110)	CR/CRu	67 (61)
	PR	24 (22)
	NR	14 (13)
	Treatment-related death	5 (5)
3 (n=64)	CR/CRu	29 (45)
	PR	11 (17)
	NR	19 (30)
	Treatment-related death	5 (8)
4, 5 (n=21)	CR/CRu	4 (19)
	PR	5 (24)
	NR	4 (19)
	Treatment-related death	8 (38)

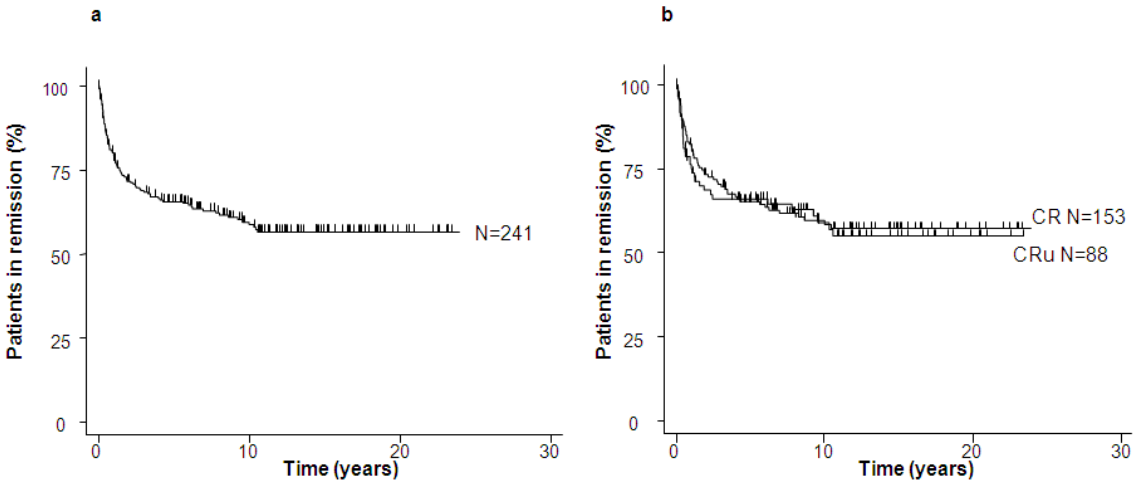

Figure 3.2 (a) Remission duration in patients achieving CR/CRu (b) Remission duration comparing patients achieving CR and CRu.

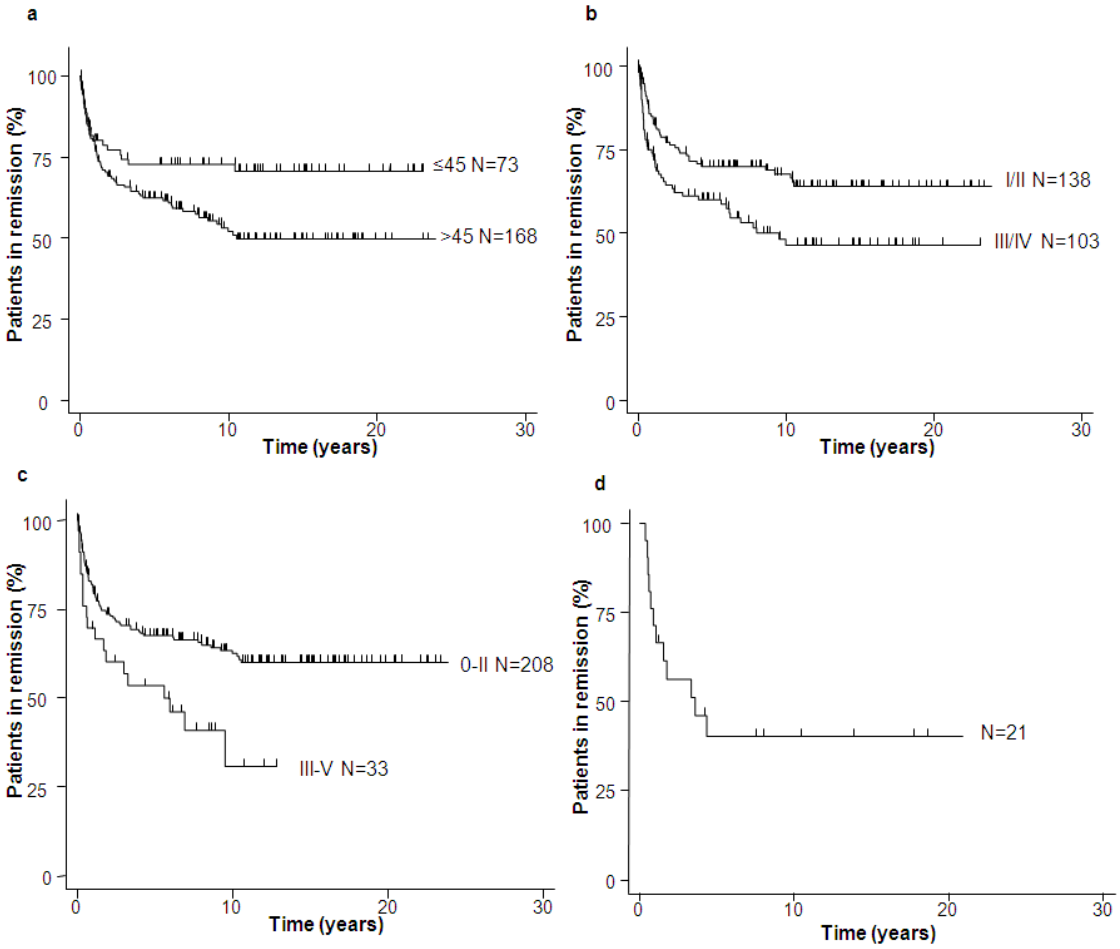

Figure 3.3 Remission duration according to (a) Age at diagnosis (b) Stage at diagnosis (c) IPI score at diagnosis (d) Remission duration in patients initially achieving PR but subsequently achieving CR/CRu with additional treatment.

3.3.2.4 Patients with 'composite' and 'discordant' lymphoma at diagnosis

Twenty-four patients had 'composite' lymphoma at diagnosis and their clinical characteristics at diagnosis are shown in Table 3.8. The histological subtype present in addition to DLBCL was: FL in 22 patients, lymphoplasmacytic lymphoma (LPL) in one, and gastric 'MALT' lymphoma in another. Seventeen patients (71%) achieved a CR/CRu after initial therapy, with a median RD of 2.6 years (Figure 3.4a). The CR/CRu rate was not significantly different from those patients with 'pure DLBCL' (p=0.5). Six patients (25%) had a PR to initial therapy and 1 had no response.

Table 3.8 Clinical characteristics of patients with 'composite' lymphoma at diagnosis

Characteristic	**Number (%)**
Number of patients	24
Age, years	
Median	58
Range	29-88
Male gender	10 (42)
B symptoms	8 (33)
Bulky disease	7 (29)
Stage	
I	5 (21)
II	2 (8)
III	6 (25)
IV	11 (46)
IPI score	
Low-risk	8 (33)
Low-intermediate	11 (46)
High-intermediate	2 (8)
High-risk	3 (13)

Seventeen patients had 'discordant' lymphoma at diagnosis; that is, DLBCL in lymph node and FL in the bone marrow and their clinical characteristics are shown in Table 3.9. Six patients (35%) achieved a CR/CRu to initial therapy. This was significantly lower than the CR/CRu rate of patients with 'pure DLBCL' (p=0.02). The median RD was 9.5 years (Figure 3.4b). Five of the 17 patients (29%) had a PR to initial therapy, 2 (12%) had no response and 4 (24%) died of treatment-related infection.

Table 3.9 Clinical characteristics of patients with 'discordant' lymphoma at diagnosis

Characteristic	Number (%)
Number of patients	17
Age, years	
Median	60
Range	46-77
Male gender	10 (59)
B symptoms	10 (59)
Bulky disease	7 (41)
IPI score	
Low-risk	1 (6)
Low-intermediate	10 (59)
High-intermediate	5 (29)
High-risk	1 (6)

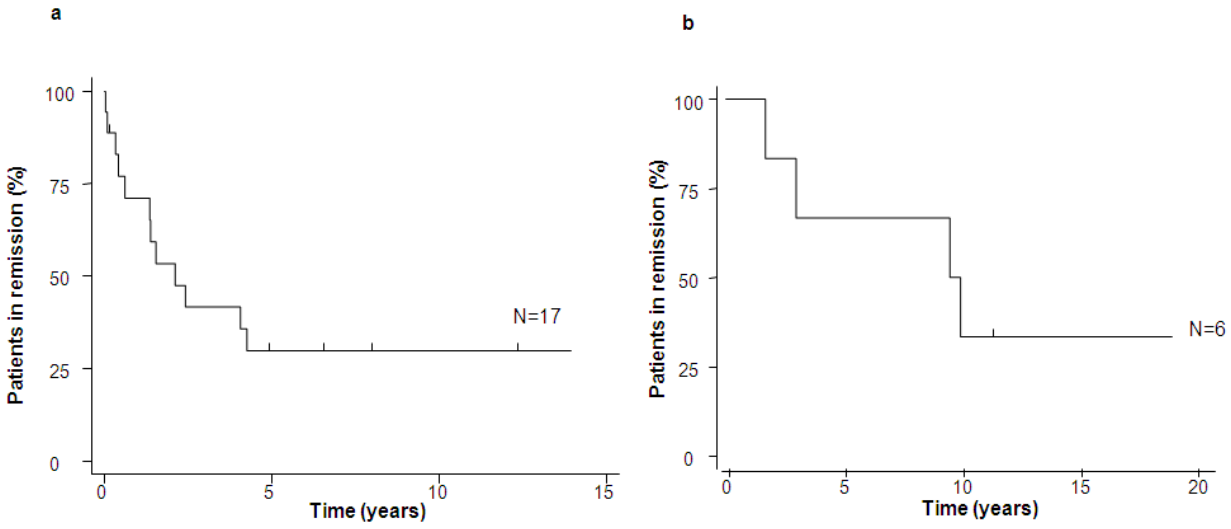

Figure 3.4 Remission duration in patients with (a) 'composite' and (b) 'discordant' lymphoma at diagnosis.

3.3.4 Recurrence

(Figure 3.5)

Ninety-two of the 241 patients (38%) in whom initial CR/CRu was achieved developed recurrent lymphoma, with a median time to recurrence of 10 months (range 2 weeks to 11 years). Eighty-two patients (89%) had a repeat biopsy at recurrence; histological subtype is shown in Table 3.2. Regarding patients with 'composite' lymphoma at diagnosis, 12/17 patients (71%) in whom CR/CRu was achieved subsequently developed recurrent disease; 3 with DLBCL, 7 with FL, 1 with 'composite' lymphoma (DLBCL and LPL) and 1 with gastric 'MALT'. Regarding patients with 'discordant' lymphoma at diagnosis, 4/6 patients in whom CR/CRu was achieved subsequently developed recurrent disease; 3 with DLBCL histology and one with FL. Thus, overall, 12 patients recurred with a different histological subtype; 11 with FL and one with gastric 'MALT' lymphoma.

Clinical characteristics at recurrence are shown in Table 3.1. Stage and the IPI score were assessable in 77/80 patients who recurred with DLBCL. Forty-one percent of patients who recurred with stage I disease had stage I at diagnosis and 73% who recurred with stage IV disease have stage IV at diagnosis (Table 3.10). Of the 9 patients who had stage I disease at diagnosis and recurrence, the site of disease was the same in 7. In total, 22 patients had stage I disease at recurrence and in 17, the site of disease was one which had been involved at diagnosis. In 23 patients (10%) recurrence of DLBCL occurred more than 2 years after CR/CRu had been achieved and in 14 (6%), after 5 years.

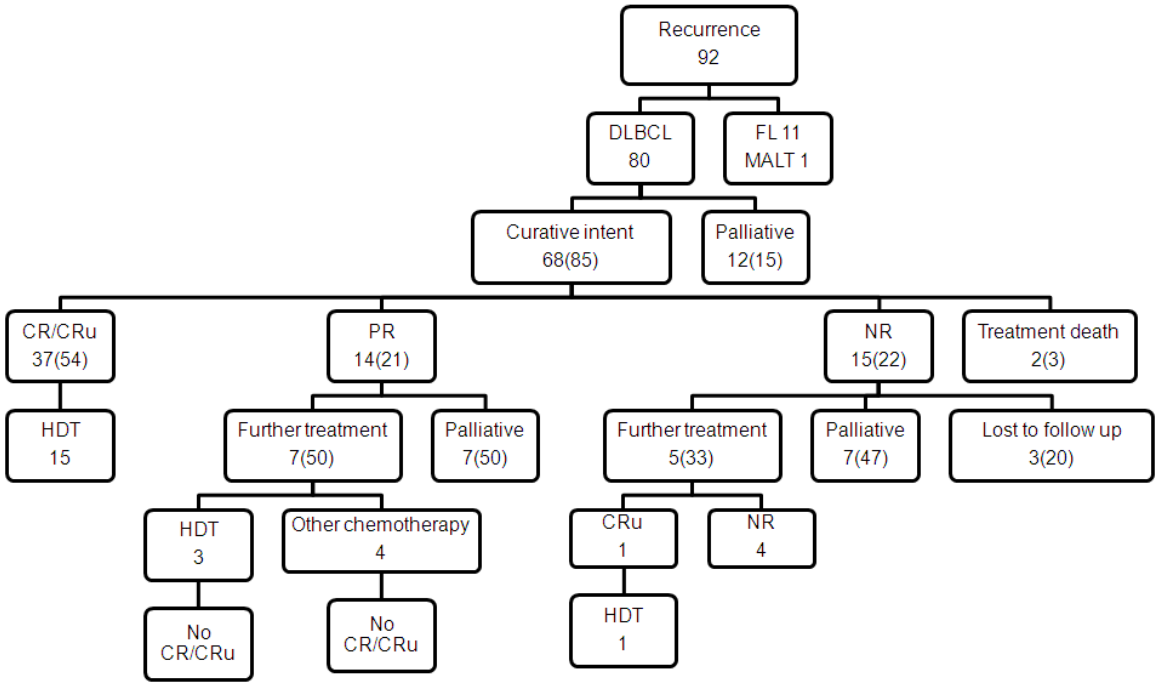

Figure 3.5 Outcome of patients with recurrent DLBCL. Numbers in brackets are percentages.

3.3.4.1 Sites of disease at recurrence

Seven patients (9%) relapsed with extra-nodal disease alone, the GIT (4%) and tonsil (3%) being the commonest sites. In patients relapsing with stage IV disease (n=26), the commonest extra-nodal sites of disease were the bone marrow (54%), GIT (42%), liver (35%), and lung (12%). Only one patient recurred with disease in the CNS.

3.3.4.2 Response to treatment at recurrence: patients treated with curative intent

Sixty-eight of the 80 patients (85%) with DLBCL at recurrence received further treatment with curative intent (Table 3.3), the most frequently used regimens being etoposide and intermediate dose cytosine arabinoside (43%) (Whelan *et al*, 1992), 'VAPEC-B' (18%)

(Radford *et al*, 1994) and 'MACOP' (15%) (Dhaliwal *et al*, 1993). Only four patients received regimens containing rituximab. Five patients with stage I disease received radiotherapy alone; all achieved a CR.

Response to treatment at recurrence is shown in Table 3.4. Overall, second CR/CRu was achieved in 37/68 patients (54%) [37/80 (46%) if all patients with recurrent DLBCL are considered]. Fourteen of 68 patients achieved a PR (21%), 15/68 patients (22%) did not respond and only one subsequently responded to an alternative therapy. Two patients (3%) died of treatment-related infection. For all patients in whom a second CR/CRu was achieved, irrespective of whether HDT was given or not (see below), the median second RD was 3 years (range 0.2-23 years; Figure 3.6a).

Seven of the 14 patients in whom only a PR was achieved after the first 'salvage' treatment went on to receive further treatment, including 3 patients who had HDT, but CR/CRu was not achieved in any of them and all died of lymphoma. Five of the seven patients who did not receive further treatment died of progressive disease and 2 died of non-lymphoma-related causes. Thus, all 14 patients have died; 12 from lymphoma.

Five of the 15 patients who failed to respond to the first 'salvage' therapy received further treatment but only one went on to have a better response (CRu) which was consolidated with HDT. However, the patient subsequently relapsed and died of lymphoma. Seven patients did not receive further treatment and all died of progressive disease. Therefore overall, 12/15 patients have died of lymphoma (3 lost to follow-up).

3.3.4.3 Patients not treated with curative intent at recurrence

Twelve of the 80 patients with DLBCL at recurrence were not treated with curative intent. All died of progressive disease with a median time to death of 2 weeks (range 2 days-6 months). Thus, overall only 10/80 patients (13%) with recurrent DLBCL are currently alive and disease-free (3 lost to follow-up).

3.3.4.4 High-dose therapy with haematopoietic stem cell support

Forty-six patients were aged 65 years or less at recurrence and therefore would have been considered for HDT with autologous haematopoietic stem cell support if a response was achieved with 'salvage' therapy. However, only nineteen (16 in CR/CRu and 3 in PR) with a median age of 46 years actually went on to receive this. In 10 patients, HDT comprised cyclophosphamide and TBI and in 9, 'BEAM'. None of the three patients receiving HDT in PR achieved CR. The median second RD for patients receiving HDT was 3.4 years. This, however, was not significantly different from the median second RD for patients in whom CR/CRu was achieved with 'salvage' chemotherapy but who did not receive HDT (2.4 years, p=0.8; Figure 3.6b)

The reasons for not proceeding with HDT in the 22/38 patients in whom a second CR/CRu were achieved were: age >65 years (9 patients), co-morbidity (4 patients), failed stem cell harvest (2 patients), rapid relapse of disease (2 patients), patient choice (2 patients) and toxicity of prior therapy (3 patients).

Table 3.10 Comparison of Stage at diagnosis and at recurrence of DLBCL

Stage at Diagnosis	**Stage at recurrence**					
	I	**II**	**III**	**IV**	**NK**	**Total**
I	9	2	3	1	1	16
II	5	6	8	2	2	23
III	3	2	6	4		15
IV	5	1	1	19		26
Total	22	11	18	26	3	80

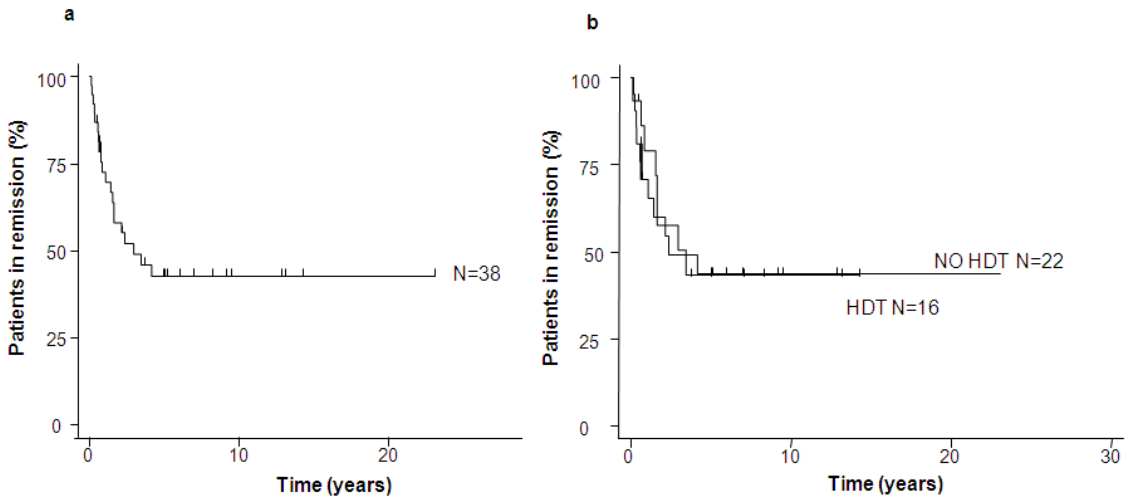

Figure 3.6 Second remission duration in (a) All patients in whom a second CR/CRu was achieved (b) Those patients in second CR/CRu that did and did not receive HDT.

3.3.4.5 Recurrence after 5 years

Fourteen patients (6%) developed recurrent DLBCL after more than 5 years in CR/CRu. The characteristics of these patients are shown in Table 3.11. Thirteen of the 14 patients had a biopsy at recurrence and in 12 the histology was DLBCL. One patient had discordant histology with 'MALT' lymphoma present in the duodenum. There were no significant differences in the stage or IPI score at diagnosis (p=0.2 and p=0.7 respectively) or recurrence (p=0.9 and p=0.98 respectively) between patients that developed recurrent DLBCL before or after 5 years of CR/CRu. Twelve of the 14 patients received treatment with curative intent. Two patients received palliative treatment only, due to advanced age and co-morbidities. Nine of the fourteen (64%) patients have died; 7 of lymphoma, 1 of treatment-related infection and 1 of a second malignancy.

Table 3.11 Clinical characteristics at diagnosis and recurrence of patients who developed recurrent DLBCL greater than 5 years after initial CR/CRu

	Diagnosis	**Recurrence**
Characteristic	**Number (%)**	**Number (%)**
Number of patients	14	14
Age, years		
Median	61	67
Range	21-74	32-83
Male gender	7 (50)	7 (50)
B symptoms	3 (21)	2 (14)
Bulky disease	6 (43)	1 (7)
Stage		
I	4 (29)	5 (36)
II	1 (7)	2 (14)
III	2 (14)	3 (21)
IV	7 (50)	4 (29)
IPI score		
Low-risk	5 (36)	7 (50)
Low-intermediate	5 (36)	5 (36)
High-intermediate	4 (29)	2 (14)
High-risk	0 (0)	0 (0)

3.3.4.6 Outcome of patients with non-DLBCL histology at recurrence

As mentioned above, 12 patients had recurrent disease with a histological subtype other than DLBCL. Eleven patients had FL; 7 of whom had 'composite' histology and 1'discordant' histology at diagnosis. The patient with a 'composite' histology of gastric DLBCL/MALT at diagnosis relapsed with gastric 'MALT' lymphoma. The median time to relapse for these 12 patients was 18 months. The patient with gastric 'MALT' lymphoma was treated with Helicobacter pylori eradication resulting in a CR which has been maintained for 5 years and 9 months. Nine of the 11 patients who recurred with FL

received treatment, some after an initial period of observation. One who was initially managed expectantly had progressive disease after 2 years and 3 months but the histology at progression was DLBCL and the patient died of lymphoma. One patient was lost to follow-up at the time of relapse.

The 'best outcomes' in the 9/11 patients with FL who received one or more treatments at recurrence were 6 CR and 1 PR. One patient did not respond and in one, the response was not recorded. Four patients received HDT with autologous stem cell support. At last follow-up, 4 of the 11 are alive, 5 have died (3 of lymphoma, 1 of treatment-related infection and 1 of a second malignancy) and 2 have been lost to follow-up.

3.3.5 Survival

3.3.5.1 Survival in all patients diagnosed with DLBCL

The median OS for all 461 patients diagnosed with DLBCL was 5.4 years. Seventy-seven patients, due to advanced age or co-morbidities, received palliative treatment, because it was deemed inappropriate for them to receive intensive, combination chemotherapy with curative intent. The median OS of these patients was 12 weeks (range 3 days to 12 years). Of interest, the patient who is currently alive and disease-free 12 years after diagnosis had severe Crohn's disease and developed primary gastrointestinal DLBCL whilst on immunosuppression. Following surgical resection, he responded to withdrawal of immunosuppression alone.

For the 384 patients treated with curative intent the median OS and cause-specific survival were 6 and 12 years respectively (Figure 3.7a). On univariate analysis, OS was significantly associated with age (≤45 years vs >45 years $p<0.001$; Figure 3.7b), stage (I vs II vs III vs IV $p<0.0001$; Figure 3.7c) and the IPI score (0/I vs II vs III vs IV/V $p<0.0001$; Figure 3.7d) at diagnosis. OS was also significantly associated with outcome to initial therapy (CR/CRu vs PR vs NR, $p<0.0001$; Figure 3.8a) but the OS for patients in whom CR was achieved versus CRu was not significantly different ($p=0.2$; Figure 3.8b).

3.3.5.2 Causes of death in patients treated with curative intent

At last follow-up, 131/384 patients (34%) were alive. Overall, 28/461 patients (6%) have been lost to follow-up. The cause of death is known for all but 4 patients and was lymphoma-related in 172/384 (45%; Table 3.12). Interestingly, 6 patients died of lymphoma-related causes >10 years after diagnosis; 5/6 patients died of recurrent DLBCL and 1/6 patients died of AML secondary to receiving cyclophosphamide/TBI.

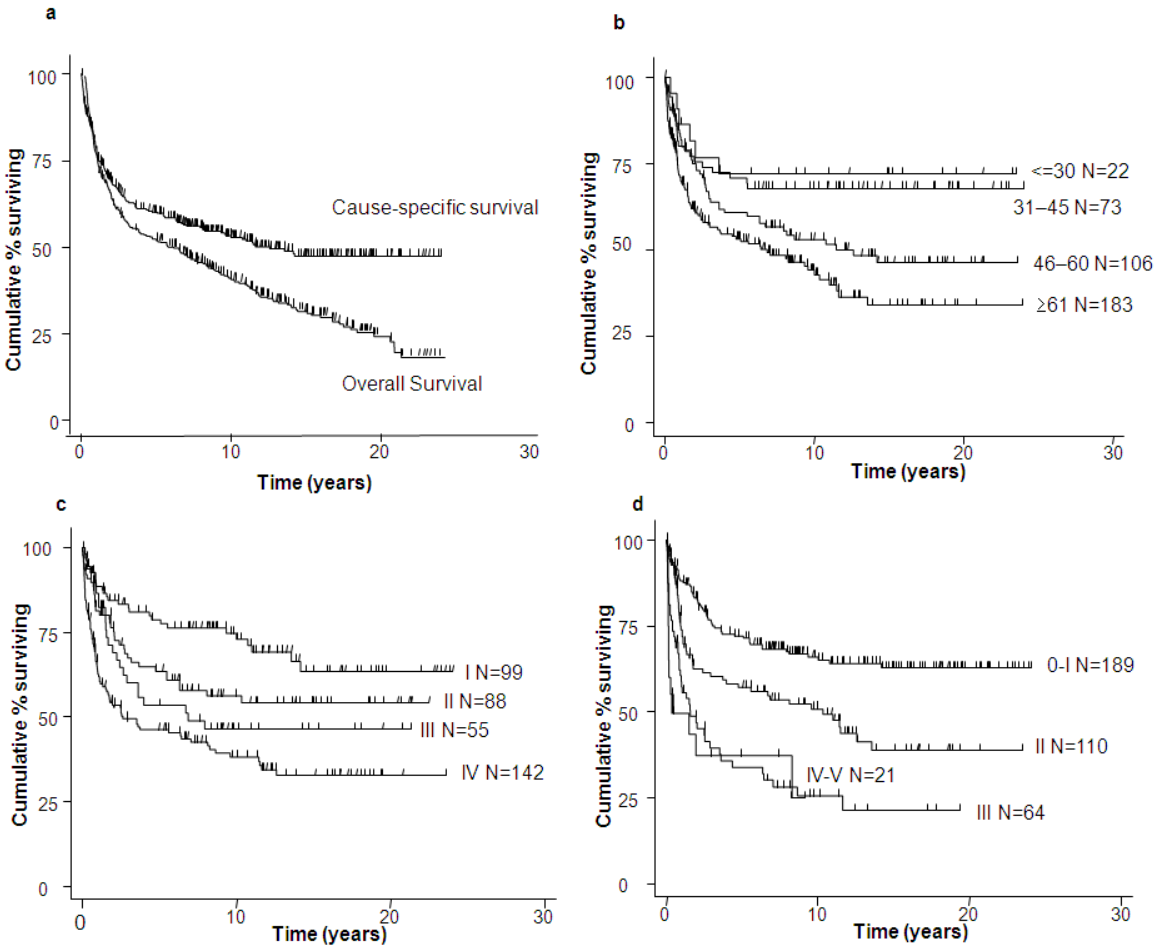

Figure 3.7 (a) Overall and cause-specific survival for all 384 patients treated with curative intent (b) Cause-specific survival according to age at diagnosis (c) Cause-specific survival according to the stage at diagnosis (d) Cause-specific survival according to the IPI score at diagnosis.

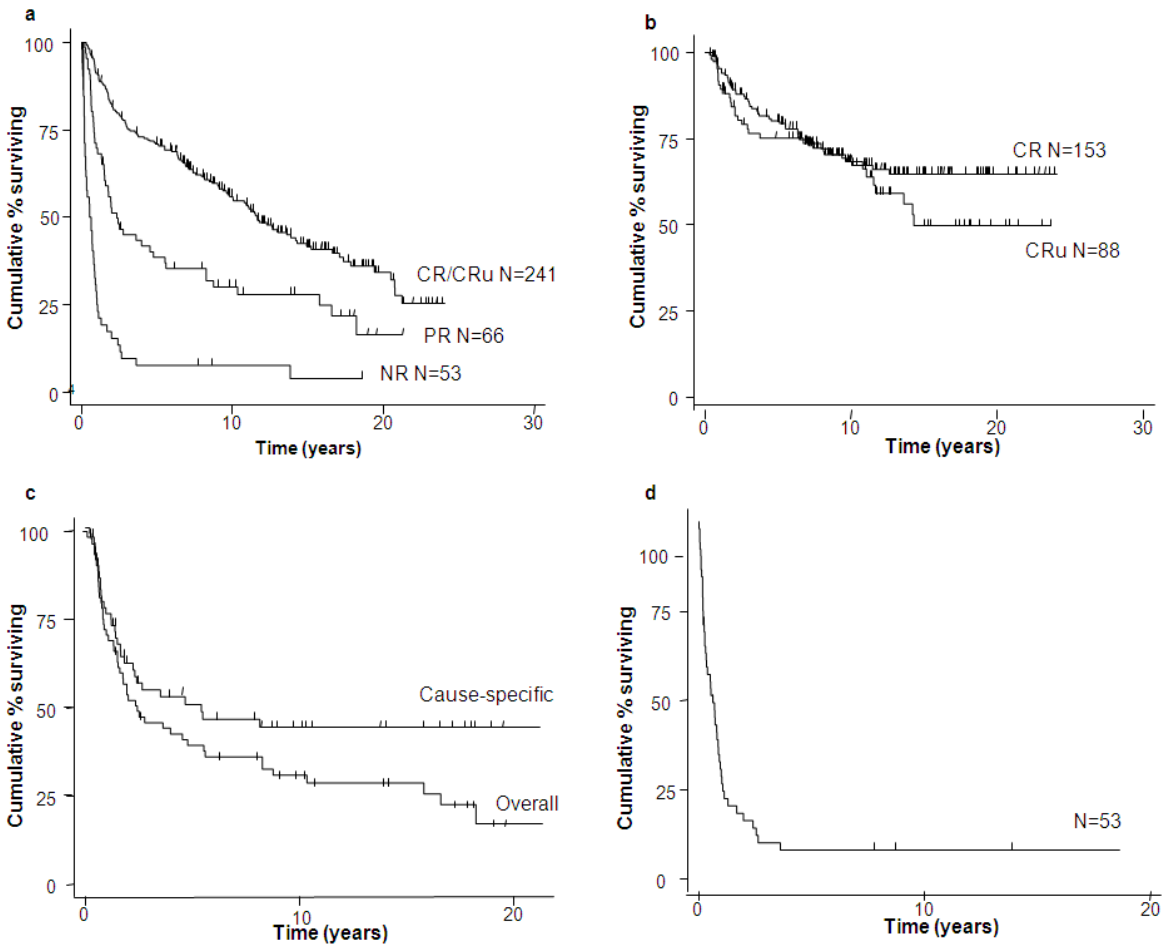

Figure 3.8 (a) Overall survival according to outcome to initial therapy (b) Overall survival in patients achieving CR and CRu after initial therapy (c) Overall survival and cause-specific survival in patients achieving PR after initial therapy (d) OS in patients not responding to initial therapy.

Table 3.12 Causes of death in patients treated with curative intent

Cause of death	Number
Lymphoma	134
Treatment-related infection	38
Second malignancy	20
Concurrent malignancy*	1
Infection	20
Haemorrhage	4
Liver failure	3
Renal failure	3
Cardiac disease	17
CVA	3
Pulmonary disease	3
Suicide	1
Old age	2
Not known	4
TOTAL	**253**

*Laryngeal carcinoma diagnosed at the same time as DLBCL. A CRu was achieved with initial therapy of DLBCL but the patient died of laryngeal carcinoma 3 years later.

3.3.5.3 Second Malignancies

Thirty-three second malignancies were diagnosed in 32 patients; 4 skin cancers, 24 solid tumours and 5 haematological malignancies (Table 3.13). The 3 patients that developed AML had all received cyclophosphamide plus TBI as HDT. Two of the 3 patients that developed breast cancer had received mediastinal radiotherapy as part of treatment for DLBCL. An additional 5 patients also received radiotherapy as part of treatment, but the second malignancy in these patients did not arise in the irradiation field. The median age at diagnosis of second malignancy was 65 years (range 34-86 years). The median time from the diagnosis of DLBCL to the diagnosis of solid tumour was 5.3 years (range 4 months-16 years) and to the diagnosis of haematological cancer, 9.7 years (range 2-14

years). In 20/32 patients the second malignancy was the cause of death (this includes all 5 patients who developed therapy-related second malignancies).

Table 3.13 Second malignancies in patients diagnosed with DLBCL

Site	Number	Number of Deaths
Basal cell (skin)	3	0
Breast	3	2
Colon	4	4
Ovary	1	1
Squamous cell (skin)	1	1
Penile (squamous cell)	1	0
Tonsil (squamous cell)	1	0
Conjunctiva (squamous cell)*	1	0
Squamous cell (site unknown)	1	0
AML	3	3
Hodgkin lymphoma	2	1
Renal	2	2
Lung	4	3
Prostate*	1	0
Liver	2	2
Bladder	2	1
Gastric	1	0
Total	**33**	**20**

* these malignancies occurred in the same patient

3.3.5.4 Survival in patients in whom partial remission was achieved after initial therapy

The median OS and cause-specific survival for the 66 patients in whom only PR was achieved after initial therapy was 2 and 4.8 years respectively (Figure 3.8c). Forty-nine patients (74%) have died and in 25 patients (38%) the cause of death was lymphoma and in 7 patients (11%), treatment-related infection.

3.3.5.5 Survival in patients in whom initial treatment failed

The median OS for the 53 patients that had no response to initial therapy was 7 months (Figure 3.8d). Only one patient is alive and disease-free, 49/53 patients have died; 45 of lymphoma (3 patients lost to follow-up).

3.3.5.6 Survival in patients with 'composite' and 'discordant' lymphoma at diagnosis

The median OS for patients with 'composite' and 'discordant' histology at diagnosis was 3.9 and 3.6 years respectively (Figure 3.9a, b). This was not significantly different from the OS of patients with 'pure DLBCL' (Figure 3.9c p=0.3).

3.3.5.7 Survival in patients with recurrent DLBCL

The median OS from recurrence for all 80 patients with recurrent DLBCL was one year (Figure 3.10a) and was significantly associated with outcome to first 'salvage' therapy (CR/CRu vs PR vs NR, p<0.0001; Figure 3.10b), and the IPI score at recurrence (0-II vs III-IV p=0.03; Figure 3.10c) but not with age and stage at recurrence or with duration of first remission (less than vs greater than 1 year, 2 years or 5 years; Figure 3.11).

In patients with recurrent disease, OS from second remission was not significantly different for those who did and those that did not receive HDT (*p*=0.7; Figure 3.12a). The median OS from second remission for all 38 patients was 6 years (Figure 3.12b). However, only 10/80 patients (13%; 3 patients lost to follow-up) with recurrent DLBCL are alive. The causes of death are shown in Table 3.14 and were lymphoma in 52 patients (65%), treatment-related infection in 5 (6%) and treatment-related AML in 2 (3%). In patients receiving HDT, 14/19 (74%) have died, the cause of death being lymphoma in 9 (47%), treatment-related infection in 2 and treatment-related AML in 2 (Table 3.15).

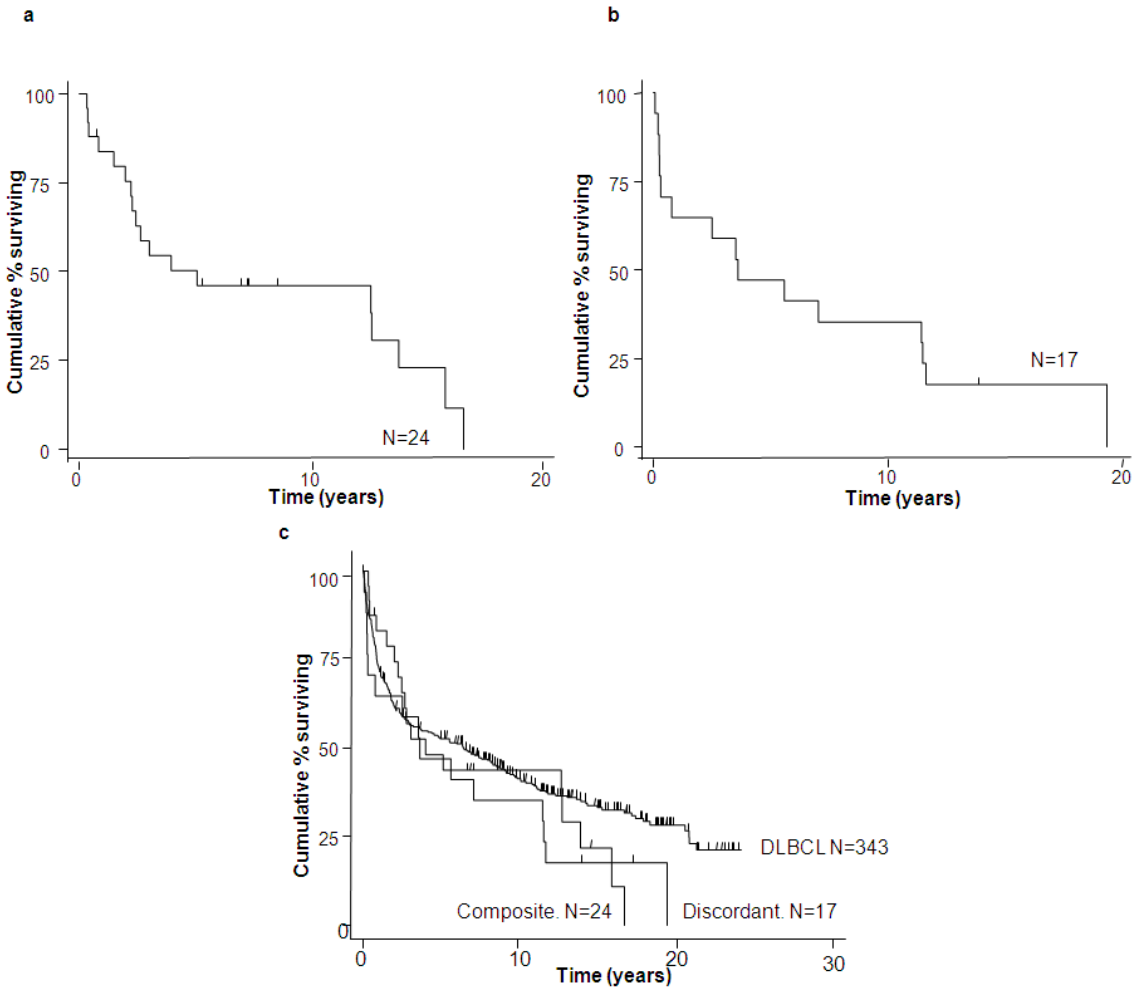

Figure 3.9 Overall survival of patients with (a) 'composite' and (b) 'discordant' lymphoma at diagnosis (c) Comparison of the overall survival of patients with 'composite', 'discordant' and 'pure' DLBCL.

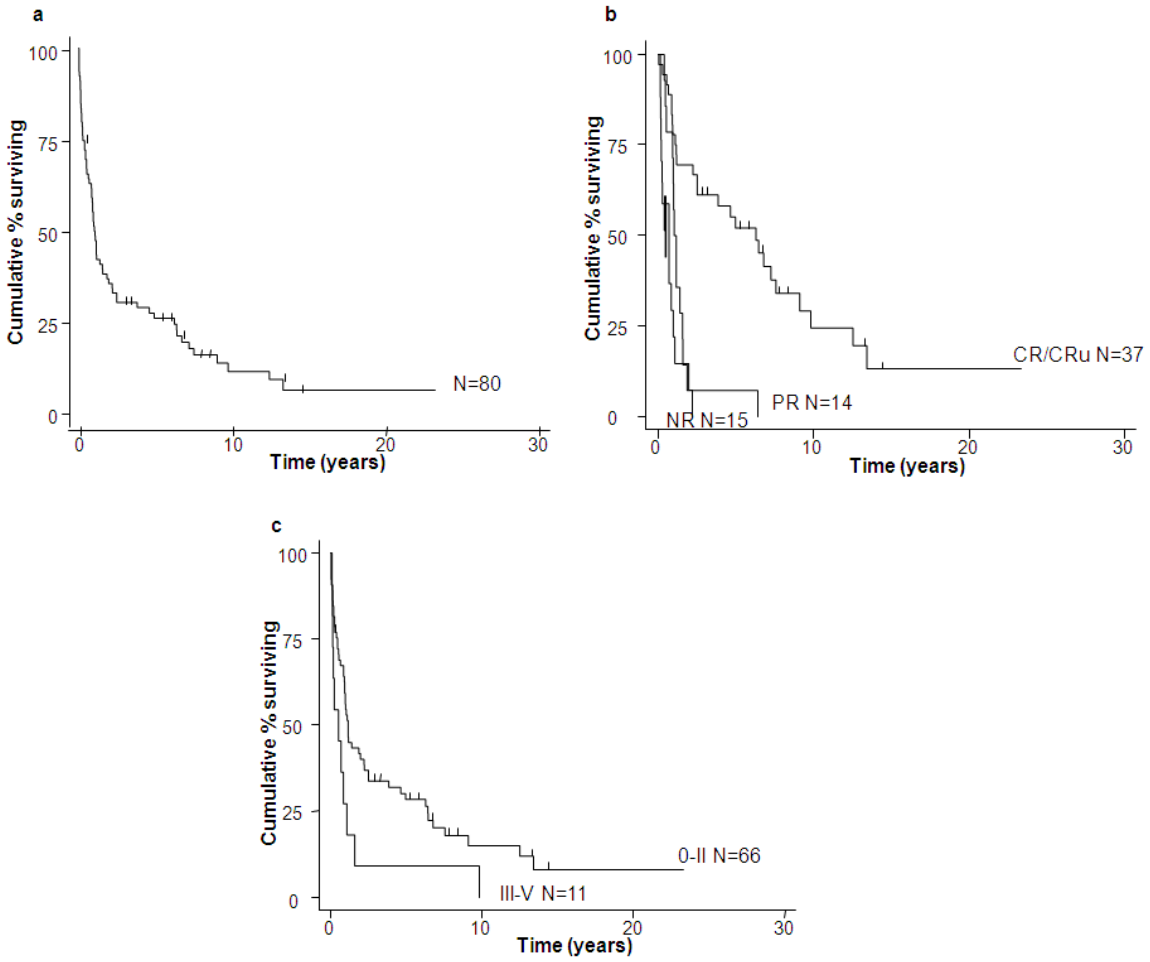

Figure 3.10 (a) Overall survival from recurrence (b) Overall survival from recurrence according to outcome to first 'salvage' chemotherapy (c) Overall survival from recurrence according to the IPI score at recurrence.

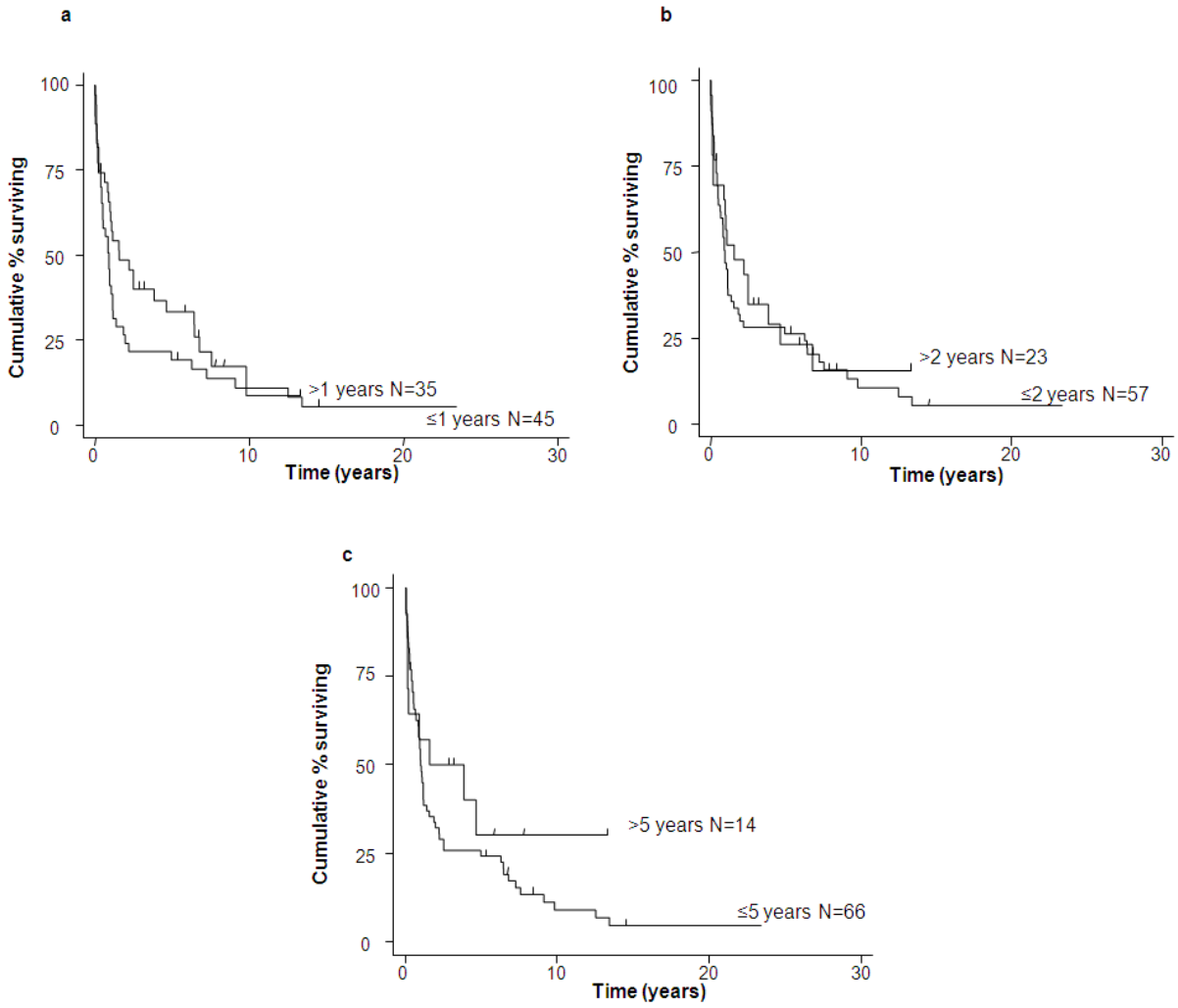

Figure 3.11 Overall survival from recurrence based on length of first RD (a) RD ≤ or > 1 year (b) RD ≤ or > 2 years (c) RD ≤ or > 5 years.

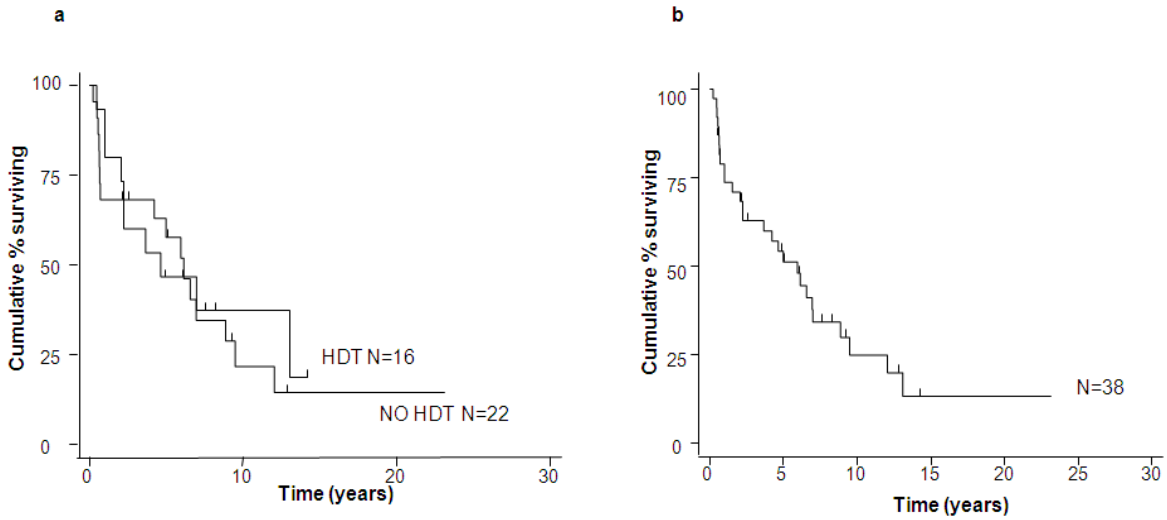

Figure 3.12 Overall survival from second remission in (a) patients that did and did not receive HDT (b) all patients achieving a second CR/CRu.

Table 3.14 Causes of death in patients with recurrent DLBCL

Cause	Number
Lymphoma	52
Treatment-related infection	5
2nd malignancy	6*
infection	1
Respiratory failure	1
Cardiac disease	1
CVA	1
TOTAL	67/80**

*including 2 patients who developed AML following cyclophosphamide/TBI. **10 patients are alive and 3 have been lost to follow-up.

Table 3.15 Causes of death in patients receiving high-dose therapy following recurrence of DLBCL

Cause	Number
Lymphoma	9
Treatment-related infection	2*
2nd malignancy	3**
TOTAL	**14/19**

*1 patient died due to complications of HDT and 1 patient from treatment-related causes following subsequent chemotherapy for progressive disease **2 patients developed AML following cyclophosphamide/TBI, 1 Hodgkin lymphoma in a patient who had not received previous radiotherapy.

3.4 DISCUSSION

This retrospective analysis reports the outcome of DLBCL in an unselected group of patients, presenting to a single centre over an 18-year period. The results draw attention to the importance of long follow-up. Whilst superficially worse than the outcome usually reported in the literature, it is important to remember that the analysis includes everyone who was referred for *consideration of treatment.* In a significant proportion of patients, it was deemed inappropriate to give chemotherapy and a palliative approach was taken. Therefore, the results truly represent outcome of patients with this illness, albeit prior to the introduction of rituximab and draw attention to the appalling prognosis of DLBCL following recurrence. In addition, it is presumed that further selection would have taken place before some patients were even referred to SBH.

The response rate to first-line therapy and the incidence of recurrence are in keeping with those reported (Dana *et al*, 1990; Fisher *et al*, 1993; Weick *et al*, 1991), but the results for patients who developed recurrent disease, irrespective of when, starkly demonstrate how bad the prognosis is. Seventy-four percent of patients with recurrent disease died of

lymphoma or treatment-related causes. The importance of performing a biopsy at the time of recurrence is also highlighted by this work as recurrence with a different histological subtype of lymphoma, mainly FL, does occur with these patients being treated differently.

Of note, the incidence of CNS recurrence in this series was very low, occurring only in one patient. When prophylaxis is not given, the incidence of CNS recurrence in DLBCL is usually around 5% (Cheung *et al*, 2005; van Besien *et al*, 1998). The low rate seen here is undoubtedly due to the fact that prior to 2001, the local policy was to give all patients CNS prophylaxis.

As reported in other studies, the IPI score at recurrence was significantly associated with survival from recurrence (Blay *et al*, 1998; Guglielmi *et al*, 2001) but the duration of first remission was not. This is in contrast to the results of most other published series in which late relapse, usually classified as relapse after more than 2 years in CR/CRu, does correlate with better OS (Guglielmi *et al*, 1998; Hoskins *et al*, 1997; Sanz *et al*, 1998). However, in a recent retrospective study, the clinical characteristics and outcome in patients developing recurrence 5 years or later following diagnosis of DLBCL were investigated. Late relapse was rare and occurred in 54/1492 patients (3.6%). The majority (83%) did recur with DLBCL histology, and in these patients the outcome was poor with a 5 year OS of 27% (Larouche *et al*, 2010).

Despite the reported cure rate of around 40% for HDT when given as consolidation of second remission (Hamlin *et al*, 2003; Philip *et al*, 1995), the great majority of such studies commence at the point of delivery of HDT and do not take into account the true 'denominator'. A significant proportion, (in fact the majority), of patients are not able to (or certainly do not) receive HDT following recurrence. The main reason for this is the high rate of chemoresistance to conventional second-line regimens; 46% of patients in this analysis did not enter CR/CRu after the first 'salvage' treatment. In addition, a significant proportion of patients with DLBCL are more than 65 years old at diagnosis

and thus at recurrence, are usually considered ineligible for HDT. However, recent studies have confirmed the feasibility and the promising efficacy of HDT in selected older patients (Jantunen *et al*, 2008).

Perhaps surprisingly, the RD and OS of patients in second CR/CRu was not significantly different in patients who did and those that did not receive HDT. Both groups had a poor outcome; 28/38 patients have died, 21 from lymphoma-related causes. Again, reflects the reality of treating an unselected group of patients with recurrent DLBCL. It is interesting to note that during the period of this analysis, 27 other patients with refractory/recurrent DLBCL were referred from peripheral hospitals, specifically to receive HDT in second remission at SBH. For these patients, by definition a more selected group, the median RD and OS were 6.8 and 11.7 years respectively (Figure 3.13).

With the advent of FDG-PET scanning it has become clear that patients with a positive FDG-PET scan prior to HDT have a much worse outcome than those in whom the scan is negative (Schot *et al*, 2007). This has led to a change in practice, at SBH and elsewhere, thus now, only patients who are FDG-PET negative after second-line 'salvage' therapy proceed to HDT. Therefore, with better patient selection it is hoped that outcome following HDT will improve.

In concordance with the results of other studies, this analysis confirms that further conventional chemotherapy is futile in patients with recurrent DLBCL in whom the first 'salvage' regimen fails to induce a response (Ardeshna *et al*, 2005; Seshadri *et al*, 2008). All patients in whom CR/CRu was not achieved after the *first* second-line treatment died from lymphoma, except for 2 patients who still had disease at the time of death from other causes. None had a durable period of remission. It would therefore be reasonable to consider such patients for experimental therapies in the context of a clinical trial as soon it is apparent that conventional therapy has failed.

However, this analysis also demonstrates that there is a group of patients, albeit small, in whom, despite only PR being achieved with initial therapy, CR and potential cure can still be achieved with an alternative chemotherapy regimen. In addition, there were 3 patients in PR who did not receive further therapy but are still alive without evidence of disease progression after a median follow-up of 9 years. All had evidence of residual abnormal lymphoid tissue on CT scanning and in retrospect it is likely that this did not represent active disease. In the era of FDG-PET, these patients would almost certainly have been classed as complete responders. In contrast, patients in whom initial therapy failed had a very poor outcome despite further therapy and again, this group of patients should be offered experimental therapies at that point.

The numbers of patients with 'composite' and 'discordant' histology in this series are small, so it is difficult to draw any firm conclusions. Literature on 'composite' lymphoma is sparse and consists mainly of case reports and case series. One retrospective study of 60 patients with DLBCL associated with a 'low-grade' component at diagnosis included 51 patients with two different histological subtypes in the same biopsy; mainly FL and marginal zone lymphoma. Compared to a matched control group with *de novo* DLBCL, the study group had a lower CR rate but comparable OS. However, the recurrence rate was high with nearly half of patients relapsing with 'low-grade' lymphoma (Ghesquieres *et al*, 2006). In this series, the CR/CRu rate in patients with composite lymphoma was similar to the overall rate of CR/CRu, but the recurrence rate was significantly higher (71% vs 36%; p=0.004) with 8/12 patients recurring with histology other than DLBCL (mainly FL). The OS, however, was not significantly different from the OS of patients with 'pure DLBCL'.

Regarding 'discordant' lymphoma, it has been generally been reported that patients with a 'low-grade' lymphoma component in the bone marrow at diagnosis have a similar outcome to patients with no bone marrow involvement (Chung *et al*, 2007; Conlan *et al*, 1990). Some studies have reported a higher rate of recurrence, particularly 'low-grade' (Robertson *et al*, 1991), whereas others have not (Hodges *et al*, 1994). In this series, the

rate of CR/CRu was significantly lower than the overall rate of CR/CRu but there were a high number of treatment-related deaths (4/17). These treatment-related deaths from infection did not occur exclusively in elderly patients, as 2 patients were <60 years and 2 patients >60 years at diagnosis. The OS of patients with 'discordant' lymphoma, however, was not significantly different from those patients with 'pure' DLBCL.

Regarding the incidence of second malignancies, there were 3 patients who developed therapy-related AML secondary to HDT with cyclophosphamide and TBI, all of whom died as a consequence. Two of the 3 patients who developed breast cancer had received mediastinal radiotherapy as part of their treatment for DLBCL, both died as a consequence. Two patients developed Hodgkin lymphoma, neither had received radiotherapy as initial therapy. If the therapy-related cases of AML and breast cancer are excluded and the incidence of second cancers is only considered relevant to those patients that achieved a CR/CRu, (having survived long enough to develop one), then there were 28 second cancers diagnosed in 264 patients (11%). In 15/264 patients (6%), this was the cause of their death.

According to the Office of National Statistics in the UK (www.statistics.gov.uk), the incidence rate of newly diagnosed cancer per 100,000 population aged between 65 to 69 years was 2125 and 1481 for males and females respectively in 2007. That is an incidence rate of around 1-2%. Although this is a very crude way of looking at the data, it seems that the incidence of second malignancy in this series of patients, with a median age of 65 years at diagnosis of their second malignancy, was higher than expected compared with that of the general population. It is difficult to tease out whether this statement is supported by published literature regarding second malignancies in patients treated for DLBCL. Radiotherapy is a known risk factor for developing a second malignancy but taking this into account, the results are conflicting; some studies have reported that the risk is not increased (Andre *et al*, 2004) whilst others have found it to be increased. (Mudie *et al*, 2006). The problem with the majority of studies addressing this issue is that they include all patients with NHL, not distinguishing between different

histological subtypes, and also the use of different study designs. However, an Italian study reported the incidence of second malignancies in a cohort of 1280 patients with DLBCL and found that only patients ≤59 years at diagnosis had an increased risk of developing a second cancer whereas patients older than 59 years had the same risk as the normal Italian population (Sacchi *et al*, 2008).

The limitations of this analysis are those associated with a retrospective analysis of any kind, which includes: missing data, modification of staging criteria over time and the heterogeneity of treatments administered. Data on the molecular subgroup of DLBCL, i.e. GCB-like or ABC-like (Alizadeh *et al*, 2000), at diagnosis and recurrence are also not available. In addition, patients in this analysis were treated prior to the routine use of rituximab. However, the expectation is that, although the addition of rituximab to initial chemotherapy has improved progression-free survival and OS, it will make recurrent disease correspondingly more difficult to treat. Interim results of the randomised 'CORAL' trial in patients with relapsed/refractory DLBCL, comparing 'R-ICE' with 'R-DHAP', suggest that prior exposure to rituximab results in a worse outcome to 'salvage' chemotherapy (Giesselbrecht C, 2007; Hagberg & Gisselbrecht, 2006). In addition, a recent retrospective analysis evaluating the influence of prior rituximab in patients with relapsed/refractory DLBCL who had received 'R-ESHAP' as salvage therapy, reported inferior progression-free survival and OS in patients previously exposed to rituximab (Martin *et al*, 2008).

Above all, this study highlights the need for new and better first-line treatments, in order to prevent recurrence in the first place, particularly in high-risk groups such as patients with an unfavourable IPI score or molecular subgroup at diagnosis. Currently, where rituximab is readily available, all patients with DLBCL are treated in the same way. Additionally, prospective randomised trials which incorporate new agents as treatment for patients with recurrent DLBCL are urgently needed. These results also emphasise the importance of reviewing outcome for all patients, not just for a selected group, as usually reported in the literature about outcome of patients treated in clinical trials.

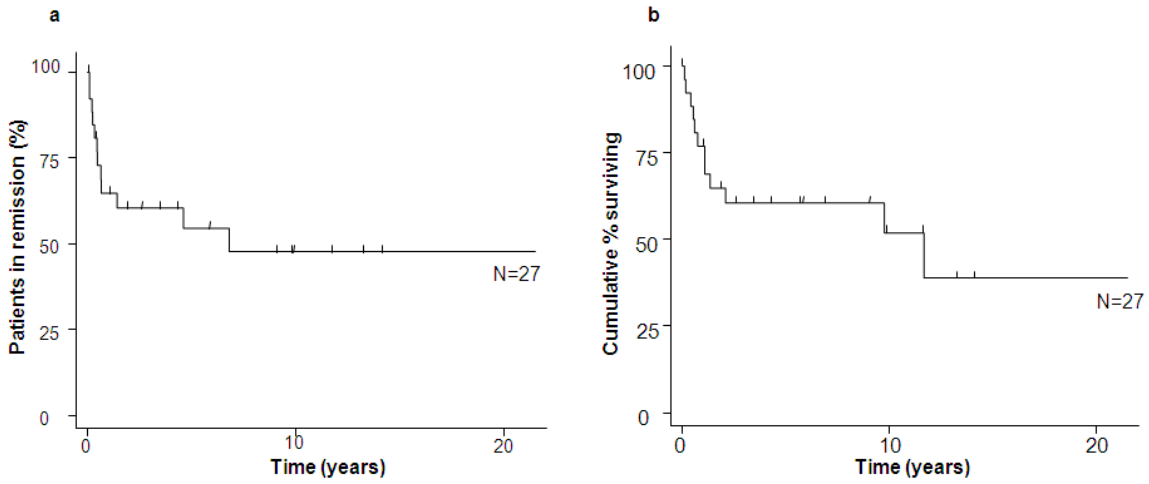

Figure 3.13 (a) Remission duration and (b) Overall survival in patients referred to St Bartholomew's Hospital from peripheral hospitals for high-dose therapy.

CHAPTER 4: The activity of selenium in B-NHL cell lines

4.1 INTRODUCTION

Work from our laboratory has previously demonstrated that Se, in the form of MSA, induces apoptosis in DLBCL cell lines but that cell lines differ markedly in their sensitivity to MSA (Last *et al*, 2006). In addition, non-toxic concentrations of MSA were found to enhance the cytotoxic effect of conventional chemotherapeutic agents and a synergistic interaction was demonstrated with doxorubicin, 4-HC and etoposide. In MSA-sensitive cell lines (RL and SUD4) a concentration of 1μmol/L MSA was chemo-sensitising, whilst in MSA-resistant cells lines (DHL4 and DoHH2) a concentration of 10μmol/L MSA was required. Best results were obtained when MSA was administered simultaneously with the cytotoxic drugs. A potential mechanism for the observed synergistic interaction was found to be a MSA-induced inhibition of NF-κB activity (Juliger *et al*, 2007). These data complement work by others, in solid tumour cell lines and xenograft models, which show that organic Se species increase the efficacy of chemotherapeutic agents whilst protecting normal tissue from chemotherapy-induced toxicity (Cao *et al*, 2004; Li *et al*, 2007b). As described extensively in Chapter 1, Se has the potential to affect the function of many cellular proteins and signalling pathways and its action differs depending on the cell type, the form of Se and the concentration. Therefore, it is likely that other, yet undefined, mechanisms will be important for the observed synergy between MSA and cytotoxic agents in DLBCL cell lines. These pre-clinical studies have led to a proposal for a phase I/II clinical trial combining MSC with 'R-ICE' immunochemotherapy in patients with relapsed/refractory DLBCL. One of the aims of this trial will be to achieve a plasma Se concentration of 20μmol/L prior to the start of chemotherapy. This plasma concentration has been extrapolated from that determined in xenograft models of solid tumours (Azrak *et al*, 2004).

Potential mechanisms of both the chemo-sensitising and cytotoxic effects of MSA are investigated in the experiments reported in this chapter.

4.2 AIMS

1) To determine the activity of MSA in DLBCL cell lines.

2) To confirm the synergistic interaction between non-toxic concentrations of MSA and conventional cytotoxic agents in DLBCL cell lines.

3) To investigate additional mechanisms by which MSA sensitises DLBCL cell lines to chemotherapy.

4) To investigate the role of p53 in the action of MSA

5) To determine the activity of MSC in B-NHL cell lines

4.3 MATERIALS AND METHODS

In these experiments, 4 DLBCL cell lines (RL, DHL4, DoHH2, and SUD4) and 1 MCL cell line (JVM2) were used. The activity of MSA and MSC was investigated using the ATP assay (Chapter 2, section 2.3.2). The results were expressed relative to the control value and were analysed using the GraphPad PRISM® software (version 5.03). The activity of MSA and MSC was summarised to an EC_{50} value which was calculated using a sigmoidal concentration-effect model with variable slope. Non-toxic concentrations of MSA were combined with cytotoxic agents, doxorubicin and 4-HC, in the RL and DHL4 cell lines and cell viability was determined using the Guava® viacount assay (Chapter 2, section 2.3.3). Intracellular GSH concentration was measured using a 96-well plate-based assay kit (Sigma-Aldrich; Chapter 2, section 2.6). Western blotting was used to investigate protein changes induced by MSA (Chapter 2, sections 2.4 and 2.5). Flow cytometry was used to determine the effect of MSA on cell cycle distribution (Chapter 2, section 2.7), MMP (Chapter 2, section 2.9) and the uptake of doxorubicin (Chapter 2, section 2.8). The 'Aktide assay' which utilises a synthetic Akt substrate peptide, RPRAAFT ('Aktide'), was used to quantify PI3K/Akt activity in whole cell extracts (Chapter 2, section 2.13).

4.4 RESULTS

4.4.1 The activity of MSA in DLBCL cell lines

The activity of MSA was studied in 4 DLBCL cell lines using the ATP assay. Two cells lines (RL and SUD4) were relatively sensitive and two cell lines (DoHH2 and DHL4) were relatively resistant to the cytotoxic effects of MSA. Figure 4.1 shows the EC_{50} concentration-effect curves following 72-hour exposure to MSA, and Table 4.1 summarises the EC_{50} values. This confirms previously published results from our group, although EC_{50} values differ slightly due to the use of different methodology (Juliger *et al*, 2007; Last *et al*, 2006). For most subsequent experiments, one MSA-sensitive cell line (RL) and one MSA-resistant cell line (DHL4) was chosen.

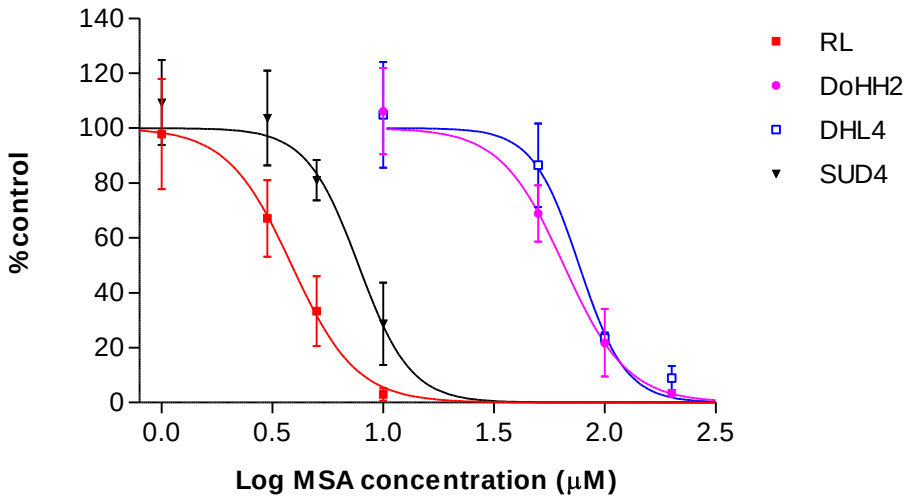

Figure 4.1 EC_{50} concentration-effect curves following 72-hour exposure to increasing concentrations of MSA in 4 DLBCL cell lines using the ATP assay. Data points are the mean +/- SD of three separate experiments.

Table 4.1 EC_{50} values in 4 DLBCL cells lines exposed to MSA for 72 hours.

Cell line	EC_{50} (µmol/L)	95% CI
RL	3.9	3.3-4.6
SUD4	7.7	6.4-9.3
DHL4	76.6	66.1-88.8
DoHH2	65.3	56.7-75.2

4.4.2 Combining MSA with standard chemotherapeutic agents

To confirm previously published data from our laboratory (Juliger *et al*, 2007), the chemo-sensitising effect of non-toxic concentrations of MSA was investigated using the Guava® viacount assay. Figure 4.2a shows that when the RL cell line was simultaneously treated with 1µmol/L MSA and increasing concentrations of doxorubicin for 48 hours, the addition of MSA significantly enhanced the cytotoxicity of doxorubicin 50nmol/L, 100nmol/L and 250nmol/L. For example, the cytotoxicity of 100nmol/L doxorubicin was increased from 24.5% (±5.7) to 47.4 (±4.9). Similarly, Figure 4.2b shows that when the DHL4 cell line was simultaneously treated with 10µmol/L MSA and increasing concentrations of 4-HC for 48 hours, the addition of MSA significantly enhanced the cytotoxicity of 4-HC 1µmol/L, 2µmol/L, 3µmol/L and 5µmol/L. For example, the cytotoxicity of 3µmol/L 4-HC was increased from 1.7% (±3.4) to 38.9% (±3.1). These experiments confirm that non-toxic concentrations of MSA result in a synergistic effect when combined with standard chemotherapeutic agents in DLBCL cell lines. In MSA-sensitive cell lines a concentration of 1µmol/L is chemo-sensitising, whilst a concentration of 10µmol/L is chemo-sensitising in MSA-resistant cell lines.

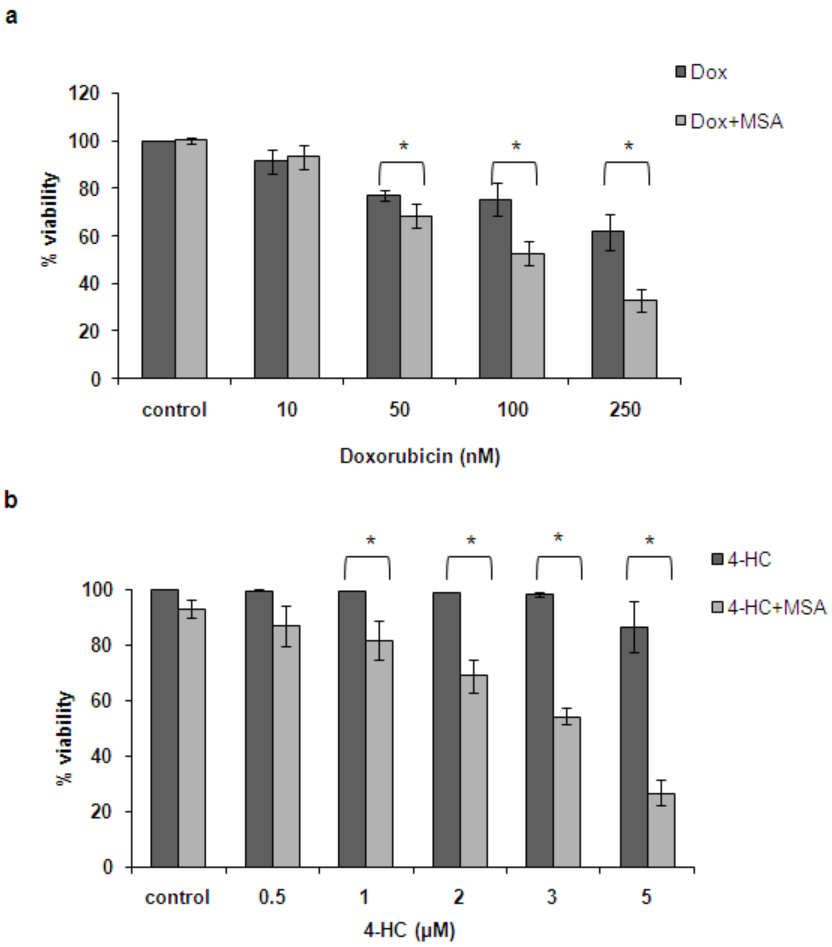

Figure 4.2 Cell viability of (a) RL cells exposed to a simultaneous combination of 1µmol/L MSA and increasing concentrations of doxorubicin (Dox) for 48 hours (b) DHL4 cells exposed to a simultaneous combination of 10µmol/L MSA and increasing concentrations of 4-HC for 48 hours. Data points are the mean +/- SD of three separate experiments. *p<0.05.

4.4.3 The effect of MSA on the generation of DNA damage

The reason for the difference in sensitivity of DLBCL cell lines to MSA is not clear. Although previous work from our laboratory did not identify ROS generation after exposure to MSA, (Last *et al*, 2006) the generation of DNA damage may contribute to MSA activity. Therefore the effect of MSA on the generation of DNA damage was investigated. Histone H2AX, a variant of the nucleosome core histone H2A, is phosphorylated on serine 139 in response to double-stranded DNA breaks and this can be

detected by western blotting (Burma *et al*, 2001). Exposure to UV light was used as a positive control. Figure 4.3 shows that in both the RL and DHL4 cell line, phosphorylation of histone H2AX was not increased when cells were exposed to MSA concentrations up to 50µmol/L for 4 hours, confirming that MSA does not induce DNA damage. In contrast, exposure to UV light clearly increased the phosphorylation of histone H2AX.

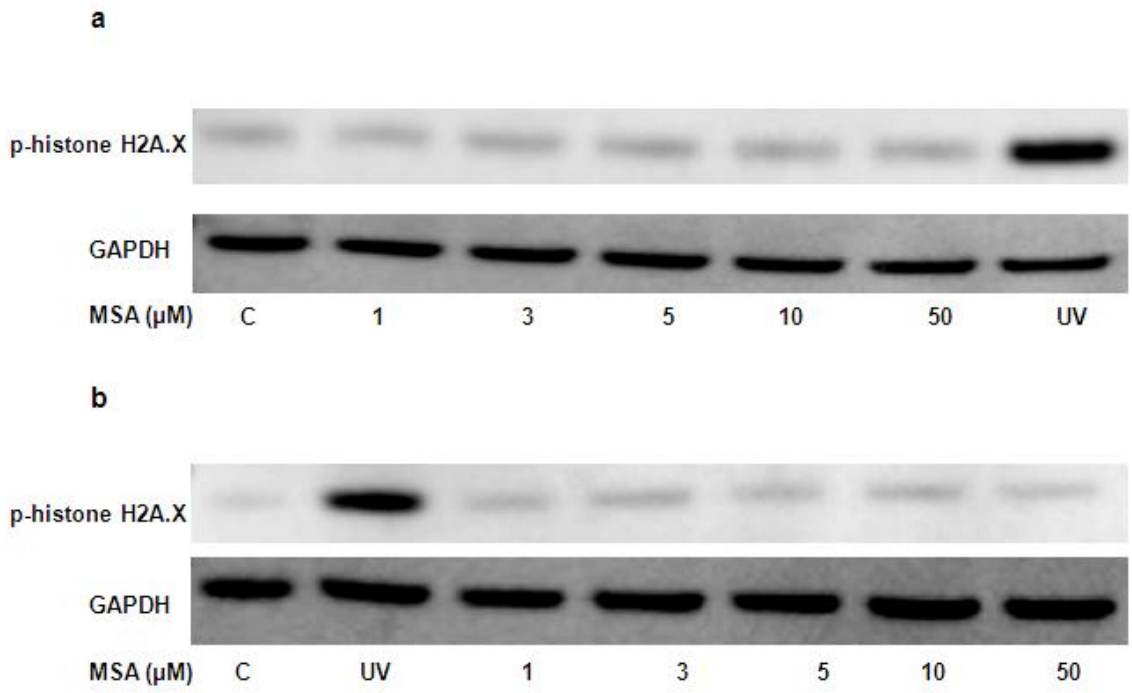

Figure 4.3 Phosphorylated histone H2AX in (a) RL cells and (b) DHL4 cells exposed to MSA for 4 hours. Exposure to UV light was used as a positive control.

4.4.4 The effect of MSA on intracellular glutathione concentration

MSA has been reported to deplete intracellular GSH (Shen *et al*, 2002). Therefore, the effect of a range of MSA concentrations (1-20µmol/L) on intracellular GSH was investigated in DLBCL cell lines. There was no difference in basal GSH levels between the three cell lines studied. Figure 4.4a shows that after a 2-hour exposure to MSA there was no change in intracellular GSH concentration in the DHL4 and RL cells lines. However, after 24-hour exposure there was a significant decrease in intracellular GSH

levels in RL cells exposed to 10µmol/L and 20µmol/L MSA but not in DHL4 cells (Figure 4.4b). Given that DHL4 and RL cells have different sensitivities to MSA, intracellular GSH was also measured in another MSA-sensitive cell line, SUD4, after 24-hour exposure to MSA. Similar results to the RL cell line were obtained, such that 24-hour exposure to 10µmol/L and 20µmol/L MSA significantly decreased intracellular GSH concentration.

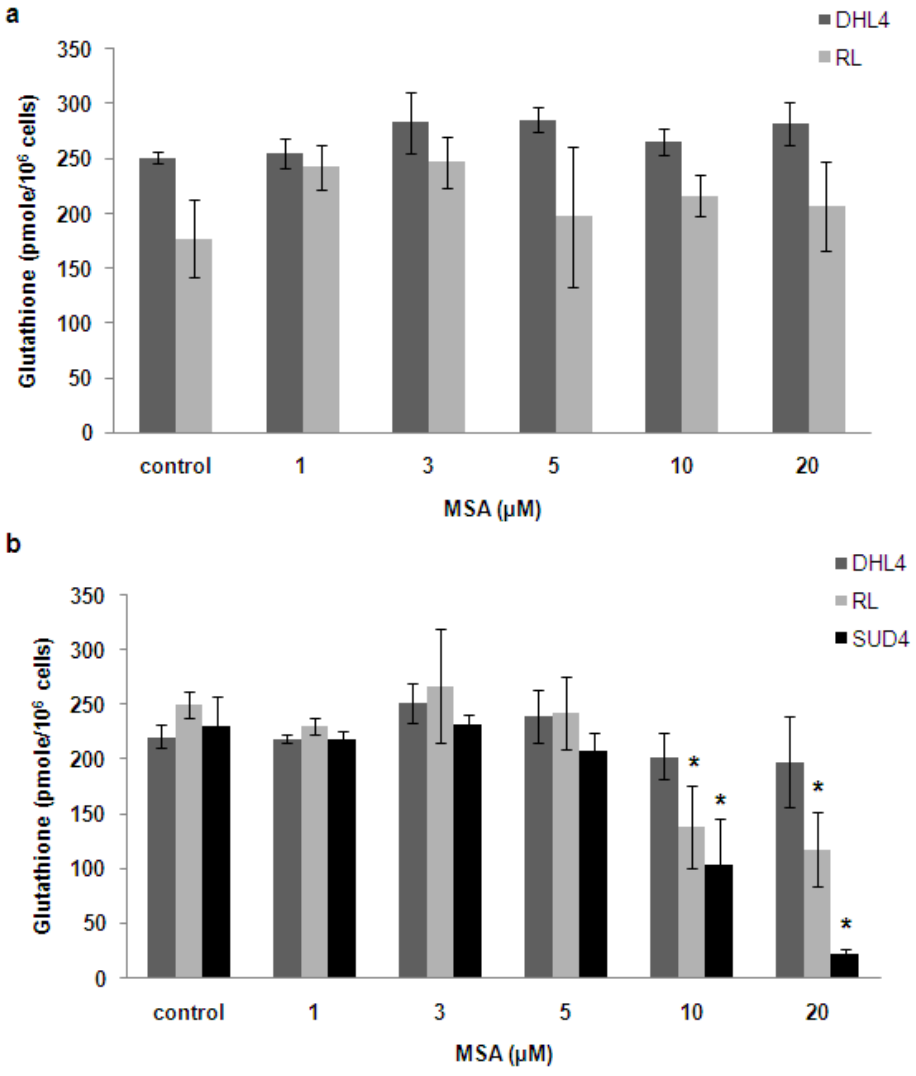

Figure 4.4 The effect of MSA on intracellular glutathione concentration in DLBCL cell lines after (a) 2-hour and (b) 24-hour exposure. Data points are the mean+/-SD of three separate experiments. *$p<0.05$ is a comparison with control using one-way ANOVA followed by Tukey's test.

4.4.5 Mitochondrial membrane potential

Previously published work from our laboratory has demonstrated that MSA induces apoptotic cell death in DLBCL cell lines (Last *et al*, 2006). To investigate whether non-toxic concentrations were able to prime cells for apoptosis, MMP was determined by JC-1 staining and flow cytometry. In non-apoptotic cells the JC-1 dye accumulates in the mitochondria forming aggregates, which fluoresce red. During apoptosis, via the intrinsic pathway, the MMP collapses, the dye no longer accumulates in the mitochondria but remains in the cytoplasm in a monomeric form, which fluoresces green.

RL and DHL4 cell lines were exposed to non-toxic and cytotoxic concentrations of MSA for 24 and 48 hours. Doxorubicin was used as a positive control as it is known to induce apoptosis via the intrinsic, mitochondrial pathway. Figures 4.5 and 4.6 show the dot plots of RL and DHL4 cells respectively exposed to MSA for 24 hours. Figure 4.7 summarises the percentage decrease in red fluorescence relative to control in cells treated with MSA. In RL cells the chemo-sensitising concentration of 1µmol/L did not alter the percentage red fluorescence. However, cytotoxic concentrations of 5µmol/L and 20µmol/L significantly decreased the percentage red fluorescence demonstrating loss of MMP. In DHL4 cells the chemo-sensitising concentration of 10µmol/L did not result in decreased red fluorescence but the cytotoxic concentration of 100µmol/L did. Similar results were obtained at 48 hours. Figures 4.8 and 4.9 show the dot plots of RL and DHL4 cell lines respectively exposed to MSA for 48 hours and results are summarised in Figure 4.10. The experiment of RL cells exposed to MSA for 48 hours was only performed twice and therefore statistical analysis is not possible. Therefore, chemo-sensitising concentrations in both cell lines did not result in loss of MMP but cytotoxic concentrations did.

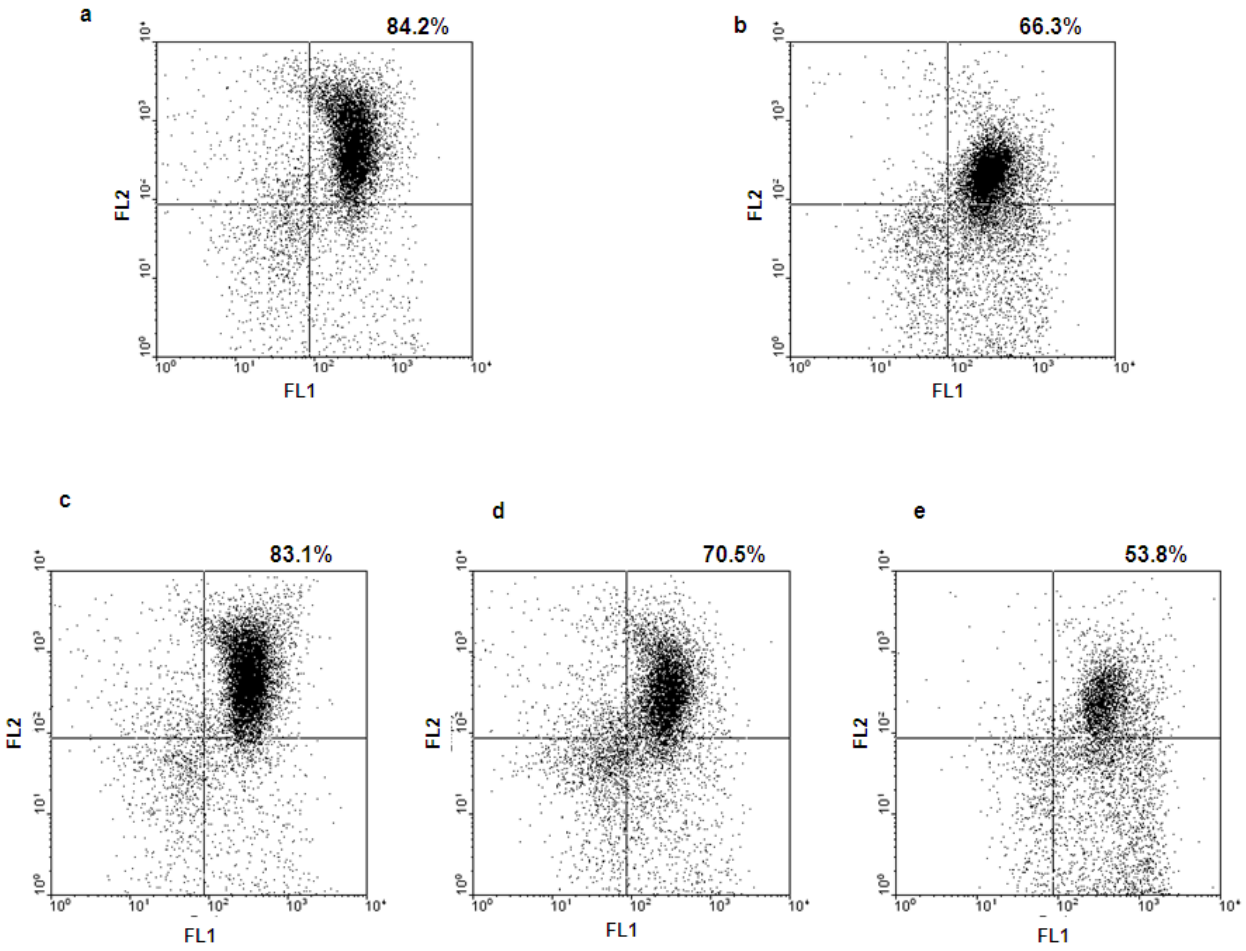

Figure 4.5 JC-1 staining in RL cells treated for 24 hours. (a) Control (b) Doxorubicin 250nmol/L (c) MSA 1µmol/L (d) MSA 5µmol/L (e) MSA 20µmol/L. Numbers represent % viable cells determined by the Guava® viacount assay. Green fluorescence is detected in the FL1 channel and red fluorescence in the FL2 channel. Cells with red fluorescence are shown in the right upper quadrant. When red fluorescence is lost, cells appear in the right lower quadrant.

.

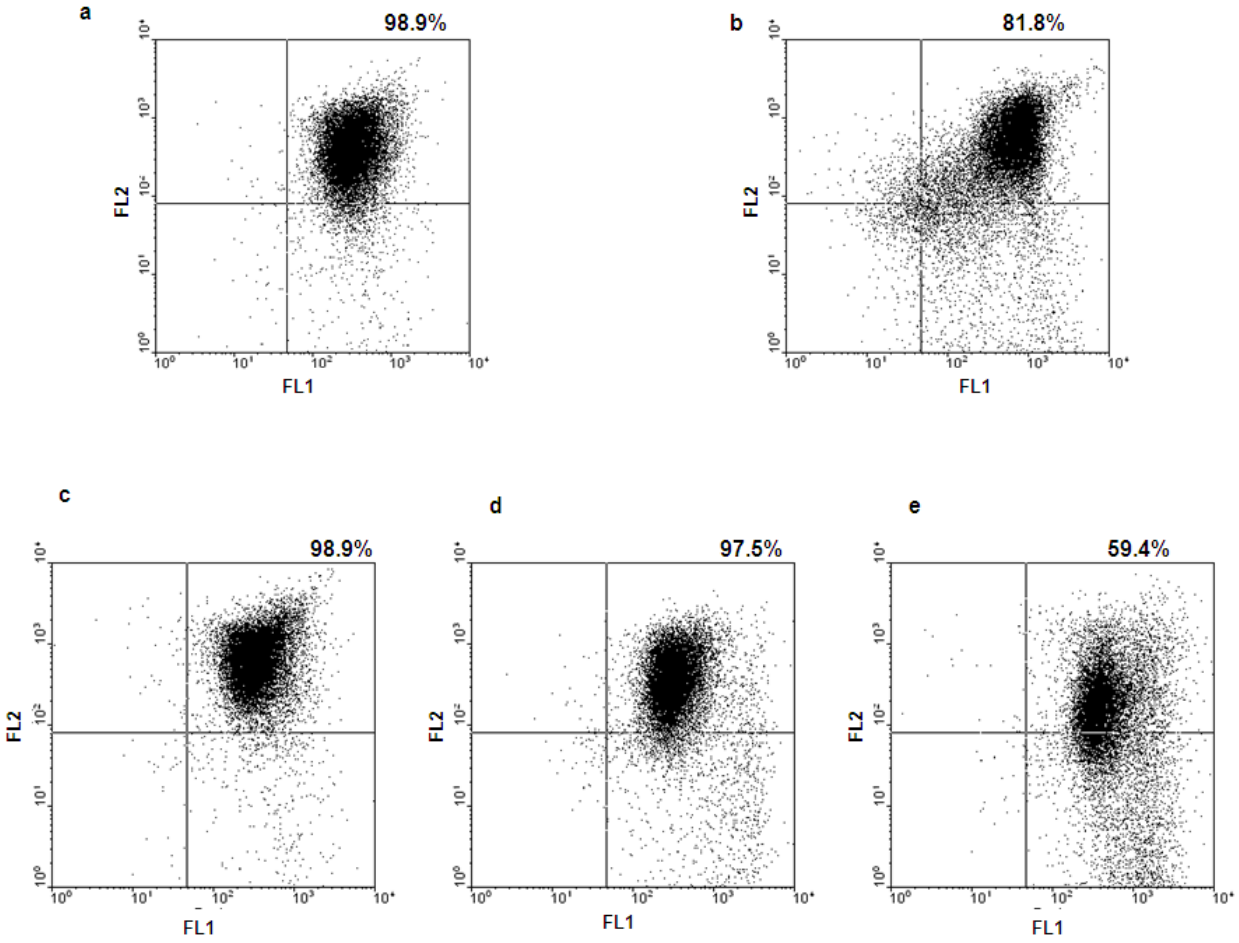

Figure 4.6 JC-1 staining in DHL4 cells treated for 24 hours. (a) Control (b) Doxorubicin 500nmol/L (c) MSA 1µmol/L (d) MSA 10µmol/L (e) MSA 100µmol/L. Numbers represent % viable cells determined by the Guava® viacount assay. Green fluorescence is detected in the FL1 channel and red fluorescence in the FL2 channel. Cells with red fluorescence are shown in the right upper quadrant. When red fluorescence is lost, cells appear in the right lower quadrant.

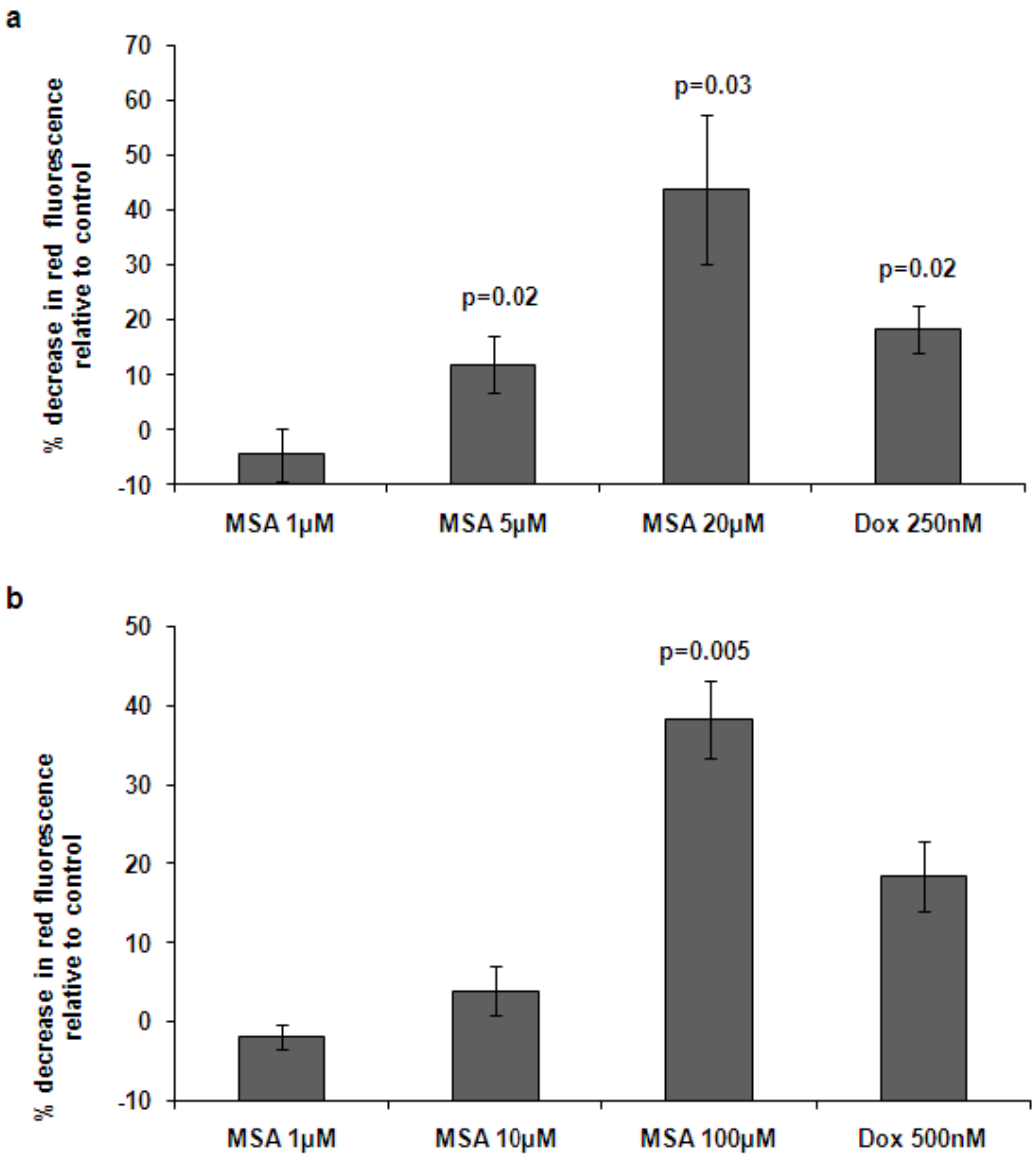

Figure 4.7 Decrease in red fluorescence in cell lines treated for 24 hours (a) RL cells (b) DHL4 cells. Data points are the mean+/-SD of at least 3 separate experiments (except DHL4+doxorucibin n=2). The p values are a comparison with control.

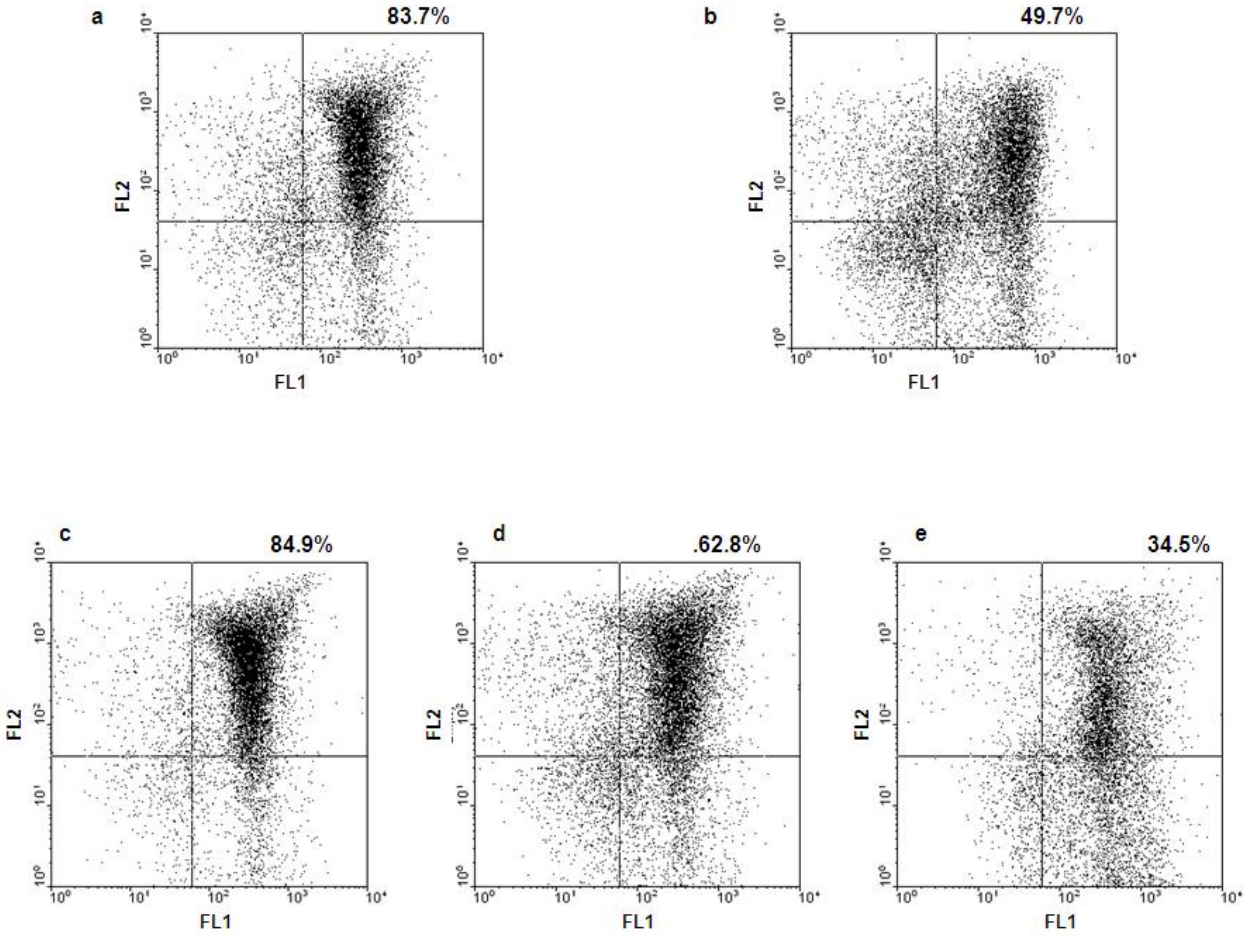

Figure 4.8 JC-1 staining in RL cells treated for 48 hours. (a) Control (b) Doxorubicin 100nmol/L (c) MSA 1µmol/L (d) MSA 5µmol/L (e) MSA 10µmol/L. Numbers represent % viable cells determined by the Guava® viacount assay. Green fluorescence is detected in the FL1 channel and red fluorescence in the FL2 channel. Cells with red fluorescence are shown in the right upper quadrant. When red fluorescence is lost, cells appear in the right lower quadrant.

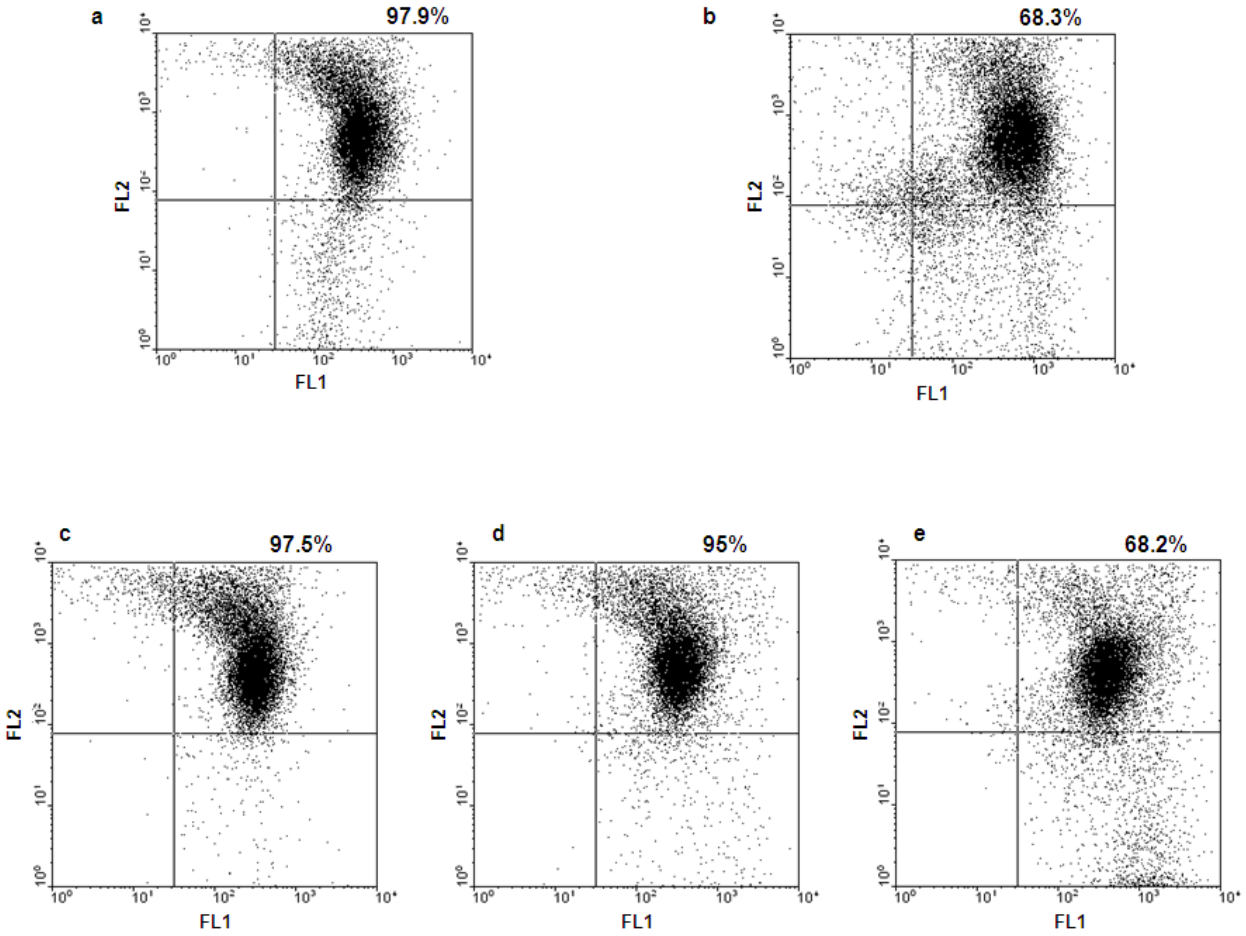

Figure 4.9 JC-1 staining in DHL4 cells treated for 48 hours. (a) Control (b) Doxorubicin 500nmol/L (c) MSA 1µmol/L (d) MSA10µmol/L (e) MSA 50µmol/L. Numbers represent % viable cells determined by the Guava® viacount assay. Green fluorescence is detected in the FL1 channel and red fluorescence in the FL2 channel. Cells with red fluorescence are shown in the right upper quadrant. When red fluorescence is lost, cells appear in the right lower quadrant.

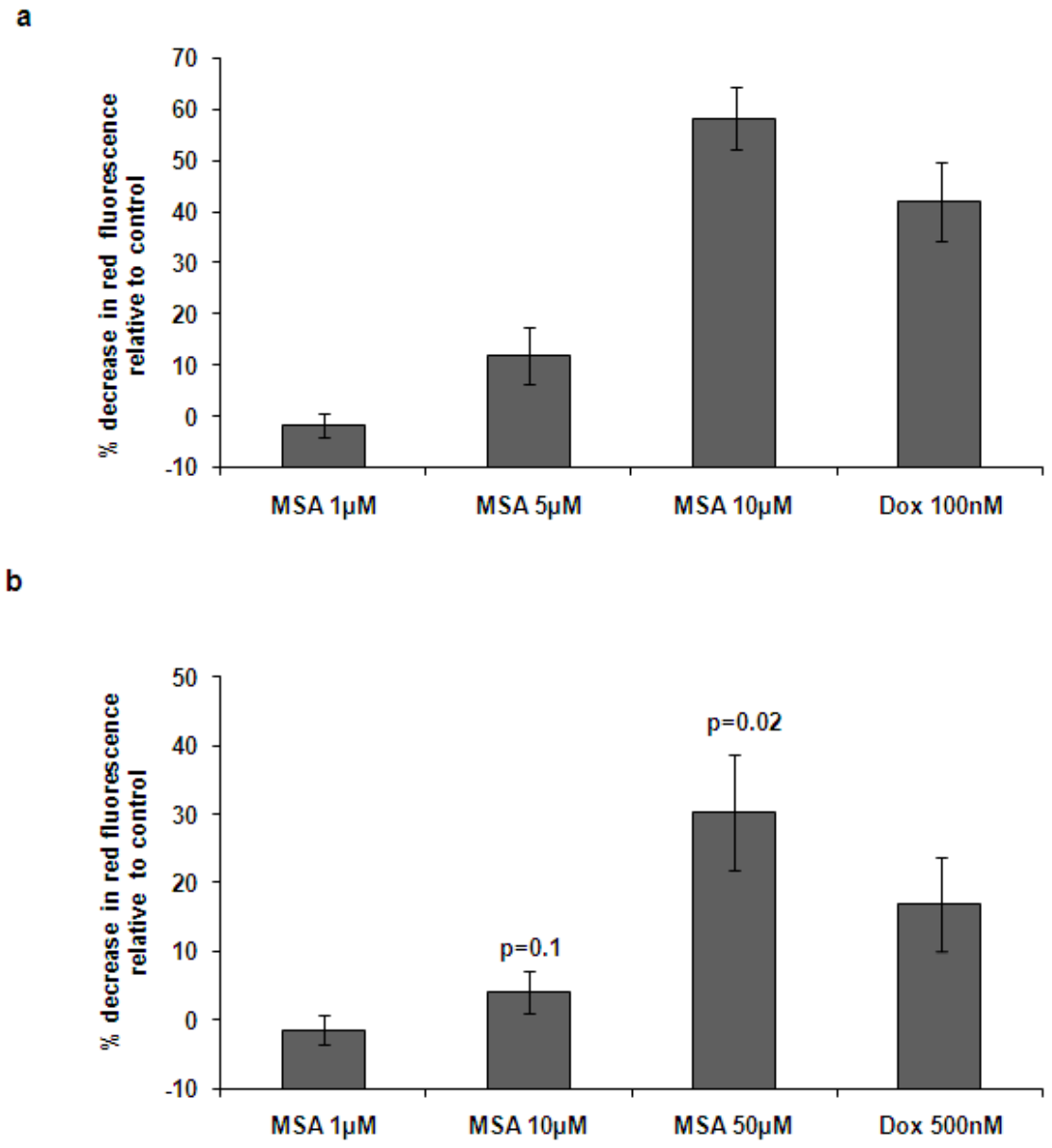

Figure 4.10 Decrease in red fluorescence in cell lines treated for 48 hours (a) RL cells, data points are the mean+/-SD of 2 separate experiments (b) DHL4 cells, data points are the mean+/-SD of 3 separate experiments. The p value is a comparison with control.

4.4.6 Pro-apoptotic signalling

The induction of apoptosis was further investigated by western blotting. Figure 4.11 shows that in RL cells, PARP cleavage occurred at the non-toxic concentration of 1µmol/L MSA after 48-hour exposure, and that the cytotoxic concentration of 5µmol/L resulted in a larger increase in cleaved PARP at the earlier time point of 24 hours. In DHL4 cells, concentrations of MSA up to 60µmol/L did not result in PARP cleavage. Staurosporine (ST) was used as a positive control.

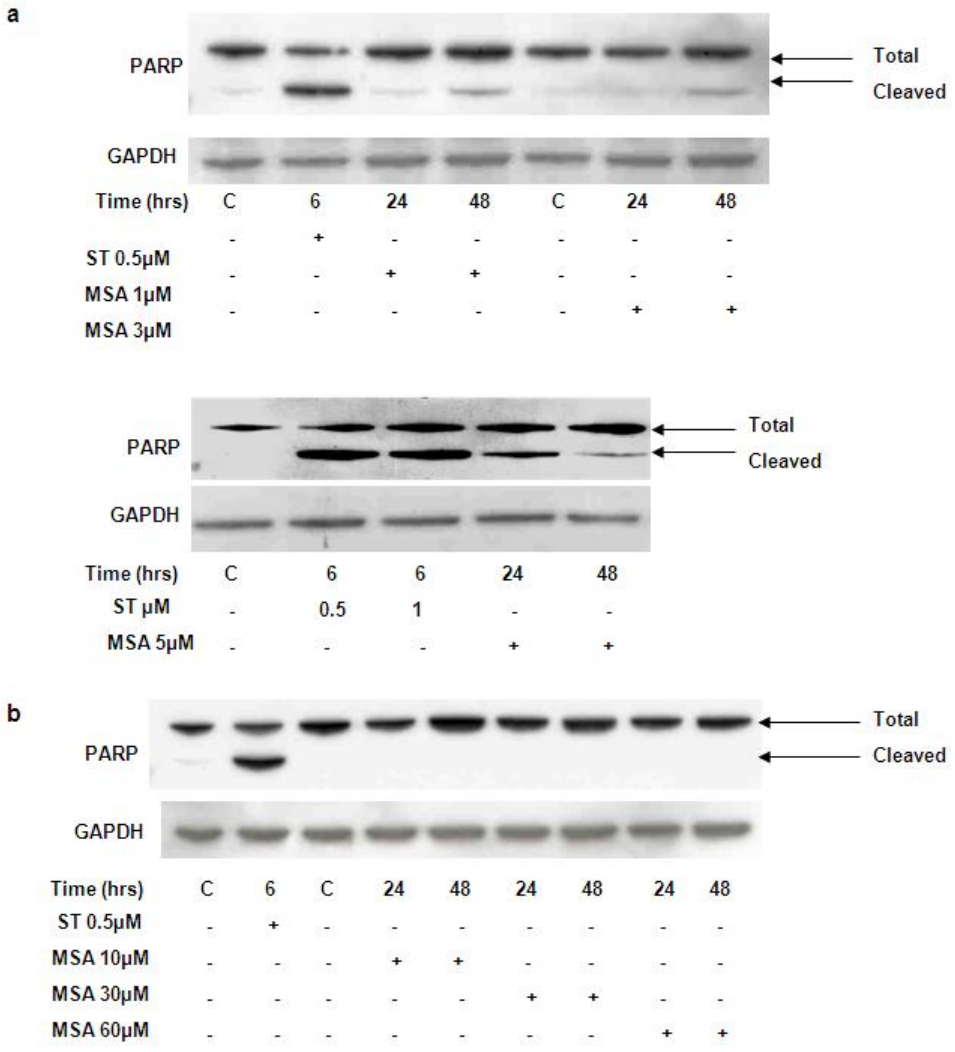

Figure 4.11 PARP cleavage in (a) RL and (b) DHL4 cell lines treated with non-toxic and cytotoxic concentrations of MSA. Cells exposed to staurosporine (ST) for 6 hours were used as a positive control.

To determine whether chemo-sensitisation by MSA was due to enhanced apoptosis, PARP cleavage was also investigated in RL and DHL4 cell lines exposed to MSA, cytotoxic chemotherapy, or both for 48 hours. Figure 4.12a shows that in DHL4 cells, doxorubicin 225nmol/L alone resulted in a small increase in cleaved PARP but MSA 10µmol/L did not. The combination of both resulted in a less than additive increase in cleaved PARP. In RL cells, doxorubicin 100nmol/L resulted in a large increase in cleaved PARP but MSA 1µmol/L only produced a small increase. The combination of both resulted in an additive increase in the amount of cleaved PARP. Figure 4.12b shows DHL4 cells exposed to a synergistic combination of MSA and 4-HC for 48 hours. However, neither MSA nor 4-HC alone or in combination resulted in PARP cleavage. It should be noted that different antibodies were used in Figures 4.12a and 4.12b as the experiments were performed at different times. This may explain why a small amount of cleaved PARP is present in DHL4 control cells in Figure 4.12a, but not in Figure 4.12b.

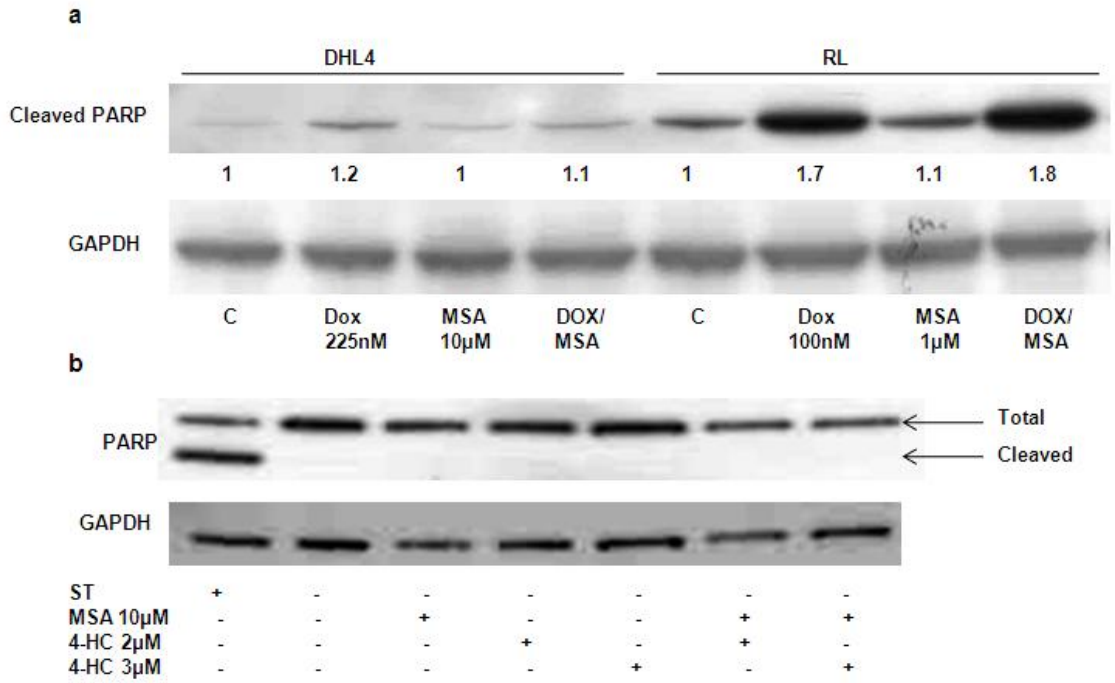

Figure 4.12 PARP cleavage in (a) RL and DHL4 cell lines exposed to MSA, doxorubicin or both for 48 hours. Densitometry values are shown. (b) DHL4 cells exposed to MSA, 4-HC or both for 48 hours. DHL4 cells exposed to staurosporine (ST) 1µmol/L for 6 hours were used as a positive control.

The effect of MSA on proteins involved in cell survival was investigated. Figure 4.13a shows that phosphorylation of Akt did not change in DHL4 and RL cells exposed to cytotoxic concentrations of MSA. Figure 4.13b shows that neither the phosphorylation of Erk1/2 nor Akt was altered in DHL4 or RL cell lines treated with synergistic combinations of MSA and doxorubicin.

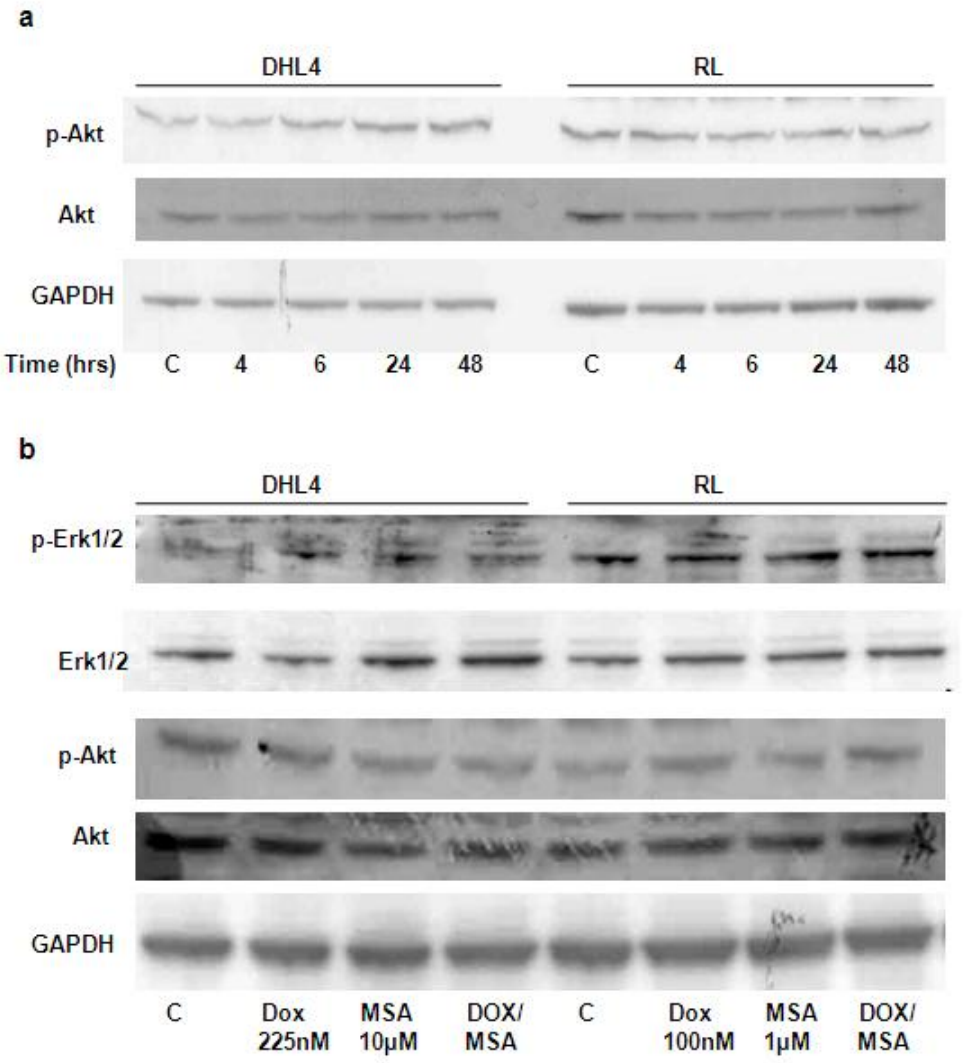

Figure 4.13 (a) p-Akt in DHL4 and RL cell lines exposed to MSA 60μmol/L and 5μmol/L respectively (b) p-Erk and p-Akt in RL and DHL4 cells exposed to MSA, doxorubicin or both for 48 hours.

The effect of chemo-sensitising and cytotoxic concentrations of MSA on the Bcl-2 family of proteins was investigated. Figure 4.14 shows that expression of the anti-apoptotic protein Bcl-2 was not clearly altered in either the RL or DHL4 cell line. In RL cells, the cytotoxic concentration of 5µmol/L increased the expression of the pro-apoptotic protein Bax but lower concentrations did not alter its expression. DHL4 cells are known not to express Bax protein (Strauss *et al*, 2007) however, 30µmol/L and 60µmol/L MSA did increase the expression of the pro-apoptotic protein Bak at 24 hours, with a further increase at 48 hours. In RL cells, the anti-apoptotic protein Mcl-1 was induced after exposure to 5µmol/L MSA for 24 hours but this decreased back to baseline by 48 hours. In DHL4 cells Mcl-1 was induced at all concentrations. With 30µmol/L and 60µmol/L MSA the increase was seen at 24 hours and returned to baseline by 48 hours but at 10µmol/L MSA the increase was sustained out to 48 hours.

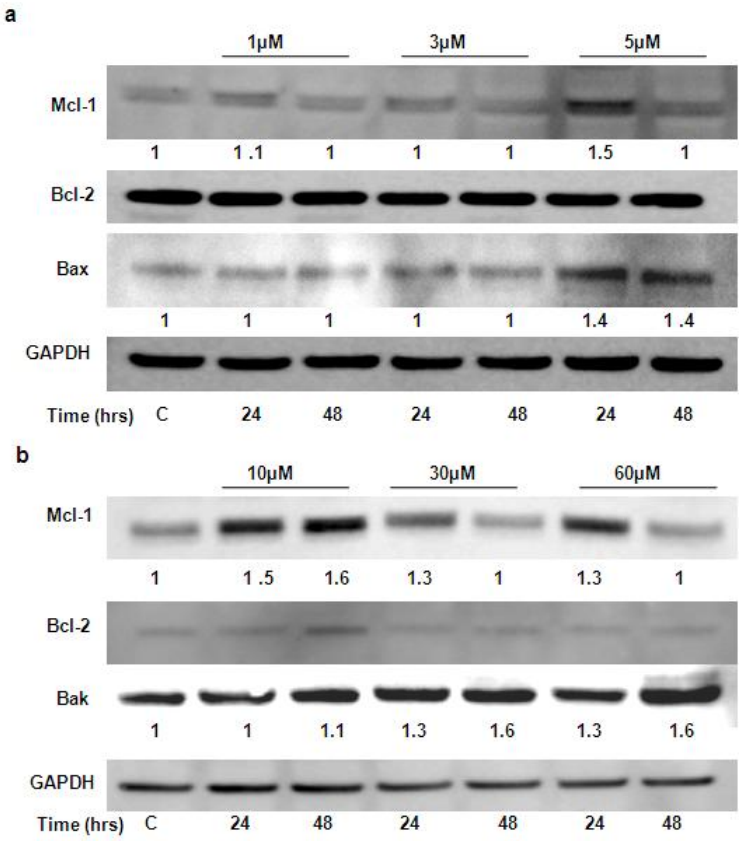

Figure 4.14 The effect of MSA on the expression of Bcl-2 family proteins. (a) RL and (b) DHL4 cell lines. Densitometry values are shown.

The effect of MSA on the expression of the anti-apoptotic protein survivin was also investigated. Figure 4.15 shows that in RL cells, survivin expression decreased in cells exposed to 5µmol/L MSA for 24 and 48 hours but lower concentrations did not alter its expression. In DHL4 cells, MSA resulted in a concentration and time-dependent decrease in survivin expression and this was seen as early as 4 hours and occurred at the chemo-sensitising concentration of 10µmol/L.

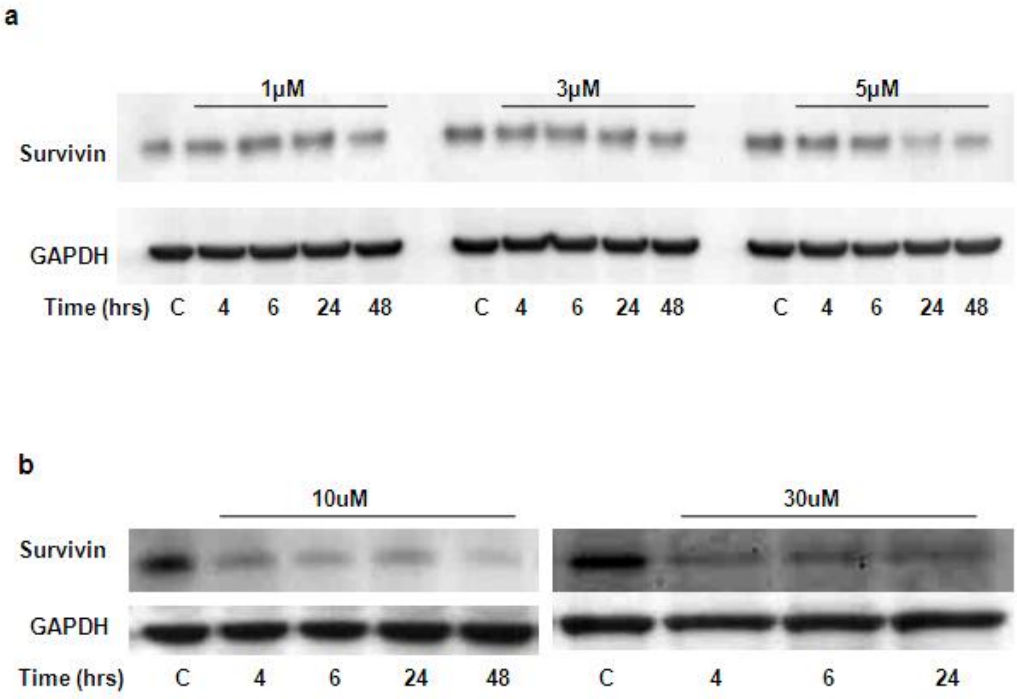

Figure 4.15 Survivin expression in (a) RL and (b) DHL4 cell lines exposed to MSA.

4.4.7 Effect of MSA on the p53 wild-type cell line JVM2

Studies have suggested that the effect of Se, mainly in the form of SLM, is dependent on the *p53* status of the cell (Goel *et al*, 2006). The cell lines studied so far all have mutations of the *p53* gene. Therefore, to investigate where the effect of MSA is also dependent on p53, the JVM2 cell line, which is *p53* wild-type, was studied. Figure 4.16 shows that the JVM2 cell line was sensitive to the cytotoxic effect of MSA, with an EC_{50} value (ATP assay) after 72-hour exposure of 3.4µmol/L (95% CI 3.1-3.9µmol/L).

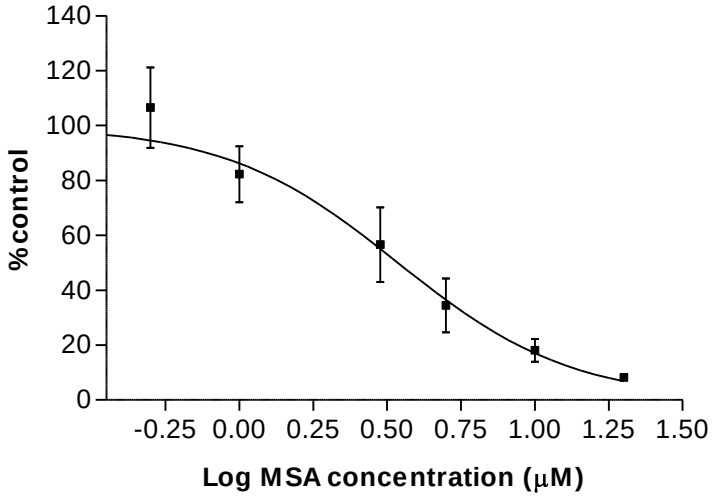

Figure 4.16 EC_{50} concentration-response curve following 72-hour exposure to increasing concentrations of MSA in the JVM2 cell line. Data points are the mean +/- SD of 8 separate experiments.

Cell cycle analysis was performed in JVM2 cells. Exposure to 3.4μmol/L MSA for 72 hours significantly increased the sub G1/apoptotic cell population (p=0.003). This was associated with a decrease in cells in all other cell cycle phases but without causing cell cycle arrest (Figure 4.17).

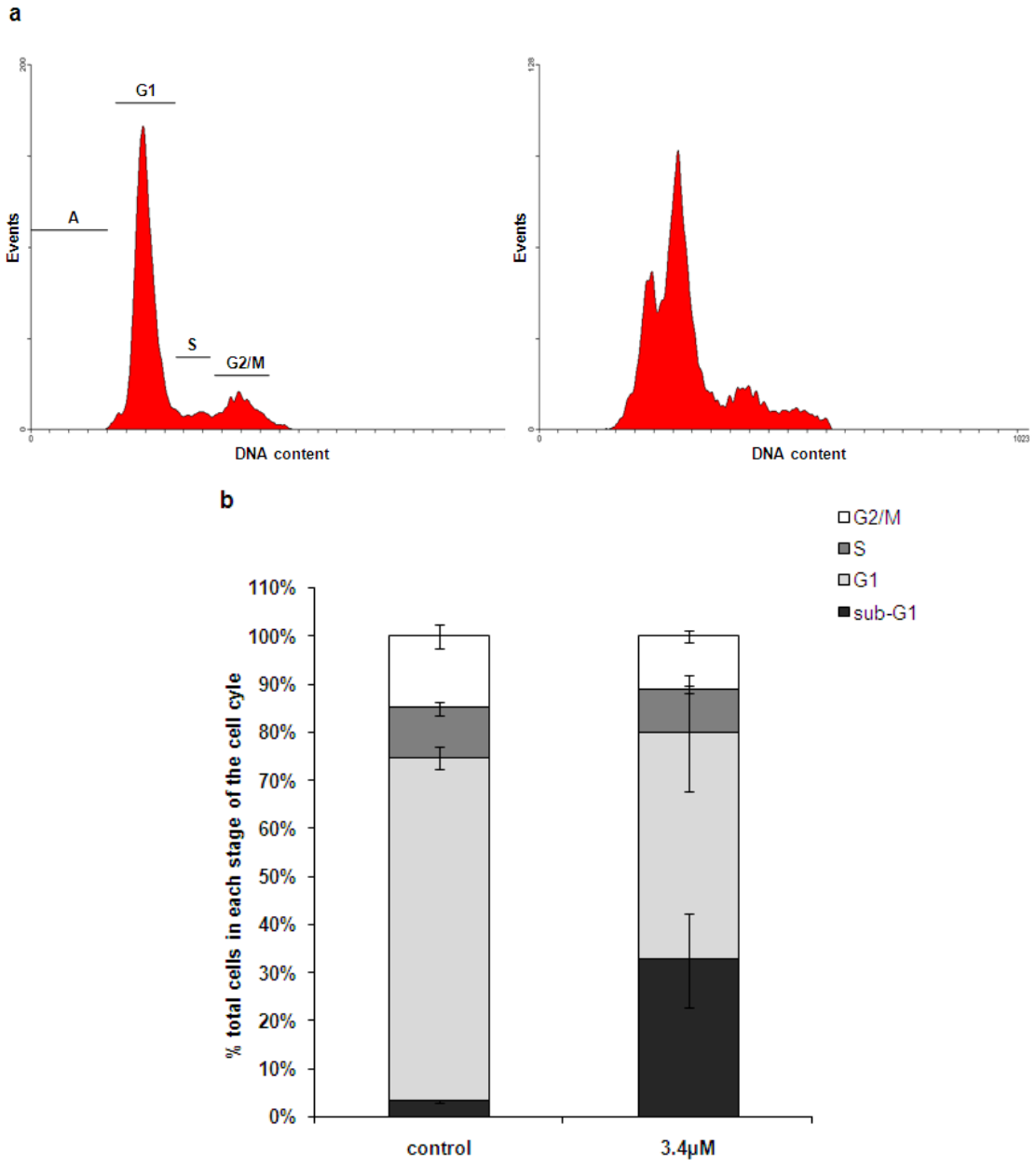

Figure 4.17 Cell cycle analysis of JVM2 cells exposed to 3.4µmol/L MSA for 72 hours. (a) Representative DNA histograms (b) Cell cycle distribution. Data points are the mean +/- SD of 3 separate experiments.

The effect of MSA on intracellular signalling pathways was studied. Figure 4.18a shows a concentration-dependent increase in PARP cleavage in JVM2 cells exposed to MSA confirming that apoptosis was induced. Staurosporine was used as a positive control. Unexpectedly, MSA decreased the expression of p53 and its downstream target p21 in a concentration-dependent manner (Figure 4.18b). This is in contrast to the RL and DHL4 cell lines, which have mutated *p53*, where MSA did not alter its expression (Figure 4.18c).

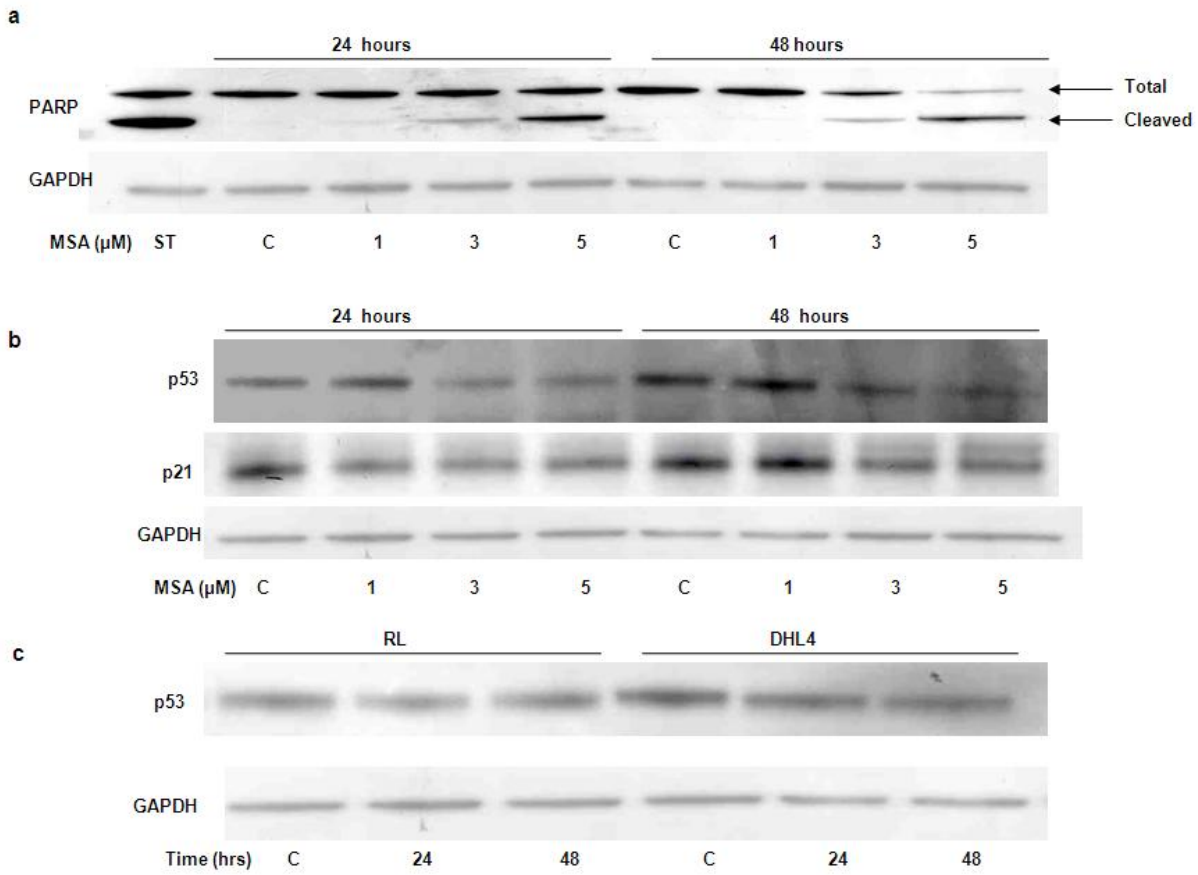

Figure 4.18 (a) PARP cleavage and (b) p53 and p21 expression in JVM2 cells exposed to MSA (c) p53 expression in RL and DHL4 cell lines exposed to MSA. Staurosporine (ST) 0.5μmol/L for 6 hours.

The induction of apoptosis was associated with concentration-dependent changes in the expression of Bcl-2 family proteins. Figure 4.19 shows that MSA increased the expression of the pro-apoptotic protein Bax and the anti-apoptotic protein Bcl-xL, whilst

decreasing the expression of the anti-apoptotic protein Mcl-1. The expression of Bcl-2 and Bak was not altered by exposure to MSA.

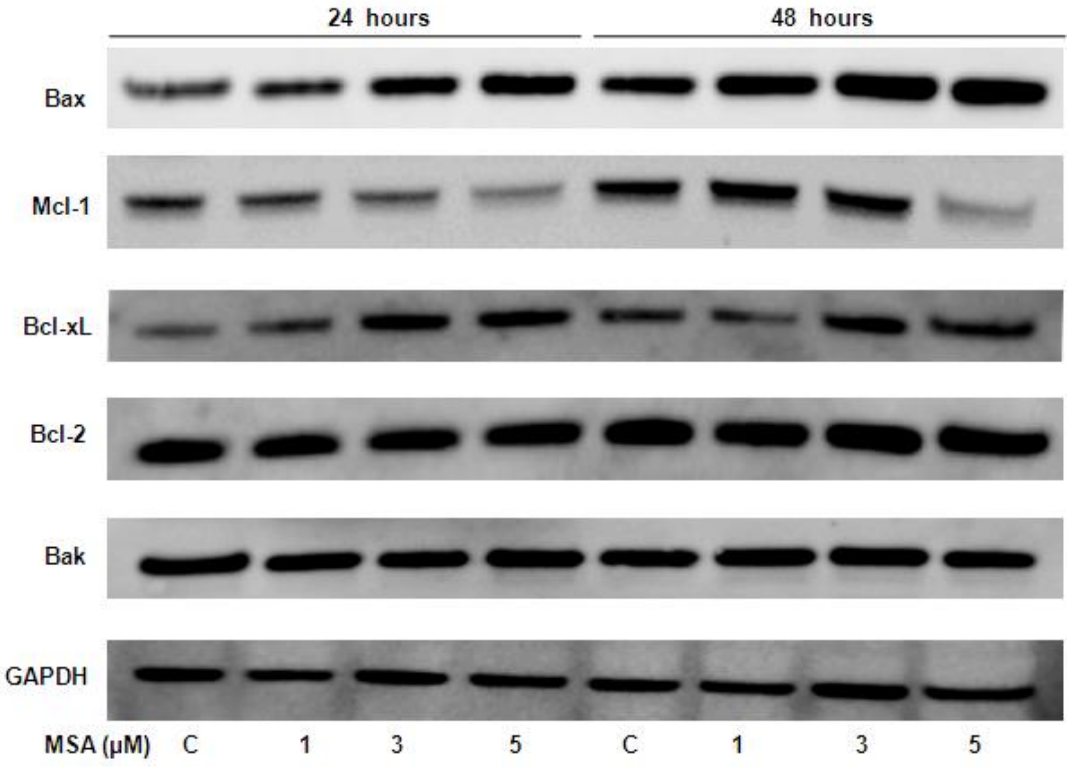

Figure 4.19 Expression of Bcl-2 family proteins in JVM2 cells exposed to MSA.

In order to confirm results in the RL and DHL4 cell lines that showed no effect of MSA on the phosphorylation of Akt, the 'Aktide assay', which was being developed in our laboratory, was used. This assay uses a synthetic Akt substrate peptide, RPRAAFT ('Aktide'), to quantify PI3K/Akt activity in whole cell extracts and has been described in Chapter 2 (section 2.13). Due to the relatively low basal levels of p-Akt in lymphoma cell lines, cells were exposed to 100μmol/L pervanadate for 30 minutes prior to exposure to a range of MSA concentrations (0.5-10μmol/L) for 30 minutes and 2 hours. Pervanadate is a phosphatase inhibitor that leads to the accumulation of phosphorylated proteins, thus activating kinases that are normally inactive in the de-phosphorylated state (Ruff *et al*, 1997). Thus, pervanadate is a potent activator of PI3K/Akt and increases the amount of p-Akt. The ability of MSA to inhibit this increase was investigated. Wortmannin 1μmol/L

was used as a positive control. Figure 4.20 shows that MSA was unable to inhibit the accumulation of p-Akt by pervanadate. Similar results were obtained by western blotting (Figure 4.21). Of note, the induction of p-Akt by pervanadate was less in the 2-hour MSA experiments compared to the 30-minute experiments, suggesting that the concentration used induced only a short term increase in p-Akt.

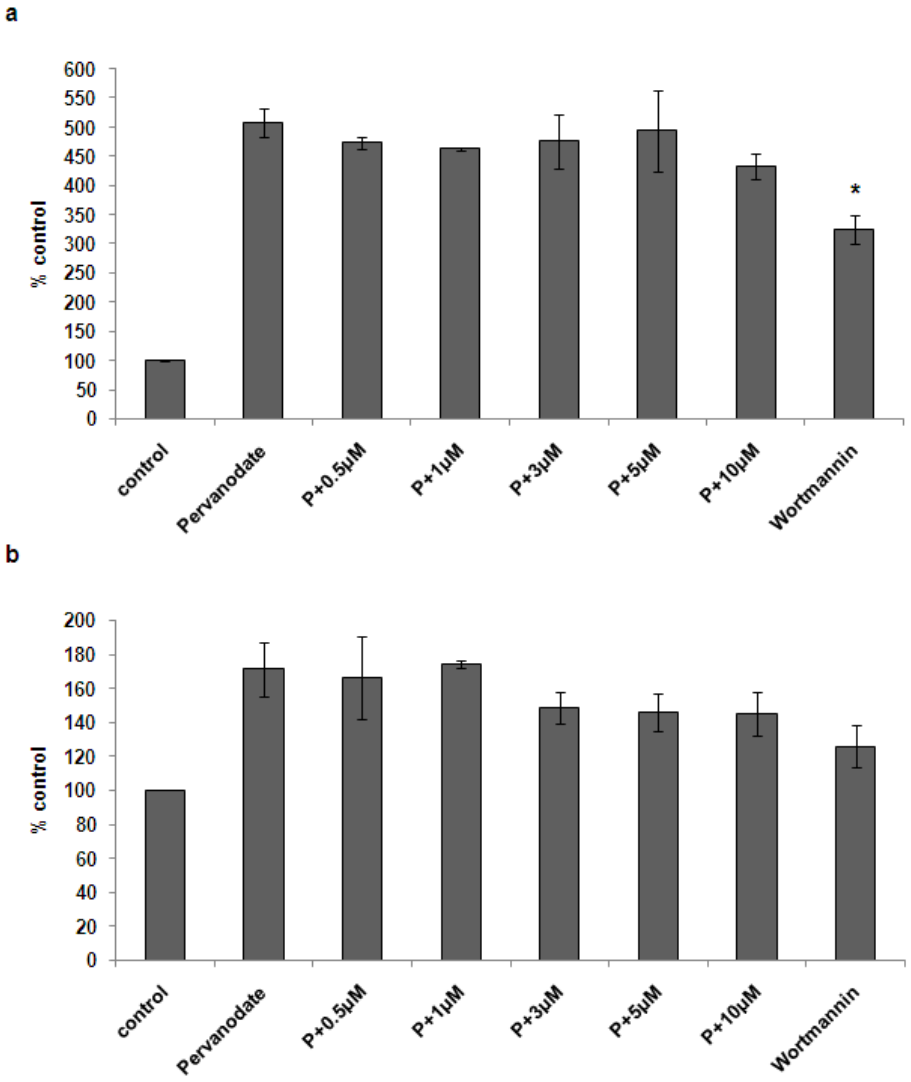

Figure 4.20 Aktide assay performed in JVM2 cells exposed to pervanadate (P) for 30 minutes followed by (a) MSA for 30 minutes, data points are the mean+/-SD of 3 separate experiments and (b) MSA for 2 hours, data points are the mean+/-SD of 2 separate experiments. *p=0.003 is a comparison with control using one way ANOVA followed by Tukey's test.

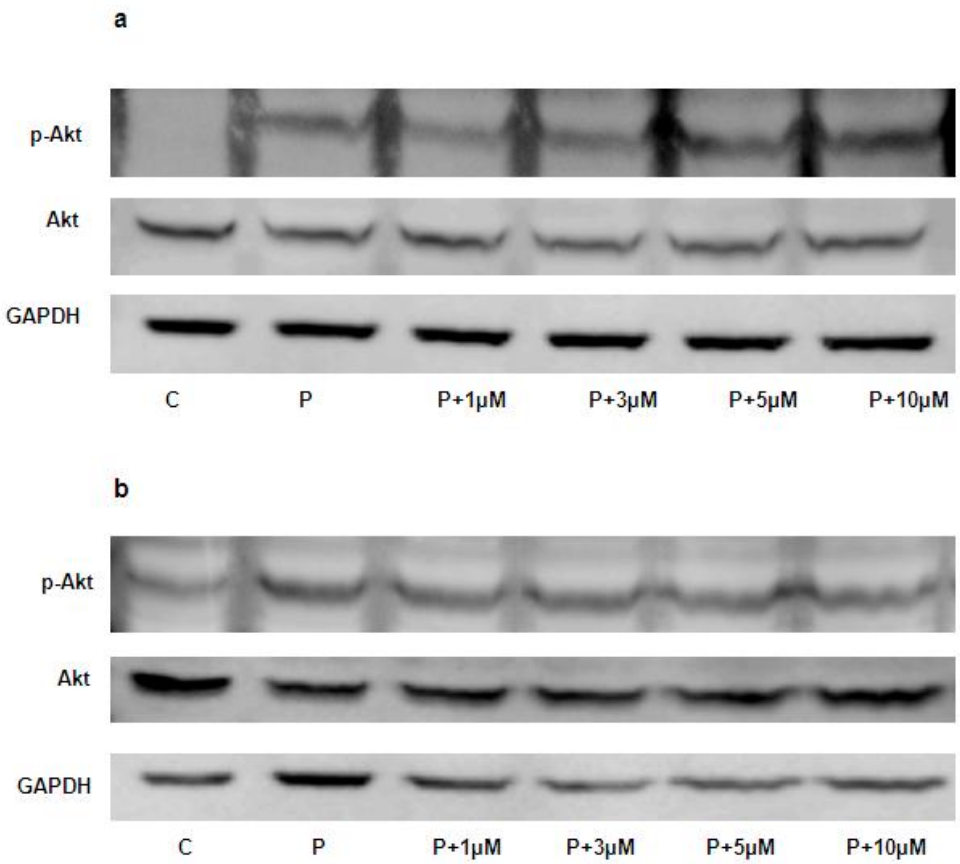

Figure 4.21 p-Akt in JVM2 cells exposed to pervanadate (P) for 30 minutes followed by (a) MSA for 30 minutes and (b) MSA for 2 hours.

4.4.8 The effect of MSA on doxorubicin uptake

To investigate whether MSA altered the uptake of cytotoxic drugs as an explanation for the observed synergy, the uptake of doxorubicin by RL and DHL cell lines with and without the addition of MSA was investigated after 24-hour exposure. Doxorubicin demonstrates auto-fluorescence and therefore can be detected by flow cytometry. Figures 4.22a and 4.23a show that exposure to increasing concentrations of doxorubicin for 24 hours in RL and DHL4 cell lines can be detected by flow cytometry. In RL and DHL4 cells, simultaneous exposure to doxorubicin and a chemo-sensitising concentration of MSA (1μmol/L and 10μmol/L respectively) did not alter the uptake of doxorubicin (Figures 4.22 and 4.23). In DHL4 cells, simultaneous exposure to doxorubicin 10nmol/L

and MSA 10µmol/L resulted in a consistently small, but statistically significant, increased uptake of doxorubicin. This was not apparent at higher doxorubicin concentrations. Figure 4.24 shows the increase in mean fluorescence intensity (MFI) relative to control.

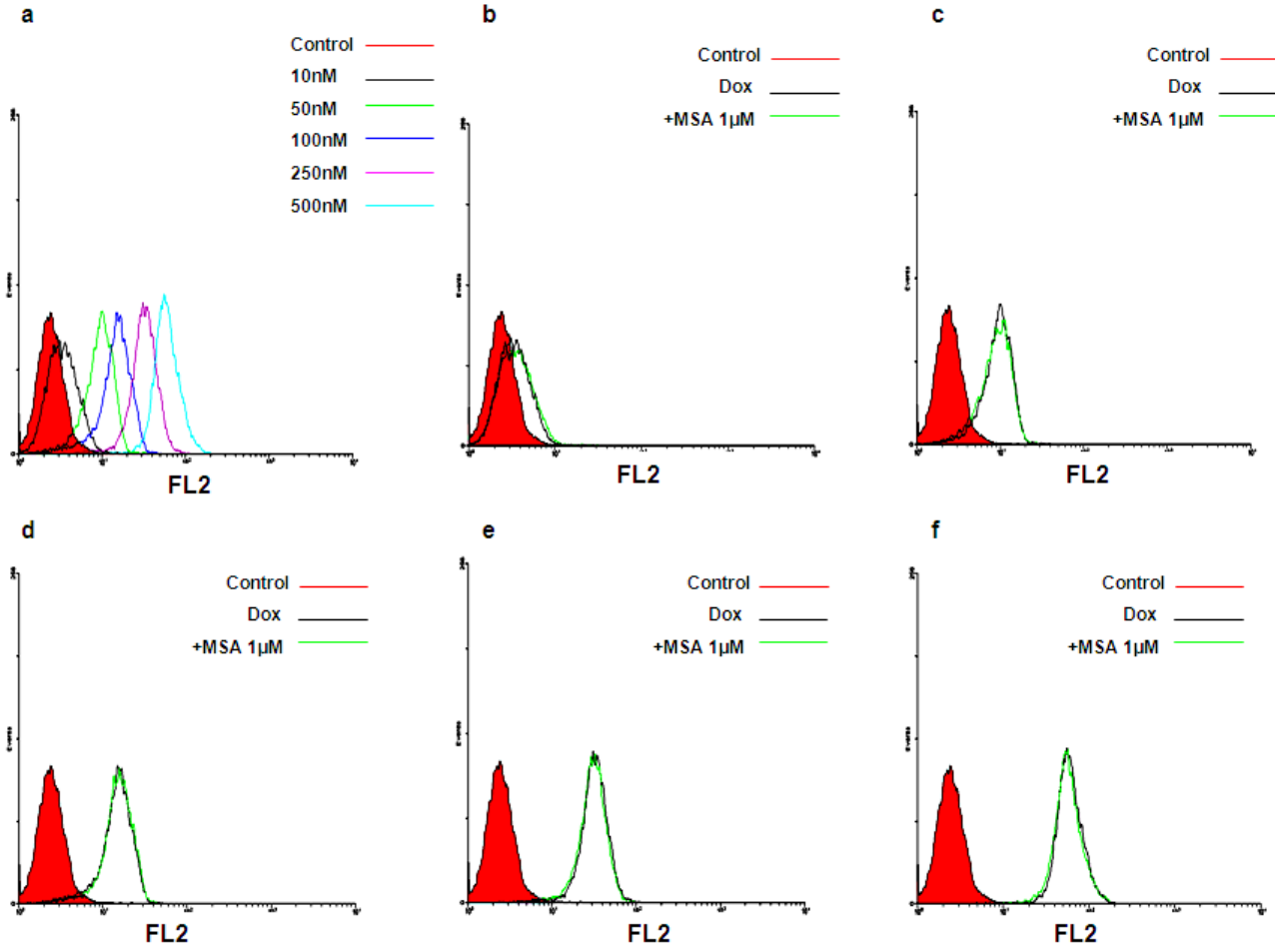

Figure 4.22 Representation histograms of RL cells exposed to doxorubicin (Dox) for 24 hours with and without simultaneous exposure to 1µmol/L MSA. (a) Increasing concentrations of doxorubicin alone, (b) Doxorubicin 10nmol/L, (c) Doxorubicin 50nmol/L, (d) Doxorubicin 100nmol/L, (e) Doxorubicin 250nmol/L, (f) Doxorubicin 500nmol/L.

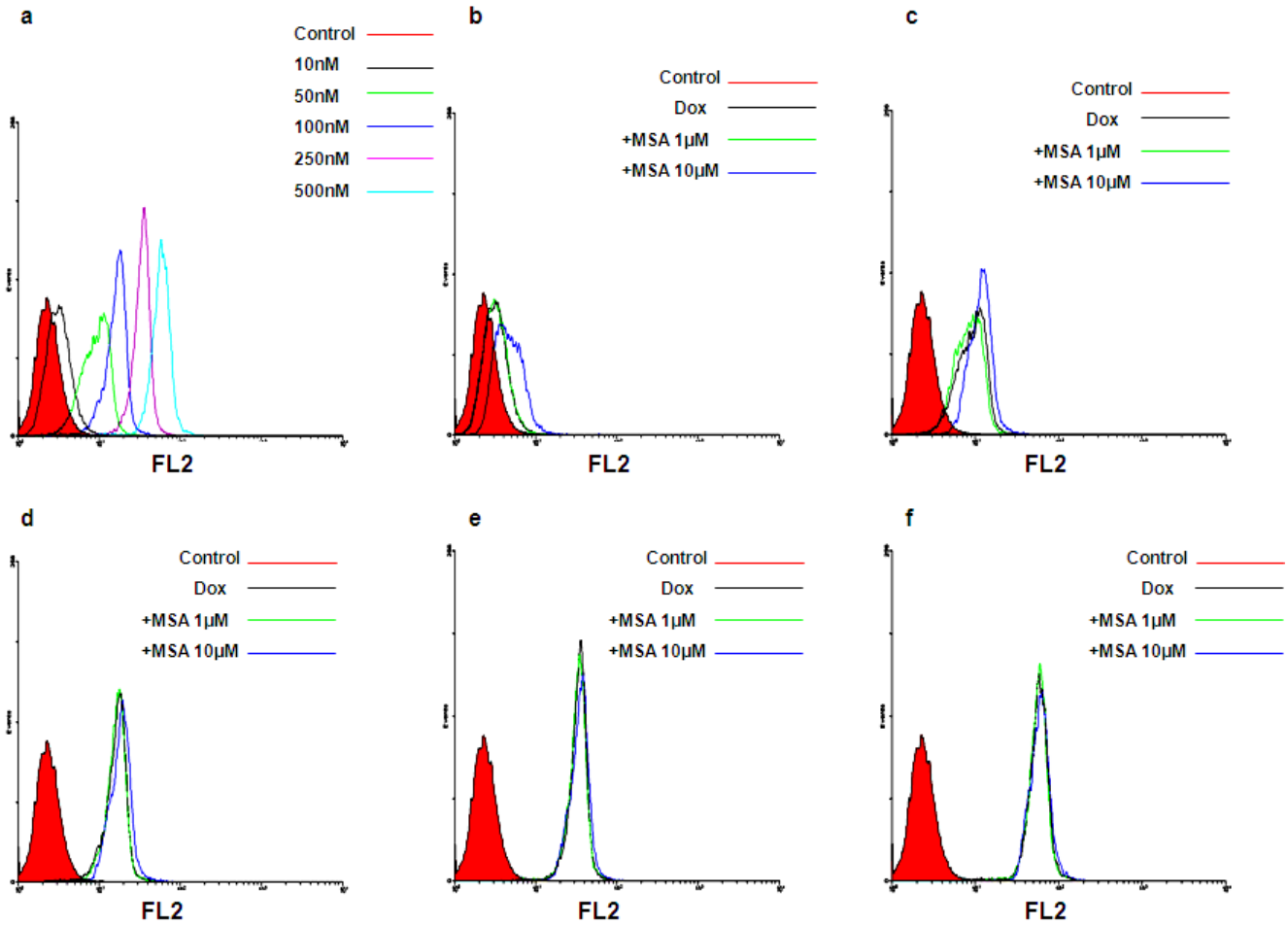

Figure 4.23 Representation histograms of DHL4 cells exposed to doxorubicin (Dox) for 24 hours with and without simultaneous exposure to 1µmol/L and 10µM MSA. (a) Increasing concentrations of doxorubicin alone, (b) Doxorubicin 10nmol/L, (c) Doxorubicin 50nmol/L, (d) Doxorubicin 100nmol/L, (e) Doxorubicin 250nmol/L, (f) Doxorubicin 500nmol/L.

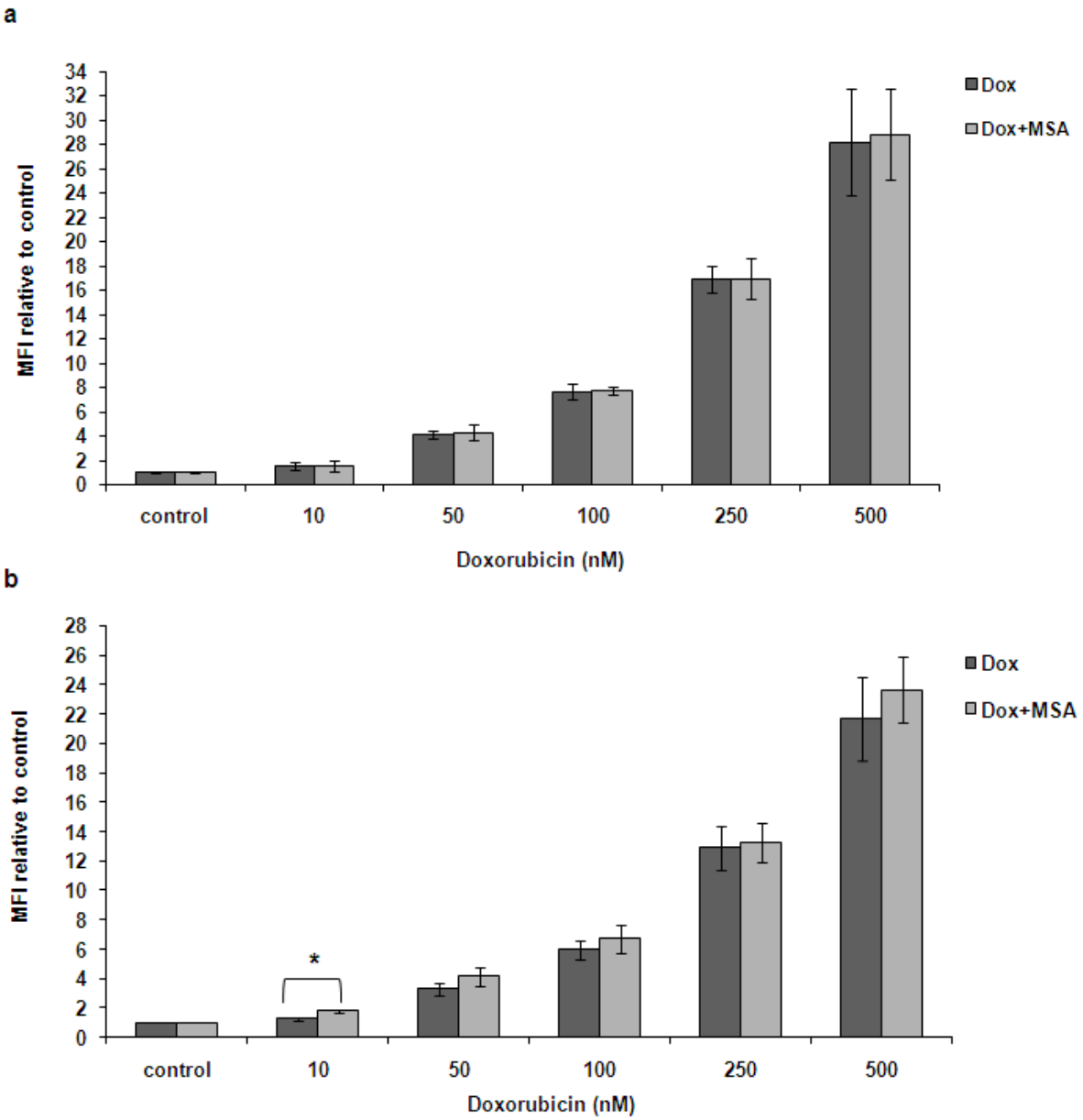

Figure 4.24 MFI in RL and DHL4 cell lines exposed to doxorubicin for 24 hours with and without simultaneous exposure to MSA (a) RL cells MSA 1µmol/L (b) DHL4 cells MSA 10µmol/L. *$p<0.05$.

4.4.9 The activity of methylselenocysteine in B-NHL cell lines

MSC is the Se compound to be used in the forthcoming clinical trial of Se supplementation in patients with DLBCL. Therefore the activity of MSC was investigated in 3 lymphoma cell lines; RL, DHL4 and JVM2. Cells were exposed to MSC

for 72 hours and cytotoxicity determined using the ATP assay. Figure 4.25 shows the concentration-effect curves and Table 4.2 the EC_{50} values

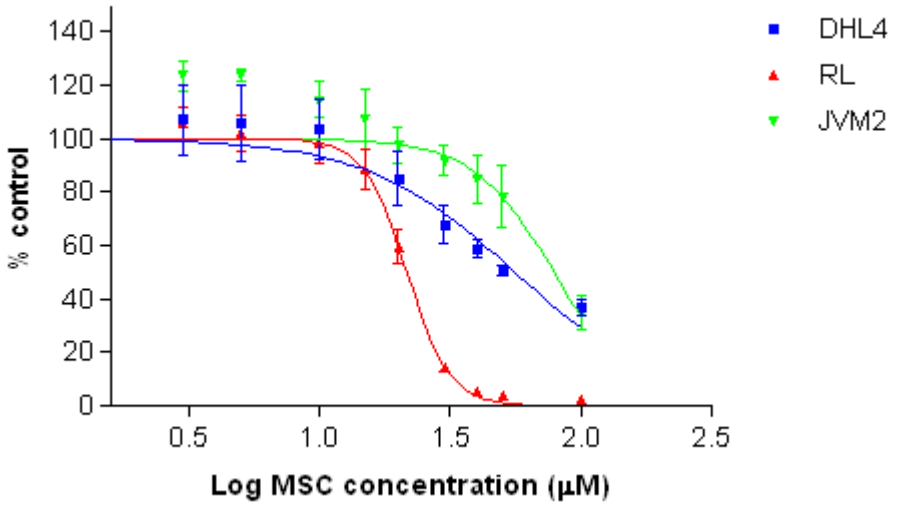

Figure 4.25 EC_{50} concentration-effect curves following 72-hour exposure to increasing concentrations of methylselenocysteine in 3 lymphoma cell lines using the ATP assay. Data points are the mean +/- SD of at least 4 separate experiments.

Table 4.2 EC_{50} values in 3 lymphoma cells lines exposed to methylselenocysteine for 72 hours

Cell line	EC_{50} (µmol/L)	95% CI
RL	21.6	20.6-22.6
DHL4	55.8	49.2-63.4
JVM2	79	65.7-95

As MSC is activated *in vivo* to methylselenol by β-lyase enzymes, the activity of MSC plus β-lyase was investigated. The enzyme L-methioninase was purchased from Wako Chemical USA, Inc (Richmond, VA) as this had previously been used in publications investigating the *in vitro* effect of MSC (Azrak *et al*, 2006). However, combining MSC

with previously published concentrations of L-methioninase (0.05 units/ml) did not alter the activity of MSC in the lymphoma cell lines (data not shown).

4.5 DISCUSSION

The cytotoxicity of MSA, through induction of apoptosis, has been reported in a number of different cancer cell lines and primary cancer samples including lymphoma (Jiang *et al*, 2001; Last *et al*, 2006). Here, the cytotoxicity of MSA in 4 DLBCL cell lines was confirmed using the ATP assay and, in keeping with previously published results, the cell lines differed in sensitivity. The reasons for this are not clear. Previous work has demonstrated that MSA does not result in the generation of ROS in DLBCL cell lines and therefore this is not a mechanism by which apoptosis is induced (Last *et al*, 2006). An alternative hypothesis studied in the experiments presented here was that apoptosis by MSA may be due to the generation of DNA damage and the extent may differ between sensitive and resistant cell lines. However, the results show that MSA does not induce DNA damage in either the RL or DHL4 cell lines as there was no increase in phosphorylation of histone H2AX. This is in keeping with previously published results in solid tumour cell lines where cytotoxic concentrations of MSA have not been associated with DNA damage (Ip *et al*, 2000).

Previously, it has been reported by our group that low non-toxic concentrations of MSA can enhance the cytotoxicity of chemotherapeutic agents in DLBCL cell lines (Juliger *et al*, 2007). Here, limited experiments were conducted to confirm these results before investigating additional potential mechanisms for the observed synergy. Thus, synergy was observed with the combination of doxorubicin and 1µmol/L MSA in RL cells and 4-HC and 10µmol/L MSA in DHL4 cells, confirming the published studies.

The effect of MSA on intracellular GSH was investigated for two reasons. Firstly, MSA has been reported to deplete intracellular GSH and increasing the intracellular GSH concentration, by treating cells with N-acetylcysteine, enhanced MSA-induced apoptosis suggesting that GSH was required as a co-factor for MSA-induced apoptosis (Shen *et al*,

2002). This is in keeping with the fact that MSA requires reduction by cellular thiols, including GSH, for conversion to its presumed active metabolite, methylselenol. However, data from our laboratory showed no effect of N-acetylcysteine on the activity of MSA (Last *et al*, 2006). Secondly, tumour cells have been found to have higher concentrations of GSH than non-tumour cells and high GSH concentrations have been associated with chemo-resistance (Friesen *et al*, 2004; Perry *et al*, 1993). In particular, some chemotherapeutic agents, including doxorubicin and cyclophosphamide, are inactivated by conjugation with GSH. Thus, GSH depletion by MSA could be responsible for its chemo-sensitising effect.

The results reported here show that basal GSH concentration in three DLBCL cell lines studied did not differ. MSA concentrations ≤20μmol/L did not alter the intracellular GSH concentration after 2-hour exposure. However, after 24-hour exposure there was a significant decrease in GSH concentration in both MSA-sensitive cell lines, RL and SUD4. This effect was not seen in the MSA-resistant cell line, DHL4. This suggests that sensitivity to MSA may be related to the degree of GSH depletion. However, GSH depletion was only seen at concentrations of 10μmol/L and 20μmol/L and the 72-hour EC_{50} of both SUD4 and RL cell lines is less than 10μmol/L; 7.7μmol/L and 3.9μmol/L respectively. Also, previous results from our laboratory did not observe an effect of increasing intracellular GSH levels on MSA activity. The reverse experiment of depleting intracellular GSH levels has not been performed and would be valuable. The MSA concentrations studied here were chosen because they are clinically relevant and in our forthcoming clinical trial the aim is to achieve a plasma Se concentration of 20μmol/l. Also, this range included the chemo-sensitising concentrations of 1μmol/L and 10μmol/L in MSA-sensitive and MSA-resistant cell lines respectively. It may, however, have been useful to study higher concentrations in the DHL4 cell line. In the study reporting the GSH-depleting effect of MSA in a hepatoma cell line, these cells were also relatively resistant to MSA and concentrations between 20μmol/L and 50μmol/L MSA were found to deplete intracellular GSH levels whereas MSA concentrations ≤10μmol/L MSA were found to increase GSH levels (Shen *et al*, 2002). The chemo-sensitising effect of MSA

cannot be explained by GSH depletion as concentrations of 1µmol/L in RL and SUD4 cells and 10µmol/L in DHL4 cells did not alter GSH concentration.

Studies in solid tumour cell lines and *in vivo* cancer models have reported that synergy between MSA and chemotherapeutic agents, is due to enhanced apoptosis (Hu *et al*, 2005a; Hu *et al*, 2008; Wu *et al*, 2009). Therefore, the induction of apoptosis by chemo-sensitising and cytotoxic concentrations of MSA in the RL and DHL4 cell lines was investigated. Cytotoxic concentrations of MSA were found to reduce the MMP, implicating the intrinsic apoptotic pathway in the cytotoxic effect of MSA. However, chemo-sensitising concentrations of MSA in both cell lines failed to alter the MMP, suggesting that MSA does not prime cells for apoptosis through this mechanism. PARP cleavage was studied as the end result of caspase-mediated apoptosis. In RL cells, PARP cleavage was apparent at the cytotoxic concentration of 5µmol/L but was also apparent at the chemo-sensitising concentration of 1µmol/L. However, when MSA and doxorubicin were combined the increase in cleaved PARP was only additive and not synergistic, suggesting that enhanced apoptosis is not the mechanism by which MSA sensitises RL cells to chemotherapy. In addition, PARP was cleaved in RL cells after exposure to 1µmol/L MSA but this concentration did not alter the MMP, suggesting that the extrinsic apoptotic pathway may also be important in the execution of apoptosis by MSA.

In DHL4 cells, the near EC_{50} concentration of 60µmol/L did not result in PARP cleavage even though similar concentrations resulted in decreased MMP. The lack of PARP cleavage in DHL4 cells may appear to be an unexpected result, however, when previous results published by our group are considered it is less so. By trypan blue exclusion, the DHL4 cell line was very sensitive to the cytostatic effect of MSA with an EC_{50} value at 72 hours of 1.7µmol/L, but very resistant to the cytotoxic effect of MSA with an EC_{50} value at 72 hours of 166µmol/L (Last *et al*, 2006). The ATP assay used here reflects both the cytostatic and cytotoxic effects of a drug and cannot distinguish between the two, thus the EC_{50} value at 72 hours of 76.6µmol/L is likely to reflect this fact. A synergistic combination of doxorubicin and 10µmol/L MSA resulted in a less than additive increase

in cleaved PARP and a synergistic combination of 4-HC and 10µmol/L MSA did not result in PARP cleavage. Thus, similar to the RL cell line, enhanced apoptosis does not appear to be the explanation for the observed synergy in DHL4 cells

Given that cytotoxic concentrations of MSA decrease the MMP, which occurs when the intrinsic apoptotic pathway is activated, changes in the expression of Bcl-2 family proteins were investigated. These proteins have both anti- and pro-apoptotic members, and the balance between them is integral in controlling the intrinsic apoptotic pathway. The synergistic interaction between MSA and cytotoxic agents has previously been reported to involve altered expression of Bcl-2 family proteins (Hu *et al*, 2008). The expression of the anti-apoptotic protein, Bcl-2, was much higher in the RL cell line compared with the DHL4 cell line, consistent with the fact that the RL cell line has the t(14;18) translocation. MSA, however, did not alter the expression of Bcl-2 in either cell line despite the fact that Bcl-2 is a downstream target of NF-κB, previously shown to be inhibited by MSA (Juliger *et al*, 2007; Tracey *et al*, 2005). In RL cells, the cytotoxic concentration of 5µmol/L MSA increased the expression of the pro-apoptotic protein Bax but lower concentrations did not. Bax is not expressed in the DHL4 cell line and therefore its expression was not studied (Strauss *et al*, 2007). In the DHL4 cell line, 30µmol/L and 60µmol/L MSA resulted in increased expression of the pro-apoptotic protein Bak at 24 hours and a further increase at 48 hours. In RL cells, Bak protein was not expressed (data not shown). The response of the anti-apoptotic protein, Mcl-1, differed between the 2 cell lines. In RL cells, 1µmol/L and 3µmol/L MSA had no effect on the expression of Mcl-1 but 5µmol/L MSA resulted in increased expression at 24 hours with a return to basal levels by 48 hours. In DHL4 cells, 10µmol/L MSA resulted in increased expression of Mcl-1 at 24 and 48 hours but 30µmol/L and 60µmol/L MSA only increased its expression at 24 hours with a return to basal levels by 48 hours.

Clearly, MSA does affect the expression of the Bcl-2 family of proteins but these effect seem to differ between the 2 cell lines. The expression of the pro-apoptotic proteins Bax and Bak in RL and DHL4 cells respectively are only increased at cytotoxic

concentrations of MSA and the anti-apoptotic protein Mcl-1 appears to be induced, mainly at 24 hours with a return to basal levels by 48 hours. Mcl-1 has a short half life of only a few hours and is degraded by the proteasome, hence it can be down-regulated rapidly in response to pro-apoptotic stimuli (Michels *et al*, 2005). It may be that Mcl-1 is induced by MSA at early time-points but once pro-apoptotic proteins are up-regulated, such as Bax in the RL cell line and Bak in the DHL4 cell line, it is rapidly degraded. In DHL4 cells exposed to 10μmol/L MSA, Mcl-1 expression increased at 24 hours and was sustained up to 48 hours, however, this concentration only resulted in a minimal increase in Bak expression which may not be enough to suppress Mcl-1 expression.

The effect of MSA on the phosphorylation of Akt and Erk1/2 was also investigated, as previous work in solid tumour cell lines have reported that cytotoxic and chemo-sensitising concentrations of MSA result in the de-phosphorylation of these two proteins, thus promoting cell death (Jiang *et al*, 2002; Li *et al*, 2007b). However, it appears that in the RL and DHL4 cell lines, neither cytotoxic nor chemo-sensitising concentrations of MSA de-phosphorylate Akt or Erk. Moreover, combining doxorubicin and MSA at synergistic concentrations did not alter the phosphorylation of Akt or Erk.

In contrast, the expression of the pro-survival protein, survivin was decreased by MSA. In the RL cell line, a cytotoxic concentration of 5μmol/L decreased survivin expression at 24 and 48 hours but lower concentrations did not. In DHL4 cell lines 10μmol/L and 30μmol/L MSA decreased the expression of survivin in a time- and concentration-dependent manner, and at an earlier time-point of 4 hours. These results are in keeping with previously published results in solid tumour cell lines that have reported decreased survivin expression by MSA and its role in chemo-sensitisation (Hu *et al*, 2008). Survivin is regulated by NF-κB and therefore these results are also in keeping with those already published by our group showing that 5μmol/L and 10μmol/L MSA inhibits the activity of NF-κB. However, down-regulation of survivin does not provide a universal explanation for the chemo-sensitising effect of MSA in DLBCL cell lines because in RL cells, 1μM MSA did not alter survivin expression. Further experiments investigating the expression

of survivin following the combination of synergistic concentrations of cytotoxic agents and MSA are needed to clarify the role of survivin in the chemo-sensitising effect of MSA.

The effect on survivin may be clinically relevant. Survivin is expressed in a large proportion of 'aggressive' B-cell lymphomas, with virtually no expression of this protein in 'small' B-cell lymphomas (Tracey *et al*, 2005). Around 60% of DLBCL cases express survivin and this has been associated with a lower OS. Survivin expression remained a prognostic factor in multivariate analysis and was independent of the IPI score (Adida *et al*, 2000). Therefore, survivin represents a rational therapeutic target in DLBCL, particularly since normal tissue does not express this protein.

To investigate the role of p53 in the action of MSA, the *p53* wild-type cell line, JVM2 was used. The JVM2 cell line was sensitive to the cytotoxic effect of MSA as determined by the ATP assay and has a very similar EC_{50} at 72 hours to the RL cell line. MSA induced apoptosis in this cell line as evidenced by PARP cleavage and an increase in the sub-G1 population with PI staining. However, MSA did not induce cell cycle arrest which is in keeping with results published in *p53*-mutated DLBCL cell lines where MSA did not affect cell cycle distribution (Last *et al*, 2006). This is in contrast, however, to a number of studies in solid tumour cell lines, in which MSA has been reported to induce G1 cell cycle arrest in association with altered expression of cell cycle regulatory proteins including p27, p21 and cyclin D1 (Jiang *et al*, 2002; Zhu *et al*, 2002). The cyclin-dependent kinase inhibitor, p21, appears to be particularly important in the G1 cell cycle arrest observed in prostate cancer cell lines as knocking-down its expression abolished the cell cycle arrest, albeit to different extents in the different cell lines tested. However, the induction of p21 was independent of p53 as the effect was apparent in *p53*-mutated cell lines (Wang *et al*, 2010).

The effect of MSA on p53 was further investigated by western blotting. It was anticipated that MSA would activate and thus increase the expression of p53 protein in keeping with

previous studies that have demonstrated p53 activation by organic Se compounds, such as SLM, in the absence of DNA damage (Goel *et al*, 2006; Seo *et al*, 2002a). Surprisingly, MSA decreased the expression of p53 in a concentration- and time-dependent manner and also decreased the expression of the down-stream protein, p21, suggesting that the induction of apoptosis in the JVM2 cell line is not dependent on functional p53 protein. The effect of MSA on the Bcl-2 family of proteins was studied in the JVM2 cell line and MSA induced a concentration- and time-dependent increase in the expression of the pro-apoptotic protein Bax but also increased the expression of the anti-apoptotic protein Bcl-xL. MSA decreased the expression of the anti-apoptotic protein Mcl-1 but had no effects on the expression of Bak or Bcl-2. Clearly, MSA alters the expression of Bcl-2 family proteins tipping the balance to apoptosis rather than survival but to better understand which proteins are crucial, knock-down and over-expression experiments are needed.

To further study the effect of MSA on Akt activity in lymphoma cell lines, 2 methods were used with JVM2 cells, the novel 'Aktide assay' and western blotting. The 'Aktide assay' measures the functional activity of Akt, based on the quantitative phosphorylation of a synthetic Akt peptide substrate. MSA, at concentrations up to 10μmol/L, was not able to inhibit the PI3K/Akt pathway at 30-minute or 2-hour exposure. Similar results were obtained by western blotting. In these experiments, phosphorylation of serine 473 was studied but full activation of Akt also requires phosphorylation at threonine 308. A study in a prostate cancer cell line found that MSA de-phosphorylated Akt as early as 1-hour post-exposure but the effect was greater at the threonine 308 site than the serine 473. It may be that in lymphoma cell lines MSA affects the threonine 308 site, however, the 'Aktide assay', which is an overall measure of Akt activity failed to demonstrate an inhibitory effect of MSA on the PI3K/Akt pathway (Wu *et al*, 2006).

Since these experiments were unable to demonstrate enhanced apoptosis as the mechanism by which MSA sensitises cells to cytotoxic agents, the effect of MSA on the uptake of doxorubicin was studied in RL and DHL4 cells. There has been an *in vivo* study published suggesting that the organo-Se compound MSC can improve the delivery

of doxorubicin to the site of tumours, mainly due to improved vascular functioning (Bhattacharya *et al*, 2008). The direct effect of Se on drug uptake *in vitro* has not been reported. The results reported here show that MSA does not alter doxorubicin uptake as determined by flow cytometry. A very small, but statistically significant, increased uptake with MSA 10μmol/L and doxorubicin 10nmol/L was not seen at higher doxorubicin concentrations.

The activity of MSC in three lymphoma cell lines was investigated, as MSC is the Se species to be used in the planned clinical trial. The EC_{50} at 72 hours ranged between 20μmol/L and 80μmol/L. These MSC concentrations were similar to those reported in solid tumour cell lines to inhibit cell growth and induce apoptosis (Ip *et al*, 2000; Yeo *et al*, 2002). The sensitivity of lymphoma cell lines to MSC did not correlate with sensitivity to MSA in that the JVM2 cell, which was very sensitive to MSA, was the most resistant of the three cell lines to MSC. Since metabolism of MSC by β-lyase enzymes is required to generate methylselenol, thought to be responsible for its anti-tumour effects, it is likely that the cell lines differ in β-lyase activity. This is addressed further in Chapter 9. Tumour cells are thought to have relatively low levels of β-lyase activity (Ip *et al*, 2000) and studies that have combined MSC with the β-lyase enzyme have induced cell death at lower concentrations (Azrak *et al*, 2006).

In summary, MSA is cytotoxic in a number of lymphoma cell lines but this cytotoxicity occurs in the absence of DNA damage and as previously reported, in the absence of ROS generation (Last *et al*, 2006). MSA, at cytotoxic concentrations, decreases MMP and affects the expression of Bcl-2 family proteins, although the pattern of changes differs between the cell lines. The reason for the difference in sensitivity between the cell lines is not clear but sensitive and resistant cell lines differ in their ability to deplete GSH in response to MSA. The synergy observed between non-toxic concentrations of MSA and chemotherapeutic agents cannot be explained by enhanced apoptosis and is not associated with effects on the Akt or Erk1/2 pathways. However, MSA does decrease the expression of survivin, which may be a downstream effect of the previously reported NF-κB

inhibition (Juliger *et al*, 2007). The effect of MSA appears to be independent of p53, as in the *p53* wild-type cell line JVM2, both p53 and its downstream target p21, were down-regulated. In addition, MSA does not alter the uptake of doxorubicin by DLBCL cell lines.

CHAPTER 5: Cellular stress induction by methylseleninic acid

5.1 INTRODUCTION

It has been demonstrated that Se induces protein misfolding, a form of cellular stress, which results in ER stress and activation of the UPR. This has been extensively discussed in Chapter 1 (section 1.3.9.11). With regards to Se in the form of MSA, induction of ER stress has been reported to be a mechanism by which high concentrations induce apoptosis (Wu *et al*, 2005; Zu *et al*, 2006) whilst non-toxic concentrations sensitise cells to chemotherapy (Wu *et al*, 2009). ER stress induction and activation of the UPR has recently been recognised as an important mechanism by which other anti-tumour agents, such as bortezomib and HSP90 inhibitors, promote tumour cell death (Davenport *et al*, 2007; Obeng *et al*, 2006). However, activation of the UPR is primarily a survival response and it is only when the cellular stress cannot be resolved that the cell undergoes apoptosis. The precise mechanism by which the cell switches from a pro-survival response to apoptosis has not been fully elucidated (Szegezdi *et al*, 2006). Recently, there has been some doubt cast about the mechanistic role of ER stress induction in the action of Se *in vivo*. In a mammary cancer model and a prostate cancer xenograft model, MSA, MSC and selenite were all able to inhibit tumour growth and induce apoptosis but this occurred in the absence of markers of ER stress (Jiang *et al*, 2009). Thus, further work is required to establish the role of Se-induced ER stress *in vivo*.

There are two main cellular protein degradation pathways that are activated by ER stress; the ubiquitin-proteasome pathway and autophagy. The process of autophagy has been discussed in Chapter 1 (section 1.3.9.12) and is generally considered to be a pro-survival pathway, but in the face of excessive cellular stress autophagy can result in cell death (Levine & Kroemer, 2008). The role of autophagy in cancer is complicated and both the induction and inhibition of autophagy has been reported to promote tumour cell death (Lambert *et al*, 2008; Zhu *et al*, 2010). There are little published data describing the effect of Se on autophagy, but it appears that the role of autophagy in the action of Se

differs between cell types. The effect of organic Se compounds on autophagy has not been investigated (Kim *et al*, 2007b; Ren *et al*, 2009).

The hypothesis being tested in the experiments described in this chapter is that Se, in the form of MSA, sensitises DLBCL cell lines to chemotherapeutic agents through the induction of ER stress.

5.2 AIMS

1) To investigate whether MSA induces protein misfolding and ER stress in DLBCL cell lines.
2) To investigate the consequences of ER stress induction.
3) To investigate whether ER stress induction is a mechanism by which MSA sensitises DLBCL cell lines to chemotherapy.

5.3 MATERIALS AND METHODS

The effects of non-toxic, chemo-sensitising and cytotoxic concentrations of MSA were investigated in the RL and DHL4 cell lines in time-course experiments. In RL cells this was 1μmol/L (chemosensitising), 3μmol/L and 5μmol/L (cytotoxic) MSA and in DHL4 cells this was 10μmol/L (chemo-sensitising), 30μmol/L and 60μmol/L (cytotoxic) MSA. Western blotting was used to investigate protein changes (Chapter 2, sections 2.4 and 2.5) and real-time PCR to investigate mRNA expression (Chapter 2, section 2.10). To investigate the process of autophagy, immunofluorescence for LC3 protein was performed (Chapter 2, section 2.11). In addition, cells were stained with AO and the formation of acidic vesicular organelles was quantified by flow cytometry (Chapter 2, section 2.12).

5.4 RESULTS

5.4.1 Induction of endoplasmic reticulum stress in RL and DHL4 cell lines exposed to MSA

To establish whether MSA induced protein misfolding, the expression of the enzyme PDI was examined. This family of enzymes catalyses protein folding through the formation of disulphide bonds and their expression is induced in response to protein misfolding, to increase the protein folding capacity of the ER (Ellgaard & Ruddock, 2005). Figure 5.1 shows that in RL cells, 1µmol/L MSA did not induce PDI expression, but induction was seen with 3µmol/L and 5µmol/L MSA at both 24- and 48-hour exposures. In DHL4 cells, 10-60µmol/L MSA induced a concentration-dependent increase in PDI expression at 24 and 48 hours.

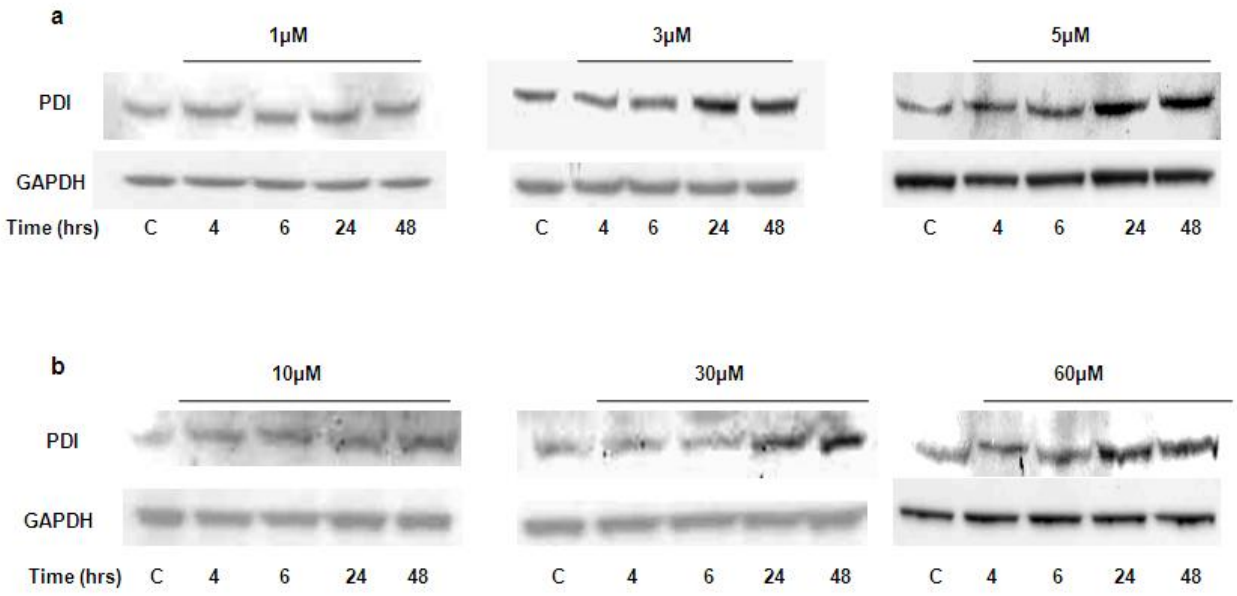

Figure 5.1 PDI expression in (a) RL and (b) DHL4 cell lines exposed to MSA.

To investigate whether protein misfolding induced ER stress, the expression of GRP78 was studied. In general, both the RL and DHL4 cell lines showed basal expression of GRP78 although there was some variability between experiments. Figure 5.2 shows that in RL cells, MSA induced GRP78 in a concentration-dependent manner. 1µmol/L MSA

resulted in only a minimal increase in GRP78 expression but 3µmol/L and 5µmol/L MSA resulted in a more obvious increase, which occurred early at 4 hours, was maximal at 6 hours and then decreased by 24 and 48 hours. 10µmol/L MSA resulted in a more sustained increase in GRP78 expression, which was maximal by 24 hours and remained at this level out to 48 hours.

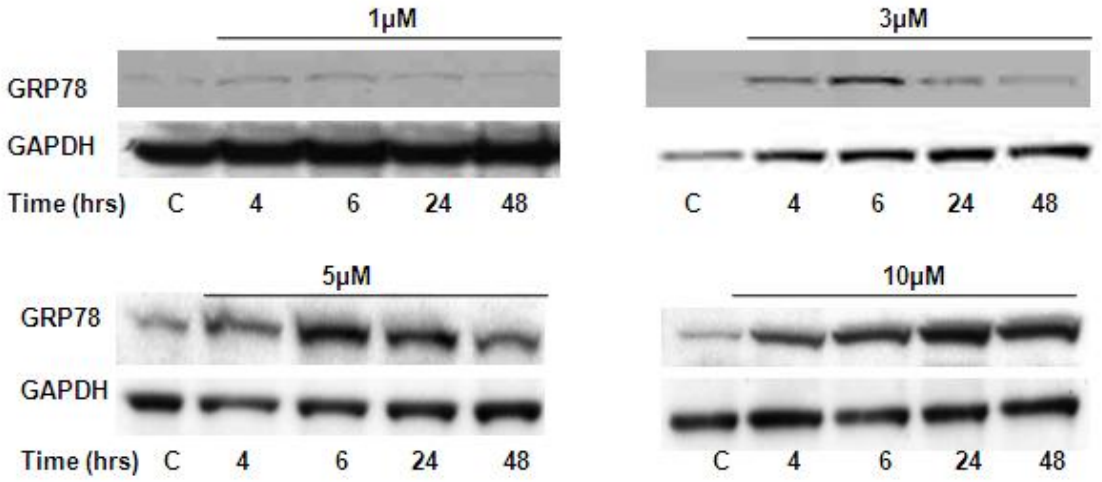

Figure 5.2 GRP78 expression in RL cells exposed to MSA.

Figure 5.3 shows that in DHL4 cells, MSA also resulted in a concentration-dependant increase in GRP78 expression which was seen as early as 4 hours. At low MSA concentrations (1-5µmol/L), the induction was greater than that seen in the RL cell line. GRP78 induction was maximal at 6 hours, and then decreased by 24-48 hours. With higher MSA concentrations of ≥10µmol/L, expression of GRP78 continued to increase with exposure time and was maximal by 24 hours remaining at this level out to 48 hours. The induction of GRP78 plateaued, with 10µmol/L, 30µmol/L and 60µmol/L MSA producing a similar effect.

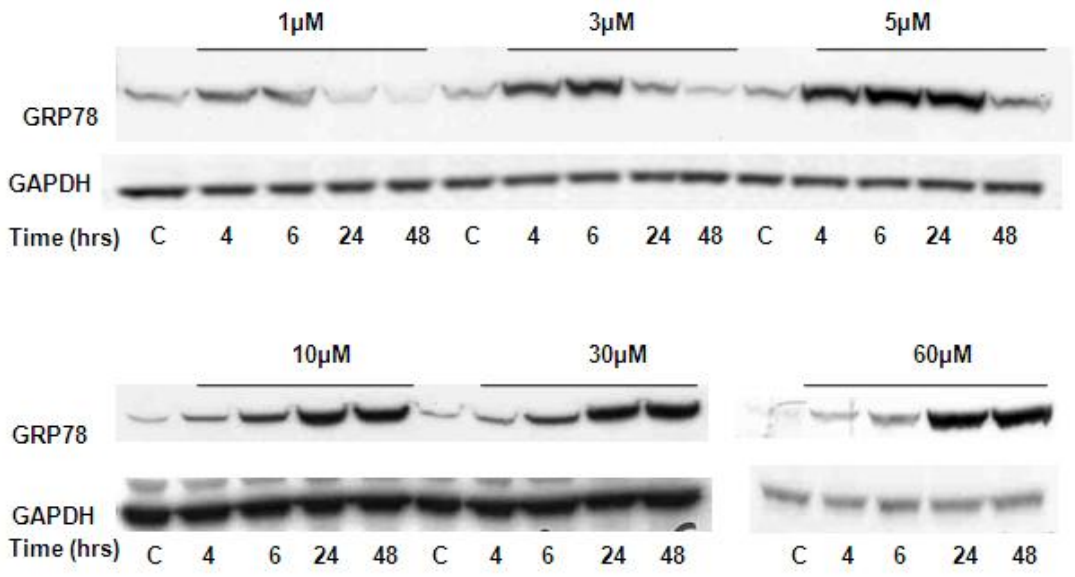

Figure 5.3 GRP78 expression in DHL4 cells exposed to MSA.

Protein misfolding activates UPR signalling, a consequence of which is activation of PERK and phosphorylation of eIF2α. Phosphorylation of eIF2α was studied in the RL and DHL4 cell lines exposed to MSA. Figure 5.4 shows that in RL cells, there was increased phosphorylation of eIF2α, which was concentration-dependent and maximal at 6-24 hours' exposure. This was due to an increase in the phosphorylation state of the protein rather than a general increase in eIF2α, as the increase was apparent when p-eIF2α was expressed relative to total eIF2α. Although the magnitude of this effect was variable, a similar trend was seen in a replicate experiment (Figure 5.4b).

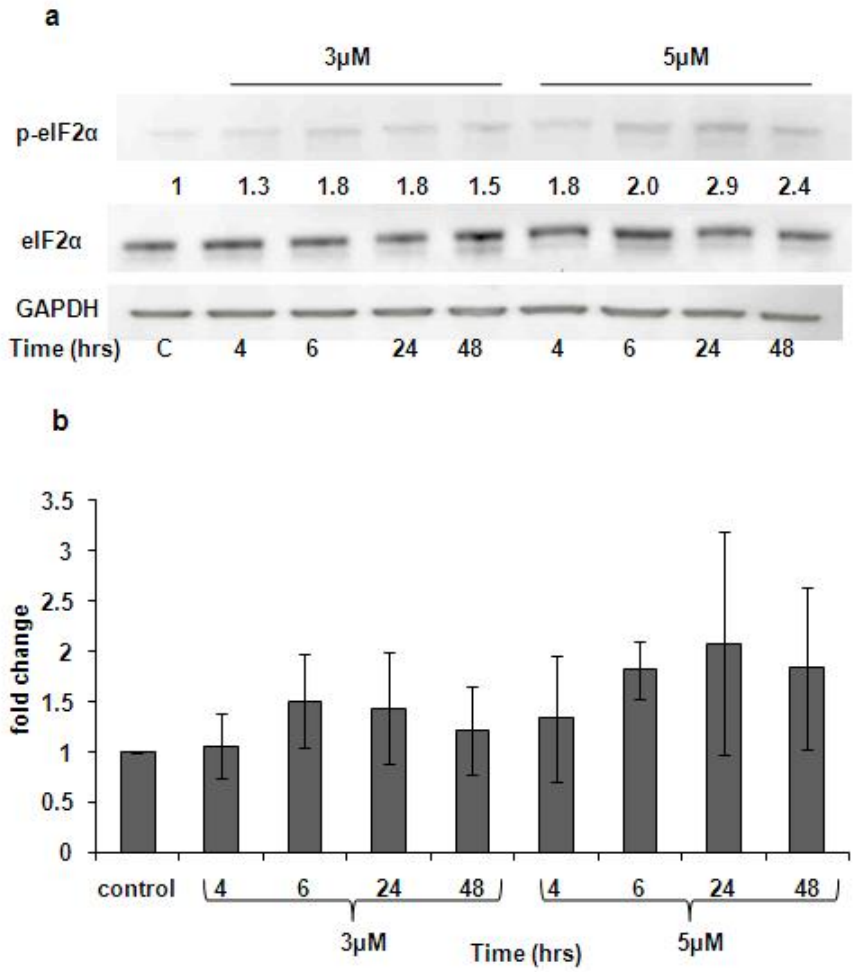

Figure 5.4 p-eIF2α in RL cells exposed to MSA. (a) Western blot with fold-change corrected to total eIF2α expression (b) Densitometry analysis corrected to total eIF2α expression. Data points are the mean+/- SD of two separate experiments.

DHL4 cells had a higher basal level of phosphorylated eIF2α compared to RL cells. In contrast to the results shown in Figure 5.4 with RL cells, in DHL4 cells there was a clear decrease in eIF2α phosphorylation, and possibly total eIF2α, which was maximal by 4-6 hours, followed by a return towards basal levels by 24-48 hours (Figure 5.5).

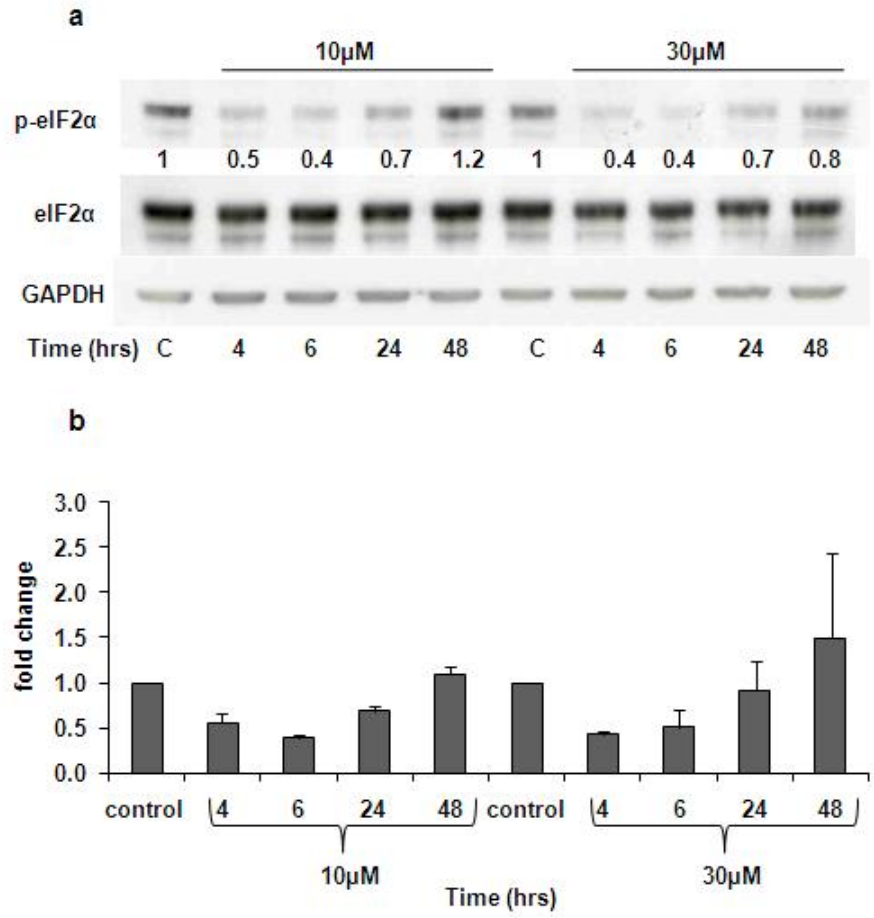

Figure 5.5 p-eIF2α in DHL4 cells exposed to MSA. (a) Western blot with fold-change corrected to total eIF2α expression (b) Densitometry analysis corrected to total eIF2α expression. Data points are the mean+/- SD of two separate experiments.

5.4.2 Endoplasmic reticulum stress-induced apoptosis

To investigate whether MSA resulted in ER-stress mediated apoptosis, expression of the pro-apoptotic gene GADD153 was studied. Despite many attempts and numerous antibodies, the expression of GADD153 in cells treated with MSA was not detected by western blotting (data not shown). However, induction of GADD153 by MSA has been demonstrated in solid tumour cell lines and therefore expression at the mRNA level was investigated by real-time PCR. Figures 5.6 and 5.7 show that MSA resulted in a concentration-dependent increase in GADD153 mRNA expression. Figure 5.6 shows that

in RL cells, the chemo-sensitising concentration of 1µmol/L MSA did not increase GADD153 mRNA expression but 5µmol/L MSA resulted in a significant increase at 4- and 6-hour exposure, which then decreased to baseline by 24-48 hours. Figure 5.7 shows that in DHL4 cells, there was a similar pattern of increased expression at 5µM MSA but higher concentrations (10-60µmol/L) resulted in further significant increases in expression of GADD153. A plateau in effect occurred at 30µmol/L with a maximal increase at 48 hours. There was no significant difference between the means for cells exposed to 30µmol/L and 60µmol/L MSA for 48 hours (p=0.5).

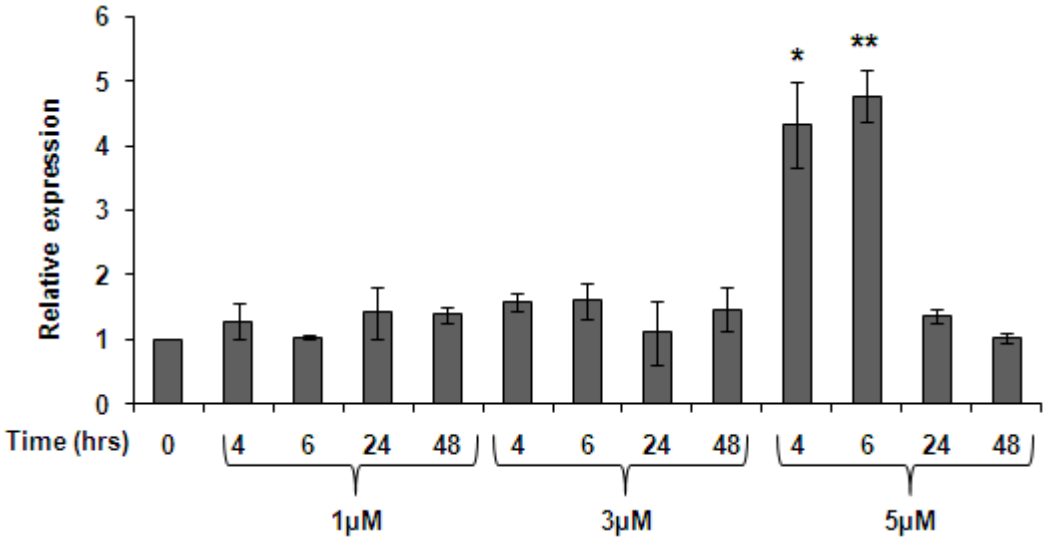

Figure 5.6 Real-time PCR for GADD153 mRNA in the RL cell line. *p=0.02, **p=0.006. Data points are the mean +/- SDs of three separate experiments. p values are a comparison with control.

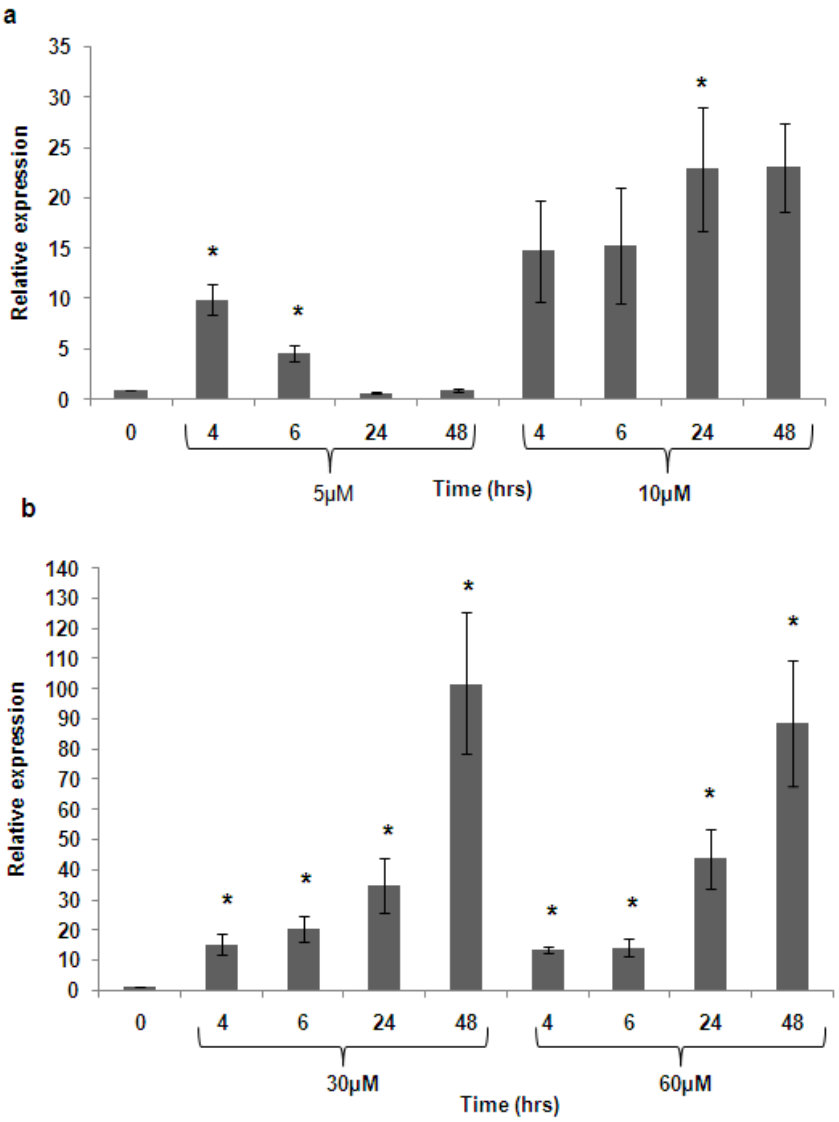

Figure 5.7 Real-time PCR for GADD153 mRNA in the DHL4 cell line (a) MSA 5μmol/L and 10μmol/L (b) MSA 30μmol/L and 60μmol/L. *p<0.05. Data points are the mean +/- SDs of three separate experiments except for 10μmol/L 48 hours, which is the mean+/-SD of 2 data points. p values are a comparison with control.

To establish whether the increase in GADD153 mRNA expression was associated with pro-apoptotic signalling at the protein level, Bcl-2 expression, phosphorylation of Jnk and PARP cleavage were studied. Staurosporine (ST), a known inducer of apoptosis, was used as a positive control for PARP cleavage. In both the RL (Figure 5.8) and DHL4

(Figure 5.9) cell lines, expression of Bcl-2 and phosphorylation of Jnk was not altered by MSA at concentrations that resulted in increased GADD153 expression. In RL cells, PARP was cleaved at concentrations as low as 1µmol/L and 3µmol/L, which did not alter GADD153 expression. Therefore, induction of apoptosis in RL cells was independent of ER stress-induced pro-apoptotic signalling. In DHL4 cells, PARP was not cleaved up to concentrations of 60µmol/L MSA.

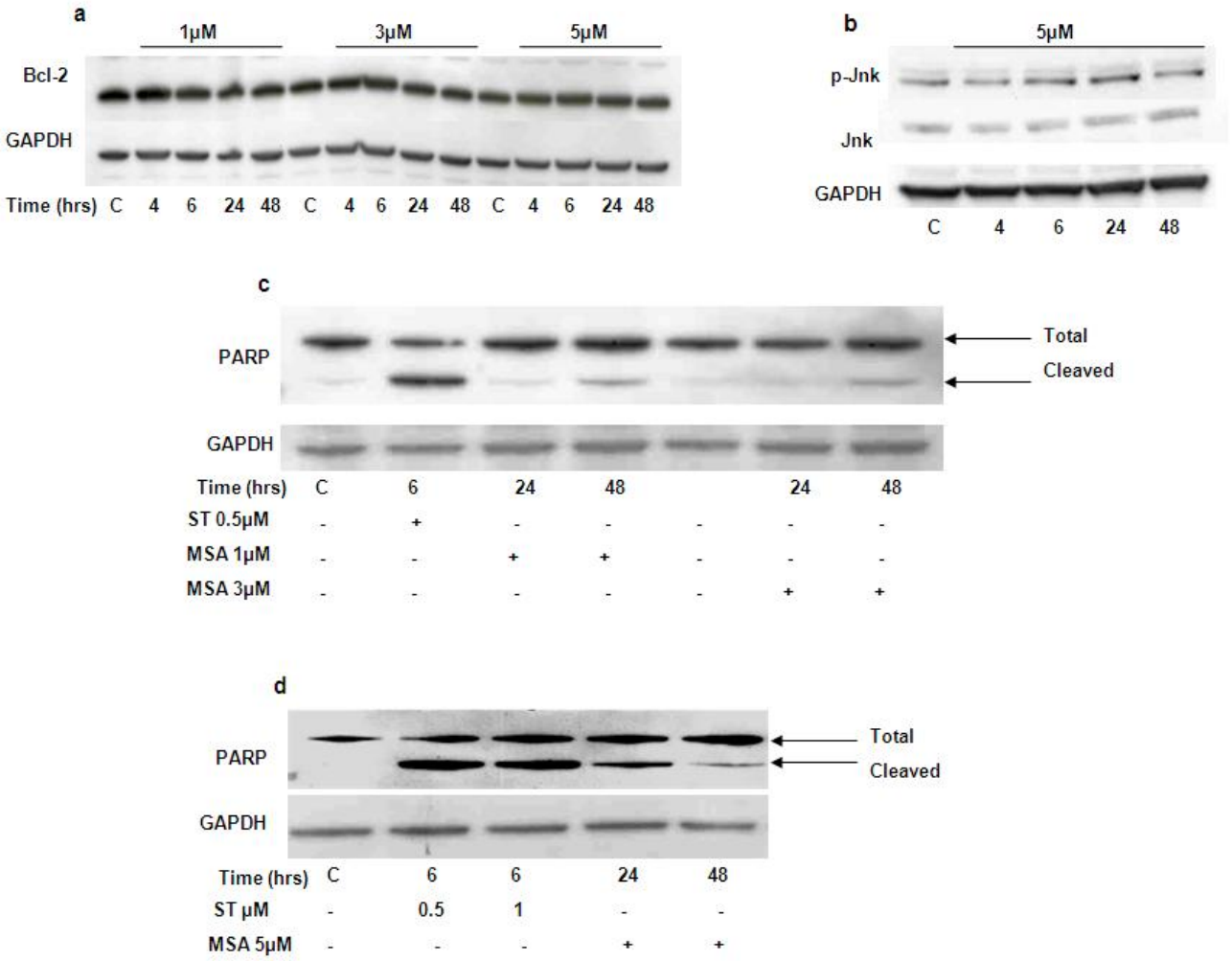

Figure 5.8 Pro-apoptotic signalling in the RL cell line exposed to MSA. (a) Bcl-2 expression (b) p-Jnk (c) and (d) PARP cleavage (as shown in Chapter 4, Figure 4.11, and repeated here). Cells exposed to staurosporine (ST) were used as a positive control.

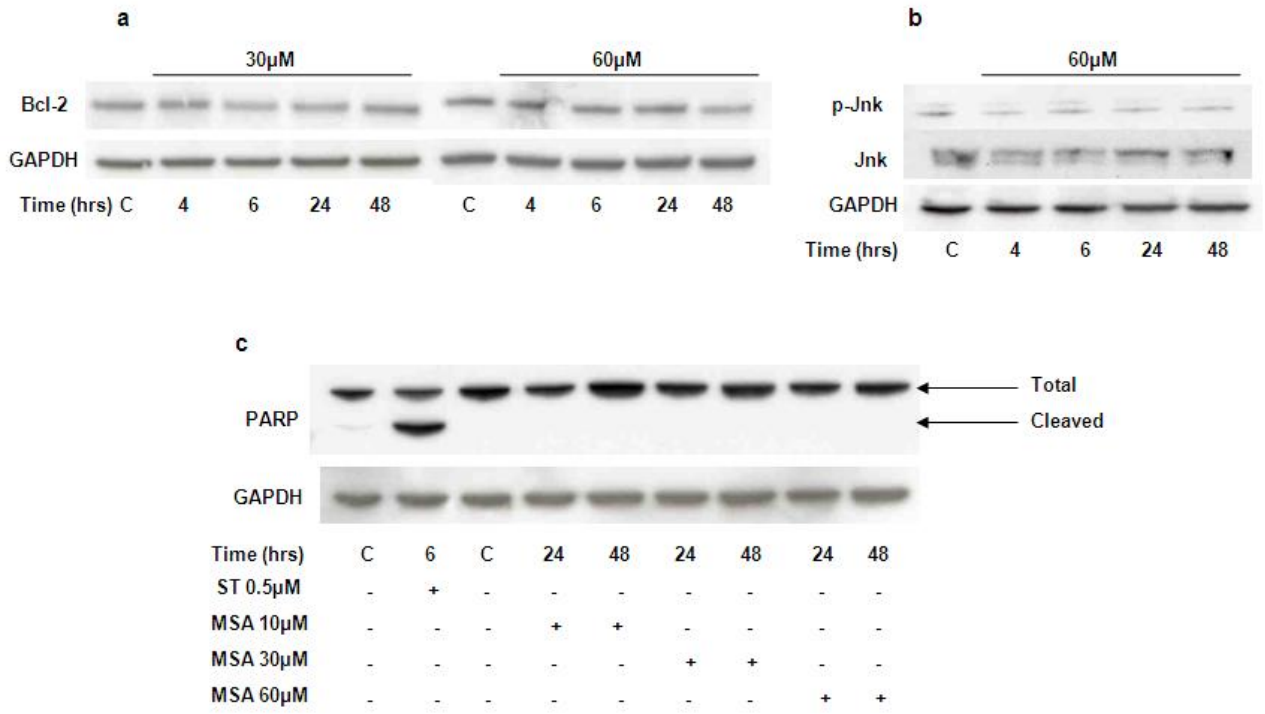

Figure 5.9 Pro-apoptotic signalling in the DHL4 cell line exposed to MSA. (a) Bcl-2 expression (b) p-Jnk (c) PARP cleavage (as shown in Chapter 4, Figure 4.11, and repeated here). Cells exposed to staurosporine (ST) were used as a positive control.

5.4.3 Protein degradation

Misfolded proteins are degraded by either the proteasome or by autophagy. Experiments to assess which mechanism was induced by MSA were conducted. Proteasomal degradation requires proteins to be ubiquitinated and therefore the level of ubiquitinated proteins in the RL and DHL4 cell lines exposed to MSA was assessed by western blotting. Cells were also exposed to bortezomib, a proteasome inhibitor, as a positive control. Figure 5.10 shows that there was not a clear increase in the amount of ubiquitinated proteins in either the RL or DHL4 cell lines after exposure to MSA, although in DHL4 cells exposed to 30μmol/L MSA there may have been a small increase. Western blotting, however, is not a very sensitive method for assessing small changes in protein levels. Exposure to bortezomib did result in a clear increase in ubiquitinated proteins.

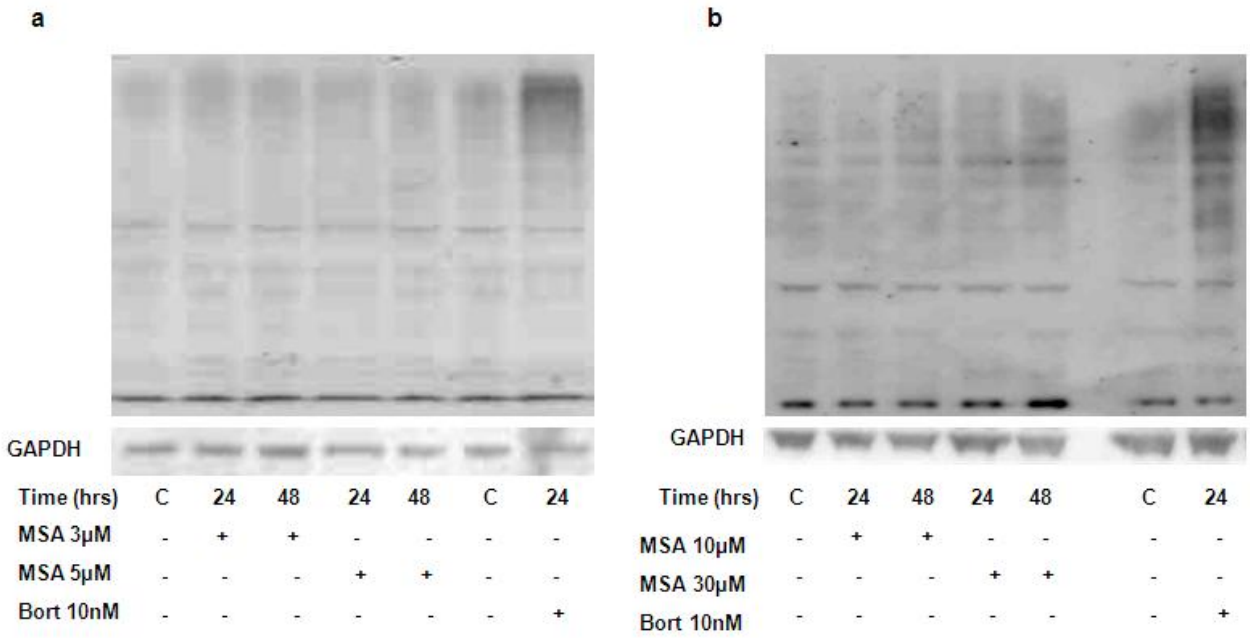

Figure 5.10 Level of ubiquitinated proteins in the (a) RL and (b) DHL4 cell lines exposed to MSA and bortezomib.

To assess whether autophagy was induced by MSA, the conversion of LC3-I to LC3-II was studied by western blotting. LC3 is microtubule-associated protein 1 light chain 3 and after post-translational modification is called LC3-I, which resides in the cytosol. When autophagy is induced, LC3-I is converted to LC3-II by conjugation to phosphatidylethanolamine and relocates specifically to associate with autophagosome membranes. There are three human isoforms of LC3; LC3A, LC3B and LC3C (Klionsky *et al*, 2008). Figure 5.11 shows that in the RL cell line, 1μmol/L and 3μmol/L MSA did not result in conversion of LC3B-I to LC3B-II but there was a small increase in LC3B-II levels in cells exposed to 5μmol/L for 24 and 48 hours. In the DHL4 cell line, exposure to 10-60μmol/L MSA did result in the conversion of LC3B-I to LC3B-II, which was apparent at 24 and 48 hours.

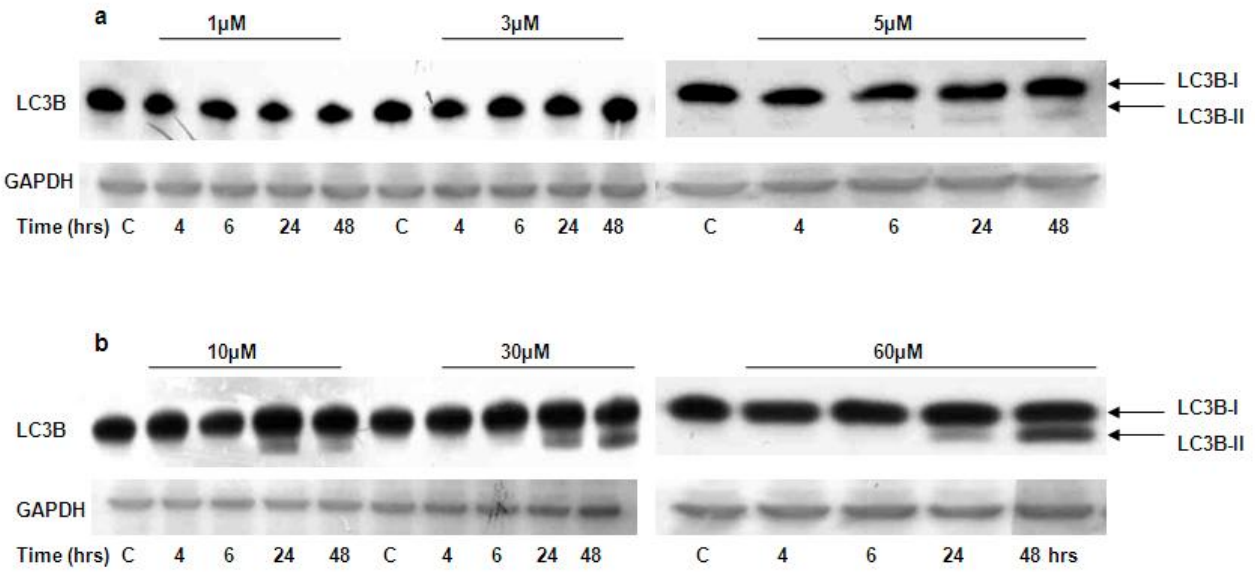

Figure 5.11 LC3B-I and -II in the (a) RL and (b) DHL4 cell lines exposed to MSA.

To confirm that autophagy was induced in the DHL4 cell line, immunofluorescence for LC3 was performed. When autophagy is induced, the distribution of LC3 protein changes from a diffuse to a punctate pattern as the protein relocates to the autophagosomes. Figure 5.12 shows that MSA did alter the pattern of LC3B distribution in DHL4 cells, with 10μmol/L and 30μmol/L MSA resulting in an increased punctate pattern.

To quantify the increase in autophagy, cells treated with MSA were stained with AO and the increase in red fluorescence, indicating an increase in acidic cytoplasmic vesicles, was determined by flow cytometry. Thapsigarin (TG), an inhibitor of the ER calcium pump and hence an inducer of ER stress and autophagy, was used as a positive control. Figure 5.13 shows the flow cytometry plots from one experiment. The numbers indicate the percentage of cells present in the upper right and left quadrants with increased red fluorescence. Figure 5.14 shows the summary of three separate experiments, demonstrating clearly that MSA significantly increased the percentage of red fluorescence compared to untreated cells, although there was no clear concentration effect.

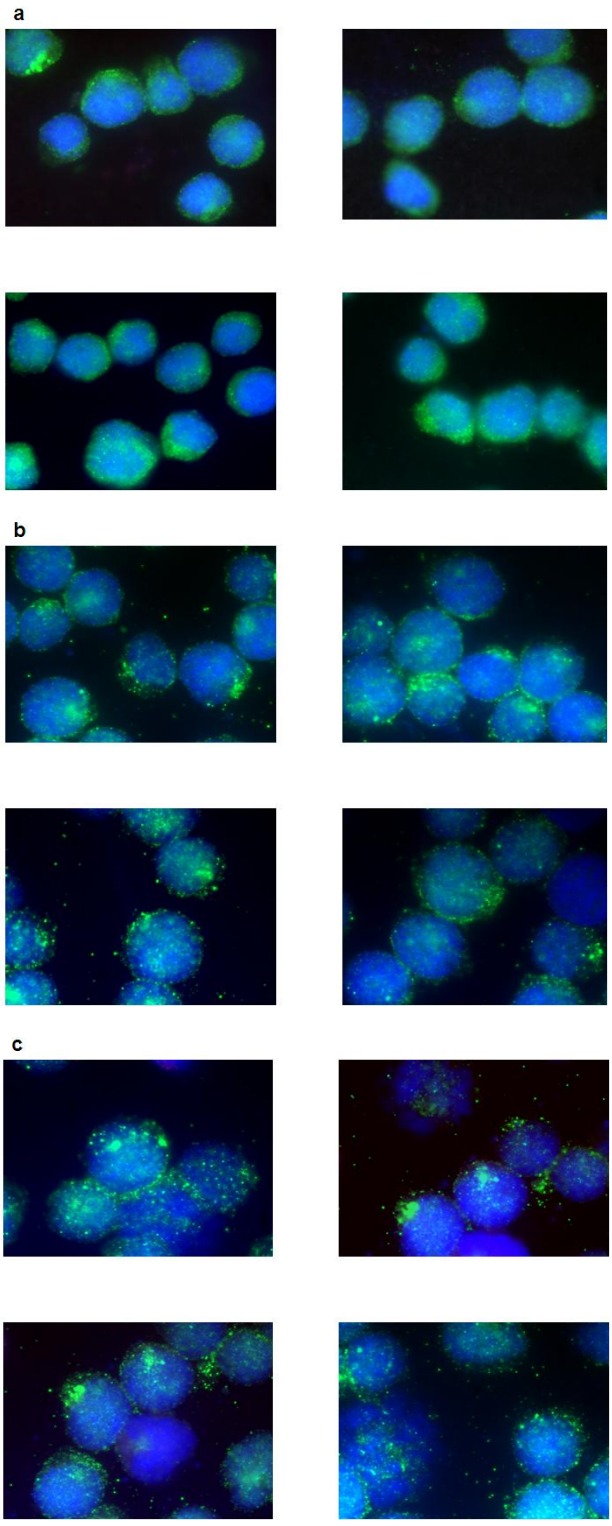

Figure 5.12 Immunofluorescence for LC3B in the DHL4 cell line exposed to MSA for 24 hours. (a) Control (b) 10μM (c) 30μM. A punctuate pattern is apparent in cells treated with MSA, indicating the formation of autophagosomes.

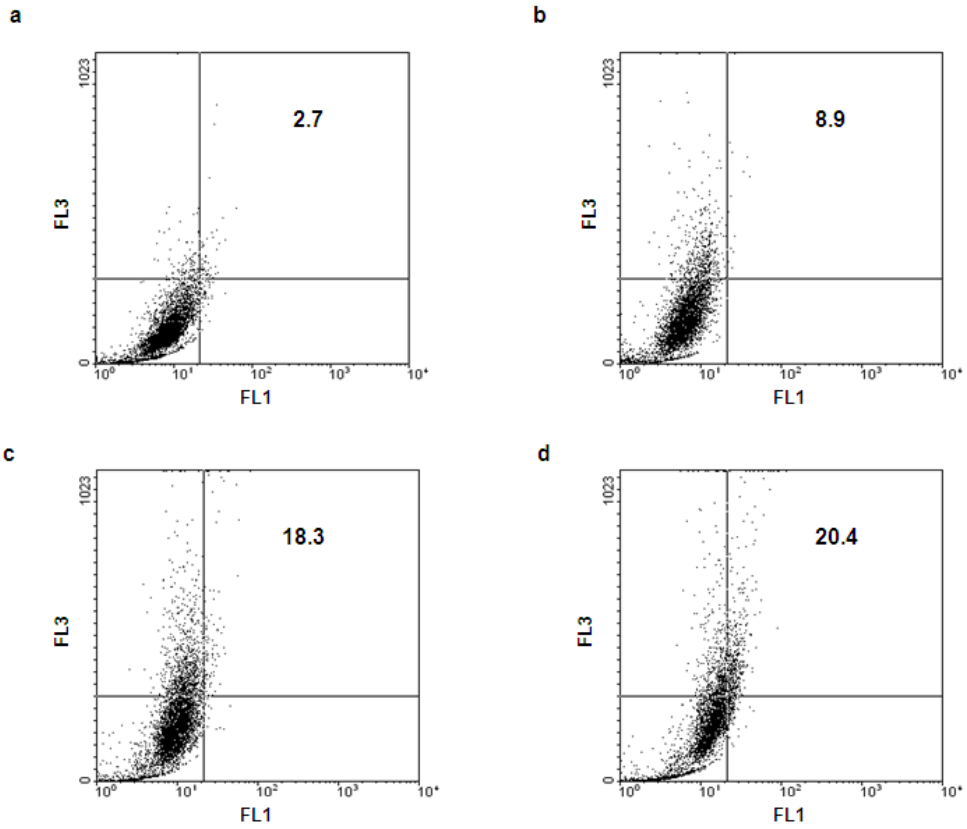

Figure 5.13 Acridine orange staining in the DHL4 cell line exposed to MSA for 24 hours. (a) Control (b) Thapsigarin 3μM, (c) MSA 10μM (d) MSA 20μM. FL1 indicates green fluorescence and FL3, red fluorescence. Cells above the horizontal line have increased red fluorescence.

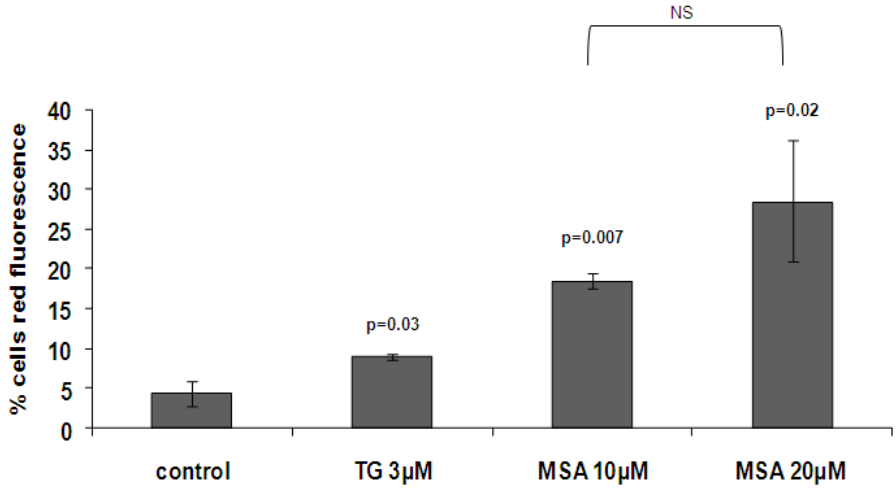

Figure 5.14 Increase in % of red fluorescent cells in DHL4 cell line stained with acridine orange after exposure to MSA or thapsigargin (TG; positive control). Data points are the mean+/-SD of 3 separate experiments. p values are a comparison with control.

To investigate the consequences of MSA-induced autophagy in the DHL4 cell line, cells were exposed to bafilomycin A1. Bafilomycin A1 is a macrolide antibiotic that inhibits vacuolar H^+-ATPase proton pumps, which are required to acidify lysosomes, therefore raising lysosomal pH (Yoshimori *et al*, 1991). It also prevents the fusion of autophagosomes with lysosomes (Yamamoto *et al*, 1998). This results in accumulation of autophagosomes and increased levels of LC3-II as LC3-II is also degraded by the process of autophagy.

To confirm that 10nmol/L bafilomycin A1 was able to inhibit autophagy, DHL4 cells were exposed to bafilomycin A1 alone. Figure 5.15a shows the accumulation of LC3B-II at 24 and 48 hours confirming the inhibition of the normal homeostatic process of autophagy in DHL4 cells. In this situation the accumulation of LC3B-II occurs because bafilomycin inhibits the degradation of autophagosomes. However, an increase in LC3-II levels also occurs as a result of autophagy induction, as seen after exposure to MSA (Figure 5.11).

DHL4 cells were then exposed to balfilomycin A1 in combination with MSA for 48 hours and cell viability assessed using the Guava® viacount assay. Figure 5.15b shows that 10nmol/L bafilomycin A1 alone did not significantly affect cell viability. However, balfilomycin A1 significantly enhanced the cytotoxicity of relatively low, non-toxic concentrations of MSA. For example, 10µmol/L MSA alone decreased cell viability by 6.3% (±1.6) but when combined with bafilomycin A1 the cell viability was decreased by 46.4% (±4.7). This suggests that autophagy is a pro-survival mechanism activated in DHL4 cells exposed to MSA. The effect of 3-methyladenine (3-MA), another inhibitor of autophagy, was also assessed in DHL4 cells. However, concentrations known from the literature to inhibit autophagy were cytotoxic to DHL4 cells (data not shown). 3-MA, in addition to inhibiting autophagy, through its action on class III PI3K, affects other signalling pathways, such as class I PI3K and MAPK (Tasdemir *et al*, 2008). Therefore, further experiments would be required to establish which of these affects resulted in cytotoxicity to the DHL4 cells.

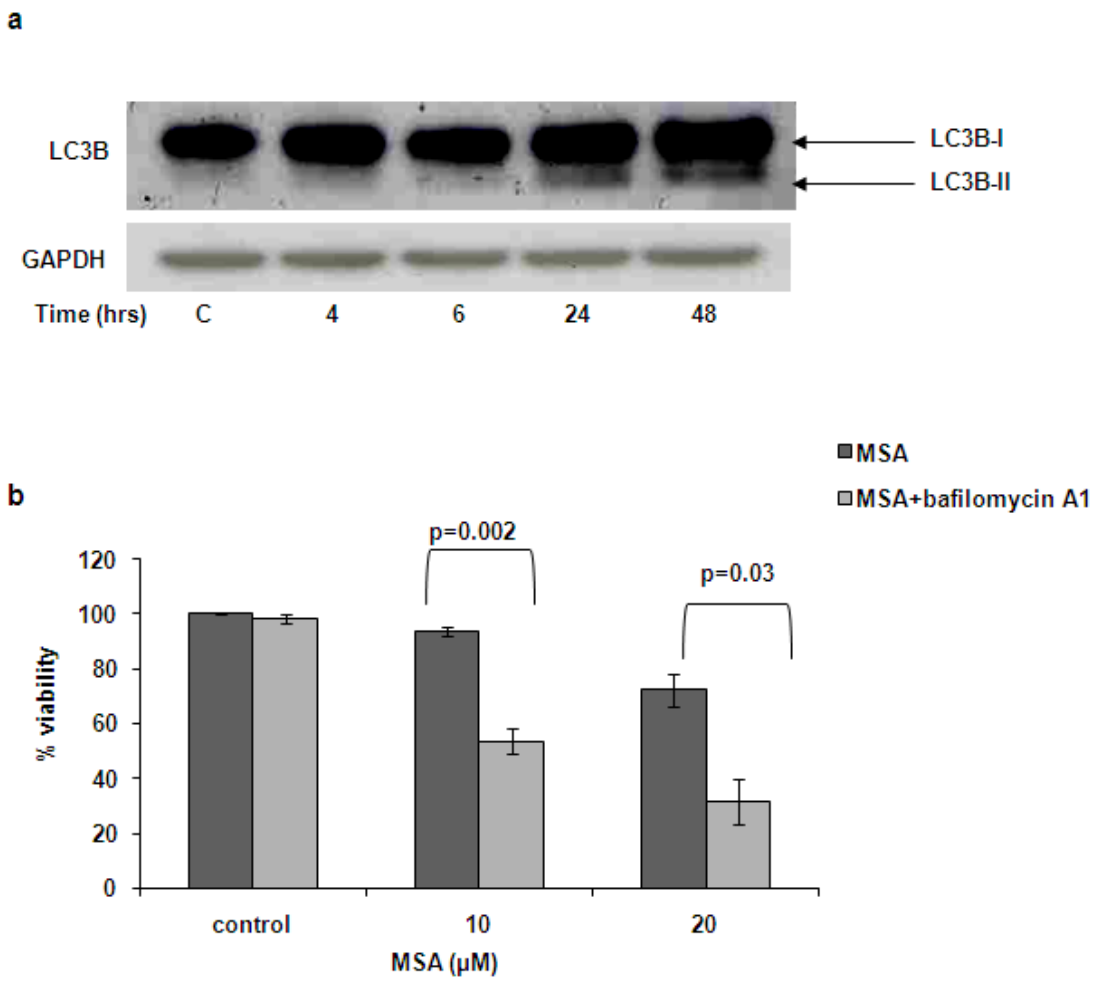

Figure 5.15 (a) Accumulation of LC3B-II in the DHL4 cell line exposed to 10nmol/L bafilomycin A1 (b) Cell viability assessed by the Guava® viacount assay in the DHL4 cell line exposed to MSA and bafilomycin A1.

5.4.4 The effect of MSA on other stress-induced proteins

The effect of MSA on other stress-induced proteins was investigated. Figure 5.16 shows that in the RL and DHL4 cell lines, MSA had no effect on the expression of cytosolic HSP70 and HSP90. This is in contrast to the marked increase in GRP78, another member of the HSP70 family, in both RL and DHL4 cells.

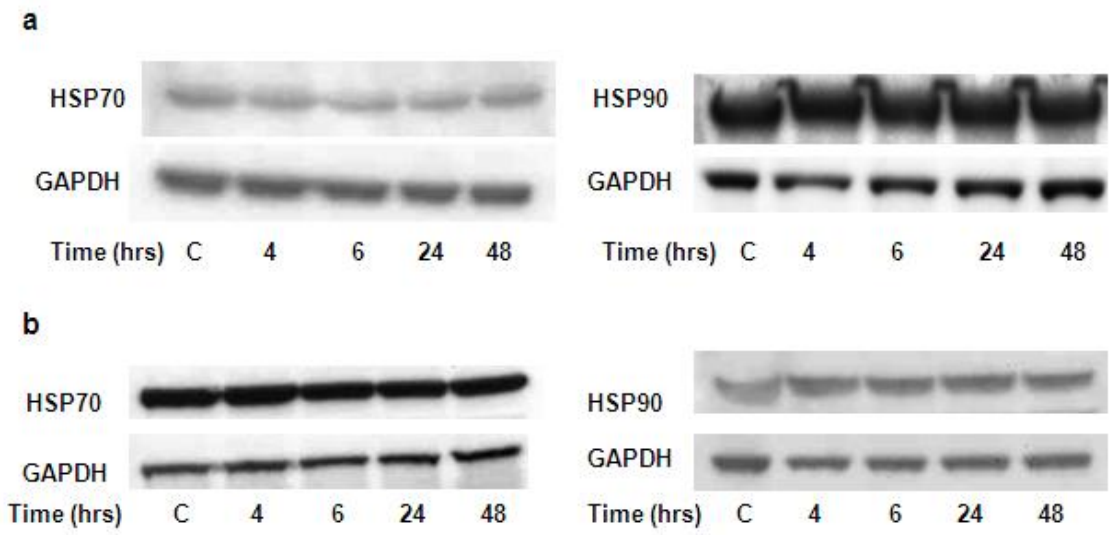

Figure 5.16 Expression of HSP70 and HSP90 in (a) RL cells exposed to 5μM MSA and (b) DHL4 cells exposed to 60μM MSA.

The effect of MSA on the transcription factor Nrf2 and the anti-oxidant protein Prx1 was also investigated. As described in Chapter 1 (Section 1.3.9.9), these proteins may be differentially affected by Se in normal and tumour cells. Figure 5.17 shows that in RL and DHL4 cells MSA had no effect on the nuclear expression of Nrf2 or the expression of Prx1 in whole cells extracts.

The Nrf2-Prx1 pathway is modulated by alterations in oxygen conditions (Kim *et al*, 2007e). Therefore the effect of hypoxia on the expression of Prx1 in cells exposed to MSA was further investigated. Figure 5.18 shows that in DHL4 cells exposed to hypoxia for 24 hours followed by MSA for a further 2 and 24 hours, there was no alteration in Prx1 expression.

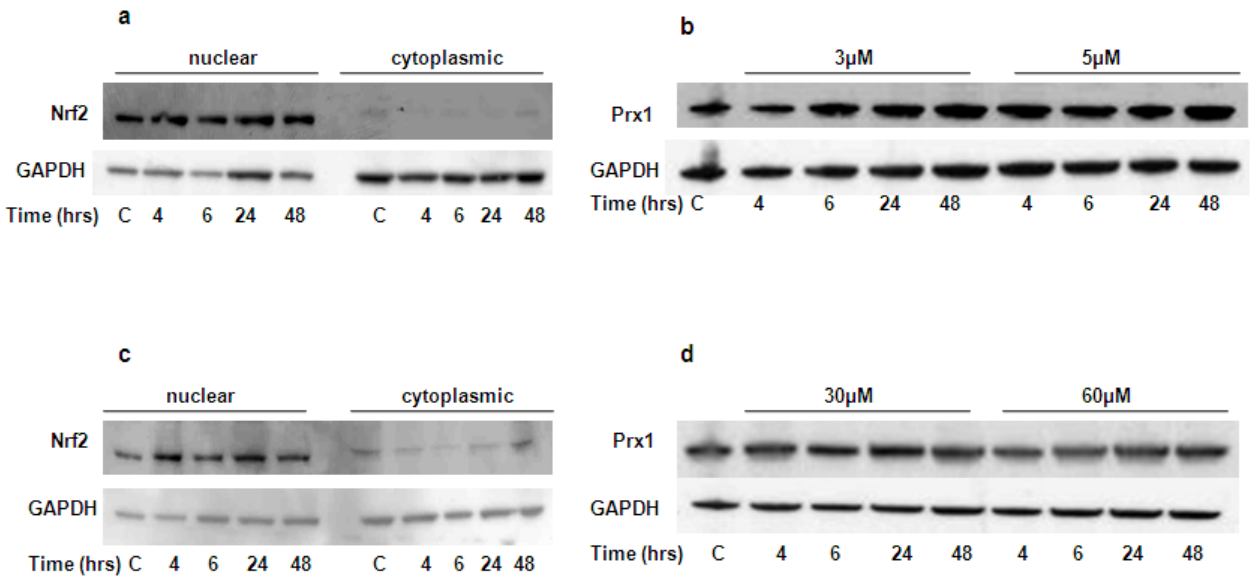

Figure 5.17 (a) Nrf2 expression in RL cells exposed to 5μM MSA; nuclear and cytoplasmic protein separation (b) Prx1 expression in RL cells exposed to 3μM and 5μM MSA (c) Nrf2 expression in DHL4 cells exposed to 60μM MSA; nuclear and cytoplasmic protein separation (d) Prx1 expression in DHL4 cells exposed to 30μM and 60μM MSA.

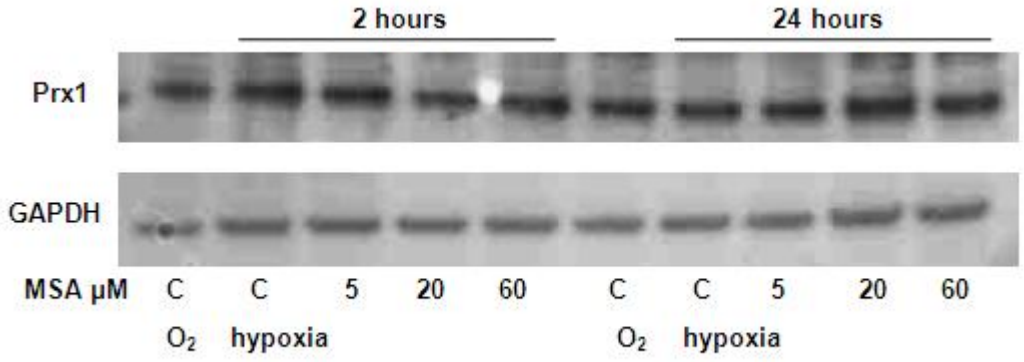

Figure 5.18 Prx1 expression in DHL4 cells exposed to MSA under hypoxic conditions (1% O_2, 5% CO_2, 94% N_2).

5.5 DISCUSSION

These experiments show that MSA induces protein misfolding in two DLBCL cell lines, resulting in ER stress and activation of the UPR. This was investigated in a MSA-sensitive (RL) and MSA-resistant (DHL4) cell line. Both cell lines demonstrated basal expression of GRP78, although there was some variability in expression between experiments. This suggests that the cells lines were already 'stressed' at baseline. The effect of MSA was concentration-dependent and changes in GRP78 expression and GADD153 mRNA levels were seen after only 4-hour exposure. The induction of PDI occurred later, at 24 and 48 hours.

In RL cells, the chemo-sensitising concentration of 1μM had very little effect on markers of ER-stress and ≥3μmol/L MSA was required to induce expression of PDI and GRP78 and 5μmol/L MSA was required to induce GADD153 mRNA. Thus, induction of ER stress is unlikely to be the mechanism by which MSA sensitises RL cells to chemotherapy. Despite the lack of ER stress induction in RL cells exposed to 1μmol/L MSA, PARP was cleaved at this concentration, suggesting ER stress is also not the mechanism of apoptosis-induction in RL cells. Of interest, 1μmol/L MSA had no effect on RL cell viability (Chapter 4, Figure 4.2a), however, PARP cleavage was clearly seen at this concentration.

In the DHL4 cell line, the induction of GRP78 at low concentrations of MSA (1-5μmol/L) was larger than in the RL cell line, but 10μmol/L MSA had a similar effect in both cell lines with the increase in GRP78 expression maintained out to 48 hours. In DHL4 cells, the increase in GRP78 plateaued at concentrations ≥10μmol/L with no further increase in expression with 30μmol/L and 60μmol/L exposure. The induction of GADD153 mRNA in DHL4 cells was also concentration-dependent and the effect plateaued at 30μmol/L MSA. In both the RL and DHL4 cells lines, 5μmol/L MSA resulted in a similar pattern of increased GADD153 mRNA expression.

GRP78 is responsible for maintaining ER calcium homeostasis, preventing the accumulation of misfolded proteins and controlling UPR signalling. GRP78 is generally considered a pro-survival protein and over-expression by tumours both promotes growth and has been implicated in chemoresistance. It has been shown that knock-down of GRP78 can inhibit the growth of cancer cells and sensitise them to chemotherapy (Pyrko *et al*, 2007). GRP78 is able to bind and inhibit the activation of caspase 7 (Reddy *et al*, 2003), inhibit pro-apoptotic members of the Bcl-2 family of proteins and prevent cytochrome *c* release from mitochondria (Fu *et al*, 2007). The MSA-resistant cell line, DHL4, induced GRP78 to a greater extent at low MSA concentrations (1-5μmol/L) compared to RL cells, which may represent a mechanism of cytotoxic drug resistance.

ER stress-induced pro-apoptotic signalling was further investigated by examining the expression of Bcl-2, phosphorylation of Jnk and cleavage of PARP. It was expected that an increase in GADD153 mRNA would decrease the expression of the anti-apoptotic protein Bcl-2 but this was not apparent in either cell line. Phosphorylation of Jnk has been reported as a downstream effect of UPR signalling via the IRE1 pathway and p-Jnk promotes apoptosis. However, increased phosphorylation of Jnk protein was also not evident in either cell line. As mentioned, in the RL cell line, PARP was cleaved independently of ER-stress induction. In the DHL4 cell line, there was no evidence of PARP cleavage even at the highest concentration of 60μmol/L. These results suggest that although ER stress is induced by MSA this does not result in pro-apoptotic signalling at the concentrations used. In addition, GADD153 mRNA levels were significantly increased by MSA but this was not demonstrated at the protein level and its downstream target, Bcl-2 was not affected. Expression of GADD153 at the protein level was investigated by western blotting on several occasions using different antibodies and antibody dilutions. However, GADD153 protein was never detected. A methodological problem cannot be excluded as a positive control was not used, but given that its down-stream targets were also unaffected by MSA it is likely that this was a true result. Therefore, in DHL4 cells, the chemo-sensitising concentration of 10μmol/L did induce ER stress but this did not appear to push the cells towards apoptosis.

Activation of the UPR was investigated further by studying the phosphorylation of eIF2α. In the RL cell line 3μmol/L and 5μmol/L MSA increased the phosphorylation of eIF2α in a concentration-dependent manner. The increase was apparent by 4-hour exposure and had decreased by 48 hours. Although there was some variability between experiments, the trend was confirmed in two independent experiments. The baseline level of p-eIF2α was higher in the DHL4 cell line compared to the RL cell line but, in contrast, there was a clear decrease in phosphorylation of p-eIF2α in DHL4 cells exposed to 10μmol/L and 30μmol/L MSA at the earliest time-point of 4 hours with a return towards baseline by 24 and 48 hours. This was an unexpected finding as phosphorylation of eIF2α is generally considered a pro-survival response resulting in decreased protein translation and has been shown to promote drug resistance (Ranganathan *et al*, 2006). Given that the DHL4 cell line is relatively resistant to MSA, increased phosphorylation of eIF2α was expected. A possible explanation for this finding is negative feed-back from GADD34, a target gene of GADD153. GADD34 can lead to the dephosphorylation of eIF2α thus removing the block on translation and promoting apoptosis (Szegezdi *et al*, 2006). It may have been that if an earlier time point than 4 hours had been investigated, an initial increase in p-eIF2α would have been seen, followed by dephosphorylation, because by 4 hours, 10μmol/L MSA had already induced a 15-fold increase in GADD153 mRNA expression. In prostate cancer cells lines, MSA increased phosphorylation of eIF2α as early as 1-hour post exposure (Wu *et al*, 2005). However, arguing against this is the observation that at the MSA concentrations investigated PARP was not cleaved in DHL4 cells, suggesting that apoptosis was not activated.

A recent study has, however, implicated the dephosphorylation of eIF2α in cell survival and resistance to bortezomib-induced cell death (Schewe & Aguirre-Ghiso, 2009). Bortezomib is known to induce ER stress and this may be one mechanism by which it induces cell death. In this study, cells surviving treatment with bortezomib were able to decrease phosphorylation of eIF2α, which was associated with a decrease in GADD153 mRNA expression. When dephosphorylation of eIF2α was inhibited, GADD153 expression was increased and cell death enhanced. As mentioned previously, UPR

signalling can simultaneously activate pro-survival and pro-apoptotic pathways and in addition to decreasing general protein translation, the phosphorylation of eIF2α can also increase GADD153 expression by increasing translation of the transcription factor ATF4 (Szegezdi *et al*, 2006). Again, this mechanism does not fully explain the findings in the DHL4 cell line as dephosphorylation of eIF2α was associated with increased expression of GADD153 mRNA.

Given that induction of ER stress by MSA in the two DLBCL cell lines was not apparently activating pro-apoptotic pathways, further downstream consequences of protein misfolding were investigated. MSA did not result in a clear increase in the level of ubiquitinated proteins suggesting that the ubiquitin-proteasome pathway may not be important in degrading the misfolded proteins. Therefore the protein degradation pathway of autophagy was investigated. MSA induced autophagy in both cell lines, but further experiments were performed only in DHL4 cells, as in the MSA-sensitive RL cell line higher than cytotoxic concentrations were required to induce ER stress and apoptosis was activated in the absence of ER stress.

In the DHL4 cell line, the chemo-sensitising concentration of 10μmol/L MSA and higher concentrations that had already been shown to induce ER stress also induced autophagy. This was shown by the conversion of LC3-I to LC3-II, which occurred later than the onset of ER stress signalling, at 24 and 48 hours. The distribution of LC3 protein was shown to change from a diffuse to a punctuate pattern by immunofluorescence indicating the formation of autophagosomes. Additionally, the increase in acidic cytoplasmic vesicles was demonstrated by an increase in AO red fluorescence by flow cytometry. When autophagy was inhibited by bafilomycin A1, the cytotoxicity of MSA was significantly enhanced, suggesting that MSA-induced autophagy is a pro-survival response in the DHL4 cell line. It has been shown that both the PERK-eIF2α and the IRE1 arms of UPR signalling can mediate ER stress-induced autophagy (Hoyer-Hansen & Jaattela, 2007), however, in DHL4 cells exposed to MSA neither of these pathways appeared to be important since MSA inhibited the phosphorylation of eIF2α and did not

increase the phosphorylation and hence activation of Jnk, which is required for IRE1-mediated autophagy.

Monitoring the cellular process of autophagy is complicated and there are drawbacks to most of the available methods, requiring several methods to be used in parallel (Klionsky *et al*, 2008). In these experiments, three different methods that are widely reported in the literature were used to establish the induction of autophagy by MSA. All of these methods demonstrate the accumulation of autophagosomes, which has been interpreted to mean increased autophagosome formation due to increased autophagic activity. However, an alternative explanation could be that there is reduced turnover of autophagosomes, which would give the same experimental results. In addition, the acidotropic dye, AO, is not specific for autophagosomes but can be taken up by any acidic vesicles. The interpretation of western blotting for LC3 protein is also not straightforward as the sensitivity of antibodies to LC3 is greater for LC3-II than LC3-I (Klionsky *et al*, 2008). Ideally, these experiments should be complemented by examining autophagic flux, hence studying the flow through the whole process of autophagy. Overall, based on evidence that ER stress is known to induce autophagy, it is likely from the data presented here that MSA is causing a real increase in autophagic activity.

This is the first report of the induction of autophagy by MSA, which, in the DHL4 cell line mediated cell survival and hence may be a mechanism of cellular resistance to MSA. Therefore, combining MSA with an inhibitor of autophagy may be a way of sensitising resistant cells to the cytotoxic effects of MSA. However, neither the induction of ER stress nor autophagy can explain the chemo-sensitising effects of MSA. In the RL cell line apoptosis is induced at concentrations that do not induce ER stress and although in the DHL4 cell line a chemo-sensitising concentration does induce ER stress and autophagy, these responses appear to protect the cell from death. The induction of autophagy was only investigated in one cell line and thus to make general conclusions these experiments would need to be conducted in more MSA-resistant cell lines.

However, these experiments were not pursued further in this work as the primary aim was to investigate mechanisms of chemo-sensitisation by MSA.

The effects of MSA on other proteins involved in the cellular response to stress were studied. HSPs are molecular chaperones that are ubiquitously expressed in the cytosol of cells and required for the function and stability of proteins implicated in cell growth, differentiation and survival. They facilitate normal protein folding and their expression is increased in response to cellular stresses such as heat, hypoxia, acidosis and protein misfolding and aggregation. HSPs, therefore, represent an adaptive response that enhances cell survival. Increased expression of these chaperone proteins, such as HSP90, is seen in many tumour types (Whitesell & Lindquist, 2005). The expression of cytosolic HSP70 and HSP90 was investigated but MSA did not alter the expression of either protein, although basal expression of at least one of these chaperones was high in both cell lines studied. Of note GRP78 is the ER homologue of HSP70 and another ER chaperone, GRP94, is the ER homologue of HSP90.

The effect of MSA on the Nrf2-Prx1 pathway was also studied. The relevance of this pathway to Se has previously been discussed (Chapter 1, section 1.3.9.9). In addition, Nrf2 has been identified as a substrate of PERK and is activated by ER stress, promoting cell survival. Nrf2 up-regulates components of the proteasome, thus facilitating protein degradation, and also increases the expression of genes involved in protein folding (Cullinan & Diehl, 2006). However, MSA did not alter the nuclear expression of Nrf2 or the expression of Prx1 in whole cell extracts. Given the hypothesis that the response of this pathway to Se may be dependent on oxygen conditions (Kim *et al*, 2007e), the effect of hypoxia on Prx1 expression was investigated. However, neither hypoxia itself nor the addition of MSA to cells grown under hypoxic conditions altered the expression of this protein.

In summary, MSA induces protein misfolding resulting in ER stress and activation of the UPR. However, in the two DLBCL cell lines studied, the induction of ER stress is neither

a mechanism by which MSA sensitises cells to chemotherapy nor induces apoptosis. Rather, in the MSA-resistance cell line, DHL4, ER stress resulted in the induction of autophagy, which was demonstrated to be a mechanism of cell survival in this cell line. Thus, combining MSA with an inhibitor of autophagy may represent a way of sensitising resistant cells to MSA.

CHAPTER 6: Inhibition of histone deacetylase activity by selenium

6.1 INTRODUCTION

In quiescent cells, DNA exists in a condensed form, wrapped around histones. This condensed chromatin structure is less accessible to transcription factors and thus leads to a transcriptionally silent state. Chromatin condensation is facilitated by histone deacetylase (HDAC) enzymes, which remove acetyl groups from histones. In contrast, histone acetylation by histone acetyltransferase (HAT) enzymes leads to a more relaxed, 'open' chromatin structure accessible to transcription factors. Thus, HDAC and HAT enzymes are involved in the regulation of gene transcription. In addition, they are involved in the regulation of a large number of non-histone proteins, including transcription factors, molecular chaperones and proteins involved in DNA repair, cell signalling and apoptosis. Protein acetylation can also affect the stability of proteins and protein-protein interactions (Glozak & Seto, 2007). Eighteen HDAC enzymes, grouped into four classes and two families, have been identified in humans. The members of the classical family comprise class I (HDAC 1, 2, 3 and 8), class II (HDAC 4, 5, 6, 7, 9, and 10) and class IV (HDAC 11). They share similarities in structure and sequence and require a zinc ion for their deacetylase activity. Class III HDACs belong to the sirtuin family and have seven members, which do not share structural or sequence similarities to members of the classical family and require NAD^+ for their activity. HDAC enzymes are not functionally redundant. Class I HDACs are localised mainly to the nucleus and are widely expressed, whereas class II HDACs are localised mainly to the cytoplasm but can move between the nucleus and cytoplasm and have tissue-specific expression. HDACs function as components of large multi-protein complexes, which are recruited to specific regions of DNA and regulate the expression of various genes (Minucci & Pelicci, 2006; Xu *et al*, 2007).

As the list of non-histone protein targets of HDACs continues to grow, it has become clear that these HDAC substrates are involved in many critical cellular processes, including the regulation of cell proliferation, differentiation and death. In addition,

dysregulation and over-expression of HDACs have been found in many cancers (Halkidou *et al*, 2004; Wilson *et al*, 2006). Therefore, inhibition of HDAC activity as a target for cancer therapy has been an area of intensive investigation in recent years and a large number of compounds are at various stages of clinical development (Figure 6.1). The HDAC inhibitor (HDACi) vorinostat is the most advanced in clinical development and has been approved by the Federal Drug Administration (FDA) in the United States for the treatment of patients with cutaneous T-cell lymphoma (Mann *et al*, 2007). HDACi are derived from both natural and synthetic routes and the main structural classes are; short chain fatty acids (e.g. valproic acid), hydroxamic acids (e.g. vorinostat), cyclic tetrapeptides (e.g. depsipeptide), aminobenzamides (e.g. MS-275) and electrophilic ketones (e.g. α-ketoamides) (Xu *et al*, 2007). HDACi are mainly directed against class I and II HDACs. Although HDACi currently in clinical trial show some differences in specificity for different HDAC isoforms, they are not particularly selective. Isoform specific HDACi are currently being developed (Marks & Xu, 2009).

The mechanism of action of HDACi is complex as these agents affect multiple cellular pathways. Studies using DNA array have found that the transcription of up to 20% of expressed genes can be altered in cells exposed to HDACi with similar numbers of genes being up- and down-regulated (Glaser *et al*, 2003; Peart *et al*, 2005). Some of the demonstrated mechanisms of action include the induction of cell cycle arrest (Ungerstedt *et al*, 2005), activation of both the intrinsic (Shao *et al*, 2004) and extrinsic apoptotic pathways (Insinga *et al*, 2005), induction of both mitotic (Robbins *et al*, 2005) and autophagic cell death (Shao *et al*, 2004) and the accumulation of ROS (Ungerstedt *et al*, 2005). In addition, inhibition of HDAC6 leads to the acetylation of HSP90, disrupting its chaperone function with consequences such as Akt dephosphorylation (Bali *et al*, 2005). HDAC6 is also a component of the aggresome, a cellular structure involved in the degradation of misfolded proteins, and thus HDAC inhibition disrupts this pathway (Kawaguchi *et al*, 2003). It appears normal cells, in contrast to tumour cells, are relatively resistant to the cytotoxic effects of HDACi (Insinga *et al*, 2005; Kim *et al*, 2003). As well as their single agent activity, HDACi have been shown to interact synergistically with a

number of conventional therapeutic drugs (Kim *et al*, 2003) and novel targeted agents (Yu *et al*, 2003)

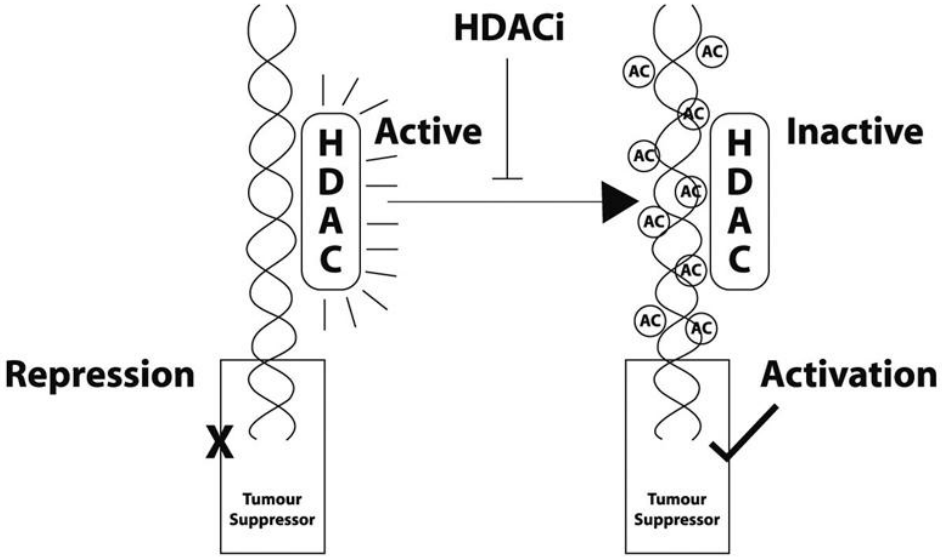

Figure 6.1 Simplified diagram representing the action of HDAC inhibitors.
Histone acetylation, through the inhibition of HDAC activity, results a more 'open' chromatin structure accessible to transcription factors.

Another potentially important property of HDACi is their ability to inhibit angiogenesis, which is required to promote tumour growth. Inhibition of new blood vessel formation is therefore a logical and promising target for cancer therapy. Angiogenesis is enhanced by hypoxia, which is commonly found in central regions of solid tumours. Hypoxia in turn regulates a number of transcription factors including HIF-1, a heterodimeric protein consisting of the subunits HIF-1α and HIF-1β. HIF-1β is constitutively expressed and not regulated by oxygen levels whilst HIF-1α expression is tightly regulated. Under normoxic conditions, certain post-translational modifications of HIF-1α and its interaction with VHL protein leads to its ubiquitination and proteasomal degradation.

However, under hypoxic conditions, HIF-1α is stabilised and moves from the cytoplasm to the nucleus of cells, where it heterodimerises with HIF-1β and initiates the transcription of a number of target genes. VEGF is one such gene whose expression is regulated by HIF-1α and is crucial in promoting angiogenesis (Semenza, 2003). HIF-1α has been found to be over-expressed in many tumour types (Zhong *et al*, 1999) and in some, but not all studies, has been associated with an inferior outcome (Birner *et al*, 2000).

Hypoxia has been found to increase the expression of HDAC proteins and it has been demonstrated that HDACs regulate HIF-1α activity through both indirect and direct mechanisms. Over-expression of HDACs leads to reduced expression of the two tumour suppressor proteins, p53 and VHL, which results in over-expression of HIF-1α and VEGF. HDAC inhibition was able to reverse this effect (Kim *et al*, 2001). HDAC inhibition can also result in HIF-1α degradation through a VHL-independent mechanism (Qian *et al*, 2006). In addition, the inhibition of HDAC6 results in acetylation of HSP90 and thus degradation of its client protein, HIF-1α (Kong *et al*, 2006). A number of studies have also found that various HDACs directly interact with HIF-1α regulating its stability and transcriptional activity (Kato *et al*, 2004; Kim *et al*, 2007c).

Se has recently been found to inhibit HDAC activity. This was first reported in the human prostate cancer cell line LNCaP, exposed to a non-cytotoxic concentration (1.5μmol/L) of the inorganic Se compound selenite for 7 days. Western blotting revealed that selenite increased levels of acetylated histone H3 without altering the levels of HDAC proteins and inhibition of HDAC activity was demonstrated using a cell-free fluorescence activity assay (Xiang *et al*, 2008). This study also found that selenite decreased the levels of methylated histone H3 and decreased general DNA methylation. In LNCaP cells, this led to the re-expression of two tumour suppressor genes known to be silenced by DNA hypermethylation. Thus, epigenetic modifications induced by Se may be important in explaining its anti-tumour effects.

The organic Se compounds, MSC and SLM, have also been reported to inhibit HDAC activity in human prostate and colon cancer cell lines (Lee *et al*, 2009a; Nian *et al*, 2009). However, it is the α-keto acid metabolites of MSC and SLM that have been shown to be responsible for this effect. As mentioned previously, the anti-cancer properties of organic Se compounds are thought to be due to the generation of methylselenol (Ip *et al*, 2000). Methylselenol is generated from MSC and SLM by the action of pyridoxal 5'-phosophate (PLP)-dependent β-lyases and γ-lyases respectively (Okuno *et al*, 2006; Suzuki *et al*, 2007). However, in addition to undergoing β- and γ-elimination, MSC and SLM are substrates for aminotransferases and L-amino oxidases resulting in the formation of α-keto acid analogues. Methylselenopyruvate (MSP) is formed by transamination and or/L-amino acid oxidase reaction of MSC and α-keto-γ-methylselenobutyrate (KMSB) is formed from SLM. Both these compounds resemble butyrate, a known HDACi, in structure (Pinto *et al*, 2010). The studies in prostate and colon cancer cell lines found that direct exposure to MSP and KMSB, generated *in vitro*, resulted in a concentration-dependent increase in histone H3 acetylation. The two studies examined different exposure times and in colon cancer cell lines, an increase in histone H3 acetylation was detected as early as 30 minutes and persisted for at least 48 hours, whereas in the prostate cancer cell lines, 5- and 24-hour exposure were examined and an increase in histone H3 acetylation was detected by 5 hours. In addition, both metabolites were able to inhibit HDAC activity in a cell-free system with an EC_{50} for HDAC inhibition around 30-50μmol/L. Much higher concentrations of MSC were required to demonstrate a similar effect, whereas SLM had no effect.

The reason for the lack of HDAC inhibitory activity of SLM was studied in prostate cancer cells and it was found that the cells contain the enzyme glutamine transaminase K (GSK), which is an aminotransferase enzyme that can convert MSC to MSP. However, SLM is a very poor substrate for this enzyme and hence the active metabolite KMSB was not produced. GSK is an enzyme that is widely distributed in mammalian tissue whereas enzymes that catalyse SLM to MSP such as glutamine transaminase L have tissue-specific expression (Pinto *et al*, 2010). These results add support to the notion that MSC

is likely to be a better anti-cancer compound than SLM. In addition to HDAC inhibition, MSP and KMSB were found to inhibit cell growth, induce cell cycle arrest and induce the expression of the cell cycle regulator p21, a known target of HDAC inhibition. From the *in vitro* studies conducted to date, it is not possible to establish whether sufficient levels of α-keto acid metabolites can be achieved *in vivo* following the administration of either MSC or SLM. Most tissues do contain aminotransferases that could potentially convert, in particular, MSC to the active metabolite but further pharmacokinetic and pharmacodynamic studies are required to confirm this. L-amino oxidases may theoretically also play a role *in vivo* in generating MSP and KMSB from MSC and SLM and enzymatic activity has been found to be present in liver, kidney and lymphoid cells however, this requires further investigation (Pinto *et al*, 2010).

In addition to naturally occurring Se compounds, two Se analogues modelled on the structure of vorinostat have been synthesised. One compound contained a Se dimer and the other selenocyanide. It was assumed that within the cell, Se would be reduced to yield selenol (SeH) which would be the active species. Both compounds were found to be more potent in their HDAC inhibitory activity in a cell-free assay than vorinostat (Desai *et al*, 2010).

6.2 AIMS

1) To determine whether MSA, a precursor of methylselenol, is able to inhibit HDAC activity in DLBCL cell lines.
2) If HDAC inhibition is observed, then to investigate downstream targets.

6.3 METHODS

The DHL4, RL and SUD4 cell lines were exposed to a range of MSA (1-30μmol/L) and MSC (20-200μmol/L) concentrations for 2, 24 and 48 hours. In addition, PBMCs harvested from healthy volunteers were exposed to MSA (1-20μmol/L) for 24 hours. Western blotting was performed to determine changes in acetylation of histone H3 and α-tubulin and expression of p21 (Chapter 2, sections 2.4 and 2.5). Cell lines were also

cultured under hypoxic conditions as described in Chapter 2 (section 2.1.2) and then exposed to MSA in order to investigate changes in HIF1α expression, by western blotting, and VEGF production, by an electrochemiluminescence assay (see below, section 6.3.3). The effect of MSA on HDAC activity in the DLBCL cell lines was investigated using a cell-free and cell-based activity assay (see below, section 6.3.1). SAHA was used as a positive control at a concentration of 1μmol/L and 3μmol/L

6.3.1 Measurement of histone deacetylase activity

HDAC activity was measured using the HDAC fluorimetric assay/discovery and the HDAC fluorimetric cellular activity kits (Biomol, Plymouth Meeting, PA, USA) according to the manufacturers' instructions. Both assays are based on the *Fluor de Lys*™ (Fluorogenic Histone deAcetylase Lysyl substrate/developer) system. The *Fluor de Lys*™ substrate has an acetylated lysine side chain, so when it is incubated with a source of HDAC activity, deacetylation occurs and sensitises the substrate. When the *Fluor de Lys*™ developer is subsequently added, a fluorescent signal is produced. The addition of an HDACi to the assay system inhibits deacetylation of the *Fluor de Lys*™ substrate thus decreasing the fluorescent signal. The assays were performed in a white 96-well format plate with each condition performed in duplicate.

For the fluorimetric assay/discovery assay, HeLa nuclear extract (provided in the assay kit) was used as the source of HDAC activity and Trichostatin A (TSA) was used as a positive control. The concentration of HeLa nuclear extract used per well was 3-4.5μg of protein. Each assay run had two blank wells (no HeLa extract added) and two control wells (no HDACi added). The HeLa extract, MSA (possible HDACi) and *Fluor de Lys*™ substrate, at a final concentration of 50μmol/L, were added to each well and the plate incubated at room temperature for 30 minutes. After this, the *Fluor de Lys*™ developer was added and the plate incubated at room temperature for a further 10-15 minutes. Of note, TSA, at a final concentration of 2μmol/L, was added to the developer to ensure that HDAC activity stopped when it was added to the wells. Fluorescence (excitation 350-380nm, emission 440-460nm) was then measured on the POLARstar OPTIMA plate

reader (BMG Labtech). The values from the blank well were deducted from the test wells and the results expressed relative to the no inhibitor control.

For the HDAC fluorimetric cellular activity assay, $1x10^5$ cells were plated in a 96-well plate. Different concentrations of MSA were added to the wells and TSA was used as a positive control. Plates were placed at 37°C in a cell culture incubator for 30 minutes. The *Fluor de Lys*™ substrate, which is cell-permeable, was then added to each well at a final concentration of 200µmol/L. The plates were once again placed at 37°C in a cell culture incubator for a further 2 hours. For this assay, the *Fluor de Lys*™ developer was diluted in cell lysis buffer (provided in the kit) and again TSA, at a final concentration of 2µmol/L, was added to ensure that HDAC activity was stopped when the developer was added to the wells. After addition of the *Fluor de Lys*™ developer, the plate was incubated at room temperature for a further 10-15 minutes. Fluorescence (excitation 350-380nm, emission 440-460nm) was then measured on the POLARstar OPTIMA plate reader (BMG Labtech). The values from the blank well were deducted from the test wells and the results expressed relative to the no inhibitor control.

6.3.2 Preparation of DHL4 cell lysates as a source of histone deacetylase activity

$4x10^6$ cells were pelleted by centrifugation at 210*g* for 6 minutes at room temperature and the supernatant discarded. Cells were then washed once in HBSS by centrifugation at 210*g* for 6 minutes. 200µl of lysis buffer [0.394g Tris HCl, 0.146g NaCl, 0.357g $MgCl_2$, 25mls glycerol, 250µl Triton X-100 made up to 250ml with deionised water, pH set to 7.4, stored at 4°C] was then added to the cell pellet and the samples sonicated in an ultrasonic bath (Grant, Cambridge, UK) for 10 minutes at room temperature. Following sonication, the sample was centrifuged at 20,800*g* for 10 minutes to remove insoluble cellular debris and the supernatant collected into a fresh tube. The cell lysate was diluted 1:1 in the HDAC kit assay buffer and used immediately. Protein concentration of the lysate was determined using the BCA™ protein assay kit as described in Chapter 2 (section 2.4.5).

6.3.3 Measurement of vascular endothelial growth factor

VEGF levels in cellular supernatants were measured using the MSD® cytokine assay (Meso Scale Discovery, Maryland, USA). This is an electrochemiluminescence assay. The custom-made 96-well microtitre plates have electrodes integrated into the bottom of the plate. The wells are pre-coated with one or several 'capture antibodies' which bind the cytokine of interest. The detection antibody has an electrochemiluminescent label (MSD SULFO-TAG™) which emits light at 620nm when electrochemically stimulated. The detection process is initiated at the electrode and only labels near the electrode are excited and detected. The light emitted is detected using a SECTOR™ Imager (Meso Scale Discovery) which uses a charge coupled device camera.

To measure VEGF levels, 25µl of the supernatant was added to each well. Samples were added in duplicate. The plate was sealed with an adhesive cover and incubated at room temperature for 1 hour with vigorous shaking (1000rpm). Following this, 25µl of the detection antibody solution (1µg/ml) was added to each well and the plate again incubated at room temperature for 1 hour with vigorous shaking. The plate was then washed 3 times with PBS and 150µl of 2x read buffer was added to each well. The plate was then analysed on a SECTOR™ Imager. A standard curve was prepared from the cytokine calibrator solution provided with the assay kit. A range of 2.4pg/ml to 1000pg/ml was used. An example of the standard curve generated is shown below (Figure 6.2, r=0.99).

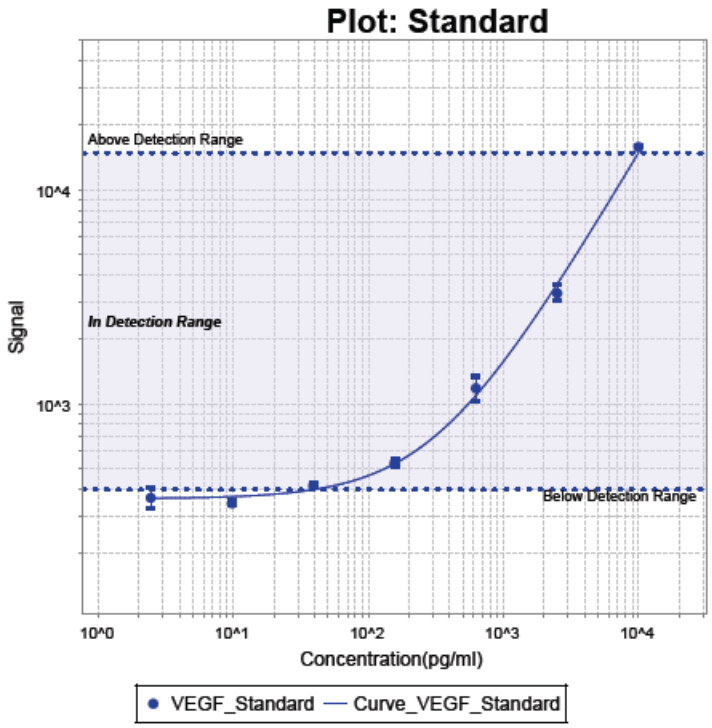

Figure 6.2 An example of the standard curve obtained for vascular endothelial growth factor using the MSD cytokine assay.

6.4 RESULTS

6.4.1 The effect of MSA on protein acetylation

A preliminary experiment was conducted in DHL4 cells to establish whether MSA induced protein acetylation. Figure 6.3 shows that MSA increased the acetylation of histone H3 at 24 hours. With 10µmol/L MSA, the effect was lost by 48 hours, whereas with 30µmol/L, the increase was sustained up to 48 hours. MSA also increased the acetylation of α-tubulin but to a lesser degree than histone H3. In addition, MSA induced the expression of the cyclin-dependent kinase inhibitor p21, a known target of HDAC inhibition. p21 expression was increased at 24 hours but by 48 hours the effect was less marked (Figure 6.3).

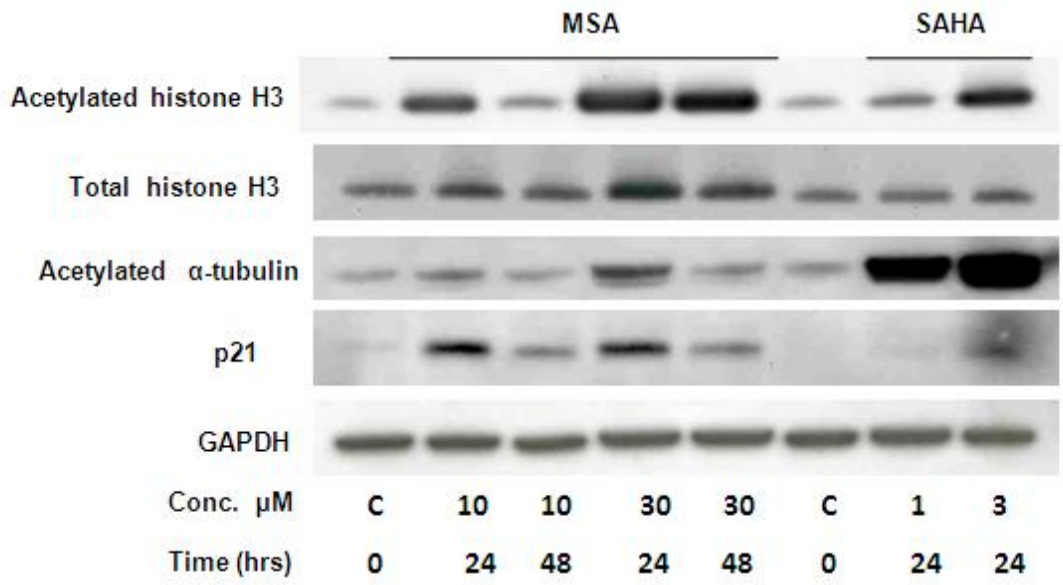

Figure 6.3 Protein acetylation and p21 expression in DHL4 cells exposed to MSA and SAHA.

Further time- and concentration-dependent experiments were conducted in SUD4, RL and DHL4 cells. Similar results were obtained in all three cell lines when exposed to MSA 1-30μmol/L for 2 and 24 hours (Figure 6.4). MSA concentrations as low as 1μmol/L increased the acetylation of histone H3 and α-tubulin as early as 2 hours, and this was sustained until 24 hours. However, the induction of acetylated histone H3 was greater at 24 hours than at 2 hours, whereas the reverse was true for acetylated α-tubulin. In addition, MSA induced the expression of p21 in RL and SUD4 cells (Figure 6.5).

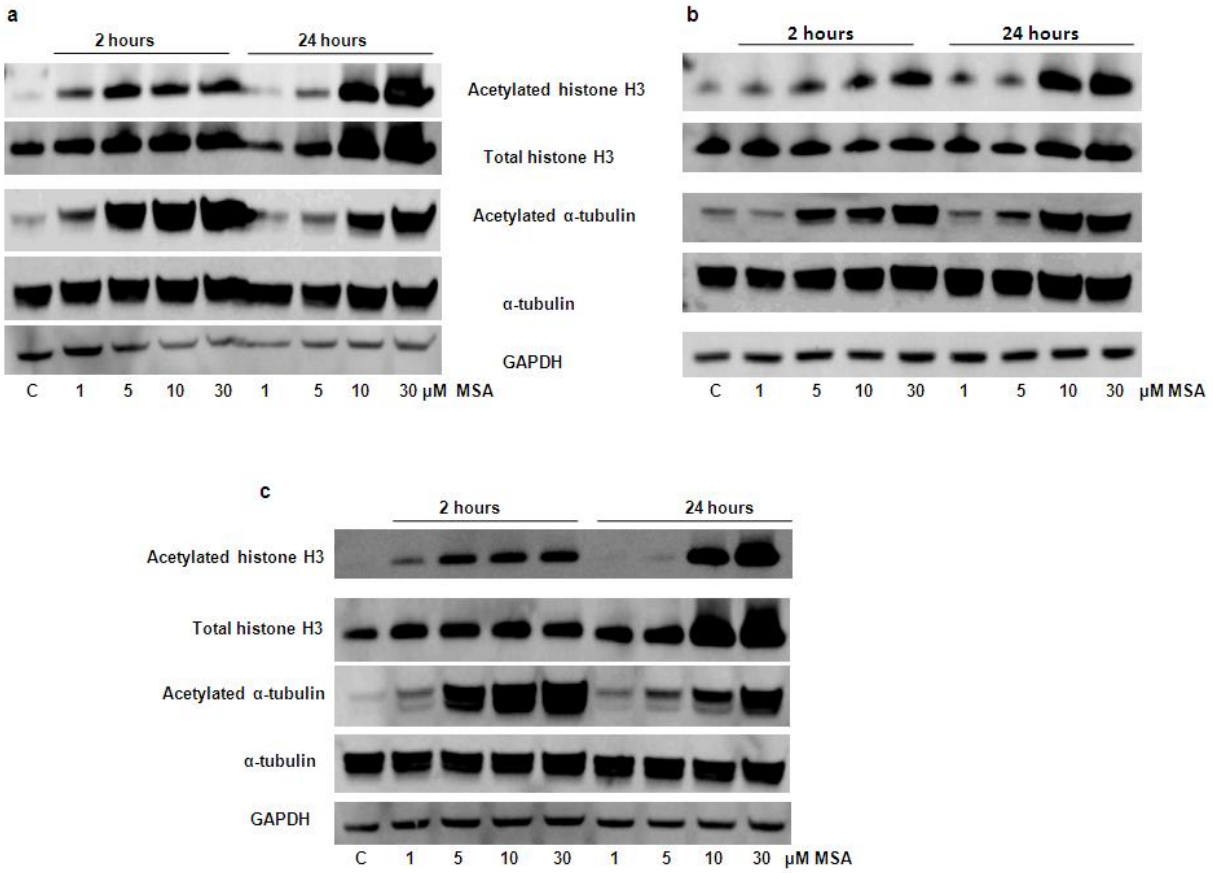

Figure 6.4 Representative western blots of protein acetylation in (a) RL, (b) SUD4 (c) DHL4 cell lines exposed to MSA for 2 and 24 hours. These experiments were performed twice.

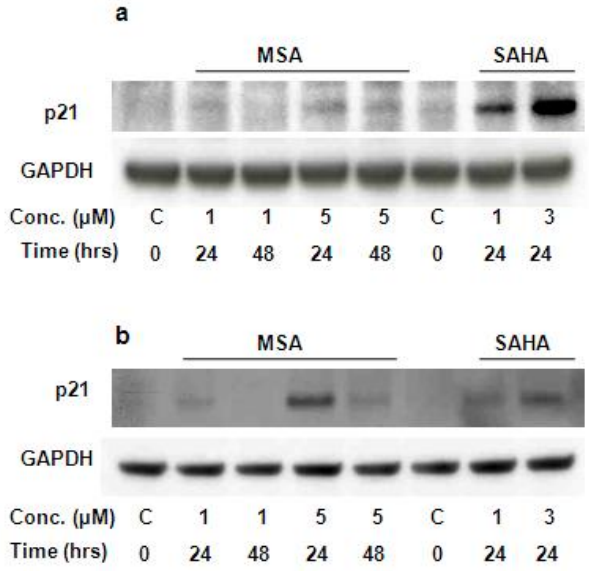

Figure 6.5 p21 expression (a) SUD4 and (b) RL cells exposed to MSA and SAHA

6.4.2 The effect of MSA on histone deacetylase activity

The effect of MSA on HDAC activity was investigated. To validate the assay kit, TSA, a known HDACi (provided in the assay kit) was first tested. TSA showed a concentration-dependent inhibition of *Fluor de Lys*™ substrate deacetylation by HeLa nuclear extract after 30 minutes incubation (Figure 6.6).

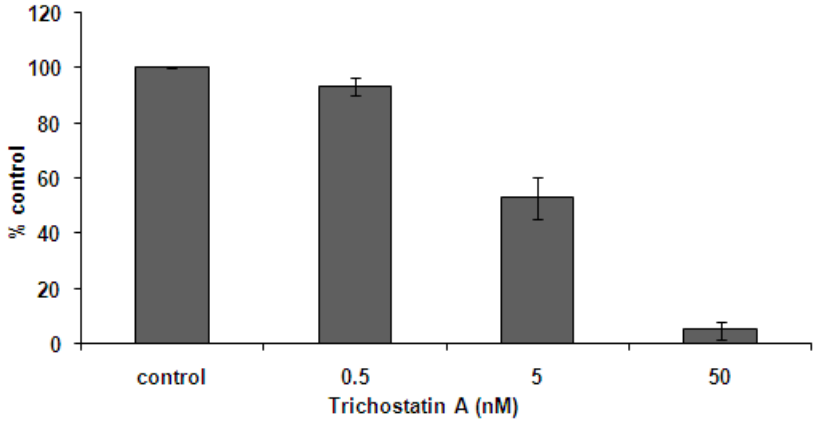

Figure 6.6 TSA inhibition of *Fluor de Lys*™ substrate deacetylation by HeLa nuclear extract. Data points are the mean+/-SD of 5 separate experiments.

However, when MSA was incubated with HeLa nuclear extract for 30 minutes, there was no inhibition of *Fluor de Lys*™ substrate deacetylation, suggesting that MSA, in this cell-free assay system, was not able to inhibit HDAC activity (Figure 6.7).

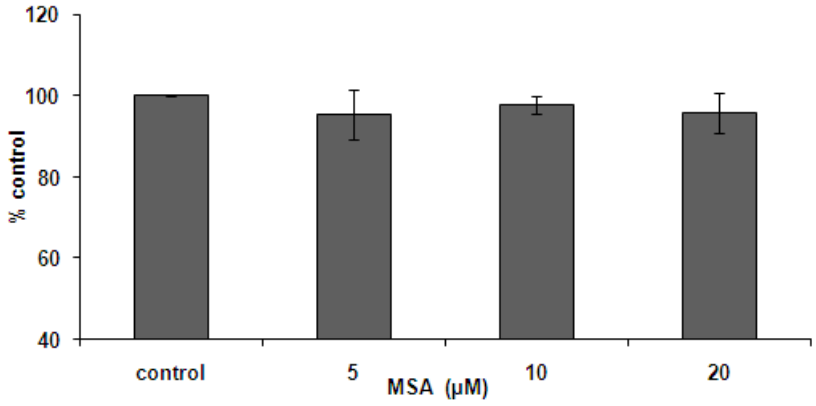

Figure 6.7 Effect of MSA on *Fluor de Lys*™ substrate deacetylation by HeLa nuclear extract. Data points are the mean+/-SD of 3 separate experiments.

Therefore, the effect of MSA on HDAC activity was tested in a cell-based assay. In this assay, MSA was able to inhibit HDAC activity in a concentration-dependent manner in all three cell lines after 2-hour exposure (Figure 6.8). 30µmol/L MSA in all three cell lines inhibited HDAC activity by around 50%. This suggests that cellular metabolism of MSA is required to generate an active metabolite.

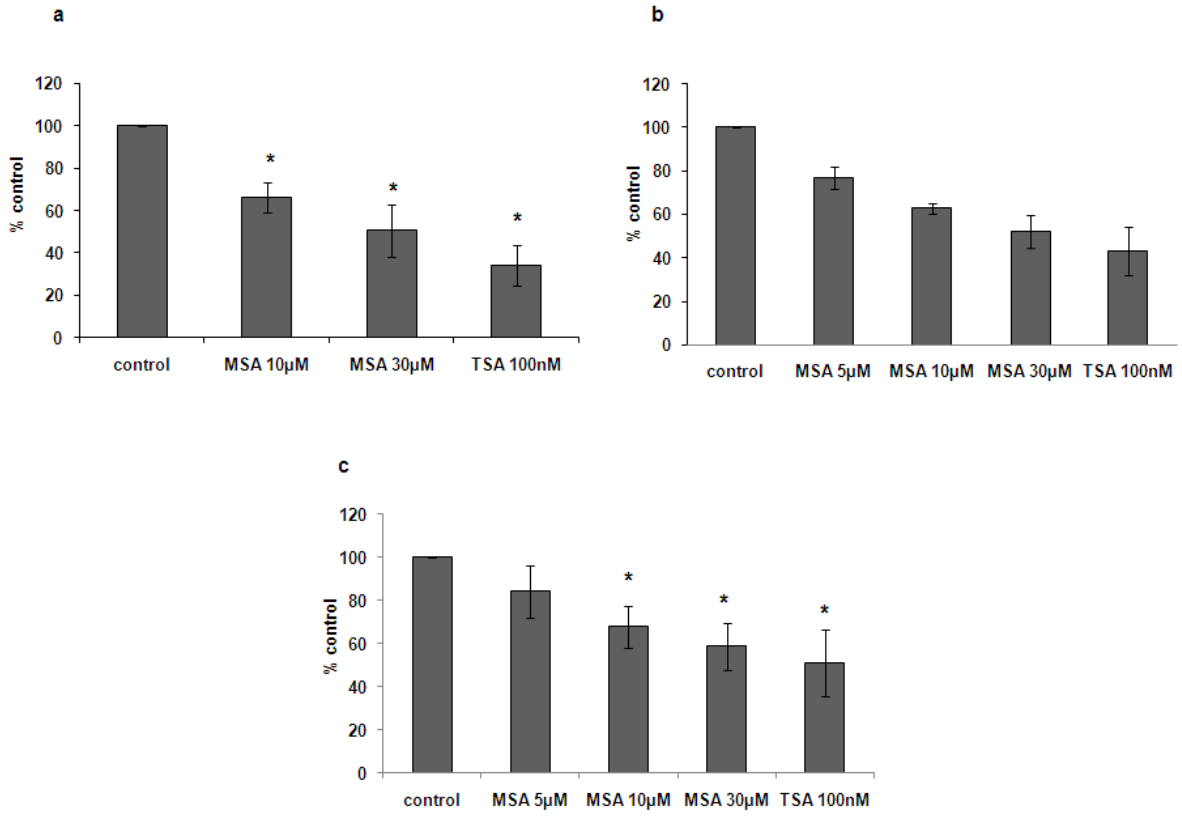

Figure 6.8 Deacetylation of *Fluor de Lys*™ substrate in (a) DHL4, (b) SUD4 and (c) RL cell lines incubated with MSA or TSA for 2 hours. Data points are the mean+/-SD of at least 3 separate experiments except in the SUD4 cells where experiments were only performed in duplicate. *$p<0.05$. p values are comparisons with control.

To confirm that HDAC inhibition did not occur in the cell-free assay even with prolonged exposure to MSA, or using an alternative HDAC source, MSA was incubated with HeLa nuclear extract and DHL4 cell lysates for 2 hours. Initially, to confirm the protein concentration of DHL4 cell lysate that produced the same fluorescence signal as the HeLa nuclear extract, different protein concentrations were used in the assay (Figure 6.9).

8µg of protein produced an equivalent fluorescence signal and therefore this concentration was used in the subsequent experiments

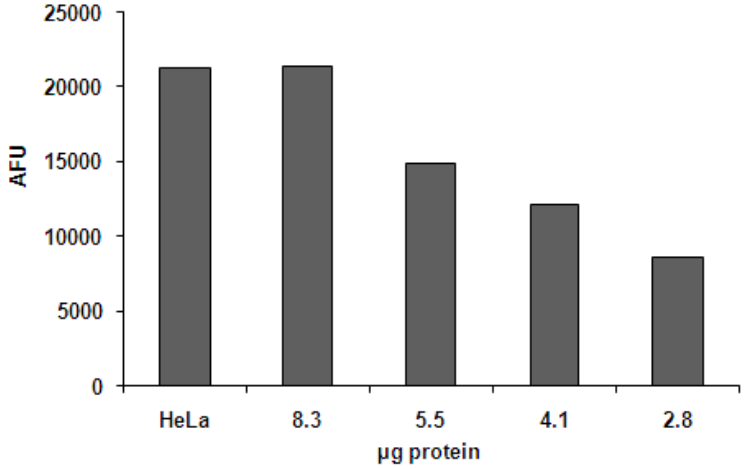

Figure 6.9 Fluorescence signal produced after incubation of *Fluor de Lys*™ substrate with different concentrations of DHL4 cell lysate compared with HeLa nuclear extract. AFU=arbitrary fluorescence units.

When MSA was incubated with either HeLa nuclear extract or DHL4 cell lysate for 2 hours there was no inhibition of *Fluor de Lys*™ substrate deacetylation. This was in contrast to incubation with TSA used as a positive control (Figure 6.10).

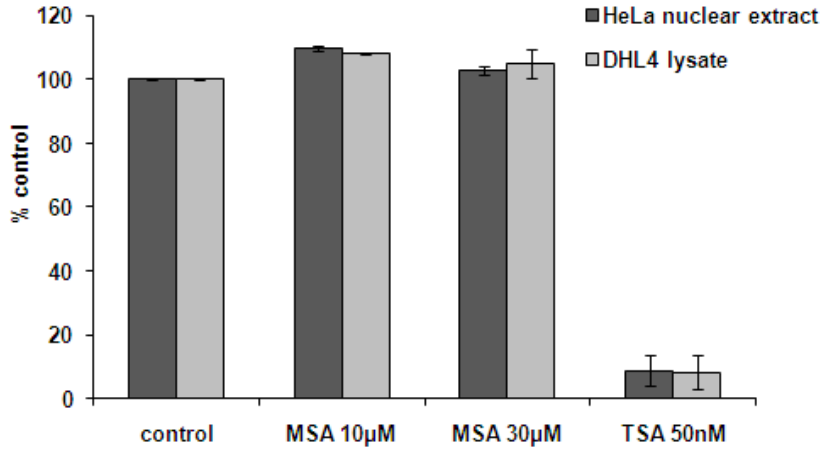

Figure 6.10 Deacetylation of *Fluor de Lys*™ substrate by HeLa nuclear extract and DHL4 cell lysate after incubation with MSA or TSA. Data points are the mean+/-SD of 2 separate experiments.

To further investigate whether a cellular metabolite of MSA was responsible for the observed HDAC inhibitory effect, medium from DHL4 cells incubated with MSA for 2 hours was tested in the cell-free HDAC assay kit. Medium from DHL4 cells incubated with 10µmol/L MSA was not able to inhibit *Fluor de Lys*™ substrate deacetylation but medium from DHL4 cells incubated with 30µmol/L MSA had a small but significant inhibitory effect of 20.6% (±4.7; Figure 6.11). This supports the hypothesis that a cellular metabolite of MSA is responsible for the effect seen.

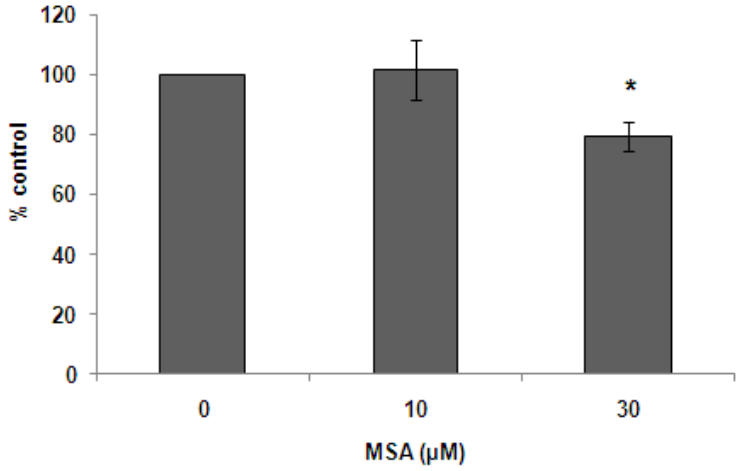

Figure 6.11 Deacetylation of *Fluor de Lys*™ substrate by HeLa nuclear extract after incubation with cell medium from DHL4 cells exposed to MSA. Data points are the mean+/-SD of 3 separate experiments. *p=0.02 is a comparison with control.

6.4.3 The effect of MSC on protein acetylation

MSC will be the Se compound used in the forthcoming clinical trial and therefore its effect on protein acetylation was also investigated. RL and DHL4 cell lines were exposed to EC_{50} and higher than EC_{50} concentrations of MSC for 24 hours (EC_{50} values of MSC shown in Chapter 4, Table 4.2). MSC increased the acetylation of histone H3 and α-tubulin and the expression of p21 in a concentration-dependent manner, suggesting that MSC also inhibits HDAC activity (Figure 6.12). A higher than EC_{50} concentration was required in RL cells to observe this effect.

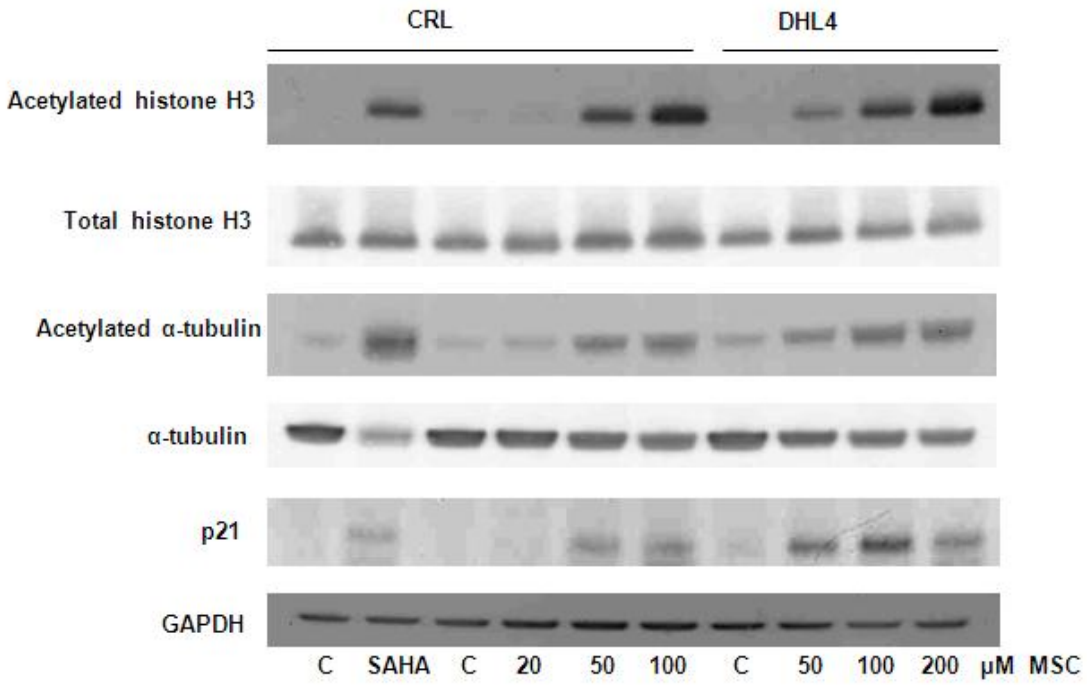

Figure 6.12 Protein acetylation and p21 expression in RL and DHL4 cell lines exposed to MSC for 24 hours. RL cells were also exposed to SAHA 3μmol/L for 24 hours

6.4.4 Effect of MSA on HIF-1α expression and vascular endothelial growth factor production

The effect of MSA on HIF-1α expression and VEGF production was investigated after culture of RL and DHL4 cells under hypoxic conditions for 24 hours. Western blotting for HIF-1α in nuclear extracts showed that hypoxia induced the expression of HIF-1α but this induction was suppressed by MSA (Figure 6.13). Hypoxia also increased the production of VEGF by RL and DHL4 cell lines, but this was also inhibited by MSA in a concentration-dependent manner (Figure 6.14)

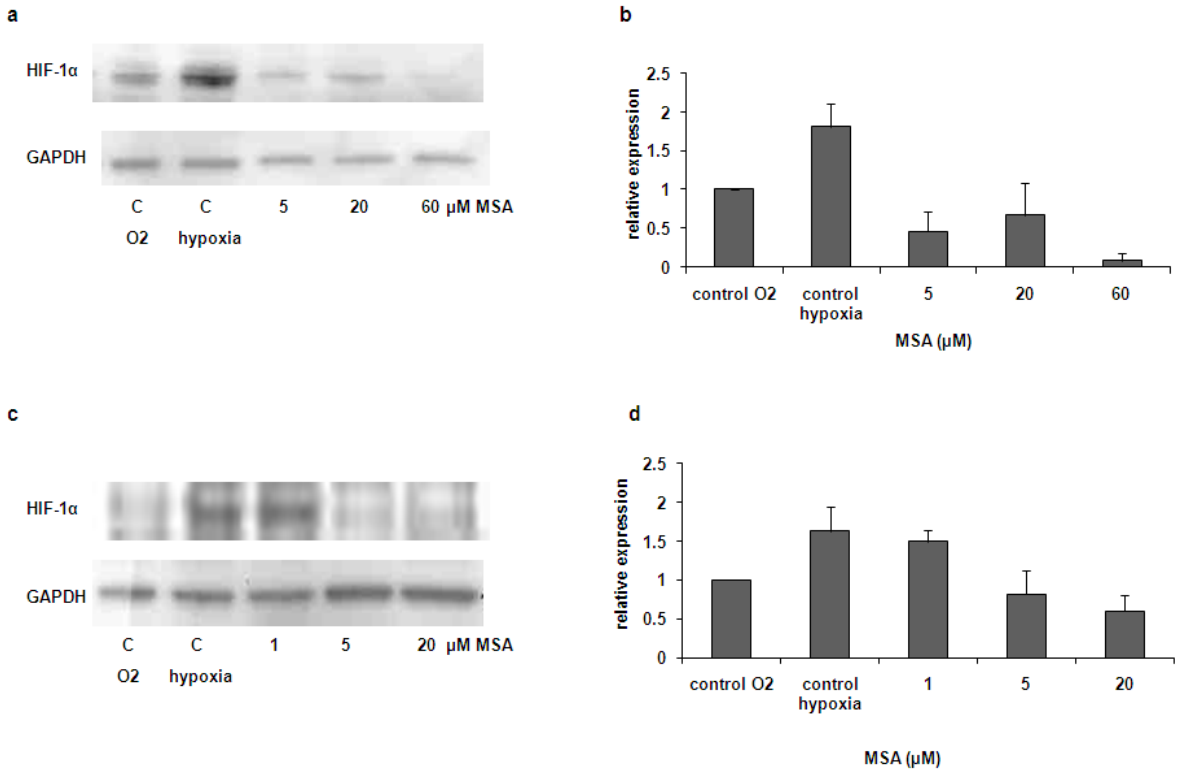

Figure 6.13 HIF-1α expression in (a, b) DHL4 cells and (c, d) RL cell lines exposed to hypoxia and MSA. Western blot and densitometry combining 2 separate experiments; data points are mean+/-SD.

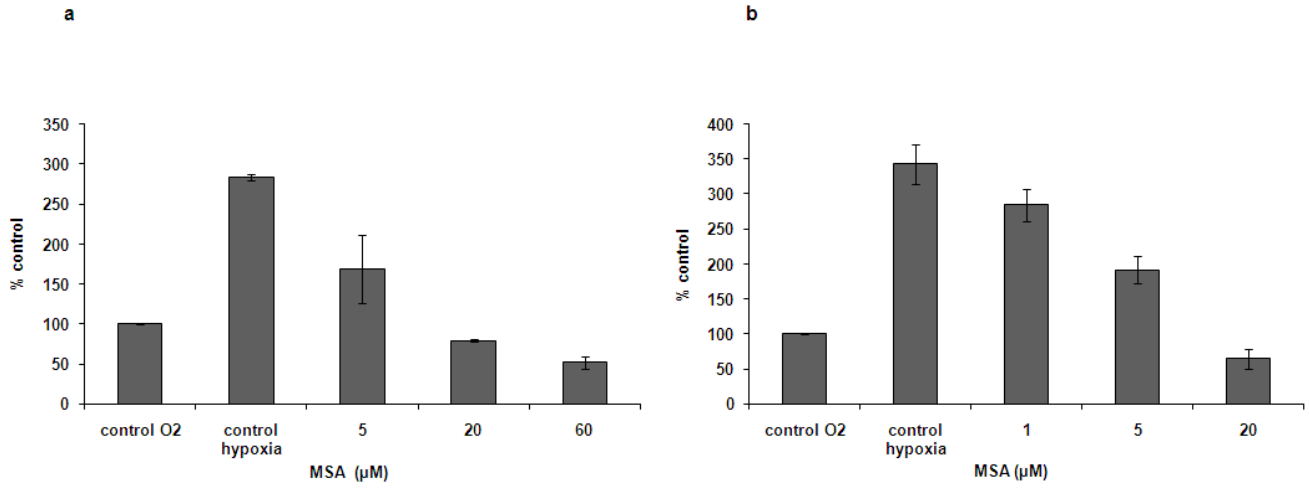

Figure 6.14 Vascular endothelial growth factor levels in the supernatant of (a) DHL4 and (b) RL cell lines exposed to hypoxia and MSA. Data points are the mean+/-SD of 2 separate experiments. Values are expressed relative to control and are corrected for cell number ($1x10^6$ cells).

6.4.5 Acetylation of Histone H3 in peripheral blood mononuclear cells

The effect of MSA in PBMCs from 3 individuals was investigated. Concentrations of 5µmol/L and above increased the acetylation of histone H3 (Figure 6.15). Unexpectedly, the expression of total histone H3 also increased.

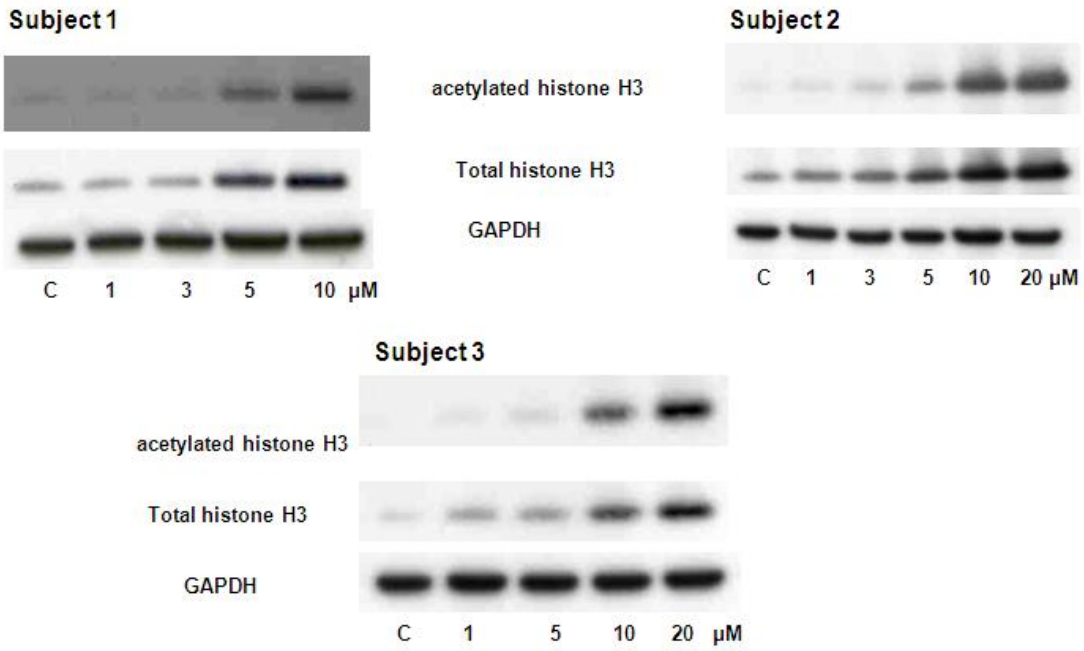

Figure 6.15 Histone H3 acetylation in peripheral blood mononuclear cells exposed to MSA for 24 hours.

6.5 DISCUSSION

These experiments have demonstrated that MSA can inhibit HDAC activity in three DLBCL cell lines. MSA increased the acetylation of histone H3 and α-tubulin in a concentration-dependent manner and the effect was apparent at concentrations as low as 1µmol/L. The pattern of protein changes was similar in all three cell lines despite the fact that RL and SUD4 cells are relatively sensitive and DHL4 cells relatively resistant to the cytotoxic effects of MSA. The increase in acetylated α-tubulin was greater at 2 hours than 24 hours and the increase in acetylated histone H3 greater at 24 hours. Acetylation of α-tubulin occurs as a result of the inhibition of HDAC6, a class II HDAC. This suggests

that MSA inhibits both class I and II HDACs but the time-course differs with an earlier effect on class II HDACs. MSA also induced the expression of p21, a cyclin-dependent kinase inhibitor, which is a well known target of HDAC inhibition. This occurs independently of p53 and is due to acetylation of histones in its gene promoter (Richon *et al*, 2000). The induction of p21 would be expected to result in cell cycle arrest, however, in these DLBCL cell lines MSA does not induce cell cycle changes (Last *et al*, 2006).

The HDAC inhibitory action of MSA was confirmed by an HDAC activity assay. However, in the cell-free assay, MSA was not able to inhibit the HDAC activity of HeLa nuclear extract. HDAC inhibition was only apparent when MSA was exposed to cells and activity measured in a cell-based assay. This is likely to be due to the intracellular activation of MSA to methylselenol, which is the metabolite thought to be responsible for its anti-tumour effect. The metabolism of MSA also results in the production of other reactive metabolites such as dimethylselenide and dimethyldiselenide (Juliger *et al*, 2007); this will be discussed further in Chapter 9. Medium from DHL4 cells exposed to 10µmol/L and 30µmol/L MSA, which in the cellular activity assay produced 34% and 50% inhibition HDAC activity respectively, was used in the cell-free assay. Only medium from DHL cells exposed to 30µmol/L MSA inhibited HDAC activity in the HeLa nuclear extract and only by 21% ($p=0.02$). This is probably due to the volatile nature of MSA metabolites which are not retained in the cell medium. These novel findings suggest that it is not only the α-keto acid metabolites of organic Se compounds that are capable of inhibiting HDAC activity but that the volatile methylated species are likely to play a role. For completeness, it would have been useful to confirm that MSA does not decrease the expression of HDAC enzymes at the protein level, which could also explain the decrease in HDAC activity. However, this is less likely, as changes in protein translation usually take longer than 2 hours. In addition, further time-course experiments are required to establish the duration of HDAC inhibition. This could include using class-specific HDAC assays to investigate the time-course of class I and class II HDAC inhibition.

MSC was also found to increase the acetylation of histone H3 and α-tubulin in two DLBCL cell lines, however, high concentrations were required. The EC_{50} of RL cells to MSC at 72 hours was 22μmol/L but concentrations higher than this were required to induce protein acetylation. The DHL4 cell line has a higher EC_{50} at 72 hours of 56μmol/L and exposure to 50μmol/L MSA did induce protein acetylation. Western blots were only performed at one time point, 24 hours, and it may be that if an earlier time point had been studied a greater effect may have been seen. However, these results are similar to those of studies in colon and prostate cancer cells in which western blotting was performed in cells exposed to 50μmol/L and 200μmol/L MSC for 24 hours (Lee *et al*, 2009a; Nian *et al*, 2009). As previously discussed, metabolism of MSC to its active metabolites methylselenol and MSP requires β-lyases and aminotransferases respectively which are likely to be present at low levels in tumour cells.

HDAC inhibition as a therapeutic strategy in lymphoma has proven to be a useful one, although it appears that T-cell lymphomas are more sensitive than B-cell lymphomas to HDAC inhibition. The best results have been seen in patients with cutaneous T-cell lymphoma (CTCL) for which vorinostat now has FDA approval. Thirty-three patients with refractory CTCL, who had received a median of 5 previous treatments, took part in a phase II trial of vorinostat. The RR rate was 24% with 8 patients achieving a PR. In addition, 11 patients had improvement in their symptoms, stable disease or both (Duvic *et al*, 2007). In DLBCL, the response to HDAC inhibition has been less impressive. A phase II study of vorinostat in 18 patients with relapsed DLBCL had only 2 responders (1 CR and one stable disease) and the remaining 16 patients discontinued treatment due to progressive disease (Crump *et al*, 2008). Although these results are disappointing, it may be, as with other targeted therapies, that combination with conventional chemotherapy, or with other novel agents may be required to achieve better responses.

There is a scientific rationale for the use of HDACi in DLBCL. It has been demonstrated by IHC staining that class I HDACs are over-expressed in tumours when compared with normal lymphoid tissue. There is, however, some discrepancy in the data about the

expression of class II HDACs, particularly HDAC6, with one study showing that it is very rarely expressed in primary tumours (Gloghini *et al*, 2009) and another showing that HDAC6 is expressed (Marquard *et al*, 2009). Furthermore, in the latter study, patients with moderate and high expression had a better outcome than patients with low expression. Class I HDACs also appear to be widely expressed in other lymphoid tumours including Hodgkin lymphoma which, in clinical trials, is more responsive than DLBCL to the HDACi MGCD0103 (Younes *et al*, 2007). HDAC expression in tumours does not however appear to be a good predictive marker for treatment response to HDACi (Gloghini *et al*, 2009). An additional role for HDAC inhibition in DLBCL is that acetylation of the transcriptional repressor, Bcl-6, inhibits its function (Bereshchenko *et al*, 2002). This protein is frequently involved in translocations and over-expressed in DLBCL thus being implicated in the pathogenesis of the disease (Swerdlow SH, 2008).

HDAC inhibition by MSA requires relatively high concentrations, with 30µmol/L for 2 hours resulting in 40-50% inhibition of activity across the three cell lines tested. HDACi currently in clinical trials inhibit activity *in vitro* at nanomolar concentrations (Khan *et al*, 2008). However, this Se concentration is potentially clinically achievable. In the phase I/II dose escalation study of SLM in patients with solid tumours, the highest dose level of 7200µg twice daily resulted in a mean plasma Se concentration after 8 days of 31µmol/L (Fakih *et al*, 2008). In the forthcoming clinical trial at SBH, the aim will be to achieve a plasma Se concentration of 20µmol/L. Despite the relatively high concentration required to inhibit HDAC enzyme activity by 50%, there is evidence (at the protein level) of an effect at concentrations as low as 1µmol/L, which resulted in increased acetylation of histone H3 and α-tubulin. However, in PBMCs, ≥5µmol/L MSA was required to increase acetylation of histone H3. It would be valuable to study an earlier time-point in PBMCs, such as 2-hour exposure, in case low concentrations of MSA increase protein acetylation early without sustaining the response to 24 hours. Acetylation of histone H3 in PBMCs at 24 hours is concentration-dependent between 5-20µmol/L and therefore may serve as a useful biomarker of Se activity in the forthcoming clinical trial. Histone acetylation in PBMCs has already been successfully used as a biomarker in clinical trials of HDACi,

however, in most studies this does not appear to be a predictive marker of response (Garcia-Manero *et al*, 2008).

Se may have a role in inhibiting angiogenesis and as described previously in Chapter 1, this has been extensively demonstrated in solid tumour xenograft models (Bhattacharya *et al*, 2008; Yin *et al*, 2006). In DLBCL cell lines exposed to hypoxia, MSA was able to suppress the induction of HIF-1α, demonstrated by western blotting of nuclear extracts, and the production of VEGF, demonstrated by an electrochemiluminescence assay of cellular supernatants. This occurred at similar concentrations to those required to inhibit HDAC activity and at concentrations that are clinically achievable. HDACi appear to target tumour angiogenesis and in addition to the pre-clinical data, there are clinical data from the phase II trial of vorinostat in CTCL to support this (Duvic *et al*, 2007). Paired skin biopsies of lymphoma lesions before and after vorinostat therapy showed a significant reduction in microvessel density in patients who responded to treatment. Although the role of hypoxia and angiogenesis in tumour progression is better established in solid tumours, these factors may also be important in lymphoma.

The most important mediator of angiogenesis is VEGF, which has several family members, including VEGF-A –B –C and –D, that interact with receptor tyrosine kinases VEGFR1 and VEGFR2. VEGF-A is produced by tumours cells and surrounding stromal cells, promoting angiogenesis through interaction with receptors on endothelial cells and bone marrow-derived endothelial precursors. In addition, VEGF-A can interact with receptors on tumour cells, resulting in cell survival and proliferation in an autocrine manner. Tumour-associated stromal cells also produce a number of other pro-angiogenic factors (Ferrara *et al*, 2003). Regarding DLBCL, it has been demonstrated that the tumour cells express both VEGF and VEGF receptors and the degree of VEGF expression correlates with the receptor expression, suggesting that autocrine and paracrine VEGF signalling may be important in lymphoma progression (Gratzinger *et al*, 2007). Targeting VEGF receptors was found to inhibit tumour growth in a xenograft model of DLBCL and both paracrine and autocrine signalling was shown to be important through the use of

species-specific VEGF receptor antibodies (Wang *et al*, 2004). The tumour microenvironment is important in lymphoma progression. A study analysing gene expression in tumour samples from patients with DLBCL found that the gene expression signature of the *non-malignant cells* influenced survival, such that tumours expressing genes related to angiogenesis, also shown to be associated with increased tumour blood-vessel density, conferred an inferior prognosis (Lenz *et al*, 2008a). When microvessel density of DLBCL samples has been studied in isolation, there have been conflicting data as to whether the degree of vascularity correlates with tumour VEGF expression and also outcome (Gratzinger *et al*, 2007; Gratzinger *et al*, 2008; Jorgensen *et al*, 2007). Most studies have shown that serum VEGF levels are increased in patients with NHL compared to controls (Passam *et al*, 2008) but whether the degree of elevation correlates with outcome is unclear, with some studies reporting an inferior outcome in patients with high serum VEGF levels at diagnosis (Salven *et al*, 2000) whereas others have not found an association (Giles *et al*, 2004). However, most studies have included patients with different types of B-cell NHL and therefore the impact on specific NHL subtypes needs to be further investigated.

There is increasing interest in targeting angiogenesis in lymphoma and bevacizumab, the humanised monoclonal antibody targeting VEGF-A, has been used in clinical trials. A phase II trial of single agent bevacizumb in 52 patients with recurrent DLBCL and MCL resulted in disease stabilisation in 25% of patients with a median time to progression of 5.2 months (Stopeck *et al*, 2009). These results are not particularly impressive but single agent therapy in patients with chemo-resistant DLBCL is unlikely to yield significant responses given the numerous pathogenic pathways involved. Therefore, bevacizumab in being investigated in combination with 'R-CHOP' in phase II/III trials. The safety and feasibility of the combination has already been established (Ganjoo *et al*, 2006).

The role of HIF-1α in lymphoma has not been extensively investigated but from the available data it appears that about 60% of tumours from patients with DLBCL express HIF-1α, with most exhibiting moderate to high expression and no difference in

expression based on the cell of origin assessed by IHC (Evens *et al*, 2008; Evens *et al*, 2010). The one study to investigate the prognostic significance of HIF-1α expression found it to be an independent predictor of good progression-free and OS in patients treated with 'R-CHOP' but not in those who received 'CHOP' without rituximab (Evens *et al*, 2010). Correlation with gene expression revealed that increased HIF-1α gene expression was associated with expression of genes forming part of the favourable stromal-1 gene signature as defined by Lenz *et al* (Evens *et al*, 2010; Lenz *et al*, 2008a). This study suggests that rituximab has a beneficial effect on HIF-1α or its downstream target genes. Further studies are required to fully understand this interaction.

Given that MSA can inhibit the induction of HIF-1α expression and the production of VEGF by DLBCL cell lines, it may have the ability to inhibit angiogenesis and other downstream targets of HIF-1α *in vivo*. However, the mechanism by which MSA inhibits HIF-1α and VEGF in DLBCL cell lines is not clear. Although MSA has been found to be an HDACi and HDACi have anti-angiogenic properties, these two observations have not been mechanistically linked by the current experimental data. In solid tumours, MSA and MSC have been reported to inhibit HIF-1α through effects on PHDs (Chintala *et al*, 2010). In order to establish whether MSA inhibits HIF-1α in DLBCL cell lines through HDAC inhibition, the experiment to perform would be to over-express HDACs and see whether this prevented the inhibition of HIF-1α expression. In addition, for the purposes of the forthcoming clinical trial, it may be possible to use plasma VEGF levels as a biomarker of Se activity.

In summary, this work has demonstrated the novel finding that a cellular metabolite of MSA is able to inhibit HDAC activity in DLBCL cell lines. MSA also inhibited the induction of HIF-1α expression and the production of VEGF in these cell lines. In addition, two potential biomarkers of Se activity have been identified that may be of value in the forthcoming clinical trial; acetylated histone H3 in PBMCs and plasma VEGF levels.

CHAPTER 7: The activity of methylseleninic acid in non-malignant cells

7.1 INTRODUCTION

There is ample evidence in the literature supporting a cyto-protective role for Se. Of particular interest to cancer medicine is its ability to protect normal cells from chemotherapy-and radiation-induced toxicity, an effect that has been demonstrated *in vitro* (Rafferty *et al*, 2003a; Santos & Takahashi, 2008), in xenograft models of human cancer (Cao *et al*, 2004) and in clinical trials (Muecke *et al*, 2010). However, the exact mechanism by which Se protects normal cells is not clear and it is apparent that different chemical forms act by different mechanisms. Evidence for the cyto-protective role of Se, and potential mechanisms by which it exerts this effect, have already been discussed in Chapter 1, but some additional points relating to organic Se compounds will be summarised here.

A number of studies have demonstrated that Se, mainly in the form of SLM, is able to activate DNA repair mechanisms when cells are exposed to DNA-damaging agents and that this is *p53*-dependent. *p53* is mutated and non-functional in a large proportion of human cancers. In the absence of functional *p53*, Se is unable to activate DNA repair mechanisms, leaving cells vulnerable to apoptosis (Fischer *et al*, 2007; Seo *et al*, 2002a; Seo *et al*, 2002b). SLM can also activate p53 by a redox mechanism in the absence of DNA damage, requiring the redox factor Ref-1 (Seo *et al*, 2002a). In addition, Ref-1 has also been found to be important in the activation of p53 in response to DNA damage (Jeong *et al*, 2009). Thus the functional status of *p53* may be one reason for the observed differential effect of Se in malignant and non-malignant cells. However, this may not be as relevant in haematological cancers because, compared to solid tumours, *p53* mutations are less common. The frequency of *p53* mutations in lymphoid malignancies at diagnosis has been reported to be 12.5% (Newcomb, 1995) although in some lymphoma subtypes this is higher, with one study in 'aggressive' B-cell lymphomas reporting a frequency of 22% (Ichikawa *et al*, 1997).

Other mechanisms that may be important include differential responses of malignant and non-malignant cells to cellular stress and, as discussed in Chapter 5, Se can induce ER stress. It has been proposed that because malignant cells, through the nature of the tumour environment, are already under a degree of cellular 'stress', any additional 'stress', such as protein misfolding in the case of Se, is tolerated less well, making them more susceptible to apoptosis. In contrast, normal cells are exposed to less 'stress' and therefore, in response to ER stress induced by Se, can mount a survival response and have a higher threshold for apoptosis (Zu *et al*, 2006).

Another cellular stress response pathway that may be differentially modulated by Se is the Nrf2-Prx1 pathway. As discussed in Chapter 1, it has been suggested that differences in oxygen conditions between the environment of normal and malignant cells may affect the cells' response to Se, with inhibition of the Nrf2-Prx1 pathway in tumour cells, thus promoting apoptosis, but induction of the pathway in normal cells, thus promoting cell survival (Kim *et al*, 2007e). In addition to cellular stress-response pathways, other survival pathways may be activated by normal cells in response to Se. A study examining the effect of MSA on tumour stage-specific mouse prostate cell lines found that tumour cells dephosphorylated Akt and Erk1/2 in response to MSA but that the non-tumourigenic cell line increased phosphorylation of Akt and Erk1/2, thus promoting cell survival (Gonzalez-Moreno *et al*, 2007).

The response of non-malignant cells to MSA has been investigated in the experiments presented in this chapter, with the aim of determining further mechanisms by which Se may protect these cells from chemotherapy-induced toxicity. The concentration of MSA used, particularly in PBMC experiments, was determined by the fact that in the forthcoming clinical trial in patients with DLBCL the aim is to achieve a plasma Se concentration of 20μM. This concentration was determined from the xenograft study by Cao *et al*, in which plasma Se concentrations of >14μmol/l and >23μmol/l were required to achieve maximum protection against chemotherapy-induced toxicity and potentiation of anti-tumour activity, respectively. These concentrations were established following SLM administration and it is likely that lower plasma Se concentrations will be adequate

following MSC administration given its more efficient conversion to methylselenol (Azrak *et al*, 2004).

7.2 AIMS

1) To investigate the activity of MSA in non-malignant cells.

2) To investigate the effect of combining MSA with cytotoxic agents in non-malignant cells.

3) To investigate mechanisms of Se-resistance in non-malignant cells.

7.3 MATERIALS AND METHODS

In these experiments, normal cells (keratinocytes, fibroblasts and PBMCs) were exposed to a range of MSA concentrations for various time points. Keratinocytes and fibroblasts were also exposed to 4-HC, the active metabolite of cyclophosphamide, and doxorubicin. Trypan blue exclusion and the ATP assay (described in Chapter 2, sections 2.3.1 and 2.3.2) were used to assess cytotoxicity. The results of the ATP assay were expressed relative to the control value and were analysed using the GraphPad PRISM® software (version 5.03). The drug activity was summarised to an EC_{50} value which was calculated using a sigmoidal concentration-effect model with variable slope.

Western blotting was performed to identify protein changes induced by MSA (described in Chapter 2, sections 2.4 and 2.5). The effect of MSA on cell cycle distribution in keratinocytes was determined by flow cytometric analysis of cells stained with PI (described in Chapter 2, section 2.7). In addition, the effect of MSA on NF-κB activity in PBMCs was determined using an ELISA kit.

7.3.1 Cell lines

Normal human keratinocytes immortalised by transfection of hTERT, the catalytic subunit of the enzyme telomerase, were purchased from Dr J. Rheinwald (Brigham and Women's Hospital and Harvard Skin Disease Centre, Harvard Medical School, MA, USA) (Dickson *et al*, 2000). These were maintained in keratinocyte serum-free medium

(GIBCO® Invitrogen™) supplemented with bovine pituitary extract (final concentration 25µg/ml), 1% penicillin (10,000units/ml) and streptomycin (10,000µg/ml), epidermal growth factor (final concentration 0.2ng/ml) and 0.3mM calcium chloride (all supplements from Invitrogen™). The HFFF2 cell line (human foetal foreskin fibroblast) was a kind gift from Dr J. Marshall (Institute of Cancer, Barts Cancer Centre, London, UK). These cells were maintained in Dulbecco's Modified Eagle Medium with high glucose (4500mg/l) and GlutaMax™ (GIBCO® Invitrogen™) supplemented with 7.6mls of GlutaMax™ (GIBCO® Invitrogen™),1% penicillin (100units/ml) and streptomycin (100µg/ml) and 10% foetal calf serum (Sigma-Aldrich). Both cell lines were kept at 37°C in a humidified atmosphere and 5% CO_2. Cell medium was changed every 2-3 days and cells were passaged once 70% confluence was reached. Cells were detached using trpsin/EDTA solution (Trypsin 0.05%, EDTA 0.01% in PBS, GIBCO® Invitrogen™).

7.3.2 Chemicals

Recombinant tissue necrosis factor alpha (TNFα; R&D systems, Europe, Ltd) was supplied as a lyophilized sample. This was reconstituted in PBS to prepare a stock solution of 100µg/ml, which was stored at -20°C. Prior to use, it was further diluted in cell culture medium to obtain a final concentration of 10ng/ml.

7.3.3 NF-κB activity in peripheral blood mononuclear cells treated with MSA

Activated NF-κB in PBMCs treated with MSA was measured by ELISA (enzyme-linked immunosorbent assay) using the TransAM™ NF-κB p65 transcription factor assay kit (Active Motif North America, Carlsbad, CA), according to the manufacturers' instructions. Six µg of protein from cell lysates was incubated in 96-well plates on which the oligonucleotide containing the NF-κB consensus (5'-GGACTTTCC-3') binding site had been immobilised. NF-κB binding to the target was detected by incubation with a primary antibody to the p65 subunit that recognised an epitope on p65 that is accessible only when NF-κB is activated and bound to its target DNA. An anti-IgG-horseradish peroxidise-conjugated secondary antibody was then added and the reaction was quantified by adding a chemiluminescent reagent and reading luminescence at a

wavelength of 450nm on the POLARstar OPTIMA plate reader (BMG Labtech). For each experiment a negative and positive control was used. The assay kit provided a positive control in the form of Jurkat nuclear extract. In addition, to monitor specificity of the assay, a wild-type consensus oligonucleotide was provided as a competitor for NF-κB binding that prevented NF-κB in the experimental sample from binding. The effect of MSA on NF-κB activation by TNFα was also studied. All samples and controls were analysed in duplicate and results were expressed relative to the control values obtained for untreated PBMCs.

7.4 RESULTS

7.4.1 The activity of MSA in three *in vitro* models of normal cells

The activity of MSA was investigated in PBMCs, hTERT-immortalised keratinocytes and the HFFF2 cell line. Previously published results from our laboratory have shown that PBMCs are relatively resistant to the cytotoxic effect of MSA with an EC_{50} at 72 hours of 84.2μmol/l (Juliger *et al*, 2007). To confirm that the concentrations of MSA to be used in subsequent PBMC experiments were not cytotoxic, cell viability of PBMCs exposed to 5μmol/L, 10μmol/L and 20μmol/L MSA for 24 and 48 hours was determined by trypan blue exclusion. Figure 7.1 shows that at these concentrations there was minimal toxicity to the cells, with 20μmol/L MSA at 48 hours reducing cell viability by 12.3% (± 3.0; p=0.02).

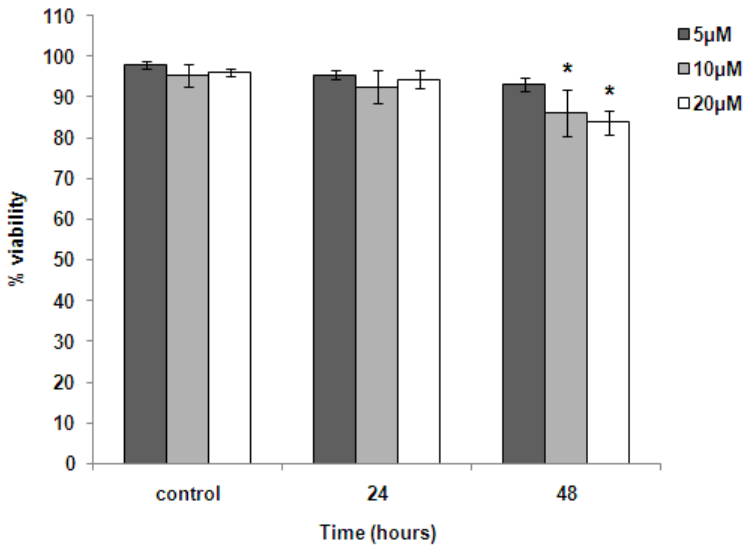

Figure 7.1 Perpipheral blood mononuclear cell viability determined by trypan blue exclusion after exposure to MSA. Data points are mean+/-SD of at least 3 separate experiments. *p<0.05. p values are a comparison with control.

The activity of MSA in keratinocytes and HFFF2 cells is shown in Figure 7.2. Both cell lines were very sensitive to the cytotoxic effect of MSA as determined by the ATP assay. For keratinocytes the EC_{50} at 48 hours was 2.4µmol/L (95% CI 2.2-2.6µmol/L) and for HFFF2 cells was 7.2µmol/L (95% CI 6.0-8.7µmol/L).

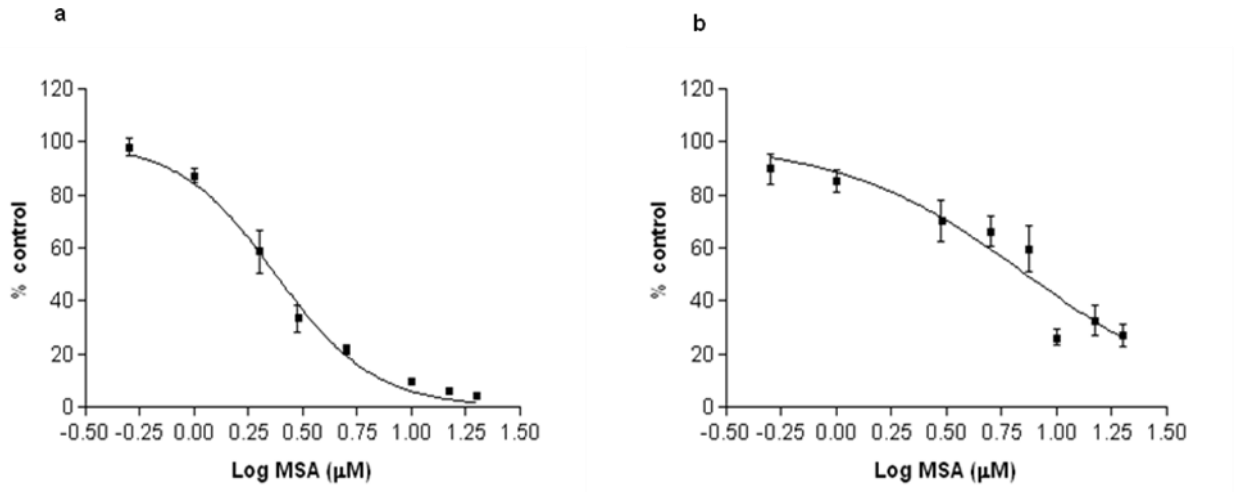

Figure 7.2 EC_{50} concentration-effect curves following 48-hour exposure to increasing concentrations of MSA in (a) Keratinocytes and (b) HFFF2 cells. Data points are the mean +/- SD of three separate experiments.

7.4.2 The activity of chemotherapeutic agents in keratinocytes and HFFF2 cells

To establish whether keratinocytes and HFFF2 cells were sensitive to other cytotoxic agents or whether this was a specific effect of MSA, cells were exposed to doxorubicin and 4-HC for 48 hours. Figure 7.3 shows that keratinocytes were relatively sensitive to both drugs. The 48-hour EC_{50} for 4-HC was 13.2µmol/L (95% CI 11.6-15.0µmol/L) and doxorubicin was 214nmol/L (95% CI 179.5-255.2nmol/L) as determined by the ATP assay. HFFF2 cells were more resistant than the keratinocytes to chemotherapeutic agents with 20µmol/L 4-HC only reducing cell viability relative to control by 19.3% (±7.3). The 48-hour EC_{50} for doxorubicin was 429.9nmol/L (95% CI 297.8-620.4nmol/L).

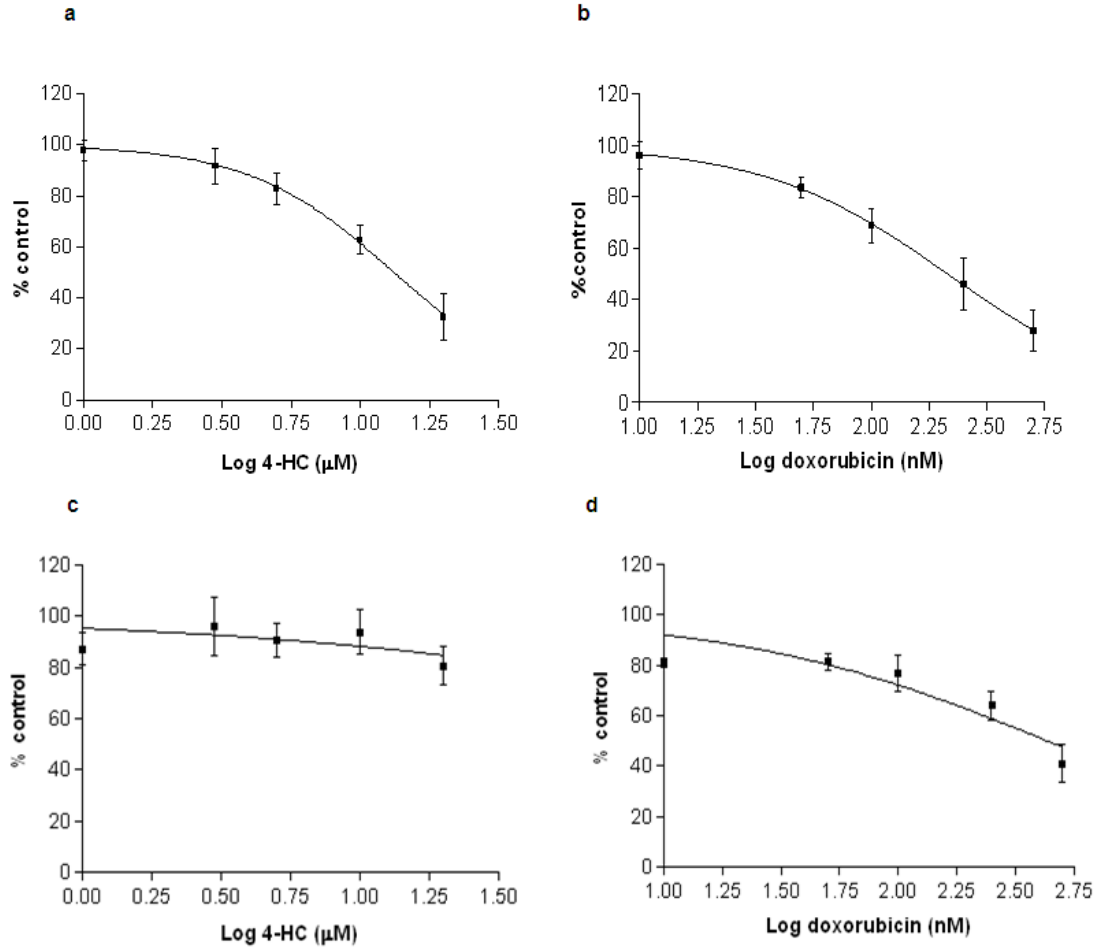

Figure 7.3 EC_{50} concentration-effect curves following 48-hour exposure to increasing concentrations of 4-HC and doxorubicin in (a, b) Keratinocytes and (c, d) HFFF2 cells. Data points are the mean +/- SD of three separate experiments.

As a comparison, the activity of doxorubicin and 4-HC in the RL cell line is shown in Figure 7.4. Although this has been performed using the Guava® viacount assay, it can be seen that the activity of the two chemotherapeutic agents in RL cells is similar to that seen in the keratinocytes and HFFF2 cells with the exception of 4-HC in HFFF2 cells. For RL cells, the 48-hour EC_{50} values for 4-HC and doxorubicin were 9.1µmol/L (95% CI 7.2-11.6µmol/L) and 314.4nmol/L (95% CI 254.7-388.2nmol/L) respectively.

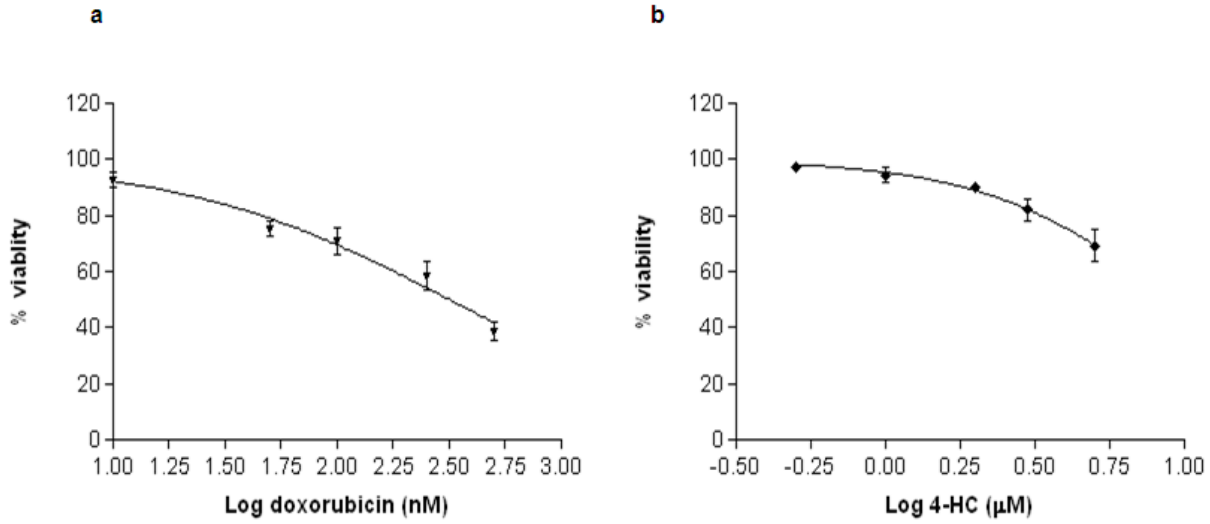

Figure 7.4 EC_{50} concentration-effect curves following 48-hour exposure to increasing concentrations of (a) 4-HC and (b) Doxorubicin in the RL cell line. Data points are the mean +/- SD of three separate experiments.

7.4.3 Cell cycle analysis in keratinocytes exposed to MSA

MSA does not induce cell cycle arrest in lymphoma cell lines. To determine whether this is the case in normal cells, the effect of MSA on cell cycle distribution in keratinocytes was investigated. Figure 7.5 shows that exposure to increasing concentrations of MSA for 24 and 48 hours increased the sub-G1 apoptotic population but did not result in cell cycle arrest.

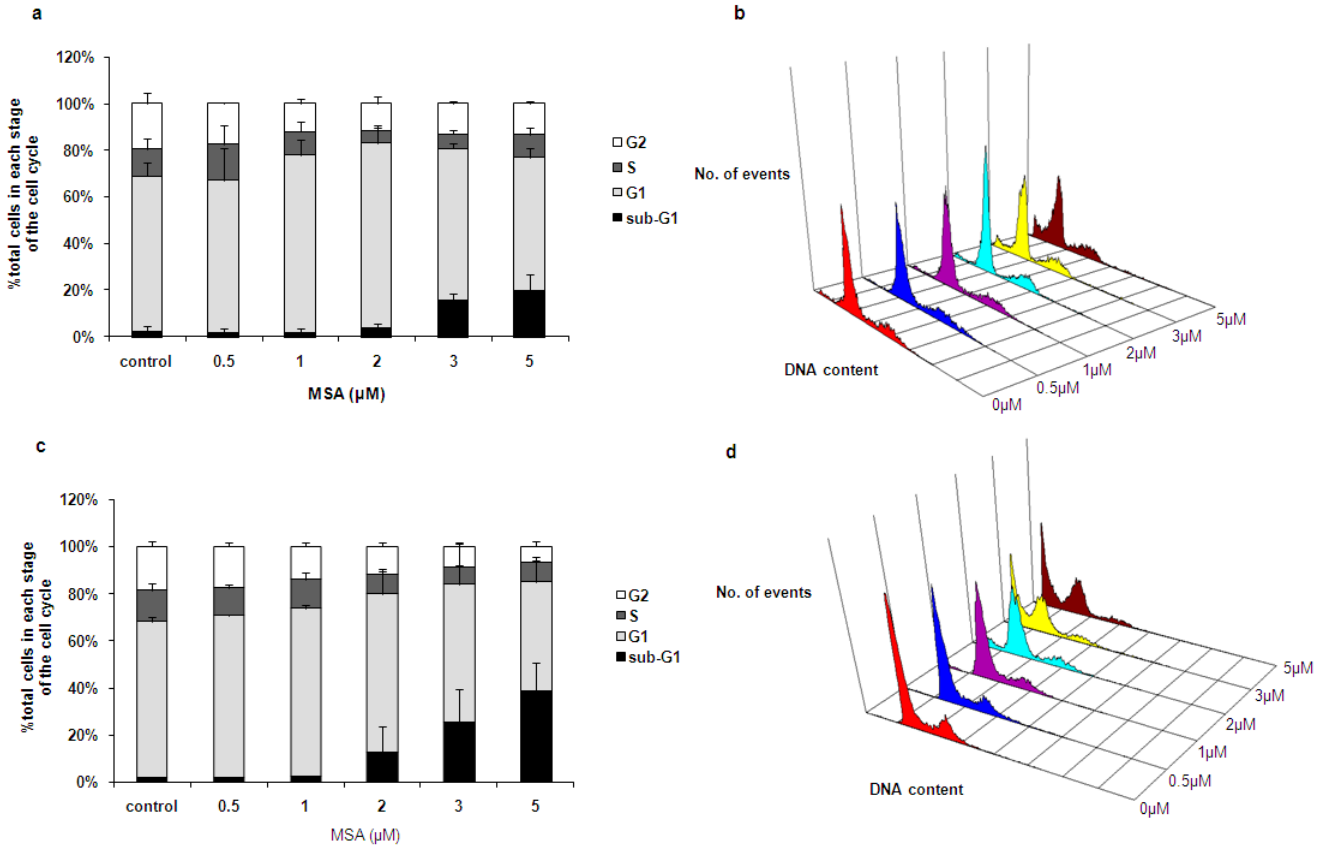

Figure 7.5 Cell cycle analysis of keratinocytes exposed to MSA (a) 24-hour exposure (b) Representative histogram of 24-hour exposure (c) 48-hour exposure (d) Representative histogram of 48-hour exposure. Data points are the mean+/-SD of at least 3 separate experiments.

7.4.4 Combining MSA and chemotherapeutic agents in keratinocytes

Given that Se has been reported to protect normal cells from chemotherapy-induced cytotoxicity, keratinocytes were treated simultaneously with a non-toxic concentration of MSA (0.5μmol/L) and either 4-HC or doxorubicin for 48 hours. However, Figure 7.6 shows that 0.5μmol/L MSA did not alter the cytotoxicity of either 4-HC or doxorubicin as determined by the ATP assay. Therefore, keratinocytes were pre-treated with 0.5μmol/L MSA for 7 days prior to exposure to either 4-HC or doxorubicin for 48 hours. Figure 7.7 shows that pre-treatment with MSA was unable to alter the cytotoxicity of either 4-HC or doxorubicin as determined by the ATP assay.

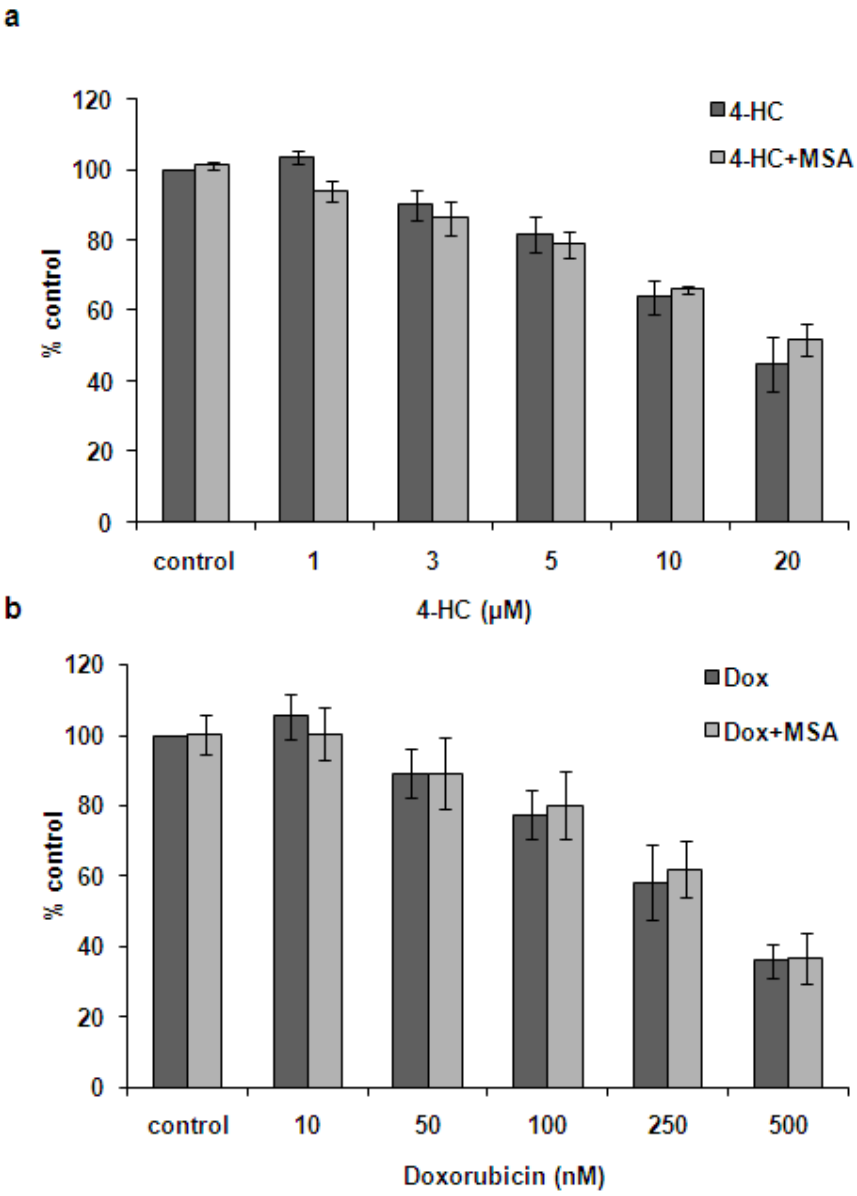

Figure 7.6 Keratinocytes exposed simultaneously to MSA 0.5μM and (a) 4-HC or (b) Doxorubicin for 48 hours. Data points are the mean+/-SD of 3 separate experiments.

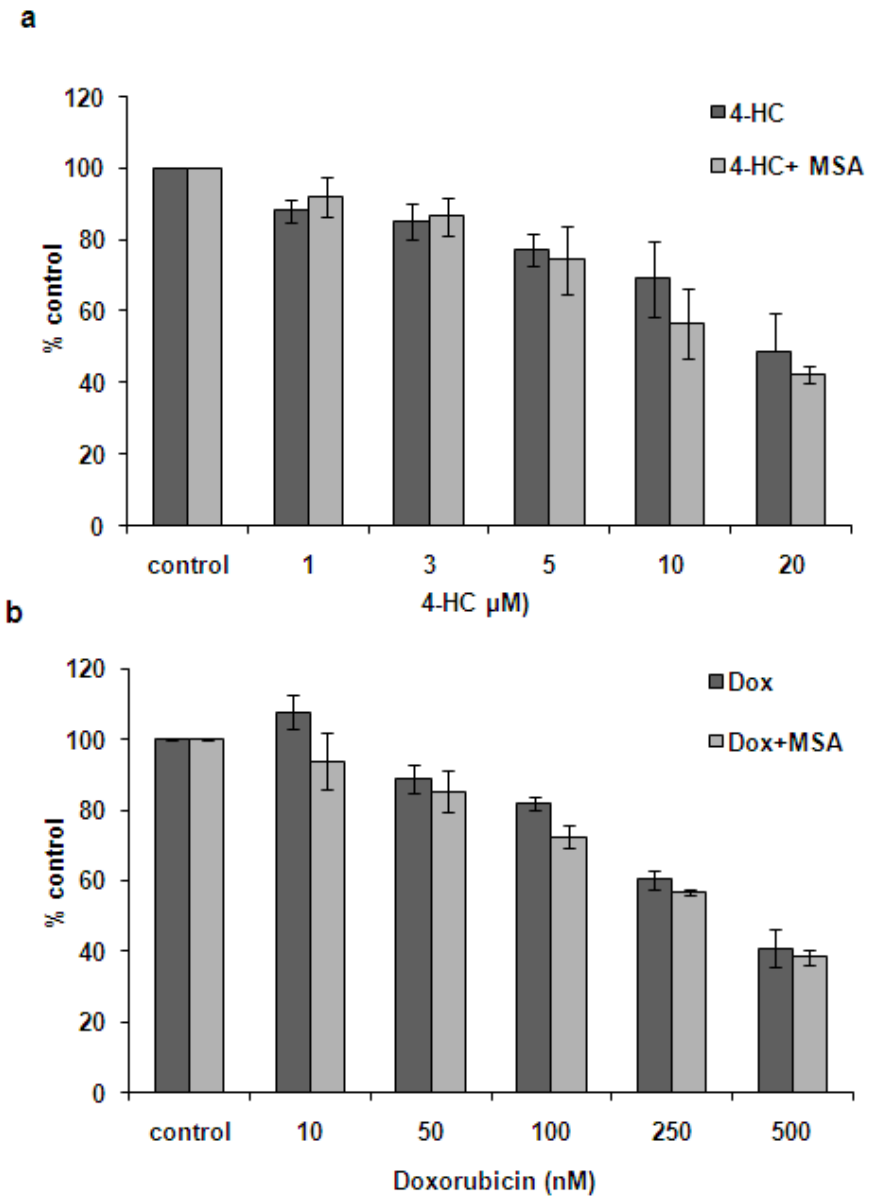

Figure 7.7 Keratinocytes pre-treated with MSA 0.5µM for 7 days followed by 48-hour exposure to (a) 4-HC or (b) Doxorubicin. Data points are the mean+/-SD of 3 separate experiments.

7.4.5 Induction of endoplasmic reticulum stress in peripheral blood mononuclear cells exposed to MSA

Given the lack of evidence for a cyto-protective action of MSA in keratinocytes and HFFF2 cells, further experiments were performed in PBMCs. Previous experiments, reported in Chapter 5, demonstrated that MSA induced ER stress and activated the UPR in DLBCL cell lines. To determine whether the response of PBMCs to MSA-induced ER stress differed, cells were exposed to a range of MSA concentrations. Initially 24- and 48-hour exposures were investigated. Figure 7.8 shows that unlike DLBCL cell lines, PBMCs have virtually no basal expression of GRP78. After 24-hour exposure to 1µmol/L MSA, there was a large increase in GRP78 expression, although a further increase in expression with higher concentrations of MSA was not apparent. A 4-hour time-point was therefore studied using 5µmol/L, 10µmol/L and 20µmol/L MSA to determine if there was a concentration effect. Figure 7.9 shows that there was induction of GRP78 at 4 hours but to a lesser extent than at 24 hours. There was also a small concentration effect between 5µmol/L and 10µmol/L MSA but between 10µmol/L and 20µmol/L the effect plateaued in some individuals.

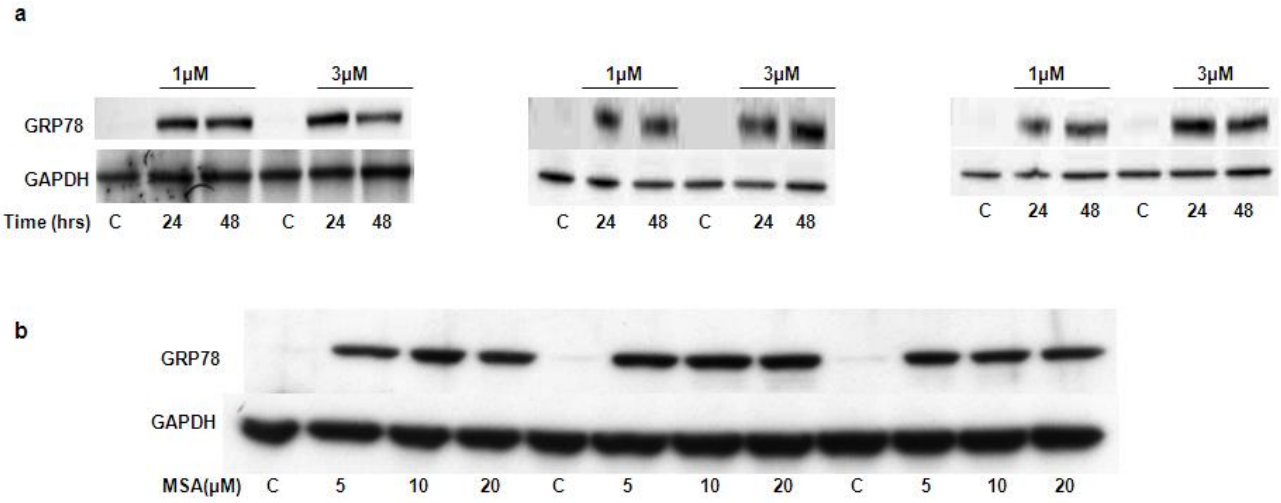

Figure 7.8 GRP78 expression in peripheral blood mononuclear cells from 3 different individuals exposed to MSA (a) 1µM and 3µM MSA for 24 and 48 hours (b) 5µM, 10µM and 20µM MSA for 24 hours.

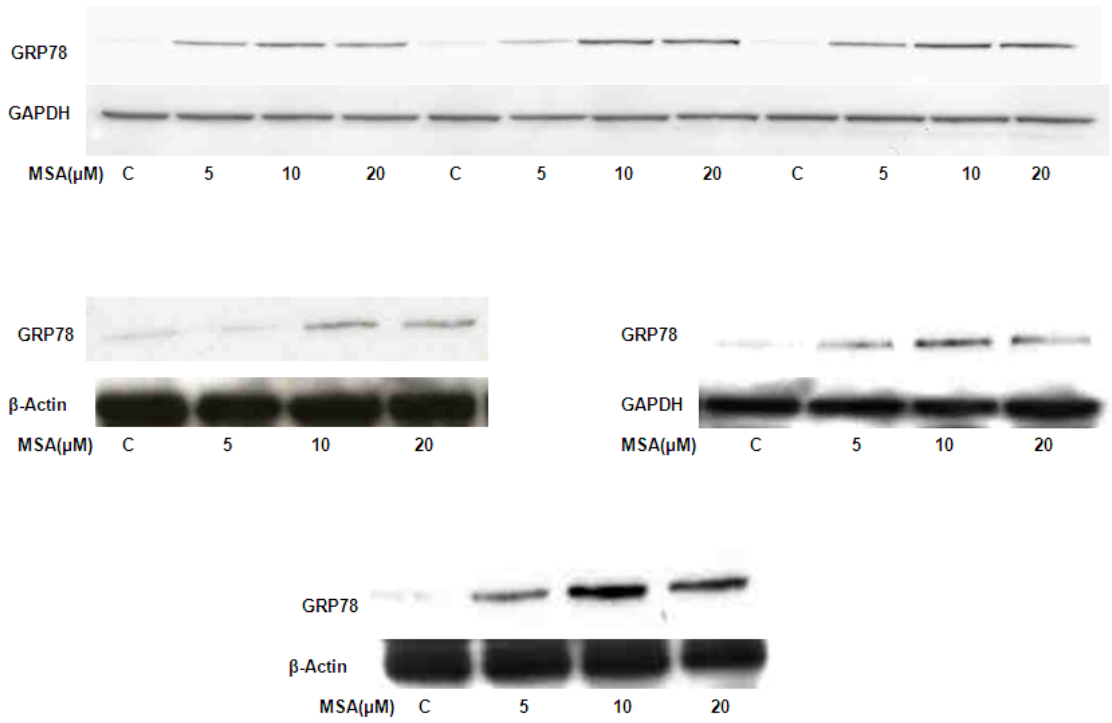

Figure 7.9 GRP78 expression in peripheral blood mononuclear cells from 6 different individuals exposed to MSA for 4 hours.

To investigate whether MSA induced the apoptotic branch of the ER stress response in a similar way to DLBCL cell lines, real-time PCR for GADD153 mRNA expression was performed in PBMCs exposed to 20μmol/L MSA. Figure 7.10 shows that GADD153 mRNA expression was induced by MSA in a time-dependent manner with the highest increase apparent at 24 hours. However, there was variability amongst individuals in the degree of induction ranging from a 4.7-fold to a 16.1-fold increase at 24 hours.

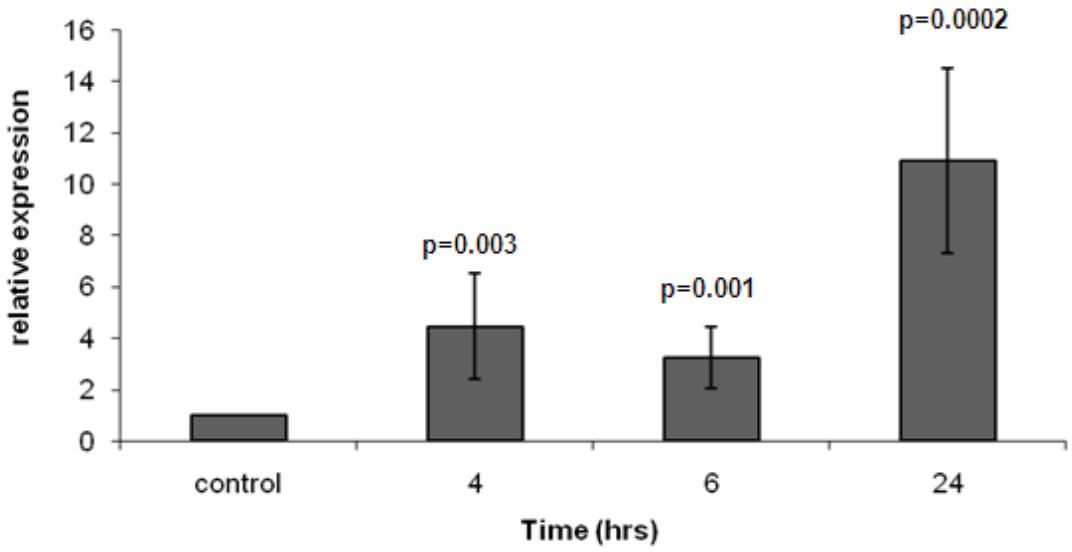

Figure 7.10 Real-time PCR for GADD153 expression in peripheral blood mononuclear cells exposed to 20μM MSA. Data points are the mean+/-SD of at least 8 separate experiments using peripheral blood mononuclear cells harvested from 10 different individuals. The p values are a comparison with control.

7.4.6 Effect of MSA on NF-κB activity in peripheral blood mononuclear cells

The effect of MSA on NF-κB was investigated for two reasons. Firstly, published results from our laboratory have demonstrated that minimally toxic concentrations of MSA can decrease NF-κB activity in DLBCL cell lines after 4-hour exposure (Juliger *et al*, 2007) and secondly, because ER stress has been reported to activate NF-κB (Nozaki *et al*, 2001; Schapansky *et al*, 2007). NF-κB activity was initially determined using the TransAM™ NF-κB p65 assay kit. The kit was first validated and Figure 7.11a shows an example of the controls used when performing the assay. Jurkat nuclear extract was provided as a positive control and produced a concentration-dependent increase in luminescence expressed as relative light units (RLU). The wild-type consensus oligonucleotide is a competitor for NF-κB binding and prevents NK-κB binding to the consensus binding site immobilised on the plate. Figure 7.11a shows that the wild-type oligonucleotide prevented an increase in luminescence. Figure 7.11b shows that increasing concentrations

of protein from PBMC whole cell lysates could produce a concentration-dependent increase in luminescence.

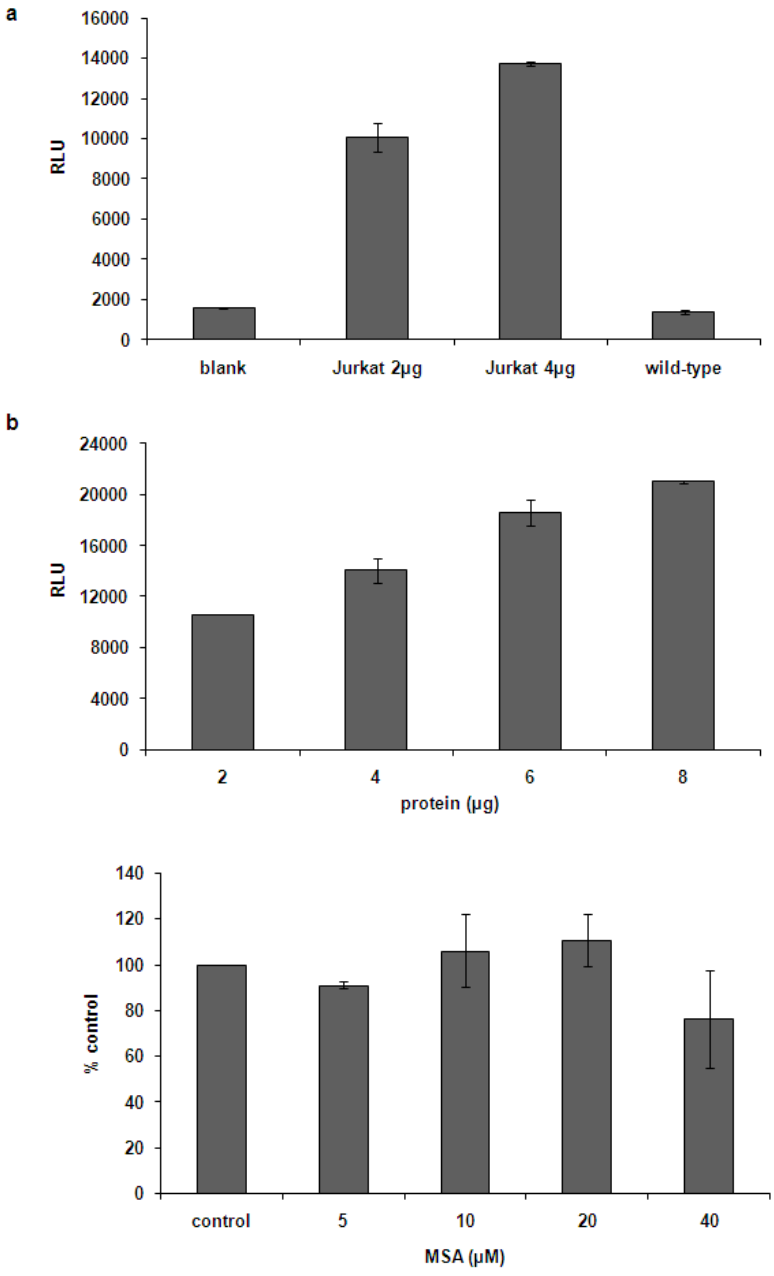

Figure 7.11 NF-κB binding activity using the TransAM™ assay kit (a) Positive and negative controls (b) Increasing protein concentration of PBMC whole cell extracts (c) Whole cell extracts of PBMCs exposed to MSA for 24 hours. Data points are the mean+/- SD of at least 2 separate experiments.

PBMCs were then exposed to a range of MSA concentrations for 24 hours and whole cell protein was extracted. Figure 7.11c shows that when whole cell lysates were used in this assay kit, there was no change in NF-κB activity. Therefore nuclear protein extracts were used for subsequent experiments.

It was expected that NF-κB activity in nuclear extracts would be relatively low and given the expectation that MSA might inhibit NF-κB activity, as seen in DLBCL cell lines, cells were first stimulated with TNFα for 1 hour prior to treating with MSA for a further 4 hours. Figure 7.12 shows experiments using PBMCs from 3 different individuals. Nuclear protein extracts were used in the TransAM™ assay kit and correlated with western blotting performed using both nuclear and cytoplasmic protein extracts. The experiments show 3 different patterns of response. In all 3 experiments TNFα increased the activity of NF-κB. In Figure 7.12a MSA further increased NF-κB activity in a concentration-dependent manner, in Figure 7.12b MSA did not further increase NF-κB activity and in Figure 7.12c MSA did further increase NF-κB activity but the effect was not concentration-dependent. In none of the 3 samples did MSA inhibit the TNFα-mediated increase in NF-κB activity. The western blotting experiments correlated very well with the results from the TransAM™ assay kit, therefore for subsequent experiments western blotting was used to confirm these preliminary results.

Since MSA activated NF-κB in PBMCs, pre-stimulation with TNFα was felt not to be necessary. Further PBMCs were exposed to 20μM MSA for 4 hours and western blotting performed on nuclear protein extracts. Figure 7.13a shows 3 examples of the results obtained. Densitometry was performed to correct for protein loading and the results of 8 separate experiments using PBMCs from 8 different individuals were combined. Figure 7.13b shows that 20μmol/L MSA for 4 hours significantly increased NF-κB activity in nuclear extracts by 2.5-fold ($p=0.02$). However, there was variability in the observed effect and in PBMCs from 2 of the 8 individuals NF-κB activity was not increased, but in none of the samples was NF-κB activity inhibited.

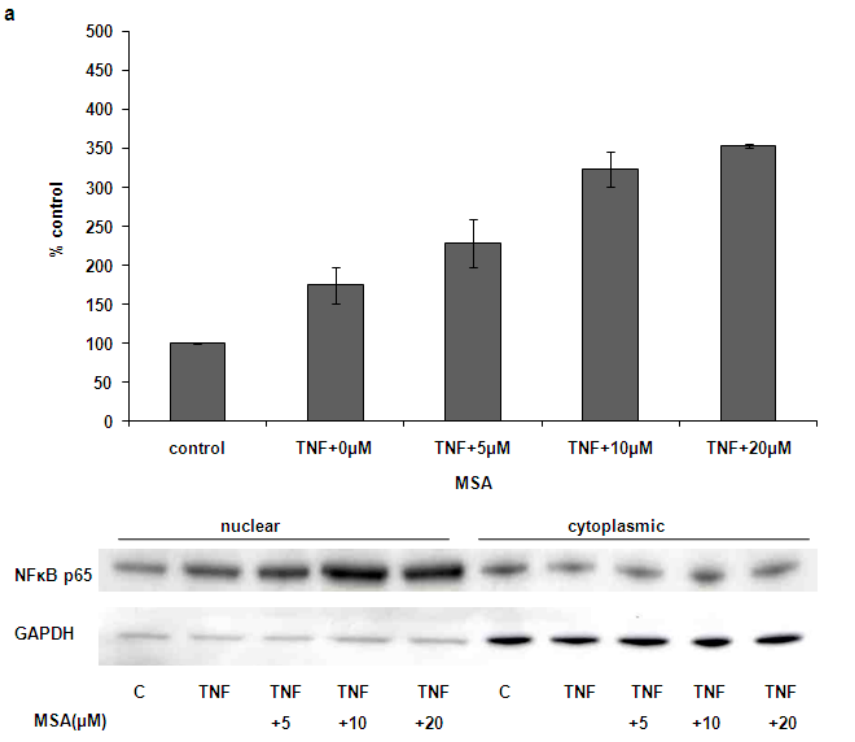
a
500
450
400
350
300
250
200
150
100
50
0
% control
control
TNF+0μM
TNF+5μM
TNF+10μM
TNF+20μM
MSA
nuclear
cytoplasmic
NFκB p65
GAPDH
C
TNF
TNF +5
TNF +10
TNF +20
MSA(μM)

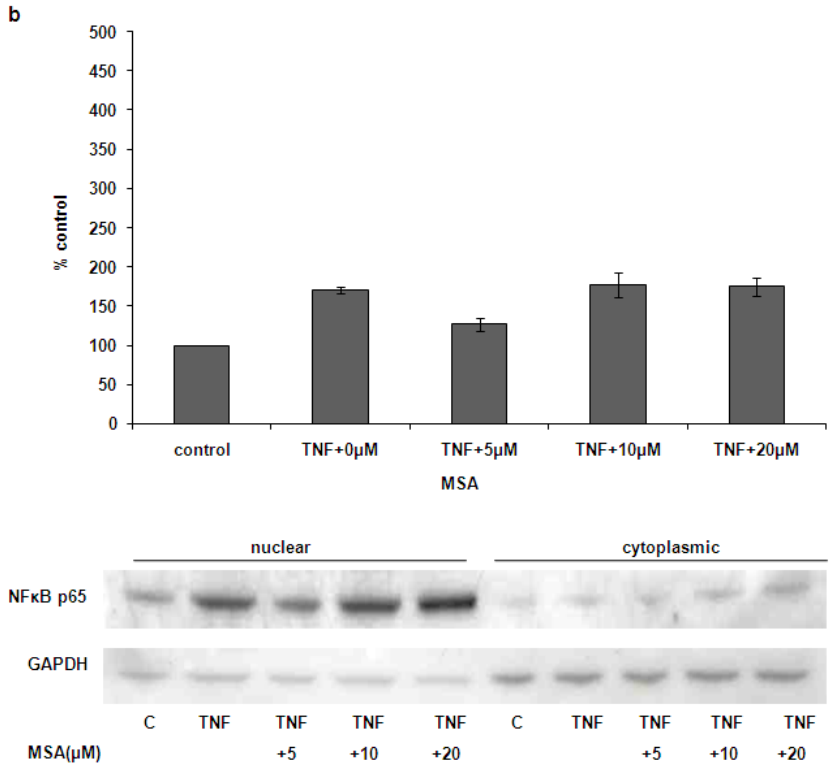
b
500
450
400
350
300
250
200
150
100
50
0
% control
control
TNF+0μM
TNF+5μM
TNF+10μM
TNF+20μM
MSA
nuclear
cytoplasmic
NFκB p65
GAPDH
C
TNF
TNF +5
TNF +10
TNF +20
MSA(μM)

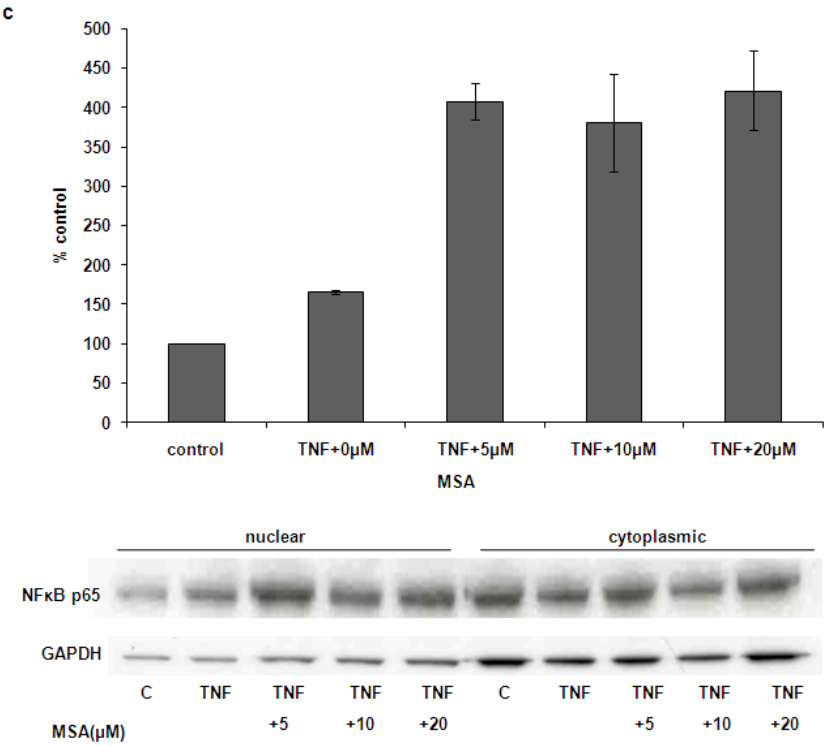

Figure 7.12 NF-κB binding activity in nuclear extracts of peripheral blood mononuclear cells exposed to TNFα 10ng/ml for 1 hour followed by MSA for a further 4 hours. Experiments on peripheral blood mononuclear cells from 3 separate individuals are shown. Data points are the mean+/-SD of one experiment performed in duplicate. Below each graph is the corresponding western blot.

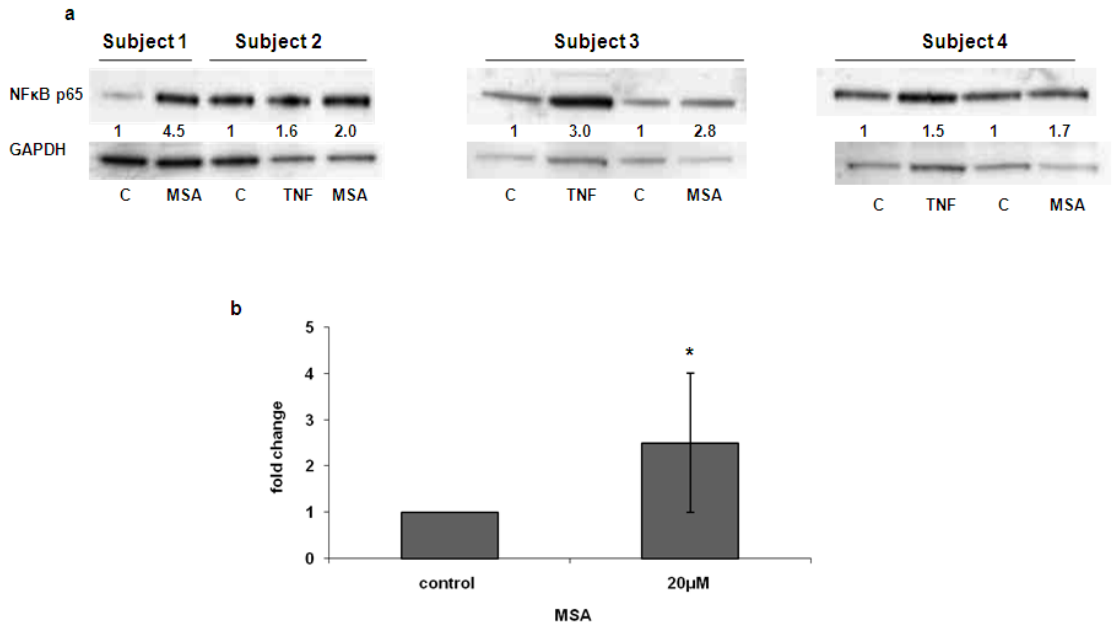

Figure 7.13 (a) NF-κB expression in nuclear extracts of peripheral blood mononuclear cells from 3 healthy subjects after exposure to MSA 20μmol/L or TNFα 10ng/ml for 4 hours (b) Densitometric analysis of western blots of 8 separate PBMC samples exposed to 20μmol/L MSA. *p=0.02.

To investigate the mechanism by which MSA activated NF-κB, phosphorylation of eIF2α and expression of IκB were determined by western blotting. It has been reported that phosphorylation of eIF2α is necessary for activation of NF-κB (Jiang *et al*, 2003) and given that IκB inhibits NF-κB activity it was expected that MSA might result in IκB degradation. However, Figure 7.14 shows that exposure to 20μmol/L MSA for 4 and 24 hours did not clearly alter the amount of phosphorylated eIF2α or the expression of IκB in PBMCs from 2 individuals.

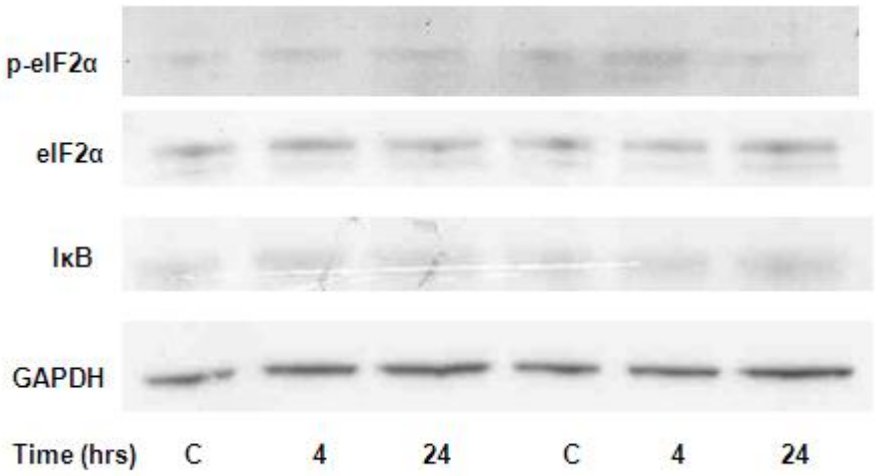

Figure 7.14 p-eIF2α and IκB in peripheral blood mononuclear cells exposed to 20μM MSA.

7.4.7 The effect of MSA on other stress-induced proteins in peripheral blood mononuclear cells

The effect of MSA on other cellular stress-induced proteins was investigated. Similar to the results obtained in DLBCL cell lines, Figure 7.15 shows that MSA did not alter the expression of HSP70, HSP90 or Prx1 in PBMCs harvested from 3 different individuals.

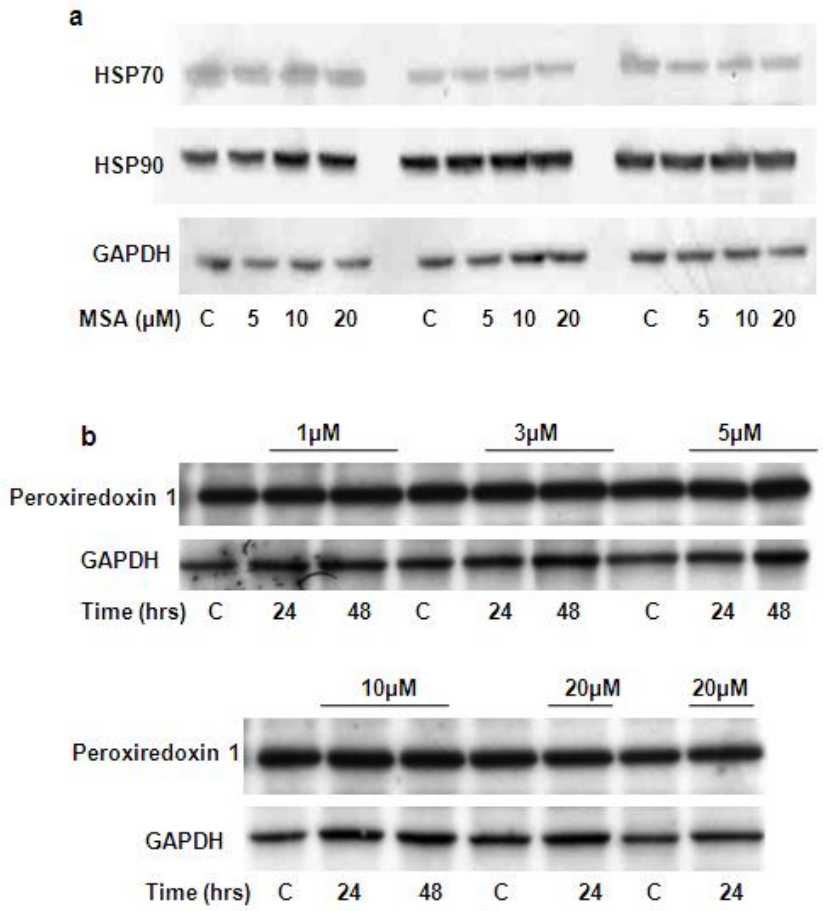

Figure 7.15 (a) HSP70 and HSP90 expression in peripheral blood mononuclear cells exposed to MSA for 24 hours (b) Peroxiredoxin-1 expression in peripheral blood mononuclear cells exposed to a range of MSA concentrations for 24 and 48 hours.

7.5 DISCUSSION

Three models of normal, non-malignant cells have been investigated. PBMCs, a mixture of lymphocytes and monocytes derived from normal volunteers, are widely used to test the cytotoxicity of novel agents in normal cells (Paoluzzi *et al*, 2010; Sterz *et al*, 2010). They have the advantage of being easily accessible, however they have the disadvantage that they are terminally differentiated and do not divide and hence may not truly reflect the action of a drug in proliferating 'normal' cells. hTERT-immortalised human keratinocytes have been reported to retain normal growth and differentiation

characteristics (Dickson *et al*, 2000) and therefore were felt to be a good model for normal proliferating cells. In addition, the HFFF2 cell line was obtained as an alternative normal cell model.

PBMCs are relatively resistant to the cytotoxic effect of MSA. Previous work published from our laboratory found that the EC_{50} for PBMCs exposed to MSA for 72 hours was 84.2μmol/L (Juliger *et al*, 2007). In the experiments reported here, MSA concentrations of up to 20μM were investigated and exposure to 20μmol/L for 48 hours resulted in minimal toxicity, reducing cell viability relative to control by 12.3%. In contrast, it was found that the keratinocytes and HFFF2 cells were relatively sensitive to the cytotoxic effect of MSA, with EC_{50} values at 48-hour exposure of 2.4μmol/L and 7.2μmol/L respectively. These cells also showed similar sensitivity to doxorubicin and 4-HC as the MSA-sensitive DLBCL cell line, RL, with the exception of HFFF2 cells exposed to 4-HC. The reason that trypan blue exclusion rather than the ATP assay was used to determine the cytotoxicity of MSA in PBMCs was to limit the number of cells required for experiments. Cell counts were performed just prior to cell lysis on a small aliquot of cells obtained from samples that had been set up for western blotting.

Most studies in the literature that have investigated the cyto-protective effect of Se in normal cells have reported the effects of selenite and SLM (Fischer *et al*, 2007; Rafferty *et al*, 2003a; Rafferty *et al*, 2003b). In addition, non-tumourigenic cell lines have been reported to be more resistant than tumour cell lines to the induction of apoptosis by MSC (Jariwalla *et al*, 2009). Very few studies have examined the effect of MSA in normal cells. In those that have, the cells studied have also been very sensitive to the cytotoxic effect of MSA. Examples include a study investigating the effect of MSA on mouse embryonic fibroblasts which found that concentrations >1μmol/L induced significant apoptosis (Fischer *et al*, 2007). In HUVECs, MSA concentrations >5μmol/L induced significant apoptosis (Wang *et al*, 2008) and human bronchial epithelial cells were also found to be very sensitive to MSA (Poerschke *et al*, 2008). In contrast, one study has reported that the non-tumourigenic prostate cell line, Pr111 was less sensitive to MSA

than prostate cancer cell lines, however, the EC_{50} for growth inhibition was 0.92μmol/L, which makes it more sensitive that any of the DLBCL cell lines studied here (Gonzalez-Moreno *et al*, 2007).

In the work presented here, MSA clearly induced apoptosis in keratinocytes at concentrations ≤5μmol/L as evidenced by the results of the ATP assay, and confirmed by an increase in the sub-G1/apoptotic population during cell cycle analysis. This suggests that the response to MSA may be cell-type dependent and that normal cells do not all respond in the same way. On the other hand, MSA may not be the correct form of Se to be studying in normal cells. MSA is highly reactive and volatile with conversion to methylselenol immediately after uptake into the cell. However, SLM and MSC require enzymatic conversion to methylselenol. *In vivo*, metabolism of SLM and MSC to methylselenol occurs predominantly in the liver and kidney, as this is where high concentrations of the relevant β- and γ-lyase enzymes are found. Other cell types generally have lower β- and γ-lyase activity and therefore conversion of SLM and MSC to methylselenol in *in vitro* cell models other than liver and kidney cells is likely to be less efficient (Cooper *et al*, 2010; Cooper & Pinto, 2006). In fact, *in vitro* studies demonstrating anti-tumour effects of SLM and MSC often supplement cultures with γ- and β-lyase respectively (Azrak *et al*, 2006; Kim *et al*, 2007a). Studies demonstrating the cyto-protective effects of SLM and MSC have not supplemented *in vitro* cell cultures with the relevant lyase enzymes suggesting that perhaps the monomethylated metabolites may not be responsible for the observed effects (Fischer *et al*, 2007). As discussed in Chapter 6, SLM and MSC can also form α-keto acid metabolites (Lee *et al*, 2009a) and therefore other metabolites could be responsible for the differing effects between MSA and other organo-Se compounds, but this requires further investigation.

In contrast, MSA has been found to be superior to SLM and selenite in respect to *in vivo* tumour growth inhibition in two xenograft models of prostate cancer. When comparing MSC and MSA in the same *in vivo* models, MSC was able to inhibit tumour growth in only one of the two xenograft models. Tumour growth inhibition by MSC was associated

with increased apoptosis whereas tumour growth inhibition by MSA was not, but instead appeared to affect angiogenesis. This suggests that although both compounds are thought to act through their common metabolite methylselenol, they appear to affect different intracellular signalling pathways (Li *et al*, 2008a). Therefore, it may be an over simplification to suggest that all Se compounds that are metabolised to methylselenol act in the same way, and it may be that other, as yet unknown, properties of these compounds are also important in mediating the effects observed.

To further investigate the effect of MSA in hTERT-immortalised keratinocytes, a non-cytotoxic concentration of MSA, 0.5μmol/L, was used. MSA was combined simultaneously with increasing concentrations of either doxorubicin or 4-HC for 48 hours. The addition of MSA did not alter the cytotoxicity of either chemotherapeutic agent. Although a cyto-protective effect of MSA was not observed, these results differed from those obtained when combining non-toxic concentrations of MSA with chemotherapeutic agents in DLBCL cell lines where a synergistic interaction was observed, as shown in Chapter 4. This suggests a differential effect between DLBCL cell lines and this normal cell line, with chemo-sensitisation observed in malignant cells, but not in normal cells. In the xenograft study that reported the protective effect of Se on chemotherapy-induced toxicity, seven days pre-treatment with Se prior to the commencement of chemotherapy was required (Cao *et al*, 2004). Therefore, keratinocytes were pre-treated with 0.5μmol/L MSA for seven days prior to treatment with increasing concentrations of doxorubicin and 4-HC for a further 48 hours. However, results were similar to those obtained after simultaneous exposure and MSA did not alter the effect of either chemotherapeutic agent. Given these negative results, further experiments were not conducted in either the hTERT immortalised keratinocytes or the HFFF2 cell line.

Further experiments were performed using PBMCs given that they appear to represent 'normal' cells that are relatively resistant to MSA. To establish whether the response to ER stress differed between normal cells and DLBCL cell lines, GRP78 expression and GADD153 mRNA expression was investigated in PBMCS exposed to MSA. In contrast

to DLBCL cell lines, PBMCs had virtually no basal expression of GRP78. Following exposure to 1μmol/L MSA for 24 hours, there was a marked increase in expression of GRP78, much larger than the effect of the same concentration in either the RL or DHL4 cell lines. In the RL cell line, 1μmol/L MSA produced a minimal increase in GRP78 expression (Chapter 5, Figure 5.2), while in DHL4 cells, 1μmol/L MSA did increase expression of GRP78 at 4- and 6-hour exposures but the effect was lost by 24 hours (Chapter 5 Figure 5.3). In PBMCs, the increase in GRP78 expression at 24 hours was maximal after exposure to only 1μmol/L MSA, with no concentration effect. Concentrations >1μmol/L MSA induced GRP78 expression to the same extent and this induction was sustained out to 48-hour exposure. In the RL and DHL4 cell lines, a maximal sustained effect in GRP78 induction was observed only after exposure to concentrations ≥10μmol/L MSA (Chapter 5, Figures 5.2 and 5.3).

Given the plateau in GRP78 expression at 24 hours with concentrations as low as 1μmol/L MSA, PBMCs were exposed to 5μmol/L, 10μmol/L and 20μmol/L MSA for 4 hours. GRP78 expression was clearly induced following 4-hour exposure but the induction was less compared with 24-hour exposure. There was a concentration effect between 5μmol/L and 10μmol/L MSA but between 10μmol/L and 20μmol/L MSA the effect was maximal in PBMCs from some but not all individuals. These results demonstrate that in PBMCs, MSA produced a larger, more sustained increase in GRP78 than in DLBCL cell lines at equivalent concentrations. Given that induction of GRP78 by cells is generally considered a pro-survival response and has been associated with chemo-resistance (Lee, 2007; Pyrko *et al*, 2007), these results suggest that PBMCs are able to induce a larger pro-survival response than DLBCL cell lines in response to MSA.

Differences were also observed in the induction of GADD153 mRNA expression by MSA between PBMCs and DLBCL cell lines. GADD153 expression was studied in PBMCs exposed to 20μmol/L MSA for 4, 6 and 24 hours. Induction of GADD153 expression was time-dependent with a maximal 11-fold increase observed at 24 hours. Although the concentrations investigated in the DHL4 cell line differed, the induction of GADD153 in PBMCs was less. In the DHL4 cell lines, 10μmol/L MSA for 24 hours

increased GADD153 expression by 23-fold and 30μmol/L MSA by 35-fold (Chapter 5, 5.7). Hence, it appears that the apoptotic response to ER stress induced by MSA in normal PBMCs is less than that seen in DLBCL cell lines.

Pre-conditioning of cells through the induction of ER stress has been demonstrated to protect cells from toxic agents. This has mainly been examined in renal cell lines and it has been reported that pre-treatment of cell lines for 16-24 hours with agents such as tunicamycin and thapsigarin, which are known inducers of ER stress, can protect cells from oxidative stress following H_2O_2 exposure and from cytotoxicity following exposure to known nephrotoxins, such as cisplatin. In these studies, ER stress induction was demonstrated by the induction of GRP78 and GRP94 and inhibiting the expression of GRP78 was found to prevent the cyto-protective response to pre-treatment with inducers of ER stress (Hung *et al*, 2003; Peyrou & Cribb, 2007). There were, however, differences between the extent of cyto-protection afforded between cell lines and the different ER stress inducers and toxic agents investigated, with the level of GRP78 induction not always correlating with the extent of cyto-protection (Bedard *et al*, 2004; Peyrou & Cribb, 2007). Thus, the mechanism of ER stress-induced cyto-protection is not fully understood and is likely to involve other molecular pathways. The MAPK and PI3K/Akt pathways have been implicated in the survival response. In renal epithelial cells, ER stress induced protection from oxidative stress caused by H_2O_2 was found to be dependent on phosphorylation and thus activation of Erk1/2 and suppression of Jnk activation, but was not dependent on the activity of the PI3K/Akt pathway (Hung *et al*, 2003). In solid tumour cell lines, ER stress-induced cell survival required phosphorylation and thus activation of Akt and Erk1/2 and also the induction of two anti-apoptotic proteins, cIAP-2 and XIAP (Hu *et al*, 2004). In addition, the induction of autophagy by ER stress may be important in the survival response. A study investigating the effect of the known nephrotoxic agent cyclosporine A reported that it induced ER stress in human renal epithelial cells and this directly led to the induction of autophagy. Inhibition of autophagy increased the cytotoxicity of cyclosporine A, implicating this pathway in cell survival (Pallet *et al*, 2008). The induction of autophagy in PBMCs by

MSA has not been investigated but given the findings in DLBCL cell lines it would be valuable to do so.

A further pro-survival protein that is activated by ER-stress is NF-κB and this is distinct from the activation of the UPR (Pahl & Baeuerle, 1995). The exact mechanism by which NF-κB is activated is not clear but phosphorylation of eIF2α is thought to be required (Jiang *et al*, 2003). NF-κB activation has been shown to inhibit the expression of GADD153 and hence promote cell survival (Nozaki *et al*, 2001; Schapansky *et al*, 2007). Given that our laboratory has demonstrated inhibition of NF-κB by MSA in DLBCL cell lines, NF-κB activity was investigated in PBMCs. The results reported here demonstrate, by two different methods, that MSA activates NF-κB. Although there was some variability in the observed effect, when results of western blotting experiments were combined, it was demonstrated that MSA increased NF-κB nuclear expression by a 2.5-fold. This may therefore explain why the induction of GADD153 was less when compared to DLBCL cell lines in which NF-κB activity is inhibited by MSA. However, the role of ER stress-induced NF-κB activation is complex and it has been reported that NF-κB can also mediate ER stress-induced cell death (Hu *et al*, 2006). To further investigate how NF-κB is activated by MSA, phosphorylation of eIF2α and expression of IκB were investigated. However, MSA did not alter the level of either protein. Further work is required to define the mechanism and role of NF-κB activation by MSA in PBMCs.

The effect of MSA on other stress-induced proteins was studied. Similar to the findings in DLBCL cells lines, MSA did not affect the expression of HSP70, HSP90 or Prx1.

The results presented in this chapter have demonstrated clear differences in the responses of PBMCs to MSA when compared with DLBCL cell lines. This was not the case with all normal cell types, with the HFFF2 cell line and normal keratinocytes showing sensitivity similar to that of some lymphoma cell lines. These results may be dependent on the Se compound used, and may reflect altered uptake or activation of MSA in normal cells compared to lymphoma cells. This is further investigated in Chapter 9.

CHAPTER 8: Combining methylseleninic acid and bortezomib in mantle cell lymphoma cell lines

8.1 INTRODUCTION

Bortezomib is a dipeptide boronic acid, 'first-in class', proteasome inhibitor (Adams *et al*, 1999). It is a specific, reversible inhibitor of the 26S proteasome, a large multi-subunit protein complex present in all eukaryotic cells. The ubiquitin-proteasome pathway (UPP) is an essential one, responsible for the degradation of intracellular proteins. To be recognised for degradation by the proteasome, proteins require the attachment of a polyubiquitin chain (Navon & Ciechanover, 2009). Proteins degraded by the UPP include those involved in key intracellular processes such as cell cycle regulation, cell growth, proliferation and survival. Therefore, inhibition of the proteasome affects multiple cellular pathways, ultimately resulting in cell death (Adams, 2004). Despite the fact that the proteasome is crucial to the functioning of all cells, it appears that malignant cells are more sensitive than normal, non-malignant cells to the cytotoxic effects of proteasome inhibition (Hideshima *et al*, 2001). The reasons for this are not entirely clear, but may include the fact that malignant cells often have abnormalities in cell cycle regulation and thus are rapidly proliferating, which may lead to the accumulation of defective proteins at a higher rate than in normal cells. Thus, malignant cells may be more dependent on the normal functioning of the UPP (Masdehors *et al*, 2000).

It has been demonstrated that bortezomib induces cell death through multiple mechanisms and that these differ depending on the tumour type. Bortezomib has been investigated most extensively in multiple myeloma and has demonstrated impressive clinical efficacy, both as a single agent and in combination with other conventional and novel agents. It is now approved in the UK and the United States for the treatment of patients with relapsed/refractory myeloma (Richardson *et al*, 2003). Initially it was thought that the key mechanism involved in the activity of bortezomib was the inhibition of NF-κB activation. The NF-κB family of transcription factors are kept in an inactive

state in the cytoplasm through binding to the inhibitor protein IκB. In order to activate NF-κB and allow its translocation to the nucleus, IκB must be phosphorylated, ubiquitinylated and degraded by the 26S proteasome. The degradation of IκB is inhibited by bortezomib, thus preventing activation of NF-κB. NF-κB activation in turn promotes cell survival, growth, proliferation and angiogenesis, by mechanisms such as induction of pro-apoptotic Bcl-2 family members, cell cycle regulators, caspase inhibitors and VEGF (Navon & Ciechanover, 2009). However, it has become apparent that bortezomib also has a number of NF-κB-independent effects. These include disruption of cell cycle progression (An *et al*, 2000), generation of ROS (Ling *et al*, 2003), activation of the extrinsic, death receptor, apoptotic pathway (Kabore *et al*, 2006), induction of ER stress and the UPR (Obeng *et al*, 2006) and cell death as a result of mitotic catastrophe (Strauss *et al*, 2007). Interestingly, a recent study has shown that bortezomib can actually induce NF-κB activation in multiple myeloma cell lines and patient-derived tumour cells through induction of IκB phosphorylation. In this study, bortezomib was still cytotoxic, suggesting that the inhibition of NF-κB activation is not the most important mechanism of bortezomib action (Hideshima *et al*, 2009). A study in endometrial cancer cell lines and primary patient samples had previously demonstrated a similar finding when examining the effects of four proteasome inhibitors, including bortezomib (Dolcet *et al*, 2006).

The other disease for which bortezomib has been approved by the FDA in the United States is for the treatment of relapsed/refractory mantle cell lymphoma (MCL). MCL is a distinct subtype of B-cell NHL and comprises about 6% of all NHL. The median age at presentation is around 60 years, it is more common in men and most patients present with advanced stage disease. It is an aggressive malignancy with a poor prognosis and currently, no curative therapy (Anon, 1997; Swerdlow SH, 2008). With the recent addition of rituximab to first-line combination chemotherapy, improvements have been made in response rates (Lenz *et al*, 2005). Impressive results have been achieved at the M.D.Anderson Cancer Centre using the intensive 'hyper-CVAD' (fractionated cyclophosphamide/vincristine/doxorubicin/ dexamethasone) regimen, alternating with

high-dose methotrexate/cytarabine plus rituximab as first-line treatment. 87% of patients achieved a CR/CRu and the 5-year OS was 65% (Fayad *et al*, 2007). However, this regimen is too toxic for the majority of patients and therefore 'CHOP' plus rituximab is the 'standard of care' in most centres. Moreover, the real problem is that the great majority of patients develop recurrent disease and bortezomib has proved to be a useful treatment option in this setting. An updated analysis (with longer follow-up) of the phase II 'PINNACLE' study, using bortezomib as a single agent in patients with relapsed/refractory MCL has recently been published. The overall response rate was 32% (CR/CRu 8%), with a median duration of response of 9.2 months. The OS was 23.5 months. In patients who responded, the median time to progression was 1 year and the OS, 3 years. These results are all the more impressive considering that almost half the patients were treated at second recurrence. (Goy *et al*, 2009).

MCL is characterised by over-expression of the protein cyclin D1, which controls cell cycle progression from G1 to S phase. MCL is characterised by the presence of the t(11;14)(q13;32) which results in the juxtaposition of the cyclin D1 gene with the immunoglobulin heavy-chain joining region. A large number of other, secondary molecular alterations have also been reported in MCL, including the constitutive activation of the NF-κB pathway (Obrador-Hevia *et al*, 2009). A study in MCL cell lines and patient-derived tumour cells reported that both bortezomib and the NF-κB inhibitor BAY 11-7082 could induce apoptosis in MCL cells and that a similar effect was observed when NF-κB activation was inhibited using a super-repressor form of IκB (Pham *et al*, 2003). Therefore, inhibition of the NF-κB pathway seems a promising therapeutic target in MCL and appears to be the main mechanism of action for bortezomib in this disease.

Bortezomib may also be of use in the treatment of DLBCL. The ABC-like molecular subgroup of DLBCL (unlike the GCB-like subgroup) is characterised by constitutive activation of the NF-κB pathway. It has a significantly worse outcome compared to the GCB-like subgroup. A recent study reported that although bortezomib had no clinical activity as a single agent in patients with relapsed/refractory DLBCL, when combined with conventional chemotherapy, it resulted in a significantly higher response rate and

OS in patients with the ABC-like subgroup compared with the GCB-like subgroup (Dunleavy *et al*, 2009).

The hypothesis being investigated by the experiments presented in this chapter is that the combination of MSA and bortezomib in MCL cell lines may lead to a synergistic interaction. The rationale is based on the following: both drugs inhibit NF-κB activity (Juliger *et al*, 2007) and both induce ER stress, through the accumulation of misfolded proteins (Wu *et al*, 2005). Furthermore, it has been reported that combining bortezomib and ER stress-inducing agents results in enhanced cell death (Hill *et al*, 2009; Kraus *et al*, 2008).

8.2 AIMS

1) To investigate the activity of MSA in MCL cell lines.
2) To investigate the combination of MSA and bortezomib in MCL cell lines.

8.3 METHODS

8.3.1 Cell lines, cell culture and treatment of cell lines

Two MCL cell lines were used in these experiments; JeKo-1 and Granta-519 obtained from Cancer Research UK cell services (Amin *et al*, 2003). They were maintained in suspension in RPMI-1640 culture medium (Sigma-Aldrich) supplemented with 10% foetal calf serum (Sigma Aldrich), and 1% penicillin (100units/ml) and streptomycin (100µg/ml) (Invitrogen™, California, USA) at 37°C in a humidified atmosphere with 5% CO_2. Cells were passaged twice weekly and reset at $2x10^5$/ml.

The cell lines were exposed to range of MSA and bortezomib concentrations and cell viability and number were determined using the Guava® viacount assay (described in Chapter 2, section 2.3.3). The results were expressed relative to the control value and were analysed using the GraphPad PRISM® software (version 5.03). The activity of MSA and bortezomib were summarised to an EC_{50} value, which was calculated using a sigmoidal concentration-effect model with variable slope.

Cell lines were then exposed to a combination of a non-toxic concentration of MSA and increasing concentrations of bortezomib. MSA and bortezomib were initially combined simultaneously for 48 hours. Subsequently, cells were pre-treated with MSA for 48 hours followed by treatment with bortezomib for a further 48 hours. Cell viability was determined using the Guava® viacount assay.

Western blotting was used to investigate protein changes induced by the combination of MSA and bortezomib.

8.3.2 Proteasome activity assay

Proteasome activity in whole cell extracts was determined by measuring the release of the fluorophore 7-amino-4-methylcoumarin (AMC) from a synthetic peptide Suc-Leu-Leu-Val-AMC (S-LLV-AMC; Alexis Biochemicals, Nottingham, UK), which is hydrolysed by the chymotryptic activity of the 20S proteasome. The assay was performed in a 96-well plate and samples analysed in triplicate.

JeKo-1 and Granta-519 cells were exposed to MSA, Bortezomib or both and then pelleted by centrifugation at 210*g* for 6 minutes. Cell were washed once in ice-cold PBS and then lysed in 'assay buffer' (20mM PIPES-KOH, pH 7.4, 10mM DTT, 10% sucrose, 1mM EDTA) to which 0.1% 3-[(3-Cholamidopropyl)dimethylammonio]-1-propanesulfonate (CHAPS; Sigma-Aldrich) was added just prior to use. Samples were incubated on ice for 20 minutes and then centrifuged at 20,800*g* for 10 minutes to remove insoluble cellular debris. The supernatant was transferred to fresh tubes and the protein concentration measured using the BCA™ protein assay kit (described in Chapter 2, section 2.4.5).

50µg of protein was diluted to 95µl in assay buffer. The reaction was initiated by the addition of 5µl of 400mmol/L (final concentration 40µmol/L) S-LLV-AMC fluorescent substrate. After incubation at 37°C for 15 minutes, fluorescence (excitation 350-360nm, emission 460nm) was measured on the POLARstar OPTIMA plate reader (BMG

Labtech). Measurements were calibrated against a standard linear regression curve of AMC (Sigma-Aldrich). Proteasome activity was defined as µmol/L AMC released per milligram protein per hour (µM/mg/hr). An example of the standard curve is shown in Figure 8.1 (r=0.99)

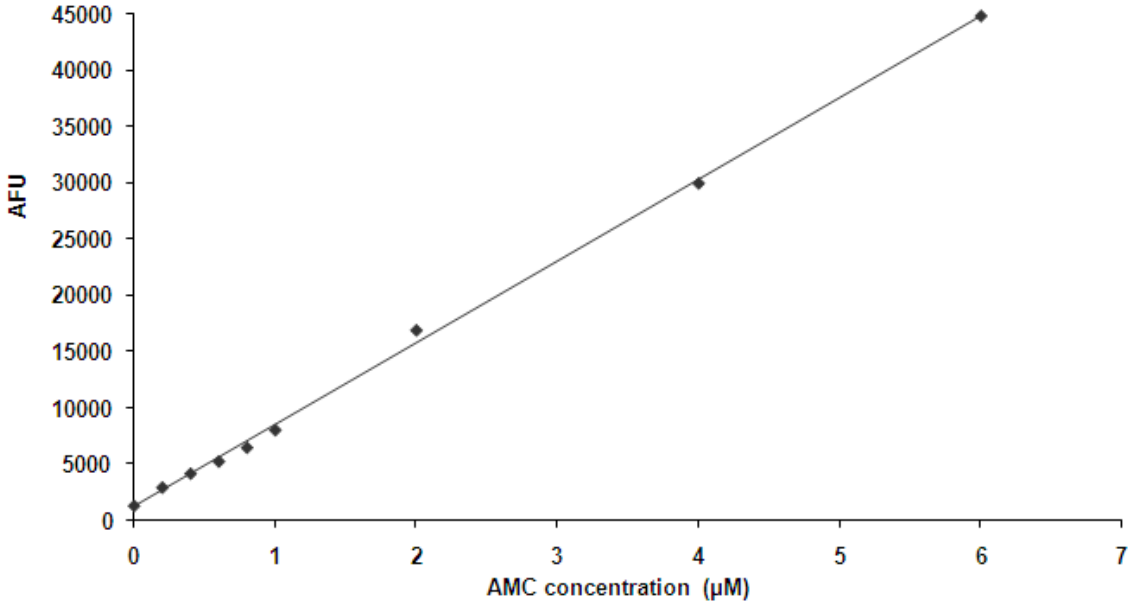

Figure 8.1 An example of a standard curve for AMC. AFU=arbitrary fluorescence units.

8.4 RESULTS

8.4.1 The effect of MSA and bortezomib on cell viability and number

JeKo-1 and Granta-519 cell lines were exposed to MSA and bortezomib for 48 hours and cell viability and number was determined. Figure 8.2 shows the EC_{50} concentration-effect curves for cell viability and number. The EC_{50} values for cell viability and cell number are summarised in Table 8.1. MSA is clearly more cytostatic than cytotoxic. This is also true for bortezomib but to a lesser degree.

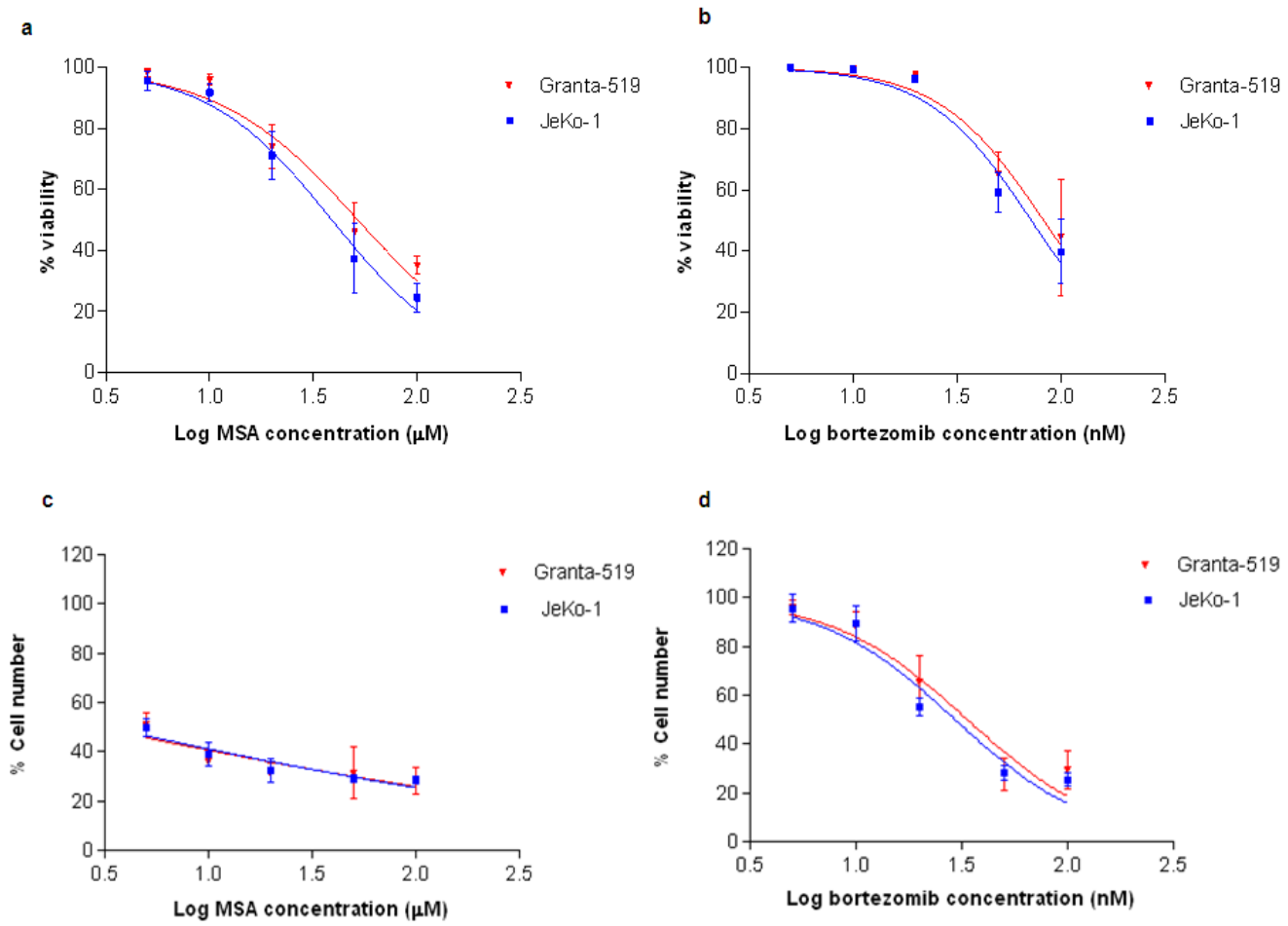

Figure 8.2 EC_{50} concentration-effect curves following 48-hour exposure to increasing concentrations of MSA and bortezomib using the Guava® viacount assay. (a) MSA cell viability (b) Bortezomib cell viability (c) MSA cell number (d) Bortezomib cell number. Data points are the mean +/- SD of three separate experiments.

Table 8.1 MSA and bortezomib EC_{50} values for cell viability and number in JeKo-1 and Granta-518 cell lines after 48-hour exposure. EC_{50} values are the mean of 3 separate experiments.

Drug	Cell lines	Cell viability EC_{50}	95% CI	Cell number EC_{50}	95% CI
MSA (µmol/L)	JeKo-1	38.9	33.2-45.5	3.2	1.6-6.1
	Granta-519	51.8	43.2-62.2	2.8	0.9-8.9
Bortezomib (nmol/L)	JeKo-1	72.2	62.3-83.7	29.4	24-36
	Granta-519	82.8	67.1-102.1	33.6	26.6-42.4

8.4.2 Simultaneous combination of MSA and bortezomib

A non-cytotoxic concentration of MSA was combined simultaneously with increasing concentrations of bortezomib for 48 hours. 10µmol/L MSA was chosen as it had minimal effect on cell viability and was the concentration in the MSA-resistant DLBCL cell lines, DHL4 and DoHH2, that resulted in a synergistic interaction with cytotoxic agents. Unexpectedly, at the highest bortezomib concentration, 50nmol/L, there was an antagonistic interaction in the combination resulting in increased cell viability compared with bortezomib alone in both MCL cell lines. In the JeKo-1 cell line, 50nmol/L bortezomib decreased the cell viability by 48.5% (±8.3) but when combined with MSA the cell viability was only decreased by 32% (±5.1). In the Granta-519 cell line, 50nmol/L bortezomib decreased the cell viability by 37.3% (±4.3) but when combined with MSA the cell viability was only decreased by 28.7% (±2.2). These effects were statistically significant (Figure 8.3 and 8.4).

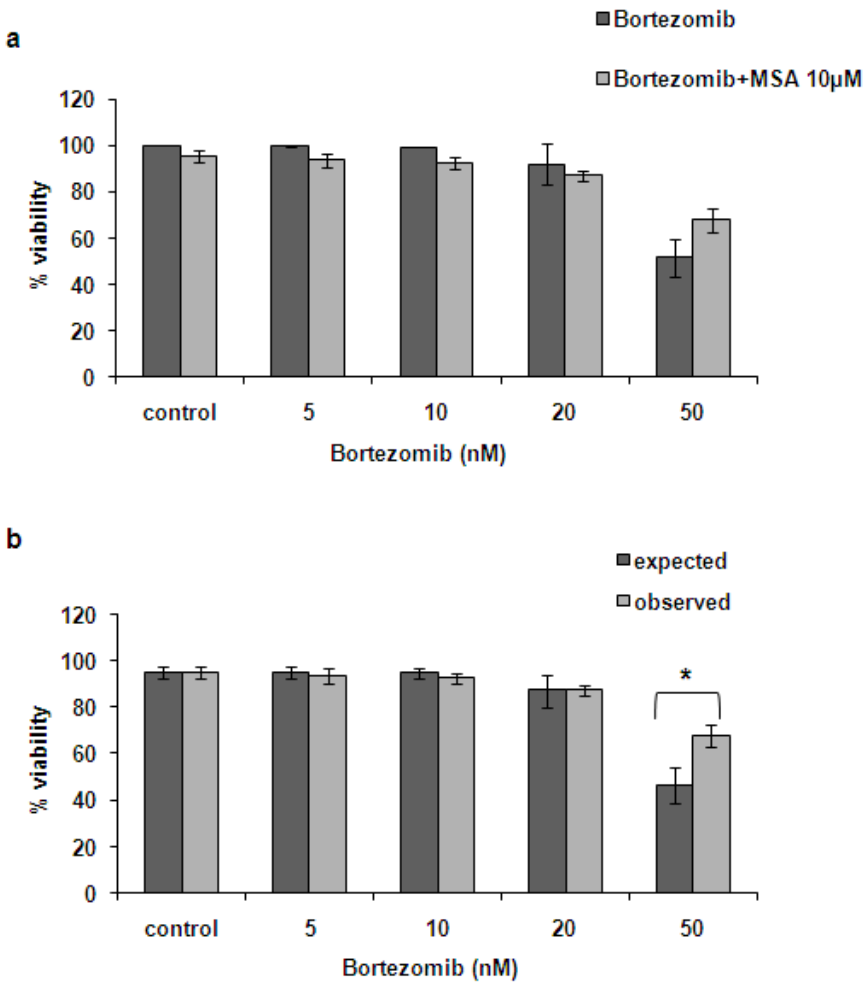

Figure 8.3 JeKo-1 cells exposed to a simultaneous combination of MSA 10μmol/L and increasing concentrations of bortezomib. (a) Cell viability with bortezomib alone and in combination with MSA (b) The expected and observed cell viability from the combination of MSA and bortezomib. Guava® viacount assay used. Data points are the mean +/- SD of three separate experiments. *p=0.006.

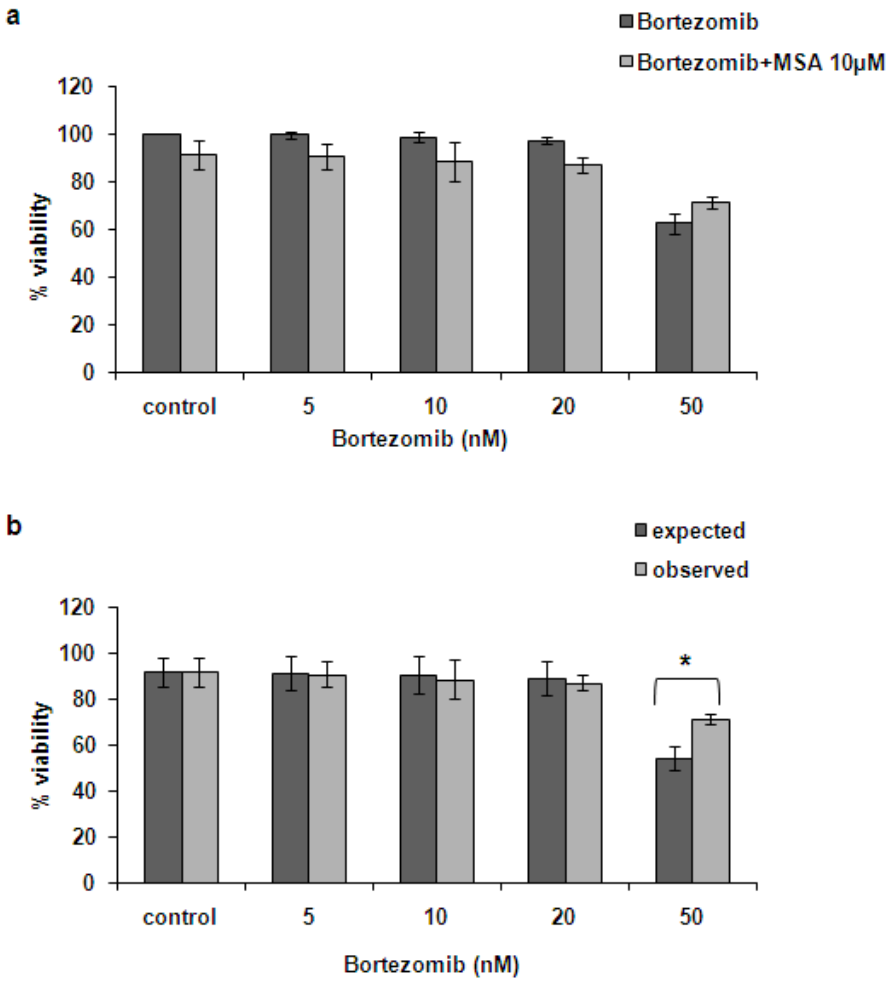

Figure 8.4 Granta-519 cells exposed to a simultaneous combination of MSA 10μmol/L and increasing concentrations of bortezomib. (a) Cell viability with bortezomib alone and in combination with MSA (b) The expected and observed cell viability from the combination of MSA and bortezomib. Guava® viacount assay used. Data points are the mean+/-SD of three separate experiments *p=0.01.

8.4.3 Pre-treatment with MSA followed by the addition of bortezomib

In order to investigate whether the scheduling of the two agents affected the observed antagonistic interaction, JeKo-1 and Granta-519 cells were pre-treated with MSA 10μmol/L for 48 hours followed by the addition of increasing concentrations of bortezomib for a further 48 hours. The results show that pre-treatment with MSA enhanced the antagonistic interaction with the effect now apparent at bortezomib

concentrations of 20nmol/L and 50nmol/L (Figure 8.5 and 8.6). In JeKo-1 cells, bortezomib 20nmol/L and 50nmol/L decreased cell viability by 15% (±2.9) and 54.5% (±7.8) respectively but when pre-treated with MSA, these bortezomib concentrations only decreased cell viability by 3.7% (± 1.0) and 14.7% (±5.7) respectively. In Granta-519 cells, bortezomib 20nmol/L and 50nmol/L decreased cell viability by a mean 17.5% (±3.0) and 68.8% (±1.5) respectively but when pre-treated with MSA these bortezomib concentrations only decreased cell viability by 3.1% (±0.6) and 12.6% (±3.4) respectively. MSA 10µmol/L alone for 96 hours decreased cell viability by <2%.

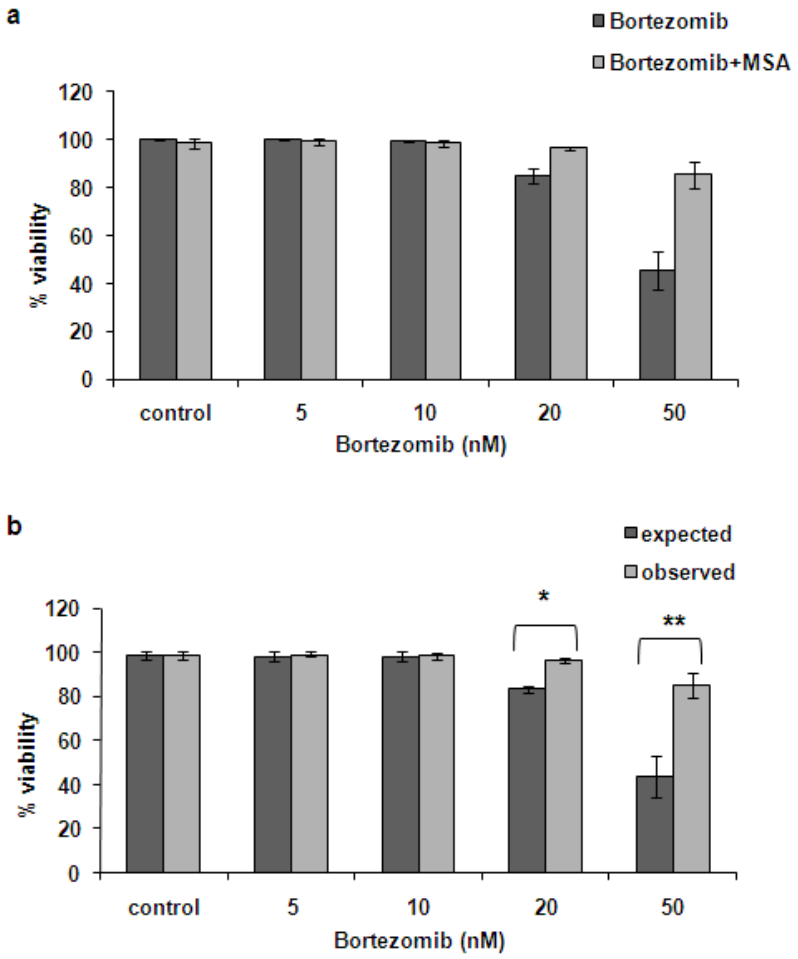

Figure 8.5 JeKo-1 cells pre-treated with MSA 10µmol/L for 48 hours, followed by increasing concentrations of bortezomib for a further 48 hours. (a) Cell viability with bortezomib alone and pre-treatment with MSA (b) The expected and observed cell viability from the combination of MSA and bortezomib. Guava® viacount assay used. Data points are the mean +/- SD of three separate experiments. *p=0.01 **p=0.04

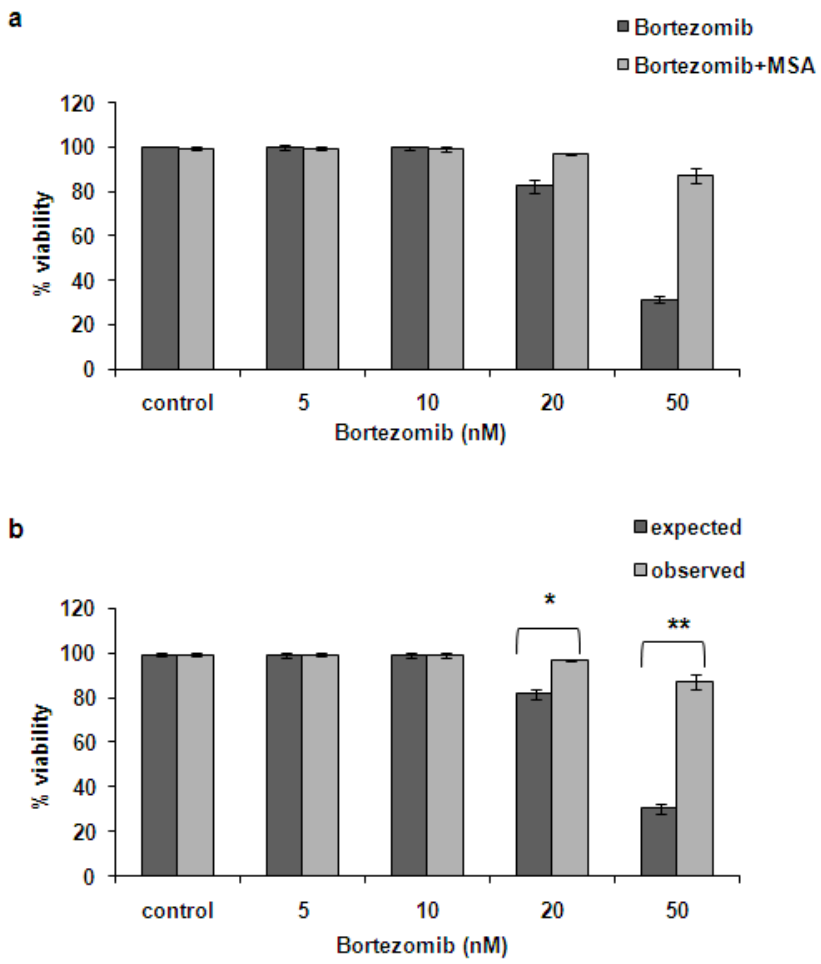

Figure 8.6 Granta-519 cells pre-treated with MSA 10µmol/L for 48 hours, followed by increasing concentrations of bortezomib for a further 48 hours. (a) Cell viability with bortezomib alone and pre-treatment with MSA. (b) The expected and observed cell viability from the combination of MSA and bortezomib. Guava® viacount assay used. Data points are the mean +/- SD of three separate experiments. *p=0.007 **p=0.002.

8.4.4 Protein changes associated with the antagonistic combination of MSA and bortezomib

To investigate the mechanism by which MSA antagonises the effect of bortezomib, western blotting was performed. Cells were exposed to MSA 10µmol/L alone at several time points (6-72 hours) and bortezomib 50nmol/L alone for 6 and 24 hours. For the

combination, cells were pre-treated with MSA for 48 hours followed by bortezmib for a further 6 and 24 hours. The results in both JeKo-1 (Figure 8.7) and Granta-519 (Figure 8.8) cells were similar. Cleavage of PARP was used to investigate the induction of apoptosis. MSA alone did not result in PARP cleavage but bortezomib at 24 hours did. However, when cells were pre-treated with MSA followed by 24 hours of bortezomib, the amount of cleaved PARP decreased, suggesting that MSA inhibits apoptosis. These results are in keeping with the cell viability data.

Both MSA and bortezomib are known to induce ER stress and autophagy which are both mechanisms of cell survival. Therefore western blotting for the ER chaparone GRP78 and the down-stream target p-eIF2α was performed and the conversion of LC3B-I to LC3B-II, as a marker of autophagy induction, was investigated. Figures 8.7 and 8.8 show that in JeKo-1 and Granta-519 cells MSA alone induced expression of GRP78 with maximal induction at 24 hours, followed by decreasing expression, although the levels did not return to baseline by 72 hours. Bortezomib also induced expression of GRP78 but the combination resulted in a less than additive increase. Both cell lines displayed phosphorylation of eIF2α at baseline. MSA alone decreased the phoshorylation of eIF2α at 6-hour exposure, which was unexpected, as induction of ER stress usually increases phosphorylation. By 24 hours, there was a return of p-eIF2α towards baseline levels. Bortezomib alone increased the phoshorylation of eIF2α as did the combination with MSA. Both MSA and Bortezomib led to the conversion of LC3B-I to LC3B-II. The amount of LC3B-II in MSA-treated cells was maximal at 24 hours. Pre-treatment with MSA prior to bortezomib actually decreased LC3B-II levels compared with bortezomib alone, suggesting that although each drug induces autophagy, the combination decreased this induction.

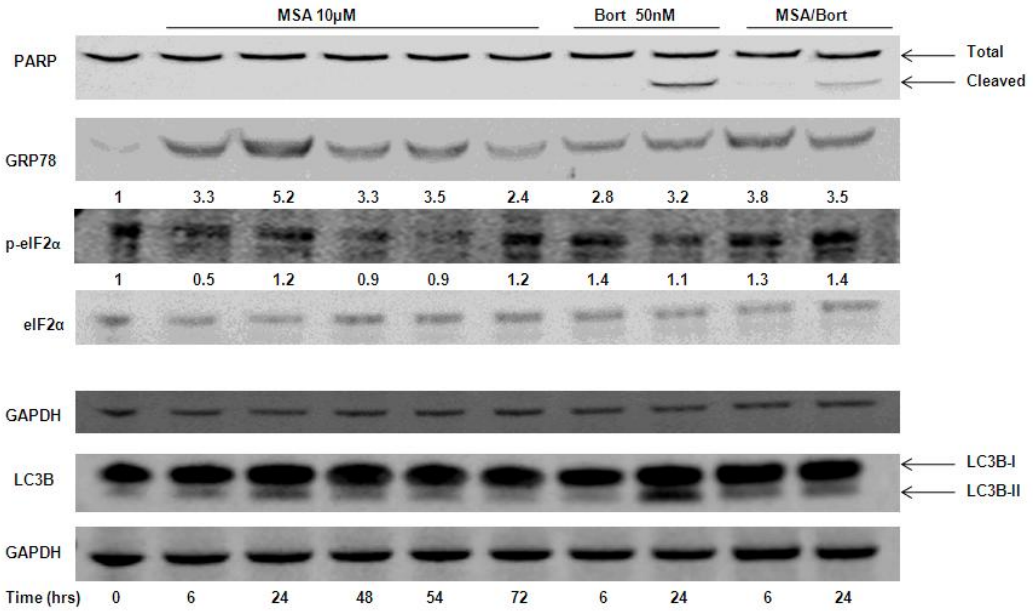

Figure 8.7 Induction of apoptosis, endoplasmic reticulum stress and autophagy in JeKo-1 cells exposed to MSA 10μmol/L and bortezomib 50nmol/L alone and in combination. Densitometry values are shown where relevant.

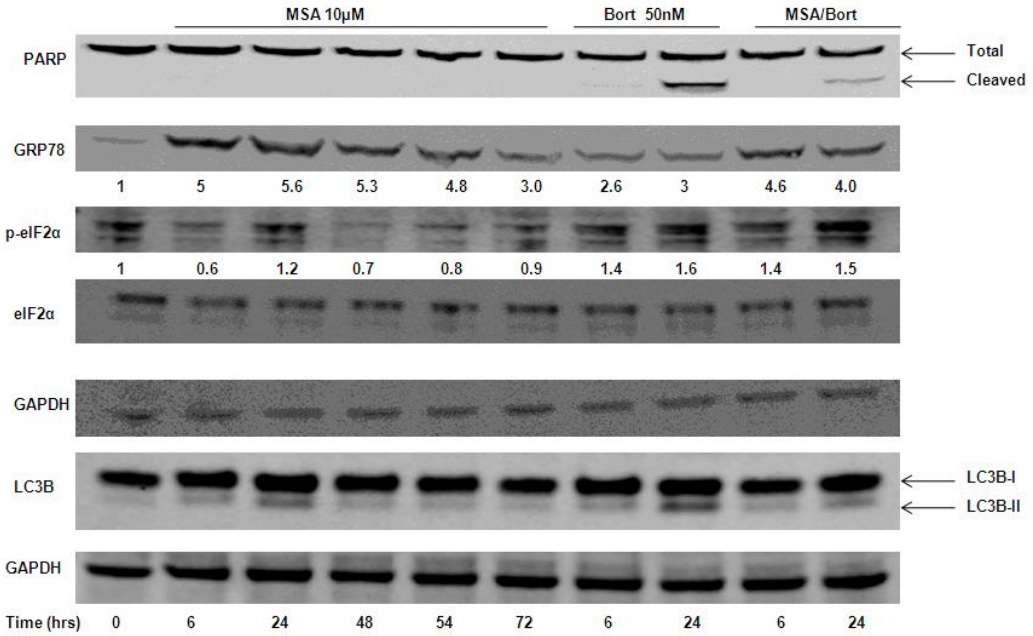

Figure 8.8 Induction of apoptosis, endoplasmic reticulum stress and autophagy in Granta-519 cells exposed to MSA 10μmol/L and bortezomib 50nmol/L alone and in combination. Densitometry values are shown where relevant.

To further investigate how MSA inhibits bortezomib-induced apoptosis, the expression of two anti-apoptotic members of the Bcl-2 family of proteins was investigated. JeKo-1 and Granta-519 cells were exposed to MSA 10µmol/L alone for 72 hours, bortezomib 50nmol/L alone for 24 hours and a combination of MSA pre-treatment for 48 hours followed by bortezomib for 24 hours. Figure 8.9 shows that MSA alone, but not bortezomib, induced the expression of Bcl-2 and the combination resulted in a larger increase in expression. Both MSA and bortezomib increased Mcl-1 expression and again the combination resulted in a further increase. This suggests that MSA inhibits bortezomib-induced apoptosis through the induction of anti-apoptotic Bcl-2 family proteins.

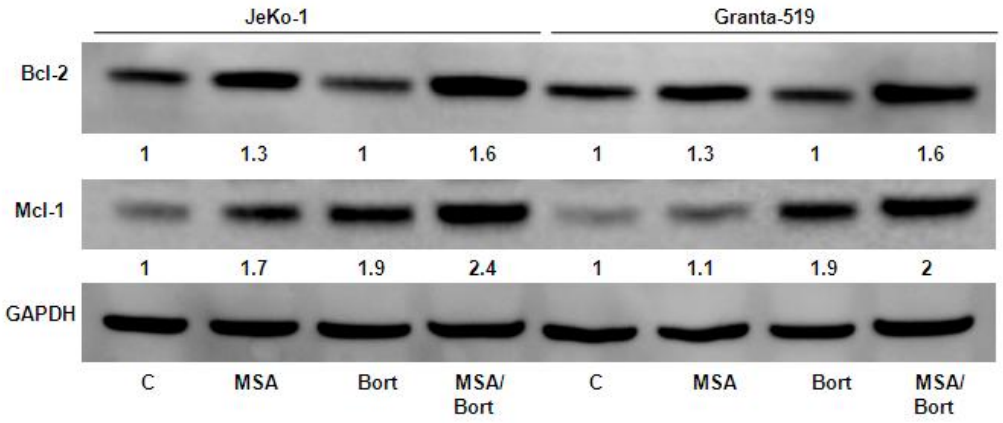

Figure 8.9 Bcl-2 and Mcl-1 expression in JeKo-1 and Granta-519 cells exposed to MSA 10µmol/L alone for 72 hours, bortezomib alone 50nmol/L for 24 hours and combined pre-treatment with MSA for 48 hours followed by bortezomib for 24 hours. Densitometry values are shown.

8.4.5 Proteasome inhibition

A further mechanism by which MSA could inhibit the action of bortezomib is by antagonising its effect on the proteasome. To investigate whether MSA prevented bortezomib from inhibiting the proteasome, two methods were used. Firstly, western blotting for total ubiquitinated proteins was performed and secondly, a proteasome activity assay was used. Figure 8.10 shows the full western blot of JeKo-1 and Granta-519 cells treated with MSA and bortezomib, in the same experiment described for

Figures 8.7 and 8.8. The blot was incubated with an anti-ubiquitin antibody. MSA did not increase the amount of ubiquitinated proteins but bortezomib did. When cells were pre-treated with MSA followed by treatment with bortezomib the amount of ubiquitinated proteins appeared the same as with bortezomib alone.

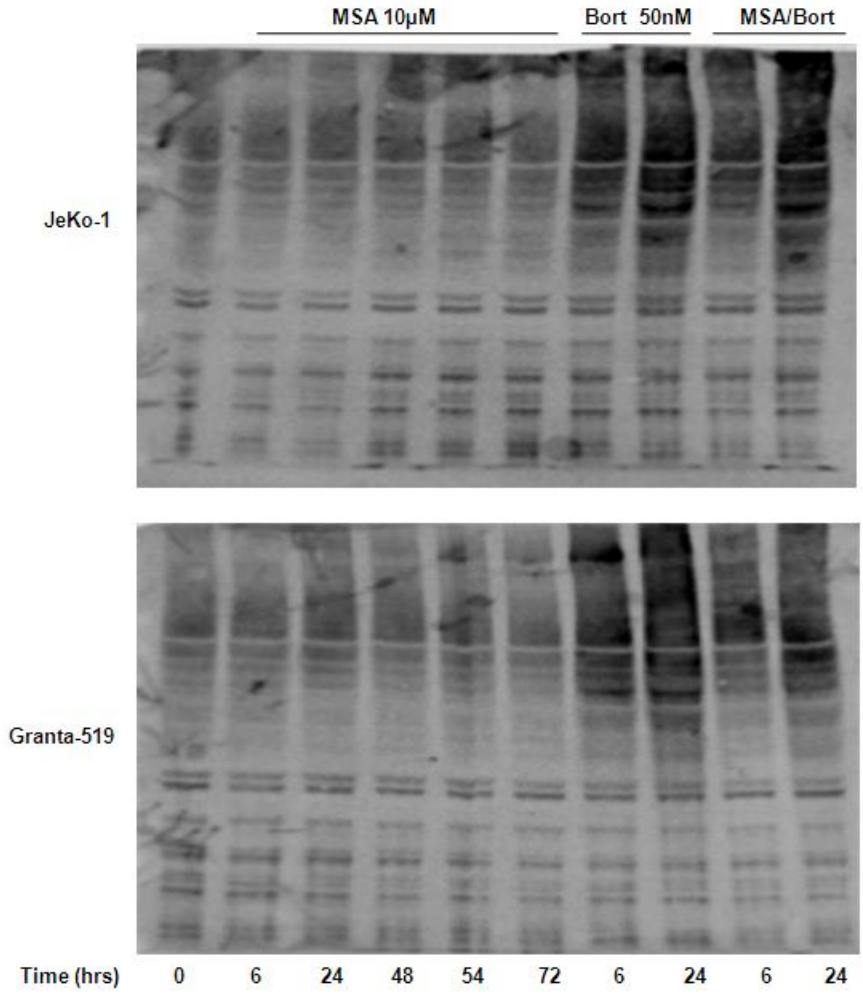

Figure 8.10 Total ubiquitinated proteins in JeKo-1 and Granta-519 cells treated with 10µmol/L MSA alone, bortezomib 50nmol/L alone and combined pre-treatment with MSA for 48 hours followed by bortezomib.

Western blotting is not a very sensitive or specific method of assessing proteasome function, therefore a proteasome activity assay was used. Cells were treated with MSA 10µmol/L alone for 72 hours, bortezomib 20nmol/L or 50nmol/L alone for 24 hours and a combination of pre-treatment with MSA for 48 hours followed by bortezomib

20nmol/L or 50nmol/L for a further 24 hours. Figure 8.11 shows that bortezomib 20 and 50nmol/L completely inhibited proteasome activity and pre-treatment with MSA did not prevent this inhibition.

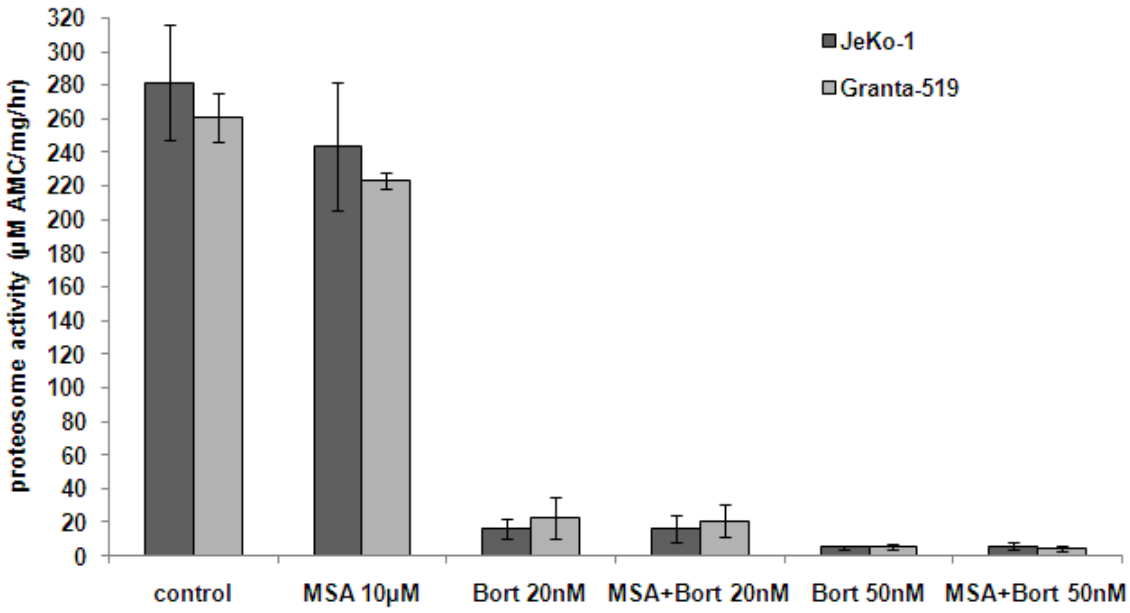

Figure 8.11 Proteasome activity assay in cells treated with MSA 10µmol/L and bortezomib alone and in combination. Bortezomib 20nmol/L, data points are the mean +/- SD of three separate experiments, Bortezomib 50nmol/L, data points are the mean +/- SD of two separate experiments.

8.5 DISCUSSION

The JeKo-1 and Granta-519 cell lines have constitutive activation of NF-κB (Shishodia *et al*, 2005) suggesting that they may be sensitive to MSA and bortezomib. Both cell lines, however, were found to be relatively resistant to the cytotoxic effects of both MSA and Bortezomib with 48-hour EC_{50} values for cell viability of >30µmol/L and >70nmol/L respectively. In comparison, the 72-hour EC_{50} value for cell viability for bortezomib in a panel of 5 B-NHL cell lines was reported to be between 6-25nmol/L (Strauss *et al*, 2007). MSA was cytostatic at much lower concentrations with EC_{50} values for cell number of 3.2µmol/L and 2.8µmol/L for JeKo-1 and Granta-519 cells respectively. Bortezomib also

had a larger effect on cell number than cell viability but not to the same degree as MSA and EC_{50} values for cell number were approximately half those for cell viability. In JVM2 cells, another MCL cell line, the 72-hour EC_{50} for MSA was found to be 3.4μM (Chapter 4, Figure 4.16). However, these results are not directly comparable to those for JeKo-1 and Granta-519 cell lines because the ATP and not the Guava® viacount assay was used. The ATP assay reflects both the cell number and viability whereas the Guava® viacount assay can assess both parameters separately. Nonetheless, in JVM2 cells, PARP cleavage was observed in cells exposed to ≥3μmol/L MSA (Chapter 4, Figure 4.18) and exposure to an EC_{50} concentration significantly increased the sub-G1/apoptotic population when performing cell cycle analysis (Chapter 4, Figure 4.17). These results suggest that the JVM2 cell line was more sensitive to the cytotoxic effects of MSA than the JeKo-1 and Granta-519 cell lines. This is the first time that the activity of MSA in MCL cell lines has been reported.

It was expected that the combination of MSA and bortezomib in MCL cell lines would result in a synergistic interaction. Unexpectedly, it was found that the opposite was true, such that MSA inhibited bortezomib-induced cell death. This was apparent when cells were treated with both drugs simultaneously but only with the highest concentration of bortezomib, 50nmol/L. However, when cells were pre-treated with MSA 10μmol/L for 48 hours and then bortezomib added for a further 48 hours the interaction was enhanced such that MSA inhibited the action of bortezomib at 20nmol/L and at 50nmol/L. In both cell lines, MSA alone for 96 hours decreased cell viability by <2%. In JeKo-1 cells, pre-treatment with MSA increased cell viability by 12.7% and 41.2% in cells treated with 20nmol/L and 50nmol/L bortezomib respectively when compared with the expected cell viability of the combination. In Granta-519 cells, pre-treatment with MSA increased cell viability by 15% and 56.8% in cells treated with 20nmol/L and 50nmol/L bortezomib respectively when compared with the expected cell viability of the combination. Decreased apoptosis was confirmed in the combination by western blotting which showed decreased PARP cleavage when cells were pre-treated with MSA compared with bortezomib alone.

There have been reports in the literature of potential therapeutic agents inhibiting the cytotoxic effect of bortezomib and the mechanism of interaction has been a chemical one with the boronic acid group of bortezomib. This has been reported for flavonoids (Liu *et al*, 2008) and polyphenols (Golden *et al*, 2009). The interaction between MSA and bortezomib is not a chemical one as pre-treatment of cells with MSA enhances the antagonism and MSA did not prevent inhibition of proteasome activity as demonstrated by western blotting and a proteasome activity assay.

Other mechanisms of resistance to bortezomib have also been reported, including the induction of GRP78. As already discussed, GRP78, a molecular chaperone found mainly in the ER, promotes cell survival and has been implicated in chemo-resistance (Lee, 2007). In addition, it has been demonstrated that GRP78 is expressed on the cell surface of tumour cells (Arap *et al*, 2004) and it can also be secreted by tumour cells (Kern *et al*, 2009). Thus, targeting GRP78 is being explored as a therapeutic option (Lee, 2007). It was recently reported that certain solid tumour cell lines secrete GRP78 and this resulted in resistance to bortezomib both *in vitro* and *in vivo*. Knockdown of GRP78 restored sensitivity to bortezomib and the addition of recombinant GRP78 to bortezomib-sensitive cell line cultures induced resistance. Direct interaction of GRP78 and bortezomib was excluded as the mechanism of resistance but it was shown that the addition of GRP78 to cell cultures induced pro-survival intracellular signalling proteins such as p-Erk and p-Akt, suggesting that GRP78 may interact with cell surface receptors (Kern *et al*, 2009).

GRP78 expression was therefore investigated in JeKo-1 and Granta-519 cells. These cell lines had a low level of basal GRP78 expression but at concentrations that resulted in antagonism both MSA and bortezomib alone resulted in induction of GRP78 expression, the mechanism of which is the accumulation of unfolded proteins (Obeng *et al*, 2006; Park *et al*, 2005). The induction by MSA was maximal at 24 hours but GRP78 had not returned to baseline by 72 hours. The combination of MSA pre-treatment followed by bortezomib resulted in a less than additive increase in GRP78 expression, although the increase was more than that with bortezomib alone. Thus, this may be a mechanism by

which MSA antagonises the effect of bortezomib. To confirm this, further experiments to knockdown the expression of GRP78 would be required.

Induction of ER stress leads to activation of the three transducers of the UPR (Szegezdi *et al*, 2006). When PERK is activated it leads to phosphorylation of eIF2α. Depending on the degree of cellular stress, phosphorylation of eIF2α can promote cell survival, by reducing the rate of protein translation and inducing growth arrest, or apoptosis, through the induction of pro-apoptotic proteins such as GADD153 (Rutkowski & Kaufman, 2007). A recent study of bortezomib in multiple myeloma reported that bortezomib-resistance was associated with eIF2α dephosphorylation and suppression of its downstream target GADD153. Treatment of myeloma cells with a chemical that induced phosphorylation of eIF2α enhanced bortezomib-induced cytotoxicity. Similar effects were seen with the proteasome inhibitor MG-132 (Schewe & Aguirre-Ghiso, 2009). Phosphorylation of eIF2α was therefore examined in the MCL cell lines and both JeKo-1 and Granta-519 cells displayed phosphorylation of eIF2α at baseline. MSA decreased the phosphorylation of eIF2α with a maximal effect at 6 hours and a return to baseline levels with longer exposure times. Bortezomib alone increased the phosphorylation of eIF2α as did the combination of MSA pre-treatment followed by bortezomib. It is difficult to know how to interpret these results without further experiments. Clearly, the combination of MSA and bortezomib increases the phosphorylation of eIF2α but pre-treatment with MSA initially decreases this. The cellular effects of this would have to be studied by either over-expressing or inhibiting p-eIF2α to see whether this reversed the protective effect of MSA.

ER stress activates autophagy, which is mainly a mechanism of cell survival whereby cells degrade long-lived proteins and protein aggregates (Ogata *et al*, 2006). However, like ER stress and the UPR, autophagy has been implicated both in cancer cell death and survival. Bortezomib has been shown to induce autophagy and in human prostate cancer cell lines this was a protective cellular response mediated by p-eIF2α. When bortezomib was combined with inhibitors of autophagy, cell death was enhanced (Zhu *et al*, 2010).

Similarly, in human breast cancer cell lines, induction of autophagy was shown to be a mechanism of resistance to bortezomib (Milani *et al*, 2009). However, the consequence of bortezomib-induced autophagy is not clear cut as some studies have reported it to result in cell death and thus the effect may be cell-type dependent (Belloni *et al*, 2010; Hoang *et al*, 2009). Both MSA and bortezomib induced autophagy in JeKo-1 and Granta-519 cells, demonstrated by an increase in LC3-II levels by western blotting. The increase in LC3-II was maximal at 24 hours in MSA treated cells and then returned to baseline. Unexpectedly, the combination of MSA pre-treatment followed by bortezomib resulted in less of an increase in LC3-II compared with bortezomib alone, suggesting that MSA inhibits bortezomib-induced autophagy. Again, the consequences of this require further investigation, for example, by combining a known inhibitor of autophagy with bortezomib to assess the effect on cell death.

Bortezomib-induced cytotoxicity is associated with altered expression of Bcl-2 family proteins although these effects differ depending on the cell type. For example, in multiple myeloma cell lines, bortezomib-induced apoptosis was associated with down-regulation of Bcl-2 (Mitsiades *et al*, 2002). However, in MCL cell lines, bortezomib did not alter Bcl-2 expression (Perez-Galan *et al*, 2006). The expression of two anti-apoptotic Bcl-2 family members, Bcl-2 and Mcl-1, was investigated by western blotting. Of note, Mcl-1 is degraded by the proteasome, so bortezomib results in its accumulation, at least in the short term (Nencioni *et al*, 2005). MSA 10μmol/L alone for 72 hours resulted in increased expression of Bcl-2 but bortezomib 50nmol/L alone for 24 hours did not. The combination of MSA pre-treatment for 48 hours, followed by bortezomib, further increased Bcl-2 expression. Both MSA and bortezomib alone increased the expression of Mcl-1 and the combination showed a larger increase. Therefore, modulation of Bcl-2 family proteins by MSA may explain, in part, the antagonism seen with bortezomib.

In summary, pre-treatment of MCL cell lines with MSA antagonises the cytotoxic effect of bortezomib. This is not through a chemical interaction as proteasome inhibition is not prevented, but may be through the modulation of Bcl-2 family proteins. Although both

drugs induce ER-stress and autophagy in the MCL cell lines it is not entirely clear from the experiments performed what role these cellular responses play in cell survival. However, it can be concluded that Se supplementation, in patients with MCL treated with bortezomib, should be avoided.

CHAPTER 9: The investigation of methylseleninic acid uptake and metabolism by diffuse large B-cell lymphoma cell lines and peripheral blood mononuclear cells.

9.1 INTRODUCTION

Methylselenol is thought to be the metabolite responsible for the anti-tumour effects of Se compounds but, because of its high volatility, it cannot be directly measured or quantified (Ip *et al*, 2000). In this thesis, the compound MSA has been used as a precursor of methylselenol to study its effects in lymphoma cell lines and normal cells. Once taken up by cells, MSA is reduced by enzymatic and non-enzymatic reactions to methylselenol. MSA reacts with cellular thiols, compounds that contain the functional group composed of a sulfur-hydrogen bond (-SH), such as GSH and cysteine-containing molecules. Intermediate compounds are formed such as methylselenenylsulfide, which is reduced to methylselenol in the presence of excess thiol, and reaction with GSH results in methylselenoglutathione, which undergoes NADPH-dependent reduction by glutathione reductase to methylselenol (Ip *et al*, 2000). Other seleno-sulphur conjugates have been detected as a result of spontaneous reaction of MSA with thiols, including S-methylselenocysteine and S-methylselenoglutathione (Gabel-Jensen *et al*, 2008). Once formed, methylselenol can be further methylated to form dimethylselenide, which *in vivo* is excreted in breath, and trimethylselenonium, which *in vivo* is excreted in urine (Ohta *et al*, 2009). Additionally, methylselenol can be demethylated to form hydrogen selenide which is the essential metabolite for the incorporation of Se into selenoproteins (Rayman *et al*, 2008; Suzuki *et al*, 2006b). Hydrogen selenide, that is not required for selenoprotein synthesis, is converted to selenosugars, which are the main Se metabolites excreted in urine after ingestion of Se compounds (Kuehnelt *et al*, 2007; Ohta *et al*, 2009). Other metabolites of MSA have also been identified. When rat hepatocytes were exposed to MSA, the major metabolite identified was MSC, with SLM identified as a minor metabolite. MSC was formed via the intermediates S-methylselenocysteine and S-methylselenoglutathione (Gabel-Jensen *et al*, 2009b). Volatile metabolites, other than methylselenol, have also been identified in the head-space of cells exposed to MSA.

These have been identified as dimethylselenide and dimethyldiselenide (Gabel-Jensen *et al*, 2009a; Goenaga-Infante *et al*, 2007a). Of interest, dimethyldiselenide can be formed by combining MSA with GSH in aqueous solution in the absence of cells indicating that it is a reaction product rather than a metabolic product (Gabel-Jensen *et al*, 2009a). Experiments, in which methylselenol was produced *in situ*, demonstrated that dimethyldiselenide is spontaneously formed by oxidation of methylselenol and hence may be a good indicator for the production of methylselenol *in vitro* (Gabel-Jensen *et al*, 2010). As an aside, these volatile species have a pungent garlic odour when working with Se compounds in the laboratory.

MSC seems to be the most promising compound for clinical use, as compared with other organic Se compounds it is more efficiently converted to methylselenol and has more potent anti-tumour properties (Ip *et al*, 1991; Ohta *et al*, 2009; Suzuki *et al*, 2006a). MSC can be directly converted to methylselenol by cysteine *S*-conjugate β-lyase (β-lyase) enzymes and the subsequent metabolic reactions are the same as those described above for MSA (Rayman *et al*, 2008). In addition, MSC can be oxidised to MSC-selenoxide and this can be converted to MSA by β-lyase enzymes (Ganther, 1999). β-lyase enzymes are pyridoxal 5'-phosophate (PLP)-dependent enzymes that primarily are involved in amino acid metabolism but catalyse β-elimination reactions as a secondary function. At least 13 mammalian enzymes with β-lyase activity have been identified, most showing a wide distribution in mammalian tissue, but with highest activity in the liver and kidney (Cooper *et al*, 2010; Cooper & Pinto, 2006). In addition, it has been demonstrated that commonly found bacterial species in the human intestine possess β-lyase activity and may play a role in the activation of selenocysteine derivatives (Schwiertz *et al*, 2008). Studies investigating the metabolism of orally administered MSC in rats have reported that MSC is taken up, intact, by a number of organs and then converted to methylselenol (Suzuki *et al*, 2006a; Suzuki *et al*, 2008). It is not clear, however, how much β-lyase activity tumour cells possess as this has not been extensively investigated. One study measured the β-lyase activity in normal and tumour tissue from patients with renal carcinoma. The enzyme activity in a large proportion of tumours was significantly higher

than in the adjacent normal tissue (Nelson *et al*, 1995). The β-lyase activity in the T-cell leukaemia cell line, Jurkat, was indirectly determined by incubating cells with MSC and measuring the generation of dimethyldiselenide, as a marker of methylselenol production, in the headspace of the cells. However, dimethyldiselenide was not detected suggesting these cells do not possess β-lyase activity (Gabel-Jensen *et al*, 2010). β-lyase activity in other human malignancies has not been reported.

The *in vitro* metabolism of MSA is, therefore, relevant to the *in vivo* use of MSC and has been investigated by our laboratory in DLBCL cell lines (Goenaga-Infante *et al*, 2007a; Juliger *et al*, 2007). This has been described in Chapter 1 (section 1.3.12) but will be briefly summarised again. These experiments used very high concentrations of MSA, 200μmol/L. Differences in baseline Se concentration were found between cell lines, with the MSA-sensitive cell line RL having a higher baseline level than two MSA-resistant cell lines (DHL4 and DoHH2). After exposure to MSA for 4 hours, the intracellular Se concentration of the DHL4 cell line increased by a larger amount compared to the RL cell line. Intracellular Se metabolites were studied in DHL4 cells and the main metabolite formed after 4-hour exposure to MSA was MSC, but SLM and γ-glutamyl-MSC were also detected as minor metabolites. In the headspace of DHL4 cells exposed to MSA, the main volatile metabolite detected was dimethyldiselenide and after longer exposure times, dimethylselenide was detected as a minor metabolite (Goenaga-Infante *et al*, 2007a; Juliger *et al*, 2007).

The experiments reported in this chapter were performed to investigate and compare the uptake and metabolism of a clinically relevant concentration of MSA (20μmol/L) in DLBCL cell lines and PBMCs collected from healthy volunteers. Given that the action of Se differs in tumour and normal cells, the hypothesis being tested in this chapter was that the uptake and metabolism of MSA may differ between lymphoma cell lines and PBMCs.

9.2 AIMS

1) To investigate the uptake of MSA in DLBCL cell lines and PBMCs.

2) To compare the intracellular metabolites of MSA in DLBCL cell lines and PBMCs using a clinically relevant concentration.

3) To compare the generation of volatile Se species in the DHL4 cell line and PBMCs.

4) To establish the feasibility of measuring intracellular Se metabolites as a pharmacokinetic end-point in patients receiving MSC in the planned clinical trial.

9.3 METHODS

9.3.1 Sample preparation for total selenium determination and intracellular selenium species

Sample preparation was performed at the Institute of Cancer, Barts Cancer Centre. Harvested PBMCs were set in culture medium at $1x10^6$ cells/ml and 10 million cells were used for each experimental condition. The DHL4 and RL cell lines were reset in fresh culture medium at $5x10^5$/ml and 10 million cells were used for each experimental condition. Cells were exposed to 20µmol/L MSA for different time periods between 10 minutes and 24 hours. This concentration of MSA was chosen because in the forthcoming clinical trial the aim is to achieve a plasma Se concentration of 20µmol/L. Cells were then lysed as described for western blot sample preparation (Chapter 2, section 2.4.3) and the lysates stored at -80°C until analysis.

9.3.2 Determination of total intracellular selenium concentration

These experiments were performed at LGC (Teddington, London, UK). The high-performance liquid chromatography (HPLC) and MS conditions are described in Table 9.1. To quantify total Se in the cell lysates the sample was initially diluted 1:1 with 2% nitric acid (LGC standards) in deionised water. 10µl of the diluted sample was then injected by flow injection into an Agilent 1200 HPLC (Agilent Technologies, Palo Alto, CA, USA). Each sample was injected in triplicate in a stream of ultra-pure water (ELGA water purification unit, ELGA, Marlow, UK) as the sample carrier. This was coupled on-line to an Agilent 7500i inductively coupled plasma (ICP)-MS for the detection of Se

isotopes. Calibration standards of Se at concentrations of 1, 2, 5, 25 and 100µg/kg were prepared in lysis buffer (the same as that used to lyse the original cell sample) and diluted 1:1 with 2% nitric acid in deionised water.

There are 6 naturally occurring isotopes of Se, and 5 are stable (^{74}Se, ^{76}Se, ^{77}Se, ^{78}Se, ^{80}Se). ^{80}Se is the most abundant isotope, but the dimer $^{40}Ar_2^+$ overlaps with its mass signal resulting in interference (B'Hymer & Caruso, 2006). Therefore, quantification was performed using the peak area measurements of the chromatographic signals for the Se isotope ^{78}Se, the second most abundant isotope. Rhodium was used as the internal standard. An example of a standard curve using ^{78}Se is shown below (Figure 9.1; r=1). Lysis buffer diluted 1:1 with 2% nitric acid in deionised water was used as a reagent blank. The lower quantification limit was set as 2.5µg/kg Se, representing 10 times the SD of at least four blank replicates. Figure 9.2 shows the chromatographic peak of one PBMC control sample in comparison with the reagent blank. Similar results were obtained for the two DLBCL cell lines, thus the basal Se concentration of the cell lines and PBMCs was below the lower quantification limit.

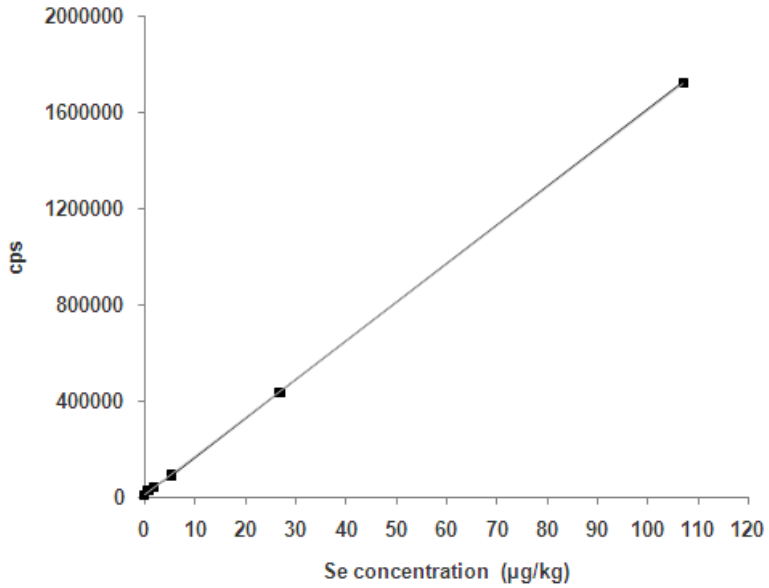

Figure 9.1 Standard curve of the Se isotope ^{78}Se, obtained by the standard addition technique (cps; counts per second).

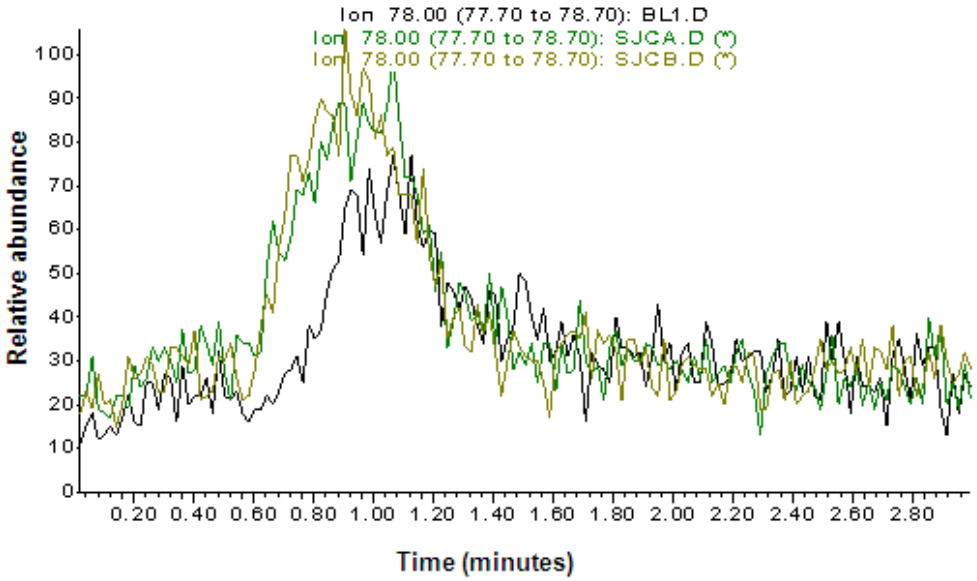

Figure 9.2 Chromatographic peak of reagent blank (black line) and 2 replicates of a peripheral blood mononuclear cell control sample (green and yellow lines).

9.3.3 Measurement of intracellular selenium species

These experiments were performed at LGC (Teddington, London, UK). HPLC and MS conditions are described in Table 9.1. Cell lysates were analysed by reverse-phase HPLC-ICP-MS. The Agilent 1200 HPLC system was used for chromatographic separations and the Agilent 7500i quadrupole ICP-MS for element-specific detection. Chromatographic data were analysed using Agilent Technologies ICP-MS chromatographic software (G1824C version C.01.00). Se standards, which included sodium selenite, SLM, MSC, dimethylselenide and dimethyldiselenide, were purchased from Sigma-Aldrich and γ-glutamyl-MSC was purchased from PharmaSe®, Inc. SLM stock solution was prepared using 0.1M hydrochloric acid. All other standards were diluted in ultra pure water and stored at 4°C. The chromatographic signal for ^{78}Se was monitored.

Verification of the presence of S-methylselenoglutathione by HPLC-ESI MS/MS

To identify an unknown Se-containing chromatographic peak, electrospray ionisation (ESI) followed by MS/MS was performed. An Agilent 1200 HPLC system coupled to an Agilent 6300 Ion Trap LC-MS were used. HPLC and MS conditions are described in Table 9.1. The cell lysate was injected into the reversed-phase column and the effluent was fed directly into the electrospray source. For ions containing Se, product ion spectra were acquired in the collision-induced dissociation mode. Confirmation of S-methylselenoglutathione was based on the MS/MS data obtained by fragmentation of the parent ion, *m/z* 402, using collision-induced dissociation. Data acquisition and processing were performed using the Agilent 6300 Ion Trap software, version 6.2.

Table 9.1 HPLC-ICP-MS and the HPLC-ESI-MS/MS operating conditions

HPLC conditions	
Column	Zorbax microbore 300SB-C_{18} (250mm length x1.0mm id x 5µm particle size)
Injection loop	5µl
Flow rate	50µl/min (30µl/min for ESI)
Mobile phase	0.1% TFA (formic acid for ESI) in 2% methanol/98% ultrapure H_2O
ICP-MS settings	
RF power	1300W
Plasma argon flow rate	15 l/min
Make-up argon flow rate	0.31 l/min
Nebuliser argon flow rate	0.81 l/min
ESI-MS/MS setting	
ESI mode	Positive
Capillary voltage	4.0 kV
Dry gas	12 l/min
Nebulisation gas	39 psi
Collision energy	20 eV
Collision gas	N_2
m/z range	200-1000

9.3.4 Measurement of volatile selenium compounds

Sample preparation

Harvested PBMCs and DHL4 cells were set in culture medium at $1x10^6$/ml and 10 million cells were used for each experimental condition. The cells were transferred into a 15ml glass vial and exposed to 20µmol/L MSA. The glass vials were placed in a cell culture incubator at 37°C in a humidified atmosphere with 5% CO_2 for a range of time-points.

Solid phase microextraction capture of volatile selenium compounds

These experiments were performed at LGC. In order to capture the volatile selenium species generated by MSA treatment, a 75µm Carboxen polydimethylsiloxane solid phase microextraction (SPME) fibre (Supelco, Sigma-Aldrich) was passed through the septum of the glass vial and placed in the 5ml headspace above the PBMCs and DHL4 cells for the last 10 minutes of the exposure. Prior to this the SPME fibre had been exposed to a conditioning temperature of 230°C for 30 minutes. The fibre was then held in the inlet liner of the gas chromatogram for the duration of the chromatographic run.

Identification of volatile Se species by Cryogenic Oven Cooling (COC) Gas Chromatography (GC) and Time of Flight Mass Spectrometry (TOFMS)

COC enables the trapping of volatile compounds on the GC column by cooling the whole oven down to temperatures as low as -60°C. GC-TOFMS measurements were performed using an Agilent 6890 GC coupled to the Leco Pegasus III TOFMS (Leco, St Joseph, Michigan, USA). The GC and TOFMS conditions are described in Table 9.2. For separation of the volatile species, a HP Ultra2 column was used. TOF mass calibration was performed using perfluorotributylamine. A splitless injection mode was used with helium as the carrier gas. The initial temperature of the column was set at -35°C for 3 minutes and reached a final temperature of 250°C with a gradient of 15°C/min. Mass spectra were recorded over a *m/z* range of 40 to 500. The LECO ChromaTOF™ software version 2.25 (optimized for Pegasus) was used for data acquisition and processing. Dimethylselenide and dimethyldiselenide were used as standards.

Table 9.2 GC-TOFMS operating conditions

GC conditions	
Column	HP ultra 2 (25m length x 0.2mm id x 0.33µm particle size)
Carrier gas	Helium
Helium flow rate	1 ml/min
Injector temperature	230°C
Splitless time	3 minutes
Purge flow	20 ml/min
Transfer line temperature	280°C
Oven programme	-35°C, 3 minutes isothermal; then 15°C/min to 250°C; then 2 minutes isothermal
TOFMS settings	
m/z range	50-400
Acquisition rate	5 spectra/second
Ion source temperature	230°C

9.3.5 Tumour selenium measurements

Samples

The request to measure Se concentration in stored tumour biopsy samples from patients with lymphoma received a favourable ethical opinion from the East London and City HA Local Research Ethics Committee. Se concentration in biopsy samples from 16 patients with DLBCL was determined. These were samples obtained from patients who were diagnosed with DLBCL at SBH between 1986 and 1996, in whom the presentation serum Se had previously been determined (Last *et al*, 2003). Fresh frozen samples had been stored in liquid nitrogen and approximately 0.1g of tissue (the weight was recorded accurately to two decimal places) was cut from the original biopsy sample, placed into glass vials and used for analysis. Further sample preparation and analysis was performed at LGC (Teddington, London, UK).

1ml of nitric acid/hydrogen peroxide (1:1) solution was added to each tumour tissue. Samples were digested in a microwave oven (CEM, UK) using the standard programme (150˚C for 10 min). Digested samples were diluted up to 10g with ultra-pure water before analysis. Certified reference material (CRM) were mineralised and analysed in duplicate

in parallel with the tumour samples to evaluate the accuracy of the procedure. The CRM used were DORM-2 dogfish muscle (National Research Council of Canada) and bovine liver (National Institute of Standards and Technology, USA) with certified concentrations for Se of 1.40 ± 0.09mg/kg and 0.73 ± 0.06mg/kg respectively.

Sample analysis

20µl of each sample was injected, in triplicate, into the Agilent 1200 HPLC (without an LC column). This was combined on-line to an Agilent 7500i ICP-MS for detection of Se isotopes. Quantification was performed by external calibration, monitoring the Se isotope ^{78}Se, and rhodium was used as the internal standard. Peak area was used for quantification.

9.3.6 β-lyase activity in lymphoma cell lines

β-lyases are PLP-dependent enzymes involved in the bioactivation of selenocysteine conjugates into selenols. β-lyase activity in lymphoma cell lines was determined by measuring the formation of pyruvate after incubating cell lyastes with MSC and PLP as per the reaction shown below. The method used was modified from a previous publication (Zhang & Hanigan, 2003).

$$\text{MSC} \xrightarrow[\text{PLP}]{\beta\text{-lyase}} \text{selenol + ammonia + pyruvate}$$

Preparation of whole cell lysates

Cell lysates were prepared from 40 million cells. DHL4, RL and JVM2 cells were used in these experiments. The renal adenocarcinoma cell line, ACHN (ATCC, VA, USA) was used as a positive control. Cells were pelleted by centrifugation at 210*g* for 6 minutes at room temperature. The supernatant was discarded and the cells washed twice in HBSS by centrifugation at 210*g* for 6 minutes at room temperature. The cells were resuspended in 250µl lysis buffer as per the western blotting protocol for cell lysis (Chapter 2, section 2.4.3). Samples were left on ice for 20 minutes and then centrifuged at 20,800*g* for 10

minutes at 4°C to remove insoluble cellular debris. The supernatant was removed and placed into fresh tubes.

Preparation of the 'reaction mix' (RM)

The RM consisted of PLP, MSC and potassium phosphate buffer pH 7.2 (K_2HPO_4). The following stock solutions were prepared and stored at -20°C until further use: 25mg/ml PLP (Sigma-Aldrich) in 1M HCl, 5mM MSC (PharmaSe® Inc.) in deionised water and 100mM K_2HPO_4 in deionised water and the pH adjusted to 7.2 with phosphoric acid. From these stock solutions 10mls of the RM was prepared by mixing 9.1ml K_2HPO_4, 910µl MSC and 1µl PLP.

β-lyase assay

200µl of the cell lysate was placed into fresh eppendorf tubes. 40µl of the RM was added to this. As a control, water was added to the cell lysate instead of the RM. The samples were then incubated for 15 minutes at 37°C. Following this, the pyruvate released was converted to pyruvate 2,4-dinitrophenylhydrazone by the addition of 2µl of 0.2M 2,4-dinitrophenylhydrazine phosphoric acid solution (Sigma-Aldrich). The samples were incubated again for 15 minutes at 37°C. This was followed by the addition of 320µl of 2M potassium hydroxide (Sigma-Aldrich). 100µl of each sample was transferred immediately to a 96-well plate and the absorbance of pyruvate 2,4-dinitrophenylhydrazone at 450nm was measured on the POLARstar OPTIMA plate reader (BMG Labtech). A standard curve was prepared using sodium pyruvate (Sigma-Aldrich) with a concentration range of 31.25 to 1000µmol/L. An example of a pyruvate standard curve is shown below (Figure 9.3; r=0.99). Results were expressed as a percentage of control.

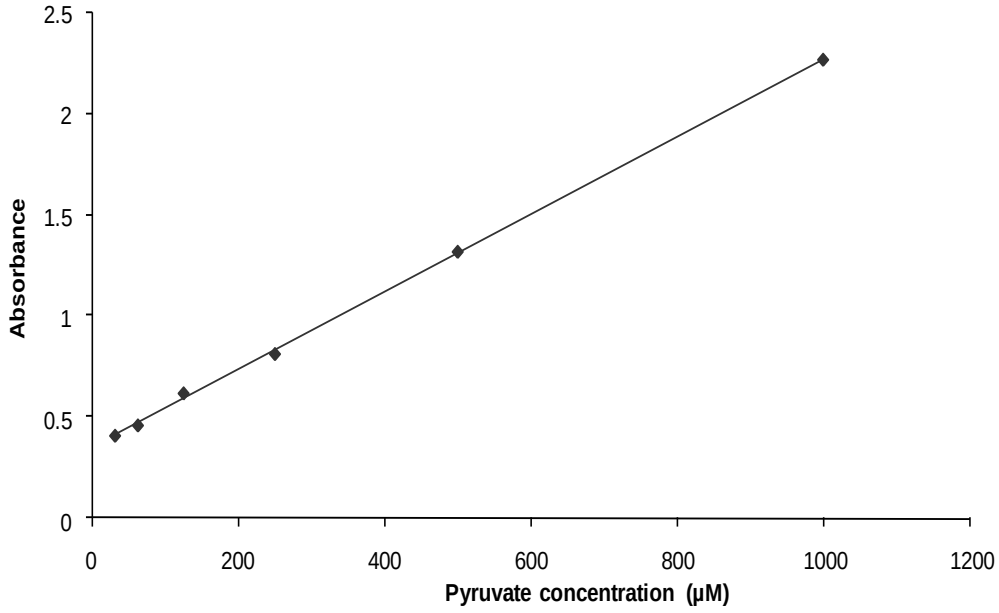

Figure 9.3 Standard curve for sodium pyruvate used to quantify β-lyase activity in cell lines.

9.4 RESULTS

9.4.1 Total intracellular selenium concentration in DLBCL cell lines and peripheral blood mononuclear cells exposed to MSA

Total intracellular Se concentration was determined in the RL and DHL4 cell lines and PBMCs exposed to 20µmol/L MSA for a range of time-points. Figure 9.4 shows the total intracellular Se concentration in the two DLBCL cell lines and Figure 9.5 shows the total intracellular Se concentration in PBMCs. The data were variable, but it appears that in the DLBCL cell lines MSA was taken up rapidly by the cells, with the maximum intracellular Se concentration reached after only 10-minute exposure. There was then a trend towards a decrease in Se concentration at 6- and 24-hour exposure, particularly in the DHL4 cell line. In contrast, the intracellular Se concentration in PBMCs increased more slowly with a maximum concentration reached at 4- to 6-hour exposure, followed by a decrease by 24 hours. The mean values at each time point were, in general, lower than those obtained in the lymphoma cell lines. In addition, the area under the curve (calculated using the GraphPad PRISM® software) for PBMCs (2236µg/kg.hrs) was

lower than that for the DLBCL cell lines (RL, 3367µg/kg.hrs; DHL4, 3102µg/kg.hrs), suggesting that overall Se uptake by PBMCs was less. However, meaningful statistical analysis was not possible due to limited data. Of note, the Se concentration in all the control samples were below estimated quantification limits, therefore these values should not be considered as exact values.

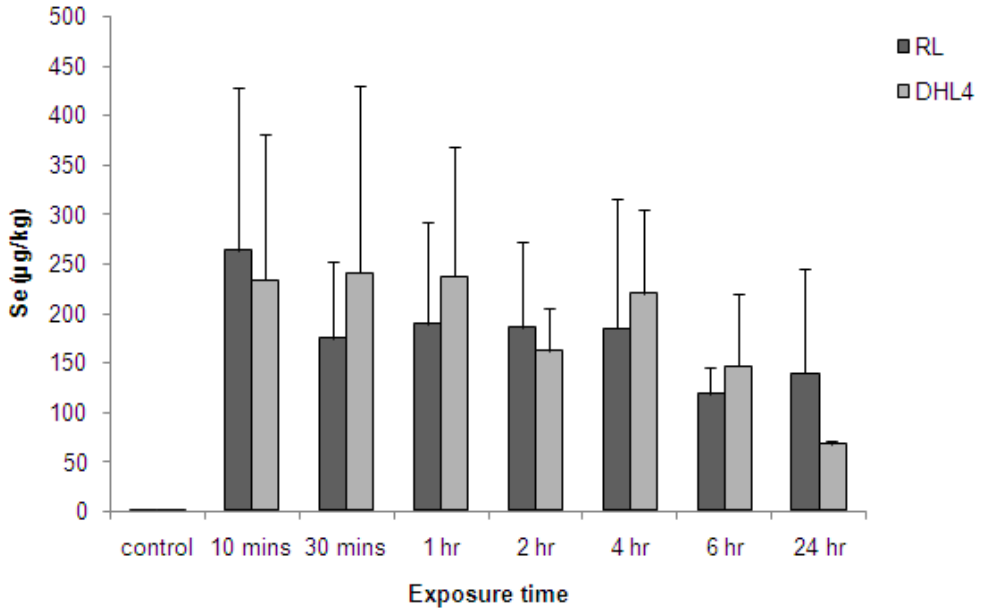

Figure 9.4 Total intracellular selenium concentration in RL and DHL4 cell lines exposed to 20µmol/L MSA. Data points are the means+/-SD of 2 separate experiments.

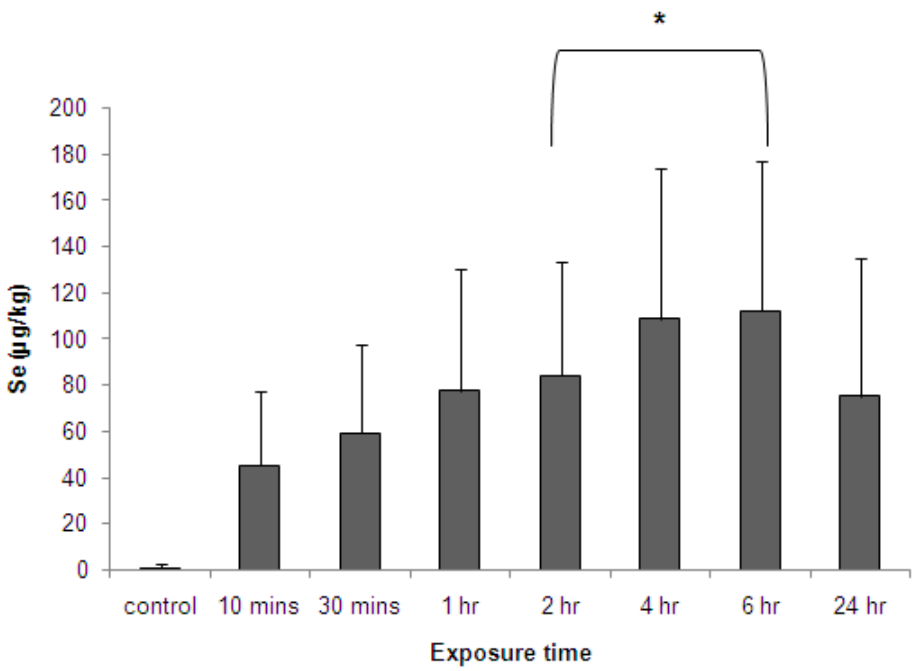

Figure 9.5 Total intracellular selenium concentration in PBMCs exposed to 20µmol/L MSA. Data points are the mean+/-SD of 5 separate experiments. *p=0.03 comparing 2- and 6-hour exposure.

9.4.2 Intracellular selenium species in DLBCL cell lines and peripheral blood mononuclear cells

DHL4 and RL cell lines exposed to 20µmol/L MSA for 1 and 2 hours

In the DHL4 cell line exposed to 20µmol/L MSA for 1 and 2 hours, three main Se-containing peaks were detected. These are shown in Figure 9.6. The peak with the highest intensity was dimethylselenide, which had a retention time of around 35 minutes (peak C). Peak A, which had a retention time of around 5 minutes, was MSC. The identity of peak D, which had a retention time of around 60 minutes, was unknown. There was also a very small peak (peak B) with a retention time of around 11 minutes, which was SLM. In the RL cell line, the same peaks were detected with the exception of MSC, which was not present in any sample (Figure 9.7). The peak with the highest intensity was again dimethylselenide.

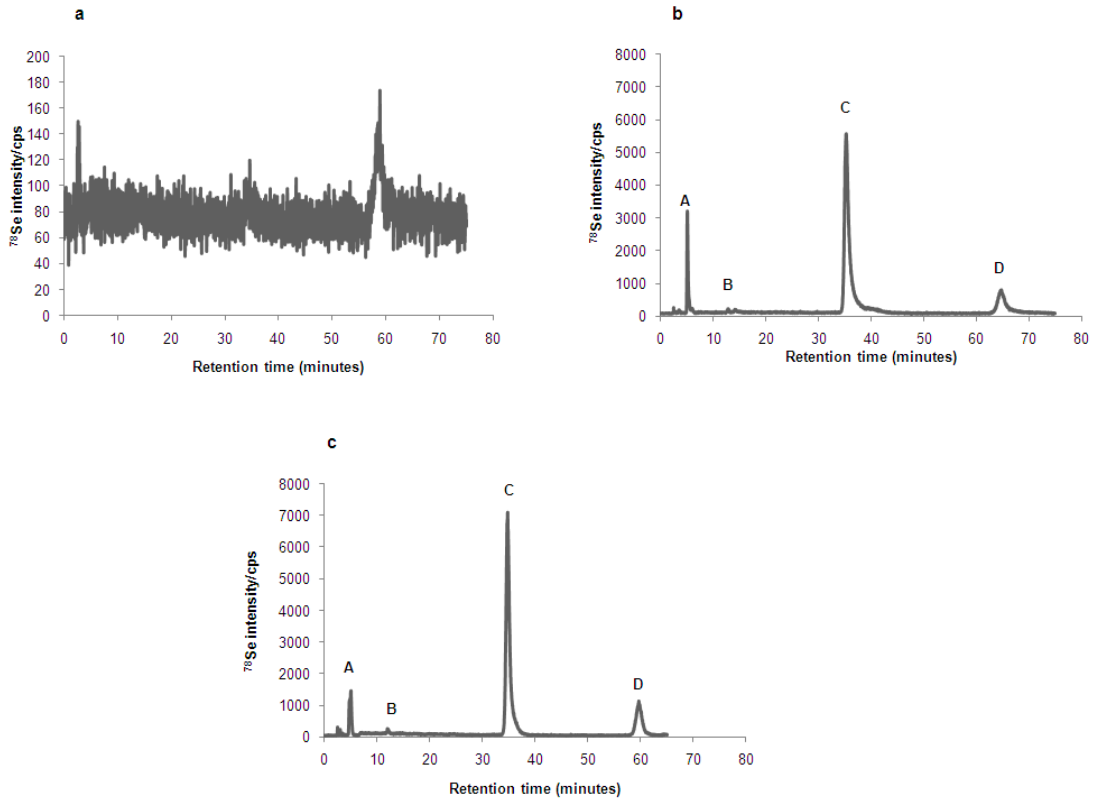

Figure 9.6 Representative chromatograms demonstrating intracellular selenium species generated in the DHL4 cell line exposed to 20µmol/L MSA (a) Control (b) 1-hour exposure (c) 2-hour exposure. Peak A is MSC, peak B is SLM, peak C is dimethylselenide and peak D is unknown. Experiments have been performed in duplicate.

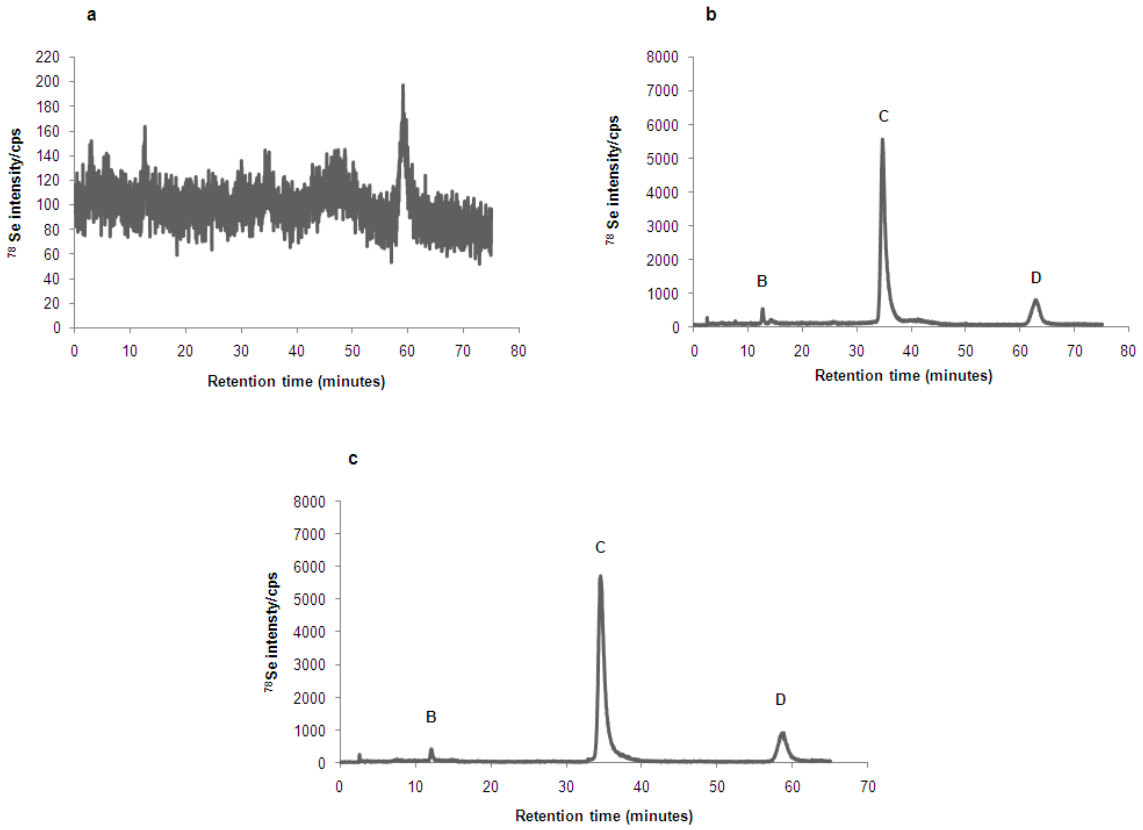

Figure 9.7 Representative chromatograms demonstrating intracellular selenium species generated in the RL cell line exposed to 20µmol/L MSA (a) Control (b) 1-hour exposure (c) 2-hour exposure. Peak B is SLM, peak C is dimethylselenide and peak D is unknown.

PBMCs exposed to 20µmol/L MSA for 1 and 2 hours

In PBMCs exposed to 20µmol/L MSA, three Se-containing peaks were detected (Figure 9.8). The peak with the highest intensity was peak D whose identity was not known. Dimethylselenide (peak C) and a small amount of SLM (peak B) were detected but similar to the RL cell line, MSC was not detected. The intensity of the dimethylselenide peak compared to the DLBCL cell lines was at least 10 times lower.

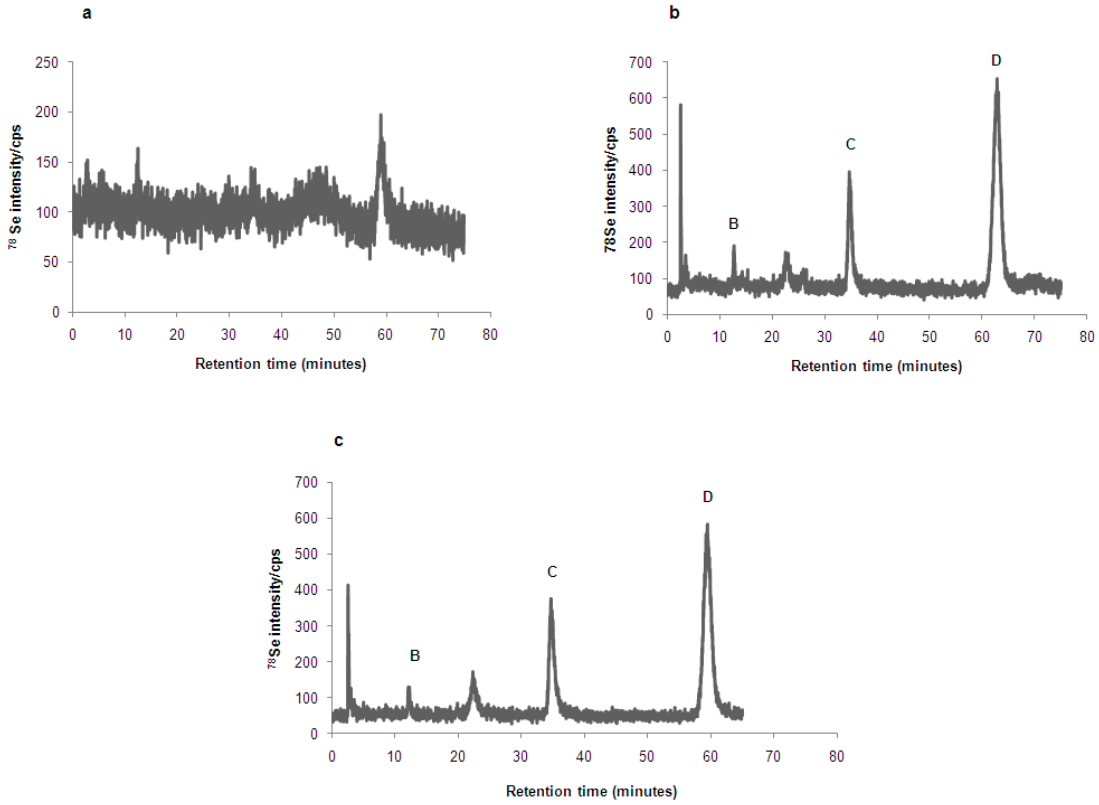

Figure 9.8 Representative chromatograms demonstrating intracellular selenium species generated in peripheral blood mononuclear cells exposed to 20µmol/L MSA (a) Control (b) 1-hour exposure (c) 2-hour exposure. Peak B is SLM, peak C is dimethylselenide and peak D is unknown. Experiments have been performed in duplicate.

Identification of the unknown peak

The unknown peak with a retention time around 60 minutes was identified using HPLC-ESI-MS/MS. In this method, the unknown Se-containing species is ionised by electro-spray and after detection of the parent ion, the parent ions are further fragmented. The fragment ions that are generated are then detected, so there are two mass detection steps, hence the MS/MS terminology. Based on the masses of the fragment ions it is possible to identify unknown elemental species by matching them with published mass spectra libraries. Figure 9.9 shows the fragmentation pattern of the unknown parent ion, *m/z* 402, which was subsequently identified as S-methylselenoglutathione.

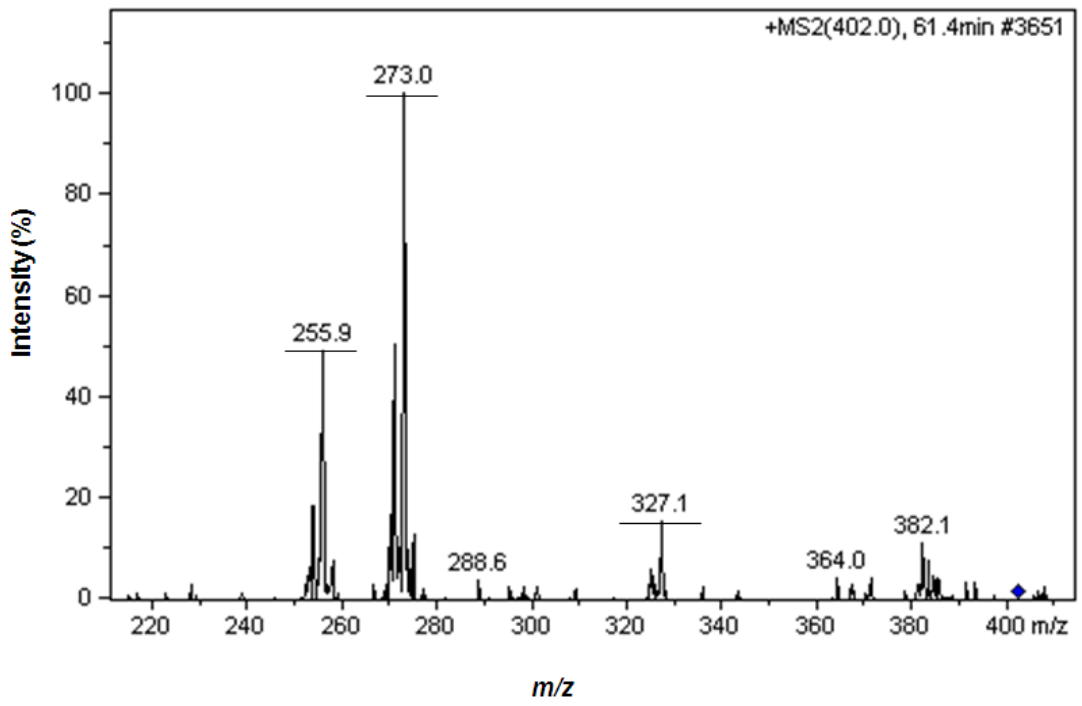

Figure 9.9 Fragmentation pattern of the unknown parent ion, *m/z* 402, consistent with S-methylselenoglutathione.

Ratio of dimethylselenide to S-methylselenoglutathione in DLBCL cell lines and PBMCs

The two Se species with the highest intensity detected in both DLBCL cell lines and PBMCS were dimethylselenide and S-methylselenoglutathione. However, in the DLBCL cell lines, dimethylselenide was the peak with the highest intensity whereas in PBMCs, S-methylselenoglutathione was the peak with the highest intensity, although the intensity was similar to that in the DLBCL cell lines. Therefore, the ratio of these 2 peaks differed between DLBCL cell lines and PBMCs, as shown in Table 9.3.

Table 9.3 The ratio of dimethylselenide to S-methylselenoglutathione in DLBCL cell lines and peripheral blood mononuclear cells

Cell type	MSA 20µmol/L	Ratio of dimethylselenide:S-methylselenoglutathione (mean+/-SD)
DHL4 cell line	1 hour (n=2)	12.5+/-6.5
	2 hours (n=2)	10.6+/-5.6
RL cell line	1 hour (n=1)	8.1
	2 hours (n=1)	7
PBMCs	1 hour (n=2)	0.8+/-0.3
	2 hours (n=3)	1.6+/-1.2

DHL4 and RL cell lines exposed to 20µmol/L MSA for 24 hours

In Chapter 4 (Figure 4.4) it was demonstrated that 24-hour exposure to MSA depleted intracellular GSH in the RL cell line but not in the DHL4 cell line. This difference could be explained by differences in the formation of S-methylselenoglutathione. Therefore, the intracellular Se species generated in the RL and DHL4 cell lines after exposure to 20µmol/L MSA for 24 hours was determined (Figure 9.10). However, in both cell lines the intensity of the S-methylselenoglutathione peak was similar at 24 hours and the peak intensity was not different from that at 1- and 2-hour exposure. Of note, both cell lines have similar basal levels of GSH (Chapter 4, Figure 4.4). The intensity of the dimethylselenide peak increased markedly at 24 hours compared with 1- and 2-hour exposure. MSC was now detected in both cell lines whereas at 1- and 2-hour exposure it was only present in the DHL4 cell line. SLM was still detected at 24 hours but at a

similar intensity to that at 1- and 2-hour exposure. An additional peak was present at 24 hours (peak C), which was identified as γ-glutamyl-MSC. Due to time constraints, PBMCs exposed to 20µmol/L MSA for 24 hours has not been analysed.

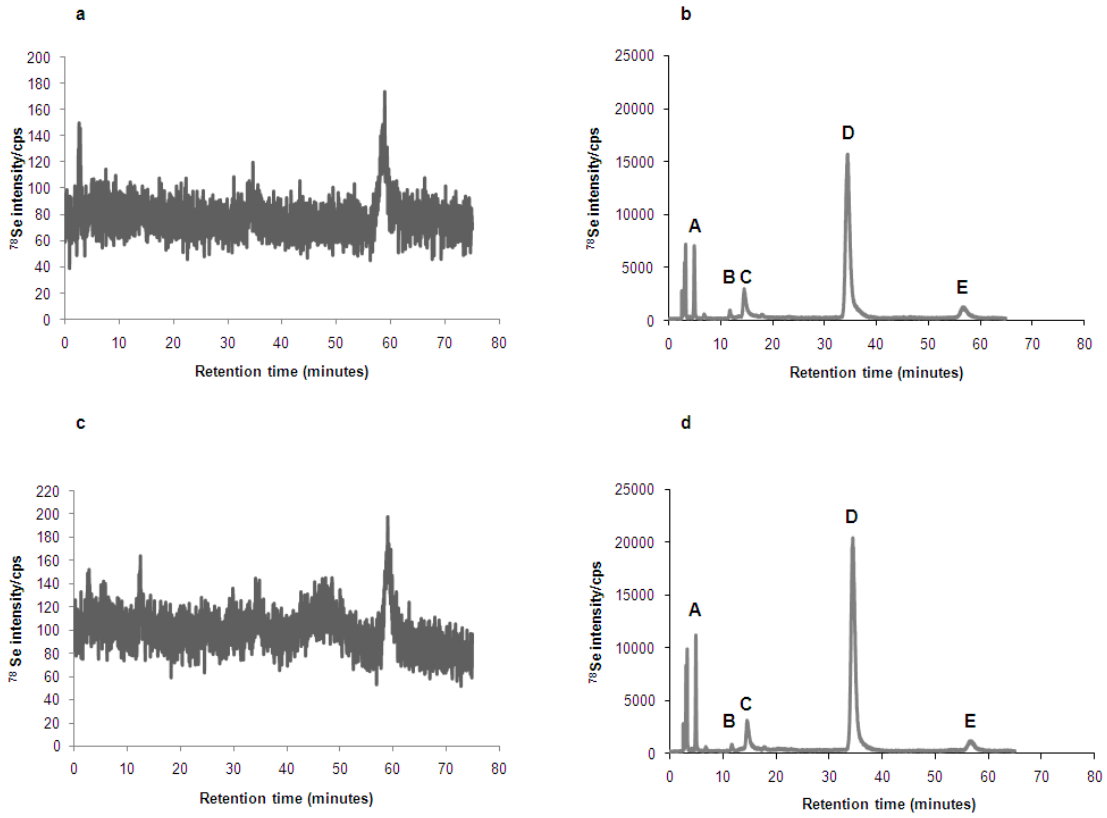

Figure 9.10 Representative chromatograms demonstrating intracellular selenium species generated in DLBCL cell lines exposed to 20µmol/L MSA for 24 hours (a) DHL4 control (b) DHL4 24 hours (c) RL control (d) RL 24 hours. Peak A is MSC, peak B is SLM, peak C is γ-glutamyl-MSC, peak D is dimethylselenide, peak E is S-methylselenoglutathione.

9.4.3 Cell lysates spiked with MSA

MSA is reduced by thiols, such as GSH, into various Se metabolites/species as described in the introduction. To determine which species were generated as a reaction product and which actually required cellular metabolism, cell lysates prepared from untreated DHL4 cells and PBMCs were spiked with MSA and then analysed by HPLC-ICP-MS. Figure 9.11 shows that when DHL4 cell lysates were spiked with MSA at a concentration of

20µmol/L, the main reaction products detected were S-methylselenoglutathione, which had the highest peak intensity, and SLM. In addition, MSA was detected early at a retention time of 3-4 minutes and a very small peak of dimethylselenide was also detected. In PBMCs, the main peak was S-methylselenoglutathione, which was present at a similar intensity to the DHL4 cell line. A very small peak of dimethylselenide was detected and SLM was also possibly formed, but because of a long tail on the peak of MSA, which extended out to the retention time of SLM, it was difficult to be certain of the presence of SLM.

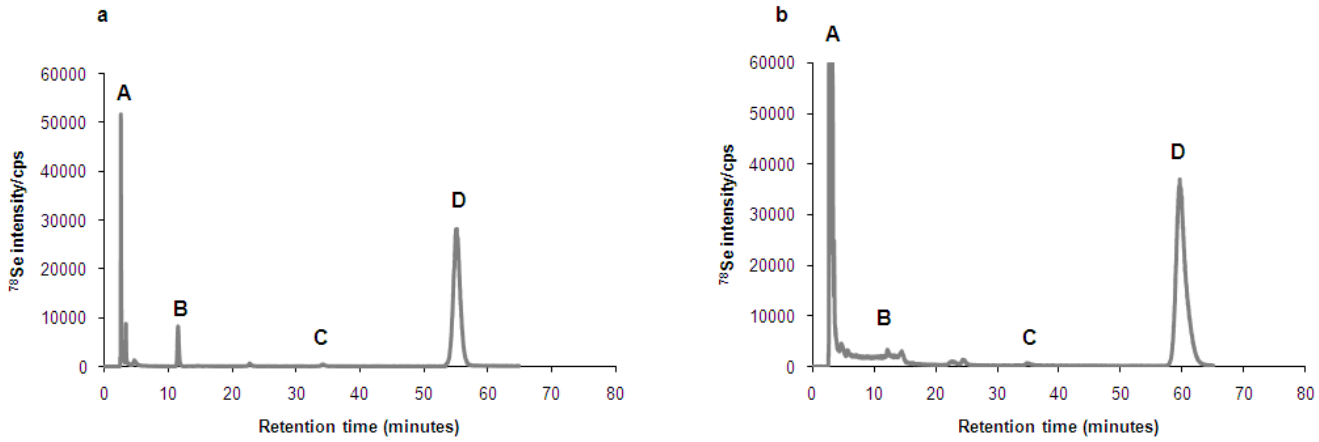

Figure 9.11 Representative chromatograms demonstrating Se species generated when cell lysates were spiked with MSA (a) DHL4 cell line (b) Peripheral blood mononuclear cells. Peak A is MSA, peak B is SLM, peak C is dimethylselenide, peak D is S-methylselenoglutathione. Experiments were performed in duplicate.

9.4.4 Volatile species generated by DHL4 cells and peripheral blood mononuclear cells exposed to 20µmol/L MSA

The volatile species generated by DHL4 and PBMCs were dimethyldiselenide and dimethylselenide. However, there were differences in the rate of generation. All experiments were performed at least in duplicate. Figure 9.12a shows the standards, dimethylselenide and dimethyldiselenide. Figure 9.12b shows the chromatogram

generated after the SPME fibre was held above the headspace of control/untreated DHL4 cells for 10 minutes.

In the DHL4 cell line exposed to MSA for 10 minutes there was generation of both volatile species, but dimethyldiselenide was the peak with the greatest intensity with only a very small peak of dimethylselenide. However, there was variability in the intensity of the dimethyldiselenide peak between replicates as shown in Figure 9.13.

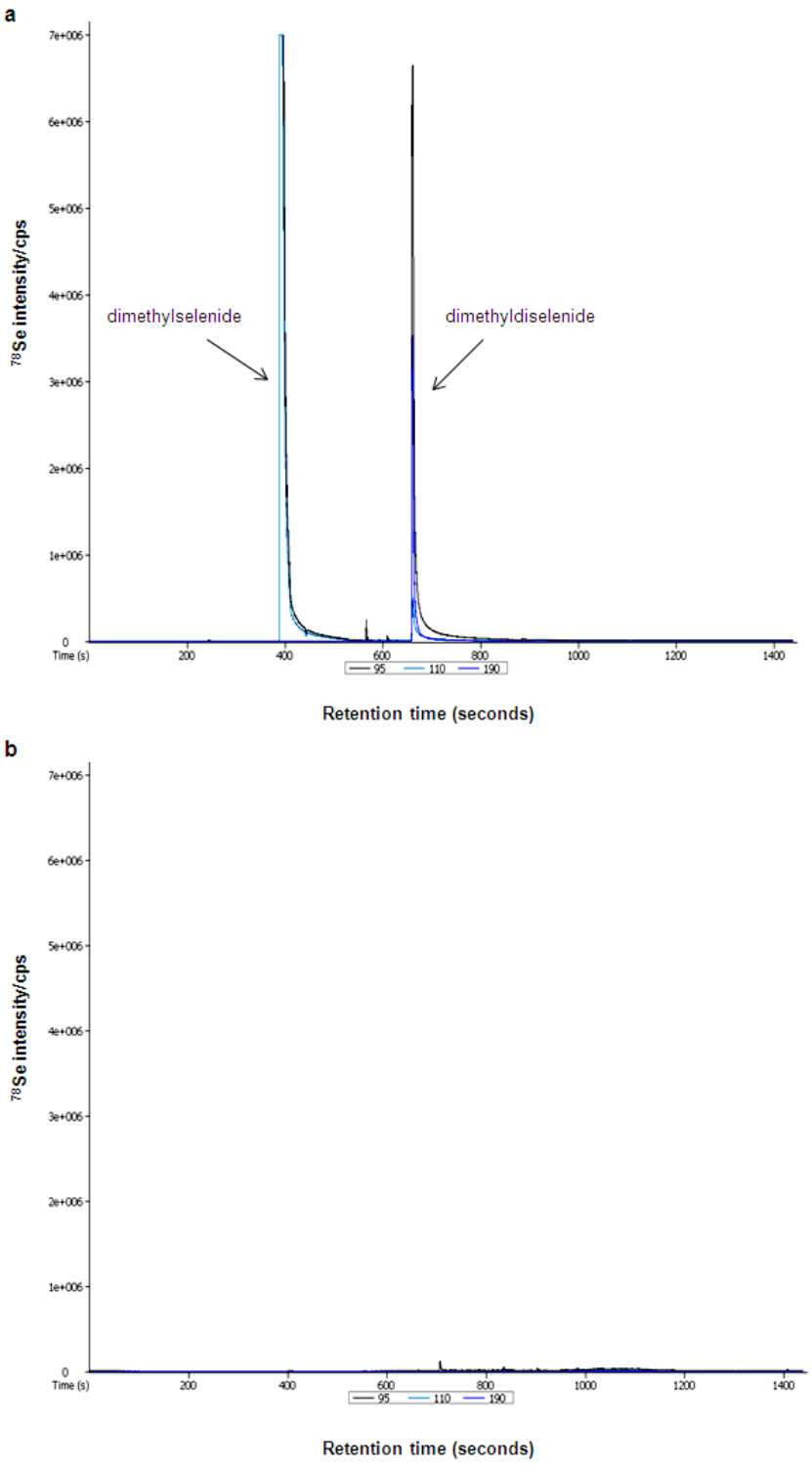

Figure 9.12 Representative chromatograms (a) Standards, dimethylselenide and dimethyldiselenide (b) Control/untreated DHL4 cells. SPME fibre held above the headspace of untreated cells and then subjected to COC-GC-TOFMS.

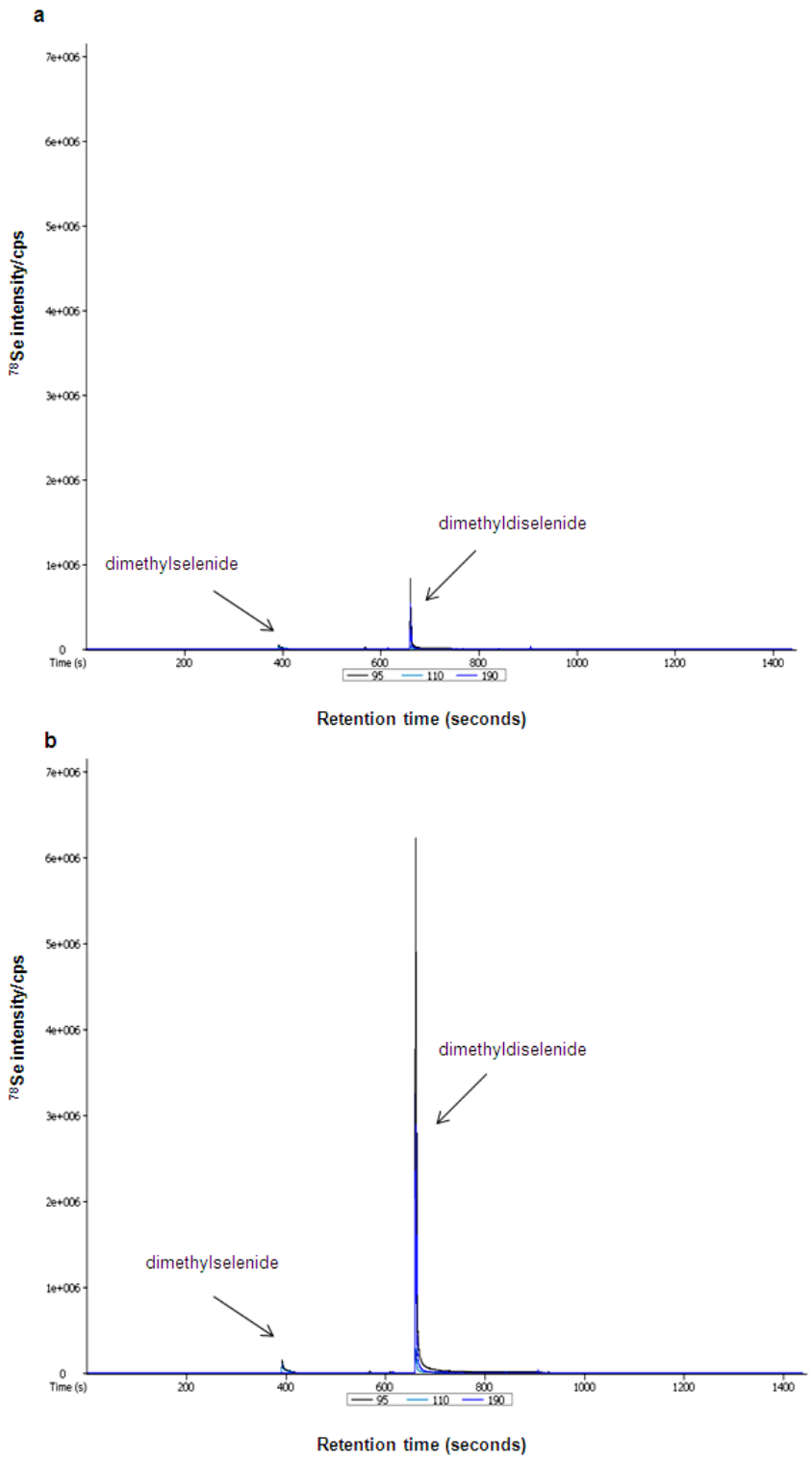

Figure 9.13 Representative chromatograms demonstrating the generation of volatile Se species in DHL4 cells exposed to 20µmol/L MSA for 10 minutes. Two replicates shown (a, b) to demonstrate the variability in the peak intensity of dimet**h**yldiselenide.

However, in PBMCs exposed to MSA for 10 minutes only very small amounts of the volatile species were generated (Figure 9.14; note the change in scale).

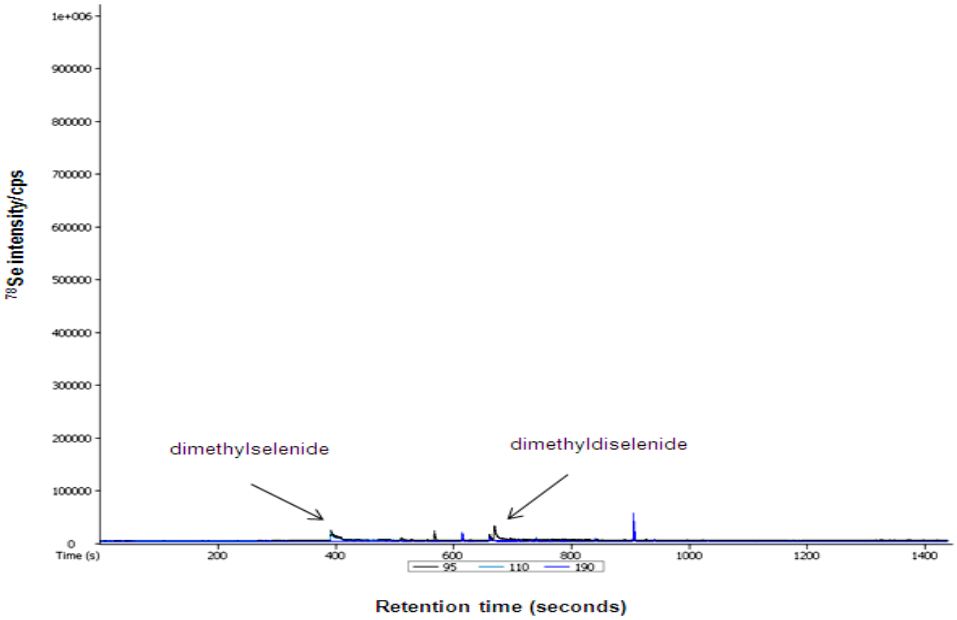

Figure 9.14 Representative chromatogram demonstrating the generation of volatile Se species in peripheral blood mononuclear cells exposed to 20µmol/L MSA for 10 minutes.

After exposure of DHL4 cells to MSA for 30 minutes, the dimethyldiselenide peak plateaued. This was either because the SPME fibre had been saturated or that the generation of this volatile species was maximal (Figure 9.15a). The dimethylselenide peak had increased in intensity compared with 10-minute exposure. In PBMCs exposed to MSA for 30 minutes (Figure 9.15b) there was an increase in intensity of the dimethyldiselenide peak compared with 10-minute exposure but dimethylselenide was still only present at a very low level.

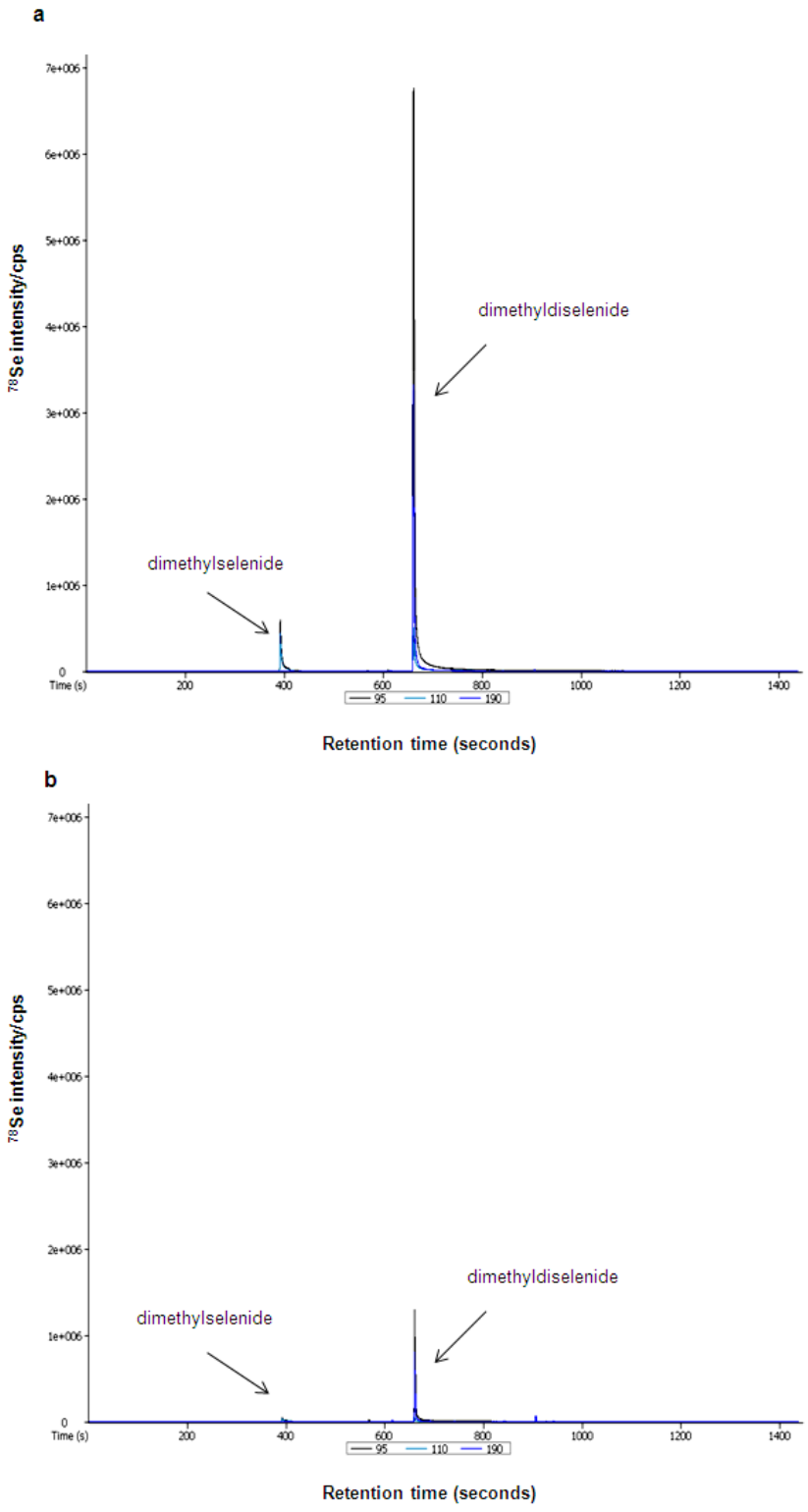

Figure 9.15 Representative chromatograms demonstrating the generation of volatile species in (a) DHL4 cells and (b) PBMCs exposed to 20µmol/L MSA for 30 minutes.

In DHL4 cells exposed to MSA for 1 hour, the dimethyldiselenide peak was stable but the dimethylselenide peak had again increased in intensity compared with 30-minute exposure (Figure 9.16a). In PBMCs exposed to MSA for 1 hour, the dimethyldiselenide peak reached the same maximum level as that generated by the DHL4 cell line. While the dimethylselenide peak had increased in intensity compared with 30-minute exposure, it was present at a much lower intensity than in the DHL4 cell line (Figure 9.16b).

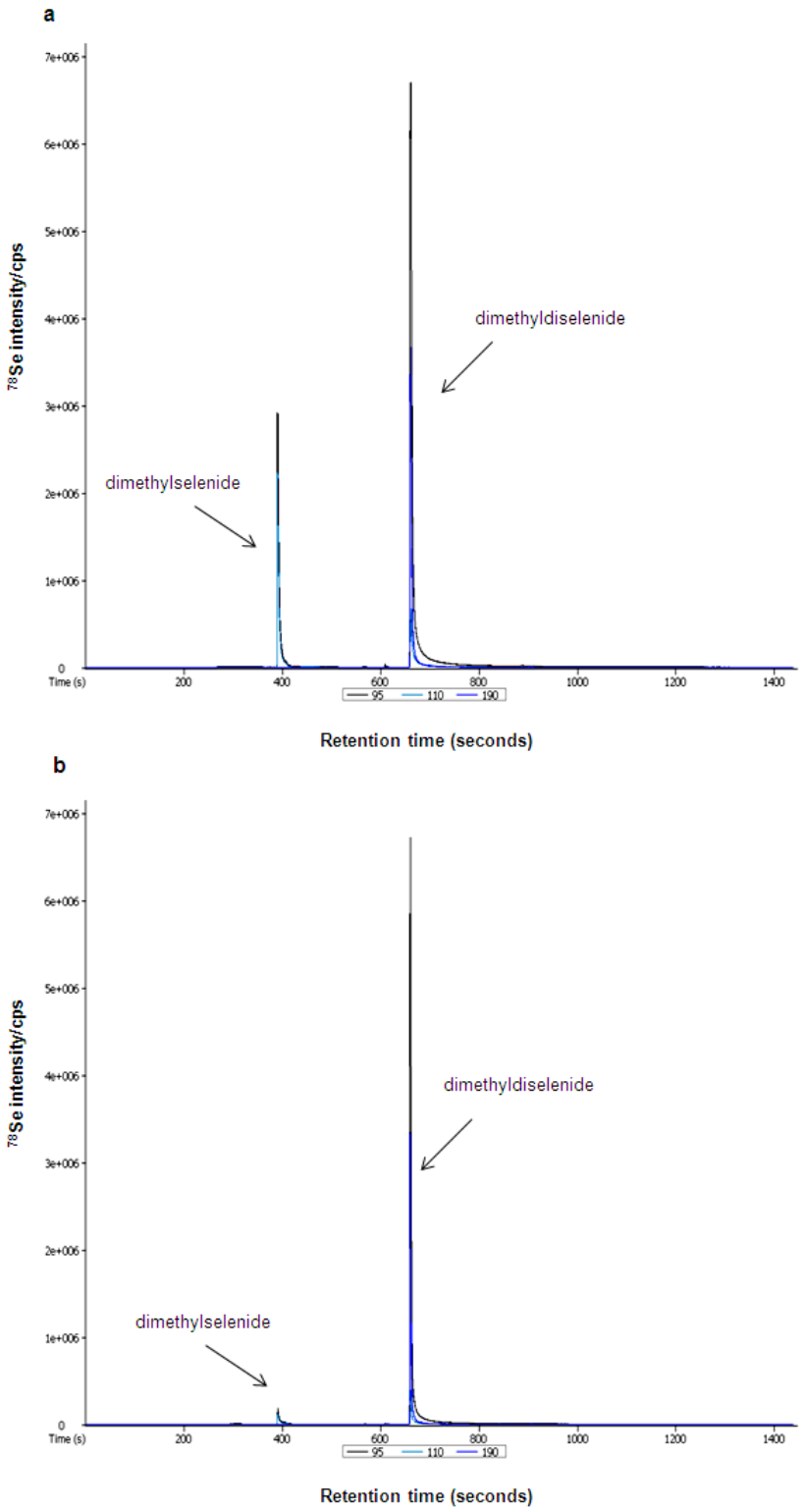

Figure 9.16 Representative chromatograms demonstrating the generation of volatile species in (a) DHL4 cell line and (b) PBMCs exposed to 20µmol/L MSA for 1 hour.

9.4.5 β-lyase activity in lymphoma cell lines

The generation of MSC differed between the DHL4 and RL cell lines after exposure to MSA and the two cell lines also differed in sensitivity to MSC. These differences may be due to differences in β-lyase activity between the cell lines and therefore this was determined in the DHL4, RL and JVM2 cell lines. In addition, the renal adenocarcinoma cell line, ACHN, was used as a positive control. The 72-hour EC_{50} of MSC in the 3 lymphoma cell lines is shown in Chapter 4 (Table 4.2). The EC_{50} values were 55.8µmol/L, 21.6µmol/L and 79µmol/L for DHL4, RL and JVM2 cells respectively. Figure 9.17 shows that the 3 lymphoma cell lines differed in their β-lyase activity as determined by pyruvate generation. The RL cell line, which was relatively sensitive to MSC, had a significant increase in pyruvate concentration after addition of the 'reaction mix' (51%±13.5 increase; p=0.005). However, there was no detectable increase in pyruvate concentration in the DHL4 and JVM2 cell lines, which were relatively resistant to MSC. The ACHN cell line had a 383% (±114.4) increase (p=0.03) in pyruvate concentration after addition of the 'reaction mix'.

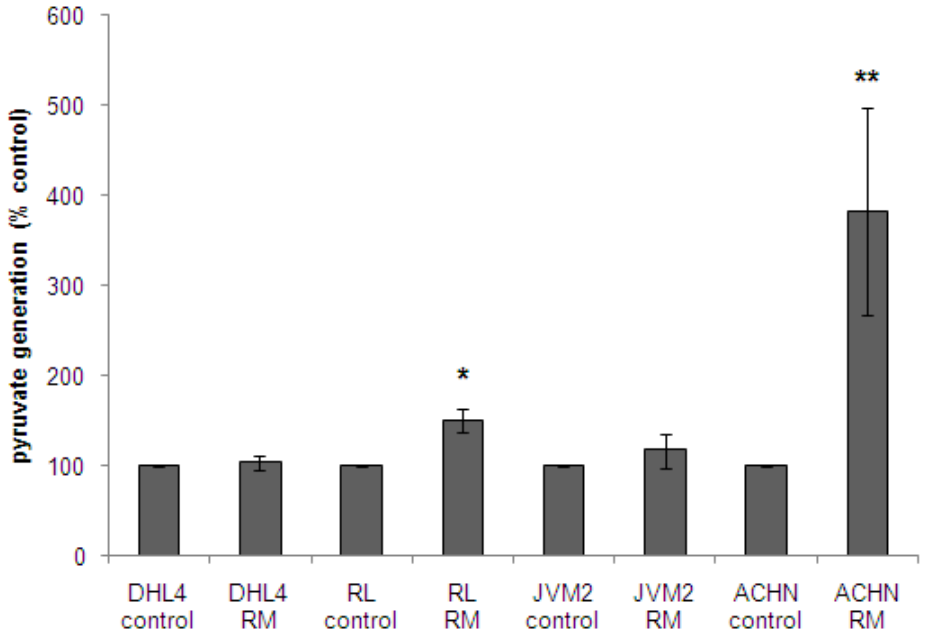

Figure 9.17 β-lyase activity in three lymphoma cell lines and the renal adenocarcinoma cell line, ACHN. Data points are the mean+/-SD of at least 3 separate experiments. *p=0.005 **p=0.03. p values are a comparison with the relevant controls.

To confirm that the sensitivity of cell lines to MSC correlated with β-lyase activity, the 72-hour EC_{50} of MSC in the ACHN cell line was determined using the ATP assay. Figure 9.18 shows that that EC_{50} was 16.4µmol/L (95% CI 14.5-18.5), which makes it the most sensitive cell line tested. The 72-hour EC_{50} for MSC and the corresponding β-lyase activity is summarised in Table 9.4.

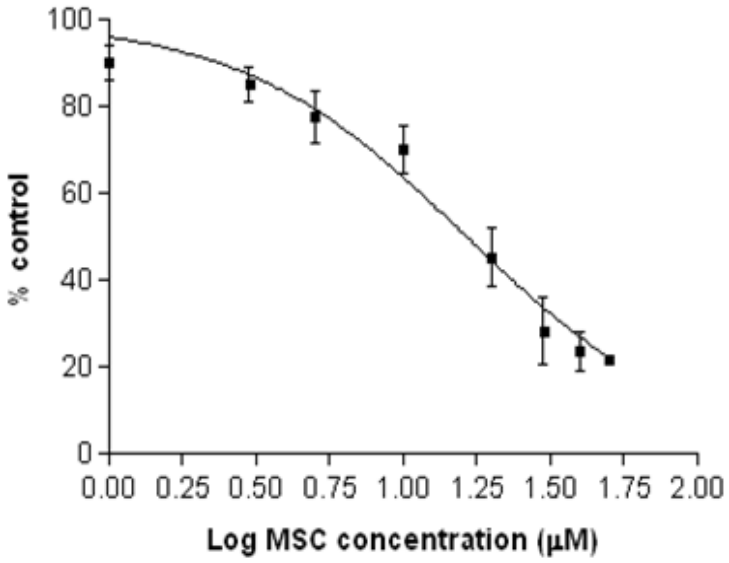

Figure 9.18 EC_{50} concentration-response curve following 72-hour exposure to increasing concentrations of MSC in the ACHN cell line. Data points are the mean+/-SD of three separate experiments.

Table 9.4 Summary of MSC EC_{50} and β-lyase activity in three lymphoma cell lines and the ACHN cell line

Cell line	**72-hour MSC EC_{50} (µmol/L)**	**% increase in pyruvate generation (Mean+/-SD)**
DHL4	55.8	3.1+/-7.9
RL	21.6	50.8+/-13.5
JVM2	79	17.2+/-18.7
ACHN	16.4	382.5+/-114.4

9.4.6 Tumour selenium concentration at diagnosis in patients with DLBCL

Our laboratory has previously reported that the serum Se concentration at diagnosis is independently predictive of treatment response and long-term survival in patients with 'aggressive' B-cell lymphoma (Last *et al*, 2003). However, it is not known whether the serum Se reflects the tumour Se concentration. Therefore, the tumour Se concentration was measured in diagnostic samples from the original cohort of patients for which serum Se had already been determined. The results are shown in Table 9.5

Table 9.5 Tumour selenium concentration in presentation tumour biopsy samples in patients with DLBCL

Sample No.	**Biopsy site**	**Serum Se (µmol/L)*#**	**Tumour Se (ng/g)**
1	Lymph node	*0.84*	177.4
2	Spleen	1.05	362
3	Lymph node	*0.6*	177
4	Lymph node	1.19	160
5	Lymph node	*0.97*	129.9
6	Spleen	*0.79*	455.4
7	Lymph node	1.51	274.3
8	Mediastinal mass	*0.89*	156.3
9	Lymph node	*0.92*	248.3
10	Lymph node	1.06	306.1
11	Lymph node	*0.97*	72.4
12	Lymph node	*0.54*	82.0
13	Lymph node	*0.97*	268.5
14	Lymph node	1.34	190.1
15	Spleen	1.05	343.6
16	Lymph node	*0.4*	343.6

*numbers in italics denote values below the UK reference range (1-1.88µmol/L)
#serum Se values were those obtained from Last *et al*, 2003

Figure 9.19 shows that there was no correlation between serum and tumour Se at diagnosis (r=0.17).

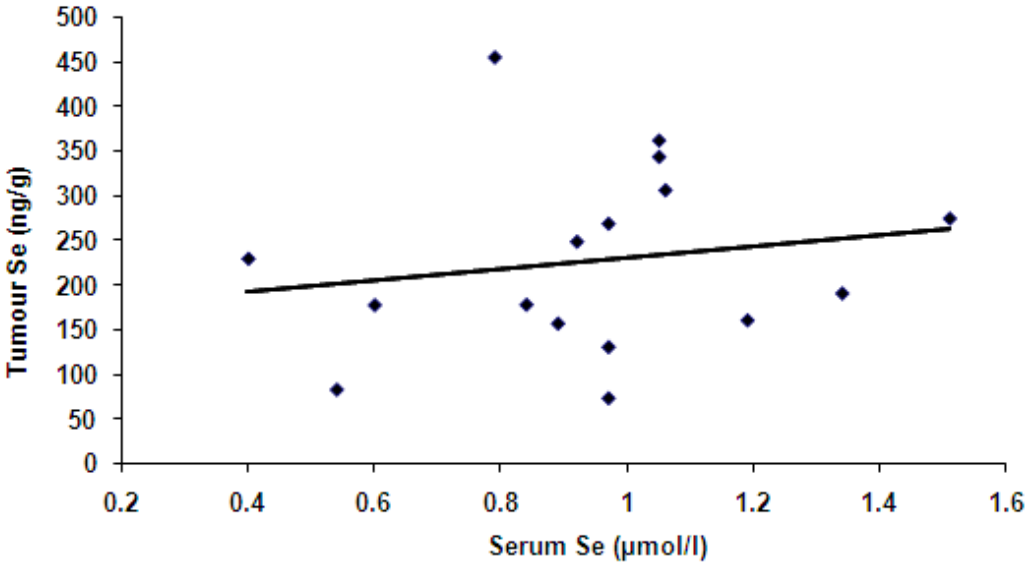

Figure 9.19 Correlation between serum and tumour selenium at diagnosis in 16 patients with DLBCL.

9.5 DISCUSSION

The results reported in this chapter have identified a number of differences in the handling of Se, in the form of MSA, between two DLBCL cell lines and PBMCs, a model for 'normal cells'. The concentration of MSA used in these experiments was 20µmol/L because in the forthcoming clinical trial, the aim is to achieve a plasma Se concentration of 20µmol/L. However, it is not entirely clear if an MSA concentration of 20µmol/L would be equivalent to a plasma Se concentration of 20µmol/L. MSA has only been used *in vivo* in rats, both orally and intravenously (Suzuki *et al*, 2006b; Suzuki *et al*, 2008). It appears that in rats, orally administered MSA and MSC produces an equivalent rise in plasma Se (Suzuki *et al*, 2008).

The predominant method used in this chapter was ICP-MS, which is a well established, robust and highly sensitive method for trace element and elemental speciation analysis. With ICP-MS it is possible to quantify elemental species even if their structure is unknown, but identification then requires matching the retention time with a known standard compound. This is because the extremely high temperature of the plasma ion source completely destroys the organic molecules present in a sample and thus ICP-MS only detects elemental ions. Therefore, it is the best method to use when quantitative data are required and reference compounds are available. However, in order to identify an unknown species for which a standard is not available, a commonly used method is ESI-MS. This is less sensitive than ICP-MS for the detection of elements but is able to provide molecular information about the elemental species and the fragmentation pattern therefore allowing identification in the absence of a standard reference compound. However, for quantification, a standard would be required. Therefore, both these methods are complimentary and together are powerful tools in the field of elemental speciation (B'Hymer & Caruso, 2006; Francesconi & Sperling, 2005; Gammelgaard *et al*, 2008). In addition to investigating differences in Se metabolism between DLBCL cell lines and PBMCs, the aim of these experiments was to establish a method for analysing and quantifying Se species in small volume samples, similar to those that will be obtained by the collection of PBMCs from patients entered into the forthcoming clinical trial.

For analysis of volatile Se species, SPME fibres were used to absorb the species as this has been demonstrated to improve the sensitivity of GC-based methods (Meija *et al*, 2002). When using conventional GC, Se compounds, such as dimethylselenide, are poorly retained because of their relatively low boiling point (58°C). Therefore COC was used to trap the volatile compounds on the GC column. This involves cooling the whole oven down to temperatures as low as -60°C (Watanabe-Suzuki *et al*, 2002).

Total intracellular Se concentration was determined in the DLBCL cell lines and PBMCs after exposure to MSA. MSA appears to be taken up into PBMCs at a slower rate than in the DLBCL cell lines. In the DLBCL cell lines, the maximum intracellular Se

concentration was reached by the earliest exposure time, 10 minutes, whereas in PBMCs the Se concentration did not plateau until 4-6 hours. In addition, it appears that the maximum intracellular concentration obtained in PBMCs was lower than in the DLBCL cell lines. However, because of the time and complexity of these experiments, analysis of DLBCL cell lines was only performed in duplicate and therefore meaningful statistical comparisons with PBMCs are not possible. The uptake of MSA by the RL and DHL4 cell lines appeared similar. This is in contrast to previously published data by our laboratory in which the DHL4 cell line accumulated more Se (Juliger *et al*, 2007). However, these previous experiments used higher concentrations of Se and thus it may be that the uptake mechanism (see below) is saturable in the RL cell line.

The results for intracellular concentration were highly variable in both the cell lines and PBMCs and thus the SD for the data points is large. It is difficult to explain the reason for this. For each experimental condition 10 million cells were lysed in the same volume of lysis buffer. There may have been variation in the degree of cell lysis between experiments and therefore it may have been prudent to have determined the protein concentration in each sample and correct the final Se concentration for protein content. It is unlikely that the method of analysis, ICP-MS, is responsible for the variation, as this is a robust method that involves the complete fragmentation of molecules into elemental ions without the need for an extraction or separation step which can contribute to variability. The calibration curves for Se were also very reproducible. It may be that the variability is actually real and that uptake of MSA by cells is variable. In addition, there may have been efflux of MSA from the cells that could have resulted in the variability.

The mechanism of MSA uptake by cells has not been extensively investigated and it is not known whether uptake is dependent on active mechanisms or is merely by diffusion. When rats were administered intravenous MSA labelled with a stable isotope, this was not detected in the plasma even at the earliest time-point post administration, 10 minutes. Instead, immediately after administration, the concentration in red cells increased dramatically suggesting that MSA was taken up rapidly. However, the Se concentration

in red cells decreased back to control levels within 30 minutes suggesting there was efflux of MSA or its metabolites (Suzuki *et al*, 2006b). Further experiments to establish the exact mechanism by which MSA is taken into cells may help to understand better the differences observed in uptake between the DLBCL cell lines and PBMCs and the data variability. These could include experiments to inhibit various cellular transporters to establish which, if any, are required for MSA uptake. To establish whether uptake is ATP dependent, membrane-bound ATPases could be inhibited. In addition, measuring the Se concentration in the culture medium to investigate efflux of MSA by cells would be valuable.

An unexpected finding was that the baseline Se concentration in both the DLBCL cell lines and PBMCs was below the lower quantification limit. However, when the same experiments were performed previously by our laboratory, it was possible to quantify the baseline Se level and differences between cell lines were reported (Goenaga-Infante *et al*, 2007a; Juliger *et al*, 2007). The reason for this is not clear as the experimental conditions used were identical to those previously reported. It is unlikely that the ICP-MS itself is responsible for these differences as it is a highly sensitive method with an extremely low detection limit. However, foetal calf serum used to supplement cell culture medium contains Se and this may differ from batch to batch depending on where the cattle are from. RPMI-1640 cell culture medium itself does not contain Se. In addition, the original experiments were only performed once and it is possible that these cell lysates could have been contaminated with Se, for example when preparing the standards for the calibration curve.

The intracellular Se species generated after exposure to MSA were determined in the DLBCL cell lines and PBMCs. Neither MSA nor methylselenol were detected. However, in DLBCL cell lines, the main intracellular species was dimethylselenide which is formed by methylation of methylselenol, suggesting that methylselenol is, as expected, the main metabolite of MSA. Dimethylselenide increased in intensity with time, being present at a higher concentration at 24 hours compared to that at 1- and 2-hour exposure. In addition,

there were other Se species detected in the DLBCL cell lines. In the DHL4 cell line, as previously reported by our laboratory, MSC and SLM were detected. In addition, a Se-containing peak, later identified as S-methylselenoglutathione was also detected. The concentration of SLM and S-methylselenoglutathione remained fairly constant between the three exposure times studied (1, 2 and 24 hours). However, there was an increase in the intensity of MSC between 1/2-hour exposure and 24 hours. At 24-hour exposure, γ-glutamyl-MSC was also detected but this was not present after 1- and 2-hour exposure. The findings were similar in the RL cell line except that MSC was not detected at 1- and 2-hour exposure but only at 24-hour exposure. In the work previously published by our group, dimethylselenide and S-methylselenoglutathione, were not detected because the chromatograms were only run for 15 minutes and these species have retention times of around 35 minutes and 60 minutes respectively. This is the first report of the detection of dimethylselenide as an intracellular, soluble metabolite of MSA. The formation of MSC, SLM and S-methylselenoglutathione have all been reported previously in hepatocytes exposed to MSA (Gabel-Jensen *et al*, 2009b).

Further experiments, involving spiking untreated DHL4 cell lysates with MSA, demonstrated that SLM and S-methylselenoglutathione were both formed as a reaction product and their production did not require intact cells. S-methylselenoglutathione was the main reaction product formed. As discussed in the introduction to this chapter, MSA is reduced by GSH and other thiols to intermediate metabolites other than methylselenol and the formation of these metabolites clearly do not require intact cells. It was thought that the extent of GSH conjugate formation may differ between the DHL4 and the RL cell lines as MSA depletes GSH in RL but not in DHL4 cells. However, both the cell lines generated the same amount of S-methylselenoglutathione, which remained relatively constant between 1/2-hour exposure and 24 hours. Therefore the generation of GSH conjugates, as a result of MSA exposure, does not explain the difference in GSH depletion observed between the two cell lines.

The chromatographic profile of PBMCs differed from that of the DLBCL cell lines. Although the same species were detected, with the exception of MSC, which was not detected, the intensity of the peaks differed. S-methylselenoglutathione was the main peak detected but this was present at a similar intensity to that seen in the DLBCL cell lines. Dimethylselenide, however, was present at a much lower intensity and the ratio of dimethylselenide to S-methylselenoglutathione was reversed in PBMCs as compared with the DLBCL cell lines. Of note, cell lysates of PBMCs exposed to MSA for 24 hours have not been analysed. Given that dimethylselenide is formed downstream of methylselenol, this suggests that PBMCs may generate less methylselenol than DLBCL cell lines. As discussed in the introduction, methylselenol can also be demethylated to hydrogen selenide, which can be used for selenoprotein synthesis. It may be that in PBMCs, methylselenol generated from MSA is metabolised through a different pathway and incorporated into selenoproteins rather than being available as methylselenol per se. This could be an explanation for the observed differences in effect of methylselenol precursors in normal and tumour cells. However, this hypothesis needs to be investigated further with additional experiments. It would be useful to determine the baseline levels of selenoproteins, such as GPx and TrxR, in harvested PBMCs and compare them to those in DLBCL cell lines. The rise in selenoprotein levels could then be measured after exposure to MSA. In addition, PBMCs may have lower concentrations of GSH than DLBCL cell lines and thus MSA is not reduced as efficiently. When cell lysates of PBMCs were spiked with MSA, the main peak detected was that of S-methylselenoglutathione confirming that this was generated as a reaction product and does not require the presence of intact cells.

Given that the generation of MSC differed between the DHL4 and RL cell lines and that they had differing sensitivities to MSC, it was hypothesised that this may be due to differences in β-lyase activity. The DHL4 cell line was relatively resistant to MSC (EC_{50} 55.8μmol/L) compared to the RL cell line, which was relatively sensitive (EC_{50} 21.6μmol/L). Therefore it was assumed that RL cells would have higher β-lyase activity than DHL4 cells. In addition, MSC was formed at 1 and 2 hours exposure to MSA in

DHL4 cells but not in RL cells and it was hypothesised that if RL cells had higher β-lyase activity, MSC would be metabolised to methylselenol and not be detected. The results clearly demonstrate that RL cells have higher β-lyase activity than DHL4 and JVM2 cells (another relatively MSC-resistant cell line). After exposure of cell lysates to MSC and PLP ('reaction mix'), RL cells had a 51% increase in pyruvate concentration indicating the conversion of MSC by β-lyases to methylselenol and pyruvate. In the DHL4 and JVM2 cells, there was no detectable increase in pyruvate concentration. These cell lines must possess some β-lyase activity as MSC is cytotoxic at high concentrations and it may be that the assay used was not sensitive enough to pick up these smaller increases in pyruvate. The other explanation may be that MSC is metabolised to its α-ketometabolite, MSP, by aminotransferases and L-amino oxidases as discussed in Chapter 6 and this metabolite may be responsible for the cytotoxicity observed at high concentrations (Pinto *et al*, 2010). It was demonstrated that the β-lyase activity of the cell lines did correlate, to a certain degree, to sensitivity to MSC. The ACHN cell line, which had high β-lyase activity demonstrated by a 383% increase in pyruvate concentration, was more sensitive than any of the lymphoma cell lines to MSC (EC_{50} 16.4μmol/L). The 95% confidence intervals for the EC_{50} of RL and ACHN cells do not overlap suggesting that the ACHN cell line is significantly more sensitive to MSC. β-lyase activity in lymphoma cell lines has not been previously reported.

The volatile species detected after exposure of the DHL4 cell line to MSA were the same as those reported previously by our laboratory (Goenaga-Infante *et al*, 2007a; Juliger *et al*, 2007). The main volatile species detected was dimethyldiselenide, which was rapidly formed after 10-minute exposure to MSA. It has been previously reported that this Se species is a reaction product and does not require the presence of intact cells as combining MSA and GSH in aqueous solution leads to rapid generation of dimethyldiselenide (Gabel-Jensen *et al*, 2009a; Gabel-Jensen *et al*, 2010). However, dimethyldiselenide is an oxidation product of methylselenol and therefore a marker of its generation (Gabel-Jensen *et al*, 2010). The intensity of the dimethyldiselenide peak was highly variable at 10-minute exposure and this was repeated at least four times with

differing results. The reason for this was felt to be the fact that dimethyldiselenide is generated so rapidly that any small variation in the time for which the SPME fibre is held in the headspace could lead to large differences in the amount of dimethyldiselenide absorbed. By 30-minute exposure, the intensity of the dimethyldiselenide peak had plateaued. A very small amount of dimethylselenide was detected at 10-minute exposure and this peak continued to increase with increasing exposure time but did not reach the maximum level of the dimethyldiselenide peak.

In PBMCs, the same volatile species were detected but the rate of generation was much slower. At 10-minute exposure there were only very tiny amounts of dimethylselenide and dimethyldiselenide detected and although the peaks had increased by 30 minutes, with the main one being dimethyldiselenide, they were present at a much lower intensity than in DHL4 cells. By 1 hour, the dimethyldiselenide peak had reached the same maximum level generated by DHL4 cells but the dimethylselenide peak was still present at a much lower intensity than in DHL4 cells. The results in PBMCs are in keeping with the other observations made in this chapter. Firstly, uptake of MSA by PBMCs is less and occurs at a slower rate than DLBCL cell lines and hence the formation of reaction products such as dimethyldiselenide is also slower. Secondly, PBMCs form less dimethylselenide than DLBCL cell lines and hence the amount of volatile dimethylselenide detected is also less. Combined with the observation that dimethyldiselenide is also formed at a slower rate in PBMCs, these results demonstrate that PBMCs form methylselenol less efficiently than DLBCL. The proposed metabolism of MSA is shown in Figure 9.20.

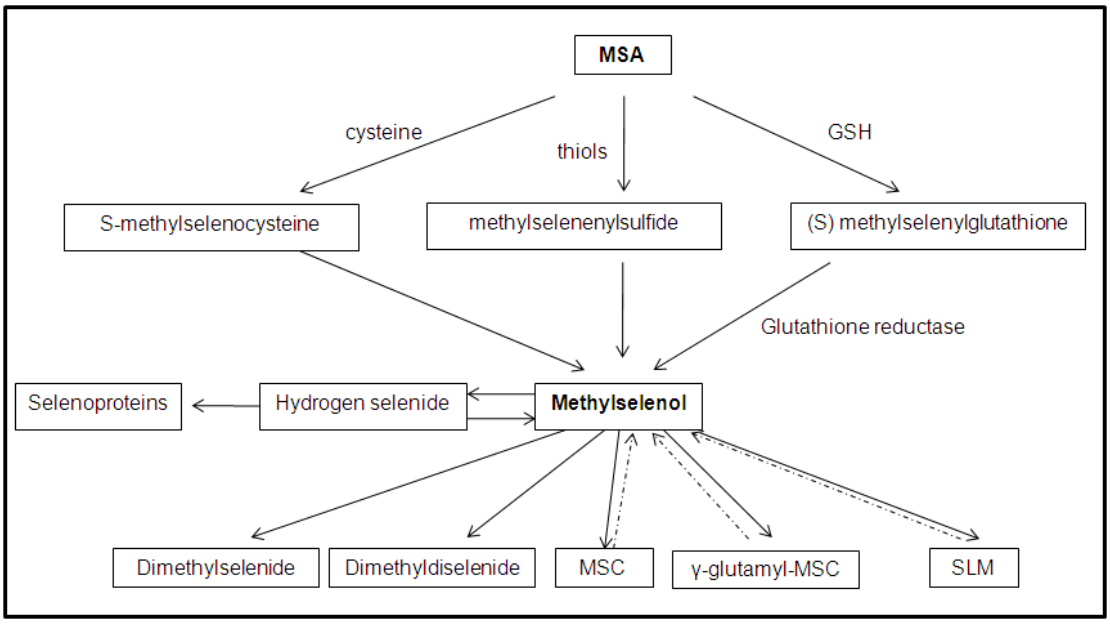

Figure 9.20 The proposed cellular metabolism of MSA.
Adapted from Gabel-Jensen, C *et al*., J. Anal. At. Spectrom, 2009 (Gabel-Jensen *et al*, 2009b). The dashed lines represent steps that would require the relevant lyase enzymes and therefore would be dependent on the cell type.

Although not directly related to the rest of the work presented in this chapter, tumour Se concentration has been included as its measurement required similar methods to those used for determining total intracellular Se concentration in cell lines and PBMCs. 16 diagnostic biopsy samples were available from the original 100 patients in whom presentation serum Se concentration had been reported (Last *et al*, 2003). In this relatively small number of samples, there was no correlation between serum Se and tumour Se at diagnosis. As discussed in Chapter 1, most studies that have reported tumour Se levels have actually found that a low serum Se concentration is associated with a significantly increased tumour Se concentration when compared with adjacent non-neoplastic tissue (Charalabopoulos *et al*, 2006a; Charalabopoulos *et al*, 2006b). Se concentration in normal or neoplastic lymphoid tissue has not previously been reported and in this study there was no non-neoplastic tissue available. Clearly it would be useful to determine tumour Se in a larger number of patients with DLBCL and this may be possible in patients entered into the forthcoming clinical trial. However, from these limited results it appears that the serum Se concentration does not reflect what is

occurring in the tumour itself which may actually support the argument that serum Se is merely a reflection of tumour burden and an acute phase response (Beguin *et al*, 1989; Sakr *et al*, 2007).

In summary, the uptake of MSA by DLBCL cell lines and PBMCs differs with slower uptake by PBMCs. In addition, PBMCs form methylselenol less efficiently than DLBCL cell lines. These differences may explain, in part, why the action of organic Se compounds differs between normal and tumour cells.

CHAPTER 10: A proteomics approach to investigating the chemo-sensitising action of methylseleninic acid

10.1 INTRODUCTION

The work presented so far in this thesis has demonstrated that Se, in the form of MSA, affects a number of cellular pathways in DLBCL cell lines. However, a unifying mechanism by which MSA sensitises these cell lines to conventional chemotherapeutic agents has not been established. Therefore, a more global approach was taken, in the form of proteomics analysis of cell lines exposed to chemo-sensitising concentrations of MSA.

A number of studies have used a genomics approach to identify molecular mechanisms of Se action. DNA microarray analysis has most frequently been performed in prostate and breast cancer cell lines exposed to organic Se compounds, precursors of mono-methylated Se species. These studies have identified a large number of genes, expression of which is altered by Se, but the results often differ depending on the form and concentration of Se used. Also, the effects of Se are dependent on the tissue type investigated. However, there are similarities in the genes identified, and commonly they are genes involved in cell cycle regulation, apoptosis and anti-oxidant function, implicating Se in the prevention of cancer initiation, progression and metastasis (El-Bayoumy & Sinha, 2005). Gene expression in prostate biopsy samples of men with prostate cancer, supplemented prior to prostatectomy with SLM, vitamin E or a combination (in a similar way to the SELECT trial), has been performed (Tsavachidou *et al*, 2009). Laser capture micro-dissection of these biopsies was used to isolate normal epithelial, normal stromal and tumour cells. The study was able to identify over 500 differentially expressed genes in the three cell types, including cell-type specific effects, thus demonstrating the potential global effect of Se *in vivo*, even at nutritional doses. There have been no studies published that have investigated gene expression in lymphoma cell lines exposed to Se. The disadvantage of a genomics approach is that mRNA expression does not always correlate with protein expression or activity. Reasons

for this include, alternative splicing of RNA, post-translational modification of proteins and protein degradation.

Like genomics, proteomics is a rapidly expanding field. It is the study of the complete protein complement of a cell/organism and MS has become the method of choice for analysing complex protein mixtures (Aebersold & Mann, 2003). A few studies have used a proteomics approach to investigate the cellular effect of Se, but again this is predominantly in prostate cancer cell lines and has not been performed in lymphoma cell lines. Although these studies have used different forms and concentrations of Se, they have all identified novel Se-targets (Roveri *et al*, 2008; Sinha *et al*, 2008). Proteomics has also been able to identify protein changes in the plasma of rats supplemented with different forms of Se and these novel proteins have the potential to be useful as biomarkers of Se intake (Mahn *et al*, 2009a; Mahn *et al*, 2009b). A study using a display thiol-proteomics approach to identify protein redox modifications by MSA has already been discussed in Chapter 1 (section 1.3.9.11) (Park *et al*, 2005). Again, this study demonstrates the large number of cellular proteins that are susceptible to modification by Se.

In addition to protein identification, MS can be used to identify post-translational modifications and this has most widely been used to study protein phosphorylation (Thingholm *et al*, 2009). Phosphorylation is one of the most common mechanisms of protein regulation, affecting both structure and function. The amino acids that are most frequently phosphorylated are serine, threonine and tyrosine and multiple residues can be phosphorylated within a protein. Protein phosphorylation is involved in the regulation of critical and diverse cellular functions such as cell division, proliferation, enzyme activity, intracellular signalling, transcription and translation (Graves & Krebs, 1999). The large numbers of protein kinases present within a cell are responsible for the phosphorylation of specific proteins and deregulated kinase activity is found in many cancers (Hunter, 1995). Thus, 'phospho-proteomics' has the potential to yield valuable information about the functioning of a cell, pathways that may be active or de-regulated within a cell and,

like proteomics itself, may identify novel therapeutic targets and biomarkers for use in cancer therapy. Interestingly, a study investigating the effect of MSA exposure on protein kinases in a mouse mammary epithelial tumour cell line found that MSA resulted in the differential expression of a number of proteins kinases, with both up- and down-regulation being observed (Singh *et al*, 2008).

A phospho-proteomics approach has been used here to study the molecular affects of MSA in DLBCL cell lines. This has not previously been reported for the investigation of Se-induced changes. This approach, however, is not without its challenges. Firstly, proteins and phospho-proteins need to be isolated from a cellular sample. Cell lysis can activate proteases and protein phosphatases making proteins susceptible to degradation and dephosphorylation. Therefore, a mixture of protease and phosphatase inhibitors is added to samples to prevent this, the choice of which is crucial. Once the isolated proteins have been digested into peptides, the sample needs to be enriched for phospho-peptides in order to improve the sensitivity of MS detection. This is because phospho-peptides are particularly difficult to analyse by MS as they are not as efficiently ionised as non-phosphorylated peptides. Thus, MS signal intensities for phospho-peptides will be lower than those for the non-phosphorylated peptides present within a sample. There are a number of methods available for phospho-enrichment of samples, each requiring validation by individual user groups prior to conducting large scale experiments. The method used in this study was immobilised metal ion affinity chromatography (IMAC). This makes uses of positively charged metal ions, such as Fe^{3+}, chelated to either nitrilotriacetic acid or iminodiacetic acid coated beads, which can bind the negatively charged phospho-peptides (Paradela & Albar, 2008; Thingholm *et al*, 2009). In addition, it has been demonstrated that larger numbers of phospho-peptides are obtained by IMAC if samples are first pre-fractionated by strong cation exchange (SCX) (Trinidad *et al*, 2006).

Samples enriched for phospho-peptides are then separated by LC and identified by tandem MS (LC-MS/MS). However, identification of phospho-peptides is not as

straightforward as the identification of non-phosphorylated peptides due to their low abundance and low ionisation efficiency, requiring very sensitive detection methods, and the potential loss of labile phosphate groups. Additionally, this results in a low number of peptide fragment ions for identification. For protein identification it is normally possible to match several MS/MS spectra to a given protein. However, for phospho-peptide identification, only one or two ion species are detected and matched to a given phospho-peptide. Thus, good quality MS/MS spectra are required to have full confidence in the findings (Alcolea *et al*, 2009; Paradela & Albar, 2008; Thingholm *et al*, 2009). The MS used in these experiments was the LTQ-Orbitrap XL (Thermo Fisher Scientific, Hemel Hempstead, UK). This is an ion-trap analyser which has the advantages of high sensitivity, resolution, mass accuracy and dynamic range in addition to performing full scans very rapidly (Aebersold & Mann, 2003). To identify the phospho-peptides present within a sample, the mass to charge ratio (*m/z* ratio) generated is compared to the *m/z* ratio within spectral reference databases to match the amino acid sequences to known peptides. However, the spectral databases for phospho-peptides are not as robust or comprehensive as those for non-phosphorylated peptides (Alcolea *et al*, 2009).

Although technically challenging for the reasons outlined above, these proteomic studies were performed to identify potentially novel mechanisms underlying the chemo-sensitising effect of MSA.

10.2 AIM

To identify novel protein changes induced by chemo-sensitising concentrations of MSA in a MSA-sensitive (RL) and MSA-resistant (DHL4) DLBCL cell line. A phospho-proteomics approach has been used to provide functional information about the signalling pathways targeted by MSA.

10.3 METHODS

A full description of the method is given in the appendix. Figure 10.1 summarises the steps involved.

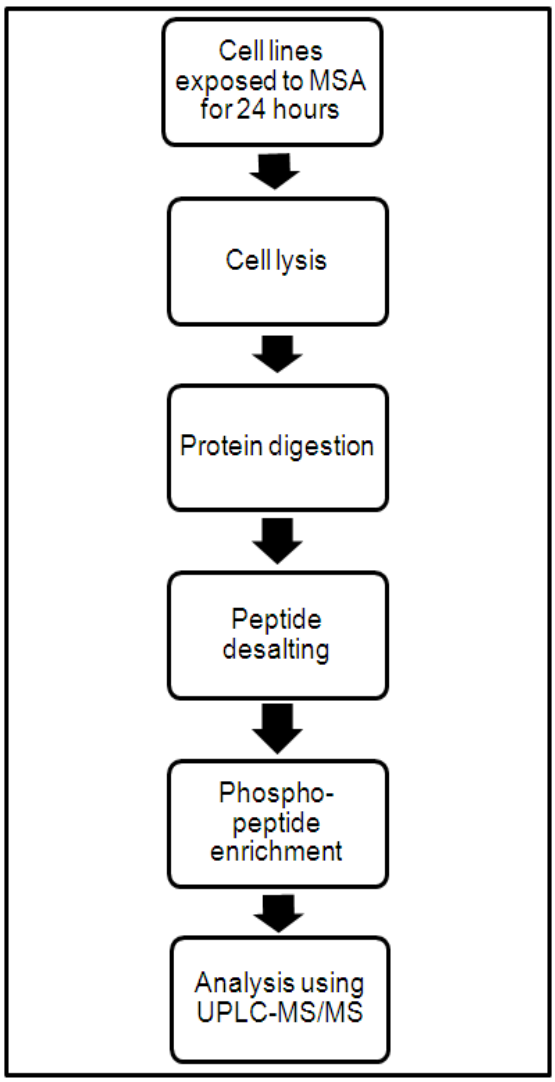

Figure 10.1 Summary of the steps involved in the phospho-proteomics experiments (UPLC; ultra high-performance liquid chromatography)

10.3.1 Sample preparation

The RL and DHL4 cell lines were exposed to 1µmol/L and 10µmol/L MSA respectively for 24 hours. Following this, 10 million cells were washed in PBS supplemented with Na_3VO_4 and NaF. Cells pellets were then snap-frozen on dry ice and stored at -20°C until further use. These experiments were performed on three separate occasions to obtain independent triplicate samples.

10.3.2 Cell lysis

The cell pellets were thawed, resuspended in 1ml of lysis buffer and the cell suspension was sonicated. Samples were centrifuged to remove cellular debris and the supernatant was recovered into protein Lobind® tubes (Eppendorf UK Limited). Where possible, samples were kept in protein LoBind® tubes from this stage onwards. Cellular proteins were reduced with DTT followed by alkylation with iodoacetamide. Protein extracts were then diluted in 20mM HEPES pH 8.0 (1:4 dilution).

10.3.3 Protein digestion

Immobilised L-1-tosylamido-2-phenylethyl chloromethyl ketone (TPCK)-trypsin beads (Thermo Fisher Scientific, Cramlington, UK) were used for protein digestion. 80µl of the beads were used per sample and beads were conditioned prior to use according to the manufacturers' instructions. Following addition of the beads, samples were incubated for 16 hours at 37°C with shaking. Digestion was stopped by adding TFA (LGC Standards) at a final concentration of 1%. The beads were removed by centrifugation.

10.3.4 Peptide desalting

Sep-Pak® C_{18} cartridges (Waters UK Ltd., Manchester, UK) were used to desalt the peptide samples.

10.3.5 Phospho-peptide enrichment by immobilised metal ion affinity chromatography

IMAC sepharose™ high performance beads (GE healthcare) were used to separate the phospho-peptide component of the peptide sample. Firstly, the beads were conditioned and charged with Fe^{3+}. The beads (300µL/sample) were then added to each sample and placed on a rotatory mixer for 1 hour. Following this, samples were centrifuged and the supernatant recovered (i.e. non-phosphorylated peptides). The phospho-peptides were eluted using ammonia water (LGC standards). Both the fractions containing the non-phosphorylated and phospho-enriched peptides were dried down in a vacuum centrifuge (Christ rotational vacuum concentrator, Osterode, Germany).

10.3.6 Nanoflow-UPLC® coupled to tandem mass spectrometry (LC-MS/MS)

Samples for analysis were reconstituted in 11µl of 0.1% FA in LC-MS grade H_2O. Samples were analysed using a nanoflow UPLC® system (nanoAquity, Waters/ Micromass UK Ltd. Manchester) coupled to a LTQ-Orbitrap XL MS (Thermo Fisher Scientific, Hemel Hempstead, UK). 3µl of each sample were injected in duplicate. The MS was operated to automatically acquire MS and MS/MS spectra. Initially, full scan survey spectra (*m/z* 375-1800) were acquired and then the five most intense ions in each full scan (every 0.6 of a second) were sequentially isolated and fragmented. Data were acquired using the Xcalibur software version 2.0.7 (Thermo Fisher Scientific).

10.3.7 Data analysis

For protein identification, the processed files were searched against the Swiss-Prot database of protein sequences using the Mascot search engine (Mascot Daemon, v2.3.0; Matrix Science). For quantitative analysis of the MS data, a program written by the Analytical Signalling Group (Institute of Cancer, Barts Cancer Centre, London, UK) known as Pescal was used (Cutillas & Vanhaesebroeck, 2007). This program generates peak intensity values for each of the peptide sequences identified by Mascot. Each experiment was performed in triplicate and therefore for each peptide the mean peak intensities for control and MSA-treated samples were calculated. If more than one peptide belonging to the same protein was present, then the peak intensity values for all peptides were combined and the mean calculated. A paired t-test was used to determine significant differences in peptide intensities between control and MSA-treated samples. $p<0.05$ was considered statistically significant. Peptides that did not change in intensity between control and MSA-treated samples were excluded from further analysis. These quantitative data were then analysed using the MetaboAnalyst software (www.metaboanalyst.ca) which performs both univariate (t-test and fold change) and multivariate analysis (principle component analysis and hierarchical cluster analysis). Network and pathway analysis was performed using Ingenuity Pathway Analysis (IPA) software™ v8.6 (Ingenuity® Systems, www.ingenuity.com). The fold-change (FC) was

calculated for the peptides that changed significantly between control and MSA-treated samples and peptides with a ≥2 FC in intensity were used in pathway analysis.

10.4 RESULTS

More than 3000 proteins were identified in each of the RL and DHL4 cell samples.

10.4.1 DHL4 cell line

In the DHL4 cell line exposed to 10µmol/L MSA, 299 proteins were identified that were differentially expressed ($p<0.05$) between control and MSA-treated samples. There were an additional 13 peptides that were differentially expressed but could not be identified. Of these 299 proteins, 87 were phosphorylated proteins (29%). 98/299 proteins had a ≥2-fold difference in expression, either up- or down-regulated, of which 39/98 (40%) were phosphorylated.

Using the MetaboAnalyst software, univariate analysis of the data was performed. FC and t-tests were calculated for the peptides identified and Figure 10.2 shows the 'volcano plot' which combines this information. The x-axis shows the FC with a threshold of +/-1-FC, and the y-axis shows the p value with a threshold of p=0.1. Note that both axes are log-transformed. The red circles represent peptides above the set thresholds for both FC and statistical significance.

Principal component analysis (PCA) was performed using the MetaboAnalyst software. This is an unsupervised, multivariate statistical method which provides a graphical representation of multi-dimensional data to determine how well calculated summary 'component' values describe differences between samples (Ringner, 2008). This is done by reducing the dimensionality of the data by identifying variables, [principal components (PC)], that account for as much of the variability in the data as possible. Thus, PC1 is associated with the greatest variation in the data and subsequent PCs for the remaining variability. Figure 10.3 shows the PCA analysis for DHL4 cells using two PCs. It shows that using these 2 summary components, the control and MSA-treated samples

can be grouped and are clearly separated, with PC1 accounting for 81% of the variability within the data and PC2, 10.2%.

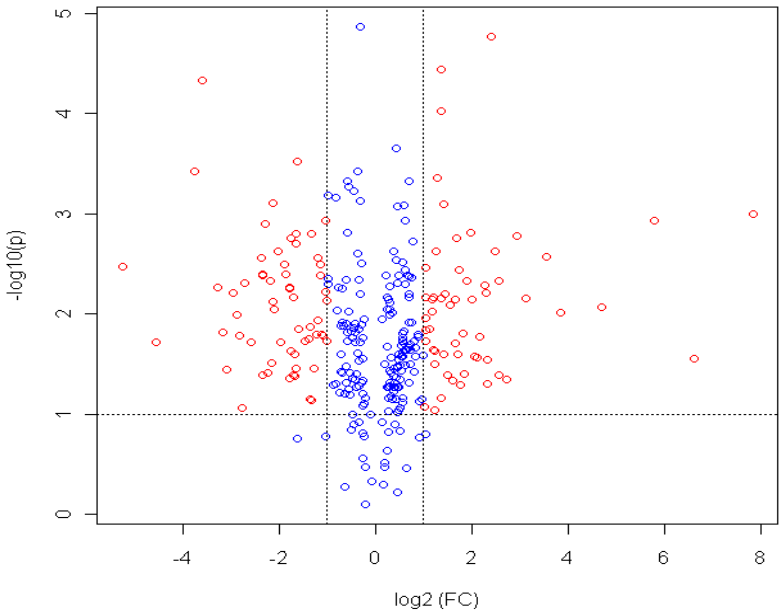

Figure 10.2 Volcano plot showing fold change and p values of peptides identified in DHL4 cells exposed to 10µmol/L MSA.

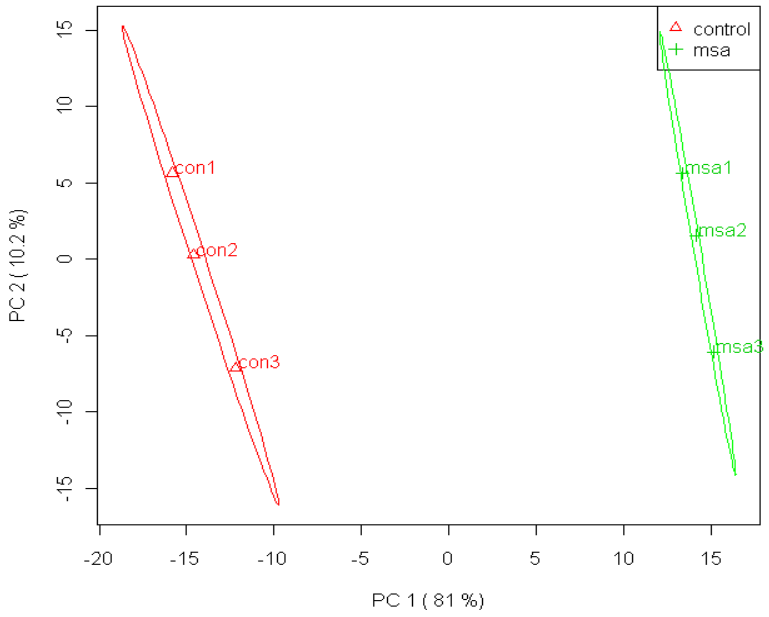

Figure 10.3 Principal component analysis plot for DHL4 cells exposed to 10µmol/L MSA.

Hierarchical cluster analysis was also performed using the MetaboAnalyst software. This again is an unsupervised analysis which begins by considering each sample as a single cluster. These clusters are then combined based on similarities until all samples belong to one cluster. Figure 10.4 shows the hierarchical clustering for the DHL4 cell line represented as a heat map. Again, the control and MSA-treated samples are clearly different and can be separated by this clustering method. The shades of blue represent peptides that are down-regulated and shades of red represent peptides that are up-regulated relative to the mean signal intensity across all samples for each peptide.

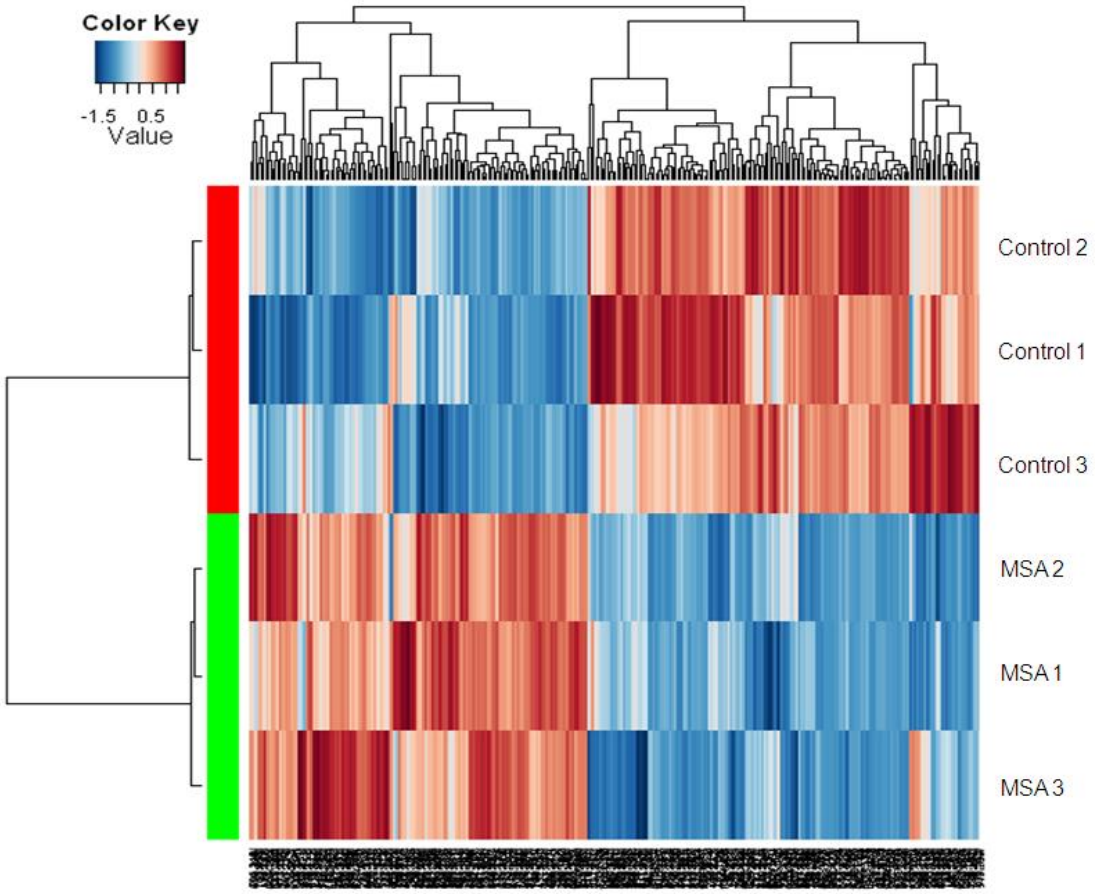

Figure 10.4 Unsupervised hierarchical clustering, shown as a heat map, of DHL4 cells exposed to 10µmol/L MSA

The data shown above clearly demonstrate that MSA results in distinct changes in peptide/protein expression in the DHL4 cell line. The top up-regulated proteins as identified by the Mascot search engine are shown in Table 10.1 and the top down-regulated proteins are shown in Table 10.2. The full list of differentially expressed proteins is shown in the appendix. Some of the protein changes were expected and confirm some of the data presented in earlier chapters. For example TrxR1, a known selenoprotein, was up-regulated. In addition, the ER chaperones GRP78 and GRP94, and the enzyme PDI were all up-regulated.

Table 10.1 The top most up-regulated proteins in DHL4 cells exposed to 10µmol/L MSA

Gene Symbol	Protein	Phospho*	FC	p value
PTPLAD1	Protein tyrosine phosphatase-like protein	ST	38.4	0.004
HNRNPA3	Isoform 1 of Heterogeneous nuclear ribonucleoprotein A3		23.7	0.02
TUBB3	Tubulin beta-3 chain		13.5	0.002
CCT8	Chaperonin containing T complex protein 1, subunit 8 (theta)		12.1	0.002
TXNRD1	Thioredoxin reductase 1		9.7	0.004
RCTPI1	Triosephosphate isomerase		9	0.02
CCT4	Chaperonin containing T complex protein 1, subunit 4 (delta)		8.5	0.02
SYNE2	Isoform 1 of Nesprin-2		7.7	0.02
PDCD4	Programmed cell death 4 isoform 2		7.3	0.009
SOD1	Superoxide dismutase		7.1	0.03
HSPA5	GRP78		6.6	0.02
HSP90B3P	GRP94		6.0	0.01

*ST, serine/threonine

Table 10.2 The top most down-regulated proteins in DHL4 cells exposed to 10µmol/L MSA

Gene Symbol	Protein	Phospho*	FC	p value
C1QBP	Complement component 1 Q subcomponent-binding protein, mitochondrial		229	0.001
MCM7	Isoform 1 of DNA replication licensing factor MCM7		98.4	0.03
VEPH1	Isoform 1 of Ventricular zone-expressed PH domain-containing protein homolog 1	ST	55.2	0.001
ALDOA	Fructose-bisphosphate aldolase A		25.8	0.008
RRM2	Ribonucleotide reductase, subunit M2	ST	14.4	0.01
GLO1	Glyoxalase 1		11.6	0.01
CDC2	Cyclin-dependent kinase 1	ST, Y	8.7	0.02
HMGCS1	Hydroxymethylglutaryl-CoA synthase,	ST	7.6	0.01
HSPH1	Heat shock protein 105 kDa (Isoform β)		6.6	0.045
RPLP0	60S acidic ribosomal protein P0	2ST	5.9	0.03

*ST, serine/threonine, Y, tyrosine

To further analyse the protein changes induced by MSA, the IPA software was used to study protein networks and signalling pathways. The proteins identified could be grouped into 3 main networks. The top network was termed 'DNA replication, recombination and repair, cell cycle and cell death' and 14 of the differentially expressed proteins could be incorporated into this network (Figure 10.5). The second network was termed 'cell-mediated immune response, cellular development, function and maintenance' and 13 proteins could be incorporated into this network (Figure 10.6). The third network was termed 'cellular growth and proliferation, cellular development and cancer' and 8 proteins could be incorporated into this network (Figure 10.7). The proteins identified were associated with a large number of canonical pathways. The three main pathways identified were glycolysis/gluconeogenesis (5 proteins), pyrimidine metabolism (5 proteins), and Nrf2-mediated oxidative stress response (5 proteins). The molecular and cellular functions of the proteins were grouped and 28 proteins were involved in cell death, 24 in cellular growth and proliferation, 7 in post-translational modification and 5 in protein folding.

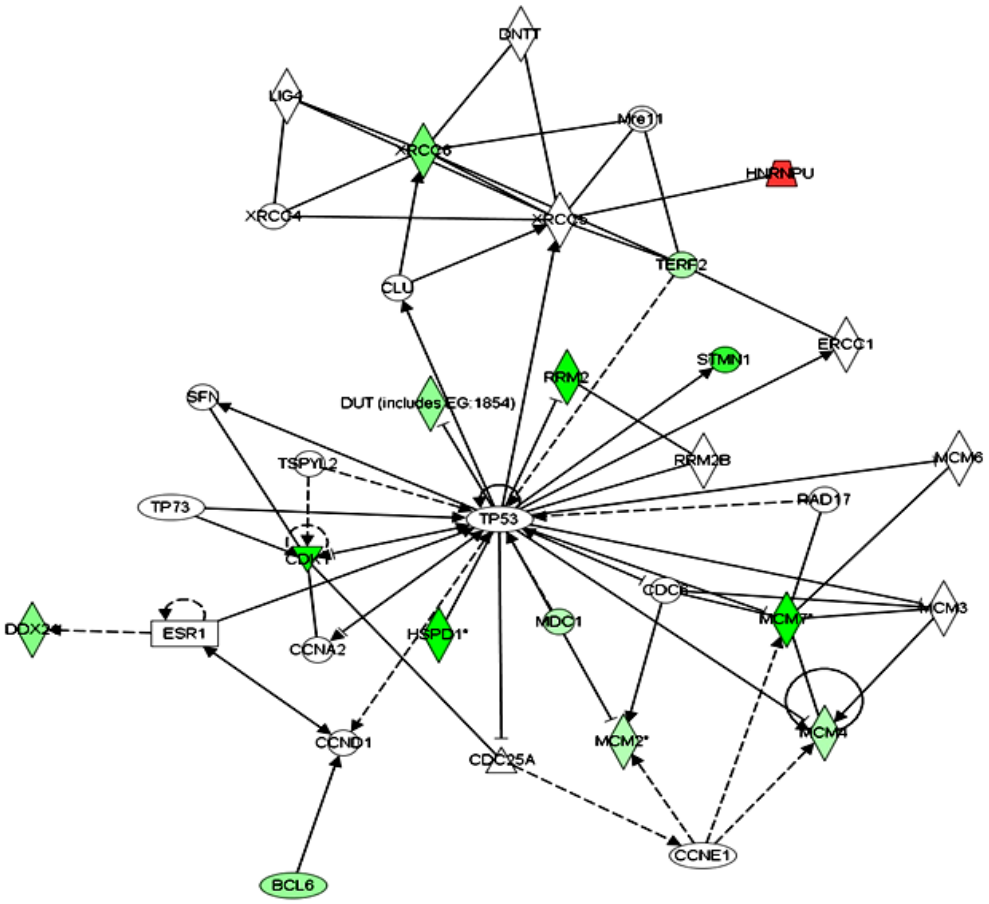

Figure 10.5 'DNA replication, recombination and repair, cell cycle and cell death' network identified by the IPA software in DHL4 cells exposed to 10µmol/L MSA. Shades of red represent proteins that were up-regulated and shades of green represent proteins that were down-regulated. The intensity of the red and green colour relates to the degree of change.

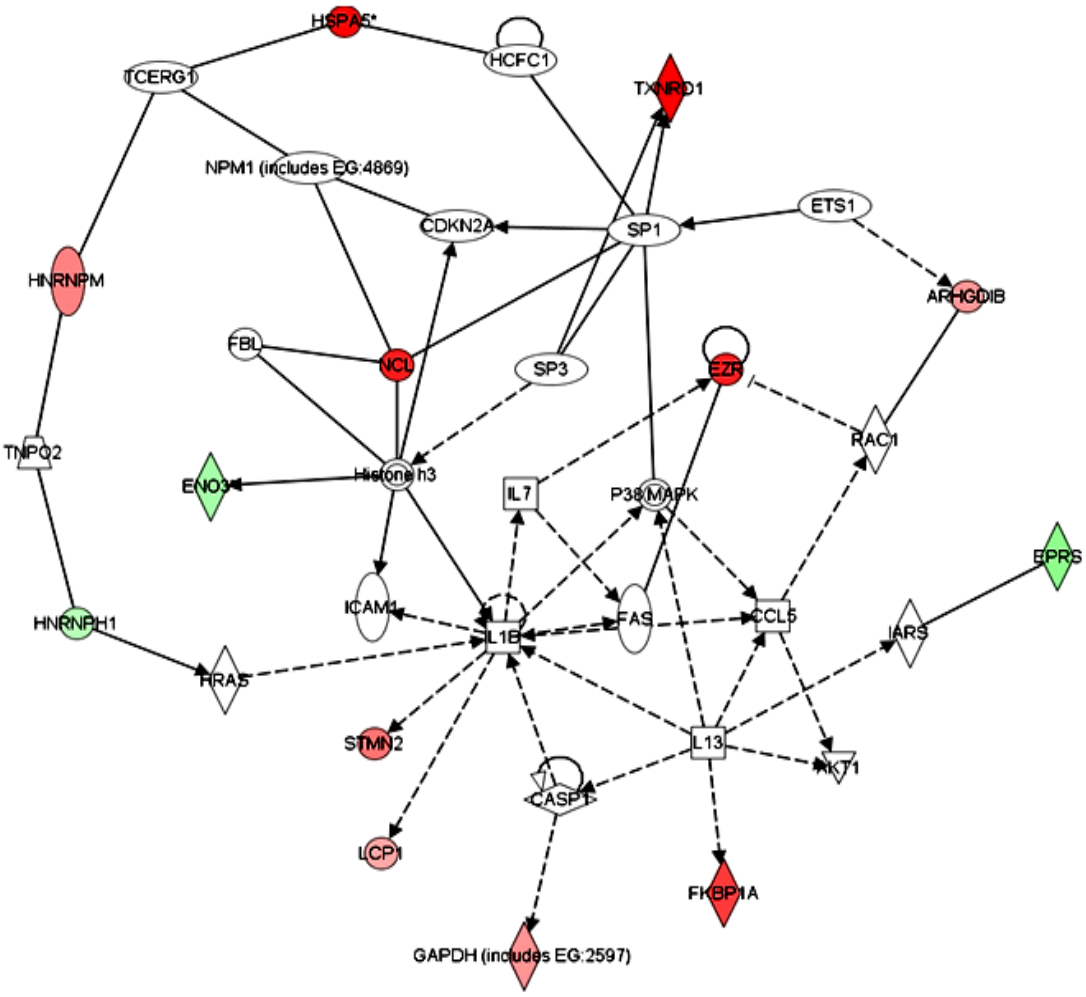

Figure 10.6 'Cell-mediated immune response, cellular development, function and maintenance' network identified by the IPA software in DHL4 cells exposed to 10µmol/L MSA. Shades of red represent proteins that were up-regulated and shades of green represent proteins that were down-regulated. The intensity of the red and green colour relates to the degree of change.

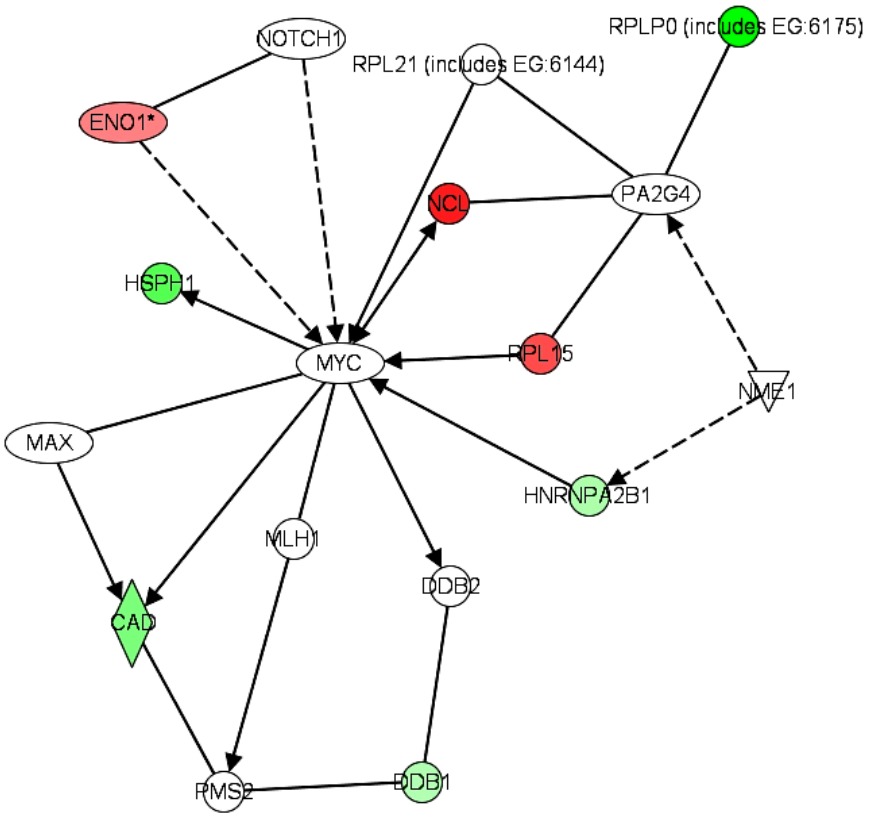

Figure 10.7 'Cellular growth and proliferation, cellular development and cancer' network identified by the IPA software in DHL4 cells exposed to 10µmol/L MSA. Shades of red represent proteins that were up-regulated and shades of green represent proteins that were down-regulated. The intensity of the red and green colour relates to the degree of change.

10.4.2 RL cell line

In the RL cell line exposed to 1µmol/L MSA, 151 proteins were identified that were differentially expressed ($p<0.05$) between control and MSA-treated samples. There were an additional 3 peptides that were differentially expressed but were unable to be identified. Of these 151 proteins, 57 were phosphorylated proteins (38%). 29/151 proteins had a ≥2-FC in expression, either up- or down-regulated, between control and MSA-treated cells of which 8/29 (28%) were phosphorylated. The same analysis using the MetaboAnalyst software was performed as for the DHL4 cell line. FC and t-tests were

calculated for the peptides identified and Figure 10.8 shows the 'volcano plot' which combines this information. The x-axis shows the FC with a threshold of +/-1-FC, and the y-axis shows the p value with a threshold of p=0.1. Note that both axes are log transformed. The red circles represent peptides above the set thresholds for both FC and statistical significance.

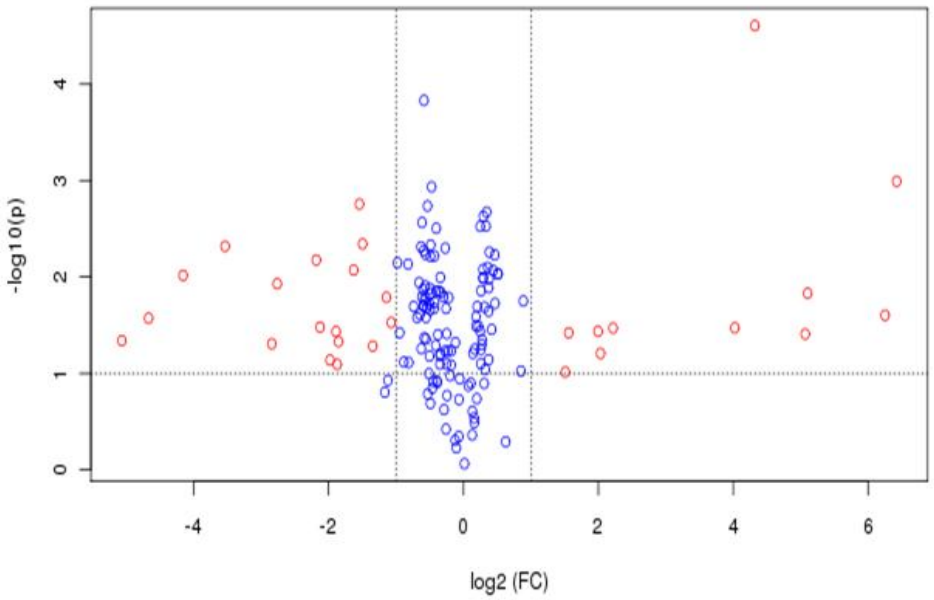

Figure 10.8 Volcano plot showing fold change and p values of peptides identified in RL cells exposed to 1µmol/L MSA.

Figure 10.9 shows the PCA analysis for RL cells using two PCs. It shows that using these 2 summary components the control and MSA-treated samples can be grouped and are clearly separated, with PC1 accounting for 75.3% of the variability within the data and PC2, 13%.

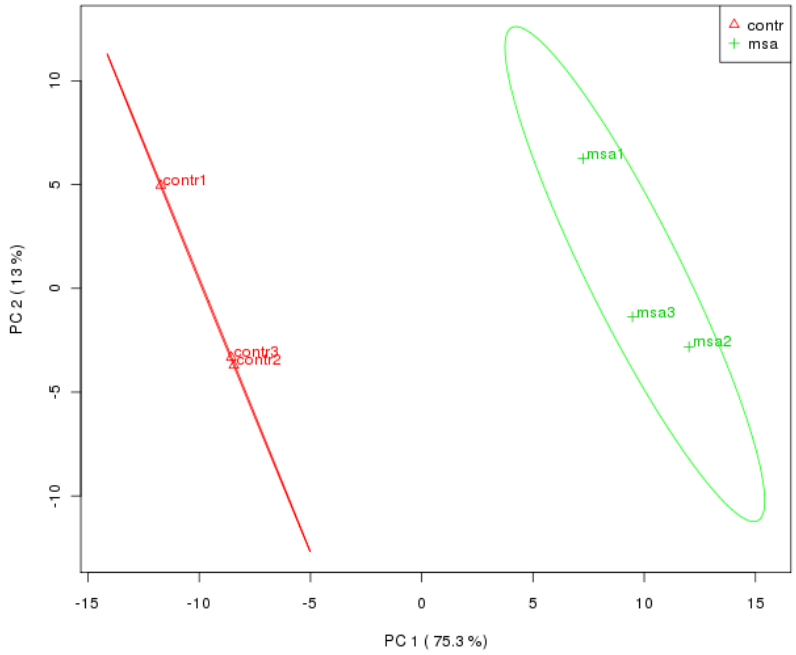

Figure 10.9 Principal component analysis plot for RL cells exposed to 1µmol/L MSA.

Figure 10.10 shows the hierarchical clustering for the RL cell line represented as a heat map. The control and MSA-treated samples are clearly different and can be separated by this clustering method. The shades of blue represent peptides that are down-regulated and shades of red represent peptides that are up-regulated relative to the mean signal intensity across all samples for each peptide.

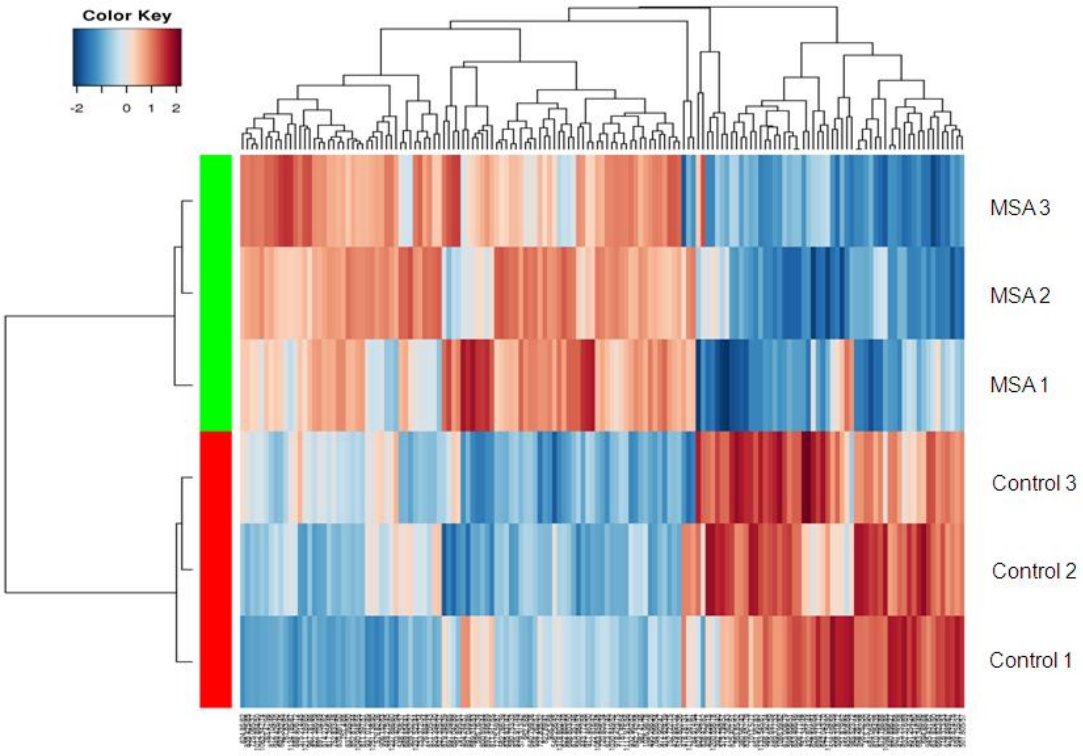

Figure 10.10 Unsupervised hierarchical clustering shown as a heat map of RL cells exposed to 1µmol/L MSA.

Compared to the DHL4 cell lines, far fewer proteins were differentially expressed by ≥2-fold between control and MSA-treated in the RL cell line. This is likely to be due to the fact that cells were exposed to only a very low concentration of MSA, 1µmol/L. However, none of the experiments performed up until this point, described in other chapters, had revealed any proteins that were altered in expression by the exposure of RL cells to 1µmol/L MSA, despite its ability to sensitise RL cells to chemotherapeutic agents. All the up-regulated proteins as identified by the Mascot search engine are shown in Table 10.3 and the down-regulated proteins are shown in Table 10.4. There were some similarities with the findings in the DHL4 cell line (see below).

Table 10.3 Up-regulated proteins in RL cells exposed to 1µmol/L MSA

Gene Symbol	Protein	Phospho*	FC	p value
NPM1	Isoform 1 of Nucleophosmin		33.4	0.047
GRHPR	Glyoxylate reductase/hydroxypyruvate reductase		25.4	0.03
EIF3B	Isoform 1 of Eukaryotic translation initiation factor 3 subunit B		17.8	0.008
ACTB	Beta actin		7.2	0.03
GAPDH	Glyceraldehyde-3-phosphate dehydrogenase	ST	6.8	0.045
RPL6	60S ribosomal protein L6		4.5	0.0004
HDGF	Hepatoma-derived growth factor isoform C	2 ST	4.4	0.02
C14orf43	49 kDa protein	ST	3.9	0.045
PPIB	Peptidyl-prolyl cis-trans isomerase B		3.7	0.04
RPLP1	60S acidic ribosomal protein P1	2 ST	3.6	0.01
DHX38	Pre-mRNA-splicing factor ATP-dependent RNA helicase PRP16		3.1	0.01
TXNRD1	Thioredoxin reductase 1		2.9	0.007
CDC2	Cyclin-dependent kinase 1	ST, Y	2.8	0.04
DHX9	ATP-dependent RNA helicase A		2.5	0.03
HSP90AB2P	Similar to Heat shock protein HSP 90-beta	ST	2.3	0.02
RPS5	40S ribosomal protein S5		2.2	0.02
HIST1H2BL	Histone H2B type 1-L		2.2	0.03
ZNF828	Zinc finger protein 828	ST	2.1	0.01

*ST, serine/threonine, Y, tyrosine

Table 10.4 Down-regulated proteins in RL cells exposed to 1µmol/L MSA

Gene Symbol	Protein	Phospho*	FC	p value
RPS14	40S ribosomal protein S14		85.8	0.001
RPS8	40S ribosomal protein S8		76.2	0.03
YWHAG	14-3-3 protein gamma		34.4	0.01
CAPZB	Isoform 1 of F-actin-capping protein subunit beta		33.5	0.04
ALDOA	Fructose-bisphosphate aldolase A		20	0.0001
PADI3	Protein-arginine deiminase type-3	ST	16.3	0.03
PHGDH	D-3-phosphoglycerate dehydrogenase		4.7	0.04
NSUN2	tRNA (cytosine-5-)-methyltransferase NSUN2		4.1	0.048
SFPQ	Isoform Long of Splicing factor, proline- and glutamine-rich		4.0	0.04
HIST1H2BN	Histone H2B type 1-N		3.0	0.04
FUS	Isoform Short of RNA-binding protein FUS		2.8	0.04

*ST, serine/threonine

The IPA software was used to group the proteins into networks and pathways. The proteins identified appeared to be spread across a large number of pathways. The proteins could be grouped into one main network termed ‘cell death, cell cycle, connective tissue development and function’ (Figure 10.11). The three main canonical pathways identified were Nrf2-mediated oxidative stress response (3 proteins), glycine, serine, threonine metabolism (2 proteins) and glycolysis/gluconeogenesis (2 proteins). Thus, 2 out of the 3 of these pathways are the same as those identified in the DHL4 cell line. The molecular and cellular functions of the proteins were grouped and 5 proteins were involved in protein synthesis, 6 in gene expression and 3 in cell cycle regulation.

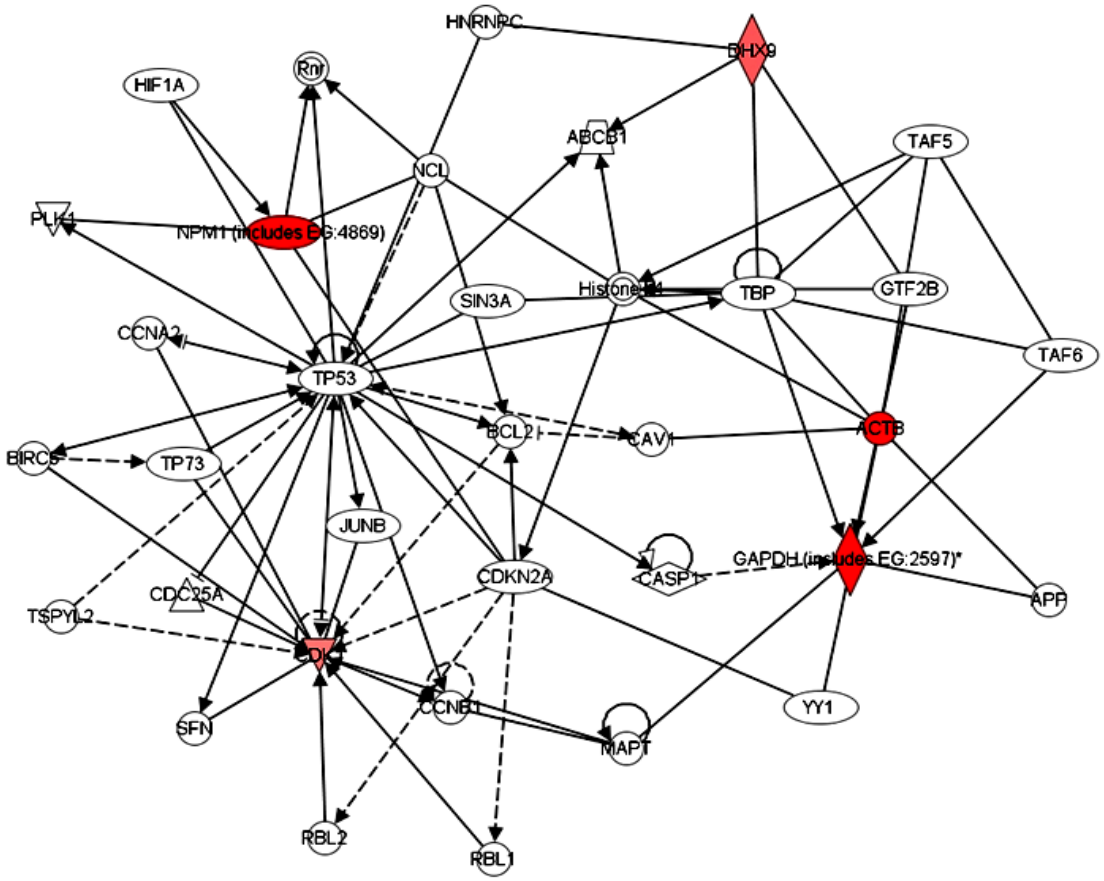

Figure 10.11 'Cell death, cell cycle, connective tissue development and function' network identified by the IPA software in RL cells exposed to 1µmol/L MSA. Shades of red represent proteins that were up-regulated and shades of green represent proteins that were down-regulated. The intensity of the red and green colour relates to the degree of change.

10.4.3 Classification of the differentially expressed proteins by function

It is possible to group the differentially expressed proteins in both the cell lines based on their function. This is shown in Table 10.5 and proteins common to both cell lines are shown in italics.

Table 10.5 Differentially expressed proteins in DHL4 and RL cell lines after exposure to MSA, based on protein function.

Function	DHL4 cell line	FC	RL cell line	FC
Protein folding	• GRP78 • GRP94 • PDI • DnaJ (HSP40) homologue • HSP60 • HSP105 (β-isoform) • Peptidyl-prolyl cis-trans isomerase FKBP1A • T-complex-1 (α-subunit) • Chaperonin containing TCP1, subunit 4 • Chaperonin containing TCP1, subunit 8 • Chaperonin containing TCP1, subunit 7	↑6.6 ↑6.0 ↑2.3 ↑2.3 ↓5.0 ↓6.6 ↑2.5 ↑4.4 ↑8.5 ↑12.1 ↓5.3	• Peptidyl-propyl cis-trans isomerase B • Protein similar to HSP90	↑3.7 ↑2.3
Protein Synthesis	• 60S acidic ribosomal protein P0 • *60S acidic ribosomal protein P1* • 60S ribosomal protein L21 • 60S ribosomal protein L15 • Nucleolin • Nucleolar RNA helicase 2 • Mitochondrial Tu translation elongation factor • Bifunctional aminoacyl-tRNA synthetase • Heterogeneous nuclear ribonucleoprotein A3 • Heterogeneous nuclear ribonucleoprotein U • Heterogeneous nuclear ribonucleoprotein M • Heterogeneous nuclear ribonucleoprotein A2/B1 • Heterogeneous nuclear ribonucleoprotein H	↓5.9 ↓2.7 ↑3.4 ↑3.1 ↑4.3 ↓3.7 ↑2.0 ↓2.3 ↑23.7 ↑3.9 ↑2.8 ↓2.6 ↓2.2	• 60S ribosomal protein L6 • *60S acidic ribosomal protein P1* • 40S ribosomal protein S5 • 40S ribosomal protein S14 • 40S ribosomal protein S8 • Eukaryotic translation initiation factor 3 • Pre-mRNA-splicing factor ATPase RNA helicase PRP16 • ATP-dependent RNA helicase A • Nucleophosmin	↑4.5 ↑3.6 ↑2.2 ↓85.8 ↓76.2 ↑17.8 ↑3.1 ↑2.5 ↑33.4

Table 10.5 continued

Function	DHL4 cell line	FC	RL cell line	FC
Metabolism	• *Fructose bisphosphate aldolase A* • *GAPDH* • Triosephosphate isomerase • Enolase 1 • Enolase 3 • Pyruvate Kinase • Asparagine synthetase • Hydroxymethylglutaryl-CoA synthase	↓25.8 ↑2.0 ↑9.0 ↑2.4 ↓2.0 ↑2.2 ↑2.2 ↓7.6	• *Fructose bisphosphate aldolase A* • *GAPDH* • Glyoxylate reductase/hydroxypyr-uvate reductase • D-3-phosphoglycerate dehydrogenase	↓20 ↑6.8 ↑25.4 ↓4.7
DNA synthesis, replication and repair	• *Cyclin-dependent kinase 1* • Ribonucleotide reductase, M2 • Deoxyuridine triphosphatase • Carbamoyl-phosphate synthetase 2 • Dyskeratosis congenita 1 • MCM2 • MCM4 • MCM5 • MCM7 • Mediator of DNA damage 1 • DNA damage-binding protein 1	↓8.7 ↓14.4 ↓3.3 ↓4.1 ↓2.1 ↓2.4 ↓2.4 ↓3.2 ↓98.4 ↓2.1 ↓2.0	• *Cyclin-dependent kinase 1*	↑2.8
Cytoskeletal/ structural proteins	• Tubulin beta-3 chain • Tubulin alpha-1C • Stathmin 2 • Stathmin • Nesprin 2 • Cofilin 2 • Ezrin	↑13.5 ↓4.0 ↑3.1 ↓3.0 ↑7.7 ↑4.5 ↑2.5	• Actin • F-actin capping protein subunit β	↑7.2 ↓33.5
Epigenetic	• Histone H4 • Histone H1.5	↑3.2 ↓5.5	• Histone H2B type 1L • Histone H2B type 1N	↑2.2 ↓3.0
Anti-oxidant	• *TrxR1* • SOD1	↑9.7 ↑7.1	• *TrxR1*	↑2.9
Lymphoma-related	• Bcl-6 • Glycolase 1	↓3.2 ↓11.6	• Nucleophosmin	↑33.4

Protein folding

As mentioned above, these results confirmed some of the earlier work presented in Chapter 5. In the DHL4 cell line the ER chaperones, GRP78 and GRP94, and the enzyme PDI were all up-regulated. These proteins are involved in the cellular response to protein misfolding. In addition, other proteins not previously studied that are involved in protein folding, were also differentially expressed. These included HSPs, mitochondrial HSP60, and HSP105 (β-isoform), which were down-regulated, and DnaJ (HSP40) homologue which was up-regulated. The enzyme peptidyl-prolyl cis-trans isomerase FKBP1A, and three members of the chaperonin containing T-complex protein (TCP) family [T-complex-1 (α-subunit), chaperonin containing TCP1, subunit 8 and chaperonin containing TCP1, subunit 4] were up-regulated, and chaperonin containing TCP1, subunit 7 was down-regulated.

In the RL cell line, two proteins that may also play a role in protein folding were up-regulated. These were the ER enzyme peptidyl-propyl cis-trans isomerase B and a protein similar to HSP90. Additionally, the phosphorylated enzyme, protein-arginine deiminase 3, was down-regulated. This enzyme is one member of a family of enzymes that catalyse the conversion of arginine in a protein to citrulline. This post-translational modification can modify the structure and function of proteins (Gyorgy *et al*, 2006).

Protein synthesis

Ribosomal proteins were differentially expressed in both cell lines. Two components of the 60S subunit were up-regulated in the RL cell line. In the DHL4 cell line, two components of the 60S subunit were down-regulated and one up-regulated. The two proteins with the largest fold-change in the RL cell line were components of the 40S ribosomal subunit and these proteins were down-regulated. In addition, the nucleolar protein, nucleophosmin, was the most up-regulated protein in the RL cell line and this protein, amongst other functions, is involved in ribosomal biogenesis (Grisendi *et al*, 2006). In the DHL4 cell line, nucleolin, another nucleolar protein involved in ribosomal biogenesis (Ginisty *et al*, 1999) , was up-regulated and nucleolar RNA helicase 2, which

is involved in the processing of ribosomal RNA, was down-regulated. Other proteins involved in protein synthesis identified included, in the RL cell line, eukaryotic translation initiation factor 3 (subunit B), pre-mRNA-splicing factor ATPase RNA helicase PRP16 and ATP-dependent RNA helicase A, which were all up-regulated. In the DHL4 cell line, mitochondrial Tu translation elongation factor was up-regulated and bifunctional aminoacyl-tRNA synthetase was down-regulated. In addition, five members of the heterogenous nuclear ribonucleoprotein family were found to be differentially expression, These proteins bind RNA and are involved in the processing of RNA however, 3 of these proteins were up-regulated and 2 down-regulated (Swanson & Dreyfuss, 1988).

Metabolism

A pathway identified by the IPA software, which was common to both cell lines was that of glycolysis/gluconeogenesis. Fructose bisphosphate aldolase A, which catalyses the reversible conversion of fructose-1,6-bisphosphate to glyceraldehyde 3-phosphate and dihydroxyacetone phosphate, was down-regulated and GAPDH, which catalyses the conversion of glyceraldehyde 3-phosphate to D-glycerate 1,3-bisphosphate, was up-regulated in both cell lines. However, in the RL cell line phosphorylated GAPDH was detected whereas in the DHL4 cell line non-phosphorylated GAPDH was detected. Phosphorylation may alter the function of GAPDH (see discussion). Additionally, in the DHL4 cell line four other enzymes in the glycolytic pathway were altered in expression; triosephosphate isomerase, enolase 1 and pyruvate kinase were up-regulated and enolase 3 was down-regulated.

Proteins involved in other cellular metabolic pathways were also differentially expressed in both cell lines. In the DHL4 cell line, asparagine synthetase was up-regulated and hydroxymethylglutaryl-CoA synthase, an enzyme involved in cholesterol synthesis, was down-regulated. In the RL cell line, the enzyme glyoxylate reductase/hydroxypyruvate reductase which catalyses the reduction of hydroxypyruvate to D-glycerate, the reduction of glyoxylate to glycolate and the oxidation of D-glycerate to hydroxypyruvate, was the

second most highly induced protein. The enzyme D-3-phosphoglycerate dehydrogenase, which catalyses the rate limiting step in serine biosynthesis, was down-regulated.

Two subunits of mitochondrial ATP synthase were up-regulated in the DHL4 cell line. This enzyme catalyses the phosphorylation of ADP to ATP (Hong & Pedersen, 2008), suggesting that in the presence of MSA there is increased generation of cellular energy.

DNA synthesis, replication and repair

In the DHL4 cell line, enzymes involved in both pyrimidine and purine synthesis, were differentially expressed. This included down-regulation of the M2 subunit of ribonucleotide reductase. This enzyme catalyses the formation of deoxyribonucleotides from ribonucleotides, hence is critical for the synthesis of DNA (Nocentini, 1996). In addition, deoxyuridine triphosphatase, carbamoyl-phosphate synthetase 2, dyskeratosis congenita 1, all proteins involved in pyrimidine metabolism, were down-regulated.

In the DHL4 cell line, four members of the mini-chromosome maintenance (MCM) family of proteins were down-regulated; MCM 2, 4, 5, and 7. This family of proteins play a critical role in DNA replication (Bochman & Schwacha, 2009). There was also down-regulation of phosphorylated mediator of DNA damage checkpoint 1 (MDC1). This protein is phosphorylated in response to DNA damage and forms complexes with phospho-histone H2AX, localising to sites of DNA damage and recruiting proteins involved in DNA repair. MDC1 also mediates both the S-phase and G2/M damage-activated cell-cycle checkpoints (Stewart *et al*, 2003). Another protein involved in DNA-damage repair, DNA damage-binding protein 1 (DDB1), was also down-regulated in the DHL4 cell line. This is a heterodimeric protein consisting of 2 subunits, the larger subunit is DDB1 and the smaller subunit is DDB2 (Dualan *et al*, 1995).

In both cell lines, there was altered expression of the cell cycle regulatory protein, CDK1, which is required mainly for transition between the G2 and mitotic phases of the cell cycle (Salaun *et al*, 2008). Phosphorylation of this kinase inactivates its activity

(Potapova *et al*, 2009); in the RL there was increased expression and in the DHL4 cell line decreased expression of the phosphorylated protein.

Cytoskeletal/structural proteins

Cytoskeletal proteins were another group of proteins that were differentially expressed in both cell lines. In the DHL4 cell line, tubulin beta-3 chain was up-regulated and the alpha-1C chain down-regulated. Tubulin is the main constituent of microtubules which are components of the cytoskeleton (Verhey & Gaertig, 2007). Stathmins are a family of proteins that bind to tubulin and inhibit microtubule formation. The proteins are regulated by phosphorylation which reduces its binding to tubulin, one consequence of which is progression of cells through mitosis (Curmi *et al*, 1999). In the DHL4 cell line, the expression of phosphorylated stathmin 1 was down-regulated and that of stathmin 2 (non-phosphorylated) was up-regulated. Actin is another component of the cytoskeleton that polymerises to form microfilaments. In the DHL4 cell line, the expression of cofilin 2, an actin-binding protein that disrupts actin assembly (Huang *et al*, 2006), was up-regulated. The protein, ezrin, was also up-regulated in DHL4 cells. This protein has a number of cellular functions including regulation of the actin cytoskeleton, control of cell shape, adhesion and motility (Brambilla & Fais, 2009). In the RL cell line β-actin was up-regulated and there was down-regulation of the β-subunit of F-actin-capping protein which binds to the growing end of actin microfilaments (Schafer *et al*, 1996). In the DHL4 cell line nesprin-2, a nuclear membrane associated protein which maintains nuclear organisation and structural integrity (Warren *et al*, 2005), was up-regulated.

Epigenetic changes

In both cell lines, histone proteins were differentially expressed, some being increased and some decreased in expression. DNA is wrapped around histones which are the main protein component of chromatin and modification of histones plays an important role in chromatin regulation, including gene transcription (Jenuwein & Allis, 2001).

Anti-oxidant enzymes

The selenoprotein, TrxR1, was up-regulated in both cell lines. Its function has been discussed in Chapter 1. In addition, in the DHL4 cell line, SOD1 expression was increased. SOD1 belongs to a family of superoxide dismutase enzymes which act to eliminate superoxide anion radicals thus combating oxidative stress (Miao & St Clair, 2009).

Lymphoma-related proteins

Two proteins associated with lymphoma pathogenesis were differentially expressed, In the DHL4 cell line phosphorylated Bcl-6 was down-regulated. This protein is a transcription factor that is frequently involved in translocations and over-expressed in DLBCL and its function is regulated by phosphorylation (Moriyama *et al*, 1997). In the RL cell line, the most up-regulated protein was nucleophosmin. This protein is frequently involved in translocations or over-expressed in a number of cancers including haematological malignancies (Grisendi *et al*, 2006). Another protein related to cancer pathogenesis, glyoxalase 1, was down-regulated in the DHL4 cell line. This enzyme catalyses the conversion of reactive α-oxoaldehydes to corresponding α-hydroxyacids (Thornalley, 2003) The gene encoding this protein, *GLO1*, has been found to be over-expressed, due to gene amplification, in a number of human cancers (Santarius *et al*, 2010).

10.5 DISCUSSION

This study has not been without its challenges, however, it has potentially identified novel proteins and pathways involved in the action of MSA in DLBCL cell lines. The main problem was that, despite several attempts, the phospho-enrichment procedure was not optimal. In these experiments, the percentage of phosphorylated peptides in enriched samples was around 30%. Previously published work using similar techniques has reported around 60% enrichment of samples (Alcolea *et al*, 2009). There are several potential reasons for this and some of these were seemingly addressed. As mentioned already, phosphate groups are labile and proteins are easily dephosphorylated. Therefore,

precautions need to be taken during sample processing such as the use of a broad range of phosphatase inhibitors and processing samples mainly at 4°C. One of the problems may have been the phospho-enrichment strategy chosen, which was the use of IMAC beads. This technique is known to have the problem of non-specific binding when complex peptide samples are used and non-phosphorylated peptides may also bind to the beads. Thereafter, when samples are analysed by MS the non-phosphorylated peptides are more efficiently ionised resulting in lowered sensitivity for phosphorylated peptides (Thingholm *et al*, 2009). There are ways to address this problem, such as sample acidification prior to IMAC enrichment and adequately raising the pH, with ammonia solution, during phospho-peptide elution, but despite these measures optimal improvements in phospho-peptide yield were not obtained (Thingholm *et al*, 2009). If these experiments are to be repeated, it may be best to use an alternate method of phospho-peptide enrichment, such as titanium dioxide chromatography, which has been reported to be a superior method to IMAC (Larsen *et al*, 2005). In addition, pre-fractionation of samples by SCX, prior to phospho-enrichment, has been shown to improve the phospho-peptide recovery, therefore this may be a useful step to add for future experiments (Trinidad *et al*, 2006).

Despite these problems, some interesting observations were made. These are, however, based mainly on the non-phosphorylated peptides present within the samples that were analysed. More differentially expressed proteins were identified in the DHL4 cell line than in the RL cell line. This is likely to be because of the higher MSA concentration used for the DHL4 cell line. Prior to these experiments, the exposure of RL cells to 1µmol/L MSA had not resulted in any detectable changes in protein expression by western blotting. However, the use of the more sensitive MS-based method has clearly demonstrated that this concentration of MSA does indeed alter protein expression. It may be that the proteins with the largest FC would also show altered expression by western blotting.

The results from the DHL4 cell line confirmed some of the work presented in earlier chapters. Mainly, that MSA alters the expression of proteins required for protein folding. In addition to identifying known targets of MSA such as ER-chaperones, other molecular chaperones including, HSPs, and enzymes required for protein folding were also identified. Of note, GADD153 was not identified as a protein that was differentially expressed, again confirming earlier results in which induction of GADD153 was only detected at the mRNA level (Chapter 5).

The IPA software identified changes within the Nrf2-mediated oxidative stress pathway as being important in both cell lines. This pathway was previously investigated by western blotting (discussed in Chapter 4) and neither the expression of Nrf2 nor its target Prx1 were altered by MSA. Nrf2 and Prx1 were not identified in these proteomics experiments either but, in the DHL4 cell line, five other down-stream targets of Nrf2 were; T-complex protein 1, subunit 7, DnaJ (HSP40) homologue, protein tyrosine phosphatase-like protein, SOD1 and TrxR1. All, except the T-complex protein 1, subunit 7, were up-regulated by MSA. However, Nrf2-mediated signalling may not be the only explanation for altered expression of these proteins. TrxR is a selenoprotein and therefore its expression is likely to be increased due to the increased availability of Se rather than being a target of Nrf2. DnaJ (HSP40) homologue expression may be related to the overall protein folding capacity of the cell. Members of the DnaJ (HSP40) homologue family have been found to be up-regulated in genomics studies of the LNCaP prostate cancer cell line exposed to MSA (Zhang *et al*, 2005; Zhao *et al*, 2004). These proteins, which are members of the HSP40 family, are co-chaperones that regulate the formation of complexes between HSP70 and its client proteins (Fan *et al*, 2003). Different SOD enzymes have also previously been identified as targets of Se in genomics studies (Dong *et al*, 2001; El-Bayoumy & Sinha, 2005) and considering that MSA results in widespread redox modifications of proteins, it is not unexpected that the expression of proteins with an antioxidant function, which themselves are redox-regulated, should be induced (Park *et al*, 2005).

In RL cells, the IPA software identified three proteins belonging to the Nrf2-mediated oxidative stress pathway, one being up-regulation of TrxR. The other two proteins which were also up-regulated, β-actin and peptidylpropyl isomerase B, could also belong to other signalling pathways. Actins are essential cytoskeletal proteins required for cell motility, structure and integrity and as mentioned above, peptidylpropyl isomerase B, in addition to other functions, is involved in protein folding. Therefore, although the Nrf2-pathway was identified as being important, many of the proteins could also belong to other pathways.

A common feature between the two cell lines was the altered expression of ribosomal proteins and other proteins involved in protein translation, suggesting that MSA affects general protein synthesis. However these proteins were both up- and down-regulated and therefore it is not entirely clear whether overall, MSA increases or decreases protein synthesis. Similar observations have been made in other genomics and proteomics studies investigating the action of Se. In a study that analysed gene expression in lymphocytes isolated from healthy volunteers supplemented with sodium selenite, there was up-regulation of genes involved in protein synthesis, including constituents of the 60s and 40S ribosomal subunits (Pagmantidis *et al*, 2008). The authors hypothesised that this may be due to enhanced incorporation of Sec into selenoproteins, several of which were also found to be up-regulated. Another study reported the down-regulation of genes coding for 40S ribosomal subunits in mammary epithelial cells in rats given MSC in addition to the carcinogen nitrosomethylurea (Dong *et al*, 2001). Two proteomics studies of LnCaP cells exposed to selenite (Roveri *et al*, 2008) and SLM (Sinha *et al*, 2008) identified up-regulation of heterogenous nuclear ribonucleoproteins. These proteins contain functional cysteine residues and are thus susceptible to redox modification by Se compounds. In the DHL4 cell lines, heterogenous nuclear ribonucleoproteins were both up- and down-regulated.

The most up-regulated protein in RL cells was nucleophosmin, a nucleolar phosphoprotein involved in many cellular functions including ribosomal biogenesis. This

protein also has a well established role in the pathogenesis of a number of cancers, including anaplastic large B-cell lymphoma and other haematological malignancies. However, evidence supports its role in both tumour promotion and tumour suppression (Grisendi *et al*, 2006). Therefore, to understand its role in the action of MSA, experiments to over-express and knockdown this protein need to be performed. In the DHL4 cell line, the protein nucleolin which is also involved in ribosomal biogenesis was up-regulated (Ginisty *et al*, 1999). Interestingly, this protein has recently been found to bind to the SECIS elements (secondary RNA stem-loop structures required for the incorporation of Sec into proteins) of a subset of selenoprotein mRNAs, including TrxR1, and positively regulate their translation. Knockdown of nucleolin resulted in decreased TrxR1 protein levels (Miniard *et al*, 2010). Therefore, the up-regulation seen in the DHL4 cell lines may be related to increased translation of TrxR.

MSA appears to affect cellular metabolic processes and a pathway, which was common to both cell lines was that of glycolysis/gluconeogenesis. Similar findings were reported in a proteomics study of the LNCaP cell line exposed to sodium selenite for 3 days. Here, GAPDH and enolase 1 were amongst the most differentially expressed proteins, both being up-regulated (Roveri *et al*, 2008). Another study reported up-regulation of enolase 2 gene expression by MSA in the prostate cancer cell line, PC-3 (Zhang *et al*, 2005). In the work presented here, enzymes involved in other metabolic pathways were also differentially expressed. These findings are supported by genomics studies reported in the literature that have identified a number of differentially expressed genes involved in several metabolic pathways in prostate cancer cell lines exposed to MSA (Gonzalez-Moreno *et al*, 2007; Zhang *et al*, 2005). However, the results presented here only overlap with respect to glycolysis.

Targeting tumour metabolic pathways for cancer therapy is currently being investigated and several compounds are in clinical trial (Tennant *et al*, 2010). It is apparent that tumour cells have altered metabolism which supports cell proliferation and survival. For example, glucose utilisation is higher compared to normal cells and inhibitors of

glycolysis have been shown to sensitise tumours to chemotherapy (Maschek *et al*, 2004). Tumour cells also utilise more amino acids and targeting of amino acid metabolism is already being used in cancer therapy. The enzyme asparaginase, which reduces plasma asparagine levels, is an integral part of therapy for acute lymphoblastic leukaemia (Masetti & Pession, 2009). Inhibitors of fatty acid metabolism have also shown promise in xenograft tumour models (Kridel *et al*, 2004). Thus, the effects of MSA on cellular metabolism could account, in part, for its chemo-sensitising effect. However, from the results obtained it is not possible to establish the exact consequences of the differentially expressed proteins as changes in pathways such as glycolysis are not consistent, with some enzymes up-regulated and some down-regulated. Further experiments, including over-expression and knock-down of these differentially expressed proteins, are required.

DNA synthesis and replication appears to be inhibited by MSA in the DHL4 cell line. Ribonucleotide reductase (M2 subunit), enzymes involved in pyrimidine synthesis and four members of the MCM family of proteins were all down-regulated. MCM proteins play a critical role in DNA replication. In particular they function as replicative helicases, unwinding double-stranded DNA into single-stranded DNA ready for the action of DNA polymerases. However, MCM proteins are crucial to all stages of the cell cycle (Bochman & Schwacha, 2009). These results are in keeping with previous data published from our laboratory demonstrating that MSA has a profound cytostatic effect in the DHL4 cell line with the 72-hour EC_{50} for cell number being 1.7µmol/L (Last *et al*, 2006), compared to a cytotoxic EC_{50}, as determined by the ATP assay, of 76.6µmol/L.

In both cell lines, there was altered expression of the cell cycle regulatory protein, CDK1, which is required mainly for transition between the G2 and mitotic phases of the cell cycle (Salaun *et al*, 2008). However, the consequences of this are difficult to explain as MSA decreased the expression of the phosphorylated/inactivated protein in DHL4 cells but increased its expression in RL cells. In addition, MSA does not result in clear cell cycle changes in either cell line (Last *et al*, 2006). A number of different cell cycle regulatory proteins, including CDK1, have been identified as targets of MSA in other

tumour cell lines but often this has been associated with cell cycle arrest (El-Bayoumy & Sinha, 2005). In the DHL4 cell line, two proteins important in maintaining genomic stability in response to DNA damage, phosphorylated MDC1 and DDB1, were down-regulated (Dualan *et al*, 1995; Stewart *et al*, 2003). MSA may therefore impair the cellular response to DNA damage, making cells more susceptible to apoptosis induced by DNA damaging agents such as doxorubicin and 4-HC.

MSA appears to result in epigenetic modifications suggested by the altered expression of histone proteins. Genomics studies of prostate cancer cell lines exposed to MSA have also described differential expression of histone proteins (Zhang *et al*, 2005; Zhao *et al*, 2004) and epigenetic modification as a mechanism of selenite action in the LnCaP cell line has also been reported (Xiang *et al*, 2008). Cytoskeletal proteins were another group of proteins that were differentially expressed in both the RL and DHL4 cell lines. Genomics studies in prostate cancer cell lines exposed to MSA also identified a number of differentially expressed genes encoding cytoskeletal proteins, none however overlapping with those identified here (Gonzalez-Moreno *et al*, 2007; Zhang *et al*, 2005). However, a proteomics study in the LNCaP cell line exposed to SLM identified the protein cofilin 2 as being up-regulated (Sinha *et al*, 2008). This protein was up-regulated in the DHL4 cell line and contains functional cysteine residues making it susceptible to redox modification. In addition, translocation of cofilin proteins from the cytosol to the mitochondria occurs during apoptosis and inhibition of these proteins using siRNA, have been found to inhibit cytochrome *c* release and apoptosis (Chua *et al*, 2003).

Of particular relevance to DLBCL was the finding that MSA decreased levels of phosphorylated Bcl-6 in the DHL4 cell line. Bcl-6 is a transcriptional repressor which is frequently over-expressed in DLBCL. This promotes cell survival, proliferation and blocks differentiation, thus targeting Bcl-6 is being investigated as a therapeutic approach in DLBCL (Parekh *et al*, 2008). Phosphorylation of the protein is known to regulate its function (Moriyama *et al*, 1997). The protein, glyoxalase 1 was also down-regulated in the DHL4 cell line. The gene encoding this protein, *GLO1*, is over-expressed in a number

of human cancers and recently this has been shown to be due to gene amplification (Santarius *et al*, 2010). Although *GLO1* over-expression has most frequently been detected in solid tumours, it has also been reported in haematological tumours, including lymphoma (Sakamoto *et al*, 2000; Santarius *et al*, 2010). Over-expression of *GLO1* is associated with drug resistance and knock-down of *GLO1* or inhibition of the glyoxalase 1 inhibits cell proliferation, increases apoptosis and reverses chemo-resistance (Sakamoto *et al*, 2000; Santarius *et al*, 2010).

Of concern in these results is the finding that MSA induces the expression of GAPDH, as this has been used as a loading control in all western blotting experiments. In the RL cell line it was the phosphorylated form of the enzyme that was detected but in the DHL4 cell line it was the non-phosphorylated protein. GAPDH is phosphorylated by protein kinase C ι/λ. GAPDH is known to associate with tubulin and it has been shown that recruitment of β-tubulin to the Golgi and ER membranes is dependent on phosphorylated GAPDH which therefore plays a role in microtubule dynamics (Tisdale, 2002). It may be that induction of GAPDH by MSA is related to its cytoskeletal function rather than its role in glycolysis. Clearly, if levels of the phosphorylated form are increased, total levels should remain the same and can still be used as a control in western blotting. The western blots presented in this thesis do not appear to show increased expression of total GAPDH therefore further western blotting experiments need to be performed to assess phosphorylated levels. This issue also highlights a limitation of the IPA software in that it does not consider the post-translational modification of proteins when performing pathway mapping. This, however, is a problem with all commercially available protein analysis software.

In summary, these results demonstrate that at chemo-sensitising concentrations, MSA alters the expression of proteins belonging to many different cellular pathways. Despite the limitations of this study, several changes reported in earlier chapters, using a western blotting approach, have been confirmed by this LC-MS method. Moreover, novel differentially expressed proteins, belonging to previously un-investigated pathways have

been identified in two DLBCL cell lines. Some of these findings are supported by published studies that have mainly investigated gene expression in solid tumour cell lines exposed to different forms of Se (El-Bayoumy & Sinha, 2005; Zhang *et al*, 2005). However, it is apparent that although there is some overlap in the functions of the genes/protein targets of Se, the effects are also very much dependent on the cell-type and the chemical form of Se. These experiments clearly need to be repeated and it would be valuable to optimise phospho-enrichment of samples to establish the effect of MSA on protein function and signalling pathways. In addition, confirmatory experiments, such as western blotting, need to be performed to be fully confident in the proteins identified in these experiments. Finally, to determine the cellular consequences of the protein changes identified, over-expression and knock-down experiments need to be conducted.

CHAPTER 11: Conclusions and future studies

DLBCL is a disease that is potentially curable with combination chemotherapy (DeVita *et al*, 1975). The addition of rituximab to first-line treatment has significantly improved both response rates and OS (Coiffier *et al*, 2002; Feugier *et al*, 2005). The work presented here analysed the outcome and patterns of survival of 384 patients, presenting to SBH over an 18-year period, for whom treatment with curative intent was deemed appropriate. Although the response rates to initial treatment were in keeping with those from other published series, the results clearly demonstrate that, in an *unselected* group of patients, the prognosis for those who develop recurrent disease is exceedingly poor. The median OS for the 80 patients with recurrent DLBCL was only one year. Similarly, for patients in whom CR was not achieved with the first 'salvage' therapy, the outcome was particularly poor, with none experiencing a durable period of remission following subsequent treatment. All, except two patients (who still had active lymphoma at the time of death), died of disease.

Despite the curative potential of HDT with autologous haematopoietic stem cell support in recurrent DLBCL, a significant proportion of patients, for several reasons, were not able to receive this treatment. Surprisingly however, in patients in whom a second CR/CRu was achieved, there was no significant difference in RD or OS between those who did and those who did not receive HDT. Clearly, this is at odds with published data that have demonstrated the superiority of HDT over standard-dose chemotherapy alone in the treatment of recurrent disease (Philip *et al*, 1995). These results, however, likely reflect the reality of treating an unselected group. The results for patients referred to SBH from peripheral hospitals, specifically to receive HDT in second remission, were considerably better and more in keeping with those achieved in clinical trials. However, most clinical trials in patients with recurrent DLBCL commence at the point of delivery of HDT and do not take into account the true 'denominator'.

This work also highlights the importance of long follow-up, as late recurrences of DLBCL do occur. In this series, recurrence of DLBCL occurred in 14 patients (6%) after

5 years of CR/CRu and these patients had a similarly poor prognosis to those in whom recurrence occurred earlier. In addition, 6 patients died of lymphoma-related causes more than 10 years after the diagnosis of DLBCL. The importance of performing a biopsy at the time of disease recurrence is also evident, as recurrence with a different histological subtype of lymphoma, mainly FL, does occur and these patients need to be treated differently.

Overall, this analysis confirms the need for new and better first-line treatments, in order to prevent recurrence in the first place. Additionally, prospective randomised trials, which incorporate new agents as treatment for patients with recurrent DLBCL, are urgently needed. With this is mind, and against this background, the remainder of the work presented has concentrated on the potential therapeutic role of Se as an adjunct to treatment for patients with DLBCL. The rationale for this project came from observational and *in vitro* studies performed in our Department. Serum Se concentration at presentation was found to be an independent prognostic factor, predicting for dose delivery, treatment response and long-term survival in patients with 'aggressive' B-cell NHL (Last *et al*, 2003). Additionally, *in vitro* studies using MSA, a precursor of methylselenol, in DLBCL cell lines demonstrated that whilst high concentrations induced apoptosis, non-cytotoxic concentrations could enhance the efficacy of a number of cytotoxic agents (Juliger *et al*, 2007; Last *et al*, 2006). Repeat experiments presented here confirm these published data. This work complements that of others, in solid tumour cell lines and xenograft models, which show that organic Se species increase the efficacy of chemotherapeutic agents, whilst protecting normal tissue from chemotherapy-induced toxicity (Cao *et al*, 2004; Hu *et al*, 2008).

MSA was shown to inhibit the activation of NF-κB in DLBCL cell lines thus providing a potential mechanism to explain its chemo-sensitising action (Juliger *et al*, 2007). However, as described extensively in Chapter 1, Se has the potential to affect the function of many cellular proteins and signalling pathways. In addition, a differential response to Se has been demonstrated in tumour and normal cells (Cao *et al*, 2004). Therefore,

further mechanisms by which Se may mediate these differential effects, was one of the main aims of the laboratory studies in this thesis.

It is perhaps surprising that the observed synergy between MSA and cytotoxic agents was not associated with increased apoptosis, as studies in solid tumour cell lines have demonstrated the ability of non-toxic concentrations of MSA to enhance apoptosis (Hu *et al*, 2005a; Hu *et al*, 2008; Wu *et al*, 2009). There are three main types of cell death; apoptosis, autophagy and necrosis. Other atypical forms of cell death exist, such as 'mitotic catastrophe' and 'anoikis', but in general, these eventually demonstrate features of apoptosis or autophagy (Kroemer *et al*, 2009). In this work, both apoptosis and autophagy were investigated. Although cytotoxic concentrations of MSA induced cell death by apoptosis (Last *et al*, 2006), non-toxic concentrations did not enhance apoptosis when combined with cytotoxic agents. The Guava® viacount assay was used to demonstrate synergy between MSA and cytotoxic drugs. This assay makes use of two dyes, one that is membrane permeable and stains all nucleated cells and one that is membrane impermeable and only enters cells when the membrane has been compromised, thus identifying apoptotic/dead cells. Cell death by necrosis could, therefore, be responsible for the observed increase in cell death as this process involves swelling of the cell with early cell membrane permeabilisation followed by membrane rupture (Kroemer *et al*, 2009). Necrosis has not been previously reported as a mechanism of cell killing by organic Se compounds, however further investigation seems warranted. Necrosis has traditionally been considered an 'accidental', unregulated form of cell death, but recent studies suggest that, under certain circumstances, it can also be a carefully regulated process (Festjens *et al*, 2006; Golstein & Kroemer, 2007). Autophagy was excluded as a mechanism of cell death in experiments reported in Chapter 5. MSA did induce autophagy but this appears, at least in one cell line, to be a mechanism of cell survival rather than cell death.

At cytotoxic concentrations, MSA activated the intrinsic apoptotic pathway as evidenced by loss of MMP and downstream effects on members of the Bcl-2 family of proteins. However, the pattern of protein changes induced by MSA differed between cell lines. In

the RL cell line, MSA increased the expression of the pro-apoptotic protein Bax and in the DHL4 cell line, the expression of the pro-apoptotic protein Bak was increased. In the JVM2 cell line, MSA increased the expression of Bax and the anti-apoptotic protein Bcl-xL, but decreased the expression of the anti-apoptotic protein Mcl-1. In all three cell lines, the expression of Bcl-2 was not altered by MSA. Of note, PARP was cleaved in the RL cell line after exposure to 1μmol/L MSA, but this concentration did not result in a loss of MMP suggesting that the extrinsic apoptotic pathway may also be involved in executing cell death. What triggers apoptosis in lymphoma cell lines exposed to MSA is not clear. Previous work from our laboratory excluded generation of ROS (Last *et al*, 2006). The generation of DNA damage and induction of ER stress (discussed further below) by MSA have now also been excluded.

The effect of MSA on intracellular GSH was investigated. MSA-resistant and MSA-sensitive DLBCL cell lines did not differ in basal GSH levels. However, in two MSA-sensitive cell lines (RL and SUD4), exposure to MSA concentrations ≥10μmol/L for 24 hours resulted in a significant decrease in GSH concentration. This effect was not observed in the MSA-resistant cell line, DHL4. The consequence of the observed MSA-induced decrease in GSH levels in RL and SUD4 cells is not entirely clear. Previous work from our laboratory has demonstrated that increasing intracellular GSH concentration, by treating DLBCL cell lines with N-acetyl cysteine, had no effect on the activity of MSA (Last *et al*, 2006). This is in contrast to a study in a hepatoma cell line, which demonstrated that N-acetylcysteine enhanced MSA-induced apoptosis (Shen *et al*, 2002). This latter finding is consistent with the fact that reduction of MSA by thiols, such as GSH, is required for its metabolism to methylselenol. To further investigate the role of GSH in determining the sensitivity of DLBCL cell lines to MSA, treatment of cells with the inhibitor of GSH synthesis, buthionine sufoxamine, would be useful. However, higher than apoptotic concentrations were required to decrease the GSH concentration in RL and SUD4 cells and this effect was not apparent at the chemo-sensitising concentration of 1μmol/L MSA. Moreover, in the DHL4 cell line, the chemo-sensitising concentration of

10µmol/L did not alter GSH levels. Therefore it is unlikely that a decrease in GSH levels is critical to the apoptotic or chemo-sensitising action of MSA in these cell lines.

A number of intracellular signalling pathways were studied in the DLBCL cell lines and JVM2 cells. Exposure to MSA did not affect the PI3K/Akt or the MAPK pathways. However, MSA decreased the expression of the anti-apoptotic protein, survivin. This protein is a target of NF-κB and its expression was suppressed at similar concentrations to those reported by our group to inhibit the activation of NF-κB; ≥5µmol/L MSA (Juliger *et al*, 2007). In RL cells, survivin expression was not altered by the chemo-sensitising concentration of 1µmol/L, therefore the effect of MSA on this protein does not provide a unifying explanation for the chemo-sensitising activity of MSA. Survivin expression in cells exposed to a combination of MSA and cytotoxic agents at synergistic concentrations was not investigated but would be valuable in order to completely exclude its role in chemo-sensitisation. The effect on survivin expression may be a clinically relevant one, as the proposed clinical trial aims to achieve a plasma Se concentration of 20µmol/L. In addition, survivin is expressed in a large proportion of 'aggressive' B-cell lymphomas with virtually no expression in normal tissue (Tracey *et al*, 2005).

p53 was not found to be important in determining the sensitivity, or action, of MSA in the lymphoma cell lines studied. All the DLBCL cell lines used have mutated *p53* and they exhibited differing sensitivities to MSA. The three MCL cell lines used, JVM2, JeKo-1 and Granta-519, all have wild-type *p53*. The JVM2 cell line was relatively sensitive to MSA with a 72-hour EC_{50} of 3.4µmol/L, whereas both the JeKo-1 and Granta-519 cell lines were relatively resistant, with 48-hour EC_{50} values for cell viability of 38.9µmol/L and 51.8µmol/L respectively. However, MSA had a greater cytostatic effect in these cell lines, with 48-hour EC_{50} values for cell number in JeKo-1 and Granta-519 cell of 3.2µmol/L and 2.8µmol/L respectively. It should be noted that different assays were used in JVM2 cells compared with JeKo-1 and Granta-519 cells. The ATP assay, which reflects both cell viability and cell number, without the ability to distinguish between these two effects, was used in experiments with JVM2 cells. For experiments with JeKo-1 and Granta-510 cells, the Guava® viacount assay was used. This assay measures cell

viability and number separately, therefore distinguishing between the cytotoxic and cytostatic effects of a drug. Given that in JVM2 cells, MSA resulted in PARP cleavage at concentrations as low as 3µmol/L and that the EC_{50} concentration of 3.4µmol/L significantly increased the sub-G1, apoptotic population, when cell cycle analysis was performed, it can be assumed that MSA was in fact cytotoxic to JVM2 cells. In JeKo-1 and Granta-519 cells, 10µmol/L MSA (the only concentration used in western blotting experiments) did not result in PARP cleavage.

Despite the presence of wild-type *p53*, MSA did not result in cell cycle arrest in JVM2 cells but rather there was a concentration-dependent decrease in p53 and p21 expression. This was unexpected, as it has been demonstrated that the organic Se compound, SLM, can activate p53 and induce cell cycle arrest in solid tumour cell lines with wild-type *p53* in the presence or absence of DNA damage (Fischer *et al*, 2007; Goel *et al*, 2006; Seo *et al*, 2002a). Of note, SLM itself is not genotoxic. Thus, it can be concluded that in lymphoma cell lines, p53 function does not have a major impact on MSA activity.

MSA was shown to induce protein misfolding and ER stress in two DLBCL cell lines. This was demonstrated by an MSA-induced increase in expression of the enzyme PDI and the ER chaperone GRP78, along with increased mRNA expression of GADD153. However, in contrast to published work in solid tumour cell lines, the induction of ER stress is unlikely to be responsible for the apoptotic or chemo-sensitising effects of MSA in DLBCL cell lines (Wu *et al*, 2009). The chemo-sensitising concentration of 1µmol/L MSA in RL cells had virtually no effect on markers of ER stress but this concentration did result in PARP cleavage suggesting that the induction of ER stress was not responsible for inducing apoptosis. In the MSA-resistant cell line, DHL4 cell line, low concentrations of MSA (1-5µmol/L) resulted in a much larger increase in GRP78 expression compared to equivalent concentrations in the RL cell line. GRP78 is generally considered a pro-survival protein and over-expression by tumours both promotes growth and has been implicated in chemo-resistance (Pyrko *et al*, 2007; Reddy *et al*, 2003). Thus, ER stress induction may represent a mechanism of MSA-resistance in this cell line. In fact, the chemo-sensitising concentration of 10µmol/L MSA, in DHL4 cells, led to the

induction of autophagy, a downstream consequence of ER stress, and this was shown to be a mechanism of cell survival. This work would need to be extended to other MSA-resistant cell lines to draw any firm conclusions, but identifying mechanisms of resistance to MSA may be useful if MSC shows value in the clinic.

A novel finding presented in this work is the observation that MSA inhibits HDAC activity in DLBCL cell lines. However, cellular metabolism of MSA was required for this effect as MSA, in a cell-free assay, was unable to inhibit the HDAC activity of HeLa nuclear extracts. It was only in a cell-based activity assay that HDAC inhibition was observed. Additionally, cell culture medium from DHL4 cells exposed to MSA had a small, but statistically significant, inhibitory effect on HDAC activity in a cell-free assay. Thus, the data demonstrate that a cellular metabolite of MSA is responsible for HDAC inhibition. It has recently been demonstrated that α-keto acid metabolites of SLM and MSC are capable of inhibiting HDAC activity in solid tumour cell lines (Lee *et al*, 2009a; Nian *et al*, 2009), however, the ability of monomethylated Se species to inhibit HDAC activity has not been reported. The main metabolite of MSA is presumed to be methylselenol, but it is difficult to detect and quantify due to its volatility.

In Chapter 9, further Se-containing metabolites of MSA were investigated. After 2-hour exposure to MSA, the same time-point as that studied for HDAC inhibition, the main intracellular metabolite detected in RL and DHL4 cells was dimethylselenide, with SLM and S-methylselenoglutathione present as minor components. Dimethylselenide is formed from the methylation of methylselenol and thus provides evidence for the conversion of MSA into its active form. This is the first time that this metabolite has been detected in solution in cells exposed to MSA. Dimethyldiselenide was the main volatile Se species detected after exposure of DHL4 cells to MSA, being detected at the earliest time-point studied, 10 minutes, when using a system that traps volatile species in the head space above cells in culture. Dimethyldiselenide is formed by the oxidation of methylselenol, thus providing further evidence for the rapid conversion of MSA to methylselenol. It is therefore assumed that either methylselenol or its methylation product, dimethylselenide,

itself a very reactive compound, may be responsible for the HDAC inhibitory activity of MSA.

The downstream consequences of HDAC inhibition were investigated. p21 expression was induced by both MSA and MSC in DLBCL cell lines, following a similar pattern to the acetylation of histone H3. This is clearly in contrast to the effect of MSA on p21 in JVM2 cells where its expression was down-regulated. The effect of MSA on HDAC activity in JVM2 cells or other MCL cell lines was not studied and it may be that this effect, like many other effects of MSA, is cell-type specific. It is also possible that the down-regulation of p53 by MSA and the resultant inhibition of p21 may exceed the opposing HDAC inhibitory effect of MSA in JVM2 cells. In DLBCL cell lines, significant HDAC inhibition in the activity assay was observed at concentrations ≥10μmol/L, whereas in the JVM2 cell, the effect on p53 was observed at concentrations ≥3μmol/L. Further work is required to clarify this.

MSA was also shown to inhibit the induction of HIF-1α and the production of VEGF in RL and DHL4 cells exposed to hypoxic conditions. Similar findings have been reported in solid tumour cell lines and xenograft models (Bhattacharya *et al*, 2008; Jiang *et al*, 2000; Yin *et al*, 2006). The mechanism by which MSA exerts these effects in DLBCL cell lines is not clear from the experiments performed. It may be a direct consequence of HDAC inhibition but further experiments would be required to confirm this. Hypoxia is known to increase the expression of several HDACs, which results, either directly or indirectly, in the deacetylation of HIF-1α, thus promoting its activity (Kim *et al*, 2001). Alternatively, HDAC inhibition may not be responsible as in solid tumours, MSA and MSC have been reported to inhibit HIF-1α through effects on prolyhydroxylases (Chintala *et al*, 2010).

The results of the experiments performed in normal cells suggest that MSA may not have been the correct Se compound to study the cyto-protective effects of Se. Most studies reporting the cyto-protective effect of organic Se compounds in normal cells have used SLM (Fischer *et al*, 2007; Seo *et al*, 2002b), with some using MSC (Cao *et al*, 2004;

Cuello *et al*, 2007). In general, when these Se compounds have been used *in vitro*, cultures have not been supplemented with the relevant lyase enzyme suggesting that formation of methylselenol would not have been maximal. A cyto-protective effect of MSA has not been reported in the literature whereas its superior *in vivo* anti-tumour effect has (Li *et al*, 2008a). It may therefore be that metabolites, other than methylselenol, are important in the cyto-protective action of Se compounds, including α-keto acid metabolites (Pinto *et al*, 2010). It is likely to be an over simplification to suppose that all Se compounds that are metabolised to methylselenol act in the same way and it may be that other, yet unknown, properties of these compounds are also important in their mechanism of action.

It has also been demonstrated that the mechanism of action of Se compounds that are precursors of methylselenol i.e. MSA, MSC and SLM may differ, and that their effects are cell-type dependent. An example is a study that compared MSC and MSA in the same *in vivo* models of prostate cancer. MSC was able to inhibit tumour growth in only one of the two xenograft models. Tumour growth inhibition by MSC was associated with increased apoptosis, whereas tumour growth inhibition by MSA was not, instead affecting angiogenesis (Li *et al*, 2008a). In contrast, in a human head and neck cancer xenograft model, MSC was found to potentiate the activity of irinotecan and hence dramatically increase cure rates but this was not associated with increased markers of apoptosis, instead, the observed synergy correlated with inhibition of angiogenesis (Yin *et al*, 2006). This demonstrates that although both MSA and MSC are thought to act through their common metabolite methylselenol, they affect different intracellular signalling pathways depending on the tumour-type or on other oncogenic alterations in the same tumour type.

It was found that PBMCs, a model for normal cells, were relatively resistant to the cytotoxic effects of MSA and were able to mount a better survival response when compared to DLBCL cell lines. Expression of GRP78, a pro-survival chaperone, was increased to a greater extent at equivalent concentrations in PBMCs than in DLBCL cell lines. In addition, MSA increased NF-κB activation in PBMCs whereas our group has

shown that MSA inhibits NF-κB activation in DLBCL cell lines (Juliger *et al*, 2007). Conversely, keratinocytes and HFFF2, two cell lines commonly used as models for normal cells, were very sensitive to the cytotoxic effects of MSA, and a non-toxic concentration of MSA was not able to protect keratinocytes from chemotherapy-induced toxicity. However, MSA did not increase the activity of cytotoxic agents in normal cells, even with 7 days' pre-exposure. It should be noted that MSA is not going to be the Se compound used in the forthcoming clinical trial, rather it will be MSC. The use of MSC *in vitro* is limited by its requirement for activation by β-lyase enzymes, which *in vivo* occurs mainly in the liver.

The experiments performed to investigate uptake and metabolism of MSA by DLBCL cell lines and PBMCs, identified differences between these cell types. In the RL and DHL4 cell lines, MSA was taken up rapidly and total intracellular Se concentration was maximal at the earliest time-point studied, 10 minutes. However, MSA was taken up at a slower rate in PBMCs with the maximal Se concentrations being achieved between 4-6 hours' exposure. In addition, the mean Se concentration at each time-point was, in general, lower in PBMCs compared with those obtained in the DLBCL cell lines. Conversion of MSA to methylselenol was found to occur less efficiently in PBMCs than in DLBCL cell lines. The formation of dimethylselenide, the methylation product of methylselenol, was less in PBMCs and the generation of volatile dimethyldiselenide, the oxidation product of methylselenol, was slower. The reason for these differences needs to be investigated further but may be because tumour cells, in general, have higher levels of GSH or because PBMCs use the Se in MSA to form selenoproteins via the intermediate hydrogen selenide. Although these experiments in themselves may not be directly clinically relevant, it has allowed the optimisation of methods to determine total intracellular Se and Se species in PBMCs. These measurements will be used to quantitate intracellular Se species in plasma and PBMCs collected from patients in the proposed clinical trial.

For clinical relevance, the conversion of MSC to methylselenol by normal and tumour cells needs to be studied. The experiments reported here show that the sensitivity of

tumour cells to MSC differs, most likely due to differences in β-lyase activity. The RL cell line and the renal adenocarcinoma cell line, ACHN, were relatively sensitive to the cytotoxic effect of MSC and these cell lines had higher β-lyase activity. Whether the β-lyase activity in lymphoma cell lines reflects that in primary lymphoma samples is not known. It is assumed that *in vivo*, MSC is converted to methylselenol, mainly in the liver and this is enough to exert its anti-tumour effect. However, there is evidence from experiments conducted in rats to suggest that MSC can also be delivered, intact, to other organs and then converted to methylselenol (Suzuki *et al*, 2008). The contribution of tumour metabolism of MSC would be interesting to investigate and it would be possible to measure β-lyase activity in tumour samples from patients entered into the proposed clinical trial. However, the current assay would have to be optimised to increase its sensitivity as 40 million cells were used per experimental condition. Additionally, it would be valuable to determine the *in vivo* anti-tumour effect of MSC in a xenograft model of lymphoma in order to confirm the results obtained in xenograft models of solid tumours.

The experiments conducted in the first part of this project did not identify further unifying mechanisms to explain the chemo-sensitising action of MSA in DLBCL cell lines. Thus, a more global approach was taken in the form of phospho-proteomics. Despite the limitations of these experiments, novel proteins and pathways of Se action were identified. In addition, in the DHL4 cell line, some of the differentially expressed proteins were those that had been identified by western blotting in earlier experiments, such as GRP78 and PDI. Further experiments are required to investigate the relevance of the more novel findings. For example, the protein nucleophosmin was the most up-regulated, by 33.4-fold, in the RL cell line. This needs to be confirmed by an alternative technique, such as western blotting, and the consequences of this up-regulation require further investigation through knock-down and over-expression experiments.

One of the aims of this work was to identify potential biomarkers for the clinical use of Se. Four such markers were identified; GRP78 expression and acetylated histone H3 by western blotting of PBMC whole cell extracts, NF-κB activity by western blotting of

PBMC nuclear extracts and plasma VEGF levels. After 24-hour exposure to MSA, GRP78 expression was maximal at 1μmol/L MSA. However, there was a concentration effect of MSA after 4-hour exposure, (mirroring the time-point of maximal Se uptake), suggesting that this potential biomarker may need to be used at early time-points in patients receiving Se supplementation. Obtaining nuclear extracts from PBMCs for NF-κB activity requires a large number of cells, around 10 million, which may limit its value. In addition, not all patients with DLBCL will have elevated VEGF levels, potentially limiting the value of this protein as a biomarker. Therefore, the true value of these potential biomarkers will have to be assessed in the forthcoming clinical trial. Differentially expressed proteins identified in the proteomics experiments may also serve as potential biomarkers but further work is required to confirm these preliminary findings.

In addition to the work performed in DLBCL cell lines, the combination of Se and bortezomib was investigated in MCL cell lines. Despite a sound rationale to suggest that this interaction would be synergistic, including the fact that both drugs inhibit the activation of NF-κB and induce ER stress, a clear antagonistic interaction was demonstrated. One potential mechanism identified for this antagonism was the induction by MSA and bortezomib of the anti-apoptotic proteins, Bcl-2 and Mcl-1. In addition, both drugs were shown to induce ER stress and autophagy in the cell lines but the role of these pathways in promoting cell survival requires further investigation. This would include over-expression and knock-down of GRP78 and combining MSA and bortezomib with an inhibitor of autophagy. However, these experiments demonstrate that the effect of MSA is dependent on cell-type and that its combination with some anti-tumour agents may in fact be detrimental. Thus, similar to its use in cancer prevention, careful selection of patients who may benefit from Se supplementation is required, since Se is clearly not going to benefit all patients receiving treatment for cancer.

In conclusion, organic Se compounds have the potential to benefit patients with DLBCL without increasing, but possibly decreasing, the toxicity of chemotherapeutic agents. Se has multiple mechanisms of action and this work has endeavoured to provide a better

understanding of its activity in DLBCL. It is hoped that this work will contribute to the successful therapeutic use of Se in patients with DLBCL.

REFERENCES

Abdulah R, Miyazaki K, Nakazawa M, Koyama H (2005) Chemical forms of selenium for cancer prevention. *J Trace Elem Med Biol* **19:** 141-50

Adams J (2004) The proteasome: a suitable antineoplastic target. *Nature reviews* **4:** 349-60

Adams J, Palombella VJ, Sausville EA, Johnson J, Destree A, Lazarus DD, Maas J, Pien CS, Prakash S, Elliott PJ (1999) Proteasome inhibitors: a novel class of potent and effective antitumor agents. *Cancer Res* **59:** 2615-22

Adida C, Haioun C, Gaulard P, Lepage E, Morel P, Briere J, Dombret H, Reyes F, Diebold J, Gisselbrecht C, Salles G, Altieri DC, Molina TJ (2000) Prognostic significance of survivin expression in diffuse large B-cell lymphomas. *Blood* **96:** 1921-5

Aebersold R, Mann M (2003) Mass spectrometry-based proteomics. *Nature* **422:** 198-207

Akbaraly NT, Arnaud J, Hininger-Favier I, Gourlet V, Roussel AM, Berr C (2005) Selenium and mortality in the elderly: results from the EVA study. *Clin Chem* **51:** 2117-23

Akbaraly TN, Arnaud J, Rayman MP, Hininger-Favier I, Roussel AM, Berr C, Fontbonne A (2010) Plasma selenium and risk of dysglycemia in an elderly French population: results from the prospective Epidemiology of Vascular Ageing Study. *Nutr Metab (Lond)* **7:** 21

Akbaraly TN, Hininger-Favier I, Carriere I, Arnaud J, Gourlet V, Roussel AM, Berr C (2007) Plasma selenium over time and cognitive decline in the elderly. *Epidemiology* **18:** 52-8

Alcolea MP, Kleiner O, Cutillas PR (2009) Increased confidence in large-scale phosphoproteomics data by complementary mass spectrometric techniques and matching of phosphopeptide data sets. *J Proteome Res* **8:** 3808-15

Alessi DR, James SR, Downes CP, Holmes AB, Gaffney PR, Reese CB, Cohen P (1997) Characterization of a 3-phosphoinositide-dependent protein kinase which phosphorylates and activates protein kinase Balpha. *Curr Biol* **7:** 261-9

Alizadeh AA, Eisen MB, Davis RE, Ma C, Lossos IS, Rosenwald A, Boldrick JC, Sabet H, Tran T, Yu X, Powell JI, Yang L, Marti GE, Moore T, Hudson J, Jr., Lu L, Lewis DB, Tibshirani R, Sherlock G, Chan WC, Greiner TC, Weisenburger DD, Armitage JO, Warnke R, Levy R, Wilson W, Grever MR, Byrd JC, Botstein D, Brown PO, Staudt LM

(2000) Distinct types of diffuse large B-cell lymphoma identified by gene expression profiling. *Nature* **403:** 503-11

Altieri DC (2003) Survivin, versatile modulation of cell division and apoptosis in cancer. *Oncogene* **22:** 8581-9

Amin HM, McDonnell TJ, Medeiros LJ, Rassidakis GZ, Leventaki V, O'Connor SL, Keating MJ, Lai R (2003) Characterization of 4 mantle cell lymphoma cell lines. *Arch Pathol Lab Med* **127:** 424-31

An WG, Hwang SG, Trepel JB, Blagosklonny MV (2000) Protease inhibitor-induced apoptosis: accumulation of wt p53, p21WAF1/CIP1, and induction of apoptosis are independent markers of proteasome inhibition. *Leukemia* **14:** 1276-83

Andre M, Mounier N, Leleu X, Sonet A, Brice P, Henry-Amar M, Tilly H, Coiffier B, Bosly A, Morel P, Haioun C, Gaulard P, Reyes F, Gisselbrecht C (2004) Second cancers and late toxicities after treatment of aggressive non-Hodgkin lymphoma with the ACVBP regimen: a GELA cohort study on 2837 patients. *Blood* **103:** 1222-8

Andreadis C, Gimotty PA, Wahl P, Hammond R, Houldsworth J, Schuster SJ, Rebbeck TR (2007) Members of the glutathione and ABC-transporter families are associated with clinical outcome in patients with diffuse large B-cell lymphoma. *Blood* **109:** 3409-16

Anon (1979) Epidemiologic studies on the etiologic relationship of selenium and Keshan disease. *Chinese medical journal* **92:** 477-82

Anon (1982) National Cancer Institute sponsored study of classifications of non-Hodgkin's lymphomas: summary and description of a working formulation for clinical usage. The Non-Hodgkin's Lymphoma Pathologic Classification Project. *Cancer* **49:** 2112-35

Anon (1993) A predictive model for aggressive non-Hodgkin's lymphoma. The International Non-Hodgkin's Lymphoma Prognostic Factors Project. *The New England journal of medicine* **329:** 987-94

Anon (1994) The effect of vitamin E and beta carotene on the incidence of lung cancer and other cancers in male smokers. The Alpha-Tocopherol, Beta Carotene Cancer Prevention Study Group. *The New England journal of medicine* **330:** 1029-35

Anon (1997) A clinical evaluation of the International Lymphoma Study Group classification of non-Hodgkin's lymphoma. The Non-Hodgkin's Lymphoma Classification Project. *Blood* **89:** 3909-18

Arap MA, Lahdenranta J, Mintz PJ, Hajitou A, Sarkis AS, Arap W, Pasqualini R (2004) Cell surface expression of the stress response chaperone GRP78 enables tumor targeting by circulating ligands. *Cancer Cell* **6:** 275-84

Ardeshna KM, Kakouros N, Qian W, Powell MG, Saini N, D'Sa S, Mackinnon S, Hoskin PJ, Goldstone AH, Linch DC (2005) Conventional second-line salvage chemotherapy regimens are not warranted in patients with malignant lymphomas who have progressive disease after first-line salvage therapy regimens. *Br J Haematol* **130:** 363-72

Arner ES (2009) Focus on mammalian thioredoxin reductases--important selenoproteins with versatile functions. *Biochimica et biophysica acta* **1790:** 495-526

Arsova-Sarafinovska Z, Matevska N, Eken A, Petrovski D, Banev S, Dzikova S, Georgiev V, Sikole A, Erdem O, Sayal A, Aydin A, Dimovski AJ (2009) Glutathione peroxidase 1 (GPX1) genetic polymorphism, erythrocyte GPX activity, and prostate cancer risk. *Int Urol Nephrol* **41:** 63-70

Asfour IA, El-Tehewi MM, Ahmed MH, Abdel-Sattar MA, Moustafa NN, Hegab HM, Fathey OM (2009) High-dose sodium selenite can induce apoptosis of lymphoma cells in adult patients with non-Hodgkin's lymphoma. *Biological trace element research* **127:** 200-10

Avanzini P, Vinceti M, Ilariucci F, Masini L, D'Inca M, Vivoli G (1995) Serum selenium concentrations in patients with newly diagnosed lymphoid malignancies. *Haematologica* **80:** 505-11

Azrak RG, Frank CL, Ghadersohi A, Rustum YM (2008) Silencing survivin results in synergy between methylseleninic acid and paclitaxel against skov3 ovarian cancer cells. *Cancer biology & therapy* **7:** 1901-8

Azrak RG, Frank CL, Ling X, Slocum HK, Li F, Foster BA, Rustum YM (2006) The mechanism of methylselenocysteine and docetaxel synergistic activity in prostate cancer cells. *Molecular cancer therapeutics* **5:** 2540-8

Azrak RP, L et al (2004) Plasma and tissue distribution of selenium after 5-methylselenocysteine or seleno-L-methionine in mice bearing human tumor xenografts. *Eur J Cancer* **2:** 613

Azrak RP, Pendyala L, Cao S, Durrani FA, Prey J, Fakih M, Rustum YM (2004) Plasma and tissue distribution of selenium after 5-methylselenocysteine or seleno-L-methionine in mice bearing human tumor xenografts. *Eur J Cancer* **2:** 613

B'Hymer C, Caruso JA (2006) Selenium speciation analysis using inductively coupled plasma-mass spectrometry. *J Chromatogr A* **1114:** 1-20

Baldwin AS, Jr. (1996) The NF-kappa B and I kappa B proteins: new discoveries and insights. *Annual review of immunology* **14:** 649-83

Bali P, Pranpat M, Bradner J, Balasis M, Fiskus W, Guo F, Rocha K, Kumaraswamy S, Boyapalle S, Atadja P, Seto E, Bhalla K (2005) Inhibition of histone deacetylase 6 acetylates and disrupts the chaperone function of heat shock protein 90: a novel basis for antileukemia activity of histone deacetylase inhibitors. *The Journal of biological chemistry* **280:** 26729-34

Barceloux DG (1999) Selenium. *Journal of toxicology* **37:** 145-72

Barrington JW, Taylor M, Smith S, Bowen-Simpkins P (1997) Selenium and recurrent miscarriage. *J Obstet Gynaecol* **17:** 199-200

Beck MA, Kolbeck PC, Rohr LH, Shi Q, Morris VC, Levander OA (1994) Benign human enterovirus becomes virulent in selenium-deficient mice. *J Med Virol* **43:** 166-70

Beckwith M, Urba WJ, Ferris DK, Freter CE, Kuhns DB, Moratz CM, Longo DL (1991) Anti-IgM-mediated growth inhibition of a human B lymphoma cell line is independent of phosphatidylinositol turnover and protein kinase C activation and involves tyrosine phosphorylation. *J Immunol* **147:** 2411-8

Bedard K, MacDonald N, Collins J, Cribb A (2004) Cytoprotection following endoplasmic reticulum stress protein induction in continuous cell lines. *Basic & clinical pharmacology & toxicology* **94:** 124-31

Beguin Y, Bours V, Delbrouck JM, Robaye G, Roelandts I, Bury J, Fillet G, Weber G (1989) Relationship of serum selenium levels to tumor activity in acute non-lymphocytic leukemia. *Carcinogenesis* **10:** 2089-91

Belloni D, Veschini L, Foglieni C, Dell'Antonio G, Caligaris-Cappio F, Ferrarini M, Ferrero E (2010) Bortezomib induces autophagic death in proliferating human endothelial cells. *Experimental cell research* **316:** 1010-8

Bentires-Alj M, Barbu V, Fillet M, Chariot A, Relic B, Jacobs N, Gielen J, Merville MP, Bours V (2003) NF-kappaB transcription factor induces drug resistance through MDR1 expression in cancer cells. *Oncogene* **22:** 90-7

Bereshchenko OR, Gu W, Dalla-Favera R (2002) Acetylation inactivates the transcriptional repressor BCL6. *Nat Genet* **32:** 606-13

Berry MJ, Banu L, Harney JW, Larsen PR (1993) Functional characterization of the eukaryotic SECIS elements which direct selenocysteine insertion at UGA codons. *The EMBO journal* **12:** 3315-22

Bewick M, Coutie W, Tudhope GR (1987) Superoxide dismutase, glutathione peroxidase and catalase in the red cells of patients with malignant lymphoma. *Br J Haematol* **65:** 347-50

Bhattacharya A, Seshadri M, Oven SD, Toth K, Vaughan MM, Rustum YM (2008) Tumor vascular maturation and improved drug delivery induced by methylselenocysteine leads to therapeutic synergy with anticancer drugs. *Clin Cancer Res* **14:** 3926-32

Bhattacharya A, Toth K, Sen A, Seshadri M, Cao S, Durrani FA, Faber E, Repasky EA, Rustum YM (2009) Inhibition of colon cancer growth by methylselenocysteine-induced angiogenic chemomodulation is influenced by histologic characteristics of the tumor. *Clin Colorectal Cancer* **8:** 155-62

Birner P, Schindl M, Obermair A, Plank C, Breitenecker G, Oberhuber G (2000) Overexpression of hypoxia-inducible factor 1alpha is a marker for an unfavorable prognosis in early-stage invasive cervical cancer. *Cancer Res* **60:** 4693-6

Blackledge G, Bush H, Chang J, Crowther D, Deakin DP, Dodge OG, Garrett JV, Palmer M, Pearson D, Scarffe JH, Todd ID, Wilkinson PM (1980) Intensive combination chemotherapy with vincristine, adriamycin and prednisolone (VAP) in the treatment of diffuse histology non-Hodgkin's lymphoma. (A report of 89 cases with extensive disease from the Manchester Lymphoma Group). *Eur J Cancer* **16:** 1459-68

Blay J, Gomez F, Sebban C, Bachelot T, Biron P, Guglielmi C, Hagenbeek A, Somers R, Chauvin F, Philip T (1998) The International Prognostic Index correlates to survival in patients with aggressive lymphoma in relapse: analysis of the PARMA trial. Parma Group. *Blood* **92:** 3562-8

Bleys J, Navas-Acien A, Guallar E (2008) Serum selenium levels and all-cause, cancer, and cardiovascular mortality among US adults. *Archives of internal medicine* **168:** 404-10

Blot WJ, Li JY, Taylor PR, Guo W, Dawsey S, Wang GQ, Yang CS, Zheng SF, Gail M, Li GY, et al. (1993) Nutrition intervention trials in Linxian, China: supplementation with specific vitamin/mineral combinations, cancer incidence, and disease-specific mortality in the general population. *Journal of the National Cancer Institute* **85:** 1483-92

Bochman ML, Schwacha A (2009) The Mcm complex: unwinding the mechanism of a replicative helicase. *Microbiol Mol Biol Rev* **73:** 652-83

Boehme V, Schmitz N, Zeynalova S, Loeffler M, Pfreundschuh M (2009) CNS events in elderly patients with aggressive lymphoma treated with modern chemotherapy (CHOP-14) with or without rituximab: an analysis of patients treated in the RICOVER-60 trial of the German High-Grade Non-Hodgkin Lymphoma Study Group (DSHNHL). *Blood* **113:** 3896-902

Bonnet C, Fillet G, Mounier N, Ganem G, Molina TJ, Thieblemont C, Ferme C, Quesnel B, Martin C, Gisselbrecht C, Tilly H, Reyes F (2007) CHOP alone compared with CHOP plus radiotherapy for localized aggressive lymphoma in elderly patients: a study by the Groupe d'Etude des Lymphomes de l'Adulte. *J Clin Oncol* **25:** 787-92

Brambilla D, Fais S (2009) The Janus-faced role of ezrin in "linking" cells to either normal or metastatic phenotype. *International journal of cancer* **125:** 2239-45

Brusamolino E, Rusconi C, Montalbetti L, Gargantini L, Uziel L, Pinotti G, Fava S, Rigacci L, Pagnucco G, Pascutto C, Morra E, Lazzarino M (2006) Dose-dense R-CHOP-14 supported by pegfilgrastim in patients with diffuse large B-cell lymphoma: a phase II study of feasibility and toxicity. *Haematologica* **91:** 496-502

Brush MH, Weiser DC, Shenolikar S (2003) Growth arrest and DNA damage-inducible protein GADD34 targets protein phosphatase 1 alpha to the endoplasmic reticulum and promotes dephosphorylation of the alpha subunit of eukaryotic translation initiation factor 2. *Molecular and cellular biology* **23:** 1292-303

Burk RF, Hill KE, Olson GE, Weeber EJ, Motley AK, Winfrey VP, Austin LM (2007) Deletion of apolipoprotein E receptor-2 in mice lowers brain selenium and causes severe neurological dysfunction and death when a low-selenium diet is fed. *J Neurosci* **27:** 6207-11

Burk RF, Norsworthy BK, Hill KE, Motley AK, Byrne DW (2006) Effects of chemical form of selenium on plasma biomarkers in a high-dose human supplementation trial. *Cancer Epidemiol Biomarkers Prev* **15:** 804-10

Burma S, Chen BP, Murphy M, Kurimasa A, Chen DJ (2001) ATM phosphorylates histone H2AX in response to DNA double-strand breaks. *The Journal of biological chemistry* **276:** 42462-7

Cai XJ, Block E, Uden PC, Zhang X, Quimby BD, Sullivan JJ (1995) Allium chemistry: Identification of selenoamino acids in ordinary and selenium-enriched garlic, onion, and broccoli using gas chromatography with atomic emission detection. *Journal of agricultural and food chemistry* **43:** 1754-1759

Calfon M, Zeng H, Urano F, Till JH, Hubbard SR, Harding HP, Clark SG, Ron D (2002) IRE1 couples endoplasmic reticulum load to secretory capacity by processing the XBP-1 mRNA. *Nature* **415:** 92-6

Cantley LC (2002) The phosphoinositide 3-kinase pathway. *Science (New York, NY* **296:** 1655-7

Cao S, Durrani FA, Rustum YM (2004) Selective modulation of the therapeutic efficacy of anticancer drugs by selenium containing compounds against human tumor xenografts. *Clin Cancer Res* **10:** 2561-9

Chan JM, Oh WK, Xie W, Regan MM, Stampfer MJ, King IB, Abe M, Kantoff PW (2009) Plasma selenium, manganese superoxide dismutase, and intermediate- or high-risk prostate cancer. *J Clin Oncol* **27:** 3577-83

Chandel NS, McClintock DS, Feliciano CE, Wood TM, Melendez JA, Rodriguez AM, Schumacker PT (2000) Reactive oxygen species generated at mitochondrial complex III stabilize hypoxia-inducible factor-1alpha during hypoxia: a mechanism of O2 sensing. *The Journal of biological chemistry* **275:** 25130-8

Chang JW, Jeon HB, Lee JH, Yoo JS, Chun JS, Kim JH, Yoo YJ (2001) Augmented expression of peroxiredoxin I in lung cancer. *Biochemical and biophysical research communications* **289:** 507-12

Charalabopoulos K, Kotsalos A, Batistatou A, Charalabopoulos A, Vezyraki P, Peschos D, Kalfakakou V, Evangelou A (2006a) Selenium in serum and neoplastic tissue in breast cancer: correlation with CEA. *British journal of cancer* **95:** 674-6

Charalabopoulos K, Kotsalos A, Karkabounas S, Vezyraki P, Kalfakakou V, Metsios A, Golias C, Charalabopoulos A, Batistatou A, Evangelou A (2006b) Low selenium levels in serum and increased concentration in neoplastic tissues in patients with colorectal cancer: Correlation with serum carcinoembryonic antigen. *Scandinavian journal of gastroenterology* **41:** 359-60

Chen MF, Keng PC, Shau H, Wu CT, Hu YC, Liao SK, Chen WC (2006) Inhibition of lung tumor growth and augmentation of radiosensitivity by decreasing peroxiredoxin I expression. *International journal of radiation oncology, biology, physics* **64:** 581-91

Cheng YY, Qian PC (1990) The effect of selenium-fortified table salt in the prevention of Keshan disease on a population of 1.05 million. *Biomed Environ Sci* **3:** 422-8

Cheson BD, Horning SJ, Coiffier B, Shipp MA, Fisher RI, Connors JM, Lister TA, Vose J, Grillo-Lopez A, Hagenbeek A, Cabanillas F, Klippensten D, Hiddemann W, Castellino R, Harris NL, Armitage JO, Carter W, Hoppe R, Canellos GP (1999) Report of an international workshop to standardize response criteria for non-Hodgkin's lymphomas. NCI Sponsored International Working Group. *J Clin Oncol* **17:** 1244

Cheson BD, Pfistner B, Juweid ME, Gascoyne RD, Specht L, Horning SJ, Coiffier B, Fisher RI, Hagenbeek A, Zucca E, Rosen ST, Stroobants S, Lister TA, Hoppe RT, Dreyling M, Tobinai K, Vose JM, Connors JM, Federico M, Diehl V (2007) Revised response criteria for malignant lymphoma. *J Clin Oncol* **25:** 579-86

Cheung CW, Burton C, Smith P, Linch DC, Hoskin PJ, Ardeshna KM (2005) Central nervous system chemoprophylaxis in non-Hodgkin lymphoma: current practice in the UK. *Br J Haematol* **131:** 193-200

Chintala S, Tomicronth K, Cao S, Durrani FA, Vaughan MM, Jensen RL, Rustum YM (2010) Se-methylselenocysteine sensitizes hypoxic tumor cells to irinotecan by targeting hypoxia-inducible factor 1alpha. *Cancer Chemother Pharmacol*

Christensen MJ, Nartey ET, Hada AL, Legg RL, Barzee BR (2007) High selenium reduces NF-kappaB-regulated gene expression in uninduced human prostate cancer cells. *Nutrition and cancer* **58:** 197-204

Chu FF, Esworthy RS, Chu PG, Longmate JA, Huycke MM, Wilczynski S, Doroshow JH (2004) Bacteria-induced intestinal cancer in mice with disrupted Gpx1 and Gpx2 genes. *Cancer Res* **64:** 962-8

Chua BT, Volbracht C, Tan KO, Li R, Yu VC, Li P (2003) Mitochondrial translocation of cofilin is an early step in apoptosis induction. *Nat Cell Biol* **5:** 1083-9

Chun JY, Hu Y, Pinder E, Wu J, Li F, Gao AC (2007) Selenium inhibition of survivin expression by preventing Sp1 binding to its promoter. *Molecular cancer therapeutics* **6:** 2572-80

Chung R, Lai R, Wei P, Lee J, Hanson J, Belch AR, Turner AR, Reiman T (2007) Concordant but not discordant bone marrow involvement in diffuse large B-cell lymphoma predicts a poor clinical outcome independent of the International Prognostic Index. *Blood* **110:** 1278-82

Clark LC, Cantor KP, Allaway WH (1991) Selenium in forage crops and cancer mortality in U.S. counties. *Archives of environmental health* **46:** 37-42

Clark LC, Combs GF, Jr., Turnbull BW, Slate EH, Chalker DK, Chow J, Davis LS, Glover RA, Graham GF, Gross EG, Krongrad A, Lesher JL, Jr., Park HK, Sanders BB, Jr., Smith CL, Taylor JR (1996) Effects of selenium supplementation for cancer prevention in patients with carcinoma of the skin. A randomized controlled trial. Nutritional Prevention of Cancer Study Group. *Jama* **276:** 1957-63

Coiffier B, Haioun C, Ketterer N, Engert A, Tilly H, Ma D, Johnson P, Lister A, Feuring-Buske M, Radford JA, Capdeville R, Diehl V, Reyes F (1998) Rituximab (anti-CD20 monoclonal antibody) for the treatment of patients with relapsing or refractory aggressive lymphoma: a multicenter phase II study. *Blood* **92:** 1927-32

Coiffier B, Lepage E, Briere J, Herbrecht R, Tilly H, Bouabdallah R, Morel P, Van Den Neste E, Salles G, Gaulard P, Reyes F, Lederlin P, Gisselbrecht C (2002) CHOP

chemotherapy plus rituximab compared with CHOP alone in elderly patients with diffuse large-B-cell lymphoma. *N Engl J Med* **346:** 235-42

COMA (1991) Dietary reference values for food energy and nutrients for the united kingdom. Report of the panel on dietary reference values. Committee on the medical aspects of food and nutrition policy. . *HMSO, London*

Conlan MG, Bast M, Armitage JO, Weisenburger DD (1990) Bone marrow involvement by non-Hodgkin's lymphoma: the clinical significance of morphologic discordance between the lymph node and bone marrow. Nebraska Lymphoma Study Group. *J Clin Oncol* **8:** 1163-72

Cooper AJ, Krasnikov BF, Niatsetskaya ZV, Pinto JT, Callery PS, Villar MT, Artigues A, Bruschi SA (2010) Cysteine S-conjugate beta-lyases: important roles in the metabolism of naturally occurring sulfur and selenium-containing compounds, xenobiotics and anticancer agents. *Amino Acids*

Cooper AJ, Pinto JT (2006) Cysteine S-conjugate beta-lyases. *Amino Acids* **30:** 1-15

Cooper ML, Adami HO, Gronberg H, Wiklund F, Green FR, Rayman MP (2008) Interaction between single nucleotide polymorphisms in selenoprotein P and mitochondrial superoxide dismutase determines prostate cancer risk. *Cancer Res* **68:** 10171-7

Copple IM, Goldring CE, Kitteringham NR, Park BK (2008) The Nrf2-Keap1 defence pathway: role in protection against drug-induced toxicity. *Toxicology* **246:** 24-33

Costa LJ, Feldman AL, Micallef IN, Inwards DJ, Johnston PB, Porrata LF, Ansell SM (2008) Germinal center B (GCB) and non-GCB cell-like diffuse large B cell lymphomas have similar outcomes following autologous haematopoietic stem cell transplantation. *Br J Haematol* **142:** 404-12

Crump M, Coiffier B, Jacobsen ED, Sun L, Ricker JL, Xie H, Frankel SR, Randolph SS, Cheson BD (2008) Phase II trial of oral vorinostat (suberoylanilide hydroxamic acid) in relapsed diffuse large-B-cell lymphoma. *Ann Oncol* **19:** 964-9

Cuello S, Ramos S, Mateos R, Martin MA, Madrid Y, Camara C, Bravo L, Goya L (2007) Selenium methylselenocysteine protects human hepatoma HepG2 cells against oxidative stress induced by tert-butyl hydroperoxide. *Analytical and bioanalytical chemistry* **389:** 2167-78

Cullinan SB, Diehl JA (2006) Coordination of ER and oxidative stress signaling: the PERK/Nrf2 signaling pathway. *Int J Biochem Cell Biol* **38:** 317-32

Cunningham D, Smith P, Mouncey W, Qian C, Pocock KM (2009) A phase III trial comparing R-CHOP 14 and R-CHOP 21 for the treatment of patients with newly diagnosed diffuse large B-cell non-Hodgkin's lymphoma. *J Clin Oncol* **27:** 8506

Curmi PA, Gavet O, Charbaut E, Ozon S, Lachkar-Colmerauer S, Manceau V, Siavoshian S, Maucuer A, Sobel A (1999) Stathmin and its phosphoprotein family: general properties, biochemical and functional interaction with tubulin. *Cell Struct Funct* **24:** 345-57

Cutillas PR, Vanhaesebroeck B (2007) Quantitative profile of five murine core proteomes using label-free functional proteomics. *Mol Cell Proteomics* **6:** 1560-73

Dana BW, Dahlberg S, Miller TP, Hartsock RJ, Balcerzak S, Coltman CA, Carden JO, Hartley K, Fisher RI (1990) m-BACOD treatment for intermediate- and high-grade malignant lymphomas: a Southwest Oncology Group phase II trial. *J Clin Oncol* **8:** 1155-62

Davenport EL, Moore HE, Dunlop AS, Sharp SY, Workman P, Morgan GJ, Davies FE (2007) Heat shock protein inhibition is associated with activation of the unfolded protein response pathway in myeloma plasma cells. *Blood* **110:** 2641-9

Davenport EL, Morgan GJ, Davies FE (2008) Untangling the unfolded protein response. *Cell Cycle* **7:** 865-9

Davis RJ (2000) Signal transduction by the JNK group of MAP kinases. *Cell* **103:** 239-52

de Jong D, Rosenwald A, Chhanabhai M, Gaulard P, Klapper W, Lee A, Sander B, Thorns C, Campo E, Molina T, Norton A, Hagenbeek A, Horning S, Lister A, Raemaekers J, Gascoyne RD, Salles G, Weller E (2007) Immunohistochemical prognostic markers in diffuse large B-cell lymphoma: validation of tissue microarray as a prerequisite for broad clinical applications--a study from the Lunenburg Lymphoma Biomarker Consortium. *J Clin Oncol* **25:** 805-12

De Paepe P, Achten R, Verhoef G, Wlodarska I, Stul M, Vanhentenrijk V, Praet M, De Wolf-Peeters C (2005) Large cleaved and immunoblastic lymphoma may represent two distinct clinicopathologic entities within the group of diffuse large B-cell lymphomas. *J Clin Oncol* **23:** 7060-8

Deffuant C, Celerier P, Boiteau HL, Litoux P, Dreno B (1994) Serum selenium in melanoma and epidermotropic cutaneous T-cell lymphoma. *Acta dermato-venereologica* **74:** 90-2

Degenhardt K, Mathew R, Beaudoin B, Bray K, Anderson D, Chen G, Mukherjee C, Shi Y, Gelinas C, Fan Y, Nelson DA, Jin S, White E (2006) Autophagy promotes tumor cell survival and restricts necrosis, inflammation, and tumorigenesis. *Cancer Cell* **10:** 51-64

Dennert G, Horneber M (2006) Selenium for alleviating the side effects of chemotherapy, radiotherapy and surgery in cancer patients. *Cochrane Database Syst Rev* **3:** CD005037

Desai D, Salli U, Vrana KE, Amin S (2010) SelSA, selenium analogs of SAHA as potent histone deacetylase inhibitors. *Bioorg Med Chem Lett* **20:** 2044-7

DeVita VT, Jr., Canellos GP, Chabner B, Schein P, Hubbard SP, Young RC (1975) Advanced diffuse histiocytic lymphoma, a potentially curable disease. *Lancet* **1:** 248-50

Dhaliwal HS, Rohatiner AZ, Gregory W, Richards MA, Johnson PW, Whelan JS, Gallagher CJ, Matthews J, Ganesan TS, Barnett MJ, et al. (1993) Combination chemotherapy for intermediate and high grade non-Hodgkin's lymphoma. *Br J Cancer* **68:** 767-74

Dhillon AS, Hagan S, Rath O, Kolch W (2007) MAP kinase signalling pathways in cancer. *Oncogene* **26:** 3279-90

Dickson MA, Hahn WC, Ino Y, Ronfard V, Wu JY, Weinberg RA, Louis DN, Li FP, Rheinwald JG (2000) Human keratinocytes that express hTERT and also bypass a p16(INK4a)-enforced mechanism that limits life span become immortal yet retain normal growth and differentiation characteristics. *Molecular and cellular biology* **20:** 1436-47

Dinkova-Kostova AT, Holtzclaw WD, Cole RN, Itoh K, Wakabayashi N, Katoh Y, Yamamoto M, Talalay P (2002) Direct evidence that sulfhydryl groups of Keap1 are the sensors regulating induction of phase 2 enzymes that protect against carcinogens and oxidants. *Proceedings of the National Academy of Sciences of the United States of America* **99:** 11908-13

Dolcet X, Llobet D, Encinas M, Pallares J, Cabero A, Schoenenberger JA, Comella JX, Matias-Guiu X (2006) Proteasome inhibitors induce death but activate NF-kappaB on endometrial carcinoma cell lines and primary culture explants. *The Journal of biological chemistry* **281:** 22118-30

Dong Y, Ganther HE, Stewart C, Ip C (2002) Identification of molecular targets associated with selenium-induced growth inhibition in human breast cells using cDNA microarrays. *Cancer Res* **62:** 708-14

Dong Y, Lee SO, Zhang H, Marshall J, Gao AC, Ip C (2004) Prostate specific antigen expression is down-regulated by selenium through disruption of androgen receptor signaling. *Cancer Res* **64:** 19-22

Dong Y, Lisk D, Block E, Ip C (2001) Characterization of the biological activity of gamma-glutamyl-Se-methylselenocysteine: a novel, naturally occurring anticancer agent from garlic. *Cancer research* **61:** 2923-8

Du K, Herzig S, Kulkarni RN, Montminy M (2003) TRB3: a tribbles homolog that inhibits Akt/PKB activation by insulin in liver. *Science (New York, NY* **300:** 1574-7

Dualan R, Brody T, Keeney S, Nichols AF, Admon A, Linn S (1995) Chromosomal localization and cDNA cloning of the genes (DDB1 and DDB2) for the p127 and p48 subunits of a human damage-specific DNA binding protein. *Genomics* **29:** 62-9

Duffield-Lillico AJ, Dalkin BL, Reid ME, Turnbull BW, Slate EH, Jacobs ET, Marshall JR, Clark LC (2003) Selenium supplementation, baseline plasma selenium status and incidence of prostate cancer: an analysis of the complete treatment period of the Nutritional Prevention of Cancer Trial. *BJU international* **91:** 608-12

Duffield-Lillico AJ, Reid ME, Turnbull BW, Combs GF, Jr., Slate EH, Fischbach LA, Marshall JR, Clark LC (2002) Baseline characteristics and the effect of selenium supplementation on cancer incidence in a randomized clinical trial: a summary report of the Nutritional Prevention of Cancer Trial. *Cancer Epidemiol Biomarkers Prev* **11:** 630-9

Duffield AJ, Thomson CD, Hill KE, Williams S (1999) An estimation of selenium requirements for New Zealanders. *The American journal of clinical nutrition* **70:** 896-903

Dunleavy K, Pittaluga S, Czuczman MS, Dave SS, Wright G, Grant N, Shovlin M, Jaffe ES, Janik JE, Staudt LM, Wilson WH (2009) Differential efficacy of bortezomib plus chemotherapy within molecular subtypes of diffuse large B-cell lymphoma. *Blood* **113:** 6069-76

Duvic M, Talpur R, Ni X, Zhang C, Hazarika P, Kelly C, Chiao JH, Reilly JF, Ricker JL, Richon VM, Frankel SR (2007) Phase 2 trial of oral vorinostat (suberoylanilide hydroxamic acid, SAHA) for refractory cutaneous T-cell lymphoma (CTCL). *Blood* **109:** 31-9

El-Bayoumy K, Sinha R (2004) Mechanisms of mammary cancer chemoprevention by organoselenium compounds. *Mutation research* **551:** 181-97

El-Bayoumy K, Sinha R (2005) Molecular chemoprevention by selenium: a genomic approach. *Mutation research* **591:** 224-36

Ellgaard L, Ruddock LW (2005) The human protein disulphide isomerase family: substrate interactions and functional properties. *EMBO reports* **6:** 28-32

Epstein AL, Levy R, Kim H, Henle W, Henle G, Kaplan HS (1978) Biology of the human malignant lymphomas. IV. Functional characterization of ten diffuse histiocytic lymphoma cell lines. *Cancer* **42:** 2379-91

Evens AM, Schumacker PT, Helenowski IB, Singh AT, Dokic D, Keswani A, Kordeluk E, Raji A, Winter JN, Jovanovic BD, Holmgren A, Nelson BP, Gordon LI (2008)

Hypoxia inducible factor-alpha activation in lymphoma and relationship to the thioredoxin family. *Br J Haematol* **141:** 676-80

Evens AM, Sehn LH, Farinha P, Nelson BP, Raji A, Lu Y, Brakman A, Parimi V, Winter JN, Schumacker PT, Gascoyne RD, Gordon LI (2010) Hypoxia-inducible factor-1 {alpha} expression predicts superior survival in patients with diffuse large B-cell lymphoma treated with R-CHOP. *J Clin Oncol* **28:** 1017-24

Fakih MG, Pendyala L, Brady W, Smith PF, Ross ME, Creaven PJ, Badmaev V, Prey JD, Rustum YM (2008) A Phase I and pharmacokinetic study of selenomethionine in combination with a fixed dose of irinotecan in solid tumors. *Cancer Chemother Pharmacol* **62:** 499-508

Fakih MG, Pendyala L, Smith PF, Creaven PJ, Reid ME, Badmaev V, Azrak RG, Prey JD, Lawrence D, Rustum YM (2006) A phase I and pharmacokinetic study of fixed-dose selenomethionine and irinotecan in solid tumors. *Clin Cancer Res* **12:** 1237-44

Fan CY, Lee S, Cyr DM (2003) Mechanisms for regulation of Hsp70 function by Hsp40. *Cell Stress Chaperones* **8:** 309-16

Faure P, Ramon O, Favier A, Halimi S (2004) Selenium supplementation decreases nuclear factor-kappa B activity in peripheral blood mononuclear cells from type 2 diabetic patients. *European journal of clinical investigation* **34:** 475-81

Fayad L, Thomas D, Romaguera J (2007) Update of the M. D. Anderson Cancer Center experience with hyper-CVAD and rituximab for the treatment of mantle cell and Burkitt-type lymphomas. *Clin Lymphoma Myeloma* **8 Suppl 2:** S57-62

Federico A, Morgillo F, Tuccillo C, Ciardiello F, Loguercio C (2007) Chronic inflammation and oxidative stress in human carcinogenesis. *International journal of cancer* **121:** 2381-6

Ferrara N, Gerber HP, LeCouter J (2003) The biology of VEGF and its receptors. *Nat Med* **9:** 669-76

Festjens N, Vanden Berghe T, Vandenabeele P (2006) Necrosis, a well-orchestrated form of cell demise: signalling cascades, important mediators and concomitant immune response. *Biochimica et biophysica acta* **1757:** 1371-87

Feugier P, Van Hoof A, Sebban C, Solal-Celigny P, Bouabdallah R, Ferme C, Christian B, Lepage E, Tilly H, Morschhauser F, Gaulard P, Salles G, Bosly A, Gisselbrecht C, Reyes F, Coiffier B (2005) Long-term results of the R-CHOP study in the treatment of elderly patients with diffuse large B-cell lymphoma: a study by the Groupe d'Etude des Lymphomes de l'Adulte. *J Clin Oncol* **23:** 4117-26

Finley JW, Ip C, Lisk DJ, Davis CD, Hintze KJ, Whanger PD (2001) Cancer-protective properties of high-selenium broccoli. *Journal of agricultural and food chemistry* **49:** 2679-83

Fischer JL, Mihelc EM, Pollok KE, Smith ML (2007) Chemotherapeutic selectivity conferred by selenium: a role for p53-dependent DNA repair. *Molecular cancer therapeutics* **6:** 355-61

Fisher RI, Gaynor ER, Dahlberg S, Oken MM, Grogan TM, Mize EM, Glick JH, Coltman CA, Jr., Miller TP (1993) Comparison of a standard regimen (CHOP) with three intensive chemotherapy regimens for advanced non-Hodgkin's lymphoma. *The New England journal of medicine* **328:** 1002-6

Flores-Mateo G, Navas-Acien A, Pastor-Barriuso R, Guallar E (2006) Selenium and coronary heart disease: a meta-analysis. *The American journal of clinical nutrition* **84:** 762-73

Foo AY, Nemesanszky E, Rosalki SB (1981) Comparison of procedures for the measurement of the anodal isoenzymes of lactate dehydrogenase in serum. *Ann Clin Biochem* **18:** 232-5

Francesconi KA, Sperling M (2005) Speciation analysis with HPLC-mass spectrometry: time to take stock. *The Analyst* **130:** 998-1001

Franke KW (1934) A New Toxicant Occurring Naturally in Certain Samples of Plant Foodstuffs. *journal of nutrition* **8:** 597-608

Friesen C, Kiess Y, Debatin KM (2004) A critical role of glutathione in determining apoptosis sensitivity and resistance in leukemia cells. *Cell Death Differ* **11 Suppl 1:** S73-85

Fu Y, Li J, Lee AS (2007) GRP78/BiP inhibits endoplasmic reticulum BIK and protects human breast cancer cells against estrogen starvation-induced apoptosis. *Cancer Res* **67:** 3734-40

Gabel-Jensen C, Bak SA, Lauritsen FR, Hanse HR, Badolo L, Gammelgaard B (2009a) *In situ* identification of dimethyl diselenide in hepatocytes treated wtih methylseleninic acid by membrane inlet mass spectrometry *J Anal At Spectrom* **24:** 949-952

Gabel-Jensen C, Lunoe K, Gammelgaard B (2010) Formation of methylselenol, dimethylselenide and dimethyldiselenide in *in vitro* metabolism models determined by headspace GC-MS. *Metallomics* **2:** 167-173

Gabel-Jensen C, Lunoe K, K.M. M, Bendix J, Cornett C, Sturup S, Hansen HR, Gammelgaard B (2008) Separation and identification of the selenium-sulfur amino acid

S-(methylseleno)cysteine in intestinal epithelial cell homogenates by LC-ICP-MS and LC-ESI-MS after incubation with methylseleninic acid. *J Anal At Spectrom* **23:** 727-732

Gabel-Jensen C, Odgaard j, Skonberg C, Badolo L, Gammelgaard B (2009b) LC-ICP-MS and LC-ESI-$(MS)^n$ identification of Se-methylselenocysteine and selenomethionine as metabolites of methylseleninic acid in rat hepatocytes. *J Anal At Spectrom* **24:** 69-75

Gall EA, Mallory TB (1942) Malignant Lymphoma: A Clinico-Pathologic Survey of 618 Cases. *Am J Pathol* **18:** 381-429

Gammelgaard B, Gabel-Jensen C, Sturup S, Hansen HR (2008) Complementary use of molecular and element-specific mass spectrometry for identification of selenium compounds related to human selenium metabolism. *Analytical and bioanalytical chemistry* **390:** 1691-706

Ganjoo KN, An CS, Robertson MJ, Gordon LI, Sen JA, Weisenbach J, Li S, Weller EA, Orazi A, Horning SJ (2006) Rituximab, bevacizumab and CHOP (RA-CHOP) in untreated diffuse large B-cell lymphoma: safety, biomarker and pharmacokinetic analysis. *Leuk Lymphoma* **47:** 998-1005

Ganther H, Ip C (2001) Thioredoxin reductase activity in rat liver is not affected by supranutritional levels of monomethylated selenium in vivo and is inhibited only by high levels of selenium in vitro. *The Journal of nutrition* **131:** 301-4

Ganther HE (1999) Selenium metabolism, selenoproteins and mechanisms of cancer prevention: complexities with thioredoxin reductase. *Carcinogenesis* **20:** 1657-66

Ganyc D, Self WT (2008) High affinity selenium uptake in a keratinocyte model. *FEBS letters* **582:** 299-304

Garcia-Manero G, Yang H, Bueso-Ramos C, Ferrajoli A, Cortes J, Wierda WG, Faderl S, Koller C, Morris G, Rosner G, Loboda A, Fantin VR, Randolph SS, Hardwick JS, Reilly JF, Chen C, Ricker JL, Secrist JP, Richon VM, Frankel SR, Kantarjian HM (2008) Phase 1 study of the histone deacetylase inhibitor vorinostat (suberoylanilide hydroxamic acid [SAHA]) in patients with advanced leukemias and myelodysplastic syndromes. *Blood* **111:** 1060-6

Gasparian AV, Yao YJ, Lu J, Yemelyanov AY, Lyakh LA, Slaga TJ, Budunova IV (2002) Selenium compounds inhibit I kappa B kinase (IKK) and nuclear factor-kappa B (NF-kappa B) in prostate cancer cells. *Molecular cancer therapeutics* **1:** 1079-87

Gerard-Marchant R, Hamlin I, Lennert, K. Rilke F, al. e (1974) Classification of non-Hodgkin's lymphomas. *Lancet* **2:** 406-408

Ghesquieres H, Berger F, Felman P, Callet-Bauchu E, Bryon PA, Traverse-Glehen A, Thieblemont C, Baseggio L, Michallet AS, Coiffier B, Salles G (2006) Clinicopathologic characteristics and outcome of diffuse large B-cell lymphomas presenting with an associated low-grade component at diagnosis. *J Clin Oncol* **24:** 5234-41

Giesselbrecht C SN, Mounier N, Ma D, trneny M, Hagberg H, et al (2007) R-ICE versus R-DHAP in relapsed patients with CD20 diffuse large B-cell lymphoma (DLBCL) followed by stem cell transplantation and maintenance treatment with rituximab or not: first interim analysis on 200 patients. CORAL study. *Blood* **110:** abstract 517

Giles FJ, Vose JM, Do KA, Johnson MM, Manshouri T, Bociek G, Bierman PJ, O'Brien SM, Kantarjian HM, Armitage JO, Albitar M (2004) Clinical relevance of circulating angiogenic factors in patients with non-Hodgkin's lymphoma or Hodgkin's lymphoma. *Leuk Res* **28:** 595-604

Ginisty H, Sicard H, Roger B, Bouvet P (1999) Structure and functions of nucleolin. *J Cell Sci* **112 (Pt 6):** 761-72

Glaser KB, Staver MJ, Waring JF, Stender J, Ulrich RG, Davidsen SK (2003) Gene expression profiling of multiple histone deacetylase (HDAC) inhibitors: defining a common gene set produced by HDAC inhibition in T24 and MDA carcinoma cell lines. *Molecular cancer therapeutics* **2:** 151-63

Glass RS, Singh WP, Jung W, Veres Z, Scholz TD, Stadtman TC (1993) Monoselenophosphate: synthesis, characterization, and identity with the prokaryotic biological selenium donor, compound SePX. *Biochemistry* **32:** 12555-9

Gloghini A, Buglio D, Khaskhely NM, Georgakis G, Orlowski RZ, Neelapu SS, Carbone A, Younes A (2009) Expression of histone deacetylases in lymphoma: implication for the development of selective inhibitors. *Br J Haematol* **147:** 515-25

Glozak MA, Seto E (2007) Histone deacetylases and cancer. *Oncogene* **26:** 5420-32

Goel A, Fuerst F, Hotchkiss E, Boland CR (2006) Selenomethionine induces p53 mediated cell cycle arrest and apoptosis in human colon cancer cells. *Cancer biology & therapy* **5:** 529-35

Goenaga-Infante H, Joel S, Warburton E, Hopley C, Hearn R, Juliger S (2007a) Investigation of the selenium species distribution in a human B-cell lymphoma lines by HPLC- and GC-ICP-MS in combination with HPLC-EMIMS/MS and GC-TOFMS after incubation with methylseleninic acid. *Journal of Analytical Atomic Spectrometry* **22:** 888-96

Goenaga-Infante H, Joel SP, Warburton E, Hopley C, Hearn R, Juliger S (2007b) Investigation of the selenium species distribution in a human B-cell lymphoma line by

HPLC- and GC-ICP-MS in combination with HPLC-EMIMS/MS and GC-TOFMS after incubation with methylseleninic acid. *Journal of Analytical Atomic Spectrometry* **22:** 888-896

Golden EB, Lam PY, Kardosh A, Gaffney KJ, Cadenas E, Louie SG, Petasis NA, Chen TC, Schonthal AH (2009) Green tea polyphenols block the anticancer effects of bortezomib and other boronic acid-based proteasome inhibitors. *Blood* **113:** 5927-37

Goldie JH, Coldman AJ (1986) Application of theoretical models to chemotherapy protocol design. *Cancer Treat Rep* **70:** 127-31

Golstein P, Kroemer G (2007) Cell death by necrosis: towards a molecular definition. *Trends Biochem Sci* **32:** 37-43

Gonzalez-Moreno O, Segura V, Serrano D, Nguewa P, de las Rivas J, Calvo A (2007) Methylseleninic acid enhances the effect of etoposide to inhibit prostate cancer growth in vivo. *International journal of cancer* **121:** 1197-204

Goy A, Bernstein SH, Kahl BS, Djulbegovic B, Robertson MJ, de Vos S, Epner E, Krishnan A, Leonard JP, Lonial S, Nasta S, O'Connor OA, Shi H, Boral AL, Fisher RI (2009) Bortezomib in patients with relapsed or refractory mantle cell lymphoma: updated time-to-event analyses of the multicenter phase 2 PINNACLE study. *Ann Oncol* **20:** 520-5

Gratzinger D, Zhao S, Marinelli RJ, Kapp AV, Tibshirani RJ, Hammer AS, Hamilton-Dutoit S, Natkunam Y (2007) Microvessel density and expression of vascular endothelial growth factor and its receptors in diffuse large B-cell lymphoma subtypes. *Am J Pathol* **170:** 1362-9

Gratzinger D, Zhao S, Tibshirani RJ, Hsi ED, Hans CP, Pohlman B, Bast M, Avigdor A, Schiby G, Nagler A, Byrne GE, Jr., Lossos IS, Natkunam Y (2008) Prognostic significance of VEGF, VEGF receptors, and microvessel density in diffuse large B cell lymphoma treated with anthracycline-based chemotherapy. *Lab Invest* **88:** 38-47

Graves JD, Krebs EG (1999) Protein phosphorylation and signal transduction. *Pharmacol Ther* **82:** 111-21

Griner EM, Kazanietz MG (2007) Protein kinase C and other diacylglycerol effectors in cancer. *Nature reviews* **7:** 281-94

Grisendi S, Mecucci C, Falini B, Pandolfi PP (2006) Nucleophosmin and cancer. *Nature reviews* **6:** 493-505

Grogan TM, Fenoglio-Prieser C, Zeheb R, Bellamy W, Frutiger Y, Vela E, Stemmerman G, Macdonald J, Richter L, Gallegos A, Powis G (2000) Thioredoxin, a putative

oncogene product, is overexpressed in gastric carcinoma and associated with increased proliferation and increased cell survival. *Human pathology* **31:** 475-81

Guglielmi C, Gomez F, Philip T, Hagenbeek A, Martelli M, Sebban C, Milpied N, Bron D, Cahn JY, Somers R, Sonneveld P, Gisselbrecht C, Van Der Lelie H, Chauvin F (1998) Time to relapse has prognostic value in patients with aggressive lymphoma enrolled onto the Parma trial. *J Clin Oncol* **16:** 3264-9

Guglielmi C, Martelli M, Federico M, Zinzani PL, Vitolo U, Bellesi G, Santini G, Tarella C, Zallio F, Pregno P, Di Renzo N, Resegotti L (2001) Risk-assessment in diffuse large cell lymphoma at first relapse. A study by the Italian Intergroup for Lymphomas. *Haematologica* **86:** 941-50

Gundimeda U, Schiffman JE, Chhabra D, Wong J, Wu A, Gopalakrishna R (2008) Locally generated methylseleninic acid induces specific inactivation of protein kinase C isoenzymes: relevance to selenium-induced apoptosis in prostate cancer cells. *The Journal of biological chemistry* **283:** 34519-31

Gundimeda U, Schiffman JE, Gottlieb SN, Roth BI, Gopalakrishna R (2009) Negation of the cancer-preventive actions of selenium by over-expression of protein kinase Cepsilon and selenoprotein thioredoxin reductase. *Carcinogenesis* **30:** 1553-61

Guo J, Verma UN, Gaynor RB, Frenkel EP, Becerra CR (2004) Enhanced chemosensitivity to irinotecan by RNA interference-mediated down-regulation of the nuclear factor-kappaB p65 subunit. *Clin Cancer Res* **10:** 3333-41

Gyorgy B, Toth E, Tarcsa E, Falus A, Buzas EI (2006) Citrullination: a posttranslational modification in health and disease. *Int J Biochem Cell Biol* **38:** 1662-77

Hagberg H, Gisselbrecht C (2006) Randomised phase III study of R-ICE versus R-DHAP in relapsed patients with CD20 diffuse large B-cell lymphoma (DLBCL) followed by high-dose therapy and a second randomisation to maintenance treatment with rituximab or not: an update of the CORAL study. *Ann Oncol* **17 Suppl 4:** iv31-2

Haioun C, Lepage E, Gisselbrecht C, Salles G, Coiffier B, Brice P, Bosly A, Morel P, Nouvel C, Tilly H, Lederlin P, Sebban C, Briere J, Gaulard P, Reyes F (2000) Survival benefit of high-dose therapy in poor-risk aggressive non-Hodgkin's lymphoma: final analysis of the prospective LNH87-2 protocol--a groupe d'Etude des lymphomes de l'Adulte study. *J Clin Oncol* **18:** 3025-30

Halkidou K, Gaughan L, Cook S, Leung HY, Neal DE, Robson CN (2004) Upregulation and nuclear recruitment of HDAC1 in hormone refractory prostate cancer. *Prostate* **59:** 177-89

Hamlin PA, Zelenetz AD, Kewalramani T, Qin J, Satagopan JM, Verbel D, Noy A, Portlock CS, Straus DJ, Yahalom J, Nimer SD, Moskowitz CH (2003) Age-adjusted

International Prognostic Index predicts autologous stem cell transplantation outcome for patients with relapsed or primary refractory diffuse large B-cell lymphoma. *Blood* **102:** 1989-96

Hans CP, Weisenburger DD, Greiner TC, Gascoyne RD, Delabie J, Ott G, Muller-Hermelink HK, Campo E, Braziel RM, Jaffe ES, Pan Z, Farinha P, Smith LM, Falini B, Banham AH, Rosenwald A, Staudt LM, Connors JM, Armitage JO, Chan WC (2004) Confirmation of the molecular classification of diffuse large B-cell lymphoma by immunohistochemistry using a tissue microarray. *Blood* **103:** 275-82

Harding HP, Zhang Y, Bertolotti A, Zeng H, Ron D (2000) Perk is essential for translational regulation and cell survival during the unfolded protein response. *Mol Cell* **5:** 897-904

Harris NL, Jaffe ES, Stein H, Banks PM, Chan JK, Cleary ML, Delsol G, De Wolf-Peeters C, Falini B, Gatter KC, et al. (1994) A revised European-American classification of lymphoid neoplasms: a proposal from the International Lymphoma Study Group. *Blood* **84:** 1361-92

Haze K, Yoshida H, Yanagi H, Yura T, Mori K (1999) Mammalian transcription factor ATF6 is synthesized as a transmembrane protein and activated by proteolysis in response to endoplasmic reticulum stress. *Molecular biology of the cell* **10:** 3787-99

He C, Klionsky DJ (2009) Regulation mechanisms and signaling pathways of autophagy. *Annu Rev Genet* **43:** 67-93

Hicks EB, Rappaport H, Winter WJ (1956) Follicular lymphoma; a re-evaluation of its position in the scheme of malignant lymphoma, based on a survey of 253 cases. *Cancer* **9:** 792-821

Hideshima T, Ikeda H, Chauhan D, Okawa Y, Raje N, Podar K, Mitsiades C, Munshi NC, Richardson PG, Carrasco RD, Anderson KC (2009) Bortezomib induces canonical nuclear factor-kappaB activation in multiple myeloma cells. *Blood* **114:** 1046-52

Hideshima T, Richardson P, Chauhan D, Palombella VJ, Elliott PJ, Adams J, Anderson KC (2001) The proteasome inhibitor PS-341 inhibits growth, induces apoptosis, and overcomes drug resistance in human multiple myeloma cells. *Cancer Res* **61:** 3071-6

Hill DS, Martin S, Armstrong JL, Flockhart R, Tonison JJ, Simpson DG, Birch-Machin MA, Redfern CP, Lovat PE (2009) Combining the endoplasmic reticulum stress-inducing agents bortezomib and fenretinide as a novel therapeutic strategy for metastatic melanoma. *Clin Cancer Res* **15:** 1192-8

Hill KE, Zhou J, McMahan WJ, Motley AK, Atkins JF, Gesteland RF, Burk RF (2003) Deletion of selenoprotein P alters distribution of selenium in the mouse. *The Journal of biological chemistry* **278:** 13640-6

Hill KE, Zhou J, McMahan WJ, Motley AK, Burk RF (2004) Neurological dysfunction occurs in mice with targeted deletion of the selenoprotein P gene. *The Journal of nutrition* **134:** 157-61

Hoang B, Benavides A, Shi Y, Frost P, Lichtenstein A (2009) Effect of autophagy on multiple myeloma cell viability. *Molecular cancer therapeutics* **8:** 1974-84

Hodges GF, Lenhardt TM, Cotelingam JD (1994) Bone marrow involvement in large-cell lymphoma. Prognostic implications of discordant disease. *Am J Clin Pathol* **101:** 305-11

Hodgkin T (1832) On some morbid experiences of the absorbant glands and spleen. *Medical-Chirurgical Trans* **17:** 68-97

Hofmann MA, Schiekofer S, Isermann B, Kanitz M, Henkels M, Joswig M, Treusch A, Morcos M, Weiss T, Borcea V, Abdel Khalek AK, Amiral J, Tritschler H, Ritz E, Wahl P, Ziegler R, Bierhaus A, Nawroth PP (1999) Peripheral blood mononuclear cells isolated from patients with diabetic nephropathy show increased activation of the oxidative-stress sensitive transcription factor NF-kappaB. *Diabetologia* **42:** 222-32

Holford NH, Sheiner LB (1982) Kinetics of pharmacologic response. *Pharmacol Ther* **16:** 143-66

Hong S, Pedersen PL (2008) ATP synthase and the actions of inhibitors utilized to study its roles in human health, disease, and other scientific areas. *Microbiol Mol Biol Rev* **72:** 590-641, Table of Contents

Horning SJ, Weller E, Kim K, Earle JD, O'Connell MJ, Habermann TM, Glick JH (2004) Chemotherapy with or without radiotherapy in limited-stage diffuse aggressive non-Hodgkin's lymphoma: Eastern Cooperative Oncology Group study 1484. *J Clin Oncol* **22:** 3032-8

Hoskins PJ, Le N, Gascoyne RD, Klasa R, Shenkier T, O'Reilly S, Connors JM (1997) Advanced diffuse large-cell lymphoma treated with 12-week combination chemotherapy: natural history of relapse after initial complete response and prognostic variables defining outcome after relapse. *Ann Oncol* **8:** 1125-32

Hoyer-Hansen M, Jaattela M (2007) Connecting endoplasmic reticulum stress to autophagy by unfolded protein response and calcium. *Cell Death Differ* **14:** 1576-82

Hu H, Jiang C, Ip C, Rustum YM, Lu J (2005a) Methylseleninic acid potentiates apoptosis induced by chemotherapeutic drugs in androgen-independent prostate cancer cells. *Clin Cancer Res* **11:** 2379-88

Hu H, Jiang C, Li G, Lu J (2005b) PKB/AKT and ERK regulation of caspase-mediated apoptosis by methylseleninic acid in LNCaP prostate cancer cells. *Carcinogenesis* **26:** 1374-81

Hu H, Li GX, Wang L, Watts J, Combs GF, Jr., Lu J (2008) Methylseleninic acid enhances taxane drug efficacy against human prostate cancer and down-regulates antiapoptotic proteins Bcl-XL and survivin. *Clin Cancer Res* **14:** 1150-8

Hu P, Han Z, Couvillon AD, Exton JH (2004) Critical role of endogenous Akt/IAPs and MEK1/ERK pathways in counteracting endoplasmic reticulum stress-induced cell death. *The Journal of biological chemistry* **279:** 49420-9

Hu P, Han Z, Couvillon AD, Kaufman RJ, Exton JH (2006) Autocrine tumor necrosis factor alpha links endoplasmic reticulum stress to the membrane death receptor pathway through IRE1alpha-mediated NF-kappaB activation and down-regulation of TRAF2 expression. *Molecular and cellular biology* **26:** 3071-84

Hu YJ, Chen Y, Zhang YQ, Zhou MZ, Song XM, Zhang BZ, Luo L, Xu PM, Zhao YN, Zhao YB, Cheng G (1997) The protective role of selenium on the toxicity of cisplatin-contained chemotherapy regimen in cancer patients. *Biological trace element research* **56:** 331-41

Hu YJ, Diamond AM (2003) Role of glutathione peroxidase 1 in breast cancer: loss of heterozygosity and allelic differences in the response to selenium. *Cancer Res* **63:** 3347-51

Hu YJ, Korotkov KV, Mehta R, Hatfield DL, Rotimi CN, Luke A, Prewitt TE, Cooper RS, Stock W, Vokes EE, Dolan ME, Gladyshev VN, Diamond AM (2001) Distribution and functional consequences of nucleotide polymorphisms in the 3'-untranslated region of the human Sep15 gene. *Cancer Res* **61:** 2307-10

Huang HC, Nguyen T, Pickett CB (2002) Phosphorylation of Nrf2 at Ser-40 by protein kinase C regulates antioxidant response element-mediated transcription. *The Journal of biological chemistry* **277:** 42769-74

Huang TY, DerMardirossian C, Bokoch GM (2006) Cofilin phosphatases and regulation of actin dynamics. *Curr Opin Cell Biol* **18:** 26-31

Hung CC, Ichimura T, Stevens JL, Bonventre JV (2003) Protection of renal epithelial cells against oxidative injury by endoplasmic reticulum stress preconditioning is mediated by ERK1/2 activation. *The Journal of biological chemistry* **278:** 29317-26
Hunter T (1995) Protein kinases and phosphatases: the yin and yang of protein phosphorylation and signaling. *Cell* **80:** 225-36

Hurst R, Armah CN, Dainty JR, Hart DJ, Teucher B, Goldson AJ, Broadley MR, Motley AK, Fairweather-Tait SJ (2010) Establishing optimal selenium status: results of a randomized, double-blind, placebo-controlled trial. *The American journal of clinical nutrition* **91:** 923-31

Hurwitz BE, Klaus JR, Llabre MM, Gonzalez A, Lawrence PJ, Maher KJ, Greeson JM, Baum MK, Shor-Posner G, Skyler JS, Schneiderman N (2007) Suppression of human immunodeficiency virus type 1 viral load with selenium supplementation: a randomized controlled trial. *Archives of internal medicine* **167:** 148-54

IARC GLOBOCAN 2002. Cancer Incidence, Mortality and Prevalence Worldwide (2002 estimates), 2006

Ichikawa A, Kinoshita T, Watanabe T, Kato H, Nagai H, Tsushita K, Saito H, Hotta T (1997) Mutations of the p53 gene as a prognostic factor in aggressive B-cell lymphoma. *The New England journal of medicine* **337:** 529-34

Imai T, Mihara H, Kurihara T, Esaki N (2009) Selenocysteine is selectively taken up by red blood cells. *Biosci Biotechnol Biochem* **73:** 2746-8

Insinga A, Monestiroli S, Ronzoni S, Gelmetti V, Marchesi F, Viale A, Altucci L, Nervi C, Minucci S, Pelicci PG (2005) Inhibitors of histone deacetylases induce tumor-selective apoptosis through activation of the death receptor pathway. *Nat Med* **11:** 71-6

Ip C, Hayes C (1989) Tissue selenium levels in selenium-supplemented rats and their relevance in mammary cancer protection. *Carcinogenesis* **10:** 921-5

Ip C, Hayes C, Budnick RM, Ganther HE (1991) Chemical form of selenium, critical metabolites, and cancer prevention. *Cancer Res* **51:** 595-600

Ip C, Lisk DJ (1997) Modulation of phase I and phase II xenobiotic-metabolizing enzymes by selenium-enriched garlic in rats. *Nutrition and cancer* **28:** 184-8

Ip C, Thompson HJ, Zhu Z, Ganther HE (2000) In vitro and in vivo studies of methylseleninic acid: evidence that a monomethylated selenium metabolite is critical for cancer chemoprevention. *Cancer research* **60:** 2882-6

Ip C, Zhu Z, Thompson HJ, Lisk D, Ganther HE (1999) Chemoprevention of mammary cancer with Se-allylselenocysteine and other selenoamino acids in the rat. *Anticancer research* **19:** 2875-80

Irons R, Tsuji PA, Carlson BA, Ouyang P, Yoo MH, Xu XM, Hatfield DL, Gladyshev VN, Davis CD (2010) Deficiency in the 15-kDa selenoprotein inhibits tumorigenicity and metastasis of colon cancer cells. *Cancer Prev Res (Phila Pa)* **3:** 630-9

Jaakkola P, Mole DR, Tian YM, Wilson MI, Gielbert J, Gaskell SJ, Kriegsheim A, Hebestreit HF, Mukherji M, Schofield CJ, Maxwell PH, Pugh CW, Ratcliffe PJ (2001) Targeting of HIF-alpha to the von Hippel-Lindau ubiquitylation complex by O2-regulated prolyl hydroxylation. *Science (New York, NY* **292:** 468-72

Jablonska E, Gromadzinska J, Reszka E, Wasowicz W, Sobala W, Szeszenia-Dabrowska N, Boffetta P (2009) Association between GPx1 Pro198Leu polymorphism, GPx1 activity and plasma selenium concentration in humans. *European journal of nutrition* **48:** 383-6

Jablonska E, Gromadzinska J, Sobala W, Reszka E, Wasowicz W (2008) Lung cancer risk associated with selenium status is modified in smoking individuals by Sep15 polymorphism. *European journal of nutrition* **47:** 47-54

Jaffe ES, Harris N, Stein H, Vardiman J (2001) Pathology and Genetics of Tumours of Haematopoietic and Lympoid Tissues: Lyon, France. *IARC Press*

Jaffe ES, Harris NL, Stein H, Isaacson PG (2008) Classification of lymphoid neoplasms: the microscope as a tool for disease discovery. *Blood* **112:** 4384-99

Jantunen E, Canals C, Rambaldi A, Ossenkoppele G, Allione B, Blaise D, Conde E, Tilly H, Cook G, Clark F, Gallamini A, Haynes A, Mounier N, Dreger P, Pfreundschuh M, Sureda A (2008) Autologous stem cell transplantation in elderly patients (> or =60 years) with diffuse large B-cell lymphoma: an analysis based on data in the European Blood and Marrow Transplantation registry. *Haematologica* **93:** 1837-42

Jariwalla RJ, Gangapurkar B, Nakamura D (2009) Differential sensitivity of various human tumour-derived cell types to apoptosis by organic derivatives of selenium. *The British journal of nutrition* **101:** 182-9

Jemal A, Siegel R, Ward E, Hao Y, Xu J, Thun MJ (2009) Cancer statistics, 2009. *CA Cancer J Clin* **59:** 225-49

Jenuwein T, Allis CD (2001) Translating the histone code. *Science (New York, NY* **293:** 1074-80

Jeong SW, Jung HJ, Rahman MM, Hwang JN, Seo YR (2009) Protective effects of selenomethionine against ionizing radiation under the modulation of p53 tumor suppressor. *J Med Food* **12:** 389-93

Jiang C, Ganther H, Lu J (2000) Monomethyl selenium--specific inhibition of MMP-2 and VEGF expression: implications for angiogenic switch regulation. *Molecular carcinogenesis* **29:** 236-50

Jiang C, Jiang W, Ip C, Ganther H, Lu J (1999) Selenium-induced inhibition of angiogenesis in mammary cancer at chemopreventive levels of intake. *Molecular carcinogenesis* **26:** 213-25

Jiang C, Wang Z, Ganther H, Lu J (2001) Caspases as key executors of methyl selenium-induced apoptosis (anoikis) of DU-145 prostate cancer cells. *Cancer Res* **61:** 3062-70

Jiang C, Wang Z, Ganther H, Lu J (2002) Distinct effects of methylseleninic acid versus selenite on apoptosis, cell cycle, and protein kinase pathways in DU145 human prostate cancer cells. *Molecular cancer therapeutics* **1:** 1059-66

Jiang HY, Wek SA, McGrath BC, Scheuner D, Kaufman RJ, Cavener DR, Wek RC (2003) Phosphorylation of the alpha subunit of eukaryotic initiation factor 2 is required for activation of NF-kappaB in response to diverse cellular stresses. *Molecular and cellular biology* **23:** 5651-63

Jiang W, Jiang C, Pei H, Wang L, Zhang J, Hu H, Lu J (2009) In vivo molecular mediators of cancer growth suppression and apoptosis by selenium in mammary and prostate models: lack of involvement of gadd genes. *Molecular cancer therapeutics* **8:** 682-91

Jimbo A, Fujita E, Kouroku Y, Ohnishi J, Inohara N, Kuida K, Sakamaki K, Yonehara S, Momoi T (2003) ER stress induces caspase-8 activation, stimulating cytochrome c release and caspase-9 activation. *Experimental cell research* **283:** 156-66

Johnson PW, Rohatiner AZ, Whelan JS, Price CG, Love S, Lim J, Matthews J, Norton AJ, Amess JA, Lister TA (1995) Patterns of survival in patients with recurrent follicular lymphoma: a 20-year study from a single center. *J Clin Oncol* **13:** 140-7

Johnson PW, Sweetenham JW, McCallum P, Norton AJ, Rohatiner AZ, Lister TA (1993) E-SHAP: inadequate treatment for poor-prognosis recurrent lymphoma. *Ann Oncol* **4:** 63-7

Jorgensen JM, Sorensen FB, Bendix K, Nielsen JL, Olsen ML, Funder AM, d'Amore F (2007) Angiogenesis in non-Hodgkin's lymphoma: clinico-pathological correlations and prognostic significance in specific subtypes. *Leuk Lymphoma* **48:** 584-95

Jost PJ, Ruland J (2007) Aberrant NF-kappaB signaling in lymphoma: mechanisms, consequences, and therapeutic implications. *Blood* **109:** 2700-7

Juliger S, Goenaga-Infante H, Lister TA, Fitzgibbon J, Joel SP (2007) Chemosensitization of B-cell lymphomas by methylseleninic acid involves nuclear factor-kappaB inhibition and the rapid generation of other selenium species. *Cancer research* **67:** 10984-92

Jung U, Zheng X, Yoon SO, Chung AS (2001) Se-methylselenocysteine induces apoptosis mediated by reactive oxygen species in HL-60 cells. *Free radical biology & medicine* **31:** 479-89

Kabore AF, Sun J, Hu X, McCrea K, Johnston JB, Gibson SB (2006) The TRAIL apoptotic pathway mediates proteasome inhibitor induced apoptosis in primary chronic lymphocytic leukemia cells. *Apoptosis* **11:** 1175-93

Kaeck M, Lu J, Strange R, Ip C, Ganther HE, Thompson HJ (1997) Differential induction of growth arrest inducible genes by selenium compounds. *Biochemical pharmacology* **53:** 921-6

Kanzawa T, Germano IM, Komata T, Ito H, Kondo Y, Kondo S (2004) Role of autophagy in temozolomide-induced cytotoxicity for malignant glioma cells. *Cell Death Differ* **11:** 448-57

Kanzawa T, Kondo Y, Ito H, Kondo S, Germano I (2003) Induction of autophagic cell death in malignant glioma cells by arsenic trioxide. *Cancer Res* **63:** 2103-8

Karin M (1999) How NF-kappaB is activated: the role of the IkappaB kinase (IKK) complex. *Oncogene* **18:** 6867-74

Karunasinghe N, Ferguson LR, Tuckey J, Masters J (2006) Hemolysate thioredoxin reductase and glutathione peroxidase activities correlate with serum selenium in a group of New Zealand men at high prostate cancer risk. *The Journal of nutrition* **136:** 2232-5

Karunasinghe N, Ryan J, Tuckey J, Masters J, Jamieson M, Clarke LC, Marshall JR, Ferguson LR (2004) DNA stability and serum selenium levels in a high-risk group for prostate cancer. *Cancer Epidemiol Biomarkers Prev* **13:** 391-7

Kato H, Tamamizu-Kato S, Shibasaki F (2004) Histone deacetylase 7 associates with hypoxia-inducible factor 1alpha and increases transcriptional activity. *The Journal of biological chemistry* **279:** 41966-74

Kawaguchi Y, Kovacs JJ, McLaurin A, Vance JM, Ito A, Yao TP (2003) The deacetylase HDAC6 regulates aggresome formation and cell viability in response to misfolded protein stress. *Cell* **115:** 727-38

Keck A, Finley J (2006) Database values do not relfect selenium contents of grain, cereals, and other foods grown or purchased in the upper Midwest of the United States. *Nutrition Research* **26:** 17-22

Kelly E, Greene CM, Carroll TP, McElvaney NG, O'Neill SJ (2009) Selenoprotein S/SEPS1 modifies endoplasmic reticulum stress in Z variant alpha1-antitrypsin deficiency. *The Journal of biological chemistry* **284:** 16891-7

Kern J, Untergasser G, Zenzmaier C, Sarg B, Gastl G, Gunsilius E, Steurer M (2009) GRP-78 secreted by tumor cells blocks the antiangiogenic activity of bortezomib. *Blood* **114:** 3960-7

Kewalramani T, Zelenetz AD, Nimer SD, Portlock C, Straus D, Noy A, O'Connor O, Filippa DA, Teruya-Feldstein J, Gencarelli A, Qin J, Waxman A, Yahalom J, Moskowitz CH (2004) Rituximab and ICE as second-line therapy before autologous stem cell transplantation for relapsed or primary refractory diffuse large B-cell lymphoma. *Blood* **103:** 3684-8

Khan N, Jeffers M, Kumar S, Hackett C, Boldog F, Khramtsov N, Qian X, Mills E, Berghs SC, Carey N, Finn PW, Collins LS, Tumber A, Ritchie JW, Jensen PB, Lichenstein HS, Sehested M (2008) Determination of the class and isoform selectivity of small-molecule histone deacetylase inhibitors. *The Biochemical journal* **409:** 581-9

Kim A, Oh JH, Park JM, Chung AS (2007a) Methylselenol generated from selenomethionine by methioninase downregulates integrin expression and induces caspase-mediated apoptosis of B16F10 melanoma cells. *J Cell Physiol* **212:** 386-400

Kim EH, Sohn S, Kwon HJ, Kim SU, Kim MJ, Lee SJ, Choi KS (2007b) Sodium selenite induces superoxide-mediated mitochondrial damage and subsequent autophagic cell death in malignant glioma cells. *Cancer Res* **67:** 6314-24

Kim MS, Blake M, Baek JH, Kohlhagen G, Pommier Y, Carrier F (2003) Inhibition of histone deacetylase increases cytotoxicity to anticancer drugs targeting DNA. *Cancer Res* **63:** 7291-300

Kim MS, Kwon HJ, Lee YM, Baek JH, Jang JE, Lee SW, Moon EJ, Kim HS, Lee SK, Chung HY, Kim CW, Kim KW (2001) Histone deacetylases induce angiogenesis by negative regulation of tumor suppressor genes. *Nat Med* **7:** 437-43

Kim SH, Jeong JW, Park JA, Lee JW, Seo JH, Jung BK, Bae MK, Kim KW (2007c) Regulation of the HIF-1alpha stability by histone deacetylases. *Oncol Rep* **17:** 647-51

Kim YJ, Ahn JY, Liang P, Ip C, Zhang Y, Park YM (2007d) Human prx1 gene is a target of Nrf2 and is up-regulated by hypoxia/reoxygenation: implication to tumor biology. *Cancer Res* **67:** 546-54

Kim YJ, Baek SH, Bogner PN, Ip C, Rustum YM, Fakih M, Ramnath N, park YM (2007e) Targeting the Nrf2-Prx1 pathway with selenium to enhance the efficacy and selectivity of cancer therapy. *Journal of Cancer Molecules* **3:** 37-73

Kiremidjian-Schumacher L, Roy M, Wishe HI, Cohen MW, Stotzky G (1994) Supplementation with selenium and human immune cell functions. II. Effect on cytotoxic lymphocytes and natural killer cells. *Biological trace element research* **41:** 115-27

Kise Y, Yoshimura S, Akieda K, Umezawa K, Okada K, Yoshitake N, Shiramizu H, Yamamoto I, Inokuchi S (2004) Acute oral selenium intoxication with ten times the lethal dose resulting in deep gastric ulcer. *The Journal of emergency medicine* **26:** 183-7

Klimo P, Connors JM (1985) MACOP-B chemotherapy for the treatment of diffuse large-cell lymphoma. *Annals of internal medicine* **102:** 596-602

Klionsky DJ, Abeliovich H, Agostinis P, Agrawal DK, Aliev G, Askew DS, Baba M, Baehrecke EH, Bahr BA, Ballabio A, Bamber BA, Bassham DC, Bergamini E, Bi X, Biard-Piechaczyk M, Blum JS, Bredesen DE, Brodsky JL, Brumell JH, Brunk UT, Bursch W, Camougrand N, Cebollero E, Cecconi F, Chen Y, Chin LS, Choi A, Chu CT, Chung J, Clarke PG, Clark RS, Clarke SG, Clave C, Cleveland JL, Codogno P, Colombo MI, Coto-Montes A, Cregg JM, Cuervo AM, Debnath J, Demarchi F, Dennis PB, Dennis PA, Deretic V, Devenish RJ, Di Sano F, Dice JF, Difiglia M, Dinesh-Kumar S, Distelhorst CW, Djavaheri-Mergny M, Dorsey FC, Droge W, Dron M, Dunn WA, Jr., Duszenko M, Eissa NT, Elazar Z, Esclatine A, Eskelinen EL, Fesus L, Finley KD, Fuentes JM, Fueyo J, Fujisaki K, Galliot B, Gao FB, Gewirtz DA, Gibson SB, Gohla A, Goldberg AL, Gonzalez R, Gonzalez-Estevez C, Gorski S, Gottlieb RA, Haussinger D, He YW, Heidenreich K, Hill JA, Hoyer-Hansen M, Hu X, Huang WP, Iwasaki A, Jaattela M, Jackson WT, Jiang X, Jin S, Johansen T, Jung JU, Kadowaki M, Kang C, Kelekar A, Kessel DH, Kiel JA, Kim HP, Kimchi A, Kinsella TJ, Kiselyov K, Kitamoto K, Knecht E, Komatsu M, Kominami E, Kondo S, Kovacs AL, Kroemer G, Kuan CY, Kumar R, Kundu M, Landry J, Laporte M, Le W, Lei HY, Lenardo MJ, Levine B, Lieberman A, Lim KL, Lin FC, Liou W, Liu LF, Lopez-Berestein G, Lopez-Otin C, Lu B, Macleod KF, Malorni W, Martinet W, Matsuoka K, Mautner J, Meijer AJ, Melendez A, Michels P, Miotto G, Mistiaen WP, Mizushima N, Mograbi B, Monastyrska I, Moore MN, Moreira PI, Moriyasu Y, Motyl T, Munz C, Murphy LO, Naqvi NI, Neufeld TP, Nishino I, Nixon RA, Noda T, Nurnberg B, Ogawa M, Oleinick NL, Olsen LJ, Ozpolat B, Paglin S, Palmer GE, Papassideri I, Parkes M, Perlmutter DH, Perry G, Piacentini M, Pinkas-Kramarski R, Prescott M, Proikas-Cezanne T, Raben N, Rami A, Reggiori F, Rohrer B, Rubinsztein DC, Ryan KM, Sadoshima J, Sakagami H, Sakai Y, Sandri M, Sasakawa C, Sass M, Schneider C, Seglen PO, Seleverstov O, Settleman J, Shacka JJ, Shapiro IM, Sibirny A, Silva-Zacarin EC, Simon HU, Simone C, Simonsen A, Smith MA, Spanel-Borowski K, Srinivas V, Steeves M, Stenmark H, Stromhaug PE, Subauste CS, Sugimoto S, Sulzer D, Suzuki T, Swanson MS, Tabas I, Takeshita F, Talbot NJ, Talloczy Z, Tanaka K, Tanida I, Taylor GS, Taylor JP, Terman A, Tettamanti G, Thompson CB,

Thumm M, Tolkovsky AM, Tooze SA, Truant R, Tumanovska LV, Uchiyama Y, Ueno T, Uzcategui NL, van der Klei I, Vaquero EC, Vellai T, Vogel MW, Wang HG, Webster P, Wiley JW, Xi Z, Xiao G, Yahalom J, Yang JM, Yap G, Yin XM, Yoshimori T, Yu L, Yue Z, Yuzaki M, Zabirnyk O, Zheng X, Zhu X, Deter RL (2008) Guidelines for the use and interpretation of assays for monitoring autophagy in higher eukaryotes. *Autophagy* **4:** 151-75

Kluin-Nelemans HC, Limpens J, Meerabux J, Beverstock GC, Jansen JH, de Jong D, Kluin PM (1991) A new non-Hodgkin's B-cell line (DoHH2) with a chromosomal translocation t(14;18)(q32;q21). *Leukemia* **5:** 221-4

Knekt P, Aromaa A, Maatela J, Alfthan G, Aaran RK, Hakama M, Hakulinen T, Peto R, Teppo L (1990) Serum selenium and subsequent risk of cancer among Finnish men and women. *Journal of the National Cancer Institute* **82:** 864-8

Kobayashi Y, Ogra Y, Ishiwata K, Takayama H, Aimi N, Suzuki KT (2002) Selenosugars are key and urinary metabolites for selenium excretion within the required to low-toxic range. *Proceedings of the National Academy of Sciences of the United States of America* **99:** 15932-6

Koch P, del Valle F, Berdel WE, Willich NA, Reers B, Hiddemann W, Grothaus-Pinke B, Reinartz G, Brockmann J, Temmesfeld A, Schmitz R, Rube C, Probst A, Jaenke G, Bodenstein H, Junker A, Pott C, Schultze J, Heinecke A, Parwaresch R, Tiemann M (2001) Primary gastrointestinal non-Hodgkin's lymphoma: I. Anatomic and histologic distribution, clinical features, and survival data of 371 patients registered in the German Multicenter Study GIT NHL 01/92. *J Clin Oncol* **19:** 3861-73

Kong X, Lin Z, Liang D, Fath D, Sang N, Caro J (2006) Histone deacetylase inhibitors induce VHL and ubiquitin-independent proteasomal degradation of hypoxia-inducible factor 1alpha. *Molecular and cellular biology* **26:** 2019-28

Korotkov KV, Kumaraswamy E, Zhou Y, Hatfield DL, Gladyshev VN (2001) Association between the 15-kDa selenoprotein and UDP-glucose:glycoprotein glucosyltransferase in the endoplasmic reticulum of mammalian cells. *The Journal of biological chemistry* **276:** 15330-6

Kouroku Y, Fujita E, Tanida I, Ueno T, Isoai A, Kumagai H, Ogawa S, Kaufman RJ, Kominami E, Momoi T (2007) ER stress (PERK/eIF2alpha phosphorylation) mediates the polyglutamine-induced LC3 conversion, an essential step for autophagy formation. *Cell Death Differ* **14:** 230-9

Kozutsumi Y, Segal M, Normington K, Gething MJ, Sambrook J (1988) The presence of malfolded proteins in the endoplasmic reticulum signals the induction of glucose-regulated proteins. *Nature* **332:** 462-4

Kraus M, Malenke E, Gogel J, Muller H, Ruckrich T, Overkleeft H, Ovaa H, Koscielniak E, Hartmann JT, Driessen C (2008) Ritonavir induces endoplasmic reticulum stress and sensitizes sarcoma cells toward bortezomib-induced apoptosis. *Molecular cancer therapeutics* **7:** 1940-8

Kridel SJ, Axelrod F, Rozenkrantz N, Smith JW (2004) Orlistat is a novel inhibitor of fatty acid synthase with antitumor activity. *Cancer Res* **64:** 2070-5

Kroemer G, Galluzzi L, Vandenabeele P, Abrams J, Alnemri ES, Baehrecke EH, Blagosklonny MV, El-Deiry WS, Golstein P, Green DR, Hengartner M, Knight RA, Kumar S, Lipton SA, Malorni W, Nunez G, Peter ME, Tschopp J, Yuan J, Piacentini M, Zhivotovsky B, Melino G (2009) Classification of cell death: recommendations of the Nomenclature Committee on Cell Death 2009. *Cell Death Differ* **16:** 3-11

Kryukov GV, Castellano S, Novoselov SV, Lobanov AV, Zehtab O, Guigo R, Gladyshev VN (2003) Characterization of mammalian selenoproteomes. *Science (New York, NY* **300:** 1439-43

Kuehnelt D, Juresa D, Francesconi KA, Fakih M, Reid ME (2007) Selenium metabolites in urine of cancer patients receiving L-selenomethionine at high doses. *Toxicology and applied pharmacology* **220:** 211-5

Kuehnelt D, Kienzl N, Traar P, Le NH, Francesconi KA, Ochi T (2005) Selenium metabolites in human urine after ingestion of selenite, L-selenomethionine, or DL-selenomethionine: a quantitative case study by HPLC/ICPMS. *Analytical and bioanalytical chemistry* **383:** 235-46

Kumaraswamy E, Malykh A, Korotkov KV, Kozyavkin S, Hu Y, Kwon SY, Moustafa ME, Carlson BA, Berry MJ, Lee BJ, Hatfield DL, Diamond AM, Gladyshev VN (2000) Structure-expression relationships of the 15-kDa selenoprotein gene. Possible role of the protein in cancer etiology. *The Journal of biological chemistry* **275:** 35540-7

Labunskyy VM, Yoo MH, Hatfield DL, Gladyshev VN (2009) Sep15, a thioredoxin-like selenoprotein, is involved in the unfolded protein response and differentially regulated by adaptive and acute ER stresses. *Biochemistry* **48:** 8458-65

Lambert LA, Qiao N, Hunt KK, Lambert DH, Mills GB, Meijer L, Keyomarsi K (2008) Autophagy: a novel mechanism of synergistic cytotoxicity between doxorubicin and roscovitine in a sarcoma model. *Cancer Res* **68:** 7966-74

Larouche JF, Berger F, Chassagne-Clement C, Ffrench M, Callet-Bauchu E, Sebban C, Ghesquieres H, Broussais-Guillaumot F, Salles G, Coiffier B (2010) Lymphoma recurrence 5 years or later following diffuse large B-cell lymphoma: clinical characteristics and outcome. *J Clin Oncol* **28:** 2094-100

Larsen MR, Thingholm TE, Jensen ON, Roepstorff P, Jorgensen TJ (2005) Highly selective enrichment of phosphorylated peptides from peptide mixtures using titanium dioxide microcolumns. *Mol Cell Proteomics* **4:** 873-86

Last K, Maharaj L, Perry J, Strauss S, Fitzgibbon J, Lister TA, Joel S (2006) The activity of methylated and non-methylated selenium species in lymphoma cell lines and primary tumours. *Ann Oncol* **17:** 773-9

Last KW, Cornelius V, Delves T, Sieniawska C, Fitzgibbon J, Norton A, Amess J, Wilson A, Rohatiner AZ, Lister TA (2003) Presentation serum selenium predicts for overall survival, dose delivery, and first treatment response in aggressive non-Hodgkin's lymphoma. *J Clin Oncol* **21:** 2335-41

Lee AH, Iwakoshi NN, Glimcher LH (2003) XBP-1 regulates a subset of endoplasmic reticulum resident chaperone genes in the unfolded protein response. *Molecular and cellular biology* **23:** 7448-59

Lee AS (2007) GRP78 induction in cancer: therapeutic and prognostic implications. *Cancer Res* **67:** 3496-9

Lee BJ, Worland PJ, Davis JN, Stadtman TC, Hatfield DL (1989) Identification of a selenocysteyl-tRNA(Ser) in mammalian cells that recognizes the nonsense codon, UGA. *The Journal of biological chemistry* **264:** 9724-7

Lee JI, Nian H, Cooper AJ, Sinha R, Dai J, Bisson WH, Dashwood RH, Pinto JT (2009a) Alpha-keto acid metabolites of naturally occurring organoselenium compounds as inhibitors of histone deacetylase in human prostate cancer cells. *Cancer Prev Res (Phila Pa)* **2:** 683-93

Lee JT, Lee TJ, Park JW, Kwon TK (2009b) Se-methylselenocysteine sensitized TRAIL-mediated apoptosis via down-regulation of Bcl-2 expression. *Int J Oncol* **34:** 1455-60

Lee SO, Nadiminty N, Wu XX, Lou W, Dong Y, Ip C, Onate SA, Gao AC (2005) Selenium disrupts estrogen signaling by altering estrogen receptor expression and ligand binding in human breast cancer cells. *Cancer Res* **65:** 3487-92

Lee SO, Yeon Chun J, Nadiminty N, Trump DL, Ip C, Dong Y, Gao AC (2006) Monomethylated selenium inhibits growth of LNCaP human prostate cancer xenograft accompanied by a decrease in the expression of androgen receptor and prostate-specific antigen (PSA). *Prostate* **66:** 1070-5

Lei K, Davis RJ (2003) JNK phosphorylation of Bim-related members of the Bcl2 family induces Bax-dependent apoptosis. *Proceedings of the National Academy of Sciences of the United States of America* **100:** 2432-7

Lenz G, Dreyling M, Hoster E, Wormann B, Duhrsen U, Metzner B, Eimermacher H, Neubauer A, Wandt H, Steinhauer H, Martin S, Heidemann E, Aldaoud A, Parwaresch R, Hasford J, Unterhalt M, Hiddemann W (2005) Immunochemotherapy with rituximab and cyclophosphamide, doxorubicin, vincristine, and prednisone significantly improves response and time to treatment failure, but not long-term outcome in patients with previously untreated mantle cell lymphoma: results of a prospective randomized trial of the German Low Grade Lymphoma Study Group (GLSG). *J Clin Oncol* **23:** 1984-92

Lenz G, Wright G, Dave SS, Xiao W, Powell J, Zhao H, Xu W, Tan B, Goldschmidt N, Iqbal J, Vose J, Bast M, Fu K, Weisenburger DD, Greiner TC, Armitage JO, Kyle A, May L, Gascoyne RD, Connors JM, Troen G, Holte H, Kvaloy S, Dierickx D, Verhoef G, Delabie J, Smeland EB, Jares P, Martinez A, Lopez-Guillermo A, Montserrat E, Campo E, Braziel RM, Miller TP, Rimsza LM, Cook JR, Pohlman B, Sweetenham J, Tubbs RR, Fisher RI, Hartmann E, Rosenwald A, Ott G, Muller-Hermelink HK, Wrench D, Lister TA, Jaffe ES, Wilson WH, Chan WC, Staudt LM (2008a) Stromal gene signatures in large-B-cell lymphomas. *The New England journal of medicine* **359:** 2313-23

Lenz G, Wright GW, Emre NC, Kohlhammer H, Dave SS, Davis RE, Carty S, Lam LT, Shaffer AL, Xiao W, Powell J, Rosenwald A, Ott G, Muller-Hermelink HK, Gascoyne RD, Connors JM, Campo E, Jaffe ES, Delabie J, Smeland EB, Rimsza LM, Fisher RI, Weisenburger DD, Chan WC, Staudt LM (2008b) Molecular subtypes of diffuse large B-cell lymphoma arise by distinct genetic pathways. *Proceedings of the National Academy of Sciences of the United States of America* **105:** 13520-5

Leung FY, Henderson AR (1981) Comparison of three serum alpha-hydroxybutyrate dehydrogenase procedures for lactate dehydrogenase isoenzyme discrimination. *Clin Chim Acta* **115:** 145-53

Levine B, Kroemer G (2008) Autophagy in the pathogenesis of disease. *Cell* **132:** 27-42

Li F, Altieri DC (1999) Transcriptional analysis of human survivin gene expression. *The Biochemical journal* **344 Pt 2:** 305-11

Li GX, Lee HJ, Wang Z, Hu H, Liao JD, Watts JC, Combs GF, Jr., Lu J (2008a) Superior in vivo inhibitory efficacy of methylseleninic acid against human prostate cancer over selenomethionine or selenite. *Carcinogenesis* **29:** 1005-12

Li H, Kantoff PW, Giovannucci E, Leitzmann MF, Gaziano JM, Stampfer MJ, Ma J (2005) Manganese superoxide dismutase polymorphism, prediagnostic antioxidant status, and risk of clinical significant prostate cancer. *Cancer Res* **65:** 2498-504

Li S, Zhou Y, Dong Y, Ip C (2007a) Doxorubicin and selenium cooperatively induce fas signaling in the absence of Fas/Fas ligand interaction. *Anticancer research* **27:** 3075-82

Li S, Zhou Y, Wang R, Zhang H, Dong Y, Ip C (2007b) Selenium sensitizes MCF-7 breast cancer cells to doxorubicin-induced apoptosis through modulation of phospho-Akt and its downstream substrates. *Molecular cancer therapeutics* **6:** 1031-8

Li Z, Carrier L, Belame A, Thiyagarajah A, Salvo VA, Burow ME, Rowan BG (2009) Combination of methylselenocysteine with tamoxifen inhibits MCF-7 breast cancer xenografts in nude mice through elevated apoptosis and reduced angiogenesis. *Breast Cancer Res Treat* **118:** 33-43

Li Z, Carrier L, Rowan BG (2008b) Methylseleninic acid synergizes with tamoxifen to induce caspase-mediated apoptosis in breast cancer cells. *Molecular cancer therapeutics* **7:** 3056-63

Liang XH, Jackson S, Seaman M, Brown K, Kempkes B, Hibshoosh H, Levine B (1999) Induction of autophagy and inhibition of tumorigenesis by beclin 1. *Nature* **402:** 672-6

Lightfoot TJ, Skibola CF, Smith AG, Forrest MS, Adamson PJ, Morgan GJ, Bracci PM, Roman E, Smith MT, Holly EA (2006) Polymorphisms in the oxidative stress genes, superoxide dismutase, glutathione peroxidase and catalase and risk of non-Hodgkin's lymphoma. *Haematologica* **91:** 1222-7

Linch DC, Yung L, Smith P, Maclennan K, Jack A, Hancock B, Cunningham D, Hoskin P, Qian W, Holte H, Boesen AM, Grigg A, Browett P, Trneny M (2010) Final analysis of the UKLG LY02 trial comparing 6-8 cycles of CHOP with 3 cycles of CHOP followed by a BEAM autograft in patients <65 years with poor prognosis histologically aggressive NHL. *Br J Haematol* **149:** 237-243

Ling YH, Liebes L, Zou Y, Perez-Soler R (2003) Reactive oxygen species generation and mitochondrial dysfunction in the apoptotic response to Bortezomib, a novel proteasome inhibitor, in human H460 non-small cell lung cancer cells. *The Journal of biological chemistry* **278:** 33714-23

Lippman SM, Klein EA, Goodman PJ, Lucia MS, Thompson IM, Ford LG, Parnes HL, Minasian LM, Gaziano JM, Hartline JA, Parsons JK, Bearden JD, 3rd, Crawford ED, Goodman GE, Claudio J, Winquist E, Cook ED, Karp DD, Walther P, Lieber MM, Kristal AR, Darke AK, Arnold KB, Ganz PA, Santella RM, Albanes D, Taylor PR, Probstfield JL, Jagpal TJ, Crowley JJ, Meyskens FL, Jr., Baker LH, Coltman CA, Jr. (2009) Effect of selenium and vitamin E on risk of prostate cancer and other cancers: the Selenium and Vitamin E Cancer Prevention Trial (SELECT). *Jama* **301:** 39-51

Lister TA, Crowther D, Sutcliffe SB, Glatstein E, Canellos GP, Young RC, Rosenberg SA, Coltman CA, Tubiana M (1989) Report of a committee convened to discuss the evaluation and staging of patients with Hodgkin's disease: Cotswolds meeting. *J Clin Oncol* **7:** 1630-6

Lister TA, Cullen MH, Brearley RB, Beard ME, Stansfeld AG, Whitehouse JM, Wrigley PF, Ford JM, Malpas JS, Crowther D (1978a) Combination chemotherapy for advanced non-Hodgkin's lymphoma of unfavourable histology. *Cancer Chemother Pharmacol* **1:** 107-12

Lister TA, Whitehouse JM, Beard ME, Brearley RL, Wrigley PF, Oliver RT, Freeman JE, Woodruff RK, Malpas JS, Paxton AM, Crowther D (1978b) Combination chemotherapy for acute lymphoblastic leukaemia in adults. *Br Med J* **1:** 199-203

Liu FT, Agrawal SG, Movasaghi Z, Wyatt PB, Rehman IU, Gribben JG, Newland AC, Jia L (2008) Dietary flavonoids inhibit the anticancer effects of the proteasome inhibitor bortezomib. *Blood* **112:** 3835-46

Luk CK, Tannock IF (1989) Flow cytometric analysis of doxorubicin accumulation in cells from human and rodent cell lines. *Journal of the National Cancer Institute* **81:** 55-9

MacFarquhar JK, Broussard DL, Melstrom P, Hutchinson R, Wolkin A, Martin C, Burk RF, Dunn JR, Green AL, Hammond R, Schaffner W, Jones TF (2010) Acute selenium toxicity associated with a dietary supplement. *Archives of internal medicine* **170:** 256-61

Maehira F, Luyo GA, Miyagi I, Oshiro M, Yamane N, Kuba M, Nakazato Y (2002) Alterations of serum selenium concentrations in the acute phase of pathological conditions. *Clinica chimica acta; international journal of clinical chemistry* **316:** 137-46

Maehira F, Miyagi I, Eguchi Y (2003) Selenium regulates transcription factor NF-kappaB activation during the acute phase reaction. *Clinica chimica acta; international journal of clinical chemistry* **334:** 163-71

Mahn AV, Toledo HM, Ruz M (2009a) Dietary supplementation with selenomethylselenocysteine produces a differential proteomic response. *J Nutr Biochem* **20:** 791-9

Mahn AV, Toledo HM, Ruz MH (2009b) Organic and inorganic selenium compounds produce different protein patterns in the blood plasma of rats. *Biol Res* **42:** 163-73

Maiuri MC, Tasdemir E, Criollo A, Morselli E, Vicencio JM, Carnuccio R, Kroemer G (2009) Control of autophagy by oncogenes and tumor suppressor genes. *Cell Death Differ* **16:** 87-93

Mann BS, Johnson JR, Cohen MH, Justice R, Pazdur R (2007) FDA approval summary: vorinostat for treatment of advanced primary cutaneous T-cell lymphoma. *Oncologist* **12:** 1247-52

Manzanares W, Biestro A, Galusso F, Torre MH, Manay N, Facchin G, Hardy G (2010) High-dose selenium for critically ill patients with systemic inflammation:

pharmacokinetics and pharmacodynamics of selenious acid: a pilot study. *Nutrition* **26:** 634-40

Marciniak SJ, Yun CY, Oyadomari S, Novoa I, Zhang Y, Jungreis R, Nagata K, Harding HP, Ron D (2004) CHOP induces death by promoting protein synthesis and oxidation in the stressed endoplasmic reticulum. *Genes & development* **18:** 3066-77

Marco P (1967) The Travels of Marco Polo, traslated by EW Marsden and revised by T Wright. *Everymans Library, London*

Mark SD, Qiao YL, Dawsey SM, Wu YP, Katki H, Gunter EW, Fraumeni JF, Jr., Blot WJ, Dong ZW, Taylor PR (2000) Prospective study of serum selenium levels and incident esophageal and gastric cancers. *Journal of the National Cancer Institute* **92:** 1753-63

Marks PA, Xu WS (2009) Histone deacetylase inhibitors: Potential in cancer therapy. *J Cell Biochem* **107:** 600-8

Marquard L, Poulsen CB, Gjerdrum LM, de Nully Brown P, Christensen IJ, Jensen PB, Sehested M, Johansen P, Ralfkiaer E (2009) Histone deacetylase 1, 2, 6 and acetylated histone H4 in B- and T-cell lymphomas. *Histopathology* **54:** 688-98

Martin A, Conde E, Arnan M, Canales MA, Deben G, Sancho JM, Andreu R, Salar A, Garcia-Sanchez P, Vazquez L, Nistal S, Requena MJ, Donato EM, Gonzalez JA, Leon A, Ruiz C, Grande C, Gonzalez-Barca E, Caballero MD (2008) R-ESHAP as salvage therapy for patients with relapsed or refractory diffuse large B-cell lymphoma: the influence of prior exposure to rituximab on outcome. A GEL/TAMO study. *Haematologica* **93:** 1829-36

Maschek G, Savaraj N, Priebe W, Braunschweiger P, Hamilton K, Tidmarsh GF, De Young LR, Lampidis TJ (2004) 2-deoxy-D-glucose increases the efficacy of adriamycin and paclitaxel in human osteosarcoma and non-small cell lung cancers in vivo. *Cancer Res* **64:** 31-4

Masdehors P, Merle-Beral H, Maloum K, Omura S, Magdelenat H, Delic J (2000) Deregulation of the ubiquitin system and p53 proteolysis modify the apoptotic response in B-CLL lymphocytes. *Blood* **96:** 269-74

Masetti R, Pession A (2009) First-line treatment of acute lymphoblastic leukemia with pegasparaginase. *Biologics* **3:** 359-68

Mathew R, Karantza-Wadsworth V, White E (2007) Role of autophagy in cancer. *Nature reviews* **7:** 961-7

McCullough KD, Martindale JL, Klotz LO, Aw TY, Holbrook NJ (2001) Gadd153 sensitizes cells to endoplasmic reticulum stress by down-regulating Bcl2 and perturbing the cellular redox state. *Molecular and cellular biology* **21:** 1249-59

McKelvey EM, Gottlieb JA, Wilson HE, Haut A, Talley RW, Stephens R, Lane M, Gamble JF, Jones SE, Grozea PN, Gutterman J, Coltman C, Moon TE (1976) Hydroxyldaunomycin (Adriamycin) combination chemotherapy in malignant lymphoma. *Cancer* **38:** 1484-93

Meija J, Montes-Bayon M, Le Duc DL, Terry N, Caruso JA (2002) Simultaneous monitoring of volatile selenium and sulfur species from se accumulating plants (wild type and genetically modified) by GC/MS and GC/ICPMS using solid-phase microextraction for sample introduction. *Anal Chem* **74:** 5837-44

Melo JV, Foroni L, Brito-Babapulle V, Luzzatto L, Catovsky D (1988) The establishment of cell lines from chronic B cell leukaemias: evidence of leukaemic origin by karyotypic abnormalities and Ig gene rearrangement. *Clin Exp Immunol* **73:** 23-8

Meplan C, Crosley LK, Nicol F, Beckett GJ, Howie AF, Hill KE, Horgan G, Mathers JC, Arthur JR, Hesketh JE (2007) Genetic polymorphisms in the human selenoprotein P gene determine the response of selenoprotein markers to selenium supplementation in a gender-specific manner (the SELGEN study). *Faseb J* **21:** 3063-74

Meplan C, Crosley LK, Nicol F, Horgan GW, Mathers JC, Arthur JR, Hesketh JE (2008) Functional effects of a common single-nucleotide polymorphism (GPX4c718t) in the glutathione peroxidase 4 gene: interaction with sex. *The American journal of clinical nutrition* **87:** 1019-27

Meplan C, Hughes DJ, Pardini B, Naccarati A, Soucek P, Vodickova L, Hlavata I, Vrana D, Vodicka P, Hesketh J (2010) Genetic variants in selenoprotein genes increase risk of colorectal cancer. *Carcinogenesis*

Miao L, St Clair DK (2009) Regulation of superoxide dismutase genes: implications in disease. *Free radical biology & medicine* **47:** 344-56

Michels J, Johnson PW, Packham G (2005) Mcl-1. *Int J Biochem Cell Biol* **37:** 267-71

Milani M, Rzymski T, Mellor HR, Pike L, Bottini A, Generali D, Harris AL (2009) The role of ATF4 stabilization and autophagy in resistance of breast cancer cells treated with Bortezomib. *Cancer Res* **69:** 4415-23

Miller TP, Dahlberg S, Cassady JR, Adelstein DJ, Spier CM, Grogan TM, LeBlanc M, Carlin S, Chase E, Fisher RI (1998) Chemotherapy alone compared with chemotherapy plus radiotherapy for localized intermediate- and high-grade non-Hodgkin's lymphoma. *The New England journal of medicine* **339:** 21-6

Miller TP, LeBlanc M, Spier C, al. e (2001) CHOP alone compared to CHOP plus radiotherapy for early aggressive non-Hodgkin's lymphoma: Update of the Southwest Oncology Group (SWOG) randomised trial. *Blood* **98:** 714a

Mills W, Chopra R, McMillan A, Pearce R, Linch DC, Goldstone AH (1995) BEAM chemotherapy and autologous bone marrow transplantation for patients with relapsed or refractory non-Hodgkin's lymphoma. *J Clin Oncol* **13:** 588-95

Miniard AC, Middleton LM, Budiman ME, Gerber CA, Driscoll DM (2010) Nucleolin binds to a subset of selenoprotein mRNAs and regulates their expression. *Nucleic Acids Res*

Minucci S, Pelicci PG (2006) Histone deacetylase inhibitors and the promise of epigenetic (and more) treatments for cancer. *Nature reviews* **6:** 38-51

Mitsiades N, Mitsiades CS, Poulaki V, Chauhan D, Fanourakis G, Gu X, Bailey C, Joseph M, Libermann TA, Treon SP, Munshi NC, Richardson PG, Hideshima T, Anderson KC (2002) Molecular sequelae of proteasome inhibition in human multiple myeloma cells. *Proceedings of the National Academy of Sciences of the United States of America* **99:** 14374-9

Moon JC, Hah YS, Kim WY, Jung BG, Jang HH, Lee JR, Kim SY, Lee YM, Jeon MG, Kim CW, Cho MJ, Lee SY (2005) Oxidative stress-dependent structural and functional switching of a human 2-Cys peroxiredoxin isotype II that enhances HeLa cell resistance to H2O2-induced cell death. *The Journal of biological chemistry* **280:** 28775-84

Moreno-Reyes R, Suetens C, Mathieu F, Begaux F, Zhu D, Rivera MT, Boelaert M, Neve J, Perlmutter N, Vanderpas J (1998) Kashin-Beck osteoarthropathy in rural Tibet in relation to selenium and iodine status. *N Engl J Med* **339:** 1112-20

Moriyama M, Yamochi T, Semba K, Akiyama T, Mori S (1997) BCL-6 is phosphorylated at multiple sites in its serine- and proline-clustered region by mitogen-activated protein kinase (MAPK) in vivo. *Oncogene* **14:** 2465-74

Moskowitz CH, Bertino JR, Glassman JR, Hedrick EE, Hunte S, Coady-Lyons N, Agus DB, Goy A, Jurcic J, Noy A, O'Brien J, Portlock CS, Straus DS, Childs B, Frank R, Yahalom J, Filippa D, Louie D, Nimer SD, Zelenetz AD (1999) Ifosfamide, carboplatin, and etoposide: a highly effective cytoreduction and peripheral-blood progenitor-cell mobilization regimen for transplant-eligible patients with non-Hodgkin's lymphoma. *J Clin Oncol* **17:** 3776-85

Moskowitz CH, Zelenetz AD, Kewalramani T, Hamlin P, Lessac-Chenen S, Houldsworth J, Olshen A, Chaganti R, Nimer S, Teruya-Feldstein J (2005) Cell of origin, germinal center versus nongerminal center, determined by immunohistochemistry on tissue

microarray, does not correlate with outcome in patients with relapsed and refractory DLBCL. *Blood* **106:** 3383-5

Mudie NY, Swerdlow AJ, Higgins CD, Smith P, Qiao Z, Hancock BW, Hoskin PJ, Linch DC (2006) Risk of second malignancy after non-Hodgkin's lymphoma: a British Cohort Study. *J Clin Oncol* **24:** 1568-74

Muecke R, Schomburg L, Glatzel M, Berndt-Skorka R, Baaske D, Reichl B, Buentzel J, Kundt G, Prott FJ, Devries A, Stoll G, Kisters K, Bruns F, Schaefer U, Willich N, Micke O (2010) Multicenter, Phase 3 Trial Comparing Selenium Supplementation With Observation in Gynecologic Radiation Oncology. *International journal of radiation oncology, biology, physics*

Muth OH, Oldfield JE, Remmert LF, Schubert JR (1958) Effects of selenium and vitamin E on white muscle disease. *Science (New York, NY* **128:** 1090

Nakanishi C, Toi M (2005) Nuclear factor-kappaB inhibitors as sensitizers to anticancer drugs. *Nature reviews* **5:** 297-309

Navon A, Ciechanover A (2009) The 26 S proteasome: from basic mechanisms to drug targeting. *The Journal of biological chemistry* **284:** 33713-8

Nelson AA, Fitzhugh OG, Calvery HO (1943) Liver tumours following cirrhosis caused by selenium in rats. *Cancer research* **3:** 230-236

Nelson JA, Pan BF, Swanson DA, Elfarra AA (1995) Cysteine conjugate beta-lyase activity in human renal carcinomas. *Cancer Biochem Biophys* **14:** 257-63

Nencioni A, Hua F, Dillon CP, Yokoo R, Scheiermann C, Cardone MH, Barbieri E, Rocco I, Garuti A, Wesselborg S, Belka C, Brossart P, Patrone F, Ballestrero A (2005) Evidence for a protective role of Mcl-1 in proteasome inhibitor-induced apoptosis. *Blood* **105:** 3255-62

Neve J (1995) Human selenium supplementation as assessed by changes in blood selenium concentration and glutathione peroxidase activity. *J Trace Elem Med Biol* **9:** 65-73

Newcomb EW (1995) P53 gene mutations in lymphoid diseases and their possible relevance to drug resistance. *Leuk Lymphoma* **17:** 211-21

Nian H, Bisson WH, Dashwood WM, Pinto JT, Dashwood RH (2009) Alpha-keto acid metabolites of organoselenium compounds inhibit histone deacetylase activity in human colon cancer cells. *Carcinogenesis* **30:** 1416-23

Nickel A, Kottra G, Schmidt G, Danier J, Hofmann T, Daniel H (2009) Characteristics of transport of selenoamino acids by epithelial amino acid transporters. *Chem Biol Interact* **177:** 234-41

Nocentini G (1996) Ribonucleotide reductase inhibitors: new strategies for cancer chemotherapy. *Crit Rev Oncol Hematol* **22:** 89-126

Noh DY, Ahn SJ, Lee RA, Kim SW, Park IA, Chae HZ (2001) Overexpression of peroxiredoxin in human breast cancer. *Anticancer research* **21:** 2085-90

Nomura AM, Lee J, Stemmermann GN, Combs GF, Jr. (2000) Serum selenium and subsequent risk of prostate cancer. *Cancer Epidemiol Biomarkers Prev* **9:** 883-7

Nozaki S, Sledge Jr GW, Nakshatri H (2001) Repression of GADD153/CHOP by NF-kappaB: a possible cellular defense against endoplasmic reticulum stress-induced cell death. *Oncogene* **20:** 2178-85

Nyman H, Adde M, Karjalainen-Lindsberg ML, Taskinen M, Berglund M, Amini RM, Blomqvist C, Enblad G, Leppa S (2007) Prognostic impact of immunohistochemically defined germinal center phenotype in diffuse large B-cell lymphoma patients treated with immunochemotherapy. *Blood* **109:** 4930-5

Obeng EA, Carlson LM, Gutman DM, Harrington WJ, Jr., Lee KP, Boise LH (2006) Proteasome inhibitors induce a terminal unfolded protein response in multiple myeloma cells. *Blood* **107:** 4907-16

Obrador-Hevia A, Fernandez de Mattos S, Villalonga P, Rodriguez J (2009) Molecular biology of mantle cell lymphoma: from profiling studies to new therapeutic strategies. *Blood Rev* **23:** 205-16

Ogata M, Hino S, Saito A, Morikawa K, Kondo S, Kanemoto S, Murakami T, Taniguchi M, Tanii I, Yoshinaga K, Shiosaka S, Hammarback JA, Urano F, Imaizumi K (2006) Autophagy is activated for cell survival after endoplasmic reticulum stress. *Molecular and cellular biology* **26:** 9220-31

Ohoka N, Yoshii S, Hattori T, Onozaki K, Hayashi H (2005) TRB3, a novel ER stress-inducible gene, is induced via ATF4-CHOP pathway and is involved in cell death. *The EMBO journal* **24:** 1243-55

Ohta Y, Kobayashi Y, Konishi S, Hirano S (2009) Speciation analysis of selenium metabolites in urine and breath by HPLC- and GC-inductively coupled plasma-MS after administration of selenomethionine and methylselenocysteine to rats. *Chem Res Toxicol* **22:** 1795-801

Okuno T, Ueno H, Nakamuro K (2006) Cystathionine gamma-lyase contributes to selenomethionine detoxification and cytosolic glutathione peroxidase biosynthesis in mouse liver. *Biological trace element research* **109:** 155-71

Olm E, Fernandes AP, Hebert C, Rundlof AK, Larsen EH, Danielsson O, Bjornstedt M (2009) Extracellular thiol-assisted selenium uptake dependent on the x(c)- cystine transporter explains the cancer-specific cytotoxicity of selenite. *Proceedings of the National Academy of Sciences of the United States of America* **106:** 11400-5

Olson GE, Winfrey VP, Hill KE, Burk RF (2008) Megalin mediates selenoprotein P uptake by kidney proximal tubule epithelial cells. *The Journal of biological chemistry* **283:** 6854-60

Olson GE, Winfrey VP, Nagdas SK, Hill KE, Burk RF (2005) Selenoprotein P is required for mouse sperm development. *Biology of reproduction* **73:** 201-11

Olson GE, Winfrey VP, Nagdas SK, Hill KE, Burk RF (2007) Apolipoprotein E receptor-2 (ApoER2) mediates selenium uptake from selenoprotein P by the mouse testis. *The Journal of biological chemistry* **282:** 12290-7

Ozgen IT, Dagdemir A, Elli M, Saraymen R, Pinarli FG, Fisgin T, Albayrak D, Acar S (2007) Hair selenium status in children with leukemia and lymphoma. *J Pediatr Hematol Oncol* **29:** 519-22

Paglin S, Hollister T, Delohery T, Hackett N, McMahill M, Sphicas E, Domingo D, Yahalom J (2001) A novel response of cancer cells to radiation involves autophagy and formation of acidic vesicles. *Cancer Res* **61:** 439-44

Pagmantidis V, Meplan C, van Schothorst EM, Keijer J, Hesketh JE (2008) Supplementation of healthy volunteers with nutritionally relevant amounts of selenium increases the expression of lymphocyte protein biosynthesis genes. *The American journal of clinical nutrition* **87:** 181-9

Pahl HL, Baeuerle PA (1995) A novel signal transduction pathway from the endoplasmic reticulum to the nucleus is mediated by transcription factor NF-kappa B. *The EMBO journal* **14:** 2580-8

Pallet N, Bouvier N, Legendre C, Gilleron J, Codogno P, Beaune P, Thervet E, Anglicheau D (2008) Autophagy protects renal tubular cells against cyclosporine toxicity. *Autophagy* **4:** 783-91

Paoluzzi L, Scotto L, Marchi E, Zain J, Seshan VE, O'Connor OA (2010) Romidepsin and belinostat synergize the antineoplastic effect of bortezomib in mantle cell lymphoma. *Clin Cancer Res* **16:** 554-65

Papp LV, Lu J, Holmgren A, Khanna KK (2007) From selenium to selenoproteins: synthesis, identity, and their role in human health. *Antioxidants & redox signaling* **9:** 775-806

Paradela A, Albar JP (2008) Advances in the analysis of protein phosphorylation. *J Proteome Res* **7:** 1809-18

Parekh S, Prive G, Melnick A (2008) Therapeutic targeting of the BCL6 oncogene for diffuse large B-cell lymphomas. *Leuk Lymphoma* **49:** 874-82

Park M-E, Choi K-S, Park S-O, Kong E-S, Zu K, Wu Y, Zhang H, Ip C, Park Y-M (2005) A display thiol-proteomics approach to characterise global redox modification of proteins by selenium: implication for the anticancer action of selenium. *Cancer Genomics and Proteomics* **2:** 25-36

Passam FH, Sfiridaki A, Pappa C, Kyriakou D, Petreli E, Roussou PA, Alexandrakis MG (2008) Angiogenesis-related growth factors and cytokines in the serum of patients with B non-Hodgkin lymphoma; relation to clinical features and response to treatment. *Int J Lab Hematol* **30:** 17-25

Peart MJ, Smyth GK, van Laar RK, Bowtell DD, Richon VM, Marks PA, Holloway AJ, Johnstone RW (2005) Identification and functional significance of genes regulated by structurally different histone deacetylase inhibitors. *Proceedings of the National Academy of Sciences of the United States of America* **102:** 3697-702

Penney KL, Schumacher FR, Li H, Kraft P, Morris JS, Kurth T, Mucci LA, Hunter DJ, Kantoff PW, Stampfer MJ, Ma J (2010) A large prospective study of SEP15 genetic variation, interaction with plasma selenium levels, and prostate cancer risk and survival. *Cancer Prev Res (Phila Pa)* **3:** 604-10

Perez-Galan P, Roue G, Villamor N, Montserrat E, Campo E, Colomer D (2006) The proteasome inhibitor bortezomib induces apoptosis in mantle-cell lymphoma through generation of ROS and Noxa activation independent of p53 status. *Blood* **107:** 257-64

Perry RR, Mazetta JA, Levin M, Barranco SC (1993) Glutathione levels and variability in breast tumors and normal tissue. *Cancer* **72:** 783-7

Persson-Moschos M, Alfthan G, Akesson B (1998) Plasma selenoprotein P levels of healthy males in different selenium status after oral supplementation with different forms of selenium. *European journal of clinical nutrition* **52:** 363-7

Peyrou M, Cribb AE (2007) Effect of endoplasmic reticulum stress preconditioning on cytotoxicity of clinically relevant nephrotoxins in renal cell lines. *Toxicol In Vitro* **21:** 878-86

Pfreundschuh M, Ho AD, Cavallin-Stahl E, Wolf M, Pettengell R, Vasova I, Belch A, Walewski J, Zinzani PL, Mingrone W, Kvaloy S, Shpilberg O, Jaeger U, Hansen M, Corrado C, Scheliga A, Loeffler M, Kuhnt E (2008a) Prognostic significance of maximum tumour (bulk) diameter in young patients with good-prognosis diffuse large-B-cell lymphoma treated with CHOP-like chemotherapy with or without rituximab: an exploratory analysis of the MabThera International Trial Group (MInT) study. *Lancet Oncol* **9:** 435-44

Pfreundschuh M, Schubert J, Ziepert M, Schmits R, Mohren M, Lengfelder E, Reiser M, Nickenig C, Clemens M, Peter N, Bokemeyer C, Eimermacher H, Ho A, Hoffmann M, Mertelsmann R, Trumper L, Balleisen L, Liersch R, Metzner B, Hartmann F, Glass B, Poeschel V, Schmitz N, Ruebe C, Feller AC, Loeffler M (2008b) Six versus eight cycles of bi-weekly CHOP-14 with or without rituximab in elderly patients with aggressive CD20+ B-cell lymphomas: a randomised controlled trial (RICOVER-60). *Lancet Oncol* **9:** 105-16

Pfreundschuh M, Trumper L, Kloess M, Schmits R, Feller AC, Rube C, Rudolph C, Reiser M, Hossfeld DK, Eimermacher H, Hasenclever D, Schmitz N, Loeffler M (2004a) Two-weekly or 3-weekly CHOP chemotherapy with or without etoposide for the treatment of elderly patients with aggressive lymphomas: results of the NHL-B2 trial of the DSHNHL. *Blood* **104:** 634-41

Pfreundschuh M, Trumper L, Kloess M, Schmits R, Feller AC, Rudolph C, Reiser M, Hossfeld DK, Metzner B, Hasenclever D, Schmitz N, Glass B, Rube C, Loeffler M (2004b) Two-weekly or 3-weekly CHOP chemotherapy with or without etoposide for the treatment of young patients with good-prognosis (normal LDH) aggressive lymphomas: results of the NHL-B1 trial of the DSHNHL. *Blood* **104:** 626-33

Pfreundschuh M, Trumper L, Osterborg A, Pettengell R, Trneny M, Imrie K, Ma D, Gill D, Walewski J, Zinzani PL, Stahel R, Kvaloy S, Shpilberg O, Jaeger U, Hansen M, Lehtinen T, Lopez-Guillermo A, Corrado C, Scheliga A, Milpied N, Mendila M, Rashford M, Kuhnt E, Loeffler M (2006) CHOP-like chemotherapy plus rituximab versus CHOP-like chemotherapy alone in young patients with good-prognosis diffuse large-B-cell lymphoma: a randomised controlled trial by the MabThera International Trial (MInT) Group. *Lancet Oncol* **7:** 379-91

Pham LV, Tamayo AT, Yoshimura LC, Lo P, Ford RJ (2003) Inhibition of constitutive NF-kappa B activation in mantle cell lymphoma B cells leads to induction of cell cycle arrest and apoptosis. *J Immunol* **171:** 88-95

Philip T, Guglielmi C, Hagenbeek A, Somers R, Van der Lelie H, Bron D, Sonneveld P, Gisselbrecht C, Cahn JY, Harousseau JL, et al. (1995) Autologous bone marrow transplantation as compared with salvage chemotherapy in relapses of chemotherapy-sensitive non-Hodgkin's lymphoma. *N Engl J Med* **333:** 1540-5

Pinto JT, Lee JI, Sinha R, Macewan ME, Cooper AJ (2010) Chemopreventive mechanisms of alpha-keto acid metabolites of naturally occurring organoselenium compounds. *Amino Acids*

Poerschke RL, Franklin MR, Moos PJ (2008) Modulation of redox status in human lung cell lines by organoselenocompounds: selenazolidines, selenomethionine, and methylseleninic acid. *Toxicol In Vitro* **22:** 1761-7

Potapova TA, Daum JR, Byrd KS, Gorbsky GJ (2009) Fine tuning the cell cycle: activation of the Cdk1 inhibitory phosphorylation pathway during mitotic exit. *Molecular biology of the cell* **20:** 1737-48

Prince HM, Imrie K, Crump M, Stewart AK, Girouard C, Colwill R, Brandwein J, Tsang RW, Scott JG, Sutton DM, Pantalony D, Carstairs K, Sutcliffe SB, Keating A (1996) The role of intensive therapy and autologous blood and marrow transplantation for chemotherapy-sensitive relapsed and primary refractory non-Hodgkin's lymphoma: identification of major prognostic groups. *Br J Haematol* **92:** 880-9

Pyrko P, Schonthal AH, Hofman FM, Chen TC, Lee AS (2007) The unfolded protein response regulator GRP78/BiP as a novel target for increasing chemosensitivity in malignant gliomas. *Cancer Res* **67:** 9809-16

Qian DZ, Kachhap SK, Collis SJ, Verheul HM, Carducci MA, Atadja P, Pili R (2006) Class II histone deacetylases are associated with VHL-independent regulation of hypoxia-inducible factor 1 alpha. *Cancer Res* **66:** 8814-21

Qiao YL, Dawsey SM, Kamangar F, Fan JH, Abnet CC, Sun XD, Johnson LL, Gail MH, Dong ZW, Yu B, Mark SD, Taylor PR (2009) Total and cancer mortality after supplementation with vitamins and minerals: follow-up of the Linxian General Population Nutrition Intervention Trial. *Journal of the National Cancer Institute* **101:** 507-18

Radford JA, Whelan JS, Rohatiner AZ, Deakin D, Harris M, Stansfeld AG, Swindell R, Wilkinson PM, James RD, Lister TA, et al. (1994) Weekly VAPEC-B chemotherapy for high grade non-Hodgkin's lymphoma: results of treatment in 184 patients. *Ann Oncol* **5:** 147-51

Rafferty TS, Beckett GJ, Walker C, Bisset YC, McKenzie RC (2003a) Selenium protects primary human keratinocytes from apoptosis induced by exposure to ultraviolet radiation. *Clin Exp Dermatol* **28:** 294-300

Rafferty TS, Green MH, Lowe JE, Arlett C, Hunter JA, Beckett GJ, McKenzie RC (2003b) Effects of selenium compounds on induction of DNA damage by broadband ultraviolet radiation in human keratinocytes. *The British journal of dermatology* **148:** 1001-9

Ranganathan AC, Zhang L, Adam AP, Aguirre-Ghiso JA (2006) Functional coupling of p38-induced up-regulation of BiP and activation of RNA-dependent protein kinase-like endoplasmic reticulum kinase to drug resistance of dormant carcinoma cells. *Cancer Res* **66:** 1702-11

Rao RV, Hermel E, Castro-Obregon S, del Rio G, Ellerby LM, Ellerby HM, Bredesen DE (2001) Coupling endoplasmic reticulum stress to the cell death program. Mechanism of caspase activation. *The Journal of biological chemistry* **276:** 33869-74

Ratnasinghe D, Tangrea JA, Andersen MR, Barrett MJ, Virtamo J, Taylor PR, Albanes D (2000) Glutathione peroxidase codon 198 polymorphism variant increases lung cancer risk. *Cancer Res* **60:** 6381-3

Rayman M, Thompson A, Warren-Perry M, Galassini R, Catterick J, Hall E, Lawrence D, Bliss J (2006) Impact of selenium on mood and quality of life: a randomized, controlled trial. *Biological psychiatry* **59:** 147-54

Rayman MP (2008) Food-chain selenium and human health: emphasis on intake. *The British journal of nutrition* **100:** 254-68

Rayman MP, Bode P, Redman CW (2003) Low selenium status is associated with the occurrence of the pregnancy disease preeclampsia in women from the United Kingdom. *Am J Obstet Gynecol* **189:** 1343-9

Rayman MP, Infante HG, Sargent M (2008) Food-chain selenium and human health: spotlight on speciation. *The British journal of nutrition***:** 1-16

Rayman MP, Rayman MP (2002) The argument for increasing selenium intake. *The Proceedings of the Nutrition Society* **61:** 203-15

Reagan-Shaw S, Nihal M, Ahsan H, Mukhtar H, Ahmad N (2008) Combination of vitamin E and selenium causes an induction of apoptosis of human prostate cancer cells by enhancing Bax/Bcl-2 ratio. *Prostate* **68:** 1624-34

Reddy RK, Mao C, Baumeister P, Austin RC, Kaufman RJ, Lee AS (2003) Endoplasmic reticulum chaperone protein GRP78 protects cells from apoptosis induced by topoisomerase inhibitors: role of ATP binding site in suppression of caspase-7 activation. *The Journal of biological chemistry* **278:** 20915-24

Reid ME, Duffield-Lillico AJ, Slate E, Natarajan N, Turnbull B, Jacobs E, Combs GF, Jr., Alberts DS, Clark LC, Marshall JR (2008) The nutritional prevention of cancer: 400 mcg per day selenium treatment. *Nutrition and cancer* **60:** 155-63

Ren Y, Huang F, Liu Y, Yang Y, Jiang Q, Xu C (2009) Autophagy inhibition through PI3K/Akt increases apoptosis by sodium selenite in NB4 cells. *BMB Rep* **42:** 599-604

Reyes F, Lepage E, Ganem G, Molina TJ, Brice P, Coiffier B, Morel P, Ferme C, Bosly A, Lederlin P, Laurent G, Tilly H (2005) ACVBP versus CHOP plus radiotherapy for localized aggressive lymphoma. *The New England journal of medicine* **352:** 1197-205

Rhee SG, Chae HZ, Kim K (2005) Peroxiredoxins: a historical overview and speculative preview of novel mechanisms and emerging concepts in cell signaling. *Free radical biology & medicine* **38:** 1543-52

Richardson PG, Barlogie B, Berenson J, Singhal S, Jagannath S, Irwin D, Rajkumar SV, Srkalovic G, Alsina M, Alexanian R, Siegel D, Orlowski RZ, Kuter D, Limentani SA, Lee S, Hideshima T, Esseltine DL, Kauffman M, Adams J, Schenkein DP, Anderson KC (2003) A phase 2 study of bortezomib in relapsed, refractory myeloma. *The New England journal of medicine* **348:** 2609-17

Richon VM, Sandhoff TW, Rifkind RA, Marks PA (2000) Histone deacetylase inhibitor selectively induces p21WAF1 expression and gene-associated histone acetylation. *Proceedings of the National Academy of Sciences of the United States of America* **97:** 10014-9

Riley T, Sontag E, Chen P, Levine A (2008) Transcriptional control of human p53-regulated genes. *Nat Rev Mol Cell Biol* **9:** 402-12

Ringner M (2008) What is principal component analysis? *Nat Biotechnol* **26:** 303-4

Robbins AR, Jablonski SA, Yen TJ, Yoda K, Robey R, Bates SE, Sackett DL (2005) Inhibitors of histone deacetylases alter kinetochore assembly by disrupting pericentromeric heterochromatin. *Cell Cycle* **4:** 717-26

Robertson LE, Redman JR, Butler JJ, Osborne BM, Velasquez WS, McLaughlin P, Swan F, Rodriguez MA, Hagemeister FB, Fuller LM, et al. (1991) Discordant bone marrow involvement in diffuse large-cell lymphoma: a distinct clinical-pathologic entity associated with a continuous risk of relapse. *J Clin Oncol* **9:** 236-42

Rohatiner AZ, Nadler L, Davies AJ, Apostolidis J, Neuberg D, Matthews J, Gribben JG, Mauch PM, Lister TA, Freedman AS (2007) Myeloablative therapy with autologous bone marrow transplantation for follicular lymphoma at the time of second or subsequent remission: long-term follow-up. *J Clin Oncol* **25:** 2554-9

Ron D, Walter P (2007) Signal integration in the endoplasmic reticulum unfolded protein response. *Nat Rev Mol Cell Biol* **8:** 519-29

Rosenwald A, Wright G, Chan WC, Connors JM, Campo E, Fisher RI, Gascoyne RD, Muller-Hermelink HK, Smeland EB, Giltnane JM, Hurt EM, Zhao H, Averett L, Yang L, Wilson WH, Jaffe ES, Simon R, Klausner RD, Powell J, Duffey PL, Longo DL, Greiner TC, Weisenburger DD, Sanger WG, Dave BJ, Lynch JC, Vose J, Armitage JO,

Montserrat E, Lopez-Guillermo A, Grogan TM, Miller TP, LeBlanc M, Ott G, Kvaloy S, Delabie J, Holte H, Krajci P, Stokke T, Staudt LM (2002) The use of molecular profiling to predict survival after chemotherapy for diffuse large-B-cell lymphoma. *The New England journal of medicine* **346:** 1937-47

Rotruck JT, Pope AL, Ganther HE, Swanson AB, Hafeman DG, Hoekstra WG (1973) Selenium: Biochemical Role as a Component of Glutathione Peroxidase *Science (New York, NY* **179:** 588-590

Roveri A, Vitale MP, Serain E, Zaccarin M, Mauri P, Di Silvestre D, De Palma A, Gion M, Toppo S, Maiorino M, Ursini F (2008) Differential liquid phase proteomic analysis of the effect of selenium supplementation in LNCaP cells. *J Chromatogr B Analyt Technol Biomed Life Sci* **865:** 63-73

Ruff SJ, Chen K, Cohen S (1997) Peroxovanadate induces tyrosine phosphorylation of multiple signaling proteins in mouse liver and kidney. *The Journal of biological chemistry* **272:** 1263-7

Rustum YM, Toth K, Seshadri M, Sen A, Durrani FA, Stott E, Morrison CD, Cao S, Bhattacharya A (2010) Architectural heterogeneity in tumors caused by differentiation alters intratumoral drug distribution and affects therapeutic synergy of antiangiogenic organoselenium compound. *J Oncol* **2010:** 396286

Rutkowski DT, Kaufman RJ (2007) That which does not kill me makes me stronger: adapting to chronic ER stress. *Trends Biochem Sci* **32:** 469-76

Sacchi S, Marcheselli L, Bari A, Marcheselli R, Pozzi S, Gobbi PG, Angrilli F, Brugiatelli M, Musto P, Federico M (2008) Second malignancies after treatment of diffuse large B-cell non-Hodgkin's lymphoma: a GISL cohort study. *Haematologica* **93:** 1335-42

Saito Y, Hayashi T, Tanaka A, Watanabe Y, Suzuki M, Saito E, Takahashi K (1999) Selenoprotein P in human plasma as an extracellular phospholipid hydroperoxide glutathione peroxidase. Isolation and enzymatic characterization of human selenoprotein p. *The Journal of biological chemistry* **274:** 2866-71

Sakamoto H, Mashima T, Kizaki A, Dan S, Hashimoto Y, Naito M, Tsuruo T (2000) Glyoxalase I is involved in resistance of human leukemia cells to antitumor agent-induced apoptosis. *Blood* **95:** 3214-8

Sakr Y, Reinhart K, Bloos F, Marx G, Russwurm S, Bauer M, Brunkhorst F (2007) Time course and relationship between plasma selenium concentrations, systemic inflammatory response, sepsis, and multiorgan failure. *Br J Anaesth* **98:** 775-84

Salaun P, Rannou Y, Prigent C (2008) Cdk1, Plks, Auroras, and Neks: the mitotic bodyguards. *Adv Exp Med Biol* **617:** 41-56

Salven P, Orpana A, Teerenhovi L, Joensuu H (2000) Simultaneous elevation in the serum concentrations of the angiogenic growth factors VEGF and bFGF is an independent predictor of poor prognosis in non-Hodgkin lymphoma: a single-institution study of 200 patients. *Blood* **96:** 3712-8

Santarius T, Bignell GR, Greenman CD, Widaa S, Chen L, Mahoney CL, Butler A, Edkins S, Waris S, Thornalley PJ, Futreal PA, Stratton MR (2010) GLO1-A novel amplified gene in human cancer. *Genes Chromosomes Cancer* **49:** 711-25

Santos RA, Takahashi CS (2008) Anticlastogenic and antigenotoxic effects of selenomethionine on doxorubicin-induced damage in vitro in human lymphocytes. *Food Chem Toxicol* **46:** 671-7

Sanz L, Lopez-Guillermo A, Martinez C, Bosch F, Esteve J, Cobo F, Montoto S, Perales M, Blade J, Cervantes F, Nomdedeu B, Campo E, Montserrat E (1998) Risk of relapse and clinico-pathological features in 103 patients with diffuse large-cell lymphoma in complete response after first-line treatment. *Eur J Haematol* **61:** 59-64

Sarbassov DD, Guertin DA, Ali SM, Sabatini DM (2005) Phosphorylation and regulation of Akt/PKB by the rictor-mTOR complex. *Science (New York, NY* **307:** 1098-101

Sasakura C, Suzuki KT (1998) Biological interaction between transition metals (Ag, Cd and Hg), selenide/sulfide and selenoprotein P. *Journal of inorganic biochemistry* **71:** 159-62

Schafer DA, Jennings PB, Cooper JA (1996) Dynamics of capping protein and actin assembly in vitro: uncapping barbed ends by polyphosphoinositides. *J Cell Biol* **135:** 169-79

Schapansky J, Olson K, Van Der Ploeg R, Glazner G (2007) NF-kappaB activated by ER calcium release inhibits Abeta-mediated expression of CHOP protein: enhancement by AD-linked mutant presenilin 1. *Experimental neurology* **208:** 169-76

Scheuner D, Song B, McEwen E, Liu C, Laybutt R, Gillespie P, Saunders T, Bonner-Weir S, Kaufman RJ (2001) Translational control is required for the unfolded protein response and in vivo glucose homeostasis. *Mol Cell* **7:** 1165-76

Schewe DM, Aguirre-Ghiso JA (2009) Inhibition of eIF2alpha dephosphorylation maximizes bortezomib efficiency and eliminates quiescent multiple myeloma cells surviving proteasome inhibitor therapy. *Cancer Res* **69:** 1545-52

Schmitz N, Nickelsen M, Ziepert M, Haenel M, Borchmann PD, Viardot A, Nickenig C, Bentz M, Peschel C, Trumper L, Loeffler M, Pfreundschuh M, Glass B (2009) Aggressive Chemotherapy (CHOEP-14) and Rituximab or High-Dose Therapy (MegaCHOEP) and Rituximab for Young, High-Risk Patients with Aggressive B-cell Lymphoma: Results of the MegaCHOEP Trial of the German High-Grade Non-Hodgkin Lymphoma Study Group (DSHNHL). *Blood* **114:** 404

Schomburg L, Schweizer U, Holtmann B, Flohe L, Sendtner M, Kohrle J (2003) Gene disruption discloses role of selenoprotein P in selenium delivery to target tissues. *The Biochemical journal* **370:** 397-402

Schonthal AH (2009) Endoplasmic reticulum stress and autophagy as targets for cancer therapy. *Cancer letters* **275:** 163-9

Schot BW, Zijlstra JM, Sluiter WJ, van Imhoff GW, Pruim J, Vaalburg W, Vellenga E (2007) Early FDG-PET assessment in combination with clinical risk scores determines prognosis in recurring lymphoma. *Blood* **109:** 486-91

Schwiertz A, Deubel S, Birringer M (2008) Bioactivation of selenocysteine derivatives by beta-lyases present in common gastrointestinal bacterial species. *Int J Vitam Nutr Res* **78:** 169-74

Scott R, MacPherson A, Yates RW, Hussain B, Dixon J (1998) The effect of oral selenium supplementation on human sperm motility. *Br J Urol* **82:** 76-80

See KA, Lavercombe PS, Dillon J, Ginsberg R (2006) Accidental death from acute selenium poisoning. *The Medical journal of Australia* **185:** 388-9

Sehn LH, Berry B, Chhanabhai M, Fitzgerald C, Gill K, Hoskins P, Klasa R, Savage KJ, Shenkier T, Sutherland J, Gascoyne RD, Connors JM (2007) The revised International Prognostic Index (R-IPI) is a better predictor of outcome than the standard IPI for patients with diffuse large B-cell lymphoma treated with R-CHOP. *Blood* **109:** 1857-61

Semenza GL (2003) Targeting HIF-1 for cancer therapy. *Nature reviews* **3:** 721-32

Seo YR, Kelley MR, Smith ML (2002a) Selenomethionine regulation of p53 by a ref1-dependent redox mechanism. *Proceedings of the National Academy of Sciences of the United States of America* **99:** 14548-53

Seo YR, Sweeney C, Smith ML (2002b) Selenomethionine induction of DNA repair response in human fibroblasts. *Oncogene* **21:** 3663-9

Seshadri T, Stakiw J, Pintilie M, Keating A, Crump M, Kuruvilla J (2008) Utility of subsequent conventional dose chemotherapy in relapsed/refractory transplant-eligible

patients with diffuse large B-cell lymphoma failing platinum-based salvage chemotherapy. *Hematology* **13:** 261-6

Shamberger RJ, Frost DV (1969) Possible protective effect of selenium against human cancer. *Can Med Assoc J* **100:** 682

Shao Y, Gao Z, Marks PA, Jiang X (2004) Apoptotic and autophagic cell death induced by histone deacetylase inhibitors. *Proceedings of the National Academy of Sciences of the United States of America* **101:** 18030-5

Shen HM, Ding WX, Ong CN (2002) Intracellular glutathione is a cofactor in methylseleninic acid-induced apoptotic cell death of human hepatoma HEPG(2) cells. *Free radical biology & medicine* **33:** 552-61

Shen HM, Yang CF, Ong CN (1999) Sodium selenite-induced oxidative stress and apoptosis in human hepatoma HepG2 cells. *International journal of cancer* **81:** 820-8

Shishodia S, Amin HM, Lai R, Aggarwal BB (2005) Curcumin (diferuloylmethane) inhibits constitutive NF-kappaB activation, induces G1/S arrest, suppresses proliferation, and induces apoptosis in mantle cell lymphoma. *Biochemical pharmacology* **70:** 700-13

Sieja K, Talerczyk M (2004) Selenium as an element in the treatment of ovarian cancer in women receiving chemotherapy. *Gynecologic oncology* **93:** 320-7

Singh U, Null K, Sinha R (2008) In vitro growth inhibition of mouse mammary epithelial tumor cells by methylseleninic acid: involvement of protein kinases. *Mol Nutr Food Res* **52:** 1281-8

Sinha R, Kiley SC, Lu JX, Thompson HJ, Moraes R, Jaken S, Medina D (1999) Effects of methylselenocysteine on PKC activity, cdk2 phosphorylation and gadd gene expression in synchronized mouse mammary epithelial tumor cells. *Cancer letters* **146:** 135-45

Sinha R, Medina D (1997) Inhibition of cdk2 kinase activity by methylselenocysteine in synchronized mouse mammary epithelial tumor cells. *Carcinogenesis* **18:** 1541-7

Sinha R, Pinto JT, Facompre N, Kilheffer J, Baatz JE, El-Bayoumy K (2008) Effects of naturally occurring and synthetic organoselenium compounds on protein profiling in androgen responsive and androgen independent human prostate cancer cells. *Nutrition and cancer* **60:** 267-75

Skarin AT, Canellos GP, Rosenthal DS, Case DC, Jr., MacIntyre JM, Pinkus GS, Moloney WC, Frei E, 3rd (1983) Improved prognosis of diffuse histiocytic and undifferentiated lymphoma by use of high dose methotrexate alternating with standard agents (M-BACOD). *J Clin Oncol* **1:** 91-8

Smith ML, Lancia JK, Mercer TI, Ip C (2004) Selenium compounds regulate p53 by common and distinctive mechanisms. *Anticancer research* **24:** 1401-8

Sterz J, Jakob C, Kuckelkorn U, Heider U, Mieth M, Kleeberg L, Kaiser M, Kloetzel PM, Sezer O, von Metzler I (2010) BSc2118 is a novel proteasome inhibitor with activity against multiple myeloma. *Eur J Haematol*

Stewart GS, Wang B, Bignell CR, Taylor AM, Elledge SJ (2003) MDC1 is a mediator of the mammalian DNA damage checkpoint. *Nature* **421:** 961-6

Stopeck AT, Unger JM, Rimsza LM, Bellamy WT, Iannone M, Persky DO, Leblanc M, Fisher RI, Miller TP (2009) A phase II trial of single agent bevacizumab in patients with relapsed, aggressive non-Hodgkin lymphoma: Southwest oncology group study S0108. *Leuk Lymphoma* **50:** 728-35

Stranges S, Marshall JR, Natarajan R, Donahue RP, Trevisan M, Combs GF, Cappuccio FP, Ceriello A, Reid ME (2007) Effects of long-term selenium supplementation on the incidence of type 2 diabetes: a randomized trial. *Annals of internal medicine* **147:** 217-23

Strauss SJ, Higginbottom K, Juliger S, Maharaj L, Allen P, Schenkein D, Lister TA, Joel SP (2007) The proteasome inhibitor bortezomib acts independently of p53 and induces cell death via apoptosis and mitotic catastrophe in B-cell lymphoma cell lines. *Cancer Res* **67:** 2783-90

Strehl J, Mey U, Glasmacher A, Djulbegovic B, Mayr C, Gorschluter M, Ziske C, Schmidt-Wolf IG (2003) High-dose chemotherapy followed by autologous stem cell transplantation as first-line therapy in aggressive non-Hodgkin's lymphoma: a meta-analysis. *Haematologica* **88:** 1304-15

Suzuki KT, Doi C, Suzuki N (2006a) Metabolism of 76Se-methylselenocysteine compared with that of 77Se-selenomethionine and 82Se-selenite. *Toxicology and applied pharmacology* **217:** 185-95

Suzuki KT, Kurasaki K, Ogawa S, Suzuki N (2006b) Metabolic transformation of methylseleninic acid through key selenium intermediate selenide. *Toxicology and applied pharmacology* **215:** 189-97

Suzuki KT, Kurasaki K, Suzuki N (2007) Selenocysteine beta-lyase and methylselenol demethylase in the metabolism of Se-methylated selenocompounds into selenide. *Biochimica et biophysica acta* **1770:** 1053-61

Suzuki KT, Shiobara Y, Itoh M, Ohmichi M (1998) Selective uptake of selenite by red blood cells. *The Analyst* **123:** 63-7

Suzuki KT, Tsuji Y, Ohta Y, Suzuki N (2008) Preferential organ distribution of methylselenol source Se-methylselenocysteine relative to methylseleninic acid. *Toxicology and applied pharmacology* **227:** 76-83

Swanson MS, Dreyfuss G (1988) Classification and purification of proteins of heterogeneous nuclear ribonucleoprotein particles by RNA-binding specificities. *Molecular and cellular biology* **8:** 2237-41

Swerdlow SH CE, Harris NL, Jaffe ES et al. (2008) WHO Classification of Tumours of Haematopoietic and Lymphoid Tissues (ed 4th). Lyon, France. *IARC Press*

Szegezdi E, Logue SE, Gorman AM, Samali A (2006) Mediators of endoplasmic reticulum stress-induced apoptosis. *EMBO reports* **7:** 880-5

Tasdemir E, Galluzzi L, Maiuri MC, Criollo A, Vitale I, Hangen E, Modjtahedi N, Kroemer G (2008) Methods for assessing autophagy and autophagic cell death. *Methods Mol Biol* **445:** 29-76

Tennant DA, Duran RV, Gottlieb E (2010) Targeting metabolic transformation for cancer therapy. *Nature reviews* **10:** 267-77

Thingholm TE, Jensen ON, Larsen MR (2009) Analytical strategies for phosphoproteomics. *Proteomics* **9:** 1451-68

Thomson CD, Robinson MF, Butler JA, Whanger PD (1993) Long-term supplementation with selenate and selenomethionine: selenium and glutathione peroxidase (EC 1.11.1.9) in blood components of New Zealand women. *The British journal of nutrition* **69:** 577-88

Thornalley PJ (2003) Protecting the genome: defence against nucleotide glycation and emerging role of glyoxalase I overexpression in multidrug resistance in cancer chemotherapy. *Biochem Soc Trans* **31:** 1372-7

Tilly H, Lepage E, Coiffier B, Blanc M, Herbrecht R, Bosly A, Attal M, Fillet G, Guettier C, Molina TJ, Gisselbrecht C, Reyes F (2003) Intensive conventional chemotherapy (ACVBP regimen) compared with standard CHOP for poor-prognosis aggressive non-Hodgkin lymphoma. *Blood* **102:** 4284-9

Tisdale EJ (2002) Glyceraldehyde-3-phosphate dehydrogenase is phosphorylated by protein kinase Ciota /lambda and plays a role in microtubule dynamics in the early secretory pathway. *The Journal of biological chemistry* **277:** 3334-41

Tome ME, Johnson DB, Rimsza LM, Roberts RA, Grogan TM, Miller TP, Oberley LW, Briehl MM (2005) A redox signature score identifies diffuse large B-cell lymphoma patients with a poor prognosis. *Blood* **106:** 3594-601

Tracey L, Perez-Rosado A, Artiga MJ, Camacho FI, Rodriguez A, Martinez N, Ruiz-Ballesteros E, Mollejo M, Martinez B, Cuadros M, Garcia JF, Lawler M, Piris MA (2005) Expression of the NF-kappaB targets BCL2 and BIRC5/Survivin characterizes small B-cell and aggressive B-cell lymphomas, respectively. *The Journal of pathology* **206:** 123-34

Trinidad JC, Specht CG, Thalhammer A, Schoepfer R, Burlingame AL (2006) Comprehensive identification of phosphorylation sites in postsynaptic density preparations. *Mol Cell Proteomics* **5:** 914-22

Tsavachidou D, McDonnell TJ, Wen S, Wang X, Vakar-Lopez F, Pisters LL, Pettaway CA, Wood CG, Do KA, Thall PF, Stephens C, Efstathiou E, Taylor R, Menter DG, Troncoso P, Lippman SM, Logothetis CJ, Kim J (2009) Selenium and vitamin E: cell type- and intervention-specific tissue effects in prostate cancer. *Journal of the National Cancer Institute* **101:** 306-20

Tucker CA, Bebb G, Klasa RJ, Chhanabhai M, Lestou V, Horsman DE, Gascoyne RD, Wiestner A, Masin D, Bally M, Williams ME (2006) Four human t(11;14)(q13;q32)-containing cell lines having classic and variant features of Mantle Cell Lymphoma. *Leuk Res* **30:** 449-57

Turker O, Kumanlioglu K, Karapolat I, Dogan I (2006) Selenium treatment in autoimmune thyroiditis: 9-month follow-up with variable doses. *J Endocrinol* **190:** 151-6

Uddin S, Hussain AR, Siraj AK, Manogaran PS, Al-Jomah NA, Moorji A, Atizado V, Al-Dayel F, Belgaumi A, El-Solh H, Ezzat A, Bavi P, Al-Kuraya KS (2006) Role of phosphatidylinositol 3'-kinase/AKT pathway in diffuse large B-cell lymphoma survival. *Blood* **108:** 4178-86

Ueno M, Masutani H, Arai RJ, Yamauchi A, Hirota K, Sakai T, Inamoto T, Yamaoka Y, Yodoi J, Nikaido T (1999) Thioredoxin-dependent redox regulation of p53-mediated p21 activation. *The Journal of biological chemistry* **274:** 35809-15

Ungerstedt JS, Sowa Y, Xu WS, Shao Y, Dokmanovic M, Perez G, Ngo L, Holmgren A, Jiang X, Marks PA (2005) Role of thioredoxin in the response of normal and transformed cells to histone deacetylase inhibitors. *Proceedings of the National Academy of Sciences of the United States of America* **102:** 673-8

Unni E, Koul D, Yung WK, Sinha R (2005) Se-methylselenocysteine inhibits phosphatidylinositol 3-kinase activity of mouse mammary epithelial tumor cells in vitro. *Breast Cancer Res* **7:** R699-707

van Besien K, Ha CS, Murphy S, McLaughlin P, Rodriguez A, Amin K, Forman A, Romaguera J, Hagemeister F, Younes A, Bachier C, Sarris A, Sobocinski KS, Cox JD, Cabanillas F (1998) Risk factors, treatment, and outcome of central nervous system

recurrence in adults with intermediate-grade and immunoblastic lymphoma. *Blood* **91:** 1178-84

Velasquez WS, Cabanillas F, Salvador P, McLaughlin P, Fridrik M, Tucker S, Jagannath S, Hagemeister FB, Redman JR, Swan F, et al. (1988) Effective salvage therapy for lymphoma with cisplatin in combination with high-dose Ara-C and dexamethasone (DHAP). *Blood* **71:** 117-22

Velasquez WS, McLaughlin P, Tucker S, Hagemeister FB, Swan F, Rodriguez MA, Romaguera J, Rubenstein E, Cabanillas F (1994) ESHAP--an effective chemotherapy regimen in refractory and relapsing lymphoma: a 4-year follow-up study. *J Clin Oncol* **12:** 1169-76

Verhey KJ, Gaertig J (2007) The tubulin code. *Cell Cycle* **6:** 2152-60

Vose JM, Rizzo DJ, Tao-Wu J, Armitage JO, Bashey A, Burns LJ, Christiansen NP, Freytes CO, Gale RP, Gibson J, Giralt SA, Herzig RH, Lemaistre CF, McCarthy PL, Jr., Nimer SD, Petersen FB, Schenkein DP, Wiernik PH, Wiley JM, Loberiza FR, Lazarus HM, van Biesen K, Horowitz MM (2004) Autologous transplantation for diffuse aggressive non-Hodgkin lymphoma in first relapse or second remission. *Biol Blood Marrow Transplant* **10:** 116-27

Wakasugi N, Tagaya Y, Wakasugi H, Mitsui A, Maeda M, Yodoi J, Tursz T (1990) Adult T-cell leukemia-derived factor/thioredoxin, produced by both human T-lymphotropic virus type I- and Epstein-Barr virus-transformed lymphocytes, acts as an autocrine growth factor and synergizes with interleukin 1 and interleukin 2. *Proceedings of the National Academy of Sciences of the United States of America* **87:** 8282-6

Walshe J, Serewko-Auret MM, Teakle N, Cameron S, Minto K, Smith L, Burcham PC, Russell T, Strutton G, Griffin A, Chu FF, Esworthy S, Reeve V, Saunders NA (2007) Inactivation of glutathione peroxidase activity contributes to UV-induced squamous cell carcinoma formation. *Cancer Res* **67:** 4751-8

Wang ES, Teruya-Feldstein J, Wu Y, Zhu Z, Hicklin DJ, Moore MA (2004) Targeting autocrine and paracrine VEGF receptor pathways inhibits human lymphoma xenografts in vivo. *Blood* **104:** 2893-902

Wang Z, Hu H, Li G, Lee HJ, Jiang C, Kim SH, Lu J (2008) Methylseleninic acid inhibits microvascular endothelial G1 cell cycle progression and decreases tumor microvessel density. *International journal of cancer* **122:** 15-24

Wang Z, Jiang C, Ganther H, Lu J (2001) Antimitogenic and proapoptotic activities of methylseleninic acid in vascular endothelial cells and associated effects on PI3K-AKT, ERK, JNK and p38 MAPK signaling. *Cancer Res* **61:** 7171-8

Wang Z, Lee HJ, Chai Y, Hu H, Wang L, Zhang Y, Jiang C, Lu J (2010) Persistent P21Cip1 induction mediates G(1) cell cycle arrest by methylseleninic acid in DU145 prostate cancer cells. *Curr Cancer Drug Targets* **10:** 307-18

Warren DT, Zhang Q, Weissberg PL, Shanahan CM (2005) Nesprins: intracellular scaffolds that maintain cell architecture and coordinate cell function? *Expert Rev Mol Med* **7:** 1-15

Watanabe-Suzuki K, Ishii A, Suzuki O (2002) Cryogenic oven-trapping gas chromatography for analysis of volatile organic compounds in body fluids. *Analytical and bioanalytical chemistry* **373:** 75-80

Wei WQ, Abnet CC, Qiao YL, Dawsey SM, Dong ZW, Sun XD, Fan JH, Gunter EW, Taylor PR, Mark SD (2004) Prospective study of serum selenium concentrations and esophageal and gastric cardia cancer, heart disease, stroke, and total death. *The American journal of clinical nutrition* **79:** 80-5

Weick JK, Dahlberg S, Fisher RI, Dana B, Miller TP, Balcerzak SP, Pierce HI (1991) Combination chemotherapy of intermediate-grade and high-grade non-Hodgkin's lymphoma with MACOP-B: a Southwest Oncology Group study. *J Clin Oncol* **9:** 748-53

Weitzel F, Ursini F, Wendel A (1990) Phospholipid hydroperoxide glutathione peroxidase in various mouse organs during selenium deficiency and repletion. *Biochimica et biophysica acta* **1036:** 88-94

West KA, Castillo SS, Dennis PA (2002) Activation of the PI3K/Akt pathway and chemotherapeutic resistance. *Drug Resist Updat* **5:** 234-48

Whelan JS, Davis CL, Rohatiner AZ, Leahy M, MacCallum PK, Gupta RK, Matthews J, Norton AJ, Amess JA, Lister TA (1992) Etoposide in combination with intermediate dose cytosine arabinoside (ID ARA C) given with the intention of further myeloablative therapy for the treatment of refractory or recurrent hematological malignancy. *Hematol Oncol* **10:** 87-94

Whitesell L, Lindquist SL (2005) HSP90 and the chaperoning of cancer. *Nature reviews* **5:** 761-72

Wilks S (1865) Cases of enlargement of the lymphatic glands and spleen (or Hodgkin’s disease), with remarks. *Guy's Hosp Rep* **11:** 56-67

Wilson AJ, Byun DS, Popova N, Murray LB, L'Italien K, Sowa Y, Arango D, Velcich A, Augenlicht LH, Mariadason JM (2006) Histone deacetylase 3 (HDAC3) and other class I HDACs regulate colon cell maturation and p21 expression and are deregulated in human colon cancer. *The Journal of biological chemistry* **281:** 13548-58

Wingler K, Bocher M, Flohe L, Kollmus H, Brigelius-Flohe R (1999) mRNA stability and selenocysteine insertion sequence efficiency rank gastrointestinal glutathione peroxidase high in the hierarchy of selenoproteins. *European journal of biochemistry / FEBS* **259:** 149-57

Wu Y, Fabritius M, Ip C (2009) Chemotherapeutic sensitization by endoplasmic reticulum stress: increasing the efficacy of taxane against prostate cancer. *Cancer biology & therapy* **8:** 146-52

Wu Y, Zhang H, Dong Y, Park YM, Ip C (2005) Endoplasmic reticulum stress signal mediators are targets of selenium action. *Cancer Res* **65:** 9073-9

Wu Y, Zu K, Warren MA, Wallace PK, Ip C (2006) Delineating the mechanism by which selenium deactivates Akt in prostate cancer cells. *Molecular cancer therapeutics* **5:** 246-52

Xia Y, Hill KE, Byrne DW, Xu J, Burk RF (2005) Effectiveness of selenium supplements in a low-selenium area of China. *The American journal of clinical nutrition* **81:** 829-34

Xiang N, Zhao R, Song G, Zhong W (2008) Selenite reactivates silenced genes by modifying DNA methylation and histones in prostate cancer cells. *Carcinogenesis* **29:** 2175-81

Xu WS, Parmigiani RB, Marks PA (2007) Histone deacetylase inhibitors: molecular mechanisms of action. *Oncogene* **26:** 5541-52

Yamamoto A, Tagawa Y, Yoshimori T, Moriyama Y, Masaki R, Tashiro Y (1998) Bafilomycin A1 prevents maturation of autophagic vacuoles by inhibiting fusion between autophagosomes and lysosomes in rat hepatoma cell line, H-4-II-E cells. *Cell Struct Funct* **23:** 33-42

Yanagawa T, Ishikawa T, Ishii T, Tabuchi K, Iwasa S, Bannai S, Omura K, Suzuki H, Yoshida H (1999) Peroxiredoxin I expression in human thyroid tumors. *Cancer letters* **145:** 127-32

Yang GQ, Wang SZ, Zhou RH, Sun SZ (1983) Endemic selenium intoxication of humans in China. *The American journal of clinical nutrition* **37:** 872-81

Yeo JK, Cha SD, Cho CH, Kim SP, Cho JW, Baek WK, Suh MH, Kwon TK, Park JW, Suh SI (2002) Se-methylselenocysteine induces apoptosis through caspase activation and Bax cleavage mediated by calpain in SKOV-3 ovarian cancer cells. *Cancer letters* **182:** 83-92

Yin MB, Li ZR, Toth K, Cao S, Durrani FA, Hapke G, Bhattacharya A, Azrak RG, Frank C, Rustum YM (2006) Potentiation of irinotecan sensitivity by Se-methylselenocysteine in an in vivo tumor model is associated with downregulation of cyclooxygenase-2,

inducible nitric oxide synthase, and hypoxia-inducible factor 1alpha expression, resulting in reduced angiogenesis. *Oncogene* **25:** 2509-19

Yoo MH, Xu XM, Carlson BA, Gladyshev VN, Hatfield DL (2006) Thioredoxin reductase 1 deficiency reverses tumor phenotype and tumorigenicity of lung carcinoma cells. *The Journal of biological chemistry* **281:** 13005-8

Yoshimori T, Yamamoto A, Moriyama Y, Futai M, Tashiro Y (1991) Bafilomycin A1, a specific inhibitor of vacuolar-type H(+)-ATPase, inhibits acidification and protein degradation in lysosomes of cultured cells. *The Journal of biological chemistry* **266:** 17707-12

Yoshizawa K, Willett WC, Morris SJ, Stampfer MJ, Spiegelman D, Rimm EB, Giovannucci E (1998) Study of prediagnostic selenium level in toenails and the risk of advanced prostate cancer. *Journal of the National Cancer Institute* **90:** 1219-24

Younes A, Wedgwood A, McLaughlin P, Andreadis C, Assouline SE, Li Z, Martell RE, Dubay M, Patterson TA, Ward MR, Crump M (2007) Treatment of relapsed or refractory lymphoma with the oral isotype-selective histone deacetylase inhibitors MGCD0103: interim results from a phase II study. *Blood* **110:** abstr. 2571

Yu C, Rahmani M, Conrad D, Subler M, Dent P, Grant S (2003) The proteasome inhibitor bortezomib interacts synergistically with histone deacetylase inhibitors to induce apoptosis in Bcr/Abl+ cells sensitive and resistant to STI571. *Blood* **102:** 3765-74

Zhang H, Dong Y, Zhao H, Brooks JD, Hawthorn L, Nowak N, Marshall JR, Gao AC, Ip C (2005) Microarray Data Mining for Potential Selenium Targets in Chemoprevention of Prostate Cancer. *Cancer Genomics Proteomics* **2:** 97-114

Zhang L, Hanigan MH (2003) Role of cysteine S-conjugate beta-lyase in the metabolism of cisplatin. *J Pharmacol Exp Ther* **306:** 988-94

Zhao H, Whitfield ML, Xu T, Botstein D, Brooks JD (2004) Diverse effects of methylseleninic acid on the transcriptional program of human prostate cancer cells. *Molecular biology of the cell* **15:** 506-19

Zhao R, Domann FE, Zhong W (2006) Apoptosis induced by selenomethionine and methioninase is superoxide mediated and p53 dependent in human prostate cancer cells. *Molecular cancer therapeutics* **5:** 3275-84

Zhong H, De Marzo AM, Laughner E, Lim M, Hilton DA, Zagzag D, Buechler P, Isaacs WB, Semenza GL, Simons JW (1999) Overexpression of hypoxia-inducible factor 1alpha in common human cancers and their metastases. *Cancer Res* **59:** 5830-5

Zhu K, Dunner K, Jr., McConkey DJ (2010) Proteasome inhibitors activate autophagy as a cytoprotective response in human prostate cancer cells. *Oncogene* **29:** 451-62

Zhu Z, Jiang W, Ganther HE, Thompson HJ (2002) Mechanisms of cell cycle arrest by methylseleninic acid. *Cancer Res* **62:** 156-64

Zhuo H, Smith AH, Steinmaus C (2004) Selenium and lung cancer: a quantitative analysis of heterogeneity in the current epidemiological literature. *Cancer Epidemiol Biomarkers Prev* **13:** 771-8

Zinszner H, Kuroda M, Wang X, Batchvarova N, Lightfoot RT, Remotti H, Stevens JL, Ron D (1998) CHOP is implicated in programmed cell death in response to impaired function of the endoplasmic reticulum. *Genes & development* **12:** 982-95

Zu K, Bihani T, Lin A, Park YM, Mori K, Ip C (2006) Enhanced selenium effect on growth arrest by BiP/GRP78 knockdown in p53-null human prostate cancer cells. *Oncogene* **25:** 546-54

APPENDIX

Appendices to Chapter 4

MSA µmol/L	Set 1	Set 2	Set 3	Mean	+/- SD
0	100	100	100	100	0
0.5	108	115.8	83.5	102.4	16.9
1	111.9	106.8	74.8	97.8	20.1
3	63.7	82.4	55.2	67.1	13.9
5	20.5	33.6	45.9	33.3	12.7
10	0.5	3.2	5.1	2.9	2.3

Table 1 Concentration-effect of the RL cell line exposed MSA for 72 hours. Results expressed relative to control values.

MSA µmol/L	Set 1	Set 2	Set 3	Mean	+/- SD
0	100	100	100	100	0
10	100.9	123.8	93.8	106.2	15.7
50	57.3	77	72.4	68.9	10.3
100	19.3	10.9	35.2	21.8	12.3
200	2	3.2	4.6	3.3	1.3
400	0.4	2.7	1.9	1.7	1.2

Table 2 Concentration-effect of the DoHH2 cell line exposed to MSA for 72 hours. Results expressed relative to control values.

MSA µmol/L	Set 1	Set 2	Set 3	Mean	+/- SD
0	100	100	100	100	0
0.5	109.2	111.5	112.3	111	1.6
1	107.4	125.6	94.9	109.3	15.4
3	97.6	90.3	123.1	103.7	17.2
5	87.7	82.2	73.2	81	7.3
10	37.7	37.1	11.4	28.7	15

Table 3 Concentration-effect of the SUD4 cell line exposed to MSA for 72 hours. Results expressed relative to control values.

MSA µmol/L	Set 1	Set 2	Set3	Mean	+/- SD
0	100	100	100	100	0
10	95.5	126.9	92	104.8	19.2
50	77.7	104	77.7	86.5	15.2
100	21.2	24	25.2	23.5	2.1
200	6.9	5.9	14	8.9	4.4
400	2.5	2.4	7.1	4	2.7

Table 4 Concentration-effect of the DHL4 cell line exposed to MSA for 72 hours. Results expressed relative to control values.

Doxorubicin nmol/L	Set 1	Set 2	Set 3	mean	SD+/-
0	100	100	100	100	0
10	92.3	86.1	96.2	91.5	5.1
50	79.2	76.4	75.0	76.9	2.2
100	68.0	81.4	77.0	75.5	6.9
250	56.4	70.1	58.5	61.6	7.4
Doxorubicin+1µmol/L MSA					
MSA alone	101.2	98.7	100.4	100.1	1.3
10	91.7	89.0	99.1	93.3	5.2
50	74.4	66.7	64.5	68.5	5.2
100	54.8	56.2	47.1	52.7	4.9
250	27.8	33.2	37.1	32.7	4.7
Doxorubicin+ 1µmol/L MSA	Expected cell viability				
MSA alone	101.2	98.7	100.4	100.1	1.3
10	93.5	84.8	96.6	91.6	6.1
50	80.4	75.1	75.4	77.0	3.0
100	69.2	80.1	77.4	75.6	5.7
250	57.6	68.8	58.9	61.7	6.1

Table 5 Cell viability of RL cells exposed to doxorubicin alone and in combination with MSA 1µmol/L for 48 hours. Results expressed relative to control.

4-HC µmol/L	Set 1	Set 2	Set 3	Mean	SD+/-
0	100	100	100	100	0
0.5	99.6	99.5	100.1	99.7	0.3
1	99.7	99.7	99.8	99.7	0.0
2	99.4	99.0	99.1	99.2	0.2
3	99.3	98.0	97.8	98.4	0.8
5	97.5	81.4	81.3	86.8	9.3
4-HC+10µmol/L MSA					
control	92.8	96.6	90.1	93.2	3.3
0.5	87.0	94.5	79.9	87.1	7.3
1	79.7	89.8	75.9	81.8	7.2
2	65.6	75.8	65.4	68.9	5.9
3	50.8	56.6	55.6	54.3	3.1
5	30.0	28.4	21.6	26.7	4.5
4-HC+10µmol/L MSA	Expected cell viability				
0	92.8	96.6	90.1	93.2	3.3
0.5	92.4	96.1	90.2	92.9	3.0
1	92.5	96.3	89.9	92.9	3.2
2	92.2	95.6	89.2	92.3	3.2
3	92.1	94.6	87.9	91.5	3.4
5	90.3	78.0	71.4	79.9	9.6

Table 6 Cell viability of DHL4 cells exposed to 4-HC alone and in combination with MSA 10µmol/L for 48 hours. Results expressed relative to control.

MSA µmol/L	Set 1	Set 2	Set 3	Mean	+/-SD
0	255.0	252.6	244.5	250.7	5.5
1	248.4	270.6	245.1	254.7	13.8
3	303.9	294.8	251.4	283.4	28.0
5	280.2	278.3	298.6	285.7	11.2
10	279.3	257.2	260.1	265.5	12.0
20	305.0	270.2	271.3	282.2	19.8

Table 7 GSH concentration in DHL4 cells exposed to MSA for 2 hours. Results expressed as pmoles/million cells.

MSA µmol/L	Set 1	Set 2	Set 3	Mean	+/-SD
0	223.8	229.4	209.2	220.8	10.4
1	215.1	222.1	219.4	218.8	3.5
3	272.9	240.2	242.7	251.9	18.2
5	246.4	212.5	258.5	239.1	23.8
10	197.7	184.8	226.2	202.9	21.2
20	197.2	155.9	239.7	197.6	41.9

Table 8 GSH concentration in DHL4 cells exposed to MSA for 24 hours. Results expressed as pmoles/million cells.

MSA µmol/L	Set 1	Set 2	Set 3	Mean	+/-SD
0	142.5	212.3	176.9	177.2	34.9
1	259.8	247.3	219.5	242.2	20.6
3	253.8	221.1	266.7	247.2	23.5
5	260.2	200.1	132.5	197.6	63.9
10	219.3	196.4	233.5	216.4	18.7
20	187.0	179.9	252.8	206.5	40.2

Table 9 GSH concentration in RL cells exposed to MSA for 2 hours. Results expressed as pmoles/million cells.

MSA µmol/L	Set 1	Set 2	Set 3	Mean	+/-SD
0	253.5	260.7	237.3	250.5	11.9
1	224.1	229.2	237.7	230.3	6.9
3	280.7	209.7	310.6	267.0	51.8
5	241.4	210.5	275.9	242.6	32.7
10	163.8	94.1	156.4	138.1	38.3
20	149.7	82.0	121.9	117.9	34.0

Table 10 GSH concentration in RL cells exposed to MSA for 24 hours. Results expressed as pmoles/million cells.

MSA µmol/L	Set 1	Set 2	Set 3	Mean	+/-SD
0	225.6	259.7	208.8	231.4	25.9
1	214.9	226.3	213.5	218.2	7.0
3	240.4	231.6	223.0	231.7	8.7
5	188.0	215.0	220.2	207.7	17.3
10	57.5	137.4	118.0	104.3	41.7
20	17.0	24.7	25.0	22.3	4.5

Table 11 GSH concentration in SUD4 cells exposed to MSA for 24 hours. Results expressed as pmoles/million cells

MSA µmol/L	Set 1	Set 2	Set 3	Set 4	Mean	+/-SD
0	0	0	0	0	0	0
1	-11.3	-0.9	-4.5	-1.3	-4.5	4.8
5	4.7	12.4	16.9	13.1	11.8	5.1
20	28.7		47.4	54.9	43.7	13.5
Doxorubicin 250nmol/L	18.3	22.7	14.1		18.4	4.3

Table 12 JC-1 staining in RL cells exposed to MSA and doxorubicin for 24 hours. Results are % decrease in red fluorescence relative to control.

MSA µmol/L	Set 1	Set 2	Set 3	Set 4	Mean	SD+/-
0	0	0	0	0	0	0
1	-2.8	0.2	-3.3	-1.6	-2.0	1.6
10	1.4	5.5	4.8	9.0	3.9	3.1
100	39.9		36.6	46.2	38.3	4.9
Doxorubicin 500nmol/L	15.3	21.5			18.4	4.4

Table 13 JC-1 staining in DHL4 cells exposed to MSA and doxorubicin for 24 hours. Results are % decrease in red fluorescence relative to control.

MSA µmol/L	Set 1	Set 2	Mean	+/-SD
0	0	0	0	0
1	-3.3	-0.1	-1.7	2.3
5	15.8	8.0	11.9	5.5
10	53.8	62.4	58.1	6.1
Doxorubicin 100nmol/L	47.4	36.6	42.0	7.6

Table 14 JC-1 staining in RL cells exposed to MSA and doxorubicin for 48 hours. Results are % decrease in red fluorescence relative to control.

MSA µmol/L	Set 1	Set 2	Set 3	Mean	+/-SD
0	0	0	0	0	0
1	-3.5	-1.6	0.7	-1.5	2.1
10	1.6	7.4	3.0	4.0	3.0
50	25.0	39.9	25.9	30.3	8.4
Doxorubicin 500nmol/L	16.6	17.4	5.2	17.0	6.8

Table 15 JC-1 staining in DHL4 cells exposed to MSA and doxorubicin for 48 hours. Results are % decrease in red fluorescence relative to control.

MSA µmol/L	Set 1	Set 2	Set 3	Set 4	Set 5	Set 6	Set 7	Set 8	Mean	+/- SD
0	100	100	100	100	100	100	100	100	100	0
0.5	100.1	96.2		123.3					106.5	14.7
1	91.1	76.6	67.5		76.8	93.7	88.3		82.3	10.2
3	75.7	60.5	71.5	65.7	40.7	41.6	49.6	48.2	56.6	13.6
5	44.6	38.4	46.6	42.7	22.9	22.3	30.9	28.4	34.5	9.8
10	21.3	18.9	21.4	24.4	13.6	12.2	16.9	17	18.1	4.2
20					8.3	6.6	9.7	9.2	8.3	1.2

Table 16 Concentration-effect of the JVM2 cell line exposed to MSA. Results expressed relative to control.

MSA µmol/L	Phase of cell cycle	Set 1	Set 2	Set 3	Mean	+/-SD
0	A	2.1	2.5	2.6	2.4	0.2
	G1	54.4	50.9	52.2	52.5	1.8
	S	6.8	8.6	7.3	7.5	0.9
	G2	13.1	10.5	9.7	11.1	1.8
3.4	A	16.7	29.2	30.9	25.6	7.8
	G1	26.4	43.9	41.5	37.3	9.5
	S	7.7	7.1	6.4	7.1	0.6
	G2	7.7	9.2	9.4	8.8	0.9

Table 17 Cell cycle analysis of JVM2 cells exposed to MSA for 72 hours. Results are % of cells in each phase of the cell cycle.

	Set 1	Set 2	Set 3	Mean	+/-SD
Control	100.0	100.0	100.0	100.0	0.0
Pervanadate 100µmol/L	478.3	535.2	511.3	508.3	23.3
Pervanadate + MSA 0.5µmol/L	458.9	477.5	483.7	473.4	10.6
Pervanadate + MSA 1µmol/L	459.5	465.9	461.9	462.4	2.6
Pervanadate +MSA 3µmol/L	443.3	541.6	441.5	475.5	46.8
Pervanadate + MSA 5µmol/L	454.0	591.5	436.8	494.1	69.2
Pervanadate + MSA 10µmol/L	410.7	463.9	426.2	433.6	22.4
Pervanadate + Wortmannin 1µmol/L	290.9	346.9	335.5	324.4	24.2

Table 18 Aktide assay in JVM2 cells exposed to pervanadate for 30 minutes followed by MSA for a further 30 minutes. Results are expressed relative to control.

	Set 1	Set 2	Mean	+/-SD
Control	100.0	100.0	100.0	0.0
Pervanadate 100µmol/L	160.3	182.9	171.6	16.0
Pervanadate + MSA 0.5µmol/L	183.7	149.1	166.4	24.5
Pervanadate + MSA 1µmol/L	175.6	173.0	174.3	1.8
Pervanadate +MSA 3µmol/L	154.9	142.1	148.5	9.1
Pervanadate + MSA 5µmol/L	138.4	153.9	146.1	10.9
Pervanadate + MSA 10µmol/L	153.9	135.7	144.8	12.9
Pervanadate + Wortmannin 1µmol/L	117.0	134.8	125.9	12.6

Table 19 Aktide assay in JVM2 cells exposed to pervanadate for 30 minutes followed by MSA for a further 2 hours. Results are expressed relative to control.

Doxorubicin nmol/L	Set 1	Set 2	Set 3	Mean	SD+/-
0	1	1	1	1	0
10	1.9	1.2	1.4	1.5	0.4
50	4.5	3.9	3.8	4.1	0.4
100	7.7	7.1	8.3	7.7	0.6
250	17.3	15.7	17.7	16.9	1.1
500	32.1	29.0	23.4	28.2	4.4
Doxorubicin+1µmol/LMSA					
0	1	1	1	1	0
10	2.1	1.2	1.4	1.5	0.4
50	5.0	3.7	4.2	4.3	0.7
100	8.1	7.4	7.7	7.7	0.4
250	18.3	15.1	17.5	17.0	1.7
500	33.1	27.6	25.9	28.9	3.7

Table 20 Intracellular doxorubicin in RL cells exposed to doxorubicin alone and in combination with 1µmol/L MSA. Results are expressed as fold change in mean fluorescence relative to control.

Doxorubicin nmol/L	Set 1	Set 2	Set 3	Mean	SD+/-
0	1	1	1	1	0
10	1.3	1.2	1.2	1.2	0.1
50	3.8	3.0	3.2	3.3	0.4
100	6.7	5.6	5.5	5.9	0.6
250	14.5	12.4	11.7	12.9	1.5
500	24.2	22.3	18.6	21.7	2.8
Doxorubicin+10µmol/L MSA					
0	1	1	1	1	0
10	2.0	1.8	1.7	1.8	0.1
50	4.9	4.0	3.6	4.1	0.6
100	7.7	6.5	5.9	6.7	0.9
250	14.5	13.4	11.9	13.3	1.3
500	26.1	23.1	21.7	23.6	2.2

Table 21 Intracellular doxorubicin in DHL4 cells exposed to doxorubicin alone and in combination with 10µmol/L MSA. Results are expressed as fold change in mean fluorescence relative to control.

MSC µmol/L	Set 1	Set 2	Set 3	Set 4	Set 5	Set 6	Set 7	Mean	+/-SD
0	100	100	100	100	100	100	100	100	0
1	98.3	99.2	114.7	100				103.1	7.8
3	97.1	93.9	117.8	118.8				106.9	13.2
5	97.4	89.8	116.3	119				105.6	14.3
10	97.3	91.1	110.4	116				103.7	11.5
20			70.2	86	81.1	93	95.7	85.2	10.2
30			55.7	69.2	72.2	72.3	70	67.9	6.9
40			53.6	57.2	60.7	62	59.5	58.6	3.3
50			48.1	49.5	52.4	53.8	51.4	51	2.3
100			37.2	33.3	41	36.7	34.9	36.6	2.9

Table 22 Concentration-effect of the DHL4 cell line exposed to MSC for 72 hours. Results expressed relative to control.

MSC μmol/L	Set 1	Set 2	Set 3	Set 4	Mean	+/-SD
0	100	100	100	100	100	0
1	109	102	107.8	116.6	108.9	6
3	100.6	102.2	106.7	113.5	105.8	5.8
5	97.8	96.6	102.4	112.4	102.3	7.2
10	95.6	90	99.5	107.2	98.1	7.2
15			83.1	94.3	88.7	7.9
20	53.3	59.5	58	68.3	59.8	6.3
30			14.8	13.4	14.1	1
40			5.3	5.4	5.4	0.1
50			3.9	3.1	3.5	0.6
100			2.2	1.6	1.9	0.4

Table 23 Concentration-effect of the RL cell line exposed to MSC for 72 hours. Results expressed relative to control.

MSC μmol/L	Set 1	Set 2	Set 3	Set 4	Set 5	Mean	+/-SD
0	100	100	100	100	100	100	0
1	112	124.6	117.2	121.8	117.8	118.7	4.8
3	125.9	125.1	119.9	131.2	116.2	123.7	5.8
5	125.2	121.3	123.7	126.6	122.1	123.7	2.2
10	116.2	106.6	123.8	109	115.7	114.3	6.8
15	96.6	99.1	112.7	124	101.7	106.8	11.4
20		97	90.6	94.9	107.1	97.4	7
30		87.8	86.2	97.1	95.7	91.7	5.5
40		79.1	82.9	98.1	79.5	84.9	9
50		77.6	77.1	94.4	65	78.5	12.1
100		63	38.4	38.7	26.2	34.9	5.9

Table 24 Concentration-effect of the JVM2 cell line exposed to MSC for 72 hours. Results expressed relative to control.

Appendices to Chapter 5

MSA µmol/L	Time (hrs)	Experiment 1	Experiment 2	Mean	+/-SD
0	Control	1.0	1.0	1.0	0.0
3	4	1.3	0.8	1.1	0.3
3	6	1.8	1.2	1.5	0.5
3	24	1.8	1.0	1.4	0.6
3	48	1.5	0.9	1.2	0.4
5	4	1.8	0.9	1.3	0.6
5	6	2.0	1.6	1.8	0.3
5	24	2.9	1.3	2.1	1.1
5	48	2.4	1.3	1.8	0.8

Table 25 Densitometry values for western blots of p-eIF2α in RL cells exposed to MSA. Results expressed as fold change relative to total eIF2α.

MSA µmol/L	Time (hrs)	Experiment 1	Experiment 2	Mean	+/-SD
0	Control	1.0	1.0	1.0	0.0
30	4	0.5	0.6	0.6	0.1
30	6	0.4	0.4	0.4	0.0
30	24	0.7	0.7	0.7	0.0
30	48	1.2	1.0	1.1	0.1
0	Control	1.0	1.0	1.0	0.0
60	4	0.4	0.5	0.4	0.0
60	6	0.4	0.6	0.5	0.2
60	24	0.7	1.1	0.9	0.3
60	48	0.8	2.2	1.5	0.9

Table 26 Densitometry values for western blots of p-eIF2α in DHL4 cells exposed to MSA. Results expressed as fold change relative to eIF2α.

MSA µmol/L	Time (hrs)	Set 1	Set 2	Set 3	Set 4	Mean	+/- SD
0	Control	1	1	1	1	1	0
1	4		1.7	1.1	1.1	1.3	0.3
1	6		1	1.1	1	1	0
1	24		1.8	1.6	0.9	1.4	0.4
1	48		1.6	1.3	1.3	1.4	0.1
3	4		1.8	1.5	1.4	1.6	0.1
3	6		1.9	1.3	1.3	1.6	0.3
3	24		1.8	0.8	0.8	1.1	0.5
3	48		1.9	1.2	1.2	1.5	0.3
5	4	3.5	5	4.5		4.3	0.7
5	6	4.3	4.7	5.3		4.8	0.4
5	24	1.4	1.2	1.4		1.4	0.1
5	48	0.9	1.1	1		1	0.1

Table 27 GADD153 mRNA expression in RL cells exposed to MSA. Results expressed as fold change relative to control.

MSA µmol/L	Time (hours)	Set 1	Set 2	Set 3	Mean	+/-SD
0		1	1	1	1	0
5	4	8.8	11	10.5	9.9	1.5
5	6	5.2	4.1	4.4	4.7	0.8
5	24	0.7	0.7	1.1	0.7	0
5	48	0.8	1.1	1.6	1.1	0.2
10	4	18.1	7.7	18.5	14.7	5
10	6	15.5	8.2	22.2	15.3	5.7
10	24	28.4	14.2	26.2	22.9	6.2
10	48	27.4	18.7		23	4.4
30	4	14.6	11.3	19.6	15.2	3.4
30	6	15.4	19.8	26	20.1	4.4
30	24	39.4	21.9	42.3	34.6	9.1
30	48	129.2	72	104.1	101.7	23.4
60	4	13.5	11.9	14.5	13.3	1.1
60	6	16	10.2	16.3	14.2	2.8
60	24	41.1	32.8	56.8	43.6	10
60	48	85.3	65.3	115.9	88.8	20.8

Table 28 GADD153 mRNA expression in DHL4 cells exposed to MSA. Results expressed as fold change relative to control.

	Set 1	Set 2	Set 3	Mean	+/-SD
Control	5.7	4.7	2.7	4.4	1.5
TG 3µmol/L	9.2	8.5	8.9	8.9	0.3
MSA 10µmol/L	17.5	19.4	18.3	18.4	1.0
MSA 20µmol/L	29.4	35.6	20.4	28.5	7.6

Table 29 Acridine orange staining in DHL4 cells exposed to MSA and Thapsigargin (TG) for 24 hours. Results represent the % increase in red fluorescence.

MSA µmol/L	Set 1	Set 2	Set 3	Mean	+/-SD
0	100	100	100	100	0
10	94.3	94.9	92.0	93.7	1.6
20	76.6	75.0	65.8	72.4	5.8
MSA+Bafilomycin 10nmol/L					SD+/-
Bafilomycin alone	99.6	99.0	96.3	98.3	1.7
10	55.6	57.1	48.2	53.6	4.7
20	22.4	35.5	37.1	31.7	8.1

Table 30 Cell viability of the DHL4 cell line exposed to MSA alone and combined with bafilomycin A1 for 48 hours. Results expressed relative to control.

Appendices to Chapter 6

TSA nmol/L	Set 1	Set 2	Set 3	Set 4	Set 5	Mean	+/-SD
0	100.0	100.0	100.0	100.0	100.0	100.0	0.0
0.5	88.7	92.6	93.2	97.9	93.8	93.2	3.3
5	47.8	60.3	60.6	43.9	51.0	52.7	7.5
50	9.9	4.3	5.8	1.7	3.2	5.0	3.1

Table 31 TSA inhibition of *Fluor de Lys*™ substrate deacetylation by HeLa nuclear extract after 30-minute exposure. Results expressed relative to control.

MSA µmol/L	Set 1	Set 2	Set 3	Mean	+/-SD
Control	100.0	100.0	100.0	100.0	0.0
5	102.6	92.6	91.5	95.6	6.1
10	96.0	97.1	100.2	97.8	2.2
20	97.3	90.5	99.9	95.9	4.9

Table 32 Effect of MSA on *Fluor de Lys*™ substrate deacetylation by HeLa nuclear extract after 30-minute exposure. Results expressed relative to control.

	Set 1	Set 2	Set 3	Mean	+/-SD
Control	100.0	100.0	100.0	100.0	0.0
MSA 10µmol/L	58.2	71.0	69.5	66.2	7.0
MSA 30µmol/L	36.4	60.0	55.1	50.5	12.4
TSA 100nmol/L	25.2	43.8	33.5	34.2	9.3

Table 33 Deacetylation of *Fluor de Lys*™ substrate in DHL4 cells exposed to MSA and TSA for 2 hours using the cellular HDAC activity assay. Results expressed relative to control.

	Set 1	Set 2	Mean	+/-SD
Control	100.0	100.0	100.0	0.0
MSA 5µmol/L	73.1	80.5	76.8	5.3
MSA 10µmol/L	61.0	64.5	62.7	2.5
MSA 30µmol/L	46.7	57.4	52.0	7.5
TSA 100nmol/L	35.2	50.9	43.1	11.1

Table 34 Deacetylation of *Fluor de Lys*™ substrate in SUD4 cells exposed to MSA and TSA for 2 hours using the cellular HDAC activity assay. Results expressed relative to control.

	Set 1	Set 2	Set 3	Set 4	Mean	+/-SD
Control	100.0	100.0	100.0	100.0	100.0	0.0
MSA 5µmol/L	75.8	90.8	97.5	72.1	84.1	12.0
MSA 10µmol/L	77.8	67.8	54.2	70.7	67.6	9.9
MSA 30µmol/L	63.6	65.3	41.9	63.3	58.5	11.1
TSA 100nmol/L	67.1	59.2	32.9	43.9	50.8	15.4

Table 35 Deacetylation of *Fluor de Lys*™ substrate in RL cells exposed to MSA and TSA for 2 hours using the cellular HDAC activity assay. Results expressed relative to control.

HeLa extract	Set 1	Set 2	Mean	+/-SD
Control	100.0	100.0	100.0	0.0
MSA 10µmol/L	110.2	109.1	109.7	0.7
MSA 30µmol/L	103.9	102.0	103.0	1.4
TSA 50nmol/L	12.1	5.4	8.8	4.7
DHL4 lysates				
Control	100.0	100.0	100.0	0.0
MSA 10µmol/L	108.1	108.5	108.3	0.3
MSA 30µmol/L	101.7	108.3	105.0	4.6
TSA 50nmol/L	11.9	4.4	8.2	5.3

Table 36 Effect of MSA and TSA on *Fluor de Lys*™ substrate deacetylation by HeLa nuclear extract and DHL4 lysates after 2-hour exposure. Results expressed relative to control.

MSA µmol/L	Set 1	Set 2	Set 3	Mean	+/-SD
0	100.0	100.0	100.0	100.0	0.0
10	92.3	112.4	100.2	101.6	10.1
30	77.6	84.7	75.8	79.4	4.7

Table 37 Effect of medium from DHL4 cells exposed to MSA for 2 hours on *Fluor de Lys*™ substrate deacetylation by HeLa nuclear extract. Results expressed relative to control.

MSA µmol/L	Experiment 1	Experiment 2	Mean	+/-SD
Control O_2	1.0	1.0	1.0	0.0
Control hypoxia	2.0	1.6	1.8	0.3
5	0.6	0.3	0.5	0.3
20	1.0	0.4	0.7	0.4
60	0.0	0.2	0.1	0.1

Table 38 Densitometry values for western blots of HIF1α expression in DHL4 cells exposed to hypoxia and MSA. Results expressed as fold change relative to control O_2.

MSA µmol/L	Experiment 1	Experiment 2	Mean	+/-SD
Control O_2	1.0	1.0	1.0	0.0
Control hypoxia	1.8	1.4	1.6	0.3
1	1.6	1.4	1.5	0.1
5	0.5	1.2	0.8	0.3
20	0.7	1.0	0.6	0.2

Table 39 Densitometry values for western blots of HIF1α expression in RL cells exposed to hypoxia and MSA. Results expressed as fold change relative to control O_2.

MSA µmol/L	Set 1	Set 2	Mean	+/-SD
Control O_2	100.0	100.0	100.0	0.0
Control hypoxia	281.4	286.1	283.8	3.4
5	139.0	199.2	169.1	42.5
20	78.2	80.6	79.4	1.7
60	46.9	57.1	52.0	7.2

Table 40 VEGF production in DHL4 cells exposed to hypoxia and MSA. Results expressed relative to control and have been corrected for cell number ($1x10^6$).

MSA µmol/L	Set 1	Set 2	Mean	+/-SD
Control O_2	100.0	100.0	100.0	0.0
Control hypoxia	322.9	363.8	343.3	28.9
1	268.6	300.7	284.6	22.7
5	177.9	206.1	192.0	19.9
20	54.3	75.2	64.7	14.8

Table 41 VEGF production in RL cells exposed to hypoxia and MSA. Results expressed relative to control and have been corrected for cell number ($1x10^6$).

Appendices to Chapter 7

MSA µmol/L	Time (hrs)	Set 1	Set 2	Set 3	Set 4	Set 5	Mean	+/-SD
0	Control	98.9	98.0	97.0			98.0	1.0
5	24	94.4	96.5	95.3			95.4	1.1
5	48	91.5	94.9	93.2			93.2	1.7
0	Control	94.4	92.9	92.9	99.2	97.3	95.3	2.8
10	24	88.1	89.2	92.9	98.0	94.1	92.5	4.0
10	48	79.2	83.3		90.0	91.5	86.0	5.8
0	Control	97.0	96.3	95.1			96.1	1.0
20	24	96.5	94.2	92.2			94.3	2.2
20	48	86.9	80.9	83.7			83.8	3.0

Table 42 Cell viability of PBMCs exposed to MSA.

MSA µmol/L	Set 1	Set 2	Set 3	Mean	SD+/-
0	100	100	100	100	0
0.5	98.8	100.7	94.7	98.1	3.1
1	83.9	88.9	88.3	87.0	2.7
2	49.7	61.3	65	58.7	8.0
3	27.4	36	36.9	33.4	5.2
5	20.2	20.7	24	21.6	2.1
10	9.1	10.7	9.5	9.8	0.8
15	6.4	6.4	5.8	6.2	0.3
20	4.2	4.9	4.6	4.6	0.4

Table 43 Concentration-effect of keratinocytes exposed to MSA for 48 hours. Results expressed relative to control.

MSA µmol/L	Set 1	Set 2	Set 3	Mean	+/-SD
0	100	100	100	100	0
0.5	94.4	91.7	83.4	89.8	5.7
1	80.5	88	87.6	85.4	4.2
3	78.3	62.8	69.6	70.2	7.8
5	67	71.6	60.3	66.3	5.7
7.5	49.8	67	62.1	59.6	8.9
10	24.2	29.6	24.6	26.1	3.0
15	26.1	36.5	35.1	32.6	5.6
20	30.8	27.6	22.3	26.9	4.3

Table 44 Concentration-effect of HFFF2 cells exposed to MSA for 48 hours. Results are expressed relative to control.

4-HC µmol/L	Set 1	Set 2	Set 3	Mean	+/-SD
0	100	100	100	100	0
1	99.9	93.2	100.2	97.8	4.0
3	83.5	94.9	96.7	91.7	7.1
5	75.4	86.0	86.7	82.7	6.3
10	56.4	67.5	64.4	62.8	5.7
20	42.6	25.7	29.3	32.6	8.9

Table 45 Concentration-effect of keratinoyctes exposed to 4-HC for 48 hours. Results are expressed relative to control.

Doxorubicin nmol/L	Set 1	Set 2	Set 3	Mean	+/-SD
0	100.0	100.0	100.0	100.0	0.0
10	99.5	90.2	99.5	96.4	5.4
50	83.5	80.1	87.7	83.8	3.8
100	74.9	61.9	70.0	68.9	6.5
250	57.1	37.2	44.4	46.2	10.0
500	36.9	21.1	26.3	28.1	8.1

Table 46 Concentration-effect of keratinocytes exposed to doxorubicin for 48 hours. Results are expressed relative to control.

4HC µmol/L	Set 1	Set 2	Set 3	Set 4	Mean	+/-SD
0	100	100	100	100	100.0	0.0
1	81.7		93.8	86.3	87.3	6.1
3	80	103.5	105.3	95.3	96.0	11.5
5	84	86.9	92	99.5	90.6	6.8
10	91	99.8	82.9	101.8	93.9	8.7
20	74.9	80.7	76.2	90.9	80.7	7.3

Table 47 Concentration-effect of HFFF2 cells exposed to 4-HC for 48 hours. Results are expressed relative to control.

Doxorubicin nmol/L	Set 1	Set 2	Set 3	Set 4	Set 5	Mean	+/-SD
0	100	100	100	100	100	100.0	0.0
10	81.4	78.7		83	80.3	80.9	1.8
50	83.1	75.9	84.4	82.4	81.2	81.4	3.3
100	76.3	76	68.5		86.3	76.8	7.3
250	61.3	72.2	59.5	59.5	67.5	64.0	5.6
500	32.5	51.8	37.5	39.5	44.6	41.2	7.4

Table 48 Concentration-effect of HFFF2 cells exposed to doxorubicin for 48 hours. Results are expressed relative to control.

Doxorubicin nmol/L	Set 1	Set 2	Set 3	Mean	+/-SD
0	100	100	100	100	0
10	95.2	89.7	93.3	92.7	2.8
50	76.6	77	72.3	75.3	2.6
100	75.2	65.3	72	70.8	5.1
250	53.8	57.7	63.6	58.4	4.9
500	35.6	37.7	42.1	38.5	3.3

Table 49 Cell viability of RL cells exposed to doxorubicin for 48 hours. Results are expressed relative to control.

4-HC µmol/L	Set 1	Set 2	Set 3	Mean	+/-SD
0	100	100	100	100	0
0.5	97.9	98.2	96.3	97.5	1.0
1	95.7	91.1	96.0	94.3	2.7
2	90.4	89.1	90.4	90.0	0.7
3	82.4	78.0	85.8	82.0	3.9
5	70.7	62.9	73.8	69.1	5.6

Table 50 Cell viability of RL cells exposed to 4-HC for 48 hours. Results are expressed relative to control.

MSA µmol/L	Phase of cell cycle	Set 1	Set 2	Set 3	Mean	+/-SD
0	A	1.0	0.7	4.6	2.1	2.2
	G1	58.4	58.8	68.4	61.9	5.6
	S	11.6	14.3	6.1	10.7	4.2
	G2	23.1	17.4	14.4	18.3	4.4
0.5	A	0.38	0.48	3.28	1.38	1.65
	G1	44.4	65.5	66.8	58.9	12.6
	S	21.8	12.5	7.2	13.8	7.3
	G2	16.4	15.6	15.4	15.8	0.5
1	A	0.8	0.2	3.7	1.6	1.9
	G1	64.4	76.4	69.7	70.2	6.0
	S	13.6	8.2	6.1	9.3	3.9
	G2	11.2	9.3	12.8	11.1	1.8
2	A	2.3	2.8	5.7	3.6	1.8
	G1	80.1	76.7	66.5	74.4	7.1
	S	3.7	6.5	3.7	4.7	1.6
	G2	10.5	8.5	14.5	11.2	3.1
3	A	13.1	14.5	18.2	15.3	2.7
	G1	66.6	63.4	62.9	64.3	2.0
	S	7.2	7.1	4.0	6.1	1.8
	G2	11.7	13.7	13.4	12.9	1.0
5	A	19.8	11.5	25.2	18.8	6.9
	G1	53.1	59.8	52.4	55.1	4.1
	S	10.5	11.7	6.6	9.6	2.7
	G2	12.0	13.9	12.4	12.8	1.0

Table 51 Cell cycle analysis of keratinocytes exposed to MSA for 24 hours. Results expressed as % of cells in each phase of the cell cycle.

MSA µmol/L	Phase of cell cycle	Set 1	Set 2	Set 3	Set 4	Mean	+/-SD
0	A	2.2	1.8	0.9	1.4	1.6	0.6
	G1	63.6	61.4	65.2	64.3	63.6	1.6
	S	10.0	16.7	11.8	12.0	12.6	2.8
	G2	19.9	15.1	18.6	16.9	17.7	2.1
0.5	A	1.4	2.2	0.9		1.5	0.6
	G1	65.9	66.6	65.7		66.1	0.5
	S	9.7	11.1	12.6		11.2	1.5
	G2	18.7	16.3	15.2		16.7	1.8
1	A	1.7	2.3	2.3		2.1	0.4
	G1	67.7	68.6	70.1		68.8	1.2
	S	14.7	10.7	8.9		11.5	3.0
	G2	11.9	15.1	13.7		13.6	1.6
2	A	3.6	3.2	14.5	25.6	11.7	10.6
	G1	70.9	68.5	65.3	50.2	63.7	9.3
	S	11.0	7.9	5.4	7.8	8.0	2.3
	G2	10.4	13.4	11.7	9.1	11.1	1.8
3	A	12.4	12.1	37.8	32.1	23.6	13.3
	G1	67.0	69.9	39.9	42.5	54.8	15.8
	S	7.6	6.1	5.7	7.4	6.7	0.9
	G2	10.1	6.6	8.4	7.4	8.1	1.5
5	A	34.4	22.5	44.3	48.6	37.5	11.6
	G1	47.5	56.1	40.6	36.3	45.1	8.6
	S	8.0	8.6	3.7	10.4	7.7	2.8
	G2	8.1	8.6	6.6	4.1	6.8	2.0

Table 52 Cell cycle analysis of keratinocytes exposed to MSA for 48 hours. Results expressed as % of cells in each phase of the cell cycle.

4-HC µmol/L	Set 1	Set 2	Set 3	Mean	+/-SD
0	100	100	100	100	0
1	104.3	101.3	105.1	103.5	2.0
3	89.3	86.1	94.2	89.9	4.1
5	77.7	80.0	87.2	81.6	4.9
10	58.7	64.3	68.4	63.8	4.9
20	37.2	45.1	52.9	45.1	7.8
4-HC+MSA 0.5µmol/L					
MSA alone	102.2	100.0	101.8	101.3	1.2
1	97.2	91.6	92.8	93.8	2.9
3	89.7	81.0	87.9	86.2	4.6
5	80.9	74.6	80.8	78.8	3.6
10	65.6	67.3	65.5	66.1	1.0
20	47.0	55.3	53.4	51.9	4.4

Table 53 Concentration-response of keratinocytes exposed to 4-HC alone and in combination with MSA for 48 hours. Results are expressed relative to control.

Doxorubicin nmol/L	Set 1	Set 2	Set 3	Mean	+/-SD
0	100	100	100	100	0
10	98.2	109.8	108.2	105.4	6.3
50	82.8	96.3	88.6	89.2	6.8
100	71.1	84.6	76.9	77.6	6.8
250	52.4	70.5	51.6	58.2	10.7
500	31.9	41.4	34.8	36.1	4.8
Doxorubicin+MSA 0.5µmol/L					
MSA alone	94.1	100.9	105.1	100.0	5.6
10	91.9	105.8	103.8	100.5	7.5
50	78.0	96.6	93.3	89.3	9.9
100	69.4	87.1	84.1	80.2	9.5
250	54.4	70.2	61.3	62.0	7.9
500	31.5	44.7	34.1	36.8	7.0

Table 54 Concentration-response of keratinocytes exposed to doxorubicin alone and in combination with MSA for 48 hours. Results expressed relative to control.

4-HC µmol/L	Set 1	Set 2	Set 3	Mean	+/-SD
0	100	100	100	100	0
1	104.3	101.3	105.1	103.5	2.0
3	89.3	86.1	94.2	89.9	4.1
5	77.7	80.0	87.2	81.6	4.9
10	58.7	64.3	68.4	63.8	4.9
20	37.2	45.1	52.9	45.1	7.8
7 days pre-treatment with 0.5µmol/L MSA					
0	102.2	100.0	101.8	101.3	1.2
1	97.2	91.6	92.8	93.8	2.9
3	89.7	81.0	87.9	86.2	4.6
5	80.9	74.6	80.8	78.8	3.6
10	65.6	67.3	65.5	66.1	1.0
20	47.0	55.3	53.4	51.9	4.4

Table 55 Concentration-effect of keratinocytes exposed to 4-HC alone for 48 hours or following pre-treatment with MSA prior to 4-HC exposure. Results expressed relative to control.

Doxorubicin nmol/L	Set 1	Set 2	Set 3	Mean	+/-SD
0	100	100	100	100	0
10	98.2	109.8	108.2	105.4	6.3
50	82.8	96.3	88.6	89.2	6.8
100	71.1	84.6	76.9	77.6	6.8
250	52.4	70.5	51.6	58.2	10.7
500	31.9	41.4	34.8	36.1	4.8
7 days pre-treatment with 0.5µmol/L MSA					
MSA alone	94.1	100.9	105.1	100.0	5.6
10	91.9	105.8	103.8	100.5	7.5
50	78.0	96.6	93.3	89.3	9.9
100	69.4	87.1	84.1	80.2	9.5
250	54.4	70.2	61.3	62.0	7.9
500	31.5	44.7	34.1	36.8	7.0

Table 56 Concentration-effect of keratinocytes exposed to doxorubicin alone for 48 hours or following pre-treatment with MSA prior to doxorubicin exposure. Results are expressed relative to control.

MSA µmol/L	Time (hours)	1	2	3	4	5	6	7	8	9	10	Mean	+/-SD
20	0	1	1	1	1	1	1	1	1	1	1	1	0
20	4	8.8		4.2	1.2	5.7	4.7	2.7	3.8	2.5	3.5	4.4	2.1
20	6	4.2		3.9	1.7	2.6	5.7	1.9	2.7	2.5	2.7	3.2	1.2
20	24	12.9	16.1	8.9		11.8		4.7	10.9	5.9	13.2	10.9	3.6

Table 57 GADD153 mRNA expression in PBMCs from 10 individuals exposed to MSA. Results are expressed as fold change relative to control.

MSA µmol/L	1	2	3	4	5	6	7	8	9	10	11	12	Mean	+/-SD
0	100	100	100	100	100	100	100	100	100	100	100	100	100	0
5								90.0		92.0			91.0	1.4
10	110.1	125.0				110.0			81.0		104.0		106.0	16.0
20	108.2	123.7	119.5				106.0					95.0	110.5	11.4
40				91.0	61.1								76.1	21.2

Table 58 NK-κB binding activity in whole cell lyastes of PBMCs exposed to MSA. Results expressed relative to control.

	Experiment 1		Mean	+/-SD
Control	100.0	100.0	100.0	0.0
TNF alone	157.7	191.3	174.5	23.7
TNF+MSA 5µmol/L	206.8	250.1	228.4	30.6
TNF+MSA 10µmol/L	339.0	308.0	323.5	21.9
TNF+MSA 20µmol/L	351.5	354.6	353.1	2.2
	Experiment 2			
Control	100	100	100	0
TNF alone	167.8	173.1	170.5	3.7
TNF+MSA 5µmol/L	121.4	133.1	127.2	8.3
TNF+MSA 10µmol/L	187.9	166.3	177.1	15.3
TNF+MSA 20µmol/L	167.2	183.5	175.3	11.5
	Experiment 3			
Control	100.0	100.0	100.0	0.0
TNF alone	167.2	163.9	165.6	2.4
TNF+MSA 5µmol/L	391.2	423.4	407.3	22.8
TNF+MSA 10µmol/L	336.8	423.5	380.1	61.3
TNF+MSA 20µmol/L	457.0	385.3	421.2	50.7

Table 59 NK-κB binding activity in nuclear extracts of PBMCs from 3 different individuals exposed to MSA. Results are expressed relative to control.

MSA µmol/L	1	2	3	4	5	6	7	8	Mean	+/-SD
Control	1	1	1	1	1	1	1	1	1	0
20	2.5	2.1	4.5	0.7	4.8	2.5	2	1	2.5	1.5

Table 60 Densitometry values of western blots of NF-κB expression in nuclear extracts of PBMCs from 8 different individuals exposed to MSA. Results are expressed as fold change relative to control.

Appendices to Chapter 8

MSA µmol/L	Set 1	Set 2	Set 3	Mean	+/-SD
0	100	100	100	100	0
5	95.4	98.7	92.4	95.5	3.2
10	91	95.1	89.2	91.8	3.0
20	64.5	79.6	69	71.0	7.8
50	30.9	50.5	30.7	37.4	11.4
100	25	28.9	19.7	24.5	4.6

Table 61 Cell viability of the JeKo-1 cell line exposed to MSA. Results expressed relative to control.

MSA µmol/L	Set 1	Set 2	Set 3	Mean	+/-SD
0	100	100	100	100	0
5	99.1	96.8	98.9	98.3	1.3
10	97.8	94.7	95.4	96.0	1.6
20	69.2	70.4	82.4	74.0	7.3
50	56.8	38.5	43.1	46.1	9.5
100	38.4	32.4	34.6	35.1	3.0

Table 62 Cell viability of the Granta-519 cell line exposed to MSA. Results expressed relative to control.

MSA µmol/L	Set 1	Set 2	Set 3	Mean	+/-SD
0	100.0	100.0	100.0	100.0	0.0
5	53.6	49.3	46.8	49.9	3.4
10	43.1	39.9	34.0	39.0	4.6
20	37.0	33.1	27.5	32.5	4.8
50	30.4	28.9	27.7	29.0	1.4
100	30.1	28.1	27.5	28.6	1.3

Table 63 Cell number of JeKo-1 cells exposed to MSA. Results expressed relative to control.

MSA µmol/L	Set 1	Set 2	Set 3	Mean	+/-SD
0	100.0	100.0	100.0	100.0	0.0
5	47.2	49.1	56.4	50.9	4.8
10	35.8	36.1	36.5	36.1	0.3
20	29.1	29.5	35.7	31.4	3.7
50	23.6	27.2	43.6	31.5	10.6
100	23.0	27.9	34.0	28.3	5.5

Table 64 Cell number of Granta-519 cells exposed to MSA. Results expressed relative to control.

Bortezomib nmol/L	Set 1	Set 2	Set 3	Mean	+/-SD
0	100	100	100	100	0
5	99.4	100.1	100.3	99.9	0.5
10	98.6	99.6	100	99.4	0.7
20	94.9	97.3	96.5	96.2	1.2
50	52.1	60.3	65.2	59.2	6.6
100	37.3	30.8	51.4	39.8	10.5

Table 65 Cell viability of the JeKo-1 cell line exposed to bortezomib. Results expressed relative to control.

Bortezomib nmol/L	Set 1	Set 2	Set 3	Mean	+/-SD
0	100	100	100	100	0
5	100.3	99.8	99.5	99.9	0.4
10	100.1	99.4	99.3	99.6	0.4
20	99.2	96.8	96.6	97.5	1.4
50	72.6	58.2	64.8	65.2	7.2
100	64.2	26.4	43.2	44.6	18.9

Table 66 Cell viability of the Granta-519 cell line exposed to bortezomib. Results expressed relative to control.

Bortezomib nmol/L	Set 1	Set 2	Set 3	Mean	+/-SD
0	100.0	100.0	100.0	100.0	0.0
5	102.2	93.5	91.3	95.6	5.8
10	89.1	96.6	82.4	89.4	7.1
20	54.9	58.9	51.9	55.2	3.5
50	30.6	29.0	24.8	28.1	3.0
100	28.5	23.3	24.4	25.4	2.8

Table 67 Cell number of JeKo-1 cells exposed to bortezomib. Results expressed relative to control.

Bortezomib nmol/L	Set 1	Set 2	Set 3	Mean	+/-SD
control	100.0	100.0	100.0	100.0	0.0
5	98.0	92.9	97.2	96.0	2.8
10	90.0	81.7	93.5	88.4	6.0
20	54.2	65.7	76.0	65.3	10.9
50	27.4	34.5	21.2	27.7	6.6
100	26.1	23.5	38.5	29.3	8.0

Table 68 Cell number of Granta-519 cells exposed to bortezomib. Results expressed relative to control.

Bortezomib nmol/L	Set 1	Set 2	Set 3	Mean	+/-SD
0	100	100	100	100	0
5	99.7	99.7	100.1	99.8	0.2
10	99.6	99.6	99.5	99.6	0.1
20	98.0	96.4	82.0	92.1	8.8
50	60.1	51.0	43.5	51.5	8.3
Bortezomib+MSA 10μmol/L					
MSA alone	95.4	92.6	97.6	95.2	2.5
5	93.5	90.8	96.9	93.7	3.1
10	91.8	90.6	95.5	92.6	2.6
20	86.2	85.6	90.0	87.3	2.3
50	73.4	67.2	63.4	68.0	5.1
Bortezomib+MSA 10μmol/L	Expected cell viability				
MSA alone	95.4	92.6	97.6	95.2	2.5
5	95.1	92.3	97.7	95.0	2.7
10	95.0	92.2	97.1	94.8	2.4
20	93.4	89.0	79.6	87.3	7.1
50	55.5	43.6	41.1	46.7	7.7

Table 69 The effect on JeKo-1 cell viability of combining MSA and bortezomib for 48 hours. Results expressed relative to control

Bortezomib nmol/L	Set 1	Set 2	Set 3	Mean	+/-SD
0	100	100	100	100	0
5	100	100.7	98.3	99.6	1.3
10	99.9	100.2	96.6	98.9	2.0
20	98.1	98.4	95.4	97.3	1.7
50	63.3	58.1	66.6	62.7	4.3
Bortezomib+MSA 10μM					
MSA alone	96.7	93.1	85.0	91.6	6.0
5	95.7	91.5	84.8	90.7	5.5
10	94.9	91.9	78.8	88.5	8.5
20	89.6	88.3	83.2	87.0	3.4
50	73.5	69.0	71.5	71.3	2.2
Bortezomib+MSA 10μM	Expected cell viability				
MSA alone	96.7	93.1	85.0	91.6	6.0
5	96.7	93.8	83.3	91.2	7.1
10	96.6	93.3	81.6	90.5	7.9
20	94.8	91.5	80.4	88.9	7.6
50	60.0	51.2	51.6	54.3	5.0

Table 70 The effect on Granta-519 cell viability of combining MSA and bortezomib for 48 hour. Results expressed relative to control.

Bortezomib nmol/L	Set 1	Set 2	Set 3	Mean	+/-SD
0	100	100	100	100	0
5	99.7	99.6	100.2	99.8	0.4
10	99.4	99.9	99.2	99.5	0.3
20	88.0	84.6	82.3	85.0	2.9
50	38.4	53.8	44.4	45.5	7.8
Bortezomib+MSA 10μmol/L					
MSA alone	96.3	100.0	99.4	98.6	2.0
5	97.9	100.3	99.4	99.2	1.2
10	97.7	100.1	97.7	98.5	1.4
20	96.3	95.4	97.3	96.3	1.0
50	91.6	80.5	84.0	85.3	5.7
Bortezomib+MSA 10μmol/L	Expected cell viability				
0	96.3	100.0	99.4	100.0	0
5	96.0	99.6	99.6	98.4	2.1
10	95.7	99.9	98.6	98.1	2.2
20	84.3	84.6	81.7	83.6	1.6
50	34.7	53.8	43.8	44.1	9.6

Table 71 The effect on JeKo-1 cell viability of pre-treatment with MSA for 48 hours followed by treatment with bortezomib for a further 48 hours. Results expressed relative to control.

Bortezomib nmol/L	Set 1	Set 2	Set 3	Mean	+/-SD
0	100	100	100	100	0
5	100.2	98.8	100.5	99.8	0.9
10	99.5	99.1	100.4	99.7	0.7
20	85.8	79.8	82.0	82.5	3.0
50	30.2	32.9	30.5	31.2	1.5
Bortezomib+MSA 10µmol/L					
MSA alone	98.4	100	99.7	99.4	0.9
5	98.4	99.5	99.8	99.2	0.8
10	98.3	99.5	100.1	99.3	0.9
20	97.3	97.4	96.2	96.9	0.6
50	91.2	86.7	84.4	87.4	3.4
Bortezomib+MSA 10µmol/L	Expected cell viability				
MSA alone	98.4	100	99.7	99.4	0.9
5	98.6	98.8	100.2	99.2	0.9
10	97.9	99.1	100.1	99.0	1.1
20	84.2	79.8	81.7	81.9	2.2
50	28.6	32.9	30.2	30.6	2.2

Table 72 The effect on Granta-519 cell viability of pre-treatment with MSA for 48 hours followed by treatment with bortezomib for a further 48 hours. Results expressed relative to control.

JeKo-1	Set 1	Set 2	Set 3	Mean	SD
Control	311.0	243.7	290.1	281.6	34.4
MSA 10µmol/L	281.6	205.4	243.6	243.6	38.1
Bortezomib 20nmol/L	19.2	9.1	19.8	16.0	6.0
MSA and bortezomib 20nmol/L	24.5	7.8	16.4	16.2	8.4
Bortezomib 50nmol/L	5.9	4.5		5.2	1.0
MSA and bortezomib 50nmol/L	7.5	4.2		5.8	2.3
Granta-519					
Control	247.3	275.8	259.4	260.8	14.3
MSA 10µmol/L	225.9	218.1	225.6	223.2	4.4
Bortezomib 20nmol/L	22.0	10.7	35.4	22.7	12.4
MSA and bortezomib	31.3	11.9	19.0	20.8	9.8
Bortezomib 50nmol/L	4.2	6.3		5.2	1.5
MSA and bortezomib 50nmol/L	3.7	6.0		4.8	1.6

Table 73 Proteasome activity in JeKo-1 and Granta-519 cell lines treated with MSA 10µmol/L and bortezomib alone and in combination. Results expressed as µM AMC/mg/hr.

Appendices to Chapter 9

RL cells	Set 1	Set 2	Mean	+/-SD
Control	0.5	1.3	0.9	0.6
10 minutes	379.5	148.0	263.8	163.7
30 minutes	230.2	120.0	175.1	77.9
1 hour	261.9	116.0	189.0	103.2
2 hours	246.7	124.0	185.3	86.8
4 hours	276.8	93.0	184.9	130.0
6 hours	136.7	100.0	118.4	26.0
24 hours	213.9	65.0	139.5	105.3
DHL4 cells				
Control	-0.3	2.1	0.9	1.7
10 minutes	337.2	130.0	233.6	146.5
30 minutes	374.8	106.0	240.4	190.0
1 hour	329.3	145.0	237.1	130.3
2 hours	192.5	132.0	162.2	42.8
4 hours	280.3	160.0	220.2	85.1
6 hours	197.7	96.0	146.8	71.9
24 hours	66.3	70.0	68.2	2.6

Table 74 Intracellular Se concentration (µg/kg) in RL and DHL4 cell lines exposed to 20µmol/L MSA.

PBMCs	Set 1	Set 2	Set 3	Set 4	Set 5	Mean	+/-SD
Control	2.8	1.3	-0.9	0.7	1.6	1.1	1.4
10 minutes	17.7	30.9	27.5	54.0	96.5	45.3	31.6
30 minutes	21.3	41.5	41.3	74.0	118.4	59.3	38.1
1 hour	31.1	51.1	39.9	115.0	150.2	77.5	52.3
2 hours	42.1	66.5	52.7	164.0	96.8	84.4	49.0
4 hours	58.9	67.1	60.9	200.0	156.1	108.6	65.3
6 hours	64.6	72.0	74.4	218.0	131.7	112.1	65.0
24 hours	29.2	33.5	33.0	153.0	127.0	75.2	59.9

Table 75 Intracellular Se concentration (µg/kg) in PBMCs exposed to 20µmol/L MSA.

	Set 1	Set 2	Set 3	Set 4	Set 5	Mean	+/-SD
DHL4 control	100.0	100.0	100.0	100.0	100.0	100.0	0.0
DHL4 + 'RM'	94.6	99.0	103.5	102.7	115.7	103.1	7.9
RL control	100.0	100.0	100.0	100.0		100.0	0.0
RL + 'RM'	169.0	137.9	143.9	152.4		150.8	13.5
JVM2 control	100.0	100.0		100.0	100.0	100.0	0.0
JVM2 + 'RM'	111.2	116.0		98.5	142.9	117.2	18.7
ACHN control	100.0	100.0			100.0	100.0	0.0
ACHN + 'RM'	293.7	511.6			342.3	382.5	114.4

Table 76 Pyruvate generation as a measure of β-lyase activity in 3 lymphoma cell lines and the renal adenocarcinoma cell line, ACHN. Results expressed relative to the relevant control. 'RM'=reaction mix

MSC µmol/L	Set 1	Set 2	Set 3	Set 4	Mean	+/-SD
0	100	100	100	100	100	0
1	90.6	84.9	90.2	94.8	90.1	4.0
3	85.1	81.0	84.0	90.2	85.1	3.8
5	79.3	82.7	68.7	79.3	77.5	6.1
10	70.7	73.0	62.2	73.9	69.9	5.3
20	45.2	54.0	37.5	44.1	45.2	6.8
30			33.8	22.7	28.2	7.9
40			26.7	20.4	23.6	4.5
50			21.9	21.0	21.4	0.7

Table 77 Concentration-response of ACHN cells exposed to MSC. Results are expressed relative to control.

Appendices to Chapter 10

Method for phospho-proteomics experiments described in full

Sample preparation

The RL and DHL4 cell lines were exposed to MSA 1μmol/L and 10μmol/L respectively for 24 hours. Following this, 10 million cells were centrifuged at 110*g* for 5 minutes at 5°C and the supernatant discarded. Cells were resuspended in ice-cold PBS containing Na_3VO_4 (Sigma-Aldrich), final concentration 100mM, and NaF (Sigma-Aldrich), final concentration 0.5M. Cells were centrifuged at 110*g* for 5 minutes at 5°C and the supernatant discarded. This step was repeated twice more after which the cell pellets were snap-frozen on dry ice and stored at -20°C until further use. These experiments were performed on 3 separate occasions to obtain independent triplicate samples. The stored samples were then all processed together as described below.

Cell lysis

The frozen cells pellets were thawed on ice and resuspended in 1 ml of lysis buffer (20mM HEPES, pH 8.0, 8M urea, 100mM Na_3VO_4, 0.5M NaF, 0.25M sodium pyrophosphate and 1M β-glycerol phosphate; all from Sigma-Aldrich). The cell suspension was then sonicated 3 times for 15 seconds to further solubilise the proteins. Samples were centrifuged at 20000*g* for 10 minutes at 5°C to remove any cellular debris and the supernatant was recovered into protein Lobind® tubes (Eppendorf UK Limited). Where possible, samples were kept in protein LoBind® tubes from this stage onwards. Cellular proteins were reduced with DTT, final concentration 4.1mM, in the dark for 15 minutes at room temperature followed by alkylation with iodoacetamide, final concentration 8.3mM in the dark for 15 minutes at room temperature. Protein extracts were then diluted in 20mM HEPES pH 8.0 (1:4 dilution).

Protein digestion

Protein digestion was achieved with the use of immobilised L-1-tosylamido-2-phenylethyl chloromethyl ketone (TPCK)-trypsin beads (Thermo Fisher Scientific, Cramlington, UK). The beads were conditioned prior to use according to the

manufacturers' instruction. 80µl of trypsin beads [≥200 TAME units per ml; (TAME Unit: One Unit hydrolyzes 1µmole of p-toluene-sulfonyl-L-arginine methyl ester (TAME) per minute at 25°C, pH 8.2, in the presence of 10mM calcium)] were used for protein extracted from 10 million cells. The appropriate amount of trypsin beads were transferred to a fresh tube and centrifuged at 2000*g* for 5 minutes at 5°C. The supernatant was discarded and the beads were re-suspended in 20mM HEPES (double the volume of beads) followed by thorough mixing. The beads were centrifuged again at 2000*g* for 5 minutes at 5°C and the supernatant discarded. This step was repeated twice more. The beads were then resuspended in 20mM HEPES at a volume equal to the original volume of beads. 80µl was added to each sample and incubated for 16 hours at 37°C with shaking. Following this, digestion was stopped by adding TFA (LGC Standards) at a final concentration of 1%. Samples were centrifuged at 2000*g* for 5 minutes at 5°C to remove the trypsin beads and the supernatant was recovered into fresh tubes.

Peptide desalting

Sep-Pak® C_{18} cartridges (Waters UK Ltd., Manchester, UK) were used to desalt the peptide samples. The cartridges were initially washed with 10mls of 100% ACN and then with 10mls of 98% H_2O/2% ACN/0.1% TFA. Following this, samples were loaded into the cartridges. Cartridges were washed again with 10mls of 98% H_2O/2% ACN/0.1% TFA. Bound peptides were then eluted with 5mls of 50% ACN/0.1% TFA and ready to use for further work.

Phospho-peptide enrichment by immobilized metal ion affinity chromatography (IMAC)

IMAC sepharose™ high performance beads (GE healthcare) were used to separate the phospho-peptide component of the peptide elution. Firstly, the beads were conditioned and charged with Fe^{3+}. 300µl of highly cross-linked agarose beads (particle size 34µm) were used for 10 million cells. All centrifugation/wash steps were at 110*g* for 1 minute at 5°C. The beads were pre-swollen in 20% ethanol and therefore the required volume was centrifuged, the supernatant discarded and the beads re-suspended in LC-MS grade H_2O

(same volume as the compacted beads). The beads were centrifuged again, the supernatant discarded and washed twice with 200mM EDTA. The beads were then washed three times with 50% ACN/0.1% TFA and the supernatant discarded. Iron chloride ($FeCl_3$; Sigma-Aldrich), 100mM, was added to the beads and incubated for 5 minutes at room temperature. The beads were centrifuged, the supernatant discarded and the same $FeCl_3$ incubation step repeated. The beads were then washed six times with 50% ACN/0.1% TFA and finally re-suspended in 50% ACN/0.1% TFA and ready for use.

300µl of the Fe^{3+} charged beads were added to each sample and placed on a rotatory mixer for 1 hour at room temperature. The samples were then centrifuged at 420*g* for 1 minute and the supernatant recovered (i.e. non-phosphorylated peptides). The beads were washed with 50% ACN/0.1% TFA and the supernatant recovered again and added to the previous supernatant sample. The phospho-peptides were eluted with ammonia water [60µl of 25% ammonia solution (LGC standards) was diluted in 940µl of ultrapure water]. 300µl was added to each sample and incubated for 5 minutes at room temperature. The samples were centrifuged at 420*g* for 1 minute and the supernatant recovered into protein LoBind® tubes. The addition of ammonia water was repeated and the supernatant recovered once again. Finally, the beads were washed twice with 100µl 50% ACN/0.1% TFA and the supernatant recovered.

Both the fractions containing the non-phosphorylated and phospho-enriched peptides were dried down in a vacuum centrifuge (Christ rotational vacuum concentrator, Osterode, Germany).

Reconstitution of samples for mass spectrometry

11µl of 0.1% FA in LC-MS grade H_2O was added to the dried samples and the sample re-suspended. The samples were incubated for 10 minutes at room temperature and then centrifuged at 2700*g* for 5 minutes at 5°C to remove any debris. 10µl of the supernatant was drawn up and placed in lubricated hydrophobic tubes (Bioquote Limited, York, UK) ready for analysis by MS

Nanoflow-UPLC® coupled to tandem MS (LC-MS/MS)

A nanoflow UPLC® system (nanoAquity, Waters/Micromass UK Ltd. Manchester) was coupled to a LTQ-Orbitrap XL MS (Thermo Fisher Scientific, Hemel Hempstead, UK). 3µl of each sample was injected into a trap column (nanoAcquity UPLC® Symmetry® C_{18} Trap; 20mm length, 180µm id, 5µm particle size; Waters/Micromass) and then into a nanoflow column (nanoAquity UPLC® BEH C_{18} column; 100mm length, 100µm id, 1.7µm particle size; Waters/Micromass). The mobile phases consisted of solution A (0.1% FA in LC-MS grade water) and solution B (0.1% FA in LC-MS grade ACN). Gradient runs were from 1% B to 35% B in 100 minutes and the flow rate was 5µl/min for loading and 0.4µl/min for elution. The spray voltage was set to 2kV, the temperature of the heated capillary to 150°C and a positive ionisation mode was used. The MS was operated in data-dependent mode to automatically acquire MS and MS/MS spectra. Full scan survey spectra (*m/z* 375-1800) were acquired in the LTQ-Orbitrap XL. The five most intense ions in each full scan (every 0.6 of a second) were sequentially isolated and fragmented by collision-induced dissociation. The collision gas was helium. Data were acquired using the Xcalibur software version 2.0.7 (Thermo Fisher Scientific).

Data analysis

LTQ-Orbitrap MS/MS data were smoothed and centroided using Mascot Distiller (v2.1.10, Matrix Science, London, UK). For protein identification, the processed files were searched against the Swiss-Prot database of protein sequences using the Mascot search engine (Mascot Daemon, v2.3.0; Matrix Science). The searches were performed choosing trypsin as digestion enzyme with two missed cleavages allowed. Carbomidomethyl (C) was set as a fixed modification and oxidation (M), phospho (ST), phospho (Y) and pyro-glu (N-term) as variable modifications. Data sets were searched with a mass tolerance of ±5ppm and a fragment mass tolerance of ±600mmu. Protein identifications were accepted when Mascot scores were above the statistically significant threshold ($p<0.05$).

For quantitative analysis of the MS data, a program written by the Analytical Signalling Group (Institute of Cancer, Barts Cancer Centre, London, UK) was used (Cutillas & Vanhaesebroeck, 2007). It is a program written in Visual Basic termed Pescal (Peak Statistic Calculator). The program uses the *m/z* and retention time values for each identified peptide ion to generate extracted ion chromatograms. Algorithms in Pescal calculate intensity at maximum peak height and area under the curve and generate peak intensity values for each of the peptide sequences identified by Mascot. These peak intensities were then normalised by dividing each peak intensity by the sum of all the peak intensities. Each experiment was performed in triplicate and therefore for each peptide the mean peak intensities for control and MSA-treated samples were calculated. If more than one peptide belonging to the same protein was present, then the peak intensity values for all peptides were combined and the mean calculated. A paired t-test was used to determine significant differences in peptide intensities between control and MSA-treated samples. $p<0.05$ was considered statistically significant. Peptides that did not change in intensity between control and MSA-treated samples were excluded from further analysis. These quantitative data were then analysed using the MetaboAnalyst software (www.metaboanalyst.ca) which performs both univariate (t-test and fold change) and multivariate analysis (principle component analysis and hierarchical cluster analysis). The data entered into this software was the *m/z*, the retention time and the peak intensity.

Network and pathway analysis was performed using Ingenuity Pathway Analysis (IPA) software™ v8.6 (Ingenuity Systems, www.ingenuity.com). The fold-change was calculated for the peptides that changed significantly between control and MSA-treated samples and peptides with a ≥ 2 fold change in intensity were used in pathway analysis.

Table 78 The complete list of differentially expressed proteins in DHL4 cells exposed to MSA 10μmol/L

Gene Symbol	Protein	Phospho	FC	p value
C1QBP	Complement component 1 Q subcomponent-binding protein, mitochondrial		↓229	0.001
MCM7	Isoform 1 of DNA replication licensing factor MCM7		↓98.4	0.03
VEPH1	Isoform 1 of Ventricular zone-expressed PH domain-containing protein homolog 1	ST	↓55.2	0.001
PTPLAD1	Protein tyrosine phosphatase-like protein	ST	↑38.4	0.004
ALDOA	Fructose-bisphosphate aldolase A		↓25.8	0.008
HNRNPA3	Isoform 1 of Heterogeneous nuclear ribonucleoprotein A3		↑23.7	0.02
RRM2	Ribonucleotide reductase, subunit M2	ST	↓14.4	0.01
TUBB3	Tubulin beta-3 chain		↑13.5	0.002
CCT8	Chaperonin containing T complex protein 1, subunit 8 (theta)		↑12.1	0.002
GLO1	Glyoxalase 1		↓11.6	0.01
TXNRD1	Thioredoxin reductase 1		↑9.7	0.004
RCTPI1	Triosephosphate isomerase		↑9	0.02
CDC2	Cyclin-dependent kinase 1	ST, Y	↓8.7	0.02
HMGCS1	Hydroxymethylglutaryl-CoA synthase, cytoplasmic	ST	↓7.6	0.01
CCT4	Chaperonin containing T complex protein 1, subunit 4 (delta)		↑8.5	0.02
SYNE2	Isoform 1 of Nesprin-2		↑7.7	0.02
PDCD4	Programmed cell death 4 isoform 2		↑7.3	0.009
SOD1	Superoxide dismutase		↑7.1	0.03
HSPA5	GRP78		↑6.6	0.02
HSPH1	Heat shock protein 105 kDa (Isoform β)		↓6.6	0.045
HSP90B3P	GRP94		↑6.0	0.01
RPLP0	60S acidic ribosomal protein P0	2ST	↓5.9	0.03
ESF1	ESF1 homolog	ST	↓5.9	0.002
HIST1H1B	Histone H1.5	ST	↓5.5	0.006
CCT7	chaperonin containing T complex protein 1, subunit 7 (eta)		↓5.3	0.0001
HLA-A	Major histocompatibility complex, class I, A		↑5.1	0.04
	Similar to Delta(3,5)-Delta(2,4)-dienoyl-		↓5.0	0.04

	CoA isomerase, mitochondrial precursor			
HSPD1	60 kDa heat shock protein, mitochondrial		↓5.0	0.04
NOP2	Putative uncharacterized protein NOP2	ST	↓4.9	0.007
	Putative uncharacterized protein RPL14P1	ST	↓4.9	0.02
CFL2	Cofilin-2		↑4.5	0.03
RAB10	Ras-related protein Rab-10		↑4.5	0.008
ANKZF1	Ankyrin repeat and zinc finger domain-containing protein 1	ST	↓4.5	0.03
ATP5B	13 kDa protein		↑4.4	0.03
TCP1	T-complex protein 1 subunit alpha		↑4.4	0.003
MCM7	Isoform 1 of DNA replication licensing factor MCM7		↓4.3	0.008
NCL	Nucleolin		↑4.3	0.008
CAD	Carbamoyl-phosphate synthetase 2	ST	↓4.1	0.004
TUBA1C	Tubulin alpha-1C chain	ST	↓4.0	0.02
HNRNPU	Isoform Short of Heterogeneous nuclear ribonucleoprotein U		↑3.9	0.03
DDX21	Isoform 1 of Nucleolar RNA helicase 2	ST	↓3.7	0.004
NOLC1	Isoform Beta of Nucleolar phosphoprotein p130		↑3.7	0.02
IGL@	Immunoglobulin lambda protein locus		↓3.7	0.02
PTPRCAP	Protein tyrosine phosphatase receptor type C-associated protein	ST	↓3.6	0.048
	Similar to Heterogeneous nuclear ribonucleoprotein A1		↑3.4	0.01
RPL21	60S ribosomal protein L21		↑3.4	0.045
XRCC6	ATP-dependent DNA helicase 2 subunit 1		↓3.4	0.048
TMPO	Isoform Beta of Lamina-associated polypeptide 2, isoforms beta/gamma	ST	↑3.4	0.008
ATP5B	ATP synthase subunit beta, mitochondrial		↑3.4	0.03
DUT	Isoform 2 of deoxyuridine triphosphatase		↓3.3	0.01
SRRM1	Isoform 1 of Serine/arginine repetitive matrix protein 1	ST	↑3.3	0.007
HIST1H4C	Histone H4		↑3.2	0.02
MCM5	DNA replication licensing factor MCM5		↓3.2	0.006
SRFBP1	Serum response factor-binding protein 1	ST	↓3.2	0.006
BCL6	B-cell lymphoma 6 protein	ST	↓3.2	0.02
RPL15	60S ribosomal protein L15		↑3.1	0.02
STMN2	Stathmin-2		↑3.1	0.02
STMN1	Stathmin	ST	↓3.0	0.04
TCOF1	Treacher Collins-Franceschetti syndrome 1 isoform a	ST	↓2.9	0.008

C17orf49	Hypothetical protein LOC124944 isoform 1	ST	↓2.8	0.04
HNRNPM	Isoform 1 of Heterogeneous nuclear ribonucleoprotein M		↑2.8	0.01
YRDC	YrdC domain-containing protein, mitochondrial	ST	↓2.7	0.006
SAMHD1	SAM domain and HD domain-containing protein 1	ST	↓2.7	0.008
RPLP1	60S acidic ribosomal protein P1	ST	↓2.7	0.04
TERF2	Isoform 1 of Telomeric repeat-binding factor 2	ST	↓2.6	0.005
HNRNPA2B1	Isoform B1 of Heterogeneous nuclear ribonucleoproteins A2/B1	ST	↓2.6	0.005
	Hypothetical short protein	ST	↓2.5	0.04
FLJ43859	FAM75-like protein FLJ43859		↓2.5	0.04
FKBP1A	Peptidyl-prolyl cis-trans isomerase FKBP1A		↑2.5	0.046
EZR	Ezrin		↑2.5	0.03
ENO1	Enolase 1		↑2.4	0.045
MCM4	DNA replication licensing factor MCM4		↓2.4	0.004
DKC1	Dyskeratosis congenital 1	ST	↓2.4	0.006
MCM2	DNA replication licensing factor MCM2	ST	↓2.4	0.03
DNAJA4	DnaJ (Hsp40) homolog, subfamily A, member 4		↑2.3	0.04
EPRS	Bifunctional aminoacyl-tRNA synthetase		↓2.3	0.01
AGAP3	CENTG3 protein	ST	↑2.3	0.01
WARS	Tryptophanyl-tRNA synthetase, cytoplasmic		↑2.3	0.01
P4HB	Protein disulfide-isomerase		↑2.3	0.04
LOC731605	Hypothetical LOC731605	ST	↑2.3	0.03
TMPO	Lamina-associated polypeptide 2, isoform alpha	2ST	↓2.3	0.04
ARHGDIB	Rho GDP-dissociation inhibitor 2		↑2.3	0.04
ACCS	1-aminocyclopropane-1-carboxylate synthase-like protein 1		↓2.2	0.01
HNRNPH1	Heterogeneous nuclear ribonucleoprotein H	ST	↓2.2	0.02
ASNS	Asparagine synthetase		↑2.2	0.007
PTMA	Putative uncharacterized protein PTMA		↓2.2	0.004
cDNA FLJ54554	highly similar to Pyruvate kinase isozymes M1/M2		↑2.2	0.02
TMC8	Isoform 1 of Transmembrane channel-like	ST	↑2.1	0.047

	protein 8			
MDC1	Mediator of DNA damage checkpoint protein 1	ST	↓2.1	0.01
ABCF1	Isoform 2 of ATP-binding cassette sub-family F member 1	2ST	↓2.1	0.009
GTF3C2	Isoform 1 of General transcription factor 3C polypeptide 2	ST	↓2.1	0.04
PI4KA	similar to PIK4CA variant protein	ST	↓2.1	0.002
ATP5A1	ATP synthase subunit alpha, mitochondrial		↑2.1	0.009
LCP1	Plastin-2		↑2.0	0.01
ENO3	Enolase 3		↓2.0	0.003
GAPDH	Glyceraldehyde-3-phosphate dehydrogenase		↑2.0	0.02
TUFM	Tu translation elongation factor, mitochondrial precursor		↑2.0	0.02
DDB1	DNA damage-binding protein 1		↓2.0	0.049

PUBLICATIONS AND PRESENTATIONS ARISING FROM THIS WORK

Shireen Kassam, Lenushka Maharaj, Crispin Hiley, Simone Juliger, Simon Joel. Methylseleninic acid (MSA) is an HDAC inhibitor and suppresses VEGF production in lymphoma cell lines. American Association for Cancer Research. Abstract No. 3651, 2010.

S. Kassam, Silvia Montoto, Andrew Wilson, Janet Matthews, Kim Last, T. Andrew Lister, and Ama Z S Rohatiner. Patterns of Outcome Following Recurrence in Patients with Diffuse Large B-Cell Lymphoma (DLBCL): Long Follow-up From a Single Centre. Blood (ASH Annual Meeting Abstracts), Nov 2009; 114: 2921.

S. Kassam, S. Juliger, H. Goenaga-Infante, E. Peachey, C. Hopley and S. Joel. Chemomodulatory effects of selenium in lymphoma and normal cells. American Association for Cancer Research. Abstract No. 5585, 2009.

H.Goenaga-Infante, S.A.Kassam, E.Peachey, C.Hopley, D.Juresa, S.P.Joel. A metallomics approach to compare element speciation of healthy with cancer cells exposed *in vitro* selenium at parts-per-billion levels. European Conference on Plasma Spectrochemistry, Abstract, 2009.

Shireen Kassam, Silvia Montoto. New treatment options for the management of non-Hodgkin Lymphoma. MEMO - Magazine of European Medical Oncology, 2009 Vol. 2 , Iss. 2 94-99.

Shireen Kassam, Silvia Montoto. Emerging Drugs in B-cell Non-Hodgkin Lymphoma. Expert Opinion on Emerging Drugs, June 2008, Vol. 13, No. 2, 323-343.